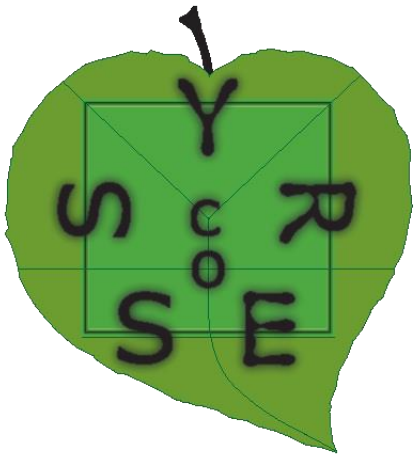

SYRCoSE 2019

Editors:

Alexander S. Kamkin, Alexander K. Petrenko, and
Andrey N. Terekhov

Preliminary Proceedings of the 13rd Spring/Summer
Young Researchers' Colloquium on Software Engineering

Saratov, May 29-31, 2019

2019

Preliminary Proceedings of the 13rd Spring/Summer Young Researchers' Colloquium on Software Engineering (SYRCoSE 2019), May 29-31, 2019 – Saratov, Russian Federation.

The issue contains papers accepted for presentation at the 13rd Spring/Summer Young Researchers' Colloquium on Software Engineering (SYRCoSE 2019) held in Saratov, Russian Federation on May 29-31, 2019.

The colloquium's topics include software development frameworks, programming languages, software and hardware verification, safety and security, automata and Petri nets, information search, and others.

The authors of the selected papers will be invited to participate in a special issue of '*The Proceedings of ISP RAS'* (http://www.ispras.ru/proceedings/), a peer-reviewed journal included into the list of periodicals recommended for publishing doctoral research results by the Higher Attestation Commission of the Ministry of Science and Higher Education of the Russian Federation.

The event is sponsored by Russian Foundation for Basic Research (Project №19-07-20042).

Contents

Foreword

Dear participants,

It is our pleasure to meet you at the 13rd Spring/Summer Young Researchers' Colloquium on Software Engineering (SYRCoSE). This year's colloquium is hosted by Saratov State University (SSU), a major higher education and research institution in Russia. The event is organized by Ivannikov Institute for System Programming of the Russian Academy of Sciences (ISP RAS), Saint-Petersburg State University (SPbSU), and SSU.

SYRCoSE 2019's Program Committee (consisting of more than 50 members from more than 25 organizations) has selected 37 papers. Each submitted paper has been reviewed independently by three referees. The authors and speakers represent well-known universities, research institutes and companies: Bauman Moscow State Technical University, Demidov Yaroslavl State University, Fraunhofer FOKUS, Higher School of Economics, INEUM, Institute YurInfor-MSU, ISP RAS, Kazan Federal University, MCST, Moscow Institute for Physics and Technology, Moscow Power Engineering Institute, Moscow State University, Peter the Great Saint Petersburg Polytechnic University, Polzunov Altai State Technical University, Rapid Telecom System Labs, Rostov Law Institute of the Ministry of Internal Affairs of the Russian Federation, Southern Federal University, SPbSU, SSU, Tomsk State University, and University of Belgrade (4 countries, 11 cities, and 21 organizations).

We would like to thank all of the participants of SYRCoSE 2019 and their advisors for interesting papers. We are also very grateful to the PC members and the external referees for their hard work on reviewing the papers and selecting the program. Our thanks go to the invited speakers, Andrey Belevantsev (ISP RAS), Jens Gerlach (Fraunhofer FOKUS), and Dmitry Koznov (SPbSU). We would also like to thank our sponsors: Russian Foundation for Basic Research (Project №19-07-20042) and Exactpro Systems. Our special thanks go to the local organizers, Dmitry Andreichenko, Inna Batraeva, Antonina Fedorova, and Alexey Geraskin, for their invaluable help in organizing the colloquium in Saratov.

Sincerely yours,

Alexander S. Kamkin
Alexander K. Petrenko
Andrey N. Terekhov

May 2019

Committees

Program Committee Chairs

Alexander K. Petrenko – Russia
Ivannikov Institute for System Programming of RAS

Andrey N. Terekhov – Russia
Saint-Petersburg State University

Program Committee

Mikhail B. Abrosimov – Russia
Saratov State University

Dmitry K. Andreichenko – Russia
Saratov State University

Elena Yu. Avdieva – Russia
Omsk State Technical University

Sergey M. Avdoshin – Russia
Higher School of Economics

Nadezhda F. Bahareva – Russia
Povolzhskiy State University of Telecommunications and Informatics

Andrey A. Belevantsev – Russia
Ivannikov Institute for System Programming of RAS

Pavel D. Drobintsev – Russia
Saint-Petersburg State Polytechnic University

Liliya Yu. Emaletdinova – Russia
Kazan National Research Technical University

Victor P. Gergel – Russia
Lobachevsky State University of Nizhny Novgorod

Susanne Graf – France
VERIMAG Laboratory

Efim M. Grinkrug – Russia
Higher School of Economics

Maxim L. Gromov – Russia
Tomsk State University

Shihong Huang – USA
Florida Atlantic University

Iosif L. Itkin – Russia
Exactpro Systems

Alexander S. Kamkin – Russia
Ivannikov Institute for System Programming of RAS

Andrei V. Klimov – Russia
Keldysh Institute of Applied Mathematics of RAS

Vsevolod P. Kotlyarov – Russia
Saint-Petersburg State Polytechnic University

Alexander N. Kovartsev – Russia
Samara State Aerospace University

Dmitry V. Koznov – Russia
Saint-Petersburg State University

Vladimir P. Kozyrev – Russia
National Research Nuclear University "MEPhI"

Daniel S. Kurushin – Russia
State National Research Polytechnic University of Perm

Peter G. Larsen – Denmark
Aarhus University

Roustam H. Latypov – Russia
Kazan Federal University

Alexander A. Letichevsky – Ukraine
Glushkov Institute of Cybernetics, NAS

Nataliya I. Limanova – Russia
Povolzhskiy State University of Telecommunications and Informatics

Alexander V. Lipanov – Ukraine
Kharkov National University of Radioelectronics

Irina A. Lomazova – Russia
Higher School of Economics

Lyudmila N. Lyadova – Russia
Higher School of Economics

Vladimir A. Makarov – Russia
Yaroslav-the-Wise Novgorod State University

Victor M. Malyshko – Russia
Moscow State University

Tiziana Margaria – Ireland
Lero – The Irish Software Research Centre

Manuel Mazzara – Russia
Innopolis University

Alexander S. Mikhaylov – Russia
RN-Inform

Alexey M. Namestnikov – Russia
Ulyanovsk State Technical University

Yaroslav R. Nedumov – Russia
Ivannikov Institute for System Programming of RAS

Valery A. Nepomniaschy – Russia
Ershov Institute of Informatics Systems of SB of RAS

Mykola S. Nikitchenko – Ukraine
Kyiv National Taras Shevchenko University

Sergey P. Orlov – Russia
Samara State Technical University

Elena A. Pavlova – Russia
Microsoft

Ivan I. Piletski – Belorussia
Belarusian State University of Informatics and Radioelectronics

Vladimir Yu. Popov – Russia
Ural Federal University

Yury I. Rogozov – Russia
Taganrog Institute of Technology, Southern Federal University

Rustam A. Sabitov – Russia
Kazan National Research Technical University

Nikolay V. Shilov – Russia
A.P. Ershov Institute of Informatics Systems of RAS

Alberto Sillitti – Russia
Innopolis University

Ruslan L. Smelyansky – Russia
Moscow State University

Valeriy A. Sokolov – Russia
Yaroslavl Demidov State University

Petr I. Sosnin – Russia
Ulyanovsk State Technical University

Veniamin N. Tarasov – Russia
Povolzhskiy State University of Telecommunications and Informatics

Andrei N. Tiugashev – Russia
Samara State Aerospace University

Sergey M. Ustinov – Russia
Saint-Petersburg State Polytechnic University

Vladimir V. Voevodin – Russia
Research Computing Center of Moscow State University

Dmitry Yu. Volkanov – Russia
Moscow State University

Mikhail V. Volkov – Russia
Ural Federal University

Nadezhda G. Yarushkina – Russia
Ulyanovsk State Technical University

Rostislav Yavorsky – Russia
Higher School of Economics

Nina V. Yevtushenko – Russia
Ivannikov Institute for System Programming of RAS

Vladimir A. Zakharov – Russia
Moscow State University

Sergey S. Zaydullin – Russia
Kazan National Research Technical University

Organizing Committee Chairs

Organizing Committee

Referees

Tolerant parsing using modified LR(1) and LL(1) algorithms with embedded ”Any” symbol

Alexey Goloveshkin
I. I. Vorovich Institute for Mathematics,
Mechanics and Computer Science
Southern Federal University
Milchakova str. 8a, 344090, Rostov-on-Don, Russia
Email: alexeyvale@gmail.com

***Abstract*—Tolerant parsing is a form of syntax analysis aimed at capturing the structure of certain points of interest presented in a source code. While these points should be well-described in a tolerant grammar of the language, other parts of the program are allowed to be described coarse-grained, thereby parser remains tolerant to the possible variations of the irrelevant area. Island grammars are one of the basic tolerant parsing techniques. ”Islands” term is used as the relevant code alias, the irrelevant code is called ”water”. Efforts required to write water rules are supposed to be as small as possible. Previously, we extended island grammars theory and introduced a novel formal concept of a simplified grammar based on the idea of eliminating water description by replacing it with a special ”Any” symbol. To work with this concept, a standard LL(1) parsing algorithm was modified and LanD parser generator was developed.**

In the paper, ”Any”-based modification is described for LR(1) parsing algorithm. In comparison with LL(1) tolerant grammars, LR(1) tolerant grammars are easier to develop and explore due to solid island rules. Supplementary ”Any” processing techniques are introduced to make this symbol easier to use while staying in the boundaries of the given simplified grammar definition. Specific error recovery algorithms are presented both for LL and LR tolerant parsing. They allow one to further minimize the number and complexity of water rules and make tolerant grammars extendible. In the experiments section, results of a large scale LL and LR tolerant parsers testing on the basis of 9 open-source project repositories are presented.

***Index Terms*—tolerant parsing, robust parsing, lightweight parsing, partial parsing, island grammars, simplified grammar, LanD parser generator**

I. Introduction

Tolerant parsing is a syntax analysis technique differing from the detailed whole-language (so-called baseline) parsing. The latter is performed by a full-featured compiler of a certain programming language to ensure the program satisfies the grammar and to prepare an internal program representation for some further steps. Tolerant parsing performs deep structural analysis only on certain parts of the program, passing other parts with minimal effort. It is achieved by generating the corresponding parser from a tolerant grammar, where these parts of interest are described in details and some minimal description of the irrelevant area is provided. From developer's perspective, tolerant parsing allows her to focus on the structure of the points valuable in the context of a current task, without worrying about irrelevant code variations. Among tolerant parsing use cases, the following ones are the most frequently mentioned:

- **Baseline grammar inaccessibility:** Full version of the language grammar can be inaccessible due to proprietary issues or manual baseline parser writing [1]. Besides, physical accessibility does not assume accessibility in terms of grammar comprehension. Baseline grammar usage requires intensive exploration to detect rules describing constructs of interest. Tolerant grammar structure and mapping between its entities and language constructs are transparent to the developer, as she writes it according to her own knowledge of the task and the language.
- **Language embedding:** Some program artifacts assume the usage of multiple languages in one source file. In this case, a parser for the relevant language must be tolerant to all the snippets written in other languages [2].
- **Domain-specific idioms:** In a certain project, some local domain-specific patterns can be applied [1], [3]. They represent a high-level abstraction layer which is not presented in the language syntax and obviously is out of scope of the whole-language parser. Nevertheless, tolerant parsers can be strictly focused at these patterns, ignoring the underlying structure.

According to the *island grammars* tolerant parsing paradigm [1], [3], parts of the program that are well-described in the grammar are called *islands*, others are called *water*. Detailed grammar rules describing islands are named *patterns*, water is presented with as few liberal productions as possible. However, sometimes it is required to describe some water parts in a fine-grained island-like style to avoid confusion with proper islands. Water parts mistaken for islands are called *false positives*, well-structured water productions are called *antipatterns*. Island grammar development is always a finite iterative process consisting of in-the-wild parser testing and subsequent patterns and antipatterns refinement. Besides, some situations, when program entity can be treated as an island and as a water at the same time, are typically solved with generalized parsing algorithms [4], [5].

The author of the current paper is interested in tolerant parsing because of the long-term goal to develop a multi-language tool for concern-based markup of software projects.

Talking about a program as a set of functionalities, so-called *concerns*, we may notice that many of them are implemented with pieces of code which are spread across solid program elements, such as classes or methods [6], [7]. These concerns are called *vertical layers* [8] or *crosscutting concerns* [9]. To work with this kind of concerns, it is vital to create and manipulate some meta-information about their location, this information should be sustainable with respect to code changes, so it cannot rely on text line and text column numbers. Abstract syntax tree is considered to be a more appropriate structure for meta-information binding, so, there must be a set of parsers for different languages, these parsers must build abstract syntax trees in one unified format. These trees should capture only the structure of program entities we plan to bind to, therefore, tolerant parsing is an option. It also should be easy to support new languages by developing additional grammars and generating tolerant parsers. Previously, to meet the requirements for parsers and trees, we developed a tolerant parser generator called LanD. It uses a modified LL(1) parsing algorithm which is theoretically and experimentally proved to be correct [10].

The contributions of this paper are: 1) a modified LR(1) parsing algorithm with incorporated notion of a special `Any` token allowing parser to match implicitly defined token sequences; 2) supplementary `Any` processing techniques for modified LL(1) and LR(1) parsing algorithms, filling the gap between the simplified grammar formal definition and real tolerant parsing use cases; 3) specific `Any`-based LL and LR error recovery mechanisms aimed at elimination of water rules and correct handling of possible ambiguities without parsing algorithm generalization; complexity analysis is also carried out; 4) lightweight LL(1) and LR(1) grammars for a broad range of languages, namely, for C#, Java, PascalABC.NET programming languages, Yacc and Lex specification formats, XML and Markdown markup languages; 5) an experimental evidence of the applicability of the generated tolerant parsers for large-scale software projects analysis.

The remainder of the paper is organized as follows. In Section II, main goals of the current research are listed. A brief overview of the previous author's research, along with closest analogues analysis, is provided in Section III. In Section IV, a modification of the standard LR(1) parsing algorithm aimed at `Any` symbol processing is introduced, `Any` implementation improvements and issues addressed are discussed, novel `Any`-based error recovery algorithms are described. Section V includes a sufficient volume of experimental data obtained by applying generated tolerant parsers for C# and Java languages to a number of real-world software repositories. In Section VI, a brief summary of the contribution of the paper is provided along with future work outlining.

II. Problem statement

The first assumption of the current research is that the concept of `Any`, previously successfully embedded into a top-down parsing, can be embedded in a bottom-up parsing too, making tolerant grammars more expressive and easy-to-write. The second assumption is that ambiguities originated in islands and water similarity can be resolved not only by adding special antipatterns or by generalized algorithms usage, but also by a special recovery mechanism embedded in a deterministic parsing.

The key goals of the current research are:

1) to design an LR(1) parsing algorithm with built-in notion of a special `Any` grammar symbol that provides skipping the token sequences that are not explicitly described in the grammar;
2) to introduce into the LanD parser generator additional capabilities for correct `Any` processing in case `Any` usage is not fully satisfies simplified grammar formalization;
3) to design specific error recovery mechanisms for LL(1) and LR(1) tolerant parsing, aimed at handling ambiguities originating in water and island similarity;
4) to implement tolerant island grammars for a broad range of languages;
5) to evaluate parser's applicability through the analysis of large-scale software projects written in C# and Java languages.

III. Related work

A. "Any" implementation

The concept of `Any` symbol is implemented in several parser generators. Historically, the first tool with embedded capability to match tokens from sets which are not directly specified in a grammar is the Coco/R recursive-descent parsers generator. According to the documentation [11, p. 14], developer can use a special symbol `ANY`, which *denotes any token that is not an alternative to that* `ANY` *symbol in the current production*. A set of admissible tokens for the position of a particular `ANY` is precomputed to make the situation when parser has to make a choice between `ANY` and some explicitly specified token unambiguously solvable in favour of the explicit option. As shown in [10], these precomputed sets are both incomplete due to the lack of nonterminal outer context analysis and excessively restrictive due to a single restriction applied to all the elements of the sequence corresponding to the iteration of `ANY`. As a result, there are grammars for which parsers generated by Coco/R do not parse programs valid from the developer's point of view. For example, a parser generated by the grammar

```
A = a b c | {ANY} d.
```

is not capable to recognize the input string `bad$` (`$` denotes the end of the input, `{ANY}` denotes zero or more `Any` tokens).

Similar `Any` implementation is built into a tool for lightweight LALR(1) parser development, called LightParse [12]. LightParse grammar is not directly used to generate a parser. Instead, it is transformed to the YACC-like format supported by the standard LALR(1) parser generator GPPG. In the transformed grammar, every entry of `Any` symbol is presented as a separate rule with single-element alternatives,

by an alternative for each of the admissible terminal symbols. To ensure these rules are valid in terms of GPPG, LightParse imposes additional restrictions on `Any` usage. It only deepens drawbacks inherited from Coco/R.

The most recent `Any` token implementation is introduced by the author of the current paper for LanD parser generator [10] aimed at LL(1) tolerant parsers generation by island grammars. In terms of the island grammars paradigm, `Any` symbol allows one not to specify the particular content of the water area, writing `Any` instead. Unlike the `ANY` symbol in Coco/R, our `Any` corresponds to a sequence of zero or more tokens, not a single token. In its implementation, all the known shortcomings are eliminated. The decision about the current token's admissibility at `Any` position is made dynamically at the parsing stage and restricts the set of admissible tokens no more than necessary to avoid ambiguities. LanD's `Any` implementation does not assume the grammar translation to the form suitable for the standard parsing algorithm. Instead, the standard LL(1) algorithm is modified to integrate the notion of `Any` and make it possible to define admissible tokens by the content of a parsing stack.

In the current paper, LanD parser generator is extended with the capability to generate LR(1) parsers with embedded notion of `Any`.

B. Formal definition of a simplified grammar

In [10], through the `Any` token, we formulate a formal concept of the *simplified grammar*. We denote by $\mathrm{lhs}(p)$ and $\mathrm{rhs}(p)$, respectively, the left and the right part of the production p. Notation $x \in \mathrm{rhs}(p)$ for $x \in N \cup T$ means that $\mathrm{rhs}(p) = \alpha_1 x \alpha_2$, where $\alpha_1 \in (N \cup T)^*$, $\alpha_2 \in (N \cup T)^*$. $\mathrm{SYMBOLS}(\gamma)$ is used for the set of terminal symbols needed to compose all the $\omega \colon \gamma \overset{*}{\Rightarrow} \omega, \gamma \in (N \cup T)^*, \omega \in T^*$.

Definition 1: Let $G = (N, T, P, S)$ be a context-free grammar, $Any \notin T$. The grammar *simplified* with respect to G is a grammar $G_s = (N_s, T_s, P_s, S_s)$ defined as follows:

1) $S_s = S$;
2) $P_s = \{p \in f(P) \mid \mathrm{lhs}(p) = S_s \vee \exists p' \in P_s \colon \mathrm{lhs}(p) \in \mathrm{rhs}(p')\}$, where
   $f : P \to \{p = A \to \alpha \mid A \in N, \alpha \in (N \cup T \cup \{Any\})^*\}$
   is the mapping that satisfies the following criteria:
   a) $\exists P' \subseteq P \colon P' = \{p \in P \mid f(p) \neq p\},\ P' \neq \emptyset$,
   b) $\forall p \in P \setminus P',\ f(p) = p$,
   c) $\forall p \in P',\ \exists n \in \mathbb{N} \colon$ p is representable in the form $A \to \alpha_1\gamma_1\beta_1\alpha_2\gamma_2\beta_2 ... \alpha_n\gamma_n\beta_n$ and $f(p)$ is representable in the form $A \to \alpha_1 Any \beta_1 \alpha_2 Any \beta_2 ... \alpha_n Any \beta_n$, where $\forall i \in [1..n],\ \alpha_i\gamma_i\beta_i \in (N \cup T)^*$, and $\forall i \in [1..n],\ \forall a \in \mathrm{FOLLOW}(A),\ \mathrm{SYMBOLS}(\gamma_i) \cap \mathrm{FIRST}(\beta_i\alpha_{i+1}\gamma_{i+1}\beta_{i+1} ... \alpha_n\gamma_n\beta_n a) = \emptyset$;
3) $N_s = \{A \in N \mid \exists p \in P_s \colon \mathrm{lhs}(p) = A\}$;
4) $T_s = \{a \in T \mid \exists p \in P_s \colon a \in \mathrm{rhs}(p)\} \cup \{Any\}$.

Intuitively, P_s contains productions for the start symbol of G_s and productions for all the nonterminals which are reachable from the start symbol. The definition of the mapping f means that some of the strings generated by G contain substrings which can be replaced with `Any`, then we obtain strings generated by G_s. Symbol `Any` can be written instead of the parts denoted by γ_i in production's right hand side, in case these parts satisfy the criterion 2c of the definition 1. Verification of this criterion is possible only when solving a direct problem: when the grammar G_s is created on the basis of some available G. In theory, G can correspond to the baseline language grammar, as well as be a more tolerant version of the baseline grammar, containing all the anti-patterns described explicitly. In practice, it is usually not available or does not exist, so direct problem is rarely considered. Writing an island grammar for a certain programming language is equivalent to solving an inverse problem. Developer writes an initial approximation in the form of a simplified grammar in which `Any` usage allows one to minimize the efforts to describe a possible water content. Then she performs an iterative refinement in accordance with parsing results, making the grammar more and more corresponding to the language generated by some baseline.

Compliance with the criterion 2c is crucial for correct `Any` processing. At the same time, it is hard to maintain while solving an inverse problem. In this paper, additional `Any` processing mechanisms are offered. They allow grammar developers to weaken the control over the consistency with the formalization.

C. LL(1) parsing algorithm modification

In Figure 1, modified algorithms from [10] are rewritten in the form more suitable for further discussion. The delta between the standard algorithms and the modified ones is highlighted with grey. As shown in Figure 1a, when no action can be performed with a current token, parser tries to interpret this token as the beginning of a sequence corresponding to `Any`. `FIRST'` set, a modified version of a standard `FIRST`, is computed for the parsing stack content to get all the tokens that are explicitly allowed in the current place. This non-static approach is inspired in some sense by full-LL(1) parsing [13, p. 247–251]. Set construction routine is shown in Figure 1c. A modification is needed to handle the consecutive `Any` problem defined in [10], this problem is explained in detail in Section IV-B1 along with a more general solution. `M` denotes a parsing table, `Stack` denotes a symbol stack which stores not just the symbols that are expected to be matched, but nodes of the syntax tree being constructed.

There are grounds for an analogy between the LL(1) parsing modification given and well-known error recovery algorithms: `Any` symbol looks similar to the `error` token denoting place in the grammar where recovered parsing can be resumed, `FIRST'` set seems like the set of synchronization tokens. Moreover, speaking in terms of the formal definition, a tolerant parser is built by a simplified grammar G_s, and a program from $L(G)$ is actually needed to be parsed. In terms of G_s, this program is erroneous. However, here also lies a fundamental difference between `Any` processing and error recovery. Recovery is performed for a program which is incorrect regarding to

```
Stack := [];
Stack.Push(new Node($));
Stack.Push(new Node(S));

X := Stack.Peek().Symbol;
t := Lexer.NextToken();
while (X ≠ $) do
  if (t = ERROR_TOKEN) then
    return false;
  end if;
  if (X = t) then
    if (t = Any) then
      t := SkipAny(true);
    else
      Stack.Pop();
      t := Lexer.NextToken();
    end if;
  elif (M[X,t] ≠ null) then
    if (t = Any) then
      if (Any ∈ FIRST'(Stack)) then
        t := SkipAny(true);
      else
        t := Error(null);
      end if;
    else
      Apply(M[X,t]);
    end if;
  elif (t = Any) then
    t := Error(null);
  else
    t := Any;
  end if;
  X := Stack.Peek().Symbol;
end while;

if (t = $) then
  Accept();
  return true;
else
  return false;
end if;
```

(a)

```
SkipAny(recoveryIsEnabled):
  t := Lexer.CurrentToken();
  idx := Lexer.CurrentTokenIndex();
  while (Stack.Peek().Symbol ∈ N_S) do
    Apply(M[Stack.Peek().Symbol, t]);
  end while;

  Stack.Pop();

  stopTokens := FIRST'(Stack);
  while (t ∉ stopTokens and t ≠ $) do
    t := Lexer.NextToken();
  end while;

  if (t ∉ stopTokens) then
    if (recoveryIsEnabled) then
      Lexer.MoveTo(idx);
      return Error(stopTokens);
    else
      return ERROR_TOKEN;
    end if;
  end if;

  return Lexer.CurrentToken();
```

(b)

```
FIRST'(α = Y_1 Y_2 ... Y_k):
  first := ∅;
  for (i from 1 to k) do
    if (Y_i ∈ T_S) then
      first ∪= {Y_i};
      if (Y_i ≠ Any) then break; end if;
    else
      first ∪= MemorizedFirst'[Y_i]\{ε};
      if (ε ∉ MemorizedFirst'[Y_i]) then break; end if;
    end if;
  end for;
  if (∀i ∈ [1..k]: ε ∈ MemorizedFirst'[Y_i] or Y_i = Any) then
    first ∪= {ε};
  end if;
  return first;
```

(c)

```
Apply( X → Y_1 Y_2 ... Y_k):
  parent := Stack.Pop();
  for (i from k to 1) do
    child := new Node(Y_i);
    Stack.Push(child);
    parent.Children.AddFirst(child);
  end for;


BuildFirst'():
  foreach (A ∈ N) do
    MemorizedFirst'[A] := ∅
  end foreach;
  changed := true;
  while (changed) do
    changed := false;
    foreach (A → α ∈ P) do
      MemorizedFirst'[A] ∪= FIRST'(α);
      if (MemorizedFirst'[A] is changed) then
        changed := true;
      end if;
    end foreach;
  end while;
```

(d)

Fig. 1: Modified LL algorithms: (a) LL(1) parsing algorithm, (b) ”Any” processing algorithm, (c) FIRST set construction, (d) Auxiliary algorithms: alternative applying and FIRST set memorization

a baseline grammar G. While success is not guaranteed, the main goal is to resume parsing at any cost, including the loss of some significant results of the previous analysis and skipping a significant part of the input stream, possibly containing some points of interest. The goal of `Any` processing is to translate a presumably valid $L(G)$ program into the language $L(G_s)$ by replacing some token sequences with `Any`. The premise that the program under consideration is correct with respect to G, in conjunction with the observance of the criterion 2c, makes input tokens skipping totally predictable. One can be sure that the parts of the input stream replaced with `Any` belongs to the water and can be discarded without loss of the land. Furthermore, predictable and correct replacement with `Any` is possible for a program that is incorrect with respect to G, in case incorrectnesses are located in water areas.

IV. Algorithms and modifications

A. LR(1) parsing

Though the modified LL(1) parsing algorithm described in Section III-C is enough to create reliable tolerant parsers, describing a real programming language with LL(1) grammar is a challenge even when this grammar is supposed to be lightweight and tolerant. Constructs of interest, such as class members, usually have a common beginning up to a certain point, so they cannot be presented as solid alternatives for a single nonterminal symbol in LL(1). Instead, we have to write rule sequences in the style of taking the common factor out of the brackets and making a separate rule for a tail:

```
entity = attribute* keyword* (class_tail | member_tail)
member_tail = type name (method_tail | property_tail)
method_tail = arguments Any (init? ';' | block)
```

As a result, the grammar structure is not transparent enough for a newcomer because the connection between existing island rules written in such a distributed manner and particular language constructs is non-obvious.

This LL(1) limitation can be overcome through switching to a more complex LR(1) parsing. A modification of the standard LR(1) algorithm is shown in Figure 2a, modified areas are highlighted with gray. Like in a standard case, two stacks exist to keep parser state. `SymbolsStack` keeps the current viable prefix [14, p. 256]. In fact, similar to LL(1) `Stack`, in our implementation, it keeps not just symbols but nodes for a tree to be build. `StatesStack` keeps the indices of the states parser passed through to obtain the current viable prefix. An

```
SymbolsStack := [];
StatesStack := [];
StatesStack.Push(0);

t := Lexer.NextToken();
while (true) do
  if(t = ERROR_TOKEN) then
    return false;
  end if;
  s := StatesStack.Peek();
  if (ACTION[s, t] ≠ null) then
    if (t = Any) then
      t := SkipAny(true);
    elif (ACTION[s, t] is ShiftAction a) then
      Shift(t, a.NextStateIdx);
      t := Lexer.NextToken();
    elif (ACTION[s, t] is ReduceAction a) then
      Reduce(a.ReductionAlternative);
    elif (ACTION[s, t] is AcceptAction) then
      Accept();
      return true;
    end if;
  elif (t ≠ Any) then
    t := Any;
  else
    t := Error(null);
  end if;
end while;
```

(a)

```
SkipAny(recoveryIsEnabled):
  s := StatesStack.Peek();
  t := Lexer.CurrentToken();
  idx := Lexer.CurrentTokenIndex();
  while (ACTION[s, Any] is ReduceAction a) do
    s := Reduce(a.ReductionAlternative);
  end while;

  s := Shift(Any, ACTION[s, Any].NextStateIdx);

  stopTokens := { t' ∈ T | ACTION[s, t'] ≠ null };
  while (t ∉ stopTokens and t ≠ $) do
    t := Lexer.NextToken();
  end while;

  if (t ∉ stopTokens) then
    if (recoveryIsEnabled) then
      Lexer.MoveTo(idx);
      return Error(stopTokens);
    else
      return ERROR_TOKEN;
    end if;
  end if;

  return Lexer.CurrentToken();
```

(b)

```
Reduce(alt = X → Y1Y2...Yk):
  parent := new Node(X);
  for (idx from k to 1) do
    StatesStack.Pop();
    child := SymbolsStack.Pop();
    parent.Children.AddFirst(child);
  end for;

  s := StatesStack.Peek();
  StatesStack.Push(GOTO[s, X]);
  SymbolsStack.Push(parent);
  return StatesStack.Peek();

Shift(token, stateIdx):
  StatesStack.Push(stateIdx);
  SymbolsStack.Push(new Node(token));
  return StatesStack.Peek();
```

(c)

Fig. 2: Modified LR algorithms: (a) Modified LR(1) parsing algorithm, (b) "Any" processing algorithm, (c) Shift and reduce algorithms

```
COMMENT : '//' ~[\n\r]* | '/*' .*? '*/'
STRING  : '"' ('\\"'|'\\\\'|.)*? '"'
CHAR    : '\'' ('\\\''|'\\\\'|.)*? '\''
MODIFIER : 'transient'|'strictfp'|'native'|'public'|'private'
    |'protected'|'static'|'final'|'synchronized'|'abstract'
    |'volatile'|'default'
ID       : [_$a-zA-Z][_$0-9a-zA-Z]*

CURVE_BRACKETED  : %left '{' %right '}'
ROUND_BRACKETED  : %left '(' %right ')'
SQUARE_BRACKETED : %left '[' %right ']'

file_content = entity*
entity = enum | class_interface | method
    | field_declaration | water_entity
enum  = common_beginning 'enum' name Any block ';'?
class_interface  = common_beginning ('class'|'interface')
    name Any '{' entity* '}' ';'?
method  = common_beginning type name arguments Any (';' | block)
field_declaration  = common_beginning type field (',' field)* ';'
field  = name ('['']')* init_value?
water_entity  = AnyInclude('@interface', 'import', 'package')
    (block | ';')+

common_beginning = (annotation|MODIFIER)*
init_value       = '=' init_part+
init_part        = Any | type_parameter

name = name_type
type = name_type
name_type_atom = type_parameter? ID type_parameter?
name_type      = name_type_atom (('.'|'::') name_type_atom) | '['']')*
type_parameter = '<' (AnyAvoid(';') | type_parameter)* '>'

arguments  = '(' Any ')'
annotation = '@' name arguments?
block      = '{' Any '}'
```

Fig. 3: Java LR(1) tolerant grammar

element `ACTIONS[s, t]` of the `ACTIONS` table keeps the knowledge of what action should be performed by the parser if token `t` is met while `s` is the parser's current state. There are two basic types of action in LR algorithm: `Shift` and `Reduce`, they are shown in Figure 2c. `GOTO[s, X]` contains the index of a state to which parser must go from `s` state after reducing some part of a viable prefix to `X`.

The essence of the parsing algorithm modification is similar to LL(1) case: tolerant parser is responsible not only for checking if the program can be derived from the start symbol, but also for translating it from a baseline language into a simplified one. In case an action for some actual combination of parser state and input token is undefined, parser tries to interpret the current token as the beginning of the subsequence of the program from $L(G)$ that corresponds to `Any` in the corresponding program from $L(G_s)$. In case there is an action available for `Any`, parser calls `SkipAny` routine (Figure 2b), where firstly all the possible `Reduce` actions are performed and secondly `Any` token is shifted. Note that we consider `ACTIONS` table to be cleared from Shift/Reduce conflicts in favour of `Shift` action. Also there is no additional checking if `Shift` action exists, because this existence follows from the standard `ACTIONS` and `GOTO` construction algorithm. Having moved `Any` to a viable prefix, parser looks for the first token which is explicitly expected in $L(G_s)$ program and then continues parsing the usual way.

In Figure 3, there is an LR(1) tolerant grammar for Java programming language written in the format supported by LanD parser generator. As it can be seen, island entities, such as enumerables, classes, methods and fields, are clearly presented as solid rules. In comparison with a baseline Java grammar, it is significantly shorter: the baseline grammar implementation for ANTLR parser generator[1] consists of 211 lines of lexer specification and 615 lines of parser description.

B. "Any" processing improvements

1) Consecutive "Any" problem: In Figure 1c, `FIRST'` algorithm, which is the modified version of the standard

[1]https://github.com/antlr/grammars-v4/tree/master/java

FIRST, is presented. It is intended to solve the problem of consecutive Any described in [10]. The problem manifests itself when two or more Any tokens directly follow each other at the beginning of the sentence which can be derived from the stack. In this case, the subsequent Any hides some stop tokens from the previous one. Consider the following grammar G:

```
A = (a|b)+ B C; B = d | ; C = (e|f)? c
```

It can be simplified to the following G_s:

```
A = Any B C; B = d | ; C = Any c
```

The string abc$ $\in L(G)$ is supposed to be successfully matched by the parser built for $L(G_s)$, because the following derivation may be performed:

$$A \Rightarrow Any\, B\, C \Rightarrow Any\, C \Rightarrow Any\, Any\, c\,.$$

Having met the token a, the tolerant parsing algorithm starts the first Any processing. If the standard FIRST is used to find stop tokens, FIRST(Stack) set equals to {d, Any}, as a result, SkipAny skips all the input and returns an error. Taking into account that Any is allowed to match an empty sequence, FIRST' modification looks beyond the second Any and, in general, beyond all the subsequent Any symbols in searching some explicitly specified tokens which may follow a sequence corresponding to these Any tokens. Stop token set found with FIRST'(Stack) equals to {d, c}, thus the first Any captures a and b tokens and stops on c, the second one matches an empty sequence, and abc$ string is admitted to be correct.

This approach is proved to be enough to build working parsers for real programming languages, such as C#, Java or PascalABC.NET. It can also be implemented for LR(1) through ACTION and GOTO static analysis. However, on closer inspection it becomes clear that algorithms modified in this way work correct only for a subclass of simplified grammars, satisfying an additional constraint:

Definition 2: Let $G_s = (N_s, T_s, P_s, S_s)$ be a grammar simplified with respect to a context-free grammar $G = (N, T, P, S)$. Enumerate as $Any_1, Any_2, ...Any_n$ all the Any entries from the right-hand sides of productions from P_s, which appeared as a result of replacement of the corresponding $\gamma_1, \gamma_2, ...\gamma_n$ subparts of the right-hand sides of productions from P in compliance with Definition 1. Derivation $S_s \overset{*}{\Rightarrow} \alpha_s Any_k Any_l ... Any_t b \beta_s$, where $k, l, ..., t \in [1..n]$, $\alpha_s, \beta_s \in (N_s \cup T_s)^*$, $b \in T_s \setminus \{Any\}$, is not acceptable in G_s if $b \in \mathrm{SYMBOLS}(\gamma_k \gamma_l ... \gamma_t)$.

Informally speaking, the token which is a stop token for the last Any in a sequence is not allowed to appear in the area corresponding to one of the preceeding Any, otherwise it will cause premature completion of Any processing. Let G has a different structure:

```
A = (a|b|c|d|e|f)+ B C; B = g | ; C = (h|i)+ a
```

It can be simplified to

```
A = Any B C; B = g | ; C = Any a
```

Herein, both replacements with Any are still satisfy the criterion 2c, but the restriction from Definition 2 is not satisfied, as a may follow the second Any, and at the same time it is a valid element of the area corresponding to the first one. As a result, while parsing abba$, the first Any is matched with an empty token sequence because FIRST'([B, C]) equals to {a, g}, the second Any also cannot include a, so, valid input is not accepted.

In practice, the most common case of consecutive Any appearance does not break the restriction mentioned: in grammars we have developed, Any is often used as one of the possible variants for an element of a list, so, all the Any tokens in the derivation of such a list originate from a single Any entry in the grammar, therefore, derivation can be rewritten as $S_s \overset{*}{\Rightarrow} \alpha_s Any_k Any_k ... Any_k b \beta_s$, and the corresponding condition $b \in \mathrm{SYMBOLS}(\gamma_k)$ is false in accordance with Definition 1. To cover the general case, we introduce a mechanism for passing an additional information at Any processing stage. Any entry can be supplemented with two options: Except and Include. For each of them, a list of literals or token names can be passed as parameters. The concept of AnyExcept initially appeared in LightParse parser generator [15], but there it was intended to compensate the lack of outer context analysis while constructing the set of admissible tokens. Our intention is different: symbols specified for Except option are supposed to compensate the lack of information in consecutive Any problem: they are supposed to be explicitly specified tokens that may follow the area corresponding to Any in $L(G)$. Include option allows one to approach this problem from a different angle, specifying tokens that shouldn't be interpreted as stop tokens despite their appearance in FIRST'(Stack). So, for the grammar above we can use one of the following simplified analogues:

```
A = AnyExcept(g,h,i) B C; B = g | ; C = Any a
A = AnyInclude(a) B C; B = g | ; C = Any a
```

Having renamed stopTokens sets built in Figure 1b and 2b to stopTokensBasic, we transform stop token set construction for both LL and LR algorithms to

```
stopTokens := anyExceptSet.Count > 0
  ? anyExceptSet
  : stopTokensBasic.Except(anyIncludeSet);
```

where anyExceptSet and anyIncludeSet denote sets of tokens passed as option parameters for Any currently being matched. For error recovery purposes discussed in Section IV-C, Any also supports Avoid option. Its arguments are tokens the presence of which in the Any-corresponding area signals about program incorrectness or wrong alternative choice. To take Avoid into account, while loop condition transforms to

t ∉ stopTokens **and** t ∉ anyAvoidSet **and** t ≠ $.

In case token skipping is interrupted because current token equals to one of the Avoid arguments, this token passes to Error routine as a second argument.

Unlike in LL(1), there can be a situation in LR(1) when we do not know for sure what particular Any entry is being

processed at the moment. This information is needed to access the corresponding options. To add support of `Any` options in LR(1), we introduce an additional type of LR(1) conflict called Any/Any conflict. It is reported when there is a state where multiple items have a dot before `Any`, and is needed to be resolved for successful parser generation.

2) Nesting level checking: While writing a tolerant grammar, developer usually has to make an additional effort to determine what bracketed areas may appear in the particular water, and if they can influence `Any` processing. Intuitively, such areas are perceived as a whole, and when `Any` is written instead of some better-grained water description, it may be missed that bracketed areas exist in that water in a real program. These areas may contain something that also appears right after that `Any` and therefore should be treated as a stop token. For example, being interested in fields of a C# class, we must capture `a`, `b`, `c` and `d` in the fragment

```
int a = 0, b = 1;
DateTime c = new DateTime(2019, 5, 29),
    d = new DateTime(2019, 5, 31);
```

At the same time, we are not interested in initializers, so, the first intention is to describe field declaration with the rules

```
fields = type name init? (',' name init?)* ';'
init = '=' Any
```

Unfortunately, these rules work only for the first declaration. The set `{',', ';'}` is a stop token set for `Any`, and in the second declaration, comma separates not only fields but also arguments bordered with round brackets. Generally speaking, `Any` does not satisfy the formalization in this case. At the same time, simplicity is the crucial property of the tolerant grammar, and the way in which water is described above is more preferable than the following one:

```
init    = '=' water
s_water = '[' (Any | s_water)+ ']'
r_water = '(' (Any | r_water)+ ')'
c_water = '{' (Any | c_water)+ '}'
water = (Any | c_water | r_water | s_water)+
```

To return the first version of `init` rule to the boundaries of the simplified grammar definition, we add to the parsing algorithms a capability to take into account nested bracketed structures. A pair of brackets is described like

```
ROUND_BRACKETED : %left '(' %right ')'
```

and nesting level is tracked by lexical analyser. If several kinds of pairs are described, it is believed that any pair can be nested in any pair. When `Any` is processed, it is allowed to end only at the same depth at which it begins. To control this situation, `SkipAny` methods are modified uniformly both for LL and LR. Firstly, at the beginning of a skip process, an additional variable is initialized:

```
depth := Lexer.CurrentDepth();
```

Secondly, in-loop `Lexer.NextToken()` call is replaced with `Lexer.NextToken(depth)`. Passing the initial nesting level to a lexer, we force it to read the input stream until the depth of the next token equals the depth of the first token in the sequence corresponding to `Any`. Thus, `Any`-corresponding area is allowed to include stop tokens in nested structures because these nested structures are invisible to the parsing algorithm. Third modification is an additional checking to prevent moving through the upper nesting level. In Figure 4, there are two cases allowed by the first two modifications. Token `a` is the beginning of `Any` area, and `b` is a stop token. Obviously, the way `Any` symbol is matched on the right breaks the semantic integrity of a bracketed area. We consider such `Any` usage to be a bad practice, so, if lexer returns a token denoting the end of some pair and rise to the level above the initial, and this token is not a stop token, parser reports an error which means that grammar should be refined.

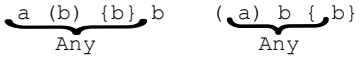

Fig. 4: Possible "Any" matching supported by nesting level tracking

C. Error recovery

1) Algorithms: As noted in Section I, in case water entities look similar to islands, developer has to refine patterns and to add some antipatterns to avoid false positives. For a deterministic parsing, the problem of water and island similarity may have unpleasant consequences not only when there is a full match between island pattern and water entity, but even if a water entity and an island have a number of common starting tokens. In this case, parser starts analysing a water entity as an island, finds a mismatch and fails to proceed analysis. It is important to note that this parsing failure indicates not the incorrect $L(G)$ program but misinterpretation of the program in terms of G_s. Generalized parsing algorithms are able to process such a situation exploring both ways an entity can be interpreted in and rejecting the failed one. To get a similar benefit from our modified deterministic parsing while preserving mostly linear complexity, we add special `Any`-based error recovery routines in both LL(1) and LR(1) algorithms. These routines are shown in Figure 5.

In the modified parsing algorithms, two types of error can occur. The first one happens when LL(1) parser cannot match the current token or apply some alternative and `Any` is not acceptable at the point, or when LR(1) parser has no shift or reduce action for the current token as well as for `Any`. The second type occurs when `Any` processing starts and no stop tokens are found till the end of the input or a token specified as `Avoid` argument is met. Recovery initiated for the first type does not influence the algorithm linearity as parsing is resumed at the token where the error occured. Acting the same way for the second type is meaningless, especially when the end of the input is reached, because significant part of islands might be uncontrollably skipped. Instead, a limited backtracking is performed. In Figure 1b and 2b, `Lexer.MoveTo(idx)` call shifts a token stream pointer to the token that triggered `Any` processing, at this point recovery is tried to be carried out. In Section IV-C2, the influence of this backtracking on parsing algorithm time complexity is analysed. In both LL(1)

```
Error(stopTokens):
  if (Lexer.CurrentTokenIndex() ∈ RecoveredIn) then
    return ERROR_TOKEN;
  end;
  RecoveredIn ∪= { Lexer.CurrentTokenIndex() };

  currentNode := Stack.Pop();
  do
    if (currentNode.Parent ≠ null) then
      maxChildIndex :=
        currentNode.Parent.Children.Count - 1;
      indexOfCurrent :=
        currentNode.Parent.Children.IndexOf(currentNode);
      for (i from indexOfCurrent + 1 to maxChildIndex) do
        Stack.Pop();
      end for;
    end if;
    currentNode := currentNode.Parent;
  while(currentNode ≠ null and (
    currentNode.Symbol ∉ RecoverySymbols or
    Any = GetDerivation(currentNode)[0] or
    IsUnsafeAny(stopTokens)
  ));

  if (currentNode ≠ null) then
    return SkipAny(false);
  else
    return ERROR_TOKEN;
  end if;
```

(a)

```
Error(stopTokens):
  if (Lexer.CurrentTokenIndex() ∈ RecoveredIn) then
    return ERROR_TOKEN;
  end;
  RecoveredIn ∪= { Lexer.CurrentTokenIndex() };

  lastMatched := ε;
  // possible derivation items
  PDI := {};
  basePDI := {};
  do
    if (SymbolsStack.Count > 0) then
      lastMatched := SymbolsStack.Pop();
    end if;
    StatesStack.Pop();
    if (StatesStack.Count > 0) then
      s := StatesStack.Peek();
      basePDI := { i = X → α•Yβ | i ∈ STATE[s], Y = lastMatched.Symbol,
        (PDI = {} ∨ ∃i' ∈ PDI : i' = X → αY•β) };
      PDI := basePDI;
      do
        PDI ∪= { i = X → α•Yβ | i ∈ STATE[s], ∃i' ∈ PDI : i' = Y → •β' };
      while (PDI changes);
    end if;
  while (StatesStack.Count > 0 and (
    |basePDI| = |PDI| or
    ∄i ∈ PDI \ basePDI : i = X → α•Yβ, Y ∈ RecoverySymbols or
    Any = GetDerivation(lastMatched)[0] or
    IsUnsafeAny(stopTokens)
  ));

  if (StatesStack.Count > 0) then
    return SkipAny(false);
  else
    return ERROR_TOKEN;
  end if;
```

(b)

Fig. 5: "Any"-based error recovery algorithms: (a) LL(1) algorithm, (b) LR(1) algorithm

and LR(1) error processing algorithms, `RecoveredIn` set stores all the indices of tokens at which recovery was once performed, so, it is guaranteed that from one recovery to another parsing process moves at least one token forward.

Like in standard recovery algorithms [16, pp. 283–285], a set of nonterminals at which recovery can be performed is defined. These nonterminals are called *recovery symbols*. Possible recovery symbols can be revealed through the static grammar analysis. Given the grammar $G_s = (N_s, T_s, P_s, S_s)$, we formally define the set as follows:

$$RecoverySymbols = \{n \in N_s \mid n \overset{*}{\Rightarrow} Any\,\alpha \wedge$$
$$\nexists n' \in N_s \colon (n \overset{*}{\Rightarrow} n'\,Any\,\alpha \wedge n' \overset{*}{\Rightarrow} \varepsilon)\}, \alpha \in (N_s \cup T_s)^*.$$

Recovery symbols are pre-computed at parser construction stage. Developer can disable recovery at all or specify particular nonterminals from this set which should be used for recovery, otherwise, all the elements of the set are taken into consideration when `Error` routine is called.

In the context of a deterministic tolerant parsing problem, recovery symbols have specific semantics. They represent decision points at which parser may choose the wrong alternative, try to match a water entity as an island, and provoke an error. Recovery itself means returning to a decision point through the grammar ancestors of the currently unmatched token or unparsed nonterminal and changing the interpretation of the part of the input that is already associated with a recovery symbol's subtree to water. More precisely, the part of the input from the first token mistaken for an island part to the first token at which the difference between an island pattern and an actual water entity manifests itself is supposed to be the beginning of the sequence corresponding to `Any` from which the water alternative starts. Backtracking to the token a wrong decision was made at is not needed in this interpretation. The end of an `Any`-corresponding sequence is looked for with a usual `SkipAny` call, then parsing continues in an ordinary way. In Figure 3, `entity` is one of the recovery symbols. It allows the parser to recognize classes, enumerables, methods, and fields as islands, while annotation definitions, constructors, initialization blocks, etc. are skipped as the water, sometimes with the involvement of recovery mechanisms.

LL(1) error recovery algorithm is presented in Figure 5a. We take advantage of the fact that at any stage of the top-down-parsing a partially built syntax tree is available, and blank nodes for what is expected are on the stack. Knowing the tree node corresponding to the unparsed symbol, we may find a recovery symbol node by moving through its ancestors. The higher we go, the wider area will be reinterpreted. Simultaneously with walking up the syntax tree, right siblings of the `currentNode` should be removed from parsing stack as they are unparsed parts of the interpretation being rejected. The appropriate recovery symbol is considered to be found if it satisfies two additional conditions. Firstly, the water alternative should not be the alternative in favor of which the decision was originally made, otherwise no reinterpreting

takes place as error actually occurred in the water. To check it, `GetDerivation` is called. It takes the built part of recovery symbol's subtree and returns a leaf sequence which is a partially revealed part of the $L(G_s)$ program, derived from this symbol. This sequence must not start with `Any`. Secondly, in case error took place at `Any` skipping, `IsUnsafeAny` prevents parsing resumption on `Any` from the recovery symbol alternative if new skipping will lead to the same erroneous situation. The decision is made on the basis of old and new stop token sets comparison and `Avoid` options analysis.

For LR(1) algorithm, recovery is more complex and heuristic due to the nature of a bottom-up parsing. Unlike in LL case, we do not know for sure what are the exact entities that are currently being analysed, so, we try to build a set of possible candidates basing on the information stored on the stacks. In Figure 5b, there is an LR(1) error recovery routine. On each iteration of `do-while` loop, one of the symbols already matched is popped along with the state parser went to after this successful matching, then `basePDI` set is constructed. It consists of the current state items having the dot before the last popped symbol. Productions of the items added to this set are possible participants of the erroneous area derivation. Basing on `basePDI`, `PDI` set is constructed in a way that looks like inverted CLOSURE [16, pp. 243–245] algorithm. Additional `PDI` items capture the higher-level grammar entities from which the area that is needed to be reinterpreted may be derived.

Recovery algorithms presented simplify the process of grammar extension and reduction. Recovery symbol alternatives become grammar building blocks: in case we are not interested in some Java island its alternative can be excluded from `entity` rule, then program areas previously corresponding to that alternative are recognized as the water, possibly through recovery algorithm application. Inversely, to add a support for class constructors in the grammar in Figure 3, we have write only one `constructor` rule and add this symbol in `entry` alternatives list, then constructors stop being interpreted as the water, because the rule appears allowing to analyse them from beginning to the end with no error occurred.

2) Complexity analysis: As noted, errors happening on `Any` processing require limited backtracking. The particular increase in running time of the algorithm depends on number and length of backtracked sequences. From the prohibition of multiple recovery at the same token, it follows that there can be only one backtracking to a particular position, so, the worst case is when the following situation repeats sequentially for each token except the first one: `Any` processing starts on the token, fails by reaching the end of the input and backtracks to that token, then recovery starts, the token matches successfully with the help of the water alternative, and the next token becomes the token under consideration. In this scenario, a number of times the token is examined equals to its sequential number counting from one. For the i_{th} token, $i-1$ examinations are occurred on `Any` skipping started at previous tokens and at the current one, and 1 examination is for some final match. As backtracking itself consists of a simple index reassignment, it does not increase this counter. It can be shown that this worst-case scenario takes place for inputs `ac$`, `aac$`, `aaac$`, etc. and a parser generated by the following LL(1) grammar:

```
S = a Any b | Any S |
```

The total number of token examinations equals to $\frac{1}{2}n^2+\frac{1}{2}n$, it means that our algorithms are $O(n^2)$ in the worst case. However, experiments show that the percentage of recoveries required backtracking is insignificant in comparison with the total number of recoveries and tokens: for example, in all the Java projects from Section V-B taken together, there are 27393 files splitting at 26255589 tokens, while total number of recoveries is 32683 for LL(1) and 31861 for LR(1), and only 20 recoveries for each type of parsing were performed after on-`Any` error.

V. Experiments

To test the algorithms described in Section IV, tolerant grammars for the following programming languages, markup languages and specification formats are developed: C#, Java, PascalABC.NET, XML, Markdown, YACC, Lex. All the sources are available on GitHub[2]. For a large-scale testing, C# and Java are chosen as the languages complex enough and having a large number of well-known open-source repositories. For both languages, LL(1) and LR(1) tolerant parsers are generated with LanD parser generator on the basis of the corresponding tolerant grammars.

As tolerant parsers are created to capture particular islands, the purpose of the experiment is to evaluate precision and recall of this capturing. Stages of the experiment are the same for both languages. For each of the projects under consideration, tolerant parser is firstly applied to parse all the project files written in the corresponding language. By traversing syntax trees built, types and names of the islands are extracted in a report files, per report for each island type. This extraction does not require some severe postprocessing: island type is actually a node type, and name is stored in one of this node's children. Secondly, the same files are parsed by a baseline parser. Roslyn is used as a baseline parser for C#, and Java parser is generated with ANTLR from the full grammar of the language[3]. Then information about program entities that are specified as islands for our tolerant parsers is extracted from trees built by these baseline parsers, so the second group of reports is obtained. At the third stage, two reports for the same type are compared in an automated way to eliminate the human factor. Matches are excluded, so only the information about entities found by one parser and not found by another one remains. It is then explored manually.

For each of the languages, there is a table whose rows correspond to projects parsed and columns correspond to island types. There is also an additional "Total files" column allowing to estimate the scale of the project. In a table cell, there is a number of islands of the corresponding type found by our tolerant parser for the corresponding project. We have

[2]https://github.com/alexeyvale/SYRCoSE-2019

[3]https://github.com/antlr/grammars-v4/tree/master/java

```
...
CURVE_BRACKETED : %left '{' %right '}'
ROUND_BRACKETED : %left '(' %right ')'
SQUARE_BRACKETED : %left ('['|GENERAL_ATTRIBUTE_START) %right ']'
...
namespace = 'namespace' name '{' namespace_content '}'
entity = enum | class_struct_interface | method
   | field_decl | property | water_entity
enum = common 'enum' name Any '{' Any '}' ';'?
class_struct_interface =
   common ('class'|'struct'|'interface') name Any '{' entity* '}' ';'?
method = common type name arguments Any (init_expression? ';' | block)
field_decl = common type field (',' field)* ';'
field = name ('[' Any ']')? init_value?
property =
   common type name (block (init_value ';')? | init_expression ';')
water_entity =
   AnyInclude('delegate', 'operator', 'this') (block | ';')+

common = entity_attribute* modifier*
modifier = MODIFIER | 'extern'
init_expression  = '=>' Any
init_value = '=' init_part+
init_part = Any | type
arguments = '(' Any ')'
block = '{' Any '}'
...
```

Fig. 6: Fragment of the C# tolerant grammar

obtained that these numbers are the same for LL(1) and LR(1) parser, so we do not need two separate tables for a single language. In case tolerant parser finds less island entities than the baseline one, the number of entities missed is specified in parentheses with a minus sign. In addition to the tables, a detailed analysis of mismatches is provided.

A. C# tolerant parsing

For C# programming language, five open-source projects from different domains are considered:

- **Roslyn** project includes C# and Visual Basic compiler sources and lots of test files capturing different complex and uncommon variants of a C# program;
- **PascalABC.NET** consists of the corresponding language compiler and IDE sources, it has a relatively long history reflected in the legacy code written by differently experienced contributors;
- **ASP.NET Core** refers to the web development domain: it is a cross-platform .NET-based web framework;
- **Entity Framework Core** is an object-relational mapper allowing to work with a database using .NET objects;
- **Mono** is an open source third-party implementation of Microsoft's .NET Framework including C# compiler, Common Language Runtime virtual machine, lots of core libraries and, again, a great number of test files.

Parsing results are presented in Table I, a fragment of the tolerant LR(1) C# grammar is presented in Figure 6. Note that classes, structures and interfaces correspond to a single grammar entity, so their total number presented in a single "Classes" column of the table. In the discussion below, footnotes contain paths to files relative to the root directory of the corresponding project.

For Roslyn sources, there are 5 methods found by Roslyn and missed by LanD. 4 of them are local[4] methods[5] (methods declared inside other methods), this feature recently appeared in C# 7.0. In case this kind of methods is important for a particular task, it is trivial to add their support in the grammar. One needs to modify the grammar above by adding `method` symbol as an alternative to `Any` inside the `block`. It is worth noting, that Roslyn project is the only project where the usage of this feature is revealed. The 5th lost method is from a test file where the text of the program is saved in Japanese Shift-JIS encoding[6]. The class name written in Japanese provokes an error which does not affect the detection of the class itself but stops parser from further class content analysis. We consider the usage of national alphabets for entity naming to be a rare case, but, if necessary, `ID` token can be adopted as needed.

2 properties from different files are not found by LanD, in both cases it is caused by missing expression for expression-bodied property preceding the uncaptured one. The expression depends on external conditional compilation symbols and is not substituted at all in case the isolated file is analysed. In the following code, `IsWindows` is not recognized by LanD, because it is interpreted as a part of expression for `Configuration`:

```
public static ExecutionConfiguration Configuration =>
#if DEBUG
    ExecutionConfiguration.Debug;
#elif RELEASE
    ExecutionConfiguration.Release;
#else
  #error Unsupported Configuration
#endif

public static bool IsWindows =>
  Path.DirectorySeparatorChar == '\\';
```

This kind of inconsistency can be partially handled by using `AnyAvoid(MODIFIER)` instead of `Any` in `init_expression` grammar rule. For the example above, this handling leads to loss of the information about `Configuration` property, as it will be treated as water, but protect the following entities starting with the one that starts with the keyword.

For PascalABC.NET and ASP.NET Core, all the entities found by Roslyn are also found by LanD. For Entity Framework Core, the difference in number of fields and methods is caused by the situation[7] similar to the one presented in the code above, and the difference in number of properties is provoked by property types containing Greek letters[8]. The latter refers us again to the national alphabets problem.

Voluminous results are obtained for Mono sources. Most losses are concentrated in files that are incorrect in terms of a full C# grammar: as an example, 26 files[9] contain unclosed conditional compilation directives and mismatch in the number and type of opening and closing brackets, half of the 122 missed classes belongs to a group of files[10] containing LINQ to SQL code written in accordance with Visual Basic syntax,

[4] src/Compilers/CSharp/Test/Emit/Emit/EndToEndTests.cs

[5] src/Compilers/CSharp/Portable/FlowAnalysis/NullableWalker.cs

[6] src/Compilers/Test/Resources/Core/Encoding/sjis.cs

[7] test/EFCore.SqlServer.FunctionalTests/Query/SimpleQuerySqlServerTest.Where.cs

[8] test/EFCore.Tests/ModelBuilding/ModelBuilder.Other.cs

[9] mcs/errors

[10] mcs/tools/sqlmetal/src/DbLinq/Test

TABLE I: Number of entities found in C# projects

Project	Total files	Enums	Classes	Fields	Properties	Methods
Roslyn	8759	482	23705	20265	23127 (-2)	116312 (-5)
PABC.NET	2802	359	5522	16739	12023	37027
ASP.NET Core	7356	333	12604	10214	16301	44163
EF Core	2997	101	7783	4687 (-1)	16941 (-2)	26421 (-135)
Mono	37224	4928 (-1)	60187 (-122)	166958 (-67)	99167 (-36)	309580 (-670)

there are also files with .cs extension written in a specific format, such as a skeleton file[11] for jay parser generator, where each line starts with a point. However, there is also a group of missed entities that illustrates a real LanD drawback. These entities are contained in `test-async`[12] and `test-partial`[13] groups of Mono test files. At grammar design and refinement stage, we did not take into consideration, that there are some keywords in C# that appeared recently and were implemented as *contextual* keywords to protect legacy code. It means that they still can be names for classes, methods, etc. For example, the following code is valid in C# (method bodies are omitted):

```
namespace async
{
   partial class async
      { partial void partial(); }

   partial class partial
   {
      // async method named 'async'
      async Task<async> async() { ... }

      // method named 'async' returning
      // an object of type 'async'
      async async(async async) { ... }
   }
}
```

Proper interpretation of a contextual keyword depends on a heavy context analysis going far beyond LL(1) or LR(1) parsing. In Roslyn sources, there is a special `ShouldAsyncBeTreatedAsModifier` method checking lots of specific conditions, each of which covers a particular `async` placement relative to non-contextual keywords, predefined types, and `partial` keyword. Besides, up to 2 additional tokens are required to make a correct decision.

Fortunately, to meet contextual keywords used as identifiers seems to be almost improbable. In our experiments, such cases were revealed only in synthetically created testing files, not in a real production code. Moreover, using `async` or `partial` contextual keywords as public entity identifiers one breaks general C# naming conventions[14] which are usually used as a basis for particular code style rules being applied inside a developers team.

B. Java tolerant parsing

For Java programming language, the following projects are considered:

- **Java Development Kit** is a toolbox consisting of Java compiler, core libraries and Java Runtime Environment;
- **Elasticsearch** is an engine for a full-text search;
- **Spring Framework** is a Java framework used to build applications for different subject domains;
- **RxJava** is a library for composing asynchronous and event-based programs.

Parsing results are presented in Table II, and a tolerant LR(1) Java grammar is presented in Figure 3.

As it can be noted, there is the only difference between baseline and tolerant parsing results. `FIND_MASK`, `NEW_MASK` and `RELEASE_MASK` fields are missed by the tolerant parser in the following code:

```
private final static int
  CREATE_MASK = 1<<CREATE,
  FIND_MASK = 1<<FIND,
  NEW_MASK = 1<<NEW,
  RELEASE_MASK = 1<<RELEASE,
  ALL_MASK = CREATE_MASK|FIND_MASK
    |NEW_MASK|RELEASE_MASK;
```

Unlike all the other types of brackets considered in Section IV-B2, angle brackets cannot be defined as a pair in the LanD grammar because they may appear in the program in different meanings, some of which assume they can be used separately from each other. However, in case they bracket type parameters, it is important to match these parameters as a whole to prevent inner commas from being interpreted as field separators. It is hard to resolve this problem correctly staying in the tolerant parsing boundaries and, actually, in the boundaries of a context-free parsing and lexing too [17]. To make a correct decision, an analysis of the context angle bracket appears at is needed. Recovery algorithm combined with `Avoid`-based error triggering helps to handle inputs like

```
private static final long ADD_WORKER =
  0x0001L << (TC_SHIFT + 15);
```

by interpreting all the angle brackets as opening for a `type_parameter` in Figure 3, triggering an error on `;` token which is forbidden in type parameters, and reinterpreting the outermost type parameter as `Any` from `init_part` water alternative. However, this processing allows the loss of some middle fields from the group of fields defined simultaneously.

C. Summary

As experiments show, both C# and Java tolerant parsers using our modified LL(1) and LR(1) algorithms are viable and allow one to find almost all the islands that can be found with a baseline parser. Mismatches can not be considered as a tolerant parsing disadvantage: the ones occurred in erroneous

[11] mcs/jay/skeleton.cs

[12] mcs/tests/test-async-*.cs

[13] mcs/tests/test-partual-*.cs

[14] https://docs.microsoft.com/en-us/dotnet/standard/design-guidelines/capitalization-conventions

TABLE II: Number of entities found in Java projects

Project	Total files	Enums	Classes	Fields	Methods
JDK	7704	151	10590	46176 (-3)	88709
Elastic	10972	387	14914	36830	94722
Spring	7063	100	12060	18402	61515
RxJava	1654	36	2728	6258	19931

C# programs are not unexpected since our algorithms are designed to work with correct programs, while for the most part of the valid programs containing lost islands, possible grammar fix can be easily suggested due to grammar simplicity and extensibility. However, there is also a tiny group of valid programs for which it is impossible to catch the missing island without performing an additional context analysis. This problem is actually not a tolerant parsing problem but a context-free analysis problem in general.

VI. Conclusion

In the present paper, several algorithms and algorithm modifications aimed at island-grammars-based deterministic tolerant parsing are proposed. LR(1) parsing algorithm modification is performed in accordance with the simplified grammar formal definition previously developed by the author of the paper. A special `Any` symbol is integrated into the algorithm to add a capability to match token sequences which are not explicitly described in the grammar. LR(1) tolerant grammars tend to be shorted and more comprehensible than their LL(1) analogues written for previously modified LL(1) algorithm. Additional restriction defining simplified grammars subclass for which LL(1) and LR(1) tolerant parsing algorithms are always able to correctly handle consecutive `Any` problem is revealed. `Any` processing mechanisms are introduced to expand correct consecutive `Any` processing to entire simplified grammars class. Nested bracketed structures tracking is implemented to give the grammar developer a possibility not to take into consideration the content of in-water bracketed areas while replacing water description with `Any`. Error recovery algorithms are proposed for LL(1) and LR(1) tolerant parsing. Unlike the standard error recovery, they are designed not to resume parsing for an incorrect program, but to find the area which was mistakenly interpreted as an island and reinterpret it as a water. Through the series of experiments with C# and Java parsers generated by tolerant grammars developed for LanD parser generator, modified LL(1) and LR(1) parsing algorithms are proved to be able to successfully analyse the source codes of industrial software products.

Though the current tolerant parsing implementation is enough to work on solution of the crosscutting concerns markup problem mentioned in Section I, an improvement of parsing results for syntactically incorrect programs may broaden the markup tool application opportunities. We have an assumption that `Any`-based recovery responsibility area may be explicitly specified for a particular grammar, and outside of this area some other recovery algorithms aimed at parsing resumption for an incorrect program can be used. Thus, our tolerant parsers will be capable to capture constructs of interest in such a program, like baseline parser successfully does in Section V-A, instead of totally failing or interpreting all of these constructs as a single water piece. Besides, as performance was not the key goal until the present, we were satisfied with the generally linear dependency between input length and running time of the algorithms. However, basing on the knowledge of LanD implementation details, we are sure that performance can be improved (not in terms of time complexity classes, but in terms of absolute values of the algorithm running time). So, algorithms and structures optimization is the second possible direction for further work on tolerant parsing.

References

[1] L. Moonen, "Generating robust parsers using island grammars," in *Proceedings of the Eighth Working Conference on Reverse Engineering (WCRE'01)*, ser. WCRE '01. Washington, DC, USA: IEEE Computer Society, 2001, pp. 13–22.

[2] A. Afroozeh, J.-C. Bach, M. van den Brand, A. Johnstone, M. Manders, P.-E. Moreau, and E. Scott, "Island grammar-based parsing using GLL and Tom," in *Software Language Engineering: 5th International Conference, Revised Selected Papers*, K. Czarnecki and G. Hedin, Eds. Berlin, Heidelberg: Springer Berlin Heidelberg, 2013, pp. 224–243.

[3] L. Moonen, "Lightweight impact analysis using island grammars," in *Proceedings of the 10th International Workshop on Program Comprehension (IWPC)*. IEEE Computer Society, 2002, pp. 219–228.

[4] E. Scott and A. Johnstone, "GLL parsing," *Electron. Notes Theor. Comput. Sci.*, vol. 253, no. 7, pp. 177–189, Sep. 2010.

[5] M. Tomita, *Efficient Parsing for Natural Language: A Fast Algorithm for Practical Systems*. Norwell, MA, USA: Kluwer Academic Publishers, 1985.

[6] A. Goloveshkin and S. Mikhalkovich, "LanD: instrumental'nyi kompleks podderzhki posloinoi razrabotki programm [LanD: a framework for layer-by-layer program development]," in *Sovremennye informatsionnye tekhnologii: tendentsii i perspektivy razvitiya [Proceedings of the 25th conference "Modern information technologies: tendencies and perspectives of evolution"]*, 2018, pp. 53–56, (in Russian).

[7] A. Goloveshkin, "Searching and analysing crosscutting concerns in marked up programming language grammar," *University News. North-Caucasian Region. Technical Sciences Series*, no. 3, pp. 29–34, Sep. 2017.

[8] A. Fuksman, *Tekhnologicheskie aspekty sozdaniya programmnykh system [Technological Aspects of Program Design]*. Moscow, Statistika, 1979.

[9] J. Conejero, J. Hernández, E. Jurado, and K. van den Berg, "Crosscutting, what is and what is not?: A formal definition based on a crosscutting pattern," Tech. Rep. 5/TR28/07, 2007.

[10] A. Goloveshkin and S. Mikhalkovich, "Tolerant parsing with a special kind of any symbol: the algorithm and practical application," *Trudy ISP RAN [Proc. ISP RAS]*, vol. 30, pp. 7–28, 2018.

[11] H. Mössenböck, "The compiler generator Coco/R," 2014. [Online]. Available: http://ssw.jku.at/Coco/Doc/UserManual.pdf

[12] M. Malevannyy, "Legkovesnyi parsing i ego ispolzovanie dlya funktsii sredy razrabotki [lightweight parsing and its application in development environment]," *Informatizatsiya i svyaz [Informatization and communication]*, vol. 3, pp. 89–94, 2015, (in Russian).

[13] D. Grune and C. J. Jacobs, *Parsing Techniques: A Practical Guide (2Nd Edition)*. New York, USA: Springer-Verlag New York, 2008.

[14] A. V. Aho, M. S. Lam, R. Sethi, and J. D. Ullman, *Compilers: Principles, Techniques, and Tools (2Nd Edition)*. Pearson Education, Inc., 2007.

[15] M. Malevannyy and S. Mikhalkovich, "Aspect markup of a source code for quick navigating a project," in *Proceedings of the 11th Central and Eastern European Software Engineering Conference in Russia*, ser. CEE-SECR '15. New York, NY, USA: ACM, 2015, pp. 4:1–4:9.

[16] A. Aho and J. Ullman, "Translations on a context free grammar," *Information and Control*, vol. 19, no. 5, pp. 439 – 475, 1971.

[17] E. R. Van Wyk and A. C. Schwerdfeger, "Context-aware scanning for parsing extensible languages," in *Proceedings of the 6th International Conference on Generative Programming and Component Engineering*, ser. GPCE '07. New York, NY, USA: ACM, 2007, pp. 63–72.

Development of a software framework for real-time management of intelligent devices

Tamara Naumović
Faculty of organizational sciences
University of Belgrade
Belgrade, Serbia
tamara@elab.rs

Lazar Živojinović
Faculty of organizational sciences
University of Belgrade
Belgrade, Serbia
lazar@elab.rs

Luka Baljak
Faculty of organizational sciences
University of Belgrade
Belgrade, Serbia
lukabaljak@elab.rs

Filip Filipović
Faculty of organizational sciences
University of Belgrade
Belgrade, Serbia
filipfilipovic@elab.rs

***Abstract*—The subject of this paper is development of software framework for real-time management of intelligent devices. The framework enables intelligent management of IoT devices in cyber-physical systems using models based on recurrence relations and differential equations. The platform was developed using Python programming language, Django framework and wide corpus of modules and libraries that support continuous simulation. The software framework incorporates application programming interface as well, for specification of system behaviour, transmission of input parameters and output results, and sending control actions via web services to the IoT system.**

Keywords—software framework, IoT, continuous simulation, python

I. INTRODUCTION

Cyber-physical systems (CPS for short) integrate devices, networks, interfaces, computer systems, and others with physical world. The fact that those elements are heterogeneous, hybrid, distributed and numerous, makes their analysis, design and implementation quite challenging and complex. In addition, CPSs are real time by their nature. Wide corpus of services, applications and interactions within CPS as well as huge growth of Internet of things further fuelled the need to change and improve existing approaches to managing those systems [1][2]. One of the most significant issues is to explore and model properties of CPS' elements, their connections and behaviour [3][4]. CPS immerged from the integration of devices with embedded systems, smart objects, people and physical environment typically connected via communication structure. Thus, it is no surprise that smart environments and systems are among the fields of CPS application.

Smart systems are integral part of CPS. The key technology for developing cyber physical systems is Internet of Things, IoT [5][6][7]. According to [8], cyber-physical systems, Internet of things and big data are related concepts of cooperative solutions, where people, autonomous devices and the environment interact with one another to achieve a certain goal. IoT technologies enable the connection of a large number of users, devices, services and applications to the Internet [9].Management of intelligent devices often needs to be done in real-time. Real-time Control System (RCS) is a reference model of architecture that defines the types of functions needed for intelligent real-time control [10]. RCS provides a comprehensive and basic methodology for design, engineering, integration and testing of control systems [11].

In RCS systems, the state of many variables changes continuously over time, so the management of these systems can be modelled using differential equations and recurrence relations. Hence, simulation enables investigation of behaviour of such dynamic systems by developing appropriate models and using these models in experiments designed to provide an insight into the future behaviour of the system under specific conditions [12][13][14]. Simulation of CPS is becoming extremely important for both academia and practice as results of simulations have huge potential to be applied in research, business and engineering. [15].

The main idea of the research is to develop a comprehensive platform that would enable modelling and simulation of different smart environments. To achieve this goal, it is vital to define a uniform formal model applicable to any smart environment whose mathematical representation can be mapped to its implementation as one-to-one correspondence. The software framework for real-time management of intelligent devices represents a cyber-physical system incorporating IoT devices as the physical component of the system and software framework accompanied with required network infrastructure as the cyber component. Having available information and input data from intelligent devices in real-time allows the simulation engine, as an integrated part of the solution, to calculate and create a plausible outcome. On the other hand, outcome created as the result of the simulation can be a trigger dispatching control actions towards the IoT system.

The formal model, implementation and example illustrating the applicability of the presented mathematical model will be explained further in the paper.

II. FORMAL MODEL

A. Continuous system simulation in IoT context

Continuous system simulation refers to experimenting with models whose states are changing continuously in time [11]. These types of simulation systems are often described by differential equitation. Time is independent variable in most cases. Continuous simulation can be used in different contexts and covers numerous types of real-world problems [16]. Considering time as an independent variable, digital computer has constraints solving differential equations,

which is why it was necessary to develop a specific language to resolve this issue.

Different specialized languages for continuous simulation were developed, such as: CSMP (Continuous Simulation Modelling Programme) ESL (European Simulation Language) ACSL (Advanced Continuous Simulation Language) CSSL4 (Continuous System Simulation Language, Simulink, Matlab, Modelica and others that have been developed to simplify modelling, and to minimize problems related to programming continuous systems [16]. However, a majority of simulation tools have limitations related to low level of flexibility and adaptability, high costs, platform dependence, maintenance difficulties, etc. [16]

CSMP/FON platform for continuous system simulation was developed following these principles [17]:

- Minimize required hardware resources and improve speed of execution
- Suitable and easy to use for educational purpose
- Simple and rich user interface
- Support for scientific research
- Saving costs

The CSMP/FON is an open source solution and can be downloaded from the web site https://elab.fon.bg.ac.rs/softver/csmp. It has been used for many years in research and teaching within simulation related courses at University of Belgrade.

Software framework for real – time management of intelligent devices and IoT systems in general is a time dependent system, which requires a tool that can overcome any time – related performance issues. Ergo, using CSMP simulation logic in the software development process can be a way of introducing control mechanism in the system.

B. Formal model of a continuous simulation system

Formal model of a continuous simulation system can be given as a tuple [18]:

$$M = (U, Y, S, \delta, \lambda, S_0) \quad (1)$$

with the following meanings:

U – set of inputs

Y – set of outputs

S – set of state variables

δ – transfer function: $\delta: U \times S \rightarrow S$

λ – output function: $\lambda: U \times S \rightarrow Y$

S_0 – set of initial states

Function of a variable φ is a mapping of a non-empty set X, of variables x, signed as domain, in non-empty set Y, of variables y, signed as scope (or codomain, set of function values) [18]:

$$\phi: X \rightarrow Y ,$$

a function of many variables is presented through mapping:

$$\phi: X \times X \times X \times \ldots \times X \rightarrow Y ,$$

a block is presented as ordered set of three elements

$$b = (\phi, X, Y),$$

each $x \in X$ is input, while $y \in Y$ is output from the block.

The process of continuous simulation is based on solving differential equations and recurrence relations [17][18]. CSMP simulation language is a block-oriented language designed for solving systems of differential equations. Each block is specified by a set of inputs and parameters and a graphic symbol [12]. The graphic display of elements in the general form is presented in Figure 1

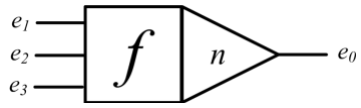

Fig1. Graphic display of an element [17]

C. Formal model of a hybrid IoT system for real-time simulation

The current simulation model describes a system that allows solving differential equation systems in the given time with predefined variables and inputs [17][18]. The software framework for real-time management of intelligent devices requires a broaden model that will be suitable for use in real-time IoT systems [19].

Figure 2 presents the concept of a hybrid IoT system for real-time simulation. This model enables having values measured in the environment in real-time included as variables of the simulation systems. In addition, the model enables managing the IoT system using variables obtained through the simulation.

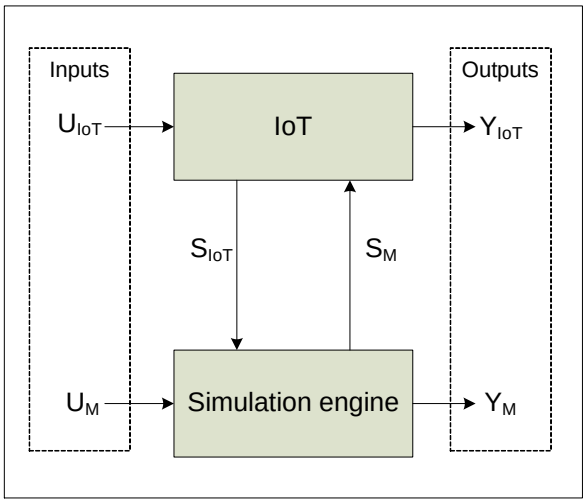

Fig2. Hybrid IoT system for real-time simulation

For mathematical modelling of the hybrid IoT system for real-time simulation, the presented formal model needs to be extended with a set of state variables, inputs and outputs from the IoT system:

$$S = S_M \cup S_{IoT} \quad (2)$$

$$U = U_M \cup U_{IoT} \quad (3)$$

$$Y = Y_M \cup Y_{IoT} \quad (4)$$

In order to have the set of state variables S in the simulation model, it is necessary to get the values of state variables from the IoT system (S_{IoT}). This is done by developing and providing API of the IoT system. This API needs to implement the following functions:

$$\rho: S_{IoT}(t) \rightarrow S(t) \quad (5)$$

$$\omega: S(t) \rightarrow S_{IoT}(t) \quad (6)$$

$$\gamma: Y_{IoT}(t) \rightarrow Y(t) \quad (7)$$

The operation ρ is the operation of reading the values of variables from IoT system. These values then can be used in

the simulation system for calculations. The operation ω enables writing the values of variables into the IoT system. These values are calculated in the simulation engine and then sent to the IoT system. These values can also be used for triggering specific actions of the IoT system. The operation γ enables reading the outputs of the IoT systems.

Having in mind that IoT systems are distributed, all these operations for interaction between the simulation and IoT systems need to be realized via web, using web services. Depending on the scenario, both PUSH and POP methods can be used.

After extending the formal model of continuous simulation system with the IoT elements, the process of continuous system simulation can be described with the finite automata equations [18]:

$$S(t) = I \times A_1 \cdot \{U(t), S(t)\} \quad (8)$$

$$Y(t) = A_2 \cdot \{U(t), S(t)\} \quad (9)$$

where A_1 and A_2 are matrix representation of algebraic functions, and I is the matrix representation of the integration operator (Fig 3).

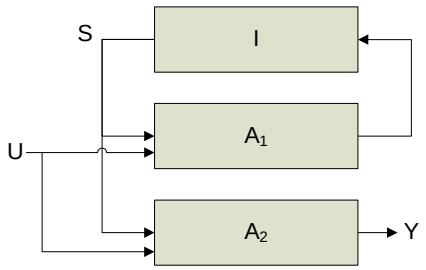

Fig3. The structure of finite automata for simulation of continuous systems [18]

A more granular structure of continuous system simulation is presented in the Figure 4.

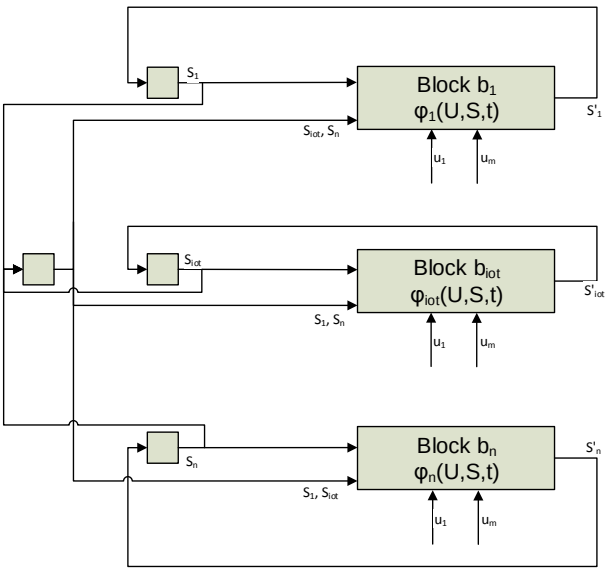

Fig4. Block diagram of granular structure of continuous systems

Figure 4 depicts the decomposition of the operator A1 to its elementary and primitive functions, represented as algebraic blocks. As explained later in section D, input of every block is an element that can come from either a set of inputs, a set of state variables or a set of the associated variables that represent inputs of the preceding algebraic blocks.

D. Orderliness

The essential feature of any non-trivial mathematical model of the continuous simulation is the feedback. The feedback occurs in the model as a result of a chain of cause-and-effect that generates a loop [20]. Considering the case of continuous simulation the model develops the feedback loop if it is impossible to mark all blocks from the set that satisfy a condition $i < j$, where block's b_i output is connected to block's b_j input [17]. The feedback loop imposes a compulsory requirement for computability of mathematical model called "orderliness", defined as:

The set A of all countable algebraic blocks (blocks that correspond to algebraic functions) of M models is called "orderly" if all distinct objects $a_j \in A$ can be ordered (sorted) in such linear list where inputs of every distinct object a_j are elements of some of the following sets [18]:

1) U – set of inputs
2) S – set of state variables
3) Subset $C' \subset C$ defined as :

$$C' = \{c \in C \mid \forall i < j, \forall a_j = (\varphi_i, X_i, Y_i): c \in X_i\}$$

III. MAPPING MATHEMATICAL MODEL TO IMPLEMENTATION

Mapping the mathematical method given in equations 1-9 is represented through series of UML sequence diagrams, where each method has its corresponding diagram.

The implementation of the software framework described through this research will be based on the concurrent computing and NoSQL concepts, such as threads and use of the MongoDB document-oriented database program.

A. Simulation engine

Figure 5 illustrates the core simulation process depicted in equations (8) and (9). The diagram represents a typical continuous simulation process: begins with loading the simulation object from the MongoDB database in the *engine*, sorting the blocks, setting the primary conditions and starting the calculation process.

The calculation process itself is a looped process where series of computations are performed on every block in the simulation model: block type analysis, output generation through block function, output appending and call for next computation. The block type analysis determines if the current block is an IoT block. If it is, the engine provides a call to the IoT service, which performs specific operations based on the type of the call. Call types can be divided into two groups: a) reading and b) writing.

The call is a software representation of functions described through equations (5), (6) and (7). Depending on the call type, the simulation system will process data sent from the IoT system and embed them as a part of the continuous simulation process, it will send a control action to the IoT system as a result of the continuous simulation process or it will read the output from the IoT system (Fig 6).

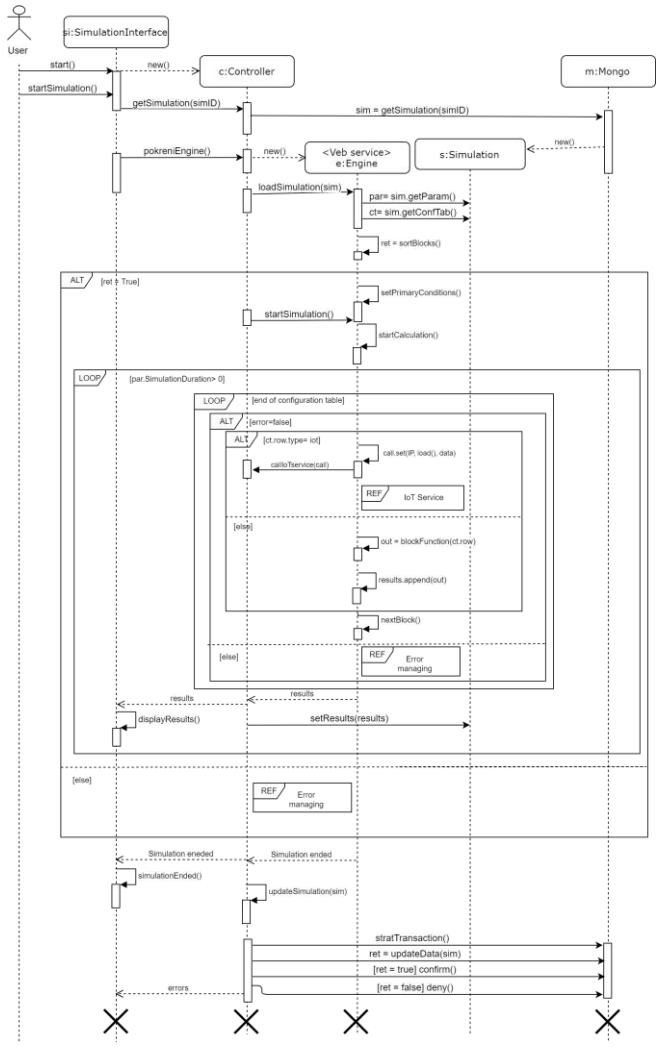

Fig5. UML sequence diagram of the core simulation process

B. *Mapping the values of state variables and output from the IoT system*

The call for executing operation ρ (5) – reading the values of variables from IoT system, is illustrated in the Figure 5, as a part of the calculation process, where simulation engine should consider IoT values as the part of the calculation.

The control actions, ω (6) – writing the values of variables into IoT system, sent to the IoT system are, also, a type of call. By connecting to the IoT system, the engine can access its API, create a call to the function provided by the user, send data from the simulation engine and thus begin the given process on the IoT platform. Such call is illustrated in the Figure 7.

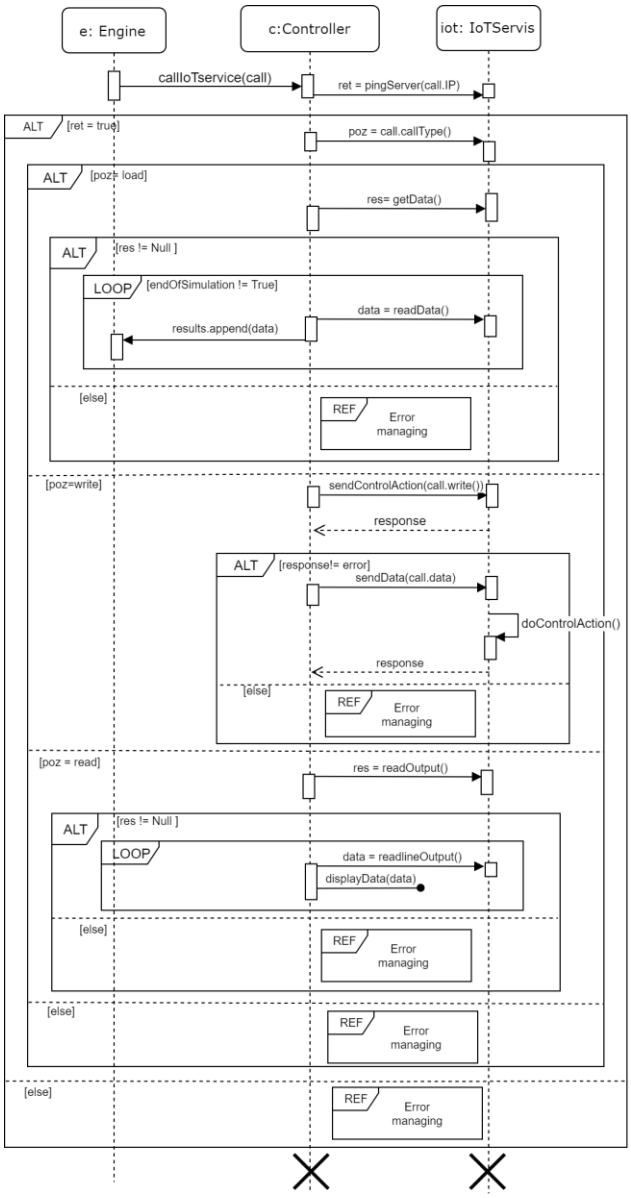

Fig6. UML sequence diagram of processing calls to IoT system

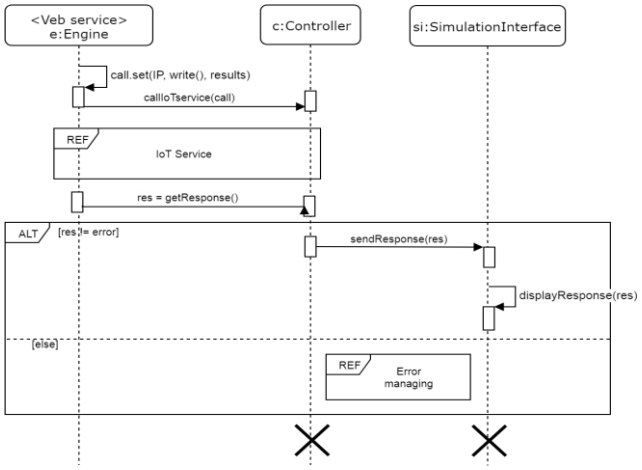

Fig7. UML sequence diagram of the operation ω – writing the values of variables into IoT system

Through the connection made to IoT system, our engine can retrieve IoT system outputs and display them though the platform interface, which is directly correlated with

mathematical operation γ (7) – reading the outputs of the IoT systems (Fig 8.).

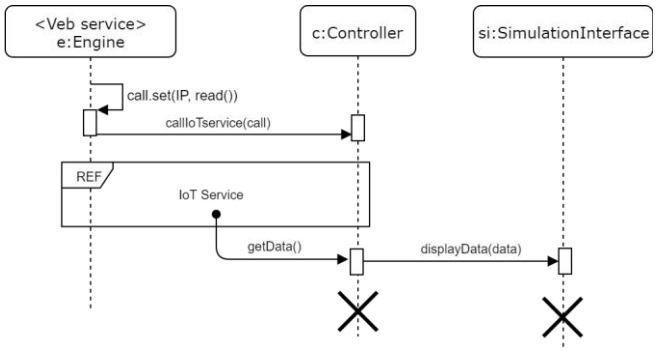

Fig8. UML sequence diagram of the operation γ – reading the outputs of the IoT systems

C. *Example: Smart watering system simulation*

The example of smart watering system simulation is an illustration of the operation ω (6), where control actions and variables are being sent to IoT system.

For this example it is necessary to create control actions that will forward the data collected through the simulation of the environment and air humidity by the simulation engine, and signal the beginning of the IoT system actions.

Smart watering system is based on air humidity predictions, provided as input parameters given by the simulation engine. If the humidity is under the marginal value set in the IoT system, the watering process begins.

CONCLUSION

Modelling hybrid IoT system for real-time simulation presents a focal point of this research. Thus, successfully mapping the values of state variables from the IoT system in the implementation process is essential.

The autonomous performance of the simulation program should be implemented using the concepts of concurrent computing – threads:

1) servicing requests for the simulation process control and error reporting,
2) servicing requests for configuration changes,
3) reading data and sending control actions to IoT system,
4) servicing requests for simulation results,
5) execution of the simulation process

Further research and work should be directed towards execution of the proposed implementation, integration of the platform in the students' educational process and evaluation and revision of the software performance. Upgrading the existing model with new modules should be considered.

ACKNOWLEDGMENT

Authors would like to thank prof. dr Bozidar Radenkovic, prof. dr Marijana Despotovic – Zrakic, prof. dr Zorica Bogdanovic, prof. dr Dusan Barac and prof. dr Aleksandra Labus for guidance and mentoring throughout this research and software development.

REFERENCES

[1] E. A. Lee, S. A. Seshia. Introduction to Embedded Systems. A Cyber-Physical Systems Approach, 2017, Second Edition

[2] Y.Z. Lun, A. D'Innocenzo, F. Smarra, I. Malavolta, M. Benedetto, Maria. State of the Art of Cyber-Physical Systems Security: an Automatic Control perspective. Journal of Systems and Software, 2018, vol. 149, pp. 174-216

[3] N. Canadas, J. Machado, F. Soares, C. Barros, L. Varela. Simulation of cyber physical systems behaviour using timed plant models. Mechatronics, 2018, vol. 54, pp.175-185

[4] J. Liu, J. Lin. Design Optimization of WirelessHART Networks in Cyber-Physical Systems. Journal of Systems Architecture, 2019, article in press

[5] K. Carruthers. Internet of Things and Beyond: Cyber-Physical Systems. 2016. Available: https://iot.ieee.org/newsletter/may-2016/internet-of-things-and-beyond-cyber-physical-systems.html

[6] L. Tan, N. Wang. Future Internet: The Internet of Things. In: Proceedings of 3rd International Conference on Advanced Computer Theory and Engineering, 2010, vol. 5, pp. 376- 380.

[7] M. Wu, T. J. Lu, F. Y. Ling, J. Sun, H. Y. Du. Research on the architecture of Internet of Things. In: Proceedings of 3rd International 8 on Advanced Computer Theory and Engineering, 2010, vol.5, pp. 484-487.

[8] S. F.Ochoaa, G. Di Fatta. Cyber-physical systems, internet of things and big data. Future Generation Computer Systems, 2017, vol. 75, pp. 82-84

[9] B. Radenković, M. Despotović-Zrakić, Z. Bogdanović, D. Barać, A. Labus, Ž. Bojović. Internet inteligentnih uređaja. Beograd: Fakultet organizacionih nauka, 2017

[10] J. S. Albus. A Reference Model Architecture for Intelligent Systems Design. Springer, 1993. Available: https://web.archive.org/web/20080916153507/http://www.isd.mel.nist.gov/documents/albus/Ref_Model_Arch345.pdf

[11] F. E. Cellier, E. Kofman. Continuous System Simulation. Springer-Verlag, 2006, First Edition.

[12] J. Banks. Handbook of Simulation: Principles, Methodology, Advances, Applications, and Practice. John Wiley & Sons, 1998.

[13] J. S. Keranen , T. D. Raty. Model-based testing of embedded systems in hardware in the loop environment. IET Software, 2012, vol. 6, no. 4, pp. 364-376.

[14] N. L. Celanovic, I. L. Celanovic, Z. R. Ivanovic. Cyber Physical Systems: A New Approach to Power Electronics Simulation, Control and Testing. Advances in Electrical and Computer Engineering, 2012, vol.12, no.1, pp.33-38, 2012

[15] P. Garraghan, D. McKee, X. Ouyang, D. Webster, J. Xu. SEED: A Scalable Approach for Cyber-Physical System Simulation. IEEE Transactions on Services Computing, 2016, vol. 9, no. 2, pp. 199-212.

[16] M. Despotović-Zrakić, D. Barać, Z. Bogdanović, B. Jovanić, B. Radenković. Software Environment for Learning Continuous System Simulation. Acta Polytechnica Hungarica, 2014, vol. 11, no 2, pp. 187-202.

[17] B. Radenković. Program za simulaciju kontinualnih i diskretnih Sistema CSMP/MICRO. Automatika, 1984, vol. 25, pp. 235-238

[18] B. Radenković, M. Stanojević, A. Marković. Chapter 6 Simulacija kontinualnih sistema. Racunarska Simulacija, 2009, IV edition, pp. 89-110.

[19] T.Naumović, B. Radenković, M. Despotović-Zrakić, D. Barać, A.Labus. A framework for real-time management of intelligent devices: an educational perspective. International Conference on New Horizons in Education, 2018, Proceedings Book Volume 1, pp 33-34

[20] A. Ford. Modeling the Environment: An Introduction To System Dynamics Modeling Of Environmental Systems, 2010, Second Edition.

Graphic DSL for Mobile Development

Artur Gudiev
Saint Petersburg State University,
7/9 University Embankment,
Saint Petersburg, 199034,
Russian Federation,
Email: arturgudiev93@gmail.com

Alexandra Grazhevskaya
Saint Petersburg State University,
7/9 University Embankment,
Saint Petersburg, 199034,
Russian Federation,
Email: sagrapro7@gmail.com

***Abstract*—Due to the increase in the number of platforms, languages and methods which are used in mobile development, the general technology elaboration problem is quite relevant nowadays. Graphic domain-specific languages (DSL) facilitate application development by use of concrete domain abstractions.**

In this work, the developed mobile application architectural template and the graphic DSL created on its basis are presented. The provided DSL allows describing the main structure of the mobile application in terms of controllers, states and transitions between them. Besides, the automatic code generation for the UbiqMobile platform is implemented.

I. Introduction

A large number of platforms, languages, and methods are used in mobile application development. Existing mobile development tools significantly differ from each other, and the common technology implementation problem is still relevant.

There are various ways of the high-level description of mobile application - architectural patterns mvc, pac, microkernel, etc.[1] All these patterns were borrowed from other software areas, are quite actively applied during mobile application development, but not quite correspond to their nature. Mobile applications differ from desktop and web programs.[2] Mobile applications are commonly used for short sessions, more focused on specific objectives performance.

Use of a suitable architectural pattern allows to increase considerably application development efficiency, but a bigger result can be achieved by graphic languages usage. DSL is the programming language in terms of the concrete subject domain which is applied to the solution of concrete type tasks[3]. Graphic DSL languages help to represent applications using visual diagrams. The result code will be generated according to these diagrams.

The purpose of this article is to develop an architectural template for mobile applications and to create graphic DSL based on it. DSL should allow describing the main logical application structure in terms of states, controllers and transition conditions between them.

II. Tools

The Modeling SDK technology is used for the graphic DSL implementation.[4] Modeling SDK is the plugin for Visual Studio intended for visual domain-specific languages development. Visual DSL development happens in the following order. At first, the metamodel (the set of all syntactically correct diagrams) is developed and edited, the implemented classes are generated. Then a DSL package compilation and debugging take place in an experimental instance of Visual Studio.

For metamodel programming, the graphic editor of Modeling SDK is used, but also it is possible to redefine or add new methods to the generated partial classes of the C# language. The T4 language is used for code generation. [5] The Dsl and DslPackage projects are automatically created in the new solution of Visual Studio. In the Dsl project, various metamodel artifacts of the created DSL are stored. DslPackage project contains the user interface settings.

III. Controllers and states model

An application state corresponds to some complete logic fragment. The result of state change is data transfer which is logically finished and clear to other states.

It is convenient to group states and transition conditions into controllers by their logical connectivity, data community, UI forms, transition frequency and data transfer between states. Grouping states into controllers gives an opportunity to define more strong transition logic, allowing transitions between states in the controller and forbidding them between conditions of unconnected controllers.

The main application cycle is run by the special mechanism starting and switching controllers of states. Each controller has an entry point and an opportunity to set input parameters when an application switches to it. There can be several exits in a state. An application can return to the caused controller, switch to the next controller, etc. Execution logic is implemented in terms of the finite-state machine in the controller. Each controller has a set of the predefined states (in particular, initial and final states), and it is possible to add new states.

Mobile application implementation by means of controllers and states model allows to centralize its logical basis, the structure of the code becomes evident. When using controllers, the aim of the mobile application developer comes down to describing the necessary logical controllers, state and conditions of transition.

IV. Graphic DSL Description

The model of controllers and states was tested on mobile applications of different classes and proved the efficiency. But

the best results can be achieved, having taken this model as a basis of graphic DSL for mobile applications. (see Fig.1)

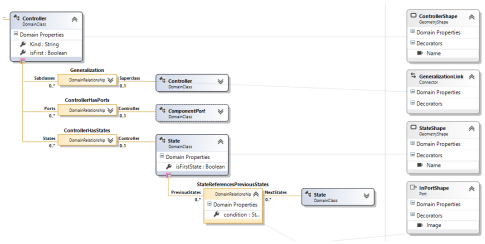

Fig. 1: Language implementation in Modelling SDK

Basic elements of the language are controllers and its states. States are placed on the controller, can connect among themselves and also to ports of the controller for the conditions description of an entrance and an exit from it.

Each state opens in the separate diagram on which conditions of an entrance, an exit from a state and its internal logic are described. The logic of states includes a display of UI forms, processing of their events, services calls, conditions checking , etc.

There is a display of a UI form for each state in the language. To connect the existing screen form with a state the ShowForm element is used.

V. Code generation

The language of T4 templates is used for code generation. The main components of the T4 language are directives, blocks of the text and control units. For a generation of the unchangeable code, text blocks are used, and dynamic parts are implemented by means of control units.

As a result of generation, the controllers' classes appear. Each controller has several states presented in the transfer type form. Process of work is implemented in terms of the finite-state machine. On links between states, the template of transitions are implemented. Controllers can also have ports. Ports are used for transitions between controllers.

The resulting code is applied to UbiqMobile platform.[6] UbiqMobile platform is aimed to cross-platform mobile development. The main features of the platform are that the business logic of all applications is executed on the server. And mobile devices have only thick clients to represent the result of application work.

VI. Samples

The purpose of the first sample is to display the train schedule for the user. The application consists of a single controller and two states. In start state, the user can choose departure and destination stations. (see Fig.2) After clicking on the button, the application will switch the current state from the first state to the second one. (see Fig.3)

The second sample allows the user to log in and receive the code which then can be used later. (see Fig. 4) There are two controllers in the application: LoginController and MainController. There is also a switching between controllers implemented by means of ports. In LoginController there is only one state. At MainController there are two states: a state with option selection and a state where a user can receive the necessary code. The UbiqMobile UI forms, corresponding to states of the application are given below. (see Fig. 5)

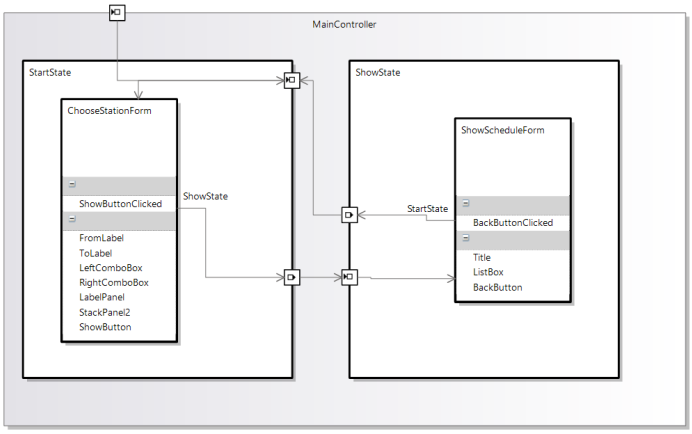

Fig. 2: Schedule application scheme

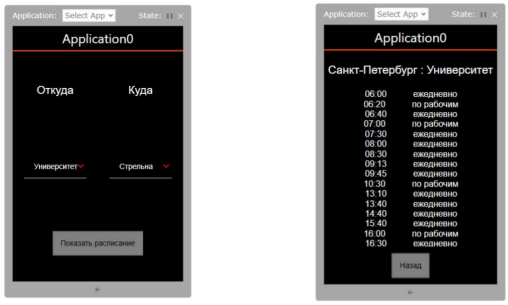

Fig. 3: Schedule application UI form

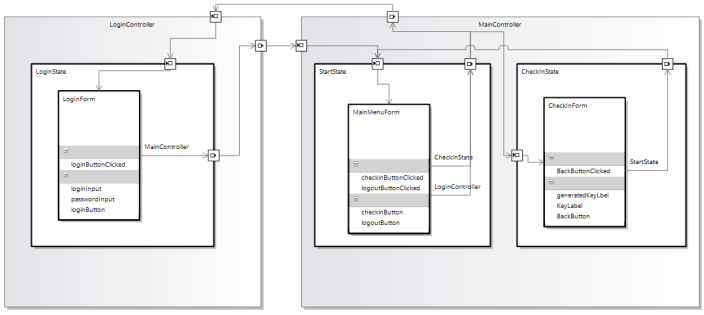

Fig. 4: Application with authorization scheme

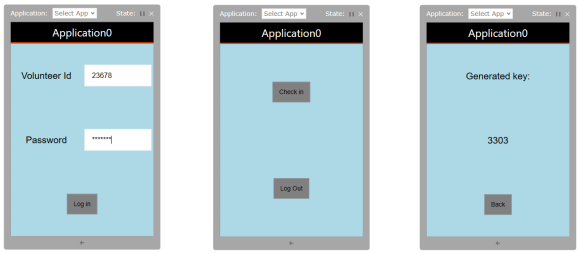

Fig. 5: UbiqMobile screens

VII. Conclusion

Within this work, the following results were achieved. The graphic DSL for mobile application development is implemented. The code generation for UbiqMobile platform feature is added. Demonstration samples are represented.

References

[1] S. D. Plakalovic D., "Applying mvc and pac patterns in mobile applications."

[2] H. K.Flora, "An investigation on the characteristics of mobile applications: A survey study."

[3] D. Koznov. Domain-specific modelling methodology and tools. [Online]. Available: http://www.math.spbu.ru/ru/mmeh/AspDok/pub/2016/koznov.pdf

[4] Modeling sdk for visual studio - domain-specific languages. [Online]. Available: https://docs.microsoft.com/ru-ru/visualstudio/modeling/modeling-sdk-for-visual-studio-domain-specific-languages

[5] Code generation and t4 text templates. [Online]. Available: https://docs.microsoft.com/ru-ru/visualstudio/modeling/code-generation-and-t4-text-templates?view=vs-2015

[6] A. Terekhov and V. Onosovski. Ubiq mobile platform for mobile development. [Online]. Available: http://www.math.spbu.ru/user/ant/all_articles/076_Terekhov_Onos_PlatformaUbiq.pdf

Graphical modeling of control systems based on Eclipse technologies

Mariia Platonova
Department of Software Engineering
St. Petersburg State University
28 Universitetsky pr., Saint-Petersburg, 198504, Russian Federation
Email: platonova.maria@outlook.com

***Abstract*—Only a few years ago Russia took the path of the digitalization and this trend is already taking active root into various areas of society. Digitalization is closely related to visualization, that is easily confirmed by the increasing popularity of graphical representation of business processes.**

This text describes the work on modeling and subsequent execution of production processes, such as document circulation, working with CNC machines and analysing production risks, by using the Eclipse IDE and the BPMN standard.

***Index Terms*—digitalization, visualization, code generation, business process, document circulation, CNC machine, bpmn, eclipse**

I. Introduction

Information revolutions that took place throughout the whole history of humanity undoubtedly made considerable changes in life of society, its culture and lifestyle [1].

For several years Russia has been confidently introducing the use of digitalization capabilities in many areas of society and showing great results, which are noticeable on the world stage [2]. Moreover, it should be noted that such processes involve the development of its own processing base, that has to comply the requirements for quality and reliability of products. In addition these processes in the near future will contribute for Russian companies specializing in software development to confidently enter the global market.

The application of digitalization, we think, begins with an intuitive presentation of business processes as they are the basis of the work of any company [3], and correspondingly it is necessary to describe them in a convenient form to use.

It is worth considering a graphical representation of the processes, because the visualization helps to reduce the efforts to understand, discuss or modify any necessary information [4]. There is an international standard BPMN (Business Process Model and Notation) intended for modeling business processes [5]. With the help of it any process can be represented in the form of a diagram, where its elements are any actions of this process. In addition, the generation of an executable program, which is necessary for many processes, becomes much easily with the use of diagram.

The main goal of this work is to create a tool to visualize processes with the subsequent generation of executable code. Due to the differences of executable programs of various processes, only three types of processes are considering in this work: document circulation, working with computer numerical control (CNC) machines and analysing production risks.

Similar study of creating a tool to visualize business processes with a code generation feature has already been conducted at the department of Software Engineering of St. Petersburg State University (department of SE) [6]. This tool is a part of the metaCASE technology based on QReal. However, the use of this practice can be justified only in the case of creating not one, but several products at once.

Based on previous experience the use of tools that are not very common, complex or have many limitations can lead to the problems with the development and support of the product, moreover, comparing it with analogues can become more complex. As IDE Eclipse was chosen, since it is a popular, free, cross-platform system, that is regularly updated, and it has large developer community, which can make it easier to solve occurring issues. Moreover, it is important to consider the differences between open-source licenses, while using ready-made products. For example, General Public License (GPL) involve the free access to source code of the product, that based on any software under this license, so it can cause some problems with commercial use [7]. On the contrary, license Apache 2.0 does not put forward any requirements or other limits for using and distributing [8]. Therefore, in this work we decided to use only ready-made product under this license.

In conclusion, it is necessary to pay attention to convenience of use the developed tool. At the department of SE a study of human-computer interaction has been conducted on the base of visual programming tools [9].

II. Graphics Editor

The main task of the graphical editor is to build diagrams using BPMN notation, another requirements involve the considerable expansion of its capabilities.

Full implementation of the editor is by no means easy, and since there are various options of ready-made solutions, it seemed to us wisely to select the appropriate editor from the existing versions and remake it according to our demands. Activiti-Designer (Activiti) was chosen from all of considered options as it is popular and evolving application based on Eclipse, that has a suitable license [10].

Activiti is represented by a canvas and an elements panel (panel), which contains 42 items separated into 9 categories: Start Event, End Event, Task, Container, Gateway, Boundary Event, Intermediate Event, Artifacts and Connection. Moreover, the editor allows to align selected elements on canvas as well as save the resulting diagrams as images. Fig. 1 is presented as an example of a business process described with this editor.

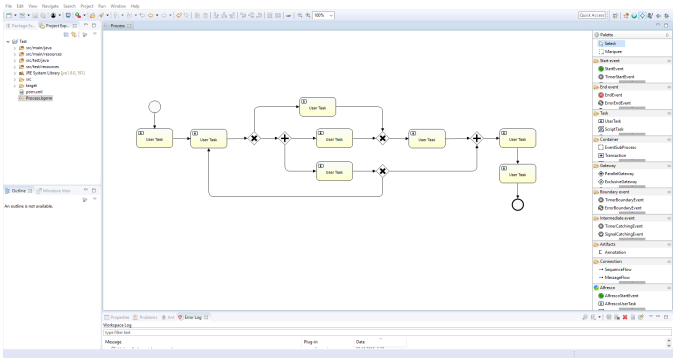

Fig. 1. Example of using Activiti.

Activiti has some drawbacks, for example, sometimes it is not possible to change the name or other attributes of an element by means of a diagram. Moreover, there is a problem with immense amount of errors that related to the hierarchy of the source code modules, the solution of this problem is addition these modules in a specific order.

In addition, Activiti does not have all required and necessary features, so it was decided to expand the capabilities of the editor. Consider in more details main added features.

A. Quick Access

An important refinement of the application was addition of the quick access feature, which allows to display any elements on the canvas without moving them from the panel.

User is provided with a set of combinations CTRL + M CTRL + N, where M is the number of a category of an element, and N is the number of the element inside this category. Thus, while using any key combination of the set, the corresponding element is added to the diagram, where the cursor is located.

B. Element Visibility

The element visibility feature is also a significant expansion of the editor capabilities. It allows to hide or expand elements of the container, that is useful in the case of large diagrams and high nesting level.

The user is provided with two functions: minimize and maximize. Depending on container visibility, one of these functions is added to the context menu of the container. Thus, while executing the minimize function, all elements of the container are hiding and the container is representing as a small rectangle. Moreover, this rectangle retains all external connections presented on its full-size version. While executing the maximize function, the container is getting its original form with all necessary edges and nodes.

III. Logical Model

A visual, that is, a user-created representation of a business process is usually called a graphical model, and an internal representation is a logical model, for example, in the form of a graph of a special type needed to generate reports, executable programs and etc.

In this work one of the main tasks is to realize a necessary representation of a logical model. Convenient and fast access to data greatly simplifies the subsequent actions according the generation of an executable program and analyzing this model.

The main reason for storing data in the form of directed graphs (graph) was the simplicity of converting user diagrams, and moreover, it is convenient to retain any additional data on their edges and nodes.

Due to the absence of any restrictions for diagrams, the complexity of working with graphs is increasing. For example, any cycles and loops make it difficult to determine the initial and final nodes of the diagram, and this is also complicating the analysis of the connections between elements. Therefore, we have adopted some restrictions that are improving the structure of the model.

In addition, a certain model of presentation was chosen, according attributes of the required graph. Consider in more details the resulting structure.

A. Base Item

Each element of the graph has unique identifier (id) and additional information of this element (info). Id is setting when the item is created and stored into info. In addition, info contains name, type, and many other components of the element. This data is definitely important for the model, and that is why id and info are formed the base class - BaseItem.

B. Types of Items

Graph consists of 3 types of elements: Container, Node, Edge. The corresponding classes provide all necessary information of the elements and their connections with others. The storage of all required information can be redundant and inefficient, so only id is using for connections between elements.

It is important to describe what a container is and what it is for. The container is provided for storing any elements of the graph and can also contains any number of other containers. Moreover, the container can also be used as a node.

Each element of the diagram contains information of the container where it is located (parent container). Edge can have 2 such containers, since its begin and end can be located in the different containers. Base container is the diagram canvas, so it means that all diagram elements are located in some parent container.

C. Graph Description

Special classes are responsible for graph representation, such as NodeUtil, EdgeUtil and ContainerUtil. These classes are static, that allows to use the same instance for any references to a class.

Each class is in charge for the current list of relevant elements. Modification of the classes has to be occurred on any diagram changes, for example, when adding, changing or deleting element.

IV. Application Examples

A. Document Circulation

For any companies are important to track its documents and check their status, that is, during the life cycle of a some document, it is necessary to know where and in what condition it is.

Such process is conveniently presented as a BPMN diagram, for example, Fig. 2. The diagram provides simple to track the document and its current status, as its movements occur along the constructed graph. There is a hierarchy system in many companies, and with this representation of the document movements, it is simple to control that only employees with the required authority can access to the document.

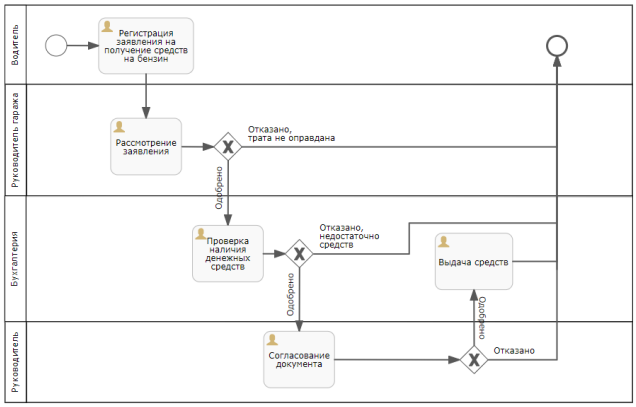

Fig. 2. Example of BPMN diagram for document circulation.

B. CNC Machines

Recent years many factories have been implementing into their working process more and more CNC machines [11], which significantly increase the automation of production and also the quality of the result.

Full automation of such processes is becoming possible in the case of using CNC machines along with industrial robots (robot), for example, cylindrical robots, packaging robots and etc. Their main task is transferring the necessary materials from one machine to another.

The question is how to program CNC machines and control the robots operations. It is important not only to specify the entire sequence of actions, but also to describe the reaction to the faulty situations, because robot can strayed or fall down due to accidental rubbish or uneven surface, which can cause the system malfunctions or the transported cargoes breakages.

Programs for CNC machines, as well as, operations of robots can be described as BPMN diagrams, for example, Fig. 3. In this way, it is convenient to set robots failure branches, that allows to quickly react to any problems and restore production process.

Fig. 3. Example of BPMN diagram for CNC machines.

C. Production Risks

Analysis of vendors and associated risks are important for any companies, since supply disruptions can significantly affect the production process, for example, it can cause increasing budget or execution time. In addition, vendors form a hierarchical structure, so it is necessary to control the whole system, due to the problem can occur on any level of the hierarchy.

One way to describe this structure is using BPMN diagrams. This will allow to implement automatic data analysis and accumulating statistics for each vendor, which will significantly reduce user actions and the influence of the human factor.

V. Code Generator

Executable programs of various types of production processes can significantly differ by its structure and end result. In this regard, code generators are implemented only for the processes described in the previous section. Each process is represented as a diagram, according to which a logical model is built with the subsequent generation of the executable code.

The main step, that preceding code generation, is analysis of the model. This intermediate step is necessary for identifying the start and end nodes, cycles, loops and etc. Data which obtained at that step is the input for code generator, so it is certainly useful to be able to visualize them, since various inaccuracies and errors can be detected that were missed during the construction of the diagram.

The user is provided with the showModel function, which executes by pressing the Show model button located in the main menu. This function can be applied to any diagram, even

if code generation is not possible. Fig. 4 shows an example of the diagram and Fig. 5 shows the visualization of its model.

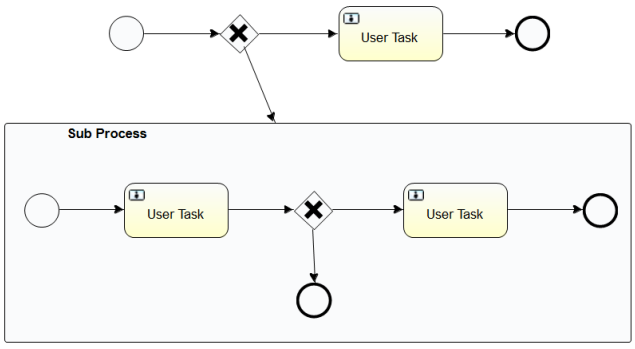

Fig. 4. Example of diagram for model visualization.

Thus, while executing showModel function to a diagram, a particular window opens where all its elements are displayed in a specific form. Recall that a child node is the destination of one of its edge and that a container can be used as a node, that is, it can have children and can be a child.

For each container, including the base one, the window displays all the corresponding elements: nodes and their children. Moreover, if the element is a container, then it is marked with a square brackets ([]), and if the element is a Gateway, then it is marked with a triangular brackets ($\langle\rangle$). In addition, all its containers, that located in the current, will be display singly with all content. Relations between elements are represented in a certain form: element1 -$\rangle$ edge -$\rangle$ element2.

Such presentation of a logical model provides easily generating code, as the task is reduced to simple linear graph traversal with a code generation for each action.

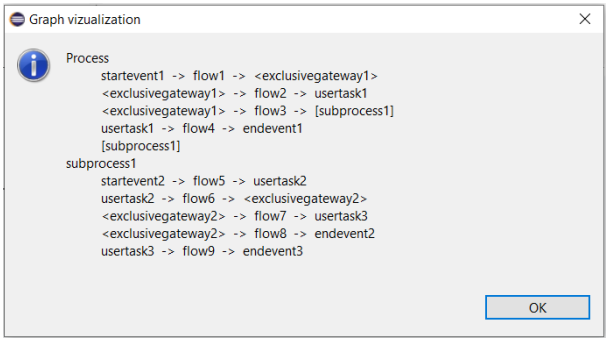

Fig. 5. Example of diagram logical model visualization.

Conclusion

In this paper we presented a description of the work on creation a tool for graphical representation of production processes with the capability of generating an executable program. The main part of the work, as the most part of the text, was focused on the modification of the Activiti graphical editor and the creation of a logical model.

References

[1] Chusyainov T.M. Informacionnaya revolyuciya i transformaciya zanyatosti. Nauka. Mysl', 2017.

[2] Chakravorti Bhaskar, Chaturvedi Ravi S. Digital Planet 2017: How Competitiveness and Trust in Digital Economies Vary Across the World. Tufts University: The Fletcher School, 2017.

[3] Plotnikov V.A. Cifrovizaciya proizvodstva: teoreticheskaya sushchnost' i perspektivy razvitiya v rossijskoj ehkonomike. Izvestiya UNECON, 2018.

[4] Afanas'ev A.A. Tekhnologiya vizualizacii dannyh kak instrument sovershenstvovaniya processa podderzhki prinyatiya reshenij. Inzhenernyj vestnik Dona, 2014.

[5] Business Process Model And Notation. Object Management Group (OMG), 2011.

[6] QReal:BP. QReal, 2013, url: http://qreal.ru/static.php?link=QRealBP.

[7] General Public License. Free Software Foundation, 2007.

[8] Apache 2.0. Apache Software Foundation, 2004.

[9] Kuzenkova A.S. Avtomatizirovannyj analiz povedeniya pol'zovatelya v QReal:Robots. 2014.

[10] Activiti-Designer. Activiti Team. url: https://github.com/Activiti/Activiti-Designer.

[11] Lovygin A.A., Teverovskij L.V. Osnovy chislovogo programmnogo upravleniya. Sovremennyj stanok s CHPU i CAD/CAM sistema, 2015.

Component-Based Software as a tool for developing complex distributed heterogeneous systems

Dmitry Kulikov
R&D Department
Rapid Telecom System Labs LLC.
Nizhny Novgorod, Russia
kulikov@ivc.nnov.ru

Vasilii Mokhin
R&D Department
Rapid Telecom System Labs LLC.
Nizhny Novgorod, Russia
mokhin@ivc.nnov.ru

Sergey Zolotov
R&D Department
Rapid Telecom System Labs LLC.
Nizhny Novgorod, Russia
sergey@ivc.nnov.ru

I. Introduction

Robotics is now one of the most sought-after and actual areas of applied sciences. More and more people are interested in this direction, thanks to which the software of robots does not stand still and evolves in huge steps, starting from the firmware of the device controllers and ending with the most complex software packages designed to solve a wide range of tasks. And, as in any software system, there can be many problems, for example, problems of architecture, development and debugging, etc. In this paper we will consider an example of the implementation of the project of automatic control system project with heterogeneous computing nodes the case of a complex hybrid, distributed computing system created on the basis of operating system based on the Linux kernel and the ROS framework [1].

II. Objective

The target of the project was to unite all the nodes of the created heterogeneous system, in which the computing nodes were used as part of a personal computer based on IBM PC x86, single-Board computers based on ARM processor (Raspberry PI3) and hardware-software based on the Atmega controller(Arduino) into a single computer network capable of receiving information in real time from various sensors, processing it in a given period of time and transmitting commands to other nodes.

III. Choosing a framework

First, it was necessary to choose a framework for heterogeneous system, because there are quite a large number of them and almost all are suitable for the task. Among all the options I chose the most common: ROS, MRDS, URBI, OROCOS, Gazebo, studied them and created a comparative table below, of the 11 most important criteria (see table I):

- open source;
- project examples;
- documentation;
- the activity of the community;
- license;
- application architecture;
- communication protocol;
- kernel;
- supported programming languages;
- supported OS;
- supported devices.

Based on the results of the studies given in the comparative table it was concluded that ROS is the best choice for the solution of the problem, because:

- it is open source;
- it has complete infrastructure;
- implemented a variety of ready-made solutions for a variety of sensors, controllers, etc;
- focused on complex tasks;
- it is possible to work in real time;
- support for a wide range of Executive computing devices.

IV. The concept of ROS

ROS is a framework for robot developing, provides functionality for distributed work and standard operating system services such as hardware abstraction, low-level device control, implementation of commonly used functions, communication between processes, and package management [2]. ROS based on a graph architecture where data is processed in nodes that can receive and transmit messages to each other. ROS supports parallel computing, has good integration with C++ and Python, can run on single-Board computers such as Raspberry Pi, BeagleBone, as well as microcontroller platforms running on the ATmega chip (such as Arduino).
The concept of ROS :

- node — is a process that performs calculations and is able to communicate with other nodes;
- message — is a type of ROS data by which nodes can communicate with each other;
- topic - is the name that is used to identify the content of the message;

TABLE I
ROSOBOTS FRAMEWORKS COMPARISON

	ROS	MRDS	URBI	OROCOS	GAZEBO
Opensource	+	-	+	+	+
Project examples	Exists an extensive and open knowledge base with ready-made projects	Exists many examples with MRDS projects	Exists many examples of working with URBO	Exists large set of ready-made libraries	Exists many pre-made components
Documentation	Well documented	Well documented	Well documented	Well documented	Well documented
Community	Active community	Inactive community	Inactive community	No community	Inactive community
License	BSD(free for research and commercial use)	Various(free for research)	BSD(Free use, except for the simulator, which is not in the URBI)	BSD((free for research and commercial use)	GNU General Public License(free for research)
Architecture	Graph architecture	Modular architecture	Client-Server	Not found	Distributed
Protocol	xmlrpc	HTTP, DSSP	Firmata	Not found	SDF
Kernel	ReactOS	KITL	Urbi SDK	Not found	Not found
Supported languages	Python, C++, Lisp and experimental libraries on Java and Lua	C#, Visual Basic .NET, JScript and IronPython	urbiscript	Not found	C, C++, Java, Tcl and Python
OS	Currently, ROS only works on Unix platforms	Works only on Windows OS	cross-platform	Not found	Linux, Mac OS X, Solaris and BSD
Supported devices	Atmega microcontroller, ARM family of processors, etc.	Atmega microcontroller, ARM family of processors, etc.	x86, ARM, MIPS, PowerPC, etc.	Not found	Atmega microcontroller, ARM family of processors, etc.

- master — is a ROS name service that allows nodes to discover each other, exchange messages, and call the necessary services;
- rosout — is a live message output;
- roscore — Master + Rosout + parameter Server.

The main concepts of ROS are nodes, messages, themes, services. Architecturally, all computing tasks are performed in ROS nodes that communicate with each other via messages. These message nodes are published to topics, which divide the messages into groups of interest indeed when a node needs to receive messages with specific data, that node subscribes to a specific topic. To implement synchronous message passing, which is necessary in certain cases, ROS defines services - a mechanism that operates on a question - answer basis.

V. PRACTICAL PART

Thanks to ROS, it was possible to link all the equipment into a single computer network with convenient debugging and rapid prototyping without any problems. Each of the microcontrollers was a separate node that received data, performed the necessary calculations, made a decision and could exchange data with other nodes at a specified frequency(see Fig.2.).

To process such a large amount of information for ROS-Master, a separate full-fledged computer(see Fig.1.), which guaranteed minimal delays in the exchange and processing of information between nodes [3]–[5]. ROS is very well documented, has an active community and a lot of ready-made examples to work with it, starting from examples of message transmission and ending with the basic projects of working with 3d SLAM, indeed it was not necessary to spend a huge amount of time searching for the necessary information, and if there were any errors during compilation, then in ROS community it was possible to find a solution to eliminate this error, which contributed to a significant acceleration of the development process.

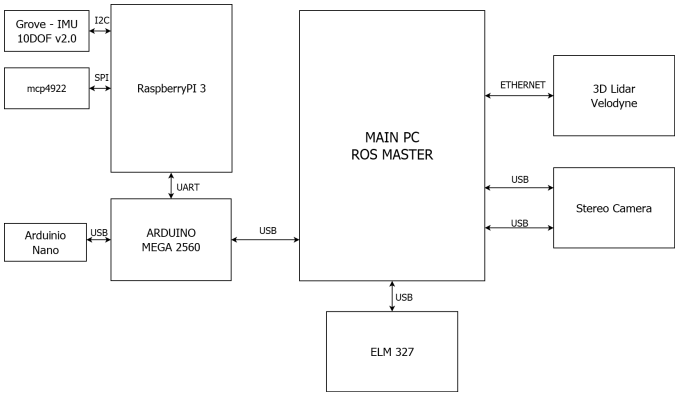

Fig. 1. Device layout.

VI. SAMPLE CODE FOR ROS

As an example of the implementation of heterogeneous nodes on the ROS framework, we present several examples of code written for different platforms (Arduino and Raspberry Pi 3). On Raspberry Pi3 nodes were written on Python, and on Arduino in C++.

A. Example code on Arduino(C++)

Using the rosserial_arduino package allows you to use ROS in conjunction with the Arduino IDE. rosserial uses a

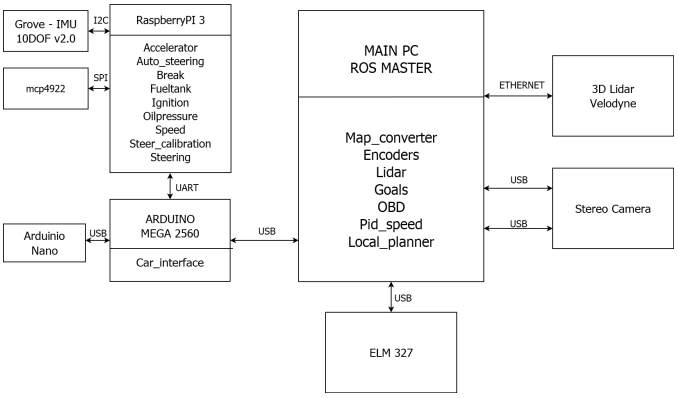

Fig. 2. Device layout with nodes.

data transfer Protocol that works through the Arduino UART (universal asynchronous transceiver). This allows Arduino to be a full ROS node that can publish and subscribe to ROS messages, publish TF (spatial) transformations, and receive ROS system time. Linking ROS to Arduino is implemented through the use of the Arduino library. To use the rosserial libraries in your code, first of all, you need to connect them:

```
#include <ros.h>
```

After we should specify the type of message:

```
#include<std_msgs/Int32.h>
std_msgs::Int32 i_msg;
```

Tell the master that we are going to be publishing a message of type std_msgs/Int32 on the topic chatter. This lets the master tell any nodes listening on chatter that we are going to publish data on that topic:

```
ros::Publisher chatter("chatter", &i_msg);
```

Subscribe to the pwm_signal topic with the master. ROS will call the msgCb() function whenever a new message arrives.

```
ros::Subscriber sub("pwm_signal",&msgCb);
```

NodeHandle::subscribe() returns a ros::Subscriber object, that you must hold on to until you want to unsubscribe. When the Subscriber object is destructed, it will automatically unsubscribe from the chatter topic:

```
nh.subscribe(sub);
```

NodeHandle::advertise() returns a ros::Publisher object, which serves two purposes: 1) it contains a publish() method that lets you publish messages onto the topic it was created with, and 2) when it goes out of scope, it will automatically unadvertised:

```
nh.advertise(chatter);
```

A ros::Rate object allows you to specify a frequency that you would like to loop at. It will keep track of how long it has been since the last call to Rate::sleep(), and sleep for the correct amount of time:

```
ros::Rate loop_rate(10);
```

Now we actually broadcast the message to anyone who is connected:

```
chatter.publish(&i_msg);
```

B. Example code on Raspberry Pi 3(Python)

You need to import rospy if you are writing a ROS Node, this is a pure Python client library for ROS. The rospy client API enables Python programmers to quickly interface with ROS Topics, Services, and Parameters. The std_msgs.msg import is so that we can reuse the std_msgs/Int32 message type (a simple string container) for publishing:

```
import rospy
from std_msgs.msg import Int32
```

After this, you must write a section of code defines the talker's interface to the rest of ROS. declares that your node is publishing to the chatter topic using the message type Int32. The queue_size argument limits the amount of queued messages indeed any subscriber is not receiving them fast enough. Rospy.init_node tells rospy the name of your node - as long as raspy does not have this information, it cannot start communicating with the ROS wizard:

```
pub = rospy.Publisher('chatter',Int32,
queue_size=10)
rospy.init_node('talker',anonymous=True)
```

This code declares that your node subscribes to the chatter topic which is of type std_msgs.msgs.Int32. When new messages are received, callback is invoked with the message as the first argument:

```
rospy.init_node('listener',anonymous=True)
rospy.Subscriber('chatter  ,Int32,callback)
```

In this example, the program operation is a call to the pub.publish(condition) that publishes Int32 in our chatter topic. The loop calls rate.sleep(), which sleeps to maintain the desired rate the loop:

```
while not rospy.is_shutdown():
    rospy.loginfo(condition)
    pub.publish(condition)
    rate.sleep(10)
```

rospy.loginfo (condition) allows you to:

- display messages on the screen
- automatically write messages to the host log file
- write messages to rosout

With using Rosout it is easier to debug because you can get messages using rqt_console, therefore, we may not to find and use the console window with the logs of your node [6].
Based on the above code examples, it becomes clear that using ROS with languages such as C++ and Python is quite easy, because after reading the documentation in detail and studying the ready-made solutions, you can easily make any of the platforms supported by ROS many nodes that will be combined into a single computer network.

VII. Conclusion

After analyzing all the currently available frameworks suitable for creating a distributed heterogeneous real-time network focused on complex tasks and supporting work with a wide range of computing devices, I came to the conclusion that ROS is the most suitable for use in solving the task set before me. ROS allows you to develop a flexible heterogeneous structure suitable for rapid prototyping, modeling and testing of various variants of real-time systems, which in turn accelerates the process of developing the final device.

At this stage, the project is completely ready, the system developed by me has been tested and confirmed its performance on an unmanned vehicle. The results obtained in the course of these studies formed the basis for the creation of an automated unmanned vehicle, and further refinement and expansion of its functionality will allow to achieve in the future more efficient use in various vehicles.

References

[1] Aaron Martinez, Enrique Fernndez. *Learning ROS for Robotics Programming*. Mumbai: Packt Publishing, 2013. ISBN 978-1-78216-144-8

[2] Jason M. OKane. *A Gentle Introduction to ROS*. Columbia: University of South Carolina, 2014. ISBN 978-14-92143-23-9

[3] Yukihiro Saito, Futoshi Sato, Takuya Azumi, Shinpei Kato, Nobuhiko Nishio . *ROSCH:Real-Time Scheduling Framework for ROS* . 2018 IEEE 24th International Conference on Embedded and Real-Time Computing Systems and Applications (RTCSA), 2018, pp. 52-58.

[4] H. Wei, Z. Huang, Q. Yu, M. Liu, Y. Guan, J. Tan. *RGMP-ROS: A real-time ROS architecture of hybrid RTOS and GPOS on multi-core processor*. 2014 IEEE International Conference on Robotics and Automation (ICRA), 2014, pp. 2482-2487.

[5] Y. Saito, T. Azumi, S. Kato, N. Nishio *Priority and Synchronization Support for ROS*. 2016 IEEE 4th International Conference on Cyber-Physical Systems Networks and Applications (CPSNA), 2016, pp. 77-82.

[6] H. Wei, Z. Shao, Z. Huang, R. Chen, Y. Guan, J. Tan, Z. Shao *RT-ROS: A real-time ROS architecture on multi-core processors*. Future Generation Computer Systems, 2016, vol.56, pp. 171-178.

An Exploration of Approaches to Instruction Pipeline Implementation for Cycle-Accurate Simulators of "Elbrus" Microprocessors

Pavel Poroshin
Department of Verification and Modelling
INEUM
Moscow, Russia
poroshin_p@mcst.ru

Alexey Meshkov
Department of Verification and Modelling
MCST, INEUM
Moscow, Russia
alex@mcst.ru

***Abstract*— Software simulation is of a big importance during development of processors as they provide access to hardware under development. Cycle-accurate simulators allow software engineers to design and optimize high-performance algorithms and programs with considerations of features and characteristics of processors being in development. One of the core aspects of a cycle-accurate simulator is the way it simulates the pipeline of the target processor. A pipeline model has high impact on an overall structure of a simulator and its potential performance and accuracy. In this paper several approaches to simulation of pipeline are described and theirs applicability to cycle-accurate simulators of "Elbrus" microprocessors are analyzed.**

Keywords*— simulation, pipeline, cycle-accurate simulator, microprocessor, Elbrus

I. Introduction

Software based simulation of hardware is a very important tool for development of computing systems. This tool is especially important for software design, as simulators can be used in place of actual still in development (or unavailable for other reasons) hardware. Also simulators can provide wide range of debugging facilities and other information about inner workings of a system being simulated.

One of the widely used classes of simulators is simulators of microprocessors. Different tasks have different needs, so there are simulators with various characteristics. Ones may be oriented at simulation performance; others are aimed at accuracy and precision.

Instruction set simulator (ISS) is a simulator of microprocessor that mostly models a program visible architecture state without considerations of microarchitecture specifics and timings. And while for many tasks this is enough, there is a need for simulators with much greater degree of accuracy which can be used for performance evaluation.

Cycle-accurate simulators (CAS) are such simulators. They are important tools for code efficiency estimation during development of performance critical software and optimizing compilers. Ability to debug performance of code is especially crucial for microprocessor architectures, which achieve high performance not by invisible to programmer microarchitectural features, but mainly by static planning of instruction execution by smart compiler. The "Elbrus" family of microprocessor architectures is such type of architectures.

Modern microprocessors achieve their high performance and clock frequency through use of pipelining. Every cycle-accurate simulator must somehow simulate this pipelining logic to achieve accuracy of its timings. The way a pipeline is represented in a simulator influences various aspects of a simulator, how its components interact and its overall design and characteristics. There are different ways to represent a pipeline and to model it.

In this paper we describe several approaches that were considered as a basis for implementation of the pipeline model during development of the cycle-accurate simulator of microprocessors belonging to the "Elbrus" family of instruction set architectures.

The remainder of this paper has following structure. Section II gives brief overview of the "Elbrus" instruction set architecture and describes an existing instruction set simulator used as base for the cycle-accurate simulator implementation. Section III formulates desired properties and requirements for the pipeline model being developed. Section IV describes in detail several considered approaches to pipeline model organization and explains its discovered advantages and drawbacks. Section V gives brief evaluation of described pipeline models. Section VI is dedicated to other approaches to pipeline simulation that can be found in literature. Section VII gives concluding remarks and briefly describes plans for further work.

II. Prerequisites

In this section we give some details of the architecture being simulated and of the available instruction set simulator that influence some design decisions around the pipeline model implementation.

A. "Elbrus" Family of Instruction Set Architectures

The "Elbrus" family of instruction set architectures is VLIW (Very Long Instruction Word) type of architectures [1]. Performance of this type of architectures is achieved by extracting ILP (Instruction Level Parallelism) through packing in one instruction several sub-operations, which are executed by hardware in parallel. "Elbrus" microprocessors are in-order and have no support of speculative execution (at least in the traditional sense).

In case of the "Elbrus", the packing format is not fixed and there are many ways several sub-operations can be packed in an instruction. Each of these sub-operations can belong to different kinds of operations: arithmetic and logical operations, control flow operations, predicate calculations, memory accesses and so on. And, while generally sub-operations observe only effects of previous instructions, there are several possible interactions of sub-operations

within one instruction, for example, in case of a predicated execution.

Another important consideration is the way pipeline stalls work. Firstly, it is worth noting, that in case one sub-operation stalls (for example, because its arguments is not ready yet), the whole instruction stalls, which is a natural result for a VLIW architecture. Secondly, which is more specific for the "Elbrus" architectures, there are a mechanism of prolonged stalls. In simple terms, in some cases (determined by a stall cause and a current pipeline stage) an instruction is not immediately stopped, but effectively after several cycles its results are discarded (as invalid) and it is returned several stages back for its repeated execution in hopes that the original stall will not occur again. This process affects not only the instruction that is not ready for execution, but also several instructions immediately after it. There are two types of such stalls: a 2-cycle one and a 4-cycle one. Moreover, it is possible for several such stalls to interleave, and for such situation there is special pipeline control logic.

Later in this paper we will refer to the pipeline stages of the "Elbrus" microprocessors by following names: F, D, B, R, E0, E1, E2 etc.

B. *Instruction Set Simulator*

Our cycle-accurate simulator was not developed completely from the ground up. An existing instruction set simulator for the "Elbrus" architecture was used as a basis and a starting point for the development of its cycle-accurate version.

This instruction set simulator supports wide range of the various "Elbrus" microprocessors of different architecture iterations via compile time configuration. It also supports both a user mode simulation (with emulation of system calls) and a full system simulation (with MMU logic, peripheral devices etc.). All of this is implemented in a shared code base.

An important feature of the instruction set simulator to consider is how it executes individual (wide) instructions. Execution is divided in two separate steps, conventionally called "read phase" and "write phase". The "read phase" prepares some intermediate data and is mostly side-effect free. Then the "write phase" uses this intermediate data to complete instruction execution. This way of organization of instruction execution greatly simplifies support of precise exceptions and of some interactions of sub-operations.

III. Requirements to CAS and Its Pipeline Model

There are multiple valid ways to implement a cycle-accurate simulator and its pipeline model, and each design have its trade-offs. So it is important to define scope and requirements to the cycle-accurate simulator being developed, including its pipeline model implementation. We define following requirements:

- Support of a user mode simulation. At this stage of development it is planned that the cycle-accurate simulator will be used mainly as a tool for debugging performance problems during software and compiler development. For such purposes a user model simulation are used.
- Code reuse with the instruction set simulator. The existing instruction set simulator implements major parts of the "Elbrus" microprocessors, and it would be wasteful to reimplement this functionality separately.
- Configurability. It should be possible to configure the simulator to support the various "Elbrus" microprocessors (like the instruction set simulator) and to enable or disable its different components (for example, for the sake of performance).
- Flexibility. It should be reasonable easy to support new features of next iterations of the "Elbrus" microprocessors. And also, when need arises, it should be possible to adapt the pipeline model for a full system simulation mode.
- Reasonable performance. The cycle-accurate simulator should not be too slow compared to the instruction set simulator. We aim at no more than tenfold slowdown.
- Reasonable accuracy. Of course, exact timing accuracy is not achievable. But the pipeline model design should not prevent possibility of further accuracy improvement and support of various microarchitectural aspects.

Some of these requirements are conflicting, and we do not expect to simultaneously meet all of them fully, but to achieve some balance between them.

IV. Pipeline Simulation of "Elbrus" Microprocessors

In this section we explore several approaches to the pipeline simulation and describe theirs advantages and disadvantages.

A. *Naïve "Direct Correspondence" Pipeline Model*

The first approach that we tried to implement was based on the simple idea of direct and faithful representation of the real pipeline stages in the simulator. These stages would be responsible both for the timing related logic and for the purely algorithmic logic of the corresponding instruction.

We implemented this approach by transforming the "read" and "write" phases of the instruction set simulator into functions representing pipeline stages. During this transformation the "read" and "write" phases were split in parts and the missing pipeline related logic was added to them. To meet the requirement of code reuse, we made code of the new cycle-accurate simulator as base, and implemented the original instruction set simulator by "glueing" stages together into the "read" and "write" phases and removing the pipeline related logic, all of this at compile time and through configuration.

Processing of such pipeline model is straightforward:

- Iterate through each pipeline stage.
- For each stage determine which instruction is at this stage and execute functions corresponding to all of the sub-operations of this instruction.
- If there are no stalls - advance instruction to the next stage. Otherwise not advance and propagate stall as necessary. In case of the prolonged stalls simulate related pipeline control logic.

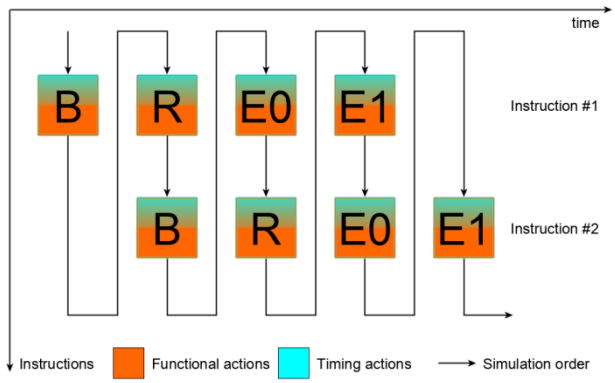

Fig. 1. Simplified illustration of pipeline stage processing in case naïve "direct correspondence" pipeline model.

This pipeline model representation should facilitate direct and straightforward support of the various microarchitectural features, as this software model is close to the actual hardware. But, although this idea is conceptually simple, during its implementation we discovered its several major drawbacks:

- Splitting of phases of the instruction set simulator into stages and glueing them back together introduce a major disturbance to the original instruction set simulator functionality. There is no clear way to avoid that. Attempts to fully restore original phases introduce much ad hoc logic, which adds fragility to the whole system. This means there is no easy way to achieve code reuse with this approach.
- In the instruction set simulator there are many unobvious interactions between phases of different sub-operations. These interactions are not easily preserved during splitting of phases.
- While for the most of the operations there is a clear correspondence of phases to pipeline stages, there are exceptions, which add complexity to the glueing process.
- Keeping track of all pipeline stages adds considerable performance overhead, although for most operations only small subset of all pipeline stages are nontrivial (at least in the context of timings).
- Splitting phases into multiple pipeline stage related functions also inhibits compiler optimizations, which impact overall simulator performance.

After this implementation attempt it became clear that for meeting our code reuse requirement we should minimize changes to the instruction set simulator.

B. Smart "Direct Correspondence" Pipeline Model

Next considered approach is a modification of previous one. Its improvements are based on the following key observations:

1. Algorithmic behavior of an operation (which is defined by an instruction set architecture and is considered by an instruction set simulator) can influence only an algorithmic behavior of operations of later (or in some cases current) instructions.

2. Algorithmic behavior of an operation determines its timing behavior.

3. Algorithmic behavior of one operation does not directly influence timing behavior of other operation.

4. Timing behavior has no direct influence on an algorithmic behavior (except in some limited number of special cases).

5. Timing behavior of one operation can influence timing behavior of other operation (but usually only in specific ways).

6. Simulator has more information about the execution process than hardware it simulates.

7. Not all details and inner workings of hardware contribute to its timing characteristics.

First six of these observations let us justify the separation of algorithmic and timing logic and moving of the algorithmic logic to the beginning of the instruction processing (right before its pipeline related processing). But we should uphold following conditions:

- Algorithmic simulation of the instruction must occur before the algorithmic simulation of the next (in program order) instruction (based on the observation 1).
- Pipeline simulation of the instruction must occur after its algorithmic simulation (based on the observation 2).
- Pipeline simulation of different instructions must occur in order determined by the pipeline state (based on the observation 5).

All of these are satisfied by this approach.

Last observation let us simplify the timing logic by removing all microarchitectural details that are not directly necessary for correctly calculating timing information, as we are interested not in inner workings of hardware, but in timing details.

These transformations should not reduce accuracy of our simulator (except in some rare special cases, which are briefly considered later in this paper).

The algorithm to process such pipeline is very similar to the previous approach. The only difference is that in the beginning of the processing of the first pipeline stage of the instruction we do all algorithmic simulation of this instruction.

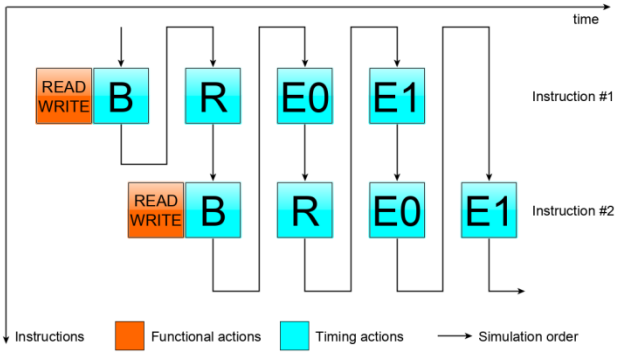

Fig. 2. Simplified illustration of pipeline stage processing in case smart "direct correspondence" pipeline model.

This approach let us use functionality of the instruction set simulator (for the algorithmic simulation of instructions) with minimal modifications, which remedy many major drawbacks of the previous approach. But we still have to address the performance concerns, as in this approach the simulator still keeps track of all pipeline stages, even if they are trivial, and the timing logic is still split into multiple independent functions.

C. *"Fully Speculative" Pipeline Model*

The next approach to the pipeline simulation is based on the assumption of stronger the observation 5:

5*. Timing behavior of operation of one instruction can influence timing behavior only of operations of the same or next instructions.

With this modified observation first five observations can be summarized as follows:

- Behavior (algorithmic and timing) of an operation of an instruction cannot depend on the behavior (algorithmic or timing) of operations of next instructions.

This assumption let us simulate all of the instruction's behavior in one go before even considering next instructions. It is just necessary to remember all effects (algorithmic and timing) of the instruction that can influence next instructions. And this is what we do in this approach.

The simulation of pipeline in this approach is as follows:

- Simulate algorithmic behavior of the instruction using the instruction set simulator functionality.
- "Speculatively" simulate timing behavior of the instruction by processing each of its nontrivial stages one by one from first to last, remembering in the process all information about produced effects and their moments in time for use by next instructions (at the same time using such information from previous instructions).
- Move to the next instruction.

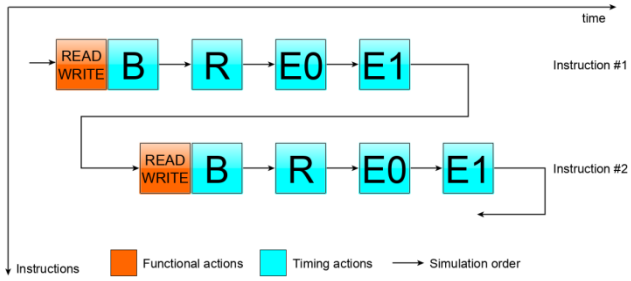

Fig. 3. Simplified illustration of pipeline stage processing in case "fully speculative" pipeline model.

Such pipeline organization is expected to be more performant, as it has less overhead related to keeping track of the individual pipeline stages, better processes trivial stages, and in general has more optimization opportunities.

At the same time, with this approach it is necessary to transform the pipeline representation in the new form that supports "speculative" accumulating of effects. This was possible in our case, but may be difficult to achieve in others.

Also, such pipeline model is more complicated and unintuitive. For example, it has no reasonable notion of the current moment in (simulation) time. Time becomes in some sense distributed around the whole pipeline model.

Pipeline is not sole contributor to timing behavior, and it must interact with other components of microprocessor, such as L1 and L2 caches, IB (Instruction Buffer, the component responsible for the fetch of instructions) and others. It may be unfeasible to simulate these components in such "speculative" fashion, and the only reasonable way is the cycle-by-cycle type of simulation. And without a clear "current moment" concept, it is not obvious, when such cycle-by-cycle simulation must occur.

Let's consider L1 cache as a concrete example. Its cycle-by-cycle simulation must occur after all its inputs are available but before its results can influence simulation of the other components (including the pipeline). After careful study of possible interactions of the L1 cache model and the pipeline model we identified that such cycle-by-cycle simulation should occur right after the simulation of the stage R of the instruction. By similar reasoning the cycle-by-cycle simulation of the IB should be placed right after the simulating of the stage F of the instruction. Additional considerations must be made in case of stalls, but overall idea is the same.

Now let's consider interactions between the IB and the L1 cache. In principle, it is possible to the IB request of the future instruction to interfere with the L1 cache state observed by the current instruction. So it is possible to the timing behavior of the future instruction to influence the timing behavior of the current instruction, which is a violation of our earlier assumption. It means that in this approach we cannot accurately simulate some interactions between various microprocessor components.

Another example of violation of our assumption is the complex interactions during the interleaving of prolonged stalls, where stall of the next instruction can influence stall latency of the current instruction.

Overall, while this approach promises performance improvement, it sacrifices accuracy and flexibility and introduces additional complexity.

D. *"Hybrid" Pipeline Model*

The last approach to the pipeline simulation considered in this paper is a combination of second and third approaches. This pipeline model tries to retain accuracy of the smart "direct correspondence" model and to achieve some of the performance benefits of the "fully speculative" model. It is based on the two additional observations:

8. Pipeline behavior of an instruction interacts with pipeline behaviors of other instructions and other components at specific pipeline stages.

9. There are continuous sequences of stages that executed uninterrupted (without stalls and influence from other instructions and components).

For example, after the stage E2 there is no possibility of any stall and all further timing behavior of the instruction is predetermined. So it is possible to simulate such continuous uninterrupted sequences of stages speculatively in a manner similar to the "fully speculative" approach, but without the risk of decreasing timing accuracy. And after the instruction

reached the pipeline stage E3, we can stop keeping track of it, as its timing behavior is completely simulated (partly normally and partly speculatively) at this point. This significantly decreases the pipeline simulation performance overhead and the overhead of dealing with trivial stages.

Processing of such pipeline model is very similar to the smart "direct correspondence" approach:

- Iterate through each pipeline stage.
- For each stage determine which instruction is at this stage.
- If it is a new instruction, then simulate its algorithmic behavior.
- If it is the first stage of an uninterrupted sequence, then speculatively simulate all stages of this sequence.
- If there are no stalls, then advance the instruction to the next stage. Otherwise not advance and propagate stall as necessary. In case of prolonged stalls simulate related pipeline control logic.

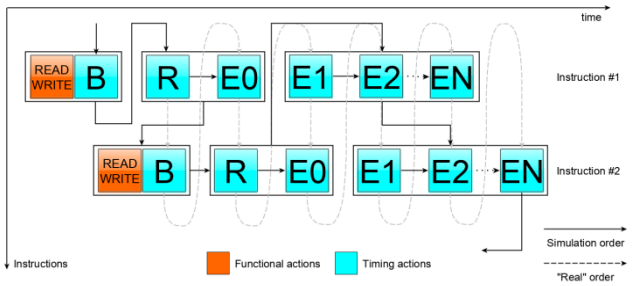

Fig. 4. Simplified illustration of pipeline stage processing in case “hybrid” pipeline model.

Overall, this approach let us partially get performance gain of the "fully speculative" approach without its major drawbacks of sacrificing accuracy.

Unfortunately, all described approaches (except the naive one) do not cover the special case of the timing behavior influencing the algorithmic behavior. Example of such situation is operations that generate a predicate based on readiness of its arguments. Researching of ways to address this is part of our future work, and we hope it will be possible to implement a solution within the "hybrid" approach.

V. Evaluation

Although the cycle-accurate simulator is still in development and there is work to be done (for example, memory subsystems are not fully implemented yet and are greatly simplified), it is worth to do some preliminary evaluation of the pipeline model implementations described in this report.

Here we will consider only the "fully speculative" and the "hybrid" models, as the "direct correspondence" models were abandoned much earlier in the development and it is hard to make a fair comparison of them to the other models.

We compare the relative performance and the total number of the simulation cycles that were needed for the test completion. The instruction set simulator is used as a baseline. Individual test cases consist of the executing on the simulator part of one of the SPEC CPU95 benchmarks. Results presented in Table 1.

At this stage of the development we do not have a reasonable cycle count reference that we can use, because, for example, our simulators do not do proper simulation of various memory accesses. Nevertheless, we hope to get rough estimate of contribution of the more detailed simulation of the pipeline by the “hybrid” model to the total cycle count.

Results show that on average the "hybrid" model is slower than the "fully speculative" model by ~20%. At the same time, average difference in total cycle count is around 0.5% with one significant outlier “146.wave5” with the cycle count difference of 6.1%. We expect that this is because less accurate simulation of the prolonged stalls in the "fully speculative" pipeline model.

It is possible to optimize both models and the performance difference after optimizations can change, but we expect that the "hybrid" model will always be slower. Despite this overall we consider the "hybrid" model as a better approach as it is more fully meets our requirements of accuracy and flexibility, and in a need of performance it should be possible to configure the "hybrid" model accordingly.

TABLE I. Performance and total cycle count relative to instruction set simulator

Test	"Hybrid" CAS		"Fully speculative" CAS	
	Relative Performance	*Relative cycle count*	*Relative Performance*	*Relative cycle count*
099.go	0,192	1,747	0,218	1,747
101.tomcatv	0,271	1,415	0,323	1,424
102.swim	0,329	1,983	0,407	1,981
103.su2cor	0,277	1,415	0,322	1,420
110.applu	0,218	1,999	0,266	2,001
124.m88ksim	0,243	1,151	0,299	1,151
126.gcc	0,291	1,376	0,341	1,378
129.compress	0,222	1,522	0,286	1,539
130.li	0,195	2,102	0,224	2,104
132.ijpeg	0,218	1,738	0,261	1,749
134.perl	0,252	1,541	0,301	1,553
141.apsi	0,248	2,364	0,286	2,379
146.wave5	0,328	1,734	0,398	1,840
147.vortex	0,250	1,600	0,308	1,601

VI. Related Work

Cycle-accurate simulation of modern microprocessors is a very active area of research. But only small portion of this research is focused on simulating of general purpose VLIW microprocessors, let alone on the "Elbrus" architecture. And many of the available approaches do not quite translate to the "Elbrus" specifics.

Approaches of simulating a pipeline of VLIW microprocessors, similar to the "direct correspondence" approaches, are described in [2][3][4]. But they do not

address the issue of code reuse in the presence of an instruction set simulator.

All of the approaches described in this paper are execution-driven. Trace-driven simulation is one of the alternatives [5][6][7][8][9]. The basic idea of the trace-driven approach is a separation of the whole simulation process in two phases: generation of some data (trace), that represents an execution path, and using that data as an input for a cycle-accurate simulation of some microprocessor aspect. Trace can be generated by real hardware or other simulator (for example, an instruction set simulator). This approach gives benefits, similar to ones we aim to achieve by separation of algorithmic logic and timing logic introduced in our second approach, but makes extremely difficult to account for a possible dependence of an algorithmic behavior on a timing behavior (which we are planning to address in future work in our approach), as these interactions cannot be captured in trace during its generation before cycle-accurate simulation.

The pipeline representation, similar to our "fully speculative" approach, is used in [10]. Authors describe in details various aspects of the pipeline simulation (occupancy of stages, operand dependencies and control flow considerations), but do not discuss limits of this approach and complexities of interaction of such pipeline model with other components of microprocessor.

VII. Conclusions and Future Work

Software based simulation of microprocessors is a very important tool. There are many possible ways to implement such simulators, each of them with its own set of advantages and disadvantages.

In this paper we explored several approaches to the pipeline simulation in the context of the cycle-accurate simulation of the "Elbrus" microprocessors. We made several simple, but general and powerful observations, which were used as the foundation for the design of the various pipeline models and for the analysis of their advantages and drawbacks. We described several of such approaches that were considered and at least partially implemented during development of our cycle-accurate simulator.

The cycle-accurate simulator described in this paper is still in active development. In the future work we are planning to address the issue of dependence of the algorithmic behavior of the instruction on the timing behavior and to explore additional ways to optimize performance of the simulation.

References

[1] Ermakov S. G., Kim A. K., Perekatov V. I. Mikroprocessory i vychislitel'nye kompleksy semejstva "Elbrus" [Микропроцессоры и вычислительные комплексы семейства "Эльбрус"], 2012 (in Russian).

[2] Cuppu, Vinodh. "Cycle accurate simulator for TMS320C62x, 8 way VLIW DSP processor." University of Maryland, College Park (1999).

[3] Barbieri I. et al. Flexibility, Speed and Accuracy in VLIW Architectures Simulation and Modeling //Simulation. – Т. 10. – №. 11. – С. 12.

[4] Barbieri I., Bariani M., Raggio M. A VLIW architecture simulator innovative approach for HW-SW co-design //2000 IEEE International Conference on Multimedia and Expo. ICME2000. Proceedings. Latest Advances in the Fast Changing World of Multimedia (Cat. No. 00TH8532). – IEEE, 2000. – Т. 3. – С. 1375-1378

[5] Uhlig R. A., Mudge T. N. Trace-driven memory simulation: A survey //ACM Computing Surveys (CSUR). – 1997. – Т. 29. – №. 2. – С. 128-170.

[6] Joshua J. Y. et al. The future of simulation: A field of dreams //Computer. – 2006. – Т. 39. – №. 11. – С. 22-29.

[7] Agarwal A., Huffman M. Blocking: Exploiting spatial locality for trace compaction. – ACM, 1990. – Т. 18. – №. 1. – С. 48-57.

[8] Cho S. et al. TPTS: A novel framework for very fast manycore processor architecture simulation //2008 37th International Conference on Parallel Processing. – IEEE, 2008. – С. 446-453.

[9] Lee H. et al. Two‐phase trace‐driven simulation (TPTS): a fast multicore processor architecture simulation approach //Software: Practice and Experience. ‐ 2010. ‐ Т. 40. ‐ №. 3. ‐ С. 239-258.

[10] Böhm I., Franke B., Topham N. Cycle-accurate performance modelling in an ultra-fast just-in-time dynamic binary translation instruction set simulator //2010 International Conference on Embedded Computer Systems: Architectures, Modeling and Simulation. – IEEE, 2010. – С. 1-10.

Approach to test program development for multilevel verification

Pavel Frolov
JSC MCST, PJSC INEUM
Moscow, Russia
Email: Pavel.V.Frolov@mcst.ru

***Abstract*—Development of system-on-chips or network-on-chips requires verification of standalone units (peripherals and commutators) and a system as a whole. An approach to test development for verification of programmable standalone units is presented. The tests are written in C++ using a specific API to program the device-under-test (DUT) and the test environment. The implementation of access to a DUT depends on the test environment structure: a standalone device, a device as a part of controllers block or a device as a part of the whole SoC. This approach gives an opportunity to use the same test both for standalone and for system-level verification (when the test is compiled as a program for execution on SoC general-purpose core). The implementation of this approach and its application to verification of microprocessors of the Elbrus family are described.**

***Index Terms*—hardware verification, simulation-based verification, test system, standalone verification, system-level verification**

I. Introduction

Typical test scenarios for programmable standalone units (peripherals and commutators) are based on estimated work patterns of the designed chip operating. Such test scenarios are an indispensable part of a standalone verification testplan. They also must be included in a device integration test suite for system-level verification to check considered device interaction with other units.

This paper describes an approach to test development for verification of programmable standalone units which allows using the same test both for standalone and system-level verification. The presented approach also enables tests run in different *execution environments* (via an RTL simulator, an FPGA-based prototype or a manufactured chip).

The rest of paper is organized as follows. Section 2 reviews the existing techniques considering the same tests reuse for different execution environments. Section 3 introduces the structure of the framework for test development, implementing presented approach. Section 4 describes API provided by the framework for tests use. Sections 5 and 6 present test transformation for system-level and standalone verification respectively. In Section 7, results are presented and in Section 8, possible/planned future work is mentioned.

II. Related work

The main target of presented approach is to reduce verification effort through the unit-level test reuse for system-level simulation.

Review works on SoC verification suppose high level of the verification components reuse [1] [2], but there is not much information about practical approaches for the test programs reuse. The problem of the stimulus reuse for different execution targets and environments is targeted by The Portable Test and Stimulus Standard (PSS) [3], but this standard provides only language for a test intent description [4].

Typical approach to unit-level verification is transaction-based verification, implemented, for example, in UVM (Universal Verification Methodoly) standard [5]. Such tests are written in SystemVerilog and commonly use constraint-random stimuli generation, implemented via external tools (RTL-simulator, for example). The reuse of such a test for system-level verification requires its additional adaptation. For example, the work [6] describes an approach which allows to get a system-level test based on the unit-level one for the separate IP-block (GPU) of the heterogeneous SoC. A trace of DUT interactions with the testbench is logged during unit-level simulation and then is compiled into assembly, ready for execution on the CPU at SoC level. The approach copes with register polling through the test driver library instumentation but DUT interrupts handling isn't described.

III. Test development framework

In the presented approach, a test is written in C++, so it can be translated to different host CPU architectures:

- to PLI-application [7] (PLI is for Program Language Interface) interacting with a simulator modeling the RTL description of the standalone unit (or the block of controllers including this unit);
- for system-level execution on one of the general-purpose cores of the verified SoC.

The system-level test runs without an operating system and this restricts usage of standard C++/C library: no explicit usage of externally linked functions is allowed. Instead, the test development framework provides a common standard API for different test execution environments. The API is described in header files as a list of C++ function prototypes. For every supported test execution environment the framework provides a corresponding *environment library* implementing these functions.

Advantages of C++ as a test implementation language mainly address system-level test execution. Firstly, C++ allows to transfer some calculations to the compilation stage via

`contexpr` specifier (since C++11 [8] version of language standard). Secondly, C++-templates allow wrap of specific assembly instructions into `inline` functions to avoid function call overhead while preserving test portability. Besides, parts of device drivers or BIOS, commonly written in C, can be relatively simply ported for test use and vice-versa.

IV. Environment library API

A typical programmable controller implements three kinds of interaction with a system: it provides access to the internal registers and memory for configuration (PIO, programmed input/output), can initiate DMA-transactions (Direct Memory Access) to the system memory and send interrupt messages. Thus the environment library API must provide means to perform, control and observe these interactions.

The API contains a description of typical operations:

- access to the registers and the internal memory of the device under test,
- system memory handling operations (allocation, pattern filling, data comparison),
- device interrupts handling,
- address translation for DMA-transactions programming,
- simulated time measuring and timeout setup,
- debug test output,
- other auxiliary procedures.

V. System-level verification

For system-level verification the test program is translated for execution on a general-purpose core of the verified SoC as well as the standard environment library. The framework also provides a bootstrap program for basic system initialization required for the test to run. The test and the library are linked into a single executable image (the system-level test). To run the test the execution environment places this image in the memory of the SoC (DRAM and/or NVRAM) and transfers control to the entry point of the environment library, which in turn calls the test function. After the test execution the environment library handles the exit code and provides diagnostic information.

The framework allows executing the same unit test with different system settings, providing comprehensive unit integration check. System settings programming is performed by the bootstrap part of the environment library; their values are described in additional files and are transmitted to the system-level test either via compilation macro definitions or as object files with initialized C-structures during linkage.

Examples of system settings to vary range from separate bits in different control registers of the verified SoC to modes which require additional nontrivial setup. For example, DMA-transactions from the tested device can work directly with system physical addresses or can be additionally redirected via IOMMU (Input/Output Memory Management Unit).

The environment library implements API with functions executed in super-user mode. Read/write access to the device registers is implemented with load/store instructions with specific attributes (memory type specifiers). In microprocessors of the Elbrus family registers of external programmable devices are placed within PCI-address spaces: memory, I/O and PCI-configuration space. The test defines a target device address in a PCI-configuration space and allocates necessary address ranges in PCI I/O or memory spaces via according API functions.

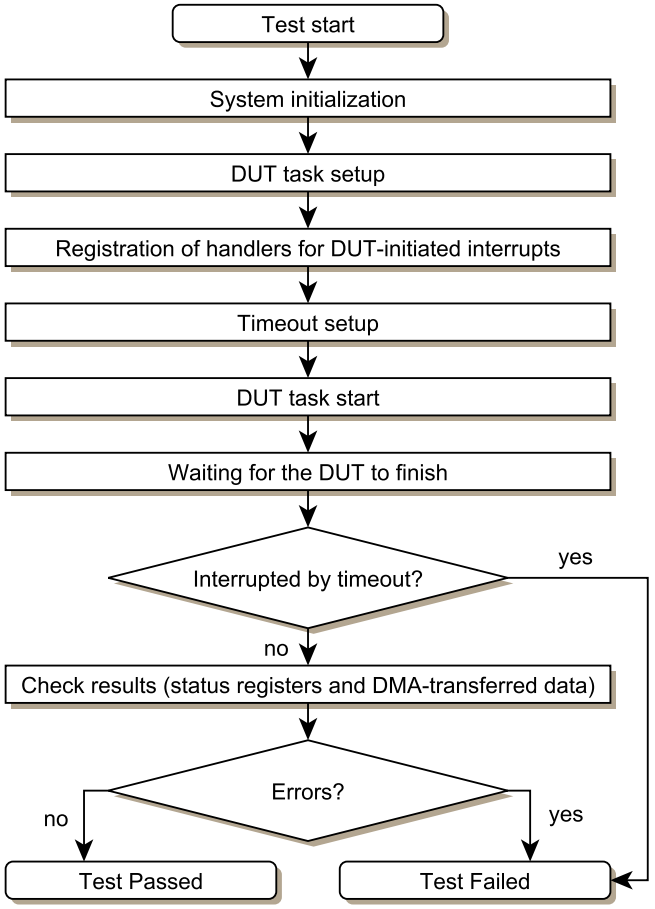

Fig. 1. Typical test algorithm

The environment library provides simple heap manager without deallocation implementation. The test program allocates data arrays in the heap for use as RAM regions accessed from the tested device by DMA-transactions.

Virtual addresses for DMA-transactions are written to the device registers and/or to descriptor tables in RAM. In the simplest case the virtual address is equal to the physical address: so-called transparent translation, but DMA-transactions from the tested device can be redirected via IOMMU, so the environment library provides functions for IOMMU configuration and in-test address translation functions. The test uses that functions for getting virtual addresses from physical ones, which are returned from the heap allocation-function.

The environment library implements functions for the system interrupt controller configuration and test-defined interrupt handling. The test configures interrupts to be sent by the tested

unit and registers callback functions handling those interrupts. During the test execution the environment library catches interrupts from the device and calls registered handlers.

Simulated time measuring is implemented via reading of the clock-counting register or programming local timer to send interrupts in defined time intervals.

The system-level test can be compiled for different execution environments: a functional model, a simulated RTL-description of the tested SoC, an FPGA-based emulator or a manufactured chip. The target execution environment determines the bootstrap procedure and the debug print support linked to the test.

The functional model allows fast execution with high observability (instruction execution trace, units programming trace), so it is used for the test and the environment library debug.

VI. Unit-level verification

The structure of the unit-level testbench is presented on Fig. 2. The testbench consists of the environment library and the test linked to the testbench as PLI-application, adaptor for the DUT-system bus interface and, possibly, a specific imitator of an external device.

The interface of the device-under-test which connects it to the rest of the SoC requires appropriate adapter for interaction with the testbench. It provides an interface-specific implementation for DUT registers access operations and redirects DUT-initiated transactions to the environment library.

There are two separate address spaces in the test: ”internal” for direct access from the test and ”external” for DMA-transactions. Memory manager returns to the test pointers with ”internal” addresses for memory allocation requests and all library functions for on-core memory processing work with ”internal” addresses.

Addresses to be targeted by DMA-transactions are wrapped by translation functions that convert internal pointers to external ones and record this translation. DMA-requests are transferred by the adaptor to the memory manager that checks DMA destination addresses against previously recorded translations. If there is an appropriate record of translation, the memory manager writes data from DMA-transactions or reads it for return to the adaptor. Otherwise an error is detected.

Interrupt messages issued by the device are registered within the environment library; when the test calls library functions, pending interrupts are handled and a user-defined callback is executed.

Simulated time measuring is implemented by means of functions DPI-exported from the part of the library written in SystemVerilog.

Different devices with one programming interface can be tested by the same test program even if they have different bus interfaces; different bus interfaces require different adaptors to be implemented. The tested controller can be connected to the adaptor not directly, but through the root commutator of the block of controllers including the unit in consideration (Figure 3). That variant of the DUT allows verification of

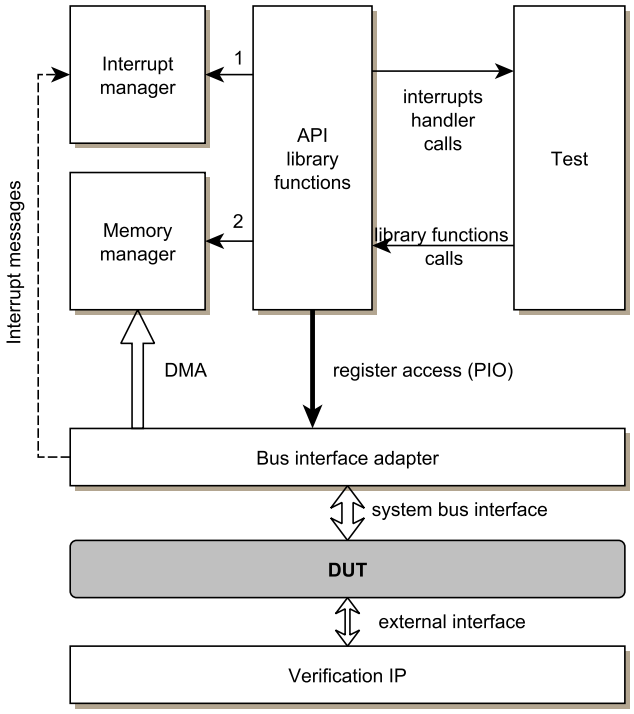

Fig. 2. Unit-level verification testbench. 1 – pending interrupts check. 2 – internal/external address translation.

interaction between system commutator and the tested controller (intermediate-level verification). Test scenarios with simultaneous work of several controllers can be implemented.

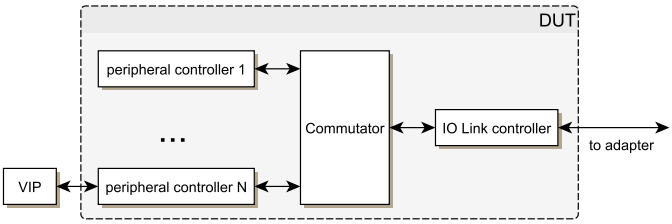

Fig. 3. DUT for intermediate-level verification

VII. Results and use experience

The described approach to test development has been applied to the verification of peripheral interfaces controllers of standalone southbridge ASICs developed in MCST [9], such as HD Audio, SATA, USB 2.0, PCI and PCI-e bridges, and multiple low-speed controllers. Now it is used for verification of embedded IOHubs being developed for a new generation of the Elbrus microprocessors. Standalone and embedded southbridges have different in-house interfaces to transfer packets based on PCI Express transaction layer packets [10], therefore different adaptors have been implemented in order to reuse the same set of tests.

MCST designs computing systems based on CPU of Elbrus and SPARC instruction set architectures, thus the environment library for system-level tests is implemented for both architectures and for different microprocessor models (starting from Elbrus-4C [13] for Elbrus-based microprocessors and R-1000 [14] for SPARC-based ones).

The typical test development and use flow consists of the following subsequent stages:

- system-level build for functional model execution and test logic debug;
- unit-level build for standalone unit verification;
- unit-level build for verification of the unit as a part of the southbridge;
- system-level build for test execution on full system-on-chip (RTL or FPGA-based prototype [11]).

The system-level environment library supports simultaneous execution of several tests for different controllers on multi-core systems. Tests are executed on different cores; shared resources are distributed between tests based on static planning [12].

VIII. Future work

The described approach for unit-level verification was implemented mainly for southbridge controllers of MCST projects. The future work is supposed to embrace adaptation of system-level tests for north-bridge integrated graphics cores to unit-level verification. It requires further development of internal system bus interface adapters for different target CPU models.

There is also an endeavor to use already developed system-level tests for verification of hardware I/O virtualization support in new microprocessors of Elbrus family. The test program is supposed to run as a simple guest OS while the environment library functions are executed in hypervisor mode. Different modes of virtual I/O support are to be implemented: emulation mode and direct device assignment.

References

[1] Anil Deshpande. Verification of IP-Core Based SoCs. 9th International Symposium on Quality Electronic Design, 2008, pp.433436. DOI: 10.1109/ISQED.2008.4479771

[2] G. Mosensoson. Practical approaches to SoC verification. Proceedings of DATE User Forum. 2002.

[3] The Portable Test and Stimulus Standard. https://www.accellera.org/downloads/standards/portable-stimulus [Accessed: 11-May-2019].

[4] Bryon Moyer. Portable Stimulus Intent. Accelleras New Standard Goes to Early Adopters. EEJournal, July 31, 2017. Available: https://www.eejournal.com/article/portable-stimulus-intent [Accessed: 11-May-2019].

[5] Standard Universal Verification Methodology. http://accellera.org/downloads/standards/uvm [Accessed: 11-May-2019].

[6] Narendra Kamat. IP Testing for Heterogeneous SOCs. 14th International Workshop on Microprocessor Test and Verification, 2013, pp. 5861. DOI: 10.1109/MTV.2013.19

[7] IEEE Standard for SystemVerilog. IEEE Std 1800-2009.

[8] ISO International Standard ISO/IEC 14882:2011(E) Programming Language C++.

[9] A.K. Kim, M.S.Mikhailov, V.M.Feldman. Podsistema vvoda-vyvoda dlya sistem na kristalle MCST-4R i Elbrus-S na osnove mikroskhemy kontrollera periferiinykh interfeisov. Voprosy radioelektroniki, seriya EVT, vypusk 3, 2012.

[10] Petrochenkov M. V., Mushtakov R. E., Stotland I. A. Verification of 10 Gigabit Ethernet controllers. Trudy ISP RAN/Proc. ISP RAS, vol. 29, issue 4, 2017, pp. 257-268. DOI: 10.15514/ISPRAS-2017-29(4)-17

[11] F. Budylin, I. Polishyk, M. Slesarev, S. Yurlin. The experience of prototyping MCST CJSC microprocessors. Voprosy radioelektroniki, 2012, no. 3.

[12] Frolov P.V. System-level test integration based on static resource allocation. Voprosy radioelektroniki, 2018, no. 2, pp. 7680.

[13] 'Centralnyj processor Elbrus-4C'. [Online]. Available: http://www.mcst.ru/elbrus-4c [Accessed: 11-May-2019].

[14] 'Centralnyj processor Elbrus-R1000'. [Online]. Available: http://www.mcst.ru/r1000 [Accessed: 11-May-2019].

Test environment for verification of multi-processor memory subsystem unit

Dmitriy Lebedev
Department of Verification and Modeling
MCST
Moscow, Russia
lebedev_d@mcst.ru

Mikhail Petrochenkov
Department of Verification and Modeling
MCST
Moscow, Russia
petroch_m@mcst.ru

***Abstract* — Ensuring the correct functioning of the memory subsystem is one of the cornerstones of modern microprocessor systems. Functional verification is used for this purpose. In this paper, we present some approaches for verification of memory subsystem units of multi-core microprocessors. Some characteristics of memory subsystems that need to be taken into account in the process of verification are described. General scheme of test environment for stand-alone verification of memory subsystem parts is presented. Classification of checking models types and their advantages and disadvantages are described. The approach of construction a standalone verification environment using Universal Verification Methodology (UVM) is presented in the paper. Some restrictions that should be taken into account when verifying memory subsystem unit are listed. Generation stimulus algorithm stages are presented. Method of using "hints" from design under verification for elimination of nondeterminism is used for implementation of checking module. Some other techniques for checking the correctness of memory subsystem units, which can be useful at different stages of projects, also reviewed. An experience of applying the suggested approaches for verification of Home Memory Unit of microprocessors with Elbrus architecture is considered. The results and further plan of the test system enhancement are presented.**

Keywords — multicore microprocessors, cache memory, coherence protocols, test system, model-based verification, stand-alone verification.

I. INTRODUCTION

With the development of microprocessor technology and growth of the number of computational cores and CPUs in systems processor performance increases rapidly. Unfortunately, the speed of memory access is not growing as fast as the speed of the processor [1]. Thus, one of the biggest bottleneck elements become the memory subsystem. To level the difference in speed, designers of microprocessor systems implement a complex memory subsystem that includes cache hierarchy. State of the art microprocessor systems usually include 3-4 levels of cache memory. This approach is able to reduce the number of accesses to main memory, and, therefore, reduce memory access instructions average execution time.

In the multicore systems if multiple cores are simultaneously allowed to contain copies of a single memory location, the problem of maintaining memory consistency arises. A mechanism must exist to ensure that all copies remain consistent when the contents of that memory location are modified. Coherence protocols support such mechanism. Usually we have higher-level caches shared between cores and lower-level caches served by a single core. Complex systems that combine several multi-core processors may also have cache memory to speed up other processors' access to their memory.

A large number of processors and processor cores and complexity of system data exchange organization makes coherence protocol very complicated. An implementation of cache coherence protocol is a complex and error-prone task. Errors of this kind are critical and difficult to detect on system-level verification. Thus, a memory subsystem and implementation of coherence protocols in HDL (Hardware Description Languages) models must be thoroughly verified [2].

There are two main methods for verification of memory subsystem: a simulation-based verification and formal verification [3]. Formal verification is used to mathematically prove the correctness of a DUV (Device Under Verification) model with respect to its specification. It is widely known that main advantage of formal methods is their exhaustiveness. Many works are devoted to this method [4-6]. Disadvantages of these methods are complexity of development and high specification requirements. Simulation-based methods are not exhaustive, but they can be applied at earlier stages of development and they are much simpler.

Verification of a memory subsystem, as a part of whole microprocessor, can be provided by means of system verification [7]. However, it is essential to mention that some of the components of a memory subsystem are invisible from the point of view of a testing program and it is hard to recreate necessary conditions for verification with proper quality. To overcome these drawbacks, a stand-alone verification of the memory subsystem is usually used.

There are a number of methods to implement a standalone functional verification of a memory subsystem. One of them is C++TESK Testing ToolKit created in ISP RAS [8]. It is an open-source C++ based toolkit intended for automated functional testing of RTL (HDL) models of digital hardware (in Verilog and VHDL). The tool included a library of C++ classes and macros that define facilities for all parts of a verification environment. Some of disadvantages of this tool are high complexity of the application and needs documentation and checking reference model high accuracy.

Another tool name is Alone-env created in the "MCST". The Alone-env provides a wrapper-class over Verilog description of the verified module. The Alone-env too has some disadvantages: the lack of collecting coverage means, high requirements for the checking reference model and the inability to reuse the test system.

Nowadays the most widespread verification methodology is Universal Verification Methodology (UVM). This is a standard verification methodology from the Accellera Systems [9]. UVM designed to enable creation of robust and reusable testbenches and their components. UVM is a class library helps to bring much automation to the SystemVerilog language. Disadvantages of UVM is learning curve is very high for new users and it takes a lot of code to create basic UVM testbench classes. Nevertheless, our team already have a number of test systems, basic classes and libraries written and debugged. Therefore, we choose UVM for developing the stand-alone verification environment of memory subsystem modules.

The rest of the paper is organized as follows. Section 2 reviews the existing techniques for standalone verification of the memory subsystem. Section 3 describes a case study suggests an approach to the problem of developing test system. Section 4 describes additional used approaches. Section 5 reveals results and Section 6 concludes the paper.

II. STANDALONE VERIFICATION METHODS OF MEMORY SUBSYSTEM

In a stand-alone verification we implement test system that allows to select a single part of the whole system and examine its behavior in the test environment that behaves in a way similar to the “real” system. Correct mechanisms of interaction with DUV are defined in its specification. One of the main advantages is that it is easier to explore edge and corner cases in the verified module.

When verifying a part of the memory subsystem with included cache, we need to take into account some features while developing the test system:

- it consists of cache lines that are fixed size blocks used to transfer data between two nodes of the system;
- logic to locate and transfer requested data;
- cache line also hold service information;
- may be several requesters which work with different cache lines
- if two or more requesters want to refer to the same cache line such request have to be serialized and completed in the same order as they received;
- controller support some of implementations of a coherence protocol;
- due to the limited amount of a memory, one of the data eviction algorithms is implemented.

Test environment (or testbench) for verifying the memory subsystem usually includes:

- generator of input stimulus;
- checker of collected reactions correctness;
- module collecting coverage information.

Generator of input stimuli is responsible not only for primary requests that perform operations with memory, it also collects reactions from verified device and generate answers from test environment - secondary requests. Generalized scheme of test environment shown on Fig. 1. Generation of stimulus can be simplified by using TLM [10] (Transaction Level Modeling) to communicate with DUV. TLM allows focusing more on the functionality of the data transmission and less on its actual implementation.

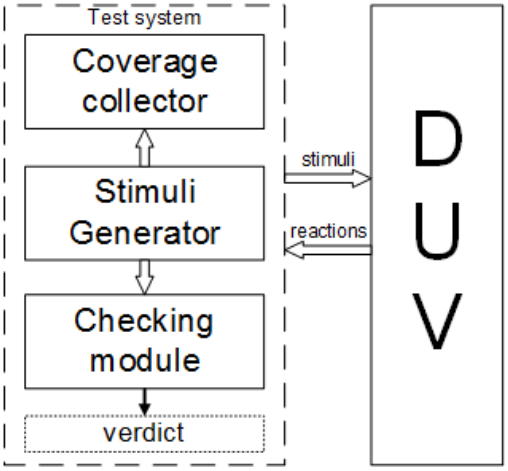

Fig 1. Generalized scheme of test environment

If the verified device has a complex structure and many states, the easiest way to check correctness of reactions is building the separate checking module. Checking module is based on the external to the test environment reference model usually written in high-level language (C, C++ or some specific languages for verification of hardware, such as SystemVerilog, SystemC or «e»). All requests and reactions from the verified device sent to the checking module where then made a conclusion about the correctness of the behavior.

The reference models could be divided into three types: cycle-accurate, discrete-event with time accounting and event models [11]. First two of them require a very accurate specification. It is hard to support design changes that happen very often on the first steps of the development. Furthermore, the similarity of the implementations of the model and the DUV can lead to duplication of errors. To check correctness of memory subsystem, it is reasonable to use event models because they require less time to develop and more flexible for changes of the design. Data interchange of the test system with reference model occurs instantly by calling appropriate functions. For some devices, there are several correct scenarios of the operation for the same input stimulus. We call those devices non-deterministic. There are two methods allowing using behavioral event models for verification of these devices [12].

The first method is dynamic refinement of transaction level model. A general approach is as follows. When a reference model gets a request and there is several possible ways to react

to the request, the model creates additional instances and executes the requests in each of them. Then the models are waiting for the reactions from the device under verification. The reaction contents service information (such as a response type, a direction of sending, etc) which helps to exclude impossible states. Absence of suitable state for reaction signals about an error. The sign of a successful completion is comparison all the reactions of the DUV and removal of all unnecessary states. The complexity of this approach is that the number of possible states potentially grows exponentially with a number of stimuli. However, this method can be implemented efficiently for memory subsystem units because all requests to a single cache line are serialized and requests to different cache lines are independent.

Second method is identification of a single correct state using hints from the verified device or a "gray box" method. This method replaces usual “black box” method. When we cannot predict the “real” sequence of interactions, we access inner interfaces of the verified device. Information from these interfaces have to be transferred to the test environment and helps to determine a single possible execution scenario and eliminate nondeterminism. This method imposes additional requirements to the device specification, but, as a result, it is quite simple to implement.

Coverage collection module extract information of functional code coverage. This information is used to identify unimplemented test cases and helps to improve stimuli generation by adding new test scenarios.

III. USING GRAY BOX APPROACH FOR VERIFICATION OF HOME MEMORY UNIT

Home Memory Unit (HMU) is a part of memory subsystem of 16-core “Elbrus” microprocessor responsible for the coherent and non-coherent access to the RAM from different requesters. HMU contains a global directory (MOSI protocol of coherence), which monitors the requests of other processors to its memory and a DMA directory which is a full copy of the DMA caches of all processors (supports the extended coherence protocol MOI). Total volume of the directory in HMU is 2.5 MB, size of entry of a cache line is 80 B, number of banks – 128, bank associativity – 16. Main functions of HMU include:

- serialization of all requests to RAM;
- reduction of coherence traffic and access time to RAM;
- support of interprocessor coherence by sending coherent requests;
- collecting short coherent responses and coherent responses with data;

Test system for stand-alone verification of the coherence protocol implementation and other functionality of HMU based on UVM. UVM helps to generate pseudo-random constrained input requests to cover possible states of the verified device.

We have to note some restrictions for generation primary, secondary stimuli and answers. The first of them is limited amount of space in input buffers. Due to process of verification, it is important not to lose some data. When generating random system settings, it is necessary to take into account that the some setup combinations may be incorrect and lead to errors. There are several types of requesters in the test system. Each of them has special identifier and a set of possible operation codes. The specific implementation of the coherence protocol also imposes restrictions on the used operation codes. Sending an inappropriate operation code may result in undefined results. Address generation is also a non-trivial task. The address have to fit the interleaving conditions. In addition, each requester have to wait for the completion of previous request when working with same cache line.

Stimuli generation is divided into several stages:

1. randomization of device configuration registers. This allows to switch different ways for handling requests and determine request routing;
2. creating list of addresses for current configuration of device with respect to routing setup;
3. choosing random requester and cache line address;
4. checking cache line availability and presence of resources needed for request transfer;
5. choosing random operation code constrained by the current state of cache line;
6. sending primary request, collecting reactions from the device under verification, sending secondary requests;
7. collecting all of necessary reactions and completion of current request;
8. transferring transaction information to checking module;

To simplify handling of requests and reactions we create models of each used cache line. Model of cache line is an object that stores information about primary request, collected reactions, data and some auxiliary functions. For generation of correct requests we created an associative memory storing current states for each cache line. The choice of the next request type is made according to the limitations imposed by the coherence protocol and the current state of the cache line. For example, one of these rules is there cannot be two requesters in a modified (M) state for a single cache line. Another feature, which was necessary to pay attention, is that one address tag corresponds to two-neighbor cache lines information. This mechanism allows increasing the ratio of the directory coverage (the ratio of the cache memory covered by the directory to the cache memory of the directory).

As noted before, there are two ways of building checking module. The choice of “gray box” method is determined by following sources of a nondeterminism inherent to HMU:

- HMU contains two input queues of primary requests what means exponential growth of possible device states size (2n+m, where n, m – number of requests inside input queues);
- cache eviction algorithm in the global directory.

HMU has two cache memories responsible for different functions of a memory subsystem: the global and DMA directories. The global directory has information only about

data belonging to the own processor and used by other processors. Along with that there is no information about presence of this cache line in cache of own processor. Such information located in the L3 cache. DMA writes are also coherent requests. For a fast and correct handling of DMA writes sent by DMA controllers the special DMA cache directory is present inside HMU. This cache directory supports extended coherence protocol MOI with substates. Its main function is processor notification about cache lines captured by DMA controllers and storing their states.

The device under verification connected with other parts of the system by means of network-on-chip and has two input channels for primary requests. All generated primary requests are sent to the DUV and the checking module simultaneously. The checking module (implemented in C++) receives requests and reactions from the verified device by means of DPI (Directed Programming Interface). Using of the DPI is necessary to match the types and classes of the test environment written in SystemVerilog hardware description language with the reference model interface functions. Inside checking module, all requests are received into two queues. Requests to the same cache line can get into the different queues. It is impossible to predict which of these requests will be handled first. Getting a sequence hint from the device under test eliminates the nondeterminism of the current state. Stable and well-described inner interfaces to the point where all request are serialized, made it possible to build simple checking module in the short time. In a similar way, an access to the eviction mechanism interface was obtained. In addition, the checking module and its behavior model may be modified if it will be needed in the future projects. Structure of the test environment with proposed "gray box" method shown in Fig. 2.

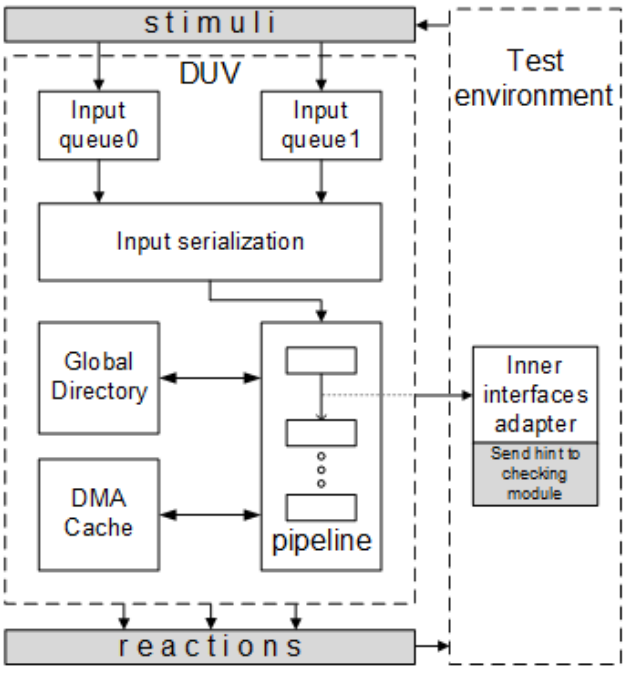

Fig 2. Simplified version of the test environment using the "gray box" method

IV. Additional Verification Methods

A. Management of transaction flow

To check if the verified device operates correctly, it is necessary to achieve multiple edge and corner cases. This involves filling all input and output primary and secondary requests queues, delaying some necessary types of answers and blocking of transactions from some modules [13]. HMU supports the credit-exchange mechanism, which indicates the devices ability to accept certain type of requests. We added the special configuration module that randomizes time delays of sending requests and credits. Management of delays setup allows to create different test scenarios with overflowing requests and responses buffers. This mechanism helps to detect livelocks and deadlocks. These types of system behavior are hard to implement during system testing.

B. Applying assertions

SystemVerilog Assertions (SVA) is an important subset of SystemVerilog [14]. The assertions are used to specify the behavior of the system. The assertions work as follows: we add some piece of verification code to the test system that monitors a design implementation for compliance with the specifications. In addition, the assertions can be used to flag that input stimuli do not conform to assumed requirements. In the beginning of the project, it may help to find more bugs and locate them faster.

In HMU verification process the assertions are used for checking for uncertain and unconnected states of signals. Usage of coherence protocols in the DUV involves certain restrictions on the stimuli generation and the state of the cache lines for different requesters. Thus, additional function of the assertions, which was used in the test system, is detection of the discrepancy between coherence protocol specification and generated requests types in the certain cache lines states. The disadvantage of this approach is the limitation of the properties of the verified device that can be checked by assertions.

C. On-the-fly ECC errors insertion

ECC bits are stored in a cell that describing the state of the cache line. Special submodules of HMU encode the data written to the RAM and decode data read from RAM. Using ECC bits allows to detect single, double, parity errors and to correct single errors. This mechanism is a potential source of errors in the device. The special module with flexible configuration was developed to insert single and double errors. This module is managed by the test system. Frequency and type of error insertion can be regulated. Detecting and correcting ECC errors additionally loaded computing logic of verified device.

V. Results

The approaches described in this paper were applied for standalone verification of Home Memory Unit of 16-core and 2-core with 6 integrated graphic boosters microprocessors with "Elbrus" architecture.

There are some difference in operating with memory subsystem in the microprocessors. The 16-core microprocessor's HMU has a global directory and DMA cache, sends coherent requests with accordance to the state in the global directory, and collects short coherent answers and coherent answers with data for write operations. For read

operations, requester (DMA or L3 cache) collects all the answers.

The 2-core microprocessor does not have a global directory in HMU but include DMA cache. HMU provides inter-core coherence. Coherence requests are sent broadcast to the cores and DMA. HMU also collects all the answers for write operations and for read operations only when requester is not DMA. Integrated graphic boosters are not snooped.

Due to the specificity of the test system construction, some part of MC controller (the MC adaptor) was also added to the verified system. Generator of responses from MC controller with randomized setups was also developed.

In the process of the standalone verification of the Home Memory Unit we found 28 errors that have not been found by other means of verification. All errors were corrected. The distribution of the number of bugs in different subsystems of the HMU are presented in Table 1. Code and functional coverage was carried out and 94% coverage was extracted. Total result indicates about effectiveness of the proposed methods of standalone verification.

TABLE 1. TYPES OF FOUND BUGS AND ITS QUANTITY

Type of bugs	Number of bugs
Coherence protocol implementation	21
Configuration registers	2
Parity checker	1
Performance improvement	2
MC adaptor	3
Total:	28

VI. CONCLUSION AND DIRECTIONS FOR FUTURE WORK

Memory subsystem is one of the most important parts of microprocessors. Its parts that support coherence protocols are especially complicated and error-prone. Verification of these types of devices is time-consuming and labor-intensive work. The stand-alone verification designed to simplify this task. The approaches mentioned in this paper can be applied for stand-alone verification memory subsystem parts regardless of their implementation.

The proposed approaches have been applied in the verification of the Home Memory Unit as a part of multi-core microprocessor memory subsystem with “Elbrus” architecture developed by "MCST". Test environment and test scenarios made it possible to detect and correct a number of logical errors that were not detected by other verification methods.

In the future, it is planned to adopt the test environment for the forthcoming projects and possible changes in coherence protocols.

REFERENCES

[1] Hennessy J.L., Patterson D.A. Computer Architecture: A Quantitative Approach. Fifth Edition. Morgan Kaufmann, 2012. 857 p.

[2] A. Kamkin, M. Petrochenkov. A Model-Based Approach to Design Test Oracles for Memory Subsystems of Multicore Microprocessors. Trudy ISP RAN /Proc. ISP RAS, vol. 27, issue 3, 2015, pp. 149-160.

[3] W.K. Lam. Hardware Design Verification: Simulation and Formal Method-Based Approaches. Prentice Hall, 2005, 624 p.

[4] Burenkov V.S. A Technique for Parameterized Verification of Cache Coherence Protocols. Trudy ISP RAN/Proc. ISP RAS, vol. 29, issue 4, 2017, pp. 231-246.

[5] Ivanov, Lubomir & Nunna, R. (2001). Modeling and verification of cache coherence protocols. 129 - 132 vol. 5. 10.1109/ISCAS.2001.922002.

[6] P. A. Abdulla, M. F. Atig, Z. Ganjeiy, A. Reziney and Y. Zhu, Verification of cache coherence protocols wrt. trace filters, 2015 Formal Methods in Computer-Aided Design (FMCAD), Austin, TX, 2015, pp. 9-16.

[7] I.A. Stotland, V.N Kutsevol, A.N. Meshkov. Problems of functional verification of Elbrus microprocessor L2-cache. Voprosy radioelektroniki [Issues of radio electronics], ser. EVT., 2015, no. 1, pp. 76-84 (in Russian).

[8] C++TESK Testing ToolKit review https://forge.ispras.ru/projects/cpptesk-toolkit (12.05.2019).

[9] Standard Universal Verification Methodology http://accellera.org/downloads/standards/uvm (12.05.2019).

[10] Kamkin A., Chupilko M. A TLM-based approach to functional verification of hardware components at different abstraction levels. Proc. of the 12th Latin-American Test Workshop (LATW), 2011, pp. 1-6.

[11] Kelton W., Law A. Imitatsionnoe modelirovanie [Simulation modeling] // Klassika CS. 3-e izd. SPb.: Piter, 2004.

[12] Petrochenkov M., Stotland I., Mushtakov R. Approaches to Stand-alone Verification of Multicore Multiprocessor Cores. Trudy ISP RAN/Proc.ISP RAS, vol. 28, issue 3, 2016, pp. 161-172. DOI: 10.15514/ISPRAS-2016-28(3)-10.

[13] Lebedev D.A., Stotland I.A. Construction of validation modules based on reference functional models in a standalone verification of communication subsystem. Trudy ISP RAN/Proc. ISP RAS, vol. 30, issue 3, 2018, pp. 183-194. DOI: 10.15514/ISPRAS-2018-30(3)-13.

[14] 1800-2017 - IEEE Standard for SystemVerilog--Unified Hardware Design, Specification, and Verification Language https://standards.ieee.org/standard/1800-2017.html (12.05.2019).

Standalone verification of IOMMU with virtualization supporting.

Anton Petrykin[1], Irina Stotland[2], Aleksey Meshkov[3]
Department of Verification and Modeling
MCST
Moscow, Russia
petrykin_a@mcst.ru[1], stotl_i@mcst.ru[2], alex@mcst.ru[3]

***Abstract* — This article presents an approach to standalone verification of I/O Memory Management Unit with virtualization supporting. We presented the base architecture of the test system. One of the key problems encountered during verification was the formation of translation table pages. The number of translation tables depends on the mode of CPU operation. As a solution of this problem the approach to the dynamic generation of translation tables is proposed. The problem of validating the translation of a virtual address into a physical one using two-level translation tables is solved. The features of the reference model implementation are considered. Reference model and test system which have been used for verification of «Elbrus-12c» microprocessor IOMMU are discribed. The methods of communication between test system and IOMMU model are presented. The results of IOMMU verification are considerd.**

Keywords — I/O Memory Management Unit, test system, reference model, «Elbrus – 12C»

I. INTRODUCTION

An I/O Memory Management Unit (IOMMU) is a hardware device that translates virtual address received from the I/O subsystem requests to proper machine physical address. IOMMUs have long been used for prohibiting devices from DMA'ing into the wrong memory and for performance optimization. With the hardware support of operating system virtualization IOMMU is also used for extending the protection and isolation properties of Vms(Virtual Machines) for I/O operations, supporting isolation of interrupts from devices and external interrupt controllers and recording of DMA and interrupt errors to system software that may corrupt memory or impact VMs isolation[1][2]. Therefore, modern IOMMUs are quite complex devices that have many modes of operation and their verification is an important step in the development of the microprocessor system.

In the paper we present a case study for functional verification IOMMU with virtualization supporting of «Elbrus-12C» microporocessor developed by MCST. The paper addresses the problem and methods of standalone verification of IOMMU with virtualization supporting.

The rest of the paper is organized as follows. Section 2 considers the problems arising from the verification of IOMMU. Section 3 suggests an approach to the problem of developing page table lines generator. Section 4 presents a common approach to the design a test system and describes its components. Section 5 reveals results. And section 6 concludes the paper.

II. IOMMU VERIFICATION CHALLENGES.

For hardware support of operating system virtualization, the translation of a virtual address into a physical one occurs according to a scheme that includes a two-level page structure. At the first level, the virtual guest OS address (GVA) is translated into the physical guest OS address (GPA) using its translation tables. At the second level, the resulting address is translated to the physical address (PA) of the hypervisor using the hypervisor translation tables. Information about the broadcast address for each device is stored in the device table. The table consists of Device Table Entry(DTE) elements. Each DTE contains information about the Domain ID, host page table root pointer (HPTP) and guest page table root pointer(GPTP). In the IOMMU of Elbrus-12C processor, DID field has an extension and is called EDID. In addition to the domain number, it contains information about whether the device belongs to the guest or the hypervisor.

The pages number of translation tables depends on the mode of device operation and the size of the page themselves. «Elbrus-12C» processors support three page sizes: 4KB, 2MB and 1GB. For guest virtual address translation through 4KB pages, the number of memory hits can reach twenty-five. Each memory hit takes a long time to process. Therefore, as part of IOMMU can be used a lot of different caches[1].

It follows from the above that the main goal of IOMMU verification is to check the correctness of all translation modes and check the following:

- Translation on pages with various size.
- Error handling.
- Caches correctness.
- Translations for the greatest possible number of addresses.
- Absence of suspensions
- Absence of unknown logic value (X-state) on output signals.

There are several main problems encountered during the IOMMU verification of Elbrus-12C processors:

- The large number of translation tables and different page size.
- Large size of the entire address space.
- Different virtual addresses can be translated into one physical.

To solve these problems, it was necessary to create the translation page tables. But their formation for the entire address space would require a large amount of computing resources. In paper [3] is presented the approach based on constraint-random generation page table entries (PTEs) which we used for IOMMU verification as a part of northbridge of our previous microprocessor. However the availability of hypervisor and guest translation caches as well as a large number of translation pages required for guest virtual address translation does not allow to use the approach described in [3]. The traditional approach is to generate a static table for a limited set of addresses which is used for verification Translation Lookaside Buffer(TLB) of MMU[4]-[6]. But with using of this approach, it is difficult to verify error handling and virtual address translation over various size pages. Therefore, for functional verification of the IOMMU of«Elbrus-12C» processor, it was decided to develop a dynamic generator of translation table pages, which generates rows of translation tables for any virtual address.

III. GENERATOR OF TRANSLATION TABLE PAGES.

The formation of pages in the generator depends on the translation mode, which is specified directly in the tests and translation request. The algorithm of the generator work could be represented in the form of several consecutive steps:

1) Receiving request for translation;
2) Translation request and mode analysis;
3) DTE formation.
4) Translation pages entry.

Translation modes are divided into single-level or native translations and two-level translations. In turn, native translations can take place in the same domain or split into different domains. Native translations in the same domain doesn't require DTE. For the rest of translation modes DTE formation is necessary. Since a unique translation identifier in Elbrus-12c processors is an EDID, each DTE element is stored in an associative array indexed by it. The formation of a DTE begins with the selection of a random EDID for a given device, after which the presence of a DTE for a given EDID in the array is checked and if it is missing, the remaining fields are formed.

Translations tables have a 4-level structure and consist of 512 elements. Each line of the table contains information about the access rights to it and whether it is the last in the translation structure. In addition, there is a field named ppn(Physical Page Number), that indicating the line from the next translation level, in case the line is on the last translation level, it contains the physical address. Hereinafter the pages of hypervisor and guest translations will be called HP(Host Page) and GP(Guest Page), respectively.

For native translation, the address of the first line is formed from the host page table index (hptp) contained in the DTE, and a part of the translated virtual address. Physical page number for each page level is calculated as follows:

$$ppn(n) = hptp + 512*(5 - n) + VA(n), \quad (1)$$

where n - host page level, VA(n) – the part of translated virtual address on level n , hptp - table root pointer.

The full list of pages for native translation is presented in Table 1.

Page level	Addres of page	Physical Page Number
HP_L4	hptp, VA(4)	hptp + 512 + VA(4)
HP_L3	ppn_L4, VA(3)	hptp + 512 * 2 + VA(3)
HP_L2	ppn_L3, VA(2)	hptp + 512 * 3 + VA(2)
HP_L1	ppn_L2, VA(1)	hptp + 512 * 4 + VA(1)

Table. 1. List of pages for native translation.

When generating rows of a two-level table for guest virtual address translation, the generator first calculates the guest physical address(GPA) for first guest page(GP_L4) according to the formula:

$$GPA(4) = GPTP + VA(4) \quad (2)$$

After that, the pages necessary for the translation of this GPA to HPA are written in the same way as the recording of the pages of translation VA to PA in the native mode. The list of pages for that translation may be seen at Table 2.

Page level	Addres of page	Physical Page Number
HP_L4	hptp, GPA(4)	hptp + 512 + GPA(4)
HP_L3	ppn_L4, GPA(3)	hptp + 512 * 2 + GPA(3)
HP_L2	ppn_L3, GPA(2)	hptp + 512 * 3 + GPA(2)
HP_L1	ppn_L2, GPA(1)	hptp + 512 * 4 + GPA(1)

Table. 2. List of pages for guest physical addres translation into host physycal address.

Then the GP_L4 page itself is written and after that the guest physical address of the next page level(GPA_3) is calculated as the sum of HP_L1 page ppn and part of virtual address:

$$GPA\_3 = ppn + VA(3), \quad (3)$$

And so on to get the GPA of the original GVA. For the obtained GPA, the pages of the last hypervisor translation are formed, which give the desired HPA. In order to avoid writing identical lines at different translation levels, guest pages addresses and ppns are configured as followed:

$$addr(x) = \{ppn, GPA\_x(0)\}, \quad (4)$$

$$ppn(x) = hptp + 512 * (9-x) + GPA\_x(1), \quad (5)$$

where x – guest page level, GPA_x(0) - the part of the guest physical address that is not translated by hypervisor structures

The list of guest pages for two-level translation is presented in the Table 3.

Page level	Addres of page	Physical Page Number
GP_L4	ppn, GPA_4(0)	hptp + 512 * 5 + GPA_4(1)
GP_L3	ppn_L4, GPA_3(0)	hptp + 512 * 6 + GPA_3(1)
GP_L2	ppn_L3, GPA_2(0)	hptp + 512 * 7 + GPA_2(2)
GP_L1	ppn_L2, GPA_1(0)	hptp + 512 * 8 + GPA_1(1)

Table. 3. List of guest pages in two-level translation.

To verify the error handling on each level of table can be prescribed a row of the page table that causing an error. That table level can be set via test parameters or randomly. In the same way, translation page sizes can be set through the PS field in a line of translation table. To verify the error handling on each level of table can be prescribed a row of the page table that causing an error. That table level can be set via test parameters or randomly. In the same way, can be setted the translation page sizes through the PS field in a line of translation table.

IV. Test System Structure.

Test system was implemented with using of SystemVerilog langueage[7] and Universal Verification Methodology[8]. Use of this language allows for an easy interface with Verilog and SystemVerilog devices, and UVM describes a general test system structure and provides a library of basic verification components.

The test system includes a set of basic components which are presented below.

A. Apb (Advanced Peripheral Bus) agent

Apb agent is used to entrance the set of configuration registers in IOMMU whose access interface is implemented according to the APB protocol.

B. Register model

A register model is an entity that encompasses and describes the hierarchical structure of class object for each register and its individual fields. Every register in the model corresponds to and actual hardware register in the design.

C. Translation agent

This is the agent in which the translations are generated and then sent on the DUT(Design Under Test) query interface and generator of table pages. Translation generation is based on constrained randomization. To specify some test scenario, one must define specific constraints for transactions that will be issued. SystemVerilog offers a native support for constrained randomization constructs. Translation agent is also receives the results of the translation from the response interface.

D. Generator of translation table pages and system memory.

Each request received from the translation agent is processed by the generator as described in Section 3. All lines of translation pages are stored in system memory.

E. Page table entries(PTE) agent

PTE agent collects information about requested and received by the device PTEs from system memory. If for any reason the requested PTE is missing, the system memory will randomly generate it.

F. Model

The IOMMU reactions were tested using its reference event model. For reconciling the types and classes of the test system written in SystemVerilog with the C++ language in which the reference model is developed the DPI(Directed Programming Interface) was used. The reference model accepts input stimuli and generates output responses, which are then sent to scoreboard.

G. Scoreboard

Scoreboard receives transactions from transaltion and page table entries interfaces. After that, they are compared with the corresponding transactions received from the model. If a mismatch is detected, the module reports an error in the test system. Test system structure is presented in Fig.1.

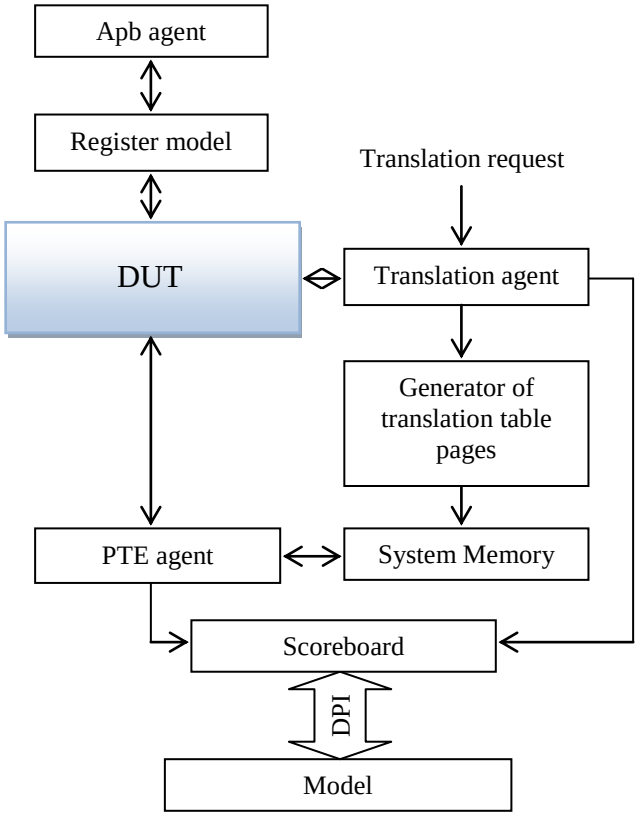

Fig. 1. Structure of a test system.

V. Results.

The approaches described above were applied to standalone verification of the IOMMU of Processor «Elbrus – 12C». Due to standalone verification of the device, 58 errors in the RTL description that have not been found by other means of verification were found and corrected. Total result indicates about effectiveness of standalone verification of I/O memory management unit.

VI. Conclusion.

I/O memory management units are among the important parts of modern microprocessor systems have to be thoroughly tested. In this article, we presented a method of translation table pages forming. The main advantages of the described approach are:

- no need to create tables for the entire address space.
- the ability to dynamically set the page size.
- convenience of exception checking due to dynamic generation of page table row fields.
- ease of obtaining maximum coverage, due to the possibility of calls to any address.

The principles described in the paper do not depend mainly on the IOMMUs implementation and allow their full standalone verification.

The proposed approaches have been applied in the verification of IOMMU as a part of microprocessor «Elbrus – 12C», developed by "MCST". The developed test system and tests made it possible to detect and correct a number of logical errors that were not detected by other test methods

References

[1] Intel Virtualization Technology for Directed I/O Architecture Specification. Intel, 2018.

[2] AMD I/O Virtualization Technology (IOMMU) Specification. AMD, 2016.

[3] Lebedev D.A., Stotland I.A. Construction of validation modules based on reference functional models in a standalone verification of communication subsystem. Trudy ISP RAN/Proc. ISP RAS, vol. 30, issue 3, 2018, pp. 183-194.

[4] Alkassar E., Cohen E., Kovalev M., Paul W.J. (2012) Verification of TLB Virtualization Implemented in C. In: Verified Software: Theories, Tools, Experiments. VSTTE 2012. Lecture Notes in Computer Science, vol 7152, pp 209-224. Springer, Berlin, Heidelberg

[5] Alkassar, E., Cohen, E., Hillebrand, M., Kovalev, M., Paul, W.: Verifying shadow page table algorithms. In: Formal Methods in Computer Aided Design (FMCAD) 2010. pp. 267-270. IEEE, Lugano, Switzerland (2010).

[6] Kamkin A., Kotsynyak A.. (2016) Specification-Based Test Program Generation for MIPS64 Memory Management Units. In: Trudy ISP RAN/Proc, vol. 28(4), 2016. pp. 99-114.

[7] IEEE Standard for SystemVerilog — Unified Hardware Design, Specification, and Verification Language. IEEE Std 1800-2012M. Young, The Technical Writer's Handbook. Mill Valley, CA: University Science, 1989.

[8] 1800.2-2017 - IEEE Standard for Universal Verification Methodology Language Reference Manual.

Digital Modelling of Production Engineering for Metalworking Machine Shops

Vsevolod Kotlyarov
Peter the Great St.Petersburg Polytechnic University
29 Politekhnicheskaya Str., Saint Petersburg
194064, Russian Federation
vpk@spbstu.ru

Alexey Maslakov
Peter the Great St.Petersburg Polytechnic University
29 Politekhnicheskaya Str., Saint Petersburg
194064, Russian Federation
alex.maslakov.ftk@gmail.com

Alexey Tolstoles
Peter the Great St.Petersburg Polytechnic University
29 Politekhnicheskaya Str., Saint Petersburg
194064, Russian Federation
gmlaletol@gmail.com

***Abstract*—Currently, the engineering industry solves the problem of implementation of efficient production methods for satisfaction of small and diverse orders. The key to the solution is to create automated, adaptable small-scale production sites, which corresponds to the paradigm of Industry 4.0. The bottleneck of the development of small-scale production is the preparation of its technological processes and their documentation.**

The technologist and the workers in the workshop use a set of technological documentation which describes the necessary technological equipment (workpieces, machines, cutting tools, mounting fixtures, etc.) and sequences of actions for the manufacturing of details.

This article presents a modular approach that reduces the labor costs for the technological preparation of small-scale metalworking production. Its idea is to formalize the technological processes, allowing generating them and their documentation from pre-prepared parameterized templates stored in the special database. Any manufactured detail or its part can be represented as the structure of its basic geometric components, such as cylinders, cones, parallelepipeds, etc., that require special processing procedures. For the template of machining operations for each component, symbolic parameters are fixed, defining the type and the material of the workpiece used, cutting tool options, machining modes, etc. The template also records restrictions on the parameters of sequences of operations used, on the usage of processing modes depending on the characteristics of instrument, etc.

The result of formalization is an automatically generated technological route in the form of an MSC diagram encoding it as a sequence of macro-operations for the machinery with symbolic parameters. This symbolic model is adapted to a specific instance of the detail being manufactured by replacing the symbolic variables with specific values set by the technologist.

The MSC diagram is supplemented with the results of calculating the time and cost of technological routes, which allows selection of the most efficient one.

The correctness of the technological routes is ensured in the process of symbolic verification by checking the permissible ranges of parameters of the MSC diagram, as well as checking the correctness of order and compatibility of operations in the sequence.

The results of the whole process obtained from the MSC diagram are the set of technological documentation of preproduction, which, in particular, includes a set of operating cards, and the fine-tuned schedule of production after its digital modeling with the real resources of the workshop taken into account.

According to technologists, by applying the described automation, the time to prepare documentation for details of medium complexity is reduced from several weeks to 1-2 days.

***Index Terms*—adaptive manufacturing, production engineering, small-scale metalworking manufacturing preparation, automation of the preparation of technological documentation**

I. Introduction

Comprehensive automation of technological processes based on information technology provides:

- Reduction of the time of pre-production.
- Optimization of labor costs and funds for the manufacture of products.
- Operational implementation of changes in the process under the external conditions (replacement of technological equipment, material, cutting tools, etc.) with automatic recalculation of the process characteristics.

Technological preparation of production (TPP) includes the following activities:

- Setting of technological problems.
- Selection of the workpiece based on its parameters.
- Development of technological processing routes.
- Selection of technological equipment.
- Formation of technological operations.
- Development of a set of technological documentation.

Fields of automation of technological preparation of production include:

- Development of technological documentation.
- Development of control programs.
- Development of technological processes.

The tasks of operational planning and automated production management are carried out by the manufacturing execution systems (MES) [1]. They occupy an intermediate place in the hierarchy of enterprise management systems between the level of information collection from equipment in workshops

done by supervisory control and data acquisition (SCADA) systems [2] and the level of operations over a large amount of administrative, financial and accounting information done by enterprise resource planning (ERP) [1] systems. The key processes for MES are as follows [3]:

1) Based on the external demand for production (which, in turn, is based on customer orders, sales plans, etc.), as well as previous production programs, taking into account all sorts of nuances and specifics of production at a particular enterprise, a detailed optimized production schedule of works and operations for machine tools, equipment, personnel is produced. In addition, automatic generation of all the documentation necessary for the work: production programs, outfits, limit maps, tables and equipment loading diagrams, etc. is also done.
2) In the course of the direct implementation of production programs, full dispatching of all operations and their results (both positive and negative - rejects, delays, etc.) is carried out.
3) If deviations from the planned programs are identified due to the external reasons, or when new demand (orders, etc.) appears, real-time re-planning is performed with all components corrected accordingly.

It should be noted that there exists an imbalance between production time and preparation time in single or small-scale productions in case of re-scheduling of the work of a production site, because it should be performed for the small batch of the details and not for the whole series of them.

Nowadays on the Russian market there are three most popular largest solutions, the products of many years of work of three scientific centers for developing systems of this class: PHOBOS system, YSB.Enterprise.Mes system and PolyPlan system. PHOBOS is traditionally used in large and medium-sized machine-building enterprises. YSB.Enterprise.Mes originated from the woodworking industry and focuses on the sector of medium and small enterprises. The PolyPlan system has a smaller set of MES functions, but is positioned as an operational scheduling system for automated and flexible manufacturing in engineering [3].

However, with all the attractiveness of such systems, due to the extensive set of functions provided and deep integration into the production processes in the enterprise at all stages, their practical implementation is a whole complex and expensive project in itself that not all enterprises, especially small-scale and individual productions, can afford. In addition to this, in order to work effectively with MES, high qualification of its operator is required. The automated workplace of the technologist given in this article is designed to solve a narrower class of problems - to simplify the TPP for small-scale machine-building production, it does not require interactions with other systems, and the results in the form of the required schedule of work distribution and a set of operating cards can be obtained in a couple of days of work of a technologist.

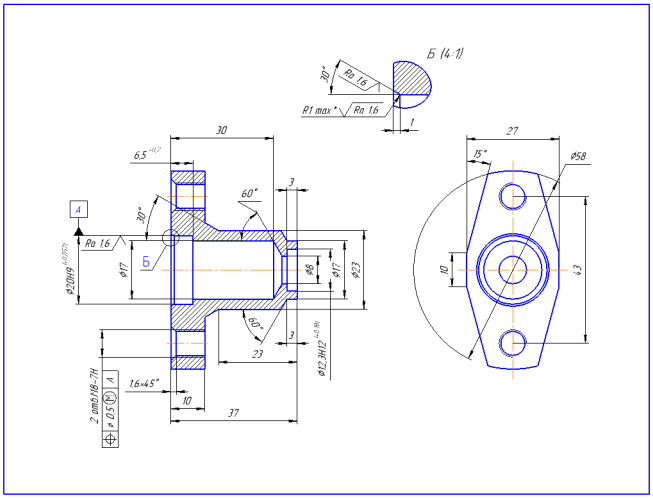

Fig. 1. Input detail drawing.

II. Formalization of the technological process

Let's look through the features of formalization based on an illustration of a specific example of work with the developed system of an automated workplace for a technologist.

The main input information for the technologist is the detail drawing. It can be done in any graphical design program, for example, in KOMPAS-3D [4]. The example of the drawing is demonstrated in the Fig. 1

To manufacture a part technologist chooses a workpiece for it. Several such workpieces may be selected; to determine the best fitting of them, all calculations of time and cost of production must be made for each selected one and compared to each other.

The next action of the technologist is the splitting of a given drawing into a set of sketches of elementary surfaces (ES), the parts of the detail. This step sets the way for the modular approach to the production technology [5]. Each of the surfaces is characterized by geometrical parameters and the number of stages required to process it. The processing stage is the smallest atomic operation, for example, turning, drilling or milling. The parameters of the processing stage are the types of machines on which it can be performed, the cutting tools to do so and the selected workpiece in the very beginning. The form for setting information about the processing stages manually is shown in the Fig. 2. The description of fields and tables of the form is as follows, from left to right and from up to down:

- The type of the elementary surface encoded by two digits.
- The unique number of the elementary surface used to distinguish between the surfaces of the same type.
- The geometrical parameters of the elementary surface, here the diameter and length are listed.
- The amount of the processing stages to be performed.
- The processing stages, divided into the following columns: the number of the stage, the name of it (here: turning), the codes of the applicable machinery for it, the

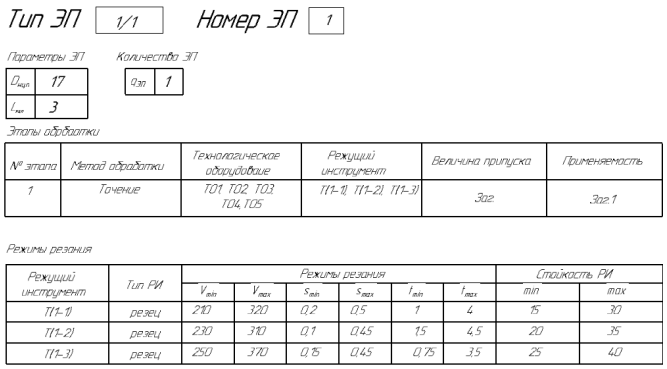

Fig. 2. Processing stage information form.

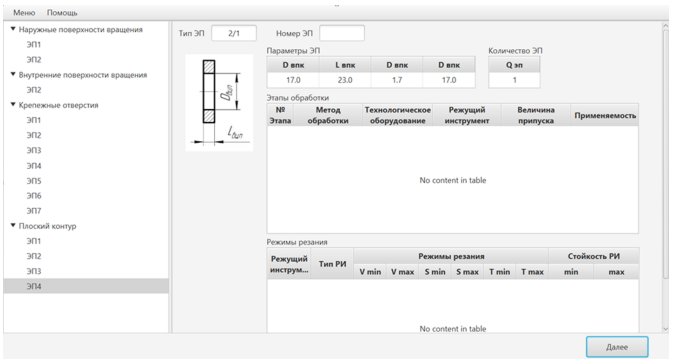

Fig. 3. The window for setting the information about an elementary surface.

codes of the applicable cutting tools for it (which are described in the table under this one), the amount of the overmeasure (here: determined by the chosen workpiece) and the name of the selected workpiece (here: the first one).

- The cutting modes, divided into the following columns: the code of the cutting tool, the type of it (here: cutter), the three technical characteristics of each cutting tool with maximum and minimum values and the minimum and maximum durabilities of the cutting tool.

To translate it into a digital form, a developed solution is used, the set of user interface screens of which forms an automated workplace for the technologist (Fig. 3). The fields and tables on the right are essentially the same, the left side shows the sorted list of the already loaded surfaces by types: inner surfaces of revolution, outer surfaces of revolution, mounting holes and flat contour. There is also a place for the sketch of the surface in the middle.

Each cutting tool added by the technologist is characterized by its cutting modes. The parameters of cutting modes affect the running time and its cost. Usually, data for the cutting tool is taken from reference catalogs in *.pdf format [6]. The user interface allows the technologist to simplify entering data from catalogs through the use of hotkeys: after selecting data in the document and pressing the CTRL + SHIFT + C combination, the data is copied directly into the table. This approach reduces the labor intensity of the manual data transfer and helps to

Fig. 4. The window for creating blocks of elementary surfaces.

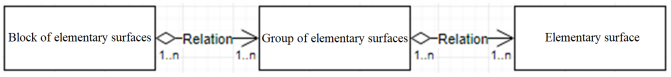

Fig. 5. The nesting hierarchy of elementary surfaces.

avoid the human factor such as errors or typos.

To determine the order of processing of elementary surfaces, further formation of blocks of elementary surfaces from them takes place. Each block is characterized by its own positioning data on the machine. The window for creating blocks of surfaces is shown in Fig. 4. The left side of it shows the list of the blocks with the button ”Create new block” at the very bottom of it, the rows on the right side consist of the surfaces corresponding to each block.

The next step of the formalization of technological process is the formation of groups of elementary surfaces inside blocks of elementary surfaces. Such group is a part of the block that can be processed in one operation without reinstalling the workpiece into the machine. Thus, the nesting hierarchy is created (Fig. 5). The operation on a group of surfaces made up from initial operations on each surface is called a machining step, each one of them has its own physical meaning, for example, turning the outer surface of revolution, drilling through hole or boring the hole. All cutting tools for all elementary surfaces within a group must be the same. The window for creating groups is shown in the Fig. 6. The three tabs on the left are created for each block, they hold lists of groups of surfaces within the block. The right side shows the elementary surfaces of each selected group with their parameters.

In addition to the windows for filling in the information, the user interface has a menu containing Help section. There is a reference catalogs searching tool which works in conjunction with a system application for viewing files in *.pdf format and is capable of two types of searches:

- The window for keyword search in catalogs is shown in Fig. 7. After entering keywords in the top field and selecting catalogs for search in the list, by pressing the leftmost button a search is performed on the selected documents. For each catalog, the following sequence of

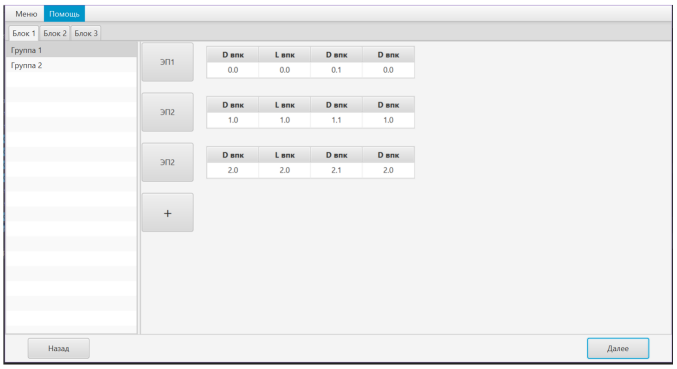

Fig. 6. The window for creating groups of elementary surfaces.

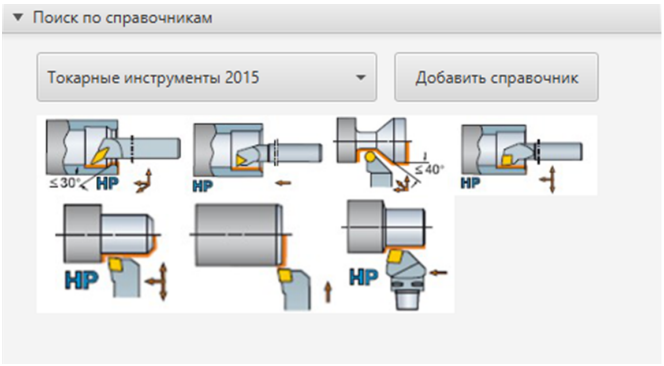

Fig. 8. Image search user interface.

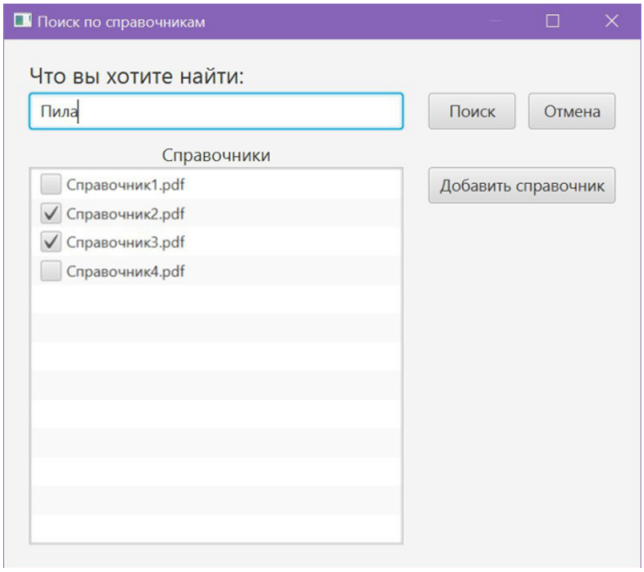

Fig. 7. Keywords search user interface.

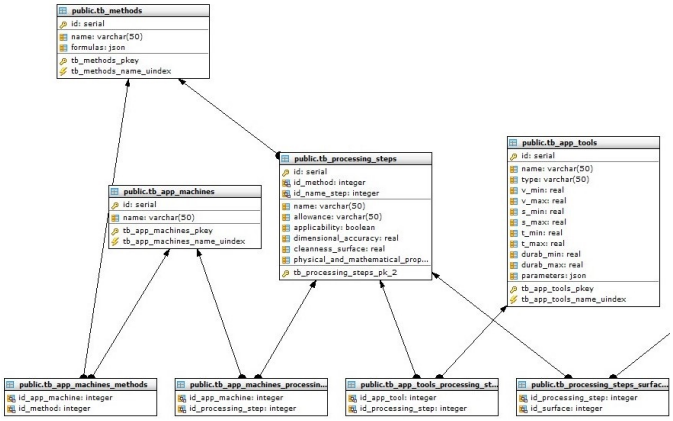

Fig. 9. Database fragment.

actions is carried out:

1) One page of document is read from disk.
2) Search for keywords is performed on this page.
3) If at least one of the keywords is detected, the page is copied into the resulting pdf document.
4) If the keywords are not found, proceed to the next page.

As soon as all pages of all catalogs are processed, a resulting document with search results is written to disk and opened in the standard pdf document viewer in the system. The right button cancels the search, the bottom one allows technologist to add a catalog to the list.

- Search by image, in contrast to search by keywords, is possible only for catalogs formatted in advance. Its interface is shown in Fig. 8. After selecting a pdf catalog from the drop-down list, if the necessary markup information exists for it, images, for example, of surfaces to be processed, are shown. By clicking on them a document containing information related only to the selected images is formed and, alike to the search by keywords, is opened in a standard pdf documents viewer. The button on the right allows technologist to add a catalog to the list.

The usage of these searching tools, especially in conjunction with copying data into tables with hotkeys, achieves a significant reduction in the complexity of data entry for elementary surfaces.

A special database based on PostgreSQL database management system [7] is used to store information entered by the technologist in the user interface [8]. The Fig. 9 shows a fragment of its tables, where:

- ”public.tb_methods” table stores information for calculating the time and cost of processing methods for elementary surfaces.
- ”public.tb_app_machines” is dedicated to applicable machines for processing methods.
- ”public.tb_processing_steps” stores the parameters of the processing methods;
- ”public.tb_app_tools” holds information about the applicable cutting tools and cutting modes.
- The four lowest tables are used for linkage between other tables.

To formulate the resulting technological route for the processing of the whole detail technologist must determine all the groups of elementary surfaces that can be processed together. There can be several routes constructed this way, the choice

of the one is made based on which machinery and which tools are available and should be used. In the approach presented here we use the MSC language [9] for the encoding of the route. MSC is a standardized language for describing behaviors using message exchange diagrams between parallel-functioning objects (machines, robots). The main unit of the diagram is a line starting with a name of a processing stage of elementary surface followed by its parameters. To construct such line, only the index parameters of the stage are used, insofar as all other necessary data can be obtained from the database based on them. Such index parameters include:

- The number of the processing stage.
- The code of the type of the elementary surface, in two digits.
- The number of the elementary surface within the same type.
- The codes of the applicable machinery for the processing stage.
- The codes of the applicable tools for the processing stage.
- The code of the workpiece used.
- The number of the block of elementary surfaces which this elementary surface corresponds to.
- The index number of the elementary surface within the block.
- The number of the group of elementary surfaces within the block.
- The index number of the elementary surface within the group.

The resulting parameterized line takes the following form, for example: *Turning(stageNumber, surfaceType1, surfaceType2, surfaceNumber, [machine1, machine2, machine3, machine4, machine5], [cuttingTool_1_1, cuttingTool_1_2, cuttingTool_1_3], workpieceParams.code, blockParams.number, numberInBlock, groupNumber, numberInGroup);* The diagram comprises a set of these lines in order set by technologist earlier. The correctness of the technological routes is ensured in the process of symbolic verification, which checks the acceptable ranges of parameters of the diagram, as well as the correctness of order of the whole sequence [10]. The actual data is taken from the database and substituted instead of parameters.

III. The usage of the formalized technological process

The MSC diagram of the route is supplemented with the results of calculating the time and cost of each processing stage. The calculations use formulas stored in the database, they are partially shown in Table I and Table II5. The individual results for each processing stage of the route are summarized, which gives an estimate of the total time and cost of the technological route. By changing the route parameters and recalculating the measurements, technologist can choose the most effective one.

The selected technological route thus meets the criteria for the time and cost but yet does not take into account the conditions and resources of the workshop in which it will be implemented. For this, it is necessary to use simulation modeling of its performance on the equipment in the workshop. To use the developed simulation algorithm, technologist inputs three files describing:

- The composition of workshop resources (CNC machines, robots, maintenance personnel, etc.). The types of operations for each machine that it can perform are defined.
- The planned technological routes. The number of manufactured parts and the sequence of operations with the amounts of time of their execution are determined for each route.
- The priorities of the routes and resources used, as well as the initial state of the workshop equipment.

The result of the simulation is a timing diagram of the distribution of operations by each machine in the form of a Gantt chart, a fragment of it is shown in the Fig. 10. Modeling allows technologist to take into account equipment downtime, the additional cost of transporting parts and machine changeover. As a result, the estimation of the time and cost of the technological route becomes more realistic. By changing the priorities of the technological routes technologist obtain several options for implementing the technological process of the workshop. By applying a hierarchy of criteria measuring the success of the work such as time, cost, equipment loading, material savings, etc. various problems of multicriteria optimization can be solved [11].

TABLE I
FORMULAS FOR TURNING TIME CALCULATIONS.

Formulas	Parameters description
$T_m = \frac{L}{n \cdot s} \cdot i$	T_m - machining time L - estimated length of processing in mm n - workpiece rounds per minute s - cutter feed per round in mm i - the number of passes of the cutter
$L = l + l_1 + l_2$	l - the length of the workpiece in the feed direction, mm $l1$ - cutting-in length of the tool $l2$ - the length of the tool exit, mm
$n = \frac{1000 \cdot v}{\pi \cdot d}$	v - the speed of the cutting, mm per minute d - the diameter of the processed workpiece, mm
$i = \frac{h}{t}$	h - the amount of overmeasure in mm t - cutting depth in mm

TABLE II
FORMULAS FOR DRILLING TIME CALCULATIONS.

Formulas	Parameters description
$T_m = \frac{L}{n \cdot s}$	T_m - machining time L - estimated length of processing in mm n - workpiece rounds per minute s - cutter feed per round in mm
$L = l + l_1 + l_2$	l - the length of the hole, mm $l1$ - cutting-in length of the tool $l2$ - the length of the tool exit, mm
$l_1 = \frac{d_t}{2} \cdot ctg(\phi)$	drilling in the solid material ϕ - the main angle in the plan, grad d_t - the diameter of the tool
$n = \frac{1000 \cdot v}{\pi \cdot d_t}$	v - the speed of the drilling, mm per minute d_t - the diameter of the tool, mm

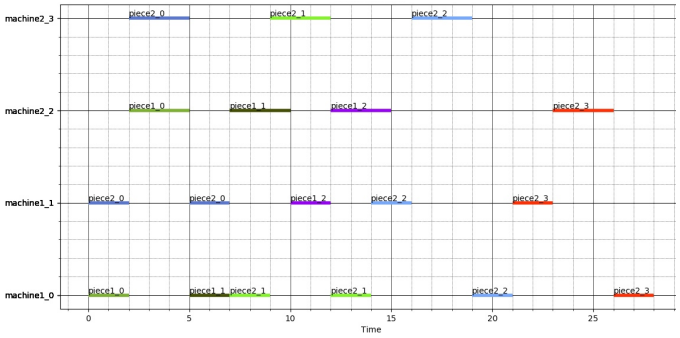

Fig. 10. Timing diagram fragment.

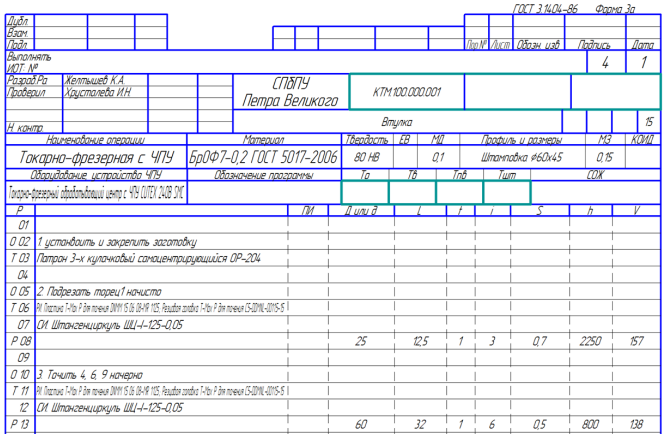

Fig. 11. Operating card.

For each selected optimized version of the technological route, technological documentation of production preparation is automatically generated in the form of the operating card [12], its example is shown in Fig. 11 [13].

IV. Conclusion

The paper considers the problem of technological preparation of single and small-scale production, which area is characterized by imbalance of work between preparation and implementation of production. The approach to its automation based on modular technology is proposed. The important properties of automation system are demonstrated:

1) The ability to adapt to specific production conditions such as different equipment, resources, orders and support staff.
2) Significant reduction of the complexity of creating a technological route for an order using a special automated workplace for the technologist
3) Operational planning and scheduling of the technological process of the workshop.
4) Selection of the optimal characteristics of production processes during hierarchical multi-criteria optimization.

According to existing estimates the platform provides a multiple increase in productivity and a reduction in labor intensity and in amount of time of the preparation of technological documentation for engineering production.

V. Acknowledgments

The work was financially supported by the Ministry of Education and Science of the Russian Federation in the framework of the Federal Targeted Program for Research and Development in Priority Areas of Advancement of the Russian Scientific and Technological Complex for 2014-2020 (14.584.21.0022, ID RFMEFI58417X0022).

References

[1] Frolov E.B. Zagidullin R.R-b. MES-sistemy, kak oni est' ili evolyutsiya sistem planirovaniya proizvodstva (chast' II) [MES as they are or the evolution of the production planning systems (part II)]. URL: http://www.fobos-mes.ru/stati/mes-sistemyi-kak-oni-est-ili-evolyutsiya-sistem-planirovaniya-proizvodstva.-chast-ii.html (Retrieved 01.04.2019) (in Russian).

[2] Davidyuk Y. SCADA-sistemy na verkhnem urovne ASUTP [SCADA systems at the top level of advanced process control systems]. Intelligent Enterprise, 2001, vol. 30, no. 13. - URL: https://www.iemag.ru/platforms/detail.php?ID=16479 (Retrieved 01.04.2019) (in Russian).

[3] Garaeva Y. Zagidullin R.R-b. Tsin S.K. Rossiiskie MES-sistemy, ili Kak vernut' proizvodstvu optimizm [Russian MES or how to return optimism to production]. SAPR i grafika [CAD and graphics], 2005, vol. 11. - URL: https://sapr.ru/article/14614 (Retrieved 01.04.2019) (in Russian).

[4] Statsenko D. Prilozheniya i rabota bez napryazheniya [Applications and work without stress]. Stremlenie [Tendency], 2017, vol. 1, no. 18. - URL: https://kompas.ru/source/articles/3.pdf (Retrived 01.04.2019) (in Russian).

[5] Bazrov B.M. Modul'naya tekhnologiya v mashinostroenii [Modular technology in mechanical engineering], Moscow "Mashinostroenie" ["Mechanical engineering"], 2001, 366 pp. (in Russian)

[6] SANDVIK COROMANT Instrument i osnastka dlya tocheniya na stankakh [Tools and equipment for turning on machines], 2015, 1253 pp. - URL: http://www.lab2u.ru/katalog-sandvik-coromant-2015-metallorezhushchii-tokarnyi-instrument-i-instrumentalnaia-osnastka-dlia-tocheniia-obrabotki-kanavok-otrezki-rezbonarezaniia-reztcy-so-smennymi-rezhushchimi-plastinami-iz-tverdogo-splava-kompanii-sandvik-koromant-lab2u.html (Retrived 01.04.2019) (in Russian).

[7] The PostgreSQL Global Development Group Postgres Pro Standard 11.2.1 Documentation, 2019. - URL: https://postgrespro.ru/docs/postgrespro/11/index (Retrived 01.04.2019)

[8] Cherepovskii D.K., Eizenakh D.C., Kotlyarov V.P. Arkhitektura bazy dannykh dlya sozdaniya tekhnologicheskikh marshrutov melkoseriinogo proizvodstva [The database architecture for the creation of the technological routes for the small-scale production], Sovremennye tekhnologii v teorii i praktike programmirovaniya [Modern technologies in the theory and practice of programming] conference proceedings, Saint-Petersburg, 2019, 3 p. (in Russian).

[9] Recommendation ITUT Z. 120. Message Sequence Chart (MSC), 11/2000.

[10] Baranov S., Kotlyarov V., Letichevsky A., Drobintsev P. The Technology of Automation Verification and Testing in Industrial Projects. Proc. of St.Petersburg IEEE Chapter, International Conference, May 18-21, St.Petersburg, Russia, 2005 - pp. 81-86.

[11] Voinov N., Chernorutsky I., Drobintsev P., Kotlyarov V. An approach to net-centric control automation of technological processes within industrial IoT systems. Advances in Manufacturing, 2017, vol. 5, no. 4, pp. 388-393.

[12] Eizenakh D.S., Cherepovskii D.K., Kotlyarov V.P. Sistema generatsii operatsionnoi karty tekhnologicheskogo protsessa dlya melkoseriinogo mashinostroitel'nogo proizvodstva [The system for generation of the operating card for the technological process for a small-scaled mechanical engineering production], Sovremennye tekhnologii v teorii i praktike programmirovaniya [Modern technologies in the theory and practice of programming] conference proceedings, Saint-Petersburg, 2019, 46 p. (in Russian).

[13] GOST 3.1404-86 Edinaya sistema tekhnologicheskoi dokumentatsii (ESTD). Formy i pravila oformleniya dokumentov na tekhnologicheskie protsessy i operatsii obrabotki rezaniem [Unified system for technological documentation (USTD). Forms and rules for paperwork on technological processes and machining operations]. - URL:

http://docs.cntd.ru/document/1200012135 (Retrieved 01.04.2019) (in Russian).

Reputation Systems in E-commerce: Comparative Analysis and Perspectives to Model Uncertainty Inherent in Them

Nosovskiy Mikhail M., Degtiarev Konstantin Y.
School of Software Engineering
National Research University Higher School of Economics
3 Kochnovsky Proezd, Moscow, Russia
mmnosovskiy@edu.hse.ru, kdegtiarev@hse.ru

***Abstract* — E-commerce is a runaway activity growing at an unprecedented rate all over the world and drawing millions of people from different spots on the globe. At the same time, e-commerce affords ground for malicious behavior that becomes a subject of principal concern. One way to minimize this threat is to use reputation systems for trust management across users of the network. Most of existing reputation systems are feedback-based, and they work with feedback expressed in the form of numbers (i.e. from 0 to 5 as per integer scale). In general, notions of trust and reputation exemplify uncertain (imprecise) pieces of information (data) that are typical for the field of e-commerce. We suggest using fuzzy logic approach to take into account the inherent vagueness of user's feedback expressing the degree of satisfaction after completion of a regular transaction. Brief comparative analysis of well-known reputation systems, such as EigenTrust, HonestPeer, Absolute Trust, PowerTrust and PeerTrust systems is presented. Based on marked out criteria like convergence speed, robustness, the presence of hyperparameters, the most robust and scalable algorithm is chosen on the basis of carried out sets of computer experiments. The example of chosen algorithm's (PeerTrust) fuzzy version is implemented and analysed.**

Keywords — E-commerce, Reputation system, Peer-to-peer computing, Trust management, Uncertainty, Fuzzy logic, Linguistic variable

I. Introduction

E-commerce is a buying-selling runaway activity, which is widening at an unprecedented rate all over the world and inveigling into fascination of various e-stores people of all ages. Ever-growing number of various websites and apps focusing on e-commerce domain makes it simple and alluring to find and to buy immediately almost anything whatever client's heart desires [23].

There is no doubt that e-commerce sales opportunities are rapidly progressing day by day. Owing to Internet, many businesses bring their products and services to customers literally in eyewink. The e-commerce share of total retail sales in the United States amounted to 10% in 2018, in expectation of attainment of 12.4% by 2020 with further strengthening its ground [28]. With such perspectives in mind it is easy to realize why e-commerce entrepreneur position becomes so attractive. With an estimated 95% of purchases that will be made online by 2040 and expected growth of year to year sales standing at the level of 15%, the opportunity to find a niche for selling products online has massive indisputable potential [22]. During the last 5 years the amount of retail sales raised from $1.3 billion to $2.8 billion. The latter is expected to nearly double (up to $4.8 billion) by the end of 2021 [20].

One of the most growing types of e-commerce is online marketplace that can be defined as a website or app that facilitates shopping from many different sources [7]. Among well-known and successful examples of online marketplaces eBay, Amazon, Rakuten (worldwide) and Avito, Ozon (in Russia) can be mentioned. Online marketplace acts as a platform integrating buyers and sellers. Being a peer-to-peer (P2P) network, it allows buyers to purchase any goods or services offered by sellers through this online platform. Usually, peers (people or businesses) communicating through online marketplace remain in the status 'strangers' with respect to each other. They don't have at their disposal reliable information about alter peer, whether it is a buyer or a seller. Therefore, peers must manage the risk associated with transactions on condition that no prior experience and knowledge concerning mutual reputation of sides exists [25]. It becomes possible to address this problem by means of developing a system on top of the network that should help peers to evaluate their past experience with other peers and to manage trust between them as well as reputation of each peer involved. This kind of systems is called *reputation systems*.

Various implementations of reputation systems exist starting with very simple to more complex ones designed mostly for P2P file-sharing networks [6,10,11,27]. No doubt that such systems have a positive impact on peer's experience as they help to distinguish trustworthy peers from ill-intentioned and unreliable opponents. For example, in reputation system used by eBay, one of e-commerce leaders, buyers and sellers have a chance to rate each other with numeric scores +1, 0 or -1 after each carried out transaction. The overall reputation of a participant is calculated as a sum of scores earned over the last six months

[10]. At that all such systems rest upon notions of *trust* and *reputation*. Trust (or, local trust) represents personal experience (attitude) of a user regarding another user, while reputation constitutes an aggregate of these individual trust values on the scale of the whole community. In the long run calculation of local trust and corresponding aggregates underlies implementations of all known reputation systems.

Despite the practical effectiveness of these systems, there is a substantial drawback inherent in them, viz. none of them can handle uncertainty "hidden" in online marketplace's data. The latter means data that relate to all transactions accomplished on the marketplace along with data collected from users after each transaction and metadata concerned with every user in the marketplace.

The primary concern of the paper is to provide the overview of best known reputation systems and to undertake their general comparative analysis on the basis of several key factors (criteria) – they are speed of convergence, complexity of calculations, use of hyperparameters expressing user's preferences, robustness and general system's suitability to handle imprecision and uncertainty of data. In the first place these factors are chosen to convey the requirements of key stakeholders who are owners and developers of a marketplace as well as its users. For the first group of stakeholders general system's effectiveness becomes important, and it is attributed above all to the efficiency of its functioning, computational resources needed to perform the work and ability for customization. Users are mostly interested in reliability of system's output and how well it suits each given user. The last factor mentioned above reflects how naturally specific implementation of the system can be extended to handle data uncertainty and imprecision, since the latter being an inherent part of virtually any system reveals itself in different forms. The recognition of such manifestation forms of uncertainty becomes a task of prime importance to represent appropriately (model) its distinctiveness. Consequently, fuzzy logic is getting one of pivotal theories that captures naturally the phenomenon of imprecision and uncertainty [34].

The rest of the paper is organized as follows: in section II notions of trust and reputation, difference between them, are considered. Uncertainty in the marketplace and verbal assessments that are inherent in reputation systems form the contents of section III. Some basic terms and definitions relating to the field of fuzzy sets and logic are covered in section IV. Section V is devoted to the brief comparison of well-known reputation systems (EigenTrust, Absolute Trust, HonestPeer, PowerTrust and PeerTrust) and stressing their key differences as well as intrinsic similarities. Setup of computer-based experimental part of the work (parameters and their values used) constitutes the material of section VI, whereas the results of carried out experiments are discussed in section VII. Thereafter, the transition from crisp to fuzzy PeerTrust algorithm (basic example and analysis of such transition's outcome) is presented in last but one section VIII. Concluding remarks and observations are drawn in section IX.

II. Trust and reputation. What is the difference between these terms?

Trust and reputation are the main concepts underlying vast majority of reputation systems. In order to clearly recognize the purpose of reputation systems, we need to define what do trust and reputation in terms of online marketplace stand for. Diverse sources give different definitions of the term 'trust'. The basic definition presented in Oxford English Dictionary reads as follows: *"Trust is a firm belief in the reliability, truth, or ability of someone or something"* [29]. However, such definition cannot lay claim to completeness, since notions of trust and reputation as applied to peculiarities of Internet-based activities must be defined in a more context-specific way. Among other things, Alam & Paul define trust as *"a belief, the trusting agent has in the trusted agent's willingness and capability to deliver the services that they are mutually agreed on in a given context and in a given time slot"* [1]. In addition, Wang & Vassileva associate term 'trust' with *"a peer's belief in another peer's capabilities, honesty and reliability based on its own direct experiences"* [24]. Starting from individual judgments and predictions, Gambetta state that *"… trust is a subjective probability that relies on context and reputation, it describes how secure a situation is even though risk is associated with it"* [5]. It can be noticed that trust is mainly linked to belief that peers (agents) mentally possess in malicious P2P environment. Thus, trust can be viewed as a soft factor of the system that is difficult to express precisely and in complete form. It is tied to distinction of numerous generally inhomogeneous interactions between peers, organization of the network, in which humans play a pivotal role.

For reputation term situation seems resembling, i.e. there is also no conventional definition that most of sources agree on. According to [24], reputation is defined as *"peer's belief in another peer's capabilities, honesty and reliability based on recommendations received from other peers"*. On the other hand, already cited above Alam & Paul propose to consider reputation as *"aggregation of all recommendations provided by the third-party recommendation agents about the quality of the trusted agent"* [1]. Abdul-Rahman & Hailes define reputation as *"an expectation about an agent's behavior based on information about its past behavior"* [2]. Kreps & Wilson link reputation to characteristic or attribute *"ascribed to one person by another person (or community)"* [3]. A complete (at least, voluminous) overview of definitions relating to trust and reputation can be found in [8]. In the present work we use definitions for terms 'trust' and 'reputation' from [24] since both definitions agree with basic concepts of reputation system and interaction within P2P community.

Even though trust and reputation are very closely related concepts, and many sources simply use them virtually as synonyms, still there is a major difference to emphasize. While trust is subjective in nature, and it expresses the *local* attitude of a peer regarding another agent on basis of his/her own past experience, reputation serves as a *global* and public perception of a given peer in the midst of other peers. With this point in mind, we may list those important (or, core) characteristics of trust and reputation that must be

taken into consideration when considering reputation systems – namely, they are:

(1) *Context awareness* (sensitivity) – trust or reputation of a peer is dependent on what the context of communication is. For instance, a peer can be really trustworthy in delivering books, but unreliable in selling electronic accessories,

(2) *Multi-faceted nature* (diversity) – even in the same context, peer can evaluate the quality of communication with another peer on the strength of several aspects. In the case of online marketplaces delivery time, quality and price of goods (services) can be mentioned. While the context-sensitivity of trust underlines the fact that the trust in the same agent may vary with reference to different situations, the multi-faceted nature characteristic stands for manifoldness of trust. It definitely plays a substantive role in deciding whether an agent is trustworthy to interact with or not [24],

(3) *Dynamism* – apparently, levels of both trust and reputation increase or decrease in view of gaining experience (direct interaction). Such changes may alternate in due course depending on arising situation in the system, with a clear-cut declining tendency observed with time [24],

(4) *Imprecision and uncertainty* – it is not very habitual for humans to operate with estimates of trust and reputation in the form of numbers. Without a doubt, it is not difficult to perform relatively simple calculations even in passing, but explanations and interpretations are usually based on verbal forms (words, phrases and short sentences in natural language). The peer can be classified as "very trustworthy", "not too trustworthy" or in some likewise manner. Thus, we express gradations (imprecise estimates) of the extent, to which the peer is reputed as trustworthy or not. The bounds of gradations (verbal granules) are inexact, but nevertheless linguistic forms are easily perceived and processed by specialists and ordinary people in talks, reasoning and decision-making process. Observing definitions above, we may conclude that trust is a subjective category, and being apparently fuzzy it can be associated with verbal assessment values (granules). The vagueness of the trust is linked outright to uncertainty of reputation as well.

III. Uncertainty in marketplace data. Verbal assessments are very natural in reputation systems

The paper is focused on reputation systems as applied to e-commerce field (and specifically online marketplaces). Because of that it is essential to consider what kind of data concerning peers and their transactions are available, and what sort of data peer's feedback about fulfilled transaction contains. In online marketplaces there are two types of peers – they are sellers and buyers; every transaction implies participation of one seller and one buyer. It is important to distinguish these types of 'players', because they gain trust and reputation that differ by their gist. In the present work we consider three types of marketplace data:

(1) *Peer data*, i.e. a set of general data pieces that relates to peer itself (personal data, registration date, etc.),

(2) *Transaction data* – general data about transaction held between seller and buyer (delivery time, payment time, total sum of transaction, date of transaction, etc.),

(3) *Feedback data* refer to data collected from both seller and buyer after completion of each transaction (goods quality, communication quality, shipping service reliability, etc.).

Most of the existing reputation systems work only with peer's feedback [6,10,11,16,27]. In general, feedback provides some subjective assessment of experience that a peer has with another peer in the course of transaction's realization. But in certain cases, such experience cannot be thoroughly expressed in terms of integers -1, 0 and +1 as it occurs in eBay system. Why do we think so? Firstly, regarding feedback as a number means neglecting diverse aspects of experience such as those mentioned above. Secondly, and this fact was also underlined earlier, it is more natural for humans to think of evaluating experience in terms of some ordinal scale stretching from "very bad" label to "very good" instead of using "good", "neutral" or "bad" plain marks as linguistic equivalents of -1, 0 and +1. It should be emphasized that in case of extended scale' use, its grades may overlap with each other, since each label or grade stands not for a single value, but for a range of values instead. For instance, there is no clear-cut border line between values (labels) "very bad" and "bad", but almost all people may differentiate these values mentally while talking about them, impacting information chunks to others.

Similar situation comes to pass with reference to transaction data. For example, let us consider delivery time of basic electronic accessories from Moscow to Saint-Petersburg. We know that they are normally delivered within N days. Is it "quickly", "slowly" or "neither slowly, nor quickly" for a client? Maybe it is a little bit slowly, but not too much? What can be said about N+2, 2N days or even 5N days? At some point it becomes obvious that delivery time can be associated with label "slowly" or even "very slowly". But what do we mean by that *some point*? For different people it occurs at different moments, which are not fixed (crisp), and this is when imprecision and uncertainty (fuzziness) of these data reveal themselves.

IV. Fuzzy Logic theory. Some basic terms and definitions used in the study

Taking into account uncertainty inherent to notions of trust and marketplace data, we need to consider its formal representation for a possible use in trust management and reputation systems (models). The concept of uncertainty is many-sided and rich; furthermore, uncertainty 'accompanies' any interactions of humans with real world [34]. In this connection, reputation systems exemplify active communication of peers based on the exchange of information that is often a matter of human perceptions and interpretations to a various extent. Much depends here on cognition and verbal assessments expressed in the natural language. Such perceived units can be mostly seen as granules with 'soft' bounds rather than exact quantities having unified meaning and interpretation by all parties involved into the process. The theory of fuzzy logic (FL) extends the ontology of mathematical research in the context of formation of a composite methodology that leverages quality and quantity [9]. It provides ample means to model

the "perceived meaning of words/phrases conveying the expert opinions (estimates) in a graded fashion" [30]. The following is a quick glance at main concepts and definitions concerned with fuzzy logic as used in the present study.

Definition 1. *Linguistic variables* (LV) – variables whose values are words, phrases or sentences (linguistic terms) expressed in natural or artificial language [26]. In short, we can state that LV constitute a form of information granulation serving as a base for further transition of those granules to computable counterparts [31]. For example, if we consider the case of delivery time from point A to point B, the label (term) "quickly" is one of possible linguistic values assigned to the variable *Delivery Time*. Its whole term-set can be represented as $\mathbf{T}_{(Delivery\ Time)}$ = "quickly" + "very quickly" + "slowly" + "more or less quickly" + … , where sign '+' denotes the aggregate of linguistic granules rather than arithmetic sum operation.

Linguistic variable *Delivery Time* is defined on the universal set U (realistic range of numeric values representing the delivery time in particular situation), i.e. each element $x \in U$ stands for the time (minutes, hours, etc.) that can be associated as a result of human's perception (judgment) with corresponding terms to various degrees.

Definition 2. Let U be a set of elements (objects) that are denoted generically as x (U={x}); *fuzzy set* $A \subseteq U$ is a set of ordered pairs $\{(x, \mu_A(x))\}$, where mapping $\mu_A : x \to [0,1]$ is a (type-1) membership function of a fuzzy set A. Value $\mu_A(x)$ is a degree (grade) of membership of x in the set A, and U is a problem's domain (universal set). Membership function (fuzzy set) represents possibility distribution of x-values over domain U. It can be expressed as aggregation $\int_{x \in U} \frac{\mu_A(x)}{x}$ or union $\sum_{x \in U} \frac{\mu_A(x)}{x}$ of pairs $(x, \mu(x))$, $\mu(x) \in [0,1]$, in continuous and discrete cases, correspondingly.

Definition 3. Let A be a fuzzy set on U, then α-*cut* of A is a crisp (non-fuzzy) set A_α composed of all $x \in U$, whose grades of membership in A are greater or equal to α [26]. Formally, A_α can be expressed as $\{x \mid \mu_A(x) \geq \alpha\}$. A fuzzy set A may be decomposed into and restored from α-cut sets through the resolution identity [12, 13], i.e. $A = \int_0^1 \alpha A_\alpha$, or $A = \sum_\alpha \alpha A_\alpha$, $\alpha \in [0,1]$.

An integral part of any formal modeling approach is closely related to the use of functions. Along with pervasive processing of non-vague objects, fuzzy quantities in last three decades became wide-spread in algorithms covering enormous circle of application domains. The need to extend the possibility for functions to operate with arguments having the form of fuzzy sets has led to formulation of extension principle [26,32,33]. As its name speaks for itself, it is directed to spreading nonfuzzy mathematical concepts to fuzzy ones [4]. It is specifically what is required to handle aspects of uncertainty (fuzziness) with reference to existing reputation systems.

Definition 4. Assume f is a mapping from universal set U to set V, and A is a fuzzy set defined on U (for the sake of simplicity we may consider finite representation of such set, i.e. $A = \mu_A(x_1)/x_1 + \mu_A(x_2)/x_2 + ... + \mu_A(x_n)/x_n$). Relying on the *extension principle*, the image $f(A)$ of A under mapping f is obtained as follows:

$$f(A) = f(\mu_A(x_1)/x_1 + \mu_A(x_2)/x_2 + ... + \mu_A(x_n)/x_n) =$$
$$= \mu_A(x_1)/f(x_1) + \mu_A(x_2)/f(x_2) + ... + \mu_A(x_n)/f(x_n).$$

In other words, the image of A under f can be deduced from the knowledge of the images $f(x_1), f(x_2), ..., f(x_n)$.

Definition 5. The process of representing initial data (e.g. linguistic values) as membership functions is called *fuzzification*; most of applications require to perform at final stages the opposite translation from fuzzy functional forms to crisp values – this is achieved through *defuzzification procedures* [30,32,34,37].

V. Brief Comparison of Existing Reputation Systems – Their Differences and Intrinsic Similarities

The number of publications devoted to trust management and reputation systems is pretty imposing, and it is growing from year to year [10,11,16,17,24,25,27]. In the paper we wittingly touch upon (just brief overview augmented with performance considerations) the most significant systems that proved themselves as effective, robust and applicable to online marketplace reputation management. It is worth mentioning that only those systems that do not use basically fuzzy logic concepts are reviewed in the paper. For instance, systems that utilize fuzzy inference schemes or other fuzzy-logic related notions [9,18,19] constitute an interesting research topic, but on level with other relevant cases it is outside of the scope of the present paper.

Results of the conducted analysis of existing sources provided a basis for selection of those criteria that can be classified as crucial from the viewpoint of systems' comparison. They can be described concisely as follows:

(1) *Speed of convergence* – iterative algorithms form a core of nearly all reputation systems. Thus, one of important aspects of such algorithms is how fast they converge and produce a result. This feature is covered as a principal one in most of papers related to reputation systems [10,11,25,27],

(2) *Robustness*, i.e. the criterion concerned outright with the main purpose of every reputation system, namely, the prevention of malicious attacks. Therefore, it becomes essential to measure how well a given system is able to hold out against malicious peers' activities. Such experiments are covered by S.D. Kamvar, M.T. Schlosser, H. Kurdi, N. Chiluka, N. Andrade, Y. Wang, L. Xiong, et al. in [10,11,16,24,25,27]; however, it is important to mention that papers referenced here cover different types of malicious behavior,

(3) *Hyperparameters* – their presence is an important point to consider in the process of system's deployment, since

they show the extent, to which the system is customizable. But at the same time, factor of their presence is a 'double-edged sword', inasmuch as, on the one hand, tuning of hyperparameters may lead to better performance of a specific system. On the other hand, it enhances significantly the complexity of deploying the system,

(4) *Handling data imprecision and uncertainty*. Most of hypothetical or artificial systems do their work in the presence of uncertainty. The latter is often linked to human factor being an integral part of a system in the context of verbally defined and/or interpreted data. The latter are elicited from active discussions with stakeholders and estimations commonly used as inputs in calculations provided for algorithms underlying system's work specifics. Those pieces of information are often 'soft' (imprecise) in their nature, and it opens manifest way for the use of fuzzy logic theory in models of reputation systems. Hence, the comparison of algorithms can be performed in the view of how well system (algorithm) adapts fuzzy logic extension.

A. EigenTrust Algorithm

EigenTrust system is originally proposed for a P2P file-sharing network by S.D. Kamvar, M. Schlosser and H. Garcia-Molina in the paper that became one of the most cited papers on reputation systems [10]. EigenTrust calculates a global trust value for each peer based on his/her past behavior by incorporating opinions of all peers in the system [16]. Opinions concerning a particular peer are represented as a local trust value. After each communication peer assesses his/her experience by the value from restricted set comprised by integers -1, 0 or 1. The local trust value is an aggregation of all communication experience assessments. It was shown how to normalize local trust values in a way that leads to elegant probabilistic interpretation similar to the Random Surfer model and efficient algorithm to aggregate these values [10,14]. Pre-trusted peers that can be seen here as a hyperparameter (it must be chosen in advance for the whole system to operate) are used to guarantee convergence and breaking up malicious collectives. What is more, the choice of pre-trusted peers is important, and it can compromise the quality of system to a marked degree [10]. As also shown in [10], for a network with 1,000 peers the algorithm converges after completion of less than 10 iterations. Theoretical base for fast convergence of EigenTrust algorithm is discussed by T.H. Haveliwala and S.D. Kamvar in [21]. Robustness of the system is evaluated under several threat models, and the system shows good overall performance in all cases [10]. For both Individual malicious peers and Malicious collectives threat models, EigenTrust system outperforms non-trust-based systems showing five to eight times better results with fraction of inauthentic downloads (FID) less than 0.2 for every setting. For Malicious collectives with camouflage case (model 3), system shows slightly less impressive results, but still Malicious Spies threat model (fourth model) tends to be the best strategy for malicious peers to attack trust-based network [10].

As already mentioned earlier, EigenTrust system uses aggregated local trust values that must be normalized beforehand to avoid system's 'demolition' due to assignment of very high and very low local trust values [10]. Normalized local trust value c_{ij} can be calculated as follows:

$$c_{ij} = \max(s_{ij}, 0) \Big/ \sum_j \max(s_{ij}, 0)$$

where s_{ij} is a local trust value. The shown way of normalization isn't free of drawbacks. For one thing, normalized values don't draw a distinction between a peer with whom a given peer *i* did not interact and a peer with respect to whom peer *i* has had a poor (negative) experience. Secondly, c_{ij} values are relative, and they cannot be interpreted easily in the absolute sense [10]. Thus, an attempt can be made to extend EigenTrust algorithm with fuzzy logic notions to obtain transparent and interpretable modification of the original computational scheme. Particularly, calculation of local trust value may be altered to accumulate different types of marketplace data, but further study that concerns the impact of fuzzification on probabilistic interpretation of EigenTrust algorithm is required.

B. HonestPeer Algorithm

HonestPeer as an enhanced version of EigenTrust algorithm is discussed by H. Kurdi [11]. The algorithm endeavors to address one of the major problems with EigenTrust system, viz. pre-trusted peers. HonestPeer minimizes the dependency on that pre-trusted set of peers by choosing one honest peer dynamically for every computation step of global trust value (GTV). This honest peer, i.e. the peer having the highest global trust value, plays a crucial role in further computations of GTV. The speed of HonestPeer's convergence is almost the same as for EigenTrust algorithm, despite the need to perform additional calculations. Following [11], two benchmarks are considered – they are EigenTrust algorithm and no algorithm. Performance of HonestPeer algorithm is estimated under different experimental settings embracing variable number of users and files as well as number of pre-trusted peers and with the examination of percentage of inauthentic file downloads by good peers and success rate of good peers (success rate of good peers equals the ratio of *#valid files received by good peers* to *#transactions attempted by good peers*).

HonestPeer algorithm surpasses EigenTrust in effectiveness and capability to 'help' good peers to download valid safe files. This fact can be attributed to the ability of HonestPeer to choose honest peers dynamically after each round, while in case of EigenTrust pre-trusted peers are chosen statically irrelative of their performance [11]. Since HonestPeer is basically an enhancement of EigenTrust algorithm, the use of fuzzy logic may be appropriate and explicable as a practical matter to address those forms of uncertainty that are typical for system under consideration.

C. PowerTrust Algorithm

The reputation system PowerTrust, which is based on power-law distribution of peer feedbacks discovered after examination of 10,000+ eBay users' transaction traces, is

covered by R. Zhou and K. Hwang [15,27]. In PowerTrust system a few power nodes are selected dynamically according to their reputation. These nodes can be dynamically replaced, if they become less active or demonstrate unacceptable behavior. Good reputation of power nodes is accumulated from the operation history of the system – functional modules of PowerTrust system as well as flow scheme that relates to collection of local trust scores and global reputation aggregation are visually demonstrated in [27]. Without going into particulars, it should be mentioned that raw data input for PowerTrust is treated as local trust scores, which are then aggregated to obtain global reputation score of each peer. The Regular Random Walk module supports the initial reputation aggregation, while Look-ahead Random Walk (LRW) module is used to update the reputation score periodically. LRW also works with Distributed Ranking Module to identify power nodes. The system leverages power nodes to update Global Reputation Scores (vector V) [27].

The experimental performance of PowerTrust in terms of reputation convergence overhead to measure aggregation speed, ranking discrepancy to measure the accuracy, and root-mean-square (RMS) aggregation error to quantify system's robustness to malicious peers shows that PowerTrust algorithm outperforms EigenTrust by more than factor 1.5 in case of convergence speed [27]. Under all settings PowerTrust exhibits its robustness against collusive peer groups of various sizes.

In much the same way as for both EigenTrust and HonestPeer, the point of fuzzy logic's application to PowerTrust algorithm is a local trust value. Several linguistic terms may be defined on [0,1] interval to be used consequently for computation of global reputation. It is of definite interest to research whether the use of fuzzy logic may affect properties of PowerTrust algorithm or not.

D. Absolute Trust Algorithm

The algorithm for aggregation of trust among peers in P2P networks (Absolute Trust algorithm) was presented by S.K. Awasthi and Y.N. Singh [17]. Most of reputation systems are built upon scenario when all peers evaluate other peers by way of assigning foregoing local trust values that are a subject for further aggregation aimed at obtaining peers global reputation scores. In general, three different types of evaluation scenarios (*one-to-many*, i.e. one person is evaluating many persons, *many-to-one* scheme, under which many persons are evaluating one person, and *one-to-one* case, which implies that one person is evaluating another person) can be identified. In an effort to strengthen feedback's reliability in many-to-one evaluation scheme, any evaluation provided must allow for the competence of evaluator (evaluating party in the system) in computations via proportional weight's factor. Global trust of j-th peer can be used by way of weight in aggregation of local trust scores in calculation of any given i-th peer's global trust. Thus, a set of peers communicating (providing services) to the i-th peer can be reduced to just one virtual representative. It results in obtaining one-to-one evaluation scheme, and the trust of a set will be dominated by peers having higher global trust [17].

The existence and uniqueness of global trust vector as an outcome of aggregation approach is proven in [17]. The closed-form peer's global trust expression lays a basis for direct comparison of global trust values calculated for any two peers in the system (network with N nodes). There is no theoretical explanation of fast algorithm's convergence, but experiments show that it converges fast (about 7 iterations for 100 peers in the network) [17].

Robustness of Absolute Trust algorithm is evaluated regarding behavior of EigenTrust and PowerTrust systems. Several network configurations are considered in [17] such as the ones under the presence of pure malicious peers, peers with unpredictable behavior as well as malicious collectives (groups of peers whose familiarity positively affects their own reputation values diminishing corresponding values of persons outside such groups). It was shown that for first two configurations the performance of Absolute Trust improves significantly as compared to counterparts (by appr. 2% to 4% of authentic transactions that relate to exchanging files between peers, respectively). As concerns malicious collectives, performances of algorithms are almost identical, with marginal superiority of Absolute Trust over its aforesaid rivals.

The local trust metric in this algorithm can be defined in many ways, and it forms prospects to develop a fuzzy local trust metric. It is worth mentioning that aggregation procedure used in the algorithm can be practically retained. The customizable local trust metric allows to use fuzzy logic approach to extend the algorithm in relatively easy and natural way.

E. PeerTrust Algorithm

PeerTrust is another example of P2P reputation system designed specifically for e-commerce communities that are characterized by distinctive problems and risks [25]. L. Xiong and L. Liu identify five important factors that relate to evaluation of peer's trustworthiness as regards supplying other peers with corresponding services. These factors are feedback obtained by a peer, feedback scope (e.g. total number of transactions occurred between peers), credibility of feedback source, transaction context aimed at drawing distinction between extremely crucial and less important or uncritical transactions, and community context to address community-wide characteristics and vulnerabilities. Based on formalization of these parameters, the authors proposed a peer's j trust value (metric) $T(\mathrm{j})$ consisting of two parts [25]. The first one is a weighted multiplicative combination of amount of satisfaction peer obtained after realization of each transaction, adaptive transaction context for i-th transaction of a peer and credibility of the feedback received from peers. Community context factor constituting the second part of $T(\mathrm{j})$'s expression increases or decreases the impart of the first part to trust value owing to allowance of distinctive community's features.

As it is emphasized in [25], the proposed metric $T(\cdot)$ should be considered as a general form, in which corresponding parts can be 'tuned' in terms of parameters and factors used. Every part of the metric can be implemented differently – alternatives of possible credibility measure metrics (trust value/TVM, personalized similarity/PSM) are presented by L. Xiong and L. Liu in

their paper.

Speed of convergence and complexity of PeerTrust algorithm appreciably depend on metrics definitions and specific implementation strategies. In general, the performance of system under PSM metric is a bit worse than in case of TVM, but on the other hand, the former provides better results as the number of peers in the network is increasing. System's robustness is assessed on the grounds of effectiveness against malicious behavior of peers comparing to conventional algorithm, in which the average of the ratings is used to measure the trustworthiness of a peer without taking into account the credibility factor. The trust computation error as a root-mean-square error (RMSE) of the computed trust value of all peers and the actual likelihood of peers performing a satisfactory transaction is computed to evaluate the performance of the algorithm. PeerTrust with PSM metric ensures striking results as calculated RMSE does not exceed the value of 0.05, and transaction success rate attains virtually unity.

It must be admitted that PeerTrust system is very flexible over the existing possibility to choose local trust metric. Therefore, it seems that the practical application of fuzzy logic approach to handle naturally nascent uncertainty (vagueness) of certain parameters and characteristics in the algorithm looks justified enough. The system also possesses a great potential to incorporate all types of marketplace data, especially through transaction and community context parts of the general metric $T(\cdot)$ that afford means of broad coverage of manifold system's peculiarities.

VI. Experimental part – setup stage

For the experimental part of the study, we implemented a simulator (in Python 3.7), and the section describes the general simulation setup, including the community setting, peer behavior pattern, and trust computation.

We assume that hypothetical (simulated) community consists of N peers, for which two peer types are defined, namely, they are *honest* and *strategic*, or malicious, peers [35]. The first one embraces those commitment long-run players focused on cooperation, since the latter maximizes player's lifetime payoffs, if the player consistently sticks to action in long-range outlook. In contrast, opportunistic player who cheats whenever the occasion is beneficial for him is bound to a strategic type [25]. The percentage of malicious peers in the community we denote by K. It is reasonable that behavior pattern of good peers is to always cooperate and provide honest feedback after each transaction. However, a correct modeling of malicious peers behavior is a bit challenging task that may require certain simplifications. In particular, we may consider that malicious peers always cheat during transactions and give dishonest ratings to other peers, i.e. they rate negatively a peer who cooperates and provides good rating to a peer who cheats. In case of EigenTrust and HonestPeer algorithms there are also pre-trusted peers that play an important role from the standpoint of algorithm's consistency. Respective PRE_TRUSTED parameter stands for the percentage of pre-trusted peers that relate to good peers only. In general, *behavior pattern of peers* is a topic on a slippery ground, i.e. it can be placed among those aspects of models of reputation systems that require close scrutiny. Why? Potentially, the above cited pattern is definitely not unique, so in order to make models viable other feasible options must be addressed hereafter with great care.

We may also assume that community has CAT categories of services that are provided by peers. From amongst these categories each peer is interested only in a specific subset having the cardinality not less than S. Each category is associated with at least P percent of peers in the community. When a peer queries a service of a specific category, only peers associated with this category can respond to such query. At that, two transaction settings are simulated – they are random and trusted. Random (or, *simple*) setting means that a peer, which responds to the query, is selected randomly (uniform distribution is used) from a set of all peers that can provide queried category of service. In trusted setting the responder is also selected randomly from all peers that can respond to the query, but it is done with respect to their reputation, i.e. a peer with higher reputation has better chances to be chosen. If there are peers with zero reputation, then there is a 10% chance that the responding peer will be chosen uniformly from those peers. It efforts the opportunity for new peers to start building up their reputation.

Binary feedback system is used to evaluate peer after each completed transaction. It means that values 0 and 1 are practised for PeerTrust and Absolute Trust algorithms, -1 and 1 are used in cases of both EigenTrust and HonestPeer approaches. Local trust and reputation computation steps as such depend on the algorithm in use. Some algorithms have their own hyperparameters that must be specified. Default values of parameters are listed in Table I. Simulation session (cycle) consists of SIM_NUM transactions. Global reputation is updated after every UPDATE_NUM transactions. Experimental results are averaged by 5 cycles of simulation. Although we simulate online marketplace community – usually it is big enough, dozens to hundreds of thousands of peers – experiments are performed under the presence of modest number of peers. It may be considered as a perceptible limitation, however, the main aim of simulation is to obtain those *prior* results that lay down the ground for further analysis of weak/strong points of models considered here in terms of deeper understanding of their potential to incorporate formal representation of uncertainty (imprecision) factors into these models. In real-life environment it seems highly unlikely that the major part of marketplace peers are malicious as it was defined earlier. Therefore, we don't consider in simulation a malicious peers share exceeding 35%.

VII. Experimental part – results and their comparison

We introduce a metric that shows the effectiveness of the reputation system as a rate of unsuccessful transactions (RUT). The unsuccess of transactions is bound up with the outcome of those transactions, in which responding peer happens to be malicious. It is obvious that the less value of the metric is the better. Besides, for the time being we *do not* consider PowerTrust algorithm in the empirical study, since it requires more close inspection and implementation cycle.

A. *Effectiveness against malicious behavior*

The objective of conducted experiments is to evaluate the robustness of the reputation systems against peers with malicious behavior. In the first experiment we alter the percentage of malicious peers in hypothetical community from 10% to 35% with other parameters keeping their default values (Table I). As is easy to see in Fig. 1, the rate of unsuccessful transactions grows almost linearly with the increase of values (axis x) for simple setting; trusted settings

TABLE I. PARAMETERS AND THEIR VALUES USED IN EXPERIMENTS

Affiliation with…	Parameter	Description	Default value
Community setting	N	number of peers	1000
	K	percentage of malicious peers	15
	CAT	number of categories	10
	S	minimal number of categories for each peer	3
	P	minimal percentage of peers associated with each category	5
Simulation setting	SIM_NUM	number of queries in a simulation	10000
	UPDATE_NUM	number of transactions in reputation update cycle	100
EigenTrust & HonestPeer	PRE_TRUSTED	percentage of pre-trusted peers	5
Absolute Trust	GOOD_W	weight of good transactions in local trust	10
	BAD_W	weight of bad transactions in local trust	1
	α	trade-off parameter between speed of convergence and quality	1/3

show better results though. EigenTrust, HonestPeer and PeerTrust algorithms show extremely moderate growth of RUT with the increase of malicious peers' percentage. Absolute Trust algorithm demonstrates quite disappointing results characterized by negligible gain (within appr. 2.1% on average) as compared to simple (random) system's case.

B. *Speed of convergence and scalability*

In this set of experiments, we take aim at evaluating the general speed of algorithms convergence and their scalability with regard to the increase of number of peers (Fig. 2). As will readily be observed, algorithms PeerTrust and Absolute Trust generally need not more than 2 iterations to converge, while EigenTrust and HonestPeer need to go through 4+ iterations. More than twofold difference on very small values practically equalizes rivals under the conditions of experiment. Thus, all algorithms seem to be quite scalable concerning the number of iterations needed to converge, since the latter does not grow substantially with the increase (from 1,000 to 3,500) of number of peers in the community.

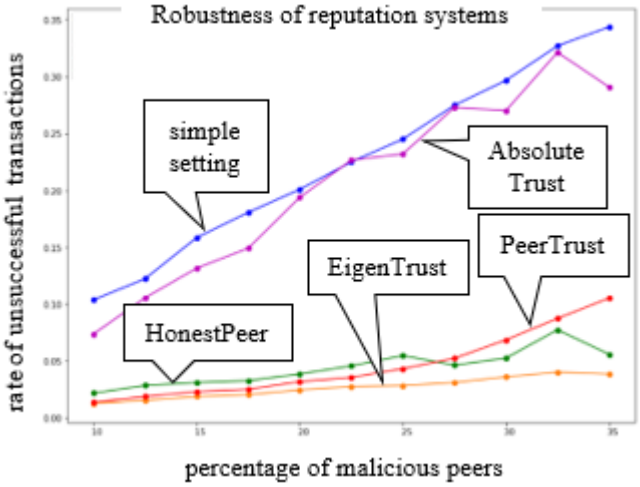

Fig. 1. The growth of rate of unsuccessful transactions depending on the increase of malicious peers' percentage (from 10% to 35%) for different algorithms

We also evaluate how consistent corresponding systems are against the background of increasing number of peers under "freezing" of other parameters (Fig. 3). It can be seen that situation remains almost indistinguishable be it small or bigger community – the rate of unsuccessful transactions mostly remains unchanged in the context of the same malicious peers percentage.

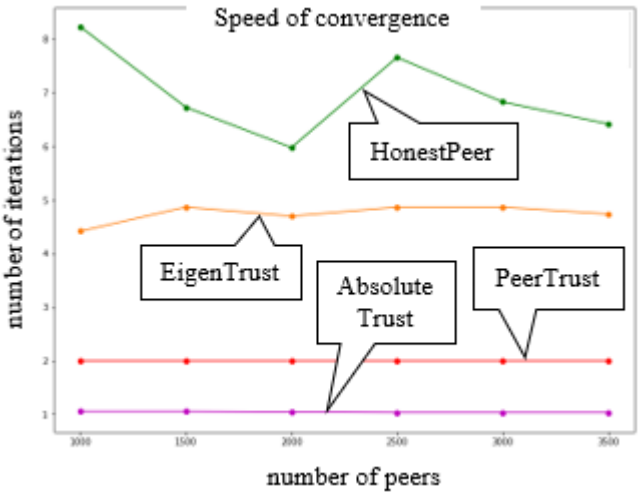

Fig. 2. The speed of convergence (number of iterations needed) of algorithms depending on the number of peers (in the range from 1,000 to 3,500)

C. *Choice of the "best" (most feasible) system*

According to the results of experiments summarized above as well as constraints and assumptions put forward, PeerTrust model appears the most robust and effective

reputation system among alternatives. It is quite stable regarding the growth of percentage of malicious peers in the community and scalable enough to handle evenly larger number of peers. What is more, local trust metric in PeerTrust system is highly customizable, and this fact simplifies the possibility to extend it with fuzzy factors in here in reputation systems. In a wide sense we can talk about *marketplace data uncertainty* that requires much attention in further development of the topic and elaboration of formal aspects of models. Thus, in this instance we opt for PeerTrust system with the object of its modification on the basis of Zadeh's extension principle.

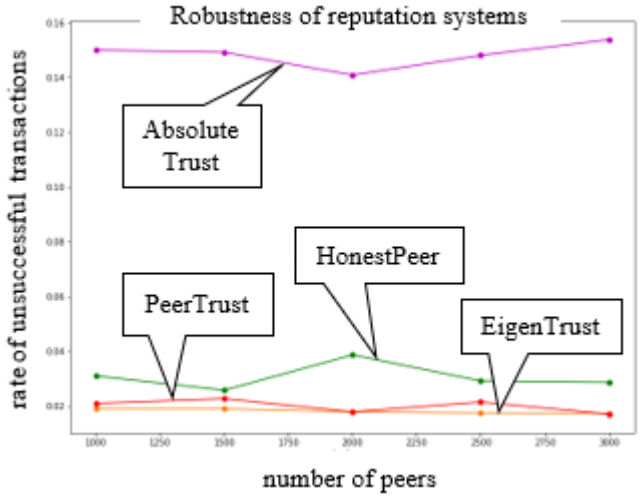

Fig. 3. The robustness (rate of unsuccessful transactions) of algorithms depending on the number of peers (in the range from 1,000 to 3,500)

VIII. Transition from crisp PeerTrust system to fuzzy PeerTrust system. Is it worthy of notice?

In order to implement fuzzy reputation system, we need to understand above all what data will be represented by fuzzy sets (numbers). In non-fuzzy version of PeerTrust algorithm binary feedback system is used. We suggest utilizing a broader scale to express degrees of satisfaction concerning transaction. It naturally arises from peculiarities of human's perception of information (comments, judgments) – it is not a very convenient and alluring way for humans to think in terms of zeros and ones (or, any other numbers). For the human mind such terms as "bad", "normal" and other resembling options look more understandable and well-suited for interpretation and processing. Being guided by this observation, the new algorithm's feedback can be represented by five verbal degrees of satisfaction, namely, they are *"very bad"*, *"bad"*, *"normal"*, *"good"* and *"very good"*. More fine granulation does not look preferable here, because it may lead to certain confusion in view of human perception of satisfaction's shades – the magic number 7±2 and the seminal paper (1956) by American psychologist George A. Miller on limits on our capacity for processing information straight away cross our mind.

Such verbal terms are treated as linguistic values of the variable *"degree of satisfaction"* or *"transaction quality"*; each value can be formally represented by trapezoidal membership function on universe of discourse U=[0, 1] as shown in Fig. 4. The type (e.g. Gaussian, bell-shaped, etc.) and the location of fuzzy sets on U may vary noticeably depending on estimates provided by expert group with reference to characteristic features and implicit shades of model under consideration [26]. The rest of the algorithm remains unchanged, and all specified operations are carried out with fuzzy numbers (intervals) instead of crisp values till the attainment of the defuzzification stage. Defuzzified reputation values are used to choose the responding peer exactly in the same way as described above. In the paper centroid method (COA) is used to obtain those values, but effectiveness and performance of the algorithm may depend distinctly on the chosen defuzzification approach [30,32].

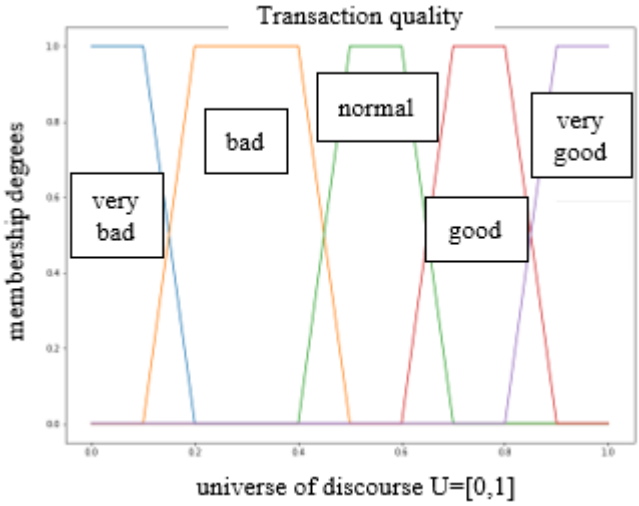

Fig. 4. Linguistic values (trapezoidal membership functions) of the variable 'Transaction quality' (universe of discourse U=[0,1])

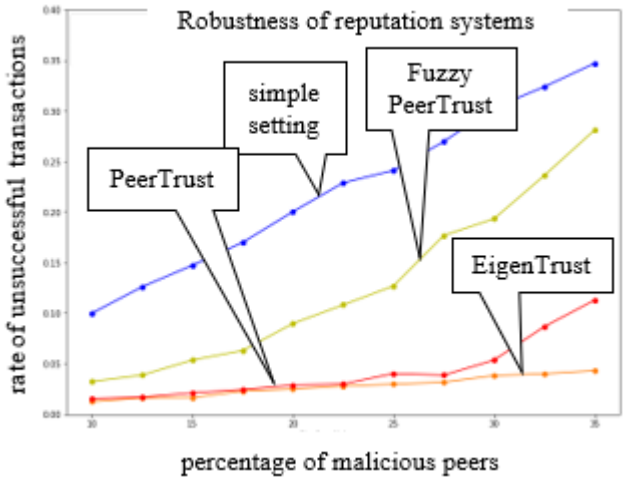

Fig. 5. The growth of rate of unsuccessful transactions depending on the increase of malicious peers percentage (from 10% to 35%) for EigenTrust, PeerTrust and Fuzzy PeerTrust algorithms

Here, special attention should be paid to the following: in the paper we consciously consider only one type of data falling under fuzzification, viz. the feedback regarding a buyer. Primarily it is connected with the amount of required modifications and scope of computational experiments to be

covered by the text of the limited size. But we are aware that other foregoing types must be addressed thoroughly in the course of the ongoing empirical study.

In conditions of maintenance of community and simulation settings (see the details of conducted experiments described above), but under the imprecision (vagueness) taken into account in the feedback system, we compare the experimental components of Fuzzy PeerTrust with original PeerTrust and EigenTrust algorithms.

A. Effectiveness against malicious behavior (fuzzy case)

In the first place, we want to evaluate the robustness of fuzzy modification of PeerTrust system. Experiment settings are retained, the percentage of malicious peers is changing within the range from 10% to 35%. The results as shown in Fig. 5 lead to the conclusion that Fuzzy PeerTrust algorithm is definitely more robust in comparison with Simple system. Under small percentage values (appr. interval [10%,17%]) of malicious peers, the performance's characteristic of Fuzzy PeerTrust is close enough to original PeerTrust and EigenTrust. However, it demonstrates worse results than crisp algorithms over the whole range of x-axis values concerned.

B. Speed of convergence and scalability

Another set of experiments was aimed at estimation of the speed of convergence of Fuzzy PeerTrust and its scalability in view of the community's growth. As expected, the speed of convergence remains the same as for original PeerTrust with two iterations on average to converge, and it differs essentially from corresponding characteristic (appr. 4.61 on average) of EigenTrust algorithm (Fig. 6). In terms

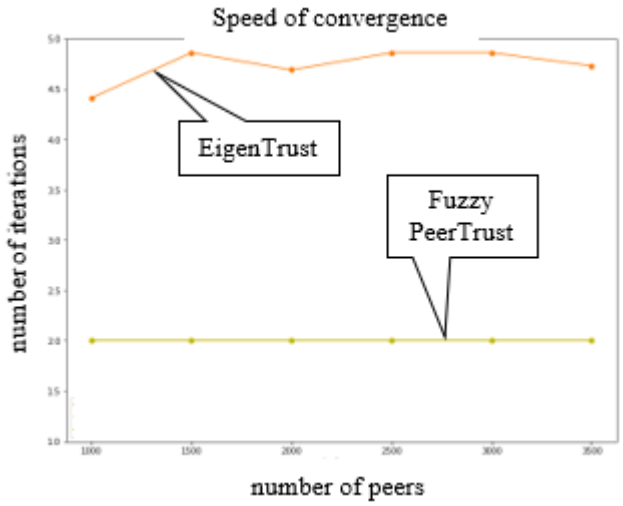

Fig. 6. The speed of convergence (number of iterations needed) of EigenTrust and Fuzzy PeerTrust algorithms depending on the number of peers (in the range from 1,000 to 3,500)

of robustness Fuzzy PeerTrust can also be pronounced scalable, since it does not show significant decrease in quality with the growth of the number of peers in the community (Fig. 7). We observe here smooth fluctuations of RUT at the level of 0.064. It is worth mentioning that all properties of crisp algorithm remain intact in comparison with its fuzzy counterpart.

Computational procedure starts with default trust vector $t^0 = \left(t_1^0, t_2^0, ..., t_N^0\right)^T = \left(\frac{1}{N}, \frac{1}{N}, ..., \frac{1}{N}\right)^T$, where N – the number of peers in the community, t_v^0 is a default trust value of a peer v, $v = \overline{1, N}$ [25]. Reputation of a peer v in the form of fuzzy set (number) is denoted as $fuzzy\left(t_v^{i+1}\right)$; $fuzzy\left(S(v, j)\right)$ stands for a feedback of peer v concerning j-th transaction, it is also represented as a fuzzy number; $defuzz(\bullet)$ signifies the reduction of a fuzzy argument to crisp value (deffuzzification step). To calculate the product of fuzzy number $fuzzy\left(S(v, j)\right)$ and crisp number $t_j^i \Big/ \sum_{k=1}^{I(v)} t_k^i$ as well as the sum (1) of thus obtained fuzzy numbers, Zadeh's extension principle is used [4,36,37]. As a result, steps to be performed (pseudocode) can be expressed as follows:

Repeat

For $v = 1$ to N do

$$fuzzy\left(t_v^{i+1}\right) = \sum_{j=1}^{I(v)} fuzzy\left(S(v, j)\right) \cdot \frac{t_j^i}{\sum_{k=1}^{I(v)} t_k^i} \quad (1)$$

$$t_v^{i+1} = defuzz\left(t_v^i\right) \quad (2)$$

$$\text{diff} = \left\| t^{i+1} - t^i \right\|$$

Until diff $\le \varepsilon$

As already mentioned, it is significant to put special emphasis on the choice of defuzzification method to use in (2). It may become a subject of separate research in the future.

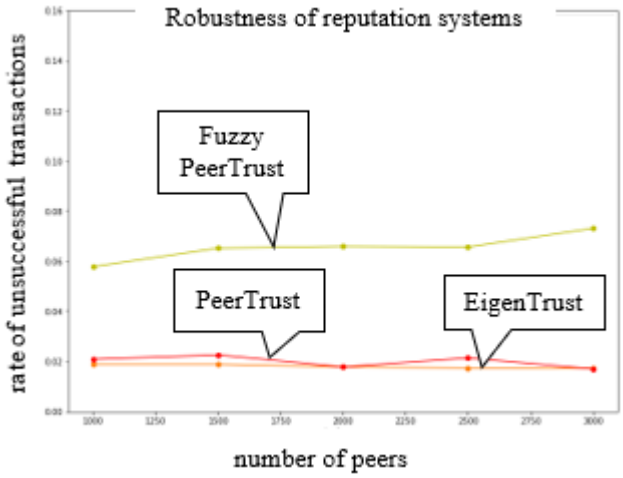

Fig. 7. The growth of rate of unsuccessful transactions depending on the number of peers (in the range from 1,000 to 3,500) for EigenTrust, PeerTrust and Fuzzy PeerTrust algorithms

At the same time, an important point of the algorithm shown is that certain aforesaid attributes of trust and reputation like context-awareness (sensitivity), decrease (of the level) with time, their multifaceted nature (diversity) are not taken into account. We may regard this version of the algorithm as *basic* one (or, *F-basic* if we consider factor of

fuzziness in its core); it paves a 'wide' way for algorithm's further revision and improvement.

The results attained enable to speak decidedly about the existing perspectives of fuzzy logic approach's application in reputation systems (corresponding algorithms). Even despite somewhat higher computational costs compared to original crisp algorithms, greater transparency, better perceptibility by humans and flexibility from a viewpoint of verbal expression and formalization of the scores provide a basis for further studying of the topic. The present paper can be considered as a mere first step in this direction.

IX. Conclusion

E-commerce is a fast-growing market that implies continual and utterly active communication between users being 'strangers' to each other on numerous occasions. Because of that it is essential to establish *reputation systems* to better handle available online information with the object to more accurately discern trustworthy and non-trustworthy players in systems creating grounds for peers to be more careful about their reputation. By the far-famed example of eBay reputation system, even relatively simple ones show themselves as very helpful from the viewpoint of malicious behavior's limitation and trustability increase. Online marketplaces that became immensely popular in the last 10-15 years as sites offering wide enough range of reasonably priced goods from various sources can be also considered as P2P networks. There is a vast range of reputation systems developed for P2P networks (mostly aimed at file-sharing) that can be adapted to e-commerce.

The main problem that is covered in the paper relates to the fact that none of these systems work with uncertainty (blurriness) of marketplace data and vagueness typical for notions of trust and reputation. Uncertainty in different forms of its manifestation is definitely inherent in reputation systems, and some of those forms can be addressed by fuzzy logic. This very inhesion, but not disconfirmed artificial desire, has served as an impellent factor to start this study.

Most likely, it can be argued that it is difficult to identify on the basis of several singled out key criteria unconditional leader among analyzed systems (algorithms EigenTrust, Absolute Trust, HonestPeer, PowerTrust and PeerTrust), since each of them has positive aspects as well as drawbacks. All algorithms, except PowerTrust, were implemented (Python 3.7) under the same conditions discussed in detail in the paper with the purpose of comparing fairly their relative performance. For reasons partially covered in the paper, Absolute Trust and PeerTrust systems were prudently regarded from the standpoint of their robustness and scalability as front-runners, i.e. candidates for fuzzification. Besides undertaking comparative analysis of those five significant and most popular reputation systems, the paper makes a mark for transition from crisp system (by the example of PeerTrust algorithm) to its fuzzy counterpart.

Corresponding fuzzy model (we call it provisionally *F-basic* algorithm) considers now only one characteristic of trust and reputation, namely, it is transaction quality or degree of peer's satisfaction. Other important attributes like context-awareness (sensitivity) or decrease of trust's level with time were not scrutinized yet. Nevertheless, initial experimental results attained in line with the fact of constant presence and active use of verbal assessments in reputation systems confirm the need to continue research in this field. Verbal forms are both habitual and convenient for human's perception despite of their intrinsic vagueness. That is why, fuzzy logic approach, to the opinion of authors, has good prospects for use in reputation systems.

At the same time, it should be mentioned that there are immediate tasks related to fuzzy models that require primary attention. The choice of membership functions and their fine tuning (shape and location on the universe of discourse), the switch from the case having dealings with marketplace data vagueness (so-called type-1 fuzzy sets used in the paper) to the case that represents uncertainty (interval type-2 fuzzy sets) and the choice of defuzzification strategy are amongst the most topical ones.

References

[1] Alam F., Paul, A., 2016. A Computational Model for Trust and Reputation Relationship in Social Network // Proc. 5th International Conference on Recent Trends in Information Technology, 1-6.

[2] Alfarez A.-R., Hailes, S., 2000. Supporting Trust in Virtual Communities // Proc. 33rd Annual Hawaii International Conference on System Sciences, 1-9.

[3] Kreps D.M., Wilson, R., 1982. Reputation and Imperfect Information // Journal of Economic Theory, vol. 27, 253-279.

[4] de Barros L.C., Bassanezi R.C., Lodwick W.A., 2017. The Extension Principle of Zadeh and Fuzzy Numbers. In: A First Course in Fuzzy Logic, Fuzzy Dynamical Systems, and Biomathematics (Studies in Fuzziness and Soft Computing), vol. 347, Springer, Berlin-Heidelberg

[5] Gambetta D., 1980. Can We Trust Trust? Chapter - Trust: Making and Breaking Co-operative Relations, 213–237, Dept. of Sociology, University of Oxford

[6] eBay, 2019. web-resource: www.ebay.com (access date 15.03.2019).

[7] Forbes.com, 2017. What Are Online Marketplaces and What Is Their Future? web-resource: https://www.forbes.com/sites/richardkestenbaum/2017/04/26/what-are-online-marketplaces-and-what-is-their-future/#704431c13284 (access date 06.02.19).

[8] Hussain J.K., Hussain O.K., Chang E., 2007. An Overview of the Interpretations of Trust and Reputation // Proc. IEEE Conference on Emerging Technologies and Factory Automation (EFTA-2007), 826-830.

[9] Zhang J., 2009. Trust Management Based on Fuzzy Sets Theory for P2P Networks // Proc. WRI World Congress on Software Engineering, 461-465.

[10] Kamvar S., Schlosser M., Garcia-Molina H., 2003. The EigenTrust Algorithm for Reputation Management in P2P Networks // Proc. 12th Int. Conference on World Wide Web, 640-651.

[11] Kurdi H., 2015. HonestPeer: An Enhanced EigenTrust Algorithm for Reputation Management in P2P Systems // Journal of King Saud University - Computer and Information Sciences, vol. 27, no. 3, 315-322.

[12] Zadeh L.A., 1972. Fuzzy Languages and Their Relation to Human and Machine Intelligence // Proc. Int. Conference on Man and Computer, 130-165.

[13] Zadeh L.A., 1971. Similarity Relations and Fuzzy Orderings // Information Sciences, vol. 3, no. 2, 177-200.

[14] Page L., Brin S., Motwani R., Winograd T., 1998. The PageRank Citation Ranking: Bringing Order to the Web, Technical Report, Stanford Digital Library Technologies Project.

[15] Faloutsos M., Faloutsos P., Faloutsos C., 1999. On Power-Law Relationship of the Internet Technology // Proc. ACM Conference on Applications, Technologies, Architectures, and Protocols for Computer Communication (SIGCOMM-1999), 251-262.

[16] Chiluka N., Andrade N., Gkorou D., Pouwelse J., 2012. Personalizing EigenTrust in the Face of Communities and Centrality Attack // Proc. IEEE 26th Int. Conference on Advanced Information Networking and Applications, 503-510.

[17] Awasthi S.K., Singh Y.N., 2016. Absolute Trust: Algorithm for Aggregation of Trust in Peer-to-peer Networks, web-resource: http://arxiv.org/abs/1601.01419 (access date 17.03.2019).

[18] Rao S., Wang Y., Tao X., 2010. The Comprehensive Trust Model in P2P Based on Improved EigenTrust Algorithm // Proc. Int. Conference on Measuring Technology and Mechatronics Automation, 822-825.

[19] Song S., Hwang K., Zhou R., Kwok Y.-K., 2005. Trusted P2P Transactions with

Fuzzy Reputation Aggregation // IEEE Internet Computing, vol. 9, no. 6, 24-34.
[20] Statista, 2018. Global Retail E-commerce Market Size 2014-2021, web-resource: https://www.statista.com/statistics/379046/worldwide-retail-e-commerce-sales/ (access date 08.02.19).
[21] Haveliwala T.H., Kamvar S.D., 2003. The Second Eigenvalue of the Google Matrix, Technical Report, Stanford University.
[22] The Next Scoop, 2018. 2019 E-commerce Trends, Statistics and Metrics, web-resource: https://thenextscoop.com/ecommerce-trends-statistics-and-metrics-2019/ (access date 14.02.19).
[23] The Next Scoop, 2018. E-Commerce is Growing at an Unprecedented Rate All over the Globe - The Next Scoop, web-resource: https://thenextscoop.com/e-commerce-is-growing-at-an-unprecedented-rate-all-over-the-globe/ (access date 17.02.19).
[24] Wang Y., Vassileva J., 2003. Bayesian Network Trust Model in Peer-to-Peer Networks // Int. Workshop on Agents and P2P Computing (Lecture Notes in Computer Science, vol. 2872, 23-34).
[25] Xiong L., Liu L., 2004. PeerTrust: Supporting Reputation-Based Trust for Peer-to-Peer Electronic Communities // Proc. IEEE Transactions on Knowledge and Data Engineering, vol. 16, no. 7, 843-857.
[26] Zadeh L., 1975. The Concept of a Linguistic Variable and Its Application to Approximate Reasoning – I // Information Sciences, vol. 8, no. 3, 199-249.
[27] Zhou R., Hwang K., 2007. PowerTrust: A Robust and Scalable Reputation System for Trusted Peer-to-Peer Computing // Proc. IEEE Transactions on Parallel and Distributed Systems, vol. 18, no. 4, 460-473.
[28] Statista, 2018. E-commerce Share of Total Retail Sales in United States from 2013 to 2021, web-resource: https://www.statista.com/statistics/379112/e-commerce-share-of-retail-sales-in-us/ (access date 26.02.19).
[29] English Oxford Living Dictionaries, web-resource: https://en.oxforddictionaries.com/ (access date 04.03.19).
[30] Semenkovich S., Kolekonova O., Degtiarev K., 2017. A Modified Scrum Story Points Estimation Method Based on Fuzzy Logic Approach // Proc. of the Institute for System Programming, vol. 29, no. 5, 19-38.
[31] Zadeh L. A., 1994. Fuzzy Logic, Neural Networks and Soft Computing // Communications of the ACM, vol. 37, no. 3, 77-84.
[32] Zimmermann H.-J., 2001. Fuzzy Set Theory – and Its Applications, 4th ed., Springer Science+Business Media, LLC.
[33] Zadeh L.A., 1965. Fuzzy Sets // Information and Control, vol. 8, no. 3, 338-353.
[34] Çelikyılmaz A., Türkşen I.B., 2009. Modeling Uncertainty with Fuzzy Logic. With Recent Theory and Applications (Studies in Fuzziness and Soft Computing, vol. 240), Springer-Verlag Berlin Heidelberg.
[35] Dellarocas C., 2003. The Digitization of Word-of-Mouth: Promise and Challenges of Online Reputation Mechanism // Management Science (Special Issue on E-Business and Management Science), vol. 49, no. 10, 1407-1424.
[36] Klir G., Yuan B., 1995. Fuzzy Sets and Fuzzy Logic Theory and Applications, Prentice-Hall/Upper Saddle River.
[37] Ross T.J., 2010. Fuzzy Logic with Engineering Applications, 3rd ed., John Wiley & Sons.

THE APPLICATION OF MACHINE LEARNING TO IMPROVE THE EFFICIENCY AND MANAGEMENT OF OIL WELLS

Zayar Aung
Applies Mathematics and Informatics
National Research University
Moscow Power Engineering Institute (MPEI)
Moscow, Russian
zayaraung53@gmail.com

Mihailov Ilya Sergeevich
Applies Mathematics and Informatics
National Research University
Moscow Power Engineering Institute (MPEI)
Moscow, Russian
fr82@mail.ru

Abstract: ***The article deals with the application of the method of data mining - support vector machine (SVM) to solve the practical problem of evaluating the efficiency of oil wells. This nonlinear method shows better analysis results than the linear regression (LR) method, which is also a machine learning method. The paper presents and analyzes the principles of solving the classification problem using logistic regression methods and support vector machines. The experiments calculated and compared the accuracy of these two algorithms under the same conditions.***

Key words: machine learning; data mining; support vector machine; oil wells.

I. INTRODUCTION

The development of digitalization of the parameters of oil wells, as sources of values of steam meters for mass production, and methods of data collection in real time, allows to optimize the process of oil production [1]. The use of machine learning for cleaning, integration, data transformation, application development and optimization of oil well data analysis is a new scientific approach to solving the problem of oil well performance analysis. Currently, the parameters of oil wells used in the data analysis algorithm are relatively simple, provided there are no parameters that depend on other groups of parameters, and standard methods for calculating the data evaluation [2-3]. The article proposes a nonlinear algorithm of SVM classification, construction of the structure of the data development system and the model of polyphyletic parameters recognition using SVM through the map of the space of features of high dimension and optimized hyper plane classification to solve the problem of nonlinear parameters analysis of oil wells and pattern recognition of parameters values sets of wells, reflecting their current state.

II. POLYPHYLETIC MODEL PARAMETERS OF PATTERN RECOGNITION OF OIL WELLS

In the process of oil production, the monitoring centre collects, transmits, analyses and provides real-time data on liquid and gas consumptions of oil well production, production water cut, pressure, temperature, electrical voltage, electric current and load, as well as other primary parameters, which helps the administrator to understand the operating conditions of the oil well and ensure its operation in the mode of high efficiency and low operating consumption [4-5]. As a rule, these parameters also include peak values of electric current and voltage, pump pressure, back pressure, oil pressure and pressure in the annular space of the well. This data is transmitted to the automated control system in real time. After performing a linear approximation and prediction of the data, the decision maker can assess the state of the well at the moment and predict its behaviour in the future, to take appropriate compensating control actions.

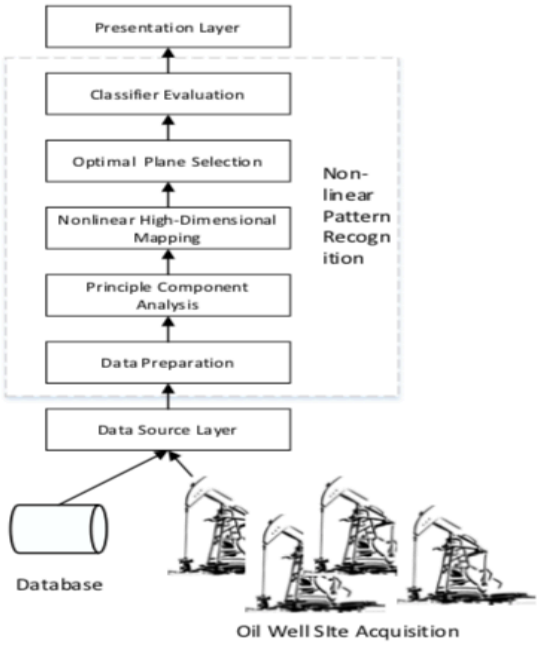

Figure. 1. Model recognition pattern of the state oil wells

Figure 1 shows the recognition process of the current situation in the oil well.

III. NONLINEAR SVM

The kernel method allows solving the problem of nonlinear classification by means of nonlinear transformation [6]. Provided that the input space is a Euclidean space and the feature space is a Hilbert space, the kernel method means the product of the feature vectors obtained by converting the input data from the input space to the feature space.

Using the method of kernels to explore non-linear data with the aim of obtaining the nonlinear SVM. The whole procedure is a work of the linear SVM method in a multidimensional feature space.

The kernel method is shown in figure 2.

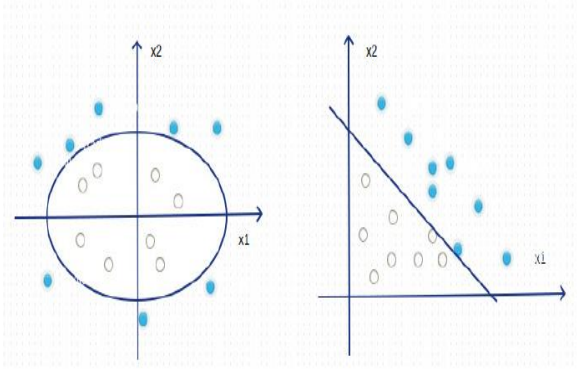

Figure. 2. Using the kernel method to solve a nonlinear problem

The General idea is to use a nonlinear transformation to change the input space into a feature space that can transform a hyper surface model in the source space into a hyper plane in the feature space. This means that the nonlinear classification problem in the source space it is transformed into a problem that can be solved by a linear SVM in the feature space.

IV. Support Vector Machine

The General idea of an SVM is to solve the problem of correctly classifying a set of data and maximizing a geometric field. There can be multiple separating hyper planes, but there is only one separating hyper plane with maximum geometric indentation. A direct explanation for maximizing the geometric field is that the hyper plane with the maximum geometric indentation derived from the classification is equal to classifying the training data by a sufficient certainty factor [7]. It is necessary not only to classify correctly, but also to separate the nearest points with a sufficient coefficient of reliability. This process can provide certain data with a good predictive ability called generalization ability.

When solving a nonlinear problem after converting to multidimensional space, it is usually difficult to find a hyper plane that can completely separate the data points, which means that there are some special points. But after removing these special points, most of the points become linearly separable. To solve this problem, we import the sliding variable into the training sample. In a soft-edged situation, the SVM learning task will look like:

$$min_{w,b,\varepsilon}\frac{1}{2}||w||^2 + C\sum_{i=1}^{N}\varepsilon_i. \quad (1)$$

$$\text{s.t. } y_i(wx_i + b) \geq 1 - \varepsilon_i. \quad (2)$$

Where C is the penalty parameter. Increasing C also increases the penalty for classification errors. You must adjust the target function to minimize the number of singular points while maximizing the offset from the hyper plane.

V. Linear logistic regression algorithm

The linear logistic regression algorithm is a classical classification method in the study of statistics related to the linear logarithmic model [8-9]. This classification model is a conditional probability distribution P (Y / X), which is a judgment model. It can be obtained from the linear regression model hw (x)= $W^T X$ and the sigmoid curve:

$$P(Y = 1|X) = \frac{1}{1+e^{-wx}}. \quad (3)$$

Where X is the input, Y is the output, W is the weighted coefficient, and WX is the internal product. The logistic regression distribution function and density function are shown in figure 3.

Figure. 3. Logistic regression distribution function and density function

Logistic regression compares the difference between two conditional probabilities and classifies the training example x into a larger probabilistic group. For the training set of data you can use maximum likelihood to estimate the parameters of the model to obtain the logistic model. The following assumptions are introduced.

$$P(Y = 1x) = f(x), P(Y\ 0 = x)\ 1 = f(x) \quad (4)$$

Likelihood function

$$\prod_{l=1}^{N}[f(x_i)]^{y_i}[1 - f(x)]^{1-y_i}. \quad (5)$$

Logarithm likelihood function

$$L(w) = \sum_{i=1}^{N}[y_i\ log\ f(x_i) + (1 - y_i)log(1 - f(x_i))]. \quad (6)$$

VI. Implementation and results of the experiment

The research main goal is to assess the efficiency of oil well planning.

The efficiency of the system is the most important factor in the quality of the production system. The efficiency of the production system is the ratio of the useful amount of produced liquid to the power consumption per unit of time, which is a significant factor in production. As a result of the experiment, the efficiency of the system was chosen as the target factor. It is assumed that the value of system efficiency above 45% is positive, less than 45% - negative.

In data mining, parameters such as pump load, temperature, and electrical voltage are suitable for solving the classification problem in the evaluation model. When analyzing the efficiency of the pumping system, the factors that affect it, listed in table 1 and table 2, are considered.

Table 1. Oil well parameters

Parameter	**Unit**	**Parameter**	**Unit**
Depth	[m]	Reactive power	[KW]
Period of work	[/]	Oil pressure	[MPa]
Max load	[KN]	Max pressure	[MPa]
Min load	[KN]	Min pressure	[MPa]
Production pressure	[MPa]	Power factor	[1]
Active power	[KW]	Voltage	[V]
Max active power	[KW]	Current	[A]

Table 2. Oil well production parameters

Parameter	Unit	Parameter	Unit
Liquid Consumption	[m^3/day]	Doppler velocity (array)	[Hz]
Gas Consumption	[m^3/day]	Gas void fraction (array)	[%]
Water cut	[%]	Sound velocity	[m/s]
Temperature	[℃]	Fluid Pressure	[MPa]

The primary data was obtained on the Perm region oil fields, on the oil wells and booster pump stations during the long period of their work.

The first data block, shown in table 1, was relatively easy to acquire, because these parameters are measured directly by the corresponding sensors. Data, shown in table 2, are the measures results of innovative ultrasonic multiphase flowmeter. It was installed on the oil wells and booster pump stations and it consists of vertical measuring pipe with two different calibrated crossections, four Doppler sensors, four gas void fraction (GVF) sensors, two sound velocity sensors, the thermometer, the gauge and the calculating unit with multilayer mathematical model. This model sets the line between primary data (Doppler velocity, GVF, sound velocity, temperature, pressure) and calculated data (liquid consumption, gas consumption, and water cut).

Liquid, gas consumption and water cut are the main oil well production efficiency parameters. However, using primary parameters the mixture flow regime can be deremined. There are four main flow regime types: bubble, slug, dispersed annular, dispersed [10]. The flow regime shows the operation oil well stability and it is also must be considered in the efficiency estimation.

In order to reduce feature space the Doppler velocity and GVF integral values can be calculated as the arithmetic mean of four corresponding parameters. Parameters are measured in the four points of two different calibrated crossections of the pipe: in the center of the minor crossecton, on the periphery of the minor crossection, in the center of the major crossecton, on the periphery of the major crossection.

According to flowmeter mathematical model liquid consumption depends on primary data twelve parameter. Nevertheless, as an example, on the figure 1 it is shown dependence between liquid consumption and integral Doppler velocity.

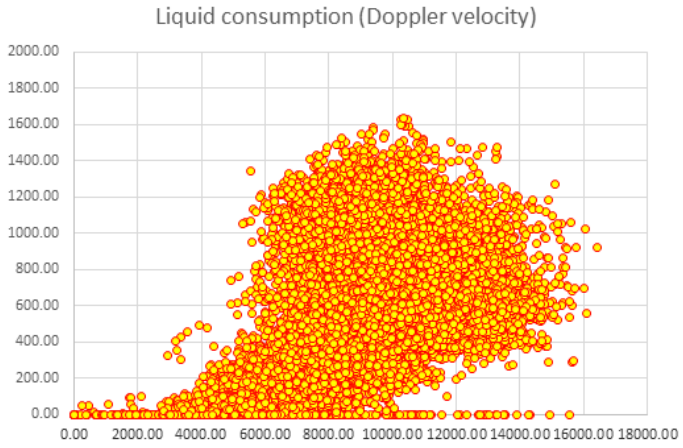

Figure. 4. Dependence between liquid consumption and integral Doppler velocity

It follows from the figure 4, that the Doppler velocity increases, the liquid consumption increases. However, liquid consumption also correlates from other parameters such as GVF, water cut, temperature, pressure and others. And the main correlation between liquid consumption and integral Doppler velocity is blurred by the influence of these parameters.

On the figure 2 it is shown dependence between gas consumption and integral gas void fraction.

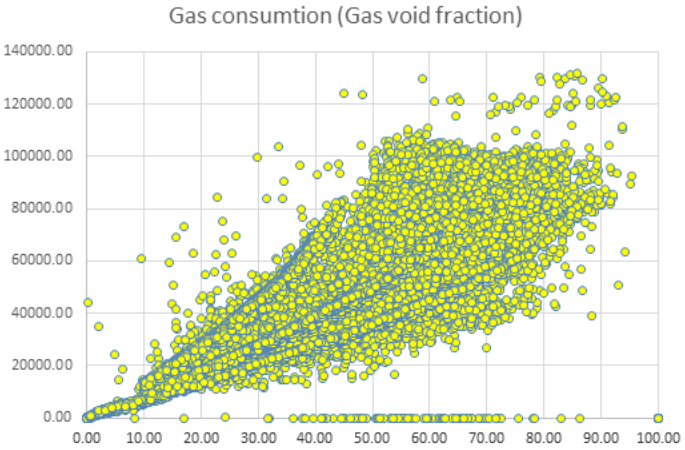

Figure. 5. Dependence between gas consumption and integral gas void fraction

It follows from the figure 5, that the GVF increases, the gas consumption increases. However, gas consumption also correlates from other parameters such as fluid velocity, water cut, temperature, pressure and others. The main correlation between gas consumption and GVF is also blurred by the influence of these parameters. Moreover, the more is the absolute value of GVF, the more is the gas consumption variation.

Therefore, after analyzing cross correlations in the training set it was determined, that all of the parameters have to be used in the research.

To improve the results of the work performed in accordance with the obtained data, the following actions were performed.

1) With the aim of improving the efficiency of data was collected with all possible related information.

2) Data set was pre-processed by smoothing, normalization and noise reduction methods.

3) An evaluation model has been created to solve real problems.

4) Evaluation of the obtained models was performed.

5) Produced an optimal modular scheme.

6) The results are compared with real data and the model is updated.

VII. Classification Results

The experiment was conducted in python on the example of oil wells data using SVM and LR algorithms [11]. Five years of measuring experience and obtained primary and calculate data where systematized and cleaned. 1980 examples of oil wells and boosting pump stations data were selected as the training set, and the 20 examples - as the test sample. According to experience, the penalty parameter C was set to 0.8, the RBF evaluation function and the standard deviation 0.5 for the SVM model; the penalty parameter C=1 for LR. A comparison of projected and actual performance is shown in table 3.

№	Real values	Forecast LR	Forecast SVM	№	Real values	Forecast LR	Forecast SVM
1	0	1	0	11	0	0	1
2	0	0	0	12	0	0	0
3	0	0	0	13	0	0	0
4	0	0	0	14	0	0	0
5	0	0	0	15	0	0	0
6	0	1	1	16	1	1	1
7	1	0	1	17	0	1	0
8	1	1	1	18	0	0	0
9	0	1	1	19	0	0	0
10	1	1	1	20	1	1	1

Using the logistic model, 15 correct classification results were found, which means that the accuracy reaches 75%. Within the framework of the SVM model, 18 correct classifications with an accuracy of 90% were found that satisfy the prediction conditions. By using the PCA dimensionality reduction method, data dimension were reduced from 17 to 2.

The result deviation forecast from real values diagram is shown in figure 6.

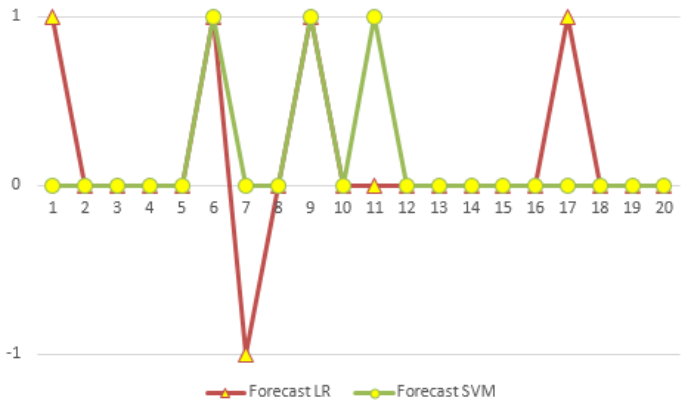

Figure.6. Results of the SVM and LR experiment

On the figure 6 the deviation between the efficiency real value and LR forecast is shown by triangles and deviation between the efficiency real value and SVM forecast is shown by circles.

In this case current flow regime of oil well production is considered automatically by the combination of primary data leading to lower or higher values of liquid and gas flow rates and to lower or higher efficiency values, without direct classifying oil wells by this parameter. However, it would be very useful to develop such classification for providing forecast of oil well behavior and to prevent emergencies.

In the subject area of oil wells, the distribution of data is complicated by the high dimension of the data space, which can have a great impact on the collection of primary data. In this situation, the possible error collection of one or more types of data, as well as uneven distribution of data. Classical manual analysis, such as the use of charts, linear analysis, or logistic regression, does not achieve high quality classification. In this case, the support vector machine using the kernel method is better suited for nonlinear complex data processing.

VIII. Conclusion

The paper presents a theoretical analysis of the support vector machine and logistic regression. It is shown, that the nonlinear SVM algorithm works better than the linear LR algorithm in the analysis of the oil well system and forecasting their efficiency.

In the future research, based on current survey, it is necessary to develop a method of multiple classification based on the support vector machine, which allows the classification of the original data set into several classes with the ability to assess the degree of proximity to each of these classes.

It is very important for the oil field technological service to determine the multiphase (oil-water-gas) stream flow regime because, for example, even high liquid flow rate in the not corresponding regime can lead to feed failure of the pump and to emergency stop of oil well. However, if this situation could be classified at the early stage, it can provide to avoid accident situation and thus to maintain oil well operating efficiency.

Literature

[1] Bashmakov, A. I., Bashmakov, I. A. Intellectual information technologies. Benefit // –M.: Publishing MGTU im. N.Uh. Bauman, 2005.

[2] Yeon Su Kim. Evaluation of the effectiveness of classification methods: comparative modeling. Expert systems with applications, 2009, 373 p.

[3] Hanuman Thota, Raghava Miriyala, Siva Prasad Akula, K. Mrithyunjaya RAO, Chandra Sekhar Vellanki, et al.. Performance comparison in classification algorithms using real data sets. Journal of computer science and systems biology, 2009, 02-01.

[4] Hung Linh AO, Junsheng Cheng, Yu Yan, Dong Khak Chuong. The method of optimization of parameters of support vectors is based on the algorithm of optimization of artificial chemical reactions and its application for diagnostics of malfunctions of roller bearings. Journal of vibration and control.2015 (12).

[5] Rimjhim Agraval, Thukaram Dhadbanjan. Identification of the fault location in distribution networks using multi-Class support vector machines. International journal of emerging electric power systems.2012 (3).

[6] Snehal A. Mulay, P. R. Devale, G. V. Garje. Intrusion detection system using support vector machine and decision tree. International journal of computer applications.2010 (3).

[7] Wang Liejun, Lai Huicheng, Zhang Taiyi. Improved least squares support vector machine algorithm. Journal Of Information Technologies.2008 (2).

[8] R. Cogdill And P. Dardenne. Least squares support vectors for Chemometrics: an introduction to andevaluation. Journal of near infrared spectroscopy.2004 (2).

[9] Ke Lin, Anirban Basudhar, Samy Missoum. Parallel construction of explicit boundaries using support vector machines. engineering calculation.2013 (1).

[10] Brill James P., Mukherjee Hemanta. Multiphase Flow in Wells. // –M.: Publishing Institute of computer research. 2006. 384 p.

[11] Ashkan Mousavian, Hojat Ahmadi, Babak, Sakhaei, Reza Labbafi. Support vector machine and K-nearest neighbor for unbalanced fault detection. Journal of quality in the field of maintenance.2014 (1).

Power dispatcher support system

Dmitri Nazarkov
BMSTU
Moscow, Russia
nazarkovdmitriy@mail.ru

Alexey Prutik
BMSTU
Moscow, Russia
alexeyprutik@gmail.com

***Abstract* — This paper is devoted to development of power dispatcher support system prototype which main purpose is to notify dispatcher in case of detecting any unplanned deviations from nominal operation mode of power equipment. System uses informational model in CIM XML/RDF format as source of knowledge about nominal operation modes.**

Keywords — power dispatcher, telemetry, CIM, XML-RDF, operational information complex, operational information complex new generation, Golang, gRPC, Redis.

I. Introduction

The operational information complex (OIC) is embedded and used in the dispatch centers of the System Operator of Unified power system (Sistemnyj operator Edinoj ehnergeticheskoj sistemy). On its platform implemented a significant count of automated subsystems to solve operational technological tasks. Analysis of the OIC subsystems' load showed that the complex has reached their limit in terms of increasing amount of processed data. In addition, present OIC architecture does not allow to improve existing technological problems solutions and to introduce new approaches.

Currently, some work as part of the unification of information models in all dispatch centers of the System Operator is carried out to put into operation information models based on IEC 61970, 61968 (Common Informational Model) standards [1]. These standards would be used for calculating power equipment's established states [2].

In connection with the above, the System Operator is working on the implementation of a new generation operational information complex (OIC NG). Implementation of the OIC NG requires modification of most automated systems that using information from the old OIC. Due to the lack of a ready solution which can replace the old OIC and its associated automated systems is necessary to organize the long-term work on the phased development and implementation of the subsystems of the new generation operational information complex and the adaptation of existing automated systems.

II. Power dispatcher support system

As part of the transition to the OIC NG, a prototype of the power dispatcher support system (DSS) is being developed, which uses common information model of the power system as a source of information necessary for estimating its state, and an Automated Integration Platform (AIP) as the telemetry source. Figure 1 shows the place of the developed support system in the described problem domain.

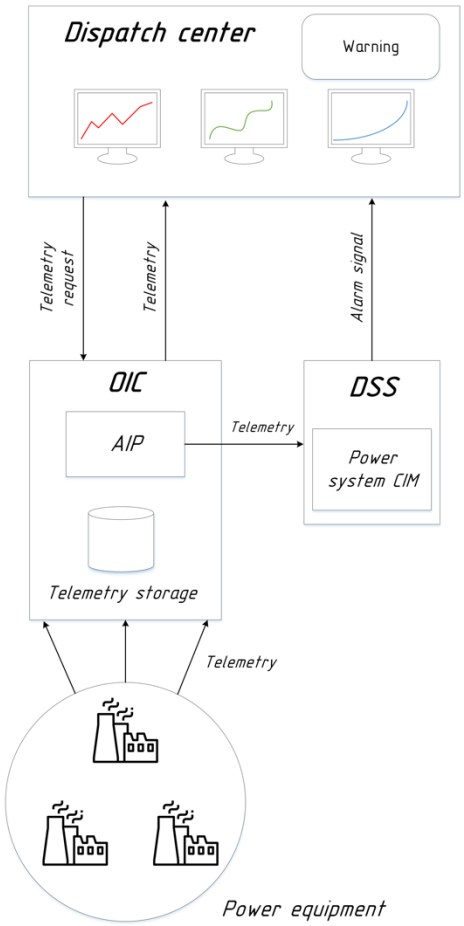

Fig. 1. The structural scheme of the subject area of the problem

Sensors are installed on the power equipment that send telemetry to the OIC NG's storage. DSS receives information from the AIP, processes it using algorithms similar to the algorithms implemented in the previous generation OIC, aimed at monitoring a certain equipment parameter (for example, the amperage in an overhead power line). During the telemetry processing DSS is guided by the CIM model of the power system.

III. Organization of storing and access to common informational model in dispatcher support system

System operator unifies information models based on CIM standards. Common Information Model (IEC 61970-301) is a standard in the field of electric power industry, designed to standardize the process of exchanging information about the electric power system between software products [1]. CIM-standard puts one or several objects of its classes in compliance with a real power equipment object [3].

One of the reasons for the transfer of System operator to OIC NG is the achievement of the limit of the amount of information processed by the previous generation OIC. Therefore, when developing DSS, it is necessary to pay special attention to the system performance criterion, use solutions and technologies that differ from analogues for the better according to this criterion.

Guided by these considerations, the Go (Golang) programming language was chosen as the main system development language, since, due to its focus on use in highly loaded multiprocessor systems, it is able to provide speed and parallelization of incoming telemetry processing.

Golang's limitation, as a language applicable to the problem, is its library for working with the XML format, which does not allow direct processing of the CIM XML/RDF file of the power system model. Therefore, the model needs to be converted to a format suitable for work in the DSS written in Go.

CIM standard represents a logical model of power systems. This model can be implemented in software and stored in different forms which depends on amount of data, how frequently data is accessed and whether the model of power system will change in the future [4].

As a rule, relational databases are used to store CIM despite the fact that CIM, as a standard, is based on an object-oriented model. This fact means that some principles of an object-oriented approach, such as inheritance or many-to-many relationships, firstly cause difficulties in designing relational database schemas, and, secondly, lead to performance problems that is critical for DSS [5]:

- Database is overloaded with a large number of tables describing the parent classes, which leads to an increase in the number of join operations.
- Tables that correspond to root classes, for example, PowerSystemResource, contain too many records, which also makes difficulties to index and query them.

Another factor influencing speed when working with information model is memory in which it is stored. The fastest type of memory is RAM. It can be used as a memory for storing the information model, since at present the full CIM of the Russia unified power system has a size of 5 GB.

The Redis DBMS was chosen as the information model storage for the following reasons:

- Stores data in RAM [6].
- Provides non-blocking data reading [7].
- Designed to be used as fast data storage which can handle thousands of simultaneous queries [8].
- Uses main memory to persist data operating when system restarts.
- Has library for Go.

Primary format for storing data in Redis is the key-value format. Each information model object has a unique GUID:

```
<cim:CurrentLimit rdf:about="#_e9a2cbc5-
6a3e-4112-8a28-40e41df3dc3b">          (1)
```

We will use it as a key entry in Redis. As an entry string value is necessary to store information model object. In order to provide reverse deserialization of the string in the Go structure, JSON format will be used.

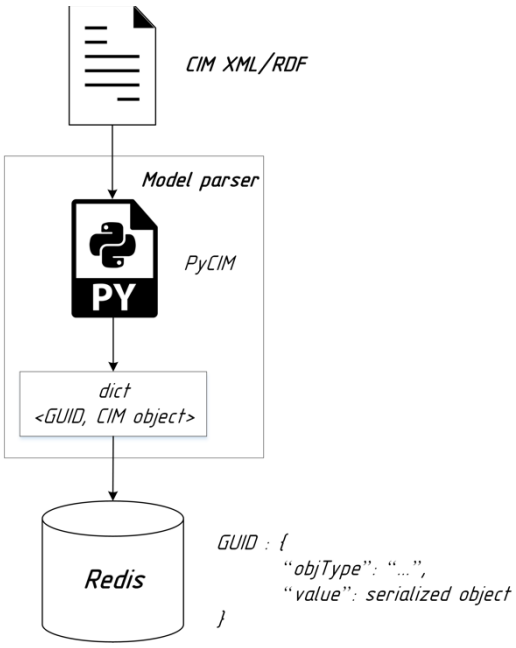

Fig. 2. Block diagram of the CIM XML / RDF file transformation process

Task of recording the information model in CIM was solved using the PyCIM Python open source library [9]. The library provides ability to read XML tree of the information model in the dictionary of objects: <GUID, CIM-object>. After processing file with the information model in this way, we serialize each object into the structure of the format indicated in Figure 2, and write it as a value to Redis. Using structures of such format eliminates problems of storing CIM in relational databases described above. Also, data in this format can be stored in single table of relational DB but this approach won't be optimal at least because Redis is specialized tool to keep key-value data oriented on high performance.

In the structure, we explicitly indicate the type of serialized data to simplify deserialization into the Go structure.

IV. Exchanging Information with Automated Integreation Platform

Interaction of the support system with Automated Integration Platform (AIP) is built using remote procedure call framework - gRPC. This framework was chosen based on the following considerations:

- Uses binary protobuf format, which allows to minimize size of the transmitted message in comparison with standard text-based XML or JSON formats [10].
- Uses HTTP / 2 as a transport. It supports bidirectional streaming.
- Supports TLS / SSL encryption of transmitted data.
- Supported in Go.

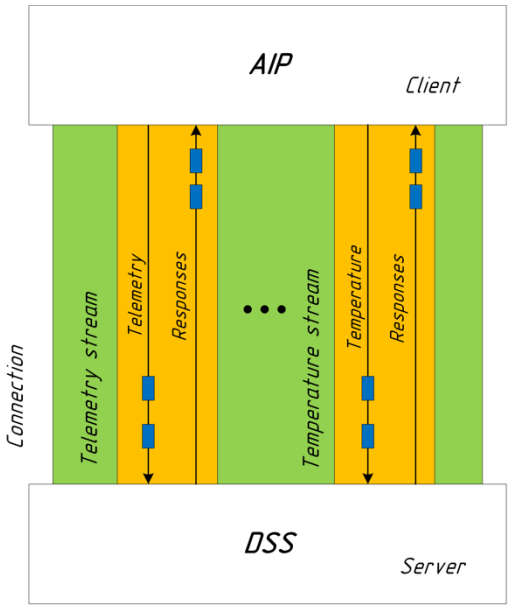

Fig. 3. Diagram of the telemetry and temperature transmission process from the automated integration platform to the power dispatcher support system

Information exchanging via HTTP / 2 protocol implies the presence of a client and a server. In the current scheme, DSS is the server, and the AIP is the client, since the AIP transmits telemetry as it changes, and DSS does not request it independently. Since the AIP is a client, there is an issue here: it must "know" about all systems that request telemetry to call their remote procedures. The set of remote procedures is constant and it is described in the protobuf-contract. Consequently, it is necessary to solve the issue, which is to organize update/add information about IP-addresses and ports of such systems.

The permanent connection is established between the support system and the platform to transfer information. Within this connection, bidirectional flows are created in which the following data are transmitted:

- Telemetry of power equipment.
- Ambient temperature.

V. Implementation of Amperage Control in Overhead Power Line

Number of algorithms were implemented in the previous generation of OIC aimed to estimate operating modes of power equipment. One of them is amperage monitoring of overhead power line.

There are three types of amperage load:

- Normal amperage - the highest amperage at which the equipment can operate indefinitely.
- Long valid amperage - amperage at which long-term operation of equipment is possible.
- Emergency amperage – this is an amperage above which the operation of the equipment is unacceptable.

In order to illustrate the operation of the support system, we consider the processing of telemetry in the order that it goes through the relevant procedures and functions of DSS. The structure and relationships of Go-packets containing telemetry processing functions are shown in figure 5.

A. Receive

The *receive* packet in the support system receives telemetry from the automated integration platform. In case of successful data acceptance, a lightweight *goroutine* is created, within which further evaluation of the equipment operation mode by the *check* package will be carried out. Processing is carried out in a separate thread, so as not to block the main stream, which receives data from the AIP. In the near future, it is planned to refuse the way of creating new goroutine for each incoming telemetry value by implementing the queue and goroutine pool mechanism, since the current mechanism theoretically can cause "10 thousand connections" problem [11], despite the fact that DSS testing in its current form is able to handle the load.

B. Check

The *check* package directly estimates operation mode of the power equipment, based on the readings of telemetry. To monitor the current load of the power line, two types of verification are implemented:

- If there are information about the ambient temperature and any amperage dependence of particular power line from ambient temperature in the CIM model (Figure 4), which appears in the descendant of the Curve class. DSS estimates operation mode using current temperature and amperage in the line with the corresponding dependency point.

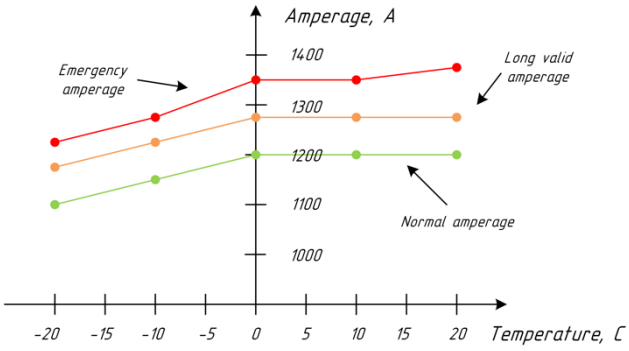

Fig. 4. Example of amperage dependence on temperature

- In the absence of temperature or amperage dependencies, the state is estimated with the set of limitations (OperationalLimitSet classes) on amperage in CIM.

The result of check is a decision on further DSS actions. When an emergency case is detected, system DSS must inform the dispatcher. If the current amperage value corresponds to the maximum permissible value, it is necessary to start the countdown. If more than one day has passed since the beginning of the countdown without reducing the current in the direction of the normal value, the dispatcher also must be notified. The *schedule* package, also pictured on the diagram in figure 5, is responsible for planning such tasks. Support system has a background thread that checks once a minute for tasks which time has come.

C. Model

Package *model* is the point of interaction with the CIM of power system. When handling request from the outside, functions of the package perform a request to Redis, which stores in memory information model. Receiving a CIM object in JSON format, using the developed library, functions convert it into a Go structure and returns it as a result. In order to reduce the number of requests to Redis cache is introduced in the package storing frequently requested model objects.

D. Notify

Package *notify* contains program code intended to transmit the result of the check to the dispatcher.

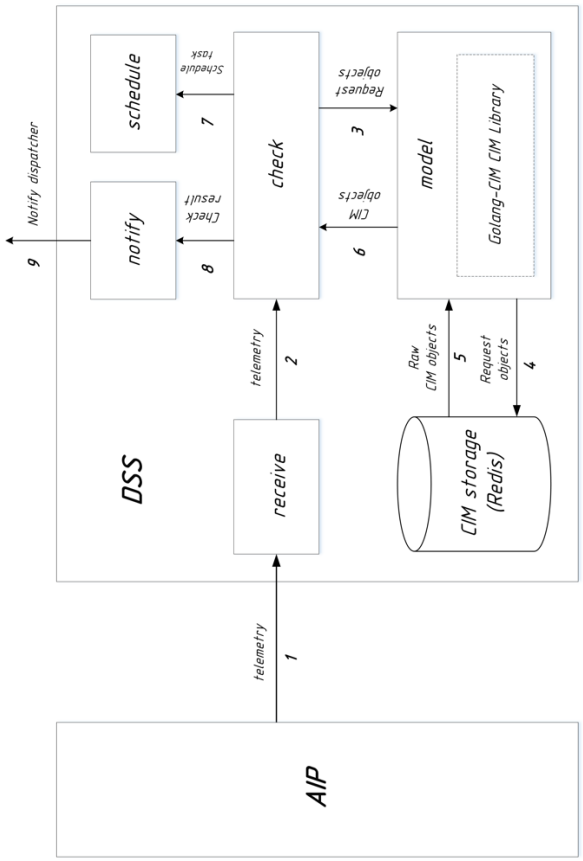

Fig. 5. Package structure and connections of the power dispatcher support system

VI. Integration Testing of Power Dispatcher Support System

In order to organize DSS testing process following set of tools was developed:

- Test version of Automated Integration Platform. It is a Golang-service with a set of test scenarios. A connection is established between the service and DSS, which allows to call remote DSS procedures for transmitting telemetry and the ambient temperature.
- Test version of power dispatcher's software. It is also a Golang-service that communicates with DSS via gRPC. Through the connection, the support system transmits the results of telemetry processing. After receiving incoming message from DSS, Golang service sends it to Centrifugo - a message server [12], which is connected via a websocket to a web page that simulates the dispatcher's interface.

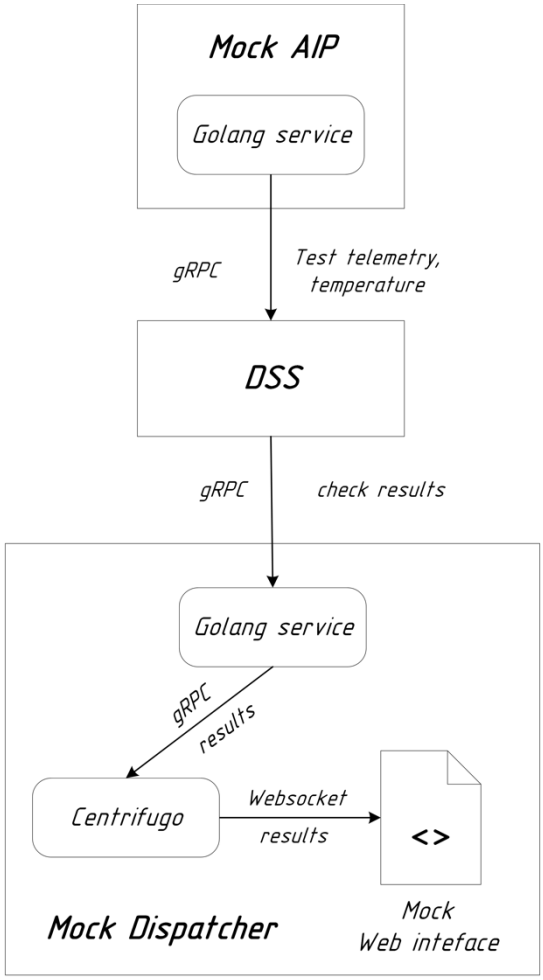

Fig. 6. Diagram of the test infrastructure of the dispatcher of the power system dispatcher

The DSS testing process is an imitation of the real mode of operation, during which the AIP transmits telemetry and temperature by calling the DSS remote procedures with the appropriate arguments. DSS receives data, processes it and, if necessary, sends a signal to the dispatcher, which is displayed in the interface.

VII. Results

Main result of solved task is a prototype of the power dispatcher support system, designed to integrate into the OIC NG.

At the moment, monitoring of the equipment amperage and voltage at the control points of the power system is implemented in the DSS prototype. In near future, it is planned to implement control over flows and restrictions in sections.

Preparation work to move to OIC NG (DSS prototype is part of it) currently is carried out. It will operate with old generation OIC in parallel when work will be completed. Transition period can last for one year and more. Duration of transition period and its events are determined by System Operator's clause «About commissioning and decommissioning of information management systems and

IT assets within JSC SO UPS» («O vvode v ekspluataciyu i vyvode iz ekspluatacii informacionno-upravlyayushchih sistem i IT-aktivov v OAO SO EES»). Transition period is intended to find defects in new system and testing it. System can be put into operation after all defects are eliminated.

Since structure and topology of power systems can change, their CIM-models also change. Currently, updating model in DSS is possible by following procedure of processing new CIM XML/RDF file described in section III. This procedure is obviously not optimal, as it will require complete rewrite of the model in Redis. It is necessary to solve problem of this process optimization. Problem is to determine changed parts of the model and update them in DBMS.

REFERENCES

[1] International Electrotechnical Commission, "Energy management system application program interface (EMS API) – Part 301: Common Information model (CIM) base", 6th ed, p. 36, December 2016.

[2] EMS for the 21st Century. System Requirements. Working Group D2.24. February 2011. ISBN: 978-2-85873-141-1., p. 6

[3] Mathias Uslar, Michael Specht, Sebastian Rohjans, Jörn Trefke, José M. González,The Common Information Model CIM: IEC 61968/61970 and 62325 – A practical introduction to the CIM, p. 23, 2012

[4] Rahul Khare, Mostafa Khadem, Sainath Moorty, Kittipong Methaprayoon, Jun Zhu «Patterns and Practices for CIM applications», 2011 IEEE Power and Energy Society General Meeting, p.5.

[5] A.W. McMorran, R.W. Lincoln, G.A. Taylor, E. M. Stewart, «Addressing Misconceptions about the Common Information Model (CIM)», 2011 IEEE Power and Energy Society General Meeting, p.2.

[6] Redis [Online]. Available: https://redis.io/ [Accessed: 31- Mar- 2019]

[7] Blocking commands in Redis modules [Online]. Available: https://redis.io/topics/modules-blocking-ops [Accessed: 31- Mar- 2019]

[8] How fast is Redis? [Online]. Available: https://redis.io/topics/benchmarks [Accessed: 30- Apr- 2019]

[9] PyCIM [Online]. Available: https://github.com/rwl/PyCIM [Accessed: 31- Mar- 2019]

[10] gRPC A high-performance, open-source universal RPC framework [Online]. Available: https://grpc.io/ [Accessed: 31- Mar- 2019]

[11] The C10K problem [Online]. Available: http://www.kegel.com/c10k.html [Accessed: 31- Mar- 2019]

[12] Centrifugo [Online]. Available: https://github.com/centrifugal/centrifugo [Accessed: 31- Mar- 2019]

Applying High-Level Function Loop Invariants for Machine Code Deductive Verification

Pavel Putro
Software Engineering Department
Ivannikov Institute for System Programming of the RAS
Moscow, Russia
pavel.putro@ispras.ru

***Abstract*—The existing tools of deductive verification allow us to successfully prove the correctness of functions written in high-level languages such as C or Java. However, this may not be enough for critical software because even fully verified code cannot guarantee the correct generation of machine code by the compiler. At the moment, developers of such systems have to accept the compiler correctness assumption, which, however, is extremely undesirable, but inevitable due to the lack of full-fledged systems of formal verification of machine code. It is also worth noting that the verification of machine code by a person directly is an extremely time-consuming task due to the high complexity and large amounts of machine code. One of the approaches to simplify the verification of machine code is automatic deductive verification reusing the formal specification of the high-level language function. The formal specification of the function consists of the specification of the pre- and postcondition, as well as loop invariants, which specify conditions that are satified at each iteration of the loop. When compiling a program into machine code, pre- and postconditions are preserved, which, however, cannot be said about loop invariants. This fact is one of the main problems of automatic verification of machine code with loops. Another important problem is that high-level function variables often have projections' to both registers and memory at the machine code level, and the verification procedure requires that invariants be described for each variable, and therefore the missing invariants must be generated. This paper presents an approach to solving these problems, based on the analysis of the control flow graph, and intelligent search of the locations of variables.**

***Index Terms*—deductive verification, formal methods, machine code**

I. Introduction

In the 1960s Floyd [1] and Hoare [2] put forward their theories that the full correctness of the program code can be proved mathematically. The proposed methods are called deductive verification, but could not immediately gain popularity due to the lack of automation, as well as low performance and the high cost of hardware computing resources. However, in recent decades, these methods are experiencing a rebirth due to the rapid development of methods for solving the SMT [3] problem, and growing performance of hardware devices. Technological leap in this area allowed to verify the application and system software by means of personal computers. In this paper, the author adheres to the use of methods of deductive verification, because unlike other methods of formal verification, such as for example model checking, deductive verification allows proving full correctness, but not only the absence of a certain class of errors.

Increasing the availability of formal verification methods has led to the fact that now formal verification is becoming a standard in the creation of systems designed to work with safety- and security-critical infrastructure. These systems are verified and tested carefully, but industrial verification tools work only at source code level when testing can't guarantee that are no errors in the program. Here we can notice a security hole when compilation of the correct code introduces errors that can't be detected by the testing system. Without anyways for solving this problem developers have to make "The assumption of the correctness of the compiler". According to a study [4] conducted in 2016, the total number of bugs found in GCC+LLVM are more than 50000. This is one of the main reasons why this assumption may not be sufficient for critical systems. There are only two ways that can allow developers to abandon this assumption: the first is to create a fully formally verified compiler, and the second is to formally verify machine code. There are some tries in recent 15 years that aimed to verify machine code or to create fully formally verified compiler but there is still no generally accepted industrial solution in machine code verification.

In this paper we consider an approach of deductive verification of machine code obtained by compiling the source code, the correctness of which has been proved by methods of deductive verification. The approach proposes to use a number of techniques designed to reuse the function specification in a high-level language to prove the correctness of the compiled machine code.

The process of deductive verification of machine code has several serious differences from deductive verification of code in high-level languages. The first difference is that in machine-independent high-level programming languages, the set of basic operations amounts to several tens, and the size of instruction sets of modern processors amounts to hundreds and may even exceed a thousand different instructions. In addition, many of these instructions can have side effects, such as setting processor flags or storing the result in a predefined register. This variety of instructions does not allow to effectively generate state-change formulas during parsing of machine code and requires a definition of the processor model and its instruction set. The second difference is that machine

code is always a sequence of instructions with operands and does not have the complex syntax that is present in modern programming languages. This feature allows you to automate the parsing of the machine code of different processors using only one tool. The third difference is that in machine code there is no explicit design to indicate the loops, such as operators ”for” or ”while” in languages C/C++. Instead, loops are organized by using a set of conditional and unconditional branches. However, the presence of such instructions does not mean that there are loops in the program because they are also used to organize any branching. This difference requires the construction and analysis of the control flow graph of the program. In this case, the control flow graph extractor should be able to distinguish branches from other processor instructions, be able to determine the target of the transition and the condition under which it will be done. If there is a control flow graph, the problem of finding loops in the program can be reduced to the problem of finding the components of strong connectivity in the oriented graph. The last significant difference is the absence of a direct connection between the names and positions of local variables in a high-level language program and their location in memory or in the registers of the program in machine code. It is necessary when we try to reuse specifications of the high-level function. A similar dependence exists when mapping function parameters to registers and stack and is determined by the target processor ABI. Using information about ABI allows you to automatically map the parameters and the result of the function to the appropriate positions in the machine code. However, the process of proving loop invariants involves the use of local variables. As a result, when trying to prove the invariants of a high-level function at the machine code level, there is a problem associated with the absence of the ability to directly associate high-level local variables with machine code. There are also other differences related to program function calls, system calls, and exception handling, but these are beyond the scope of this paper. As you can see the first two considered differences are common and observed in the processing of any machine code, while the second two appear only in the case of processing functions with loops. In this paper, the most attention is paid to the solution of the problems caused by the second two differences while the previous author's paper is devoted to the first two [5].

II. Related work

In [6], the HOL4 proof assistant [7] is used to verify machine programs in subsets of ARM, PowerPC, and x86 (IA-32). These ISAs were specified independently: the ARM and x86 models [8], [9] were written in HOL4, while the PowerPC model [10] was written in Coq [11] and then manually translated to HOL4. There are four levels of abstraction. Machine code (level 1) is automatically decompiled into the low-level function model in HOL4 (level 2). A user describes the high-level function model (level 3) as well as the functional specification (level 4). By proving the equivalence between the levels, the user ensures that the machine code complies with the functional specification. In our opinion, automation can be increased by using specialized ISA description languages and SMT solvers. For proving the correctness of the programs with loops, it uses loops to recursive functions translation technique. This technique is available only for interactive provers due to efficiency problems of automatic solvers while processing programs with loops.

An interesting approach aimed at verifying machine code against ACSL [12] specifications is presented in [13]. The general scheme is as follows: first, the ACSL annotations are rewritten as an inline assembly; second, the modified sources are compiled into assembly language; third, the assembly code is translated into a Why program; finally, the Why environment generates verification conditions and proves them with external solvers. The approach looks similar to the proposed one; however, there some distinctions. E.g., there are separate primitives for storing/loading variables of a different type (32- and 64-bit integers, single and double floating-point numbers, etc.), which leads to certain limitations in dealing with pointers. It is also worth noting that verification at the assembly level does not allow us to abandon the compiler correctness assumption, as the assembly code is an intermediate form and needs additional translation. This approach relies on the compiler while processing programs with loops, as compiler places rewritten as inline assembly loop invariants into the beginning of the loop and automatically bind local variables to the registers or memory.

In [14], there have been demonstrated the possibility of reusing correctness proofs of high-level programs for the related machine code verification. The approach is illustrated on the example of a Java-like source language and a bytecode target language. The paper describes a scenario of using such a technology in the context of proof-carrying code (PCC) and shows (in a particular setting) that compilation preserves proof obligations, i.e. source code proofs (built either automatically or interactively) can be transformed to the machine code proofs. The problem we are solving is different (though some ideas may be useful); moreover, we would like to make our solution architecture and compiler independent. In the case of the processing of the programs with loops, if loop invariants are preserved by compilation, their proving will be a trivial process.

III. Using the control flow graph for VC generation

In deductive verification of programs in high-level languages, various syntactic constructions allow determining the presence of loops in the program, their contents, as well as the conditions of exit from the loop. However, when processing the machine code such structures do not exist, and to search for loops and other branch operations need to build a control flow graph (CFG). As part of the study for the processing of machine code used MicroTESK toolkit [15] (full justification for the use of MicroTESK for deductive verification of machine code is given in article [5]). The use of this tool, in particular, allows to describe the processor model in the language of nML [16], and on the basis of this model to

automatically analyze the binary code and build its behavior model in the logical language SMT-LIB [17]. In addition, CFG extractor has been added to this tool over the past year.

A. The format of the CFG

MicroTESK toolkit is able to determine whether the instruction described in nML is a branch instruction, determine the branch condition and the target address. In addition, MicroTESK has an advanced algorithm for calculating the target address of the transition, which allows it to calculate indirect targets, such as in a situation where the target address is preloaded into the register and the branch is carried out already on the register. Such capabilities in combination with the use of nML processor models allow you to automatically generate CFG for any processor modeled using nML. The generated CFG is saved in JSON format [18], and has the following format:

1) All basic blocks are placed in the list with the name ”blocks”.
2) Each basic block has an index in the ” blocks” list and has the following format:
   a) The ”range” list that includes the sequence number of the first and last instruction of the base block in the context of the entire function being analyzed. Used for extraction of the SMT-LIB representation of the block from the SMT-LIB representation of machine code.
   b) The ”asm” list that contains instructions of a basic block in the assembler language of the target processor.
   c) The ”vars_start” list, which contains the SMT-LIB versions of the main variables of the nML model of the processor such as registers and memory, but not temporary and auxiliary variables. Versions are specified for the entry point of the basic block.
   d) The ”vars_end” list, contains values similar to the list of ”vars_start”, however, the version specified for the exit point of the basic block.
   e) The field ”condition” contains the branch condition. The MicroTESK nML internal representation syntax is used to write the condition. ”true” for unconditional branches and in the case when there is no branch in the block.
   f) The field ”condition_smt” same as ”condition”, however, is recorded using SMT-LIB.
   g) The field ”target_taken” containing the index of the basic block in the ”blocks” list, which will be passed to the control in the case when ”condition” is met. ”null” for blocks in which is the function exit point.
   h) Optional field ”target_ntaken” containing the index of the basic block in the ”blocks” list, which will be passed to the control in the case when ”condition” is not met. Defined only for blocks with a conditional branch.

This structure of the graph contains all the necessary information for generating verification conditions. Below is an example of the extracted CFG for the function of calculating the sum of numbers from 0 to N (Table I).

```
{
"blocks": [
{
"range": [0, 8],
"vars_start": ["MEM!1","XREG!1"],
"vars_end": ["MEM!37","XREG!15"],
"asm": [
"addi␣sp,␣sp,␣-48",
"sd␣s0,␣40(sp)",
"addi␣s0,␣sp,␣48",
"addi␣a5,␣a0,␣0",
"sw␣a5,␣-36(s0)",
"sw␣zero,␣-20(s0)",
"addi␣a5,␣zero,␣1",
"sw␣a5,␣-24(s0)",
"jal␣zero,␣0x10"
],
"condition": "true",
"target_taken": 1
},
{
"range": [16, 20],
"vars_start": ["MEM!53","XREG!27"],
"vars_end": ["MEM!53","XREG!36"],
"asm": [
"lw␣a4,␣-24(s0)",
"lw␣a5,␣-36(s0)",
"addiw␣a4,␣a4,␣0",
"addiw␣a5,␣a5,␣0",
"bge␣a5,␣a4,␣-22"
],
"condition": "i1␣sge␣i64␣a5,␣a4",
"condition_smt": "op_20_instruction.operation.action.block_0!1",
"target_taken": 2,
"target_ntaken": 3
},
{
"range": [9, 15],
"vars_start": ["MEM!37","XREG!15"],
"vars_end": ["MEM!53","XREG!27"],
"asm": [
"lw␣a4,␣-20(s0)",
"lw␣a5,␣-24(s0)",
"addw␣a5,␣a4,␣a5",
"sw␣a5,␣-20(s0)",
"lw␣a5,␣-24(s0)",
"addiw␣a5,␣a5,␣1",
"sw␣a5,␣-24(s0)"
],
"condition": "true",
"target_taken": 1
},
{
"range": [21, 25],
"vars_start": ["MEM!53","XREG!36"],
"vars_end": ["MEM!53","XREG!45"],
"asm": [
"lw␣a5,␣-20(s0)",
"addi␣a0,␣a5,␣0",
"ld␣s0,␣40(sp)",
"addi␣sp,␣sp,␣48",
"jalr␣zero,␣ra,␣0"
],
"condition": "true",
"target_taken": null
}
]
}
```

B. Joining basic blocks for verification conditions generation

The basic blocks themselves are not suitable targets for generating verification conditions (VC), as they may not contain specific targets, but only state change formulas. There

ACSL-ANNOTATED C CODE	ASSEMBLY CODE	BINARY CODE

`/*@ axiomatic Sum {`
`*@  logic integer sum(integer n);`
`*@  axiom sum_init:`
`*@   \forall integer n;`
`*@     n <= 0 ==> sum(n) == 0;`
`*@  axiom sum_step_dec:`
`*@   \forall integer n;`
`*@     n > 0 ==> sum(n) == sum(n-1) + n;`
`*@ }`
`*/`
 	
`/*@ requires 0 <= n <= 65535;`
`*@ ensures \result == sum(n);`
`*/`
`int sum(int n) {`
`int s = 0;`
 	
`/*@ loop invariant 1 <= i <= n+1;`
`*@ loop invariant s == sum(i-1);`
`*@ loop variant n-i;`
`*/`
`for(int i = 1; i <= n; i++) {`
`s += i;`
`}`
`return s;`
`}`
	`addi  sp, sp, -48`
	`sd  s0, 40(sp)`
	`addi  s0, sp, 48`
	`addi  a5, a0, 0`
	`sw  a5, -36(s0)`
	`sw  zero, -20(s0)`
	`addi  a5, zero, 1`
	`sw  a5, -24(s0)`
	`jal  zero, 0x10`
	`lw  a4, -20(s0)`
	`lw  a5, -24(s0)`
	`addw  a5, a4, a5`
	`sw  a5, -20(s0)`
	`lw  a5, -24(s0)`
	`addiw a5, a5, 1`
	`sw  a5, -24(s0)`
	`lw  a4, -24(s0)`
	`lw  a5, -36(s0)`
	`addiw a4, a4, 0`
	`addiw a5, a5, 0`
	`bge  a5, a4, -22`
	`lw  a5, -20(s0)`
	`addi  a0, a5, 0`
	`ld  s0, 40(sp)`
	`addi  sp, sp, 48`
	`jalr  zero, ra, 0`
		`fd01 0113`
		`0281 3423`
		`0301 0413`
		`0005 0793`
		`fcf4 2e23`
		`fe04 2623`
		`0010 0793`
		`fef4 2423`
		`0200 006f`
		`fec4 2703`
		`fe84 2783`
		`00f7 07bb`
		`fef4 2623`
		`fe84 2783`
		`0017 879b`
		`fef4 2423`
		`fe84 2703`
		`fdc4 2783`
		`0007 071b`
		`0007 879b`
		`fce7 dae3`
		`fec4 2783`
		`0007 8513`
		`0281 3403`
		`0301 0113`
		`0000 8067`

TABLE I
EXAMPLE: ACSL-ANNOTATED C CODE, RISC-V ASSEMBLY CODE, AND BINARY CODE GENERATED BY GCC FOR RISC-V

are several types of verification conditions in deductive verification. The first and foremost is the postcondition. Also as VC can be used various custom asserts or conditions for checking the security of the program execution, such as for example the absence of indexing out of range of the array. Also, as VC uses invariants of loops. In this case, each invariant can be further divided into checking the initialization of this invariant that is, checking the condition of the invariant before the execution of the loop code, as well as checking the preservation of the invariant - the preservation of the compliance of the invariant for the next iteration of the loop, provided that all the invariants are compliances on the current one. Therefore, the basic blocks must be joined and marked so that one or more of these conditions can be matched to each of them. Accordingly, the algorithm for combining the base blocks can be defined as follows. In the first step, using the fields ”target_taken” and ”target_ntaken”, the array of edges of the CFG is selected from the set of basic blocks. In the second step, to search for loops in the program, the graph uses an algorithm to search for strongly related components in a directed graph. The author’s implementation uses Tarjan’s algorithm [19] implemented by the ocaml-containers library [20]. To find nested loops, this step must be repeated recursively for all found base block sets, and the relationship between the first and last base block in the loop must be broken. In the third step, you need to depth-first search the graph for marking and joining blocks. The traversal must start from the zero base block the program entry point. At the input, there is a set of basic blocks, as well as a set of chains of strongly related component - loops. The output is a set of joined and marked basic blocks suitable for VC generation.

1) If the block has two targets, they must be processed separately, and the results combined.
2) If the current block and its target is not in the loop it is necessary to ”join” these blocks and proceed to the processing of the joined block.
3) If the current block is not included in the loop, and its target is included in the loop, it must be marked as the loop entry point. Next, proceed to the processing of its target.
4) If the block and its target are in the same loop and do not make a loop, they must be joined and proceed to the processing of the joined block.
5) If the block and its targets are in the same loop and thus make a loop, they must be combined and the result is returned.
6) If the unit is part of the loop, and its target is included in a nested loop it is necessary to mark as a loop entry point and proceed to the processing its target.
7) If the block is included in the nested loop, and its target in the outer loop, then the block must be marked as the loop exit point and joined with the target and proceed to the processing of the joined block.
8) If the block in the loop but its target is no, then the block must be marked as the exit point of the loop and joined with the target and proceed to process the joined block.
9) If the block target is null, the result must be returned.

The procedure of joining blocks is the base for the graph traversal and is carried out according to the following rules:

1) The procedure allows you to create a new block based on two existing ones.

2) Joining is possible if the target (”target_taken” or ”target_ntaken”) of the first block is the second block. In all other cases, the result of the join is not determined.
3) The targets of the joined block will be the targets of the second block.
4) Condition (”condition_smt”) of the joined block will be the condition of the second block.
5) If the second block is a loop exit point, the initial state ”vars_start” of the combined block will be the initial state of the second block, otherwise the initial state of the first block.
6) If at least one of the joining blocks is marked as the loop exit point, the joined block must also be marked as the loop exit point.
7) If the second block is marked as the loop entry point, the result should be marked as the loop entry point.
8) If the second block ”closes” the loop, i.e. its target is the first block, its SMT-LIB representation should be changed so that all elements of the final state ”vars_end” of the second block should get new unique names. Any other conflicts between any variables in SMT-LIB representations of the joining blocks must be resolved in the same way.
9) SMT-LIB the representation of the joined block must be obtained by concatenating the SMT-LIB representations of the merged blocks. In this case, if the condition ”condition” of the first block is not empty (”true”), it must be added as SMT-LIB assert to the representation code of the joined block. Also, if the join follows the ”target_ntaken” branch, the condition must be inverted. Also, if the blocks do not follow each other in the program, the final state of the first block also needs to be associated with the initial state of the second block at the level of the SMT-LIB representation.

As a result of following this algorithm, in most cases, you can create a set of code blocks on which you can directly prove various verification conditions. The algorithm allows processing machine code with loops, nested loops, sequential loops, as well as code generated by the presence of the brake and continue statements in the program, but is not able to cope with tasks when, for example, several entries to one loop and other non-trivial situations caused by the use of transition instructions are detected in the control flow graph. However, such situations cause difficulties already at the stage of verification of the source code, and the construction of an algorithm that allows you to automatically deductively verify any machine code is an unsolvable task.

If we apply the algorithm to the CFG function of the sum of the numbers presented above, we will be able to allocate three blocks to prove VC. The first block will have index 0, have loop entry status and be used to prove the correctness of the initialization of the loop invariants. The second block will be a join of blocks 1 and 2 and will be used to prove the preservation of loop invariants. The third block will be a join of blocks 1 and 3 and will be used to prove the postcondition provided the invariants are correct.

IV. Automatic binding of high- and low-level local variables

In general, to describe loop invariants, high-level functions use local variable names that are not available when working with machine code. In general, information about binding local variables to specific positions on the stack or registers is not available. Of course, you can require the user to manually provide this data and even give examples where such requirements will have a positive impact on system performance. However, in most cases, manual mapping of local variables to their positions will be a bottleneck in the performance of the verification system, as well as reduce the degree of automation. From the above, we can conclude that the system should automatically determine the location of local variables, and the possibility of their manual input should be optional. To determine the positions of local variables, the author has developed an algorithm for efficient search of positions in the VC generation, which includes the following steps:

1) All potential positions of local variables are calculated. This can be done both by means of machine code analysis (similar to those used by modern disassemblers and debuggers) and with the help of an existing logical model of machine code and SMT-solver. The author proposes to use the second option because it is a more universal approach. In this approach, for each memory write instruction it is required to prove by solver that there are no positions on the stack that could change as a result of the operation. If solver managed to generate a counterexample, the position found is a potential position for the local variable. This algorithm allows you to find positions for local variables, but it can be difficult if there is an array on the stack. In this case, if solver fails to determine which position of the array was recorded, the result may not be determined and the user will have to specify the position himself. Similarly, you can calculate the registers to which the local variable can be mapped.
2) Each local variable is assigned a potential positions set, which may depend on its size in bytes.
3) For each invariant from the list of invariants for the proof, the ”cost” of proving its correct initialization should be calculated. Here, the cost is the number of all possible combinations of potential positions of local variables involved in the description of this invariant. Here it is necessary to take into account that each variable has its own unique memory location, therefore, combinations of potential positions should consist only of unique values. It is also worth noting that this step should be carried out only when proving the initialization of the invariants, since the initialization of the invariant is proved independently of the other loop invariants, and the proof of preserving the loop invariant must be proved given that all other invariants must be satisfied. Thus, when proving the correct initialization of

the invariant, it is possible to reduce the number of local variables necessary for binding, and, as a consequence, the "cost" of the proof may differ for different invariants. If it is necessary to prove the loop invariant preservation the cost of all invariants should be considered equal to.

4) For the least cost invariant, it is necessary to try to prove correctness for each possible combinations of potential positions of local variables on which the invariant depends. The results ("unsat"/"unknown"/"sat" verdicts) should be saved in a separate list.
5) If there was no one verdict is "unsat", it is necessary to mark the invariant unproven. If at least one verdict "unsat" has been obtained, then the invariant should be considered proved and the potential positions of local variables on which the proved invariant depends should be filtered, leaving only those positions that consist in combinations of potential positions for which the invariant has been proved (the "unsat" verdict).
6) Remove the proved invariant from the list of invariants for the proof and (if there are still invariants in the list) proceed to step 3.

Using this algorithm, it is possible in some cases to significantly reduce the number of generated targets relative to a complete search. As an example, let's take a function with 3 different local variables with values $s = -1$, $i = 0$, $n = 90$ at the loop entry point and three potential positions on the stack: $sp - 0x10$, $sp - 0x18$, $sp - 0x24$, respectively. For simplicity, the size of variables and positions will be considered equal to 4 bytes. Initially, the correspondence between the positions of local variables is not known. Based on these data, we try to prove the initialization of the following invariants: "$0 <= i < 100$", "$s == 2 * i - 1$" and "$s < n + i$". According to the algorithm, we calculate the cost of proving the invariants, which will be equal to 3, 6 and 6, respectively. Next, try to prove the correctness of the first invariant with the cost of 3 and will find two potential positions ($sp - 0x18$ and $sp - 0x24$) for the variable i (we will also be able to prove the invariant for variable n). Second, we perform filtering to remove the position of the $sp - 0x10$ for the variable i. Recalculate the costs of the remaining invariants: the result of 4 and 4 (the cause of reducing the cost is reducing the number of potential positions for the variable i, on which the invariants depend). When proving the correctness of the initialization of the second invariant, only one set of potential positions for the variables s and i is $sp - 0x10$ and $sp - 0x18$, respectively, will be selected. We filter and proceed to the proof of the last invariant. It is possible to select only one target for it the position for n will be selected by the elimination method. We prove the invariant, perform filtering and get the same correspondence between variables and their positions on the stack, which was set by the compiler.

V. Evaluation

At the time of writing, the approach proposed by the author was partially implemented in the system of deductive verification of machine code [5]. Using this approach, the machine code of the function of the sum of numbers from 0 to N (Table I), as well as some other functions with loops, was successfully verified. For each generated VC, a verdict was obtained confirming its correctness. In addition, the positions of local variables on the function stack were strictly determined by the computer during the verification process. More complex testing is planned after the full implementation of the approach.

VI. Conclusion

Verification of functions with loops is one of the main stumbling blocks in the verification of machine code. Various research groups have proposed various solutions that however impose serious limitations, such as the need to use interactive proof assistants or the introduction of dependency on the target compiler. However, due to the high complexity of the machine code structure, the use of interactive proof assistants can significantly slow down the verification process and require very experienced staff. Dependency on the target compiler also reduces the universality of the approach and requires its integration into the source code compilation process, which can cause some difficulties. In contrast to these works, the author proposes to use a compiler-independent approach based on the use of automatic SMT-solvers. To implement the approach, we propose to use two main algorithms, as well as a tool for CFG extraction. The first algorithm allows the basic blocks of the function CFG to be joined in such a way that they become suitable for VC proving. The second algorithm allows restoring the lost links between the local variables of the high-level function and their positions in memory or on the processor registers at the machine code level. Using this approach allows in most cases to generate such VC, which will be sufficient for deductive verification of the machine code of the function with loops.

The work is in progress. At the moment, the approach has been partially implemented in the system of deductive verification of machine code. Its full implementation and testing is the nearest direction for further work. Also among the possible areas for further research can be identified the study of problems arising in the proof of the correctness of functions containing calls to other functions or system calls. There is a separate issue with the security check of the machine code execution, i.e. the absence of exceptions at the processor level, incorrect memory readings or stack overflows. Also of great importance is the study of the applicability of the machine code deductive verification system for solving real industrial problems.

References

[1] R.W. Floyd. *Assigning Meanings to Programs*. Mathematical Aspects of Computer Science. Proceedings of Symposia in Applied Mathematics, 19, 1967. P. 19-32. DOI: 10.1090/psapm/019/0235771.

[2] C.A.R. Hoare. *An Axiomatic Basis for Computer Programming*. Communications of the ACM, 12(10), 1969. P. 576-585. DOI: 10.1145/363235.363259.

[3] C Barrett, R Sebastiani, S Seshia, and C Tinelli. *Satisfiability Modulo Theories*. Handbook of Satisfiability, vol. 185 of Frontiers in Artificial Intelligence and Applications, (A Biere, M J H Heule, H van Maaren, and T Walsh, eds.), IOS Press, Feb. 2009, pp. 825885.

[4] C. Sun, V. Le, Q. Zhang, Z. Su *Toward understanding compiler bugs in gcc and llvm*. ISSTA 2016, pp. 294-305.
[5] Putro P.A. *Combining ACSL Specifications and Machine Code*. Trudy ISP RAN/Proc. ISP RAS, vol. 30, issue 4, 2018. pp. 95-106. DOI: 10.15514/ISPRAS-2018-30(4)-6
[6] M.O. Myreen. *Formal Verification of Machine-Code Programs*. Ph.D. Thesis. University of Cambridge, 2009. 131 p.
[7] K. Slind, M. Norrish. *A Brief Overview of HOL4*. Theorem Proving in Higher Order Logics (TPHOLs). Lecture Notes in Computer Science (LNCS), 5170, 2008. P. 28-32. DOI: 10.1007/978-3-540-71067-7_6.
[8] A. Fox. *Formal Specification and Verification of ARM6*. Theorem Proving in Higher Order Logics (TPHOLs). Lecture Notes in Computer Science (LNCS), 2758, 2003. P. 25-40. DOI: 10.1007/10930755_2.
[9] K. Crary, S. Sarkar. *Foundational Certified Code in a Metalogical Framework*. Technical Report CMU-CS-03-108. Carnegie Mellon University, 2003. 19 p.
[10] X. Leroy. *Formal Certification of a Compiler Back-End or: Programming a Compiler with a Proof Assistant*. Principles of Programming Languages (POPL), 2006. P. 42-54, DOI: 10.1145/1111037.1111042.
[11] Y. Bertot. *A Short Presentation of Coq*. Theorem Proving in Higher Order Logics (TPHOLs). Lecture Notes in Computer Science, 5170, 2008. P. 12-16. DOI: 10.1007/978-3-540-71067-7_3.
[12] P. Baudin, P. Cuoq, J.-C. Filliâtre, C. Marché, B. Monate, Y. Moy, V. Prevosto. *ACSL: ANSI/ISO C Specification Language*. Version 1.13, 2018. 114 p.
[13] T.M.T. Nguyen, C. Marché. *Hardware-Dependent Proofs of Numerical Programs*. Certified Programs and Proofs (CPP), 2011. Lecture Notes in Computer Science 7086. P. 314-329. DOI: 10.1007/978-3-642-25379-9_23.
[14] G. Barthe, T. Rezk, A. Saabas. *Proof Obligations Preserving Compilation*. Formal Aspects in Security and Trust (FAST), 2005. Lecture Notes in Computer Science 3866. P. 112-126. DOI: 10.1007/11679219_9.
[15] *MicroTESK Framework* – http://www.microtesk.org
[16] M. Freericks. *The nML Machine Description Formalism*. Technical Report TR SM-IMP/DIST/08, TU Berlin CS Department, 1993. 47 p.
[17] C. Barrett, P. Fontaine, C. Tinelli. *The SMT-LIB Standard Version 2.6*. Release 2017-07-18. 104 p.
[18] *JavaScript Object Notation* – https://www.json.org/
[19] R. E. Tarjan, *Dep-first search and linear graph algorithms* SIAM J. Comput., vol. 1, no. 2, pp. 146-160, June 1972.
[20] *ocaml-containers library* – https://github.com/c-cube/ocaml-containers

Extracting Assertions for Conflicts in HDL Descriptions

Alexander Kamkin[1, 2, 3, 4], Mikhail Lebedev[1], Sergey Smolov[1]
[1]Ivannikov Institute for System Programming of the Russian Academy of Sciences
[2]Lomonosov Moscow State University
[3]Moscow Institute for Physics and Technology
[4]National Research University Higher School of Economics
E-mail: {kamkin, lebedev, smolov}@ispras.ru

***Abstract*—Data access conflicts may arise in hardware designs. We propose a static analysis based approach to data conflicts extraction from HDL descriptions. Conflicts are formulated as conditions on variables. Bounded model checking is used to check whether these conditions are reachable. If true, counterexamples are generated and then translated to HDL testbenches. The proposed approach was applied to several open source HDL benchmarks.**

Keywords—hardware design; hardware description language; functional verification; static analysis; test generation; data access conflict; guarded action; model checking.

I. Introduction

Modern hardware designs contain multiple modules and processes operating on the common set of internal variables. In this case *conflicts*, i.e. illegal accesses from different processes to the same data, may appear. Requirements on how to operate with modules and avoid conflicts in a communication protocol can be described both in *formal* (machine-readable) and *informal* (human-readable) ways.

In this paper a formal verification based approach to conflict extraction is proposed. The idea is to analyze an HDL description aimed at finding *data access conflicts* [1]. Both the conflicts and the target description are then automatically translated into the input format of a *model checking* tool. The tool generates counterexamples for the feasible conflicts.

II. Related work

In [1] several categories of data conflicts are described: *read after write* (RAW), *write after read* (WAR) and *write after write* (WAW). The HOL verification system [2] was used to check a RISC processor's pipeline. The formal specification of pipeline was implemented manually that is hard to be done for modern processors because of their complexity.

In [3], a GoldMine methodology is presented for automatic generation of hardware assertions. The method uses a combination of data mining and static analysis techniques. First, the HDL design is simulated to generate data about the design's dynamic behavior. Then, the generated data are mined for "candidate assertions" that are likely to be *invariants*. The data mining technique used is a decision-tree-based supervised learning algorithm. The candidate assertions are then passed through the Cadence Incisive Formal Verifier [4] tool to filter out the spurious candidates. The disadvantages of GoldMine are: 1) usage of commercial tool; 2) invariants' incompleteness because of random simulation usage at an early stage.

III. Assertion extraction method

We propose a new approach to data access conflicts extraction in HDL descriptions. Our goal is to detect conflicts and provide proofs that they may happen. The method is aimed at conflicts of the following types:

1) *read-write* (RW): on the same clock tick one process writes the variable and the other process reads it;
2) *write-write* (WW): on the same clock tick at least two processes write the same variable;
3) *write-read-write* (WRW): we assume that a variable should be read between two writes;
4) *undefined* (UNDEF): variable is read before it was written.

The method consists of the following steps: 1) *Control Flow Graph* (CFG) extraction; 2) transformation to *Guarded Actions Decision Diagram* (GADD); 3) process invariants and conflict assertions extraction; 4) invariants and assertions translation into an input format of a model checking tool; 5) counterexample generation. All method steps are made automatically. The CFG representation is built for every process of the HDL model using an abstract syntax tree traversal compiler-like approach [5]. From the structural view, CFG is a directed graph. Nodes of the graph contain HDL operators; edges of the graph mean control flows. On the left side of Fig. 1 the fragment of Verilog code is shown; the related CFG is shown on the right side. Branch operators are shown as diamond nodes and called as C^i. Basic block operators are shown as rectangles and called as B^i. Graph edges contain the values that the branch conditions should be equal to for edges to be passed. CFG is supposed to be acyclic: HDL loops with constant numbers of iteration are unrolled into sequences of operators.

```
if (state_bank3[inst_addr] > 1) // C1
        prediction[3] <= 1;     // B1
else
        prediction[3] = 0;      // B2
if (state_bank2[inst_addr] > 1) // C2
        prediction[2] <= 1;     // B3
else
        prediction[2] <= 0;     // B4
if (state_bank1[inst_addr] > 1) // C3
        prediction[1] <= 1;     // B5
else
        prediction[1] <= 0;     // B6
```

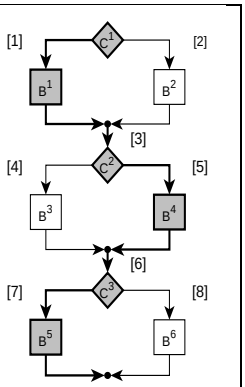

Fig. 1. Control Flow Graph Example

The next step is the transformation of the CFG to a GADD that is a labeled DAG of guarded actions. A pair $\{\gamma, \delta\}$, where γ is a guard and δ is an action, is called a *guarded action* (GA) [6]. The main idea of the CFG-GADD transformation method is in extraction of branch-free sub-paths from the CFG. Every such sub-path (GA) contains a condition (*guard*) and a sequence of assignment operators (*action*). For action to be executed the guard should be satisfied. Actions are represented in the *static single assignment* (*SSA*) form [7]. To connect subsequent GAs into a complete CFG path an auxiliary *phase* variable is used.

To illustrate this step of the approach, let us take the previous example (see Fig. 1). The CFG model contains the following execution path: $C^1 \to B^1 \to C^2 \to B^4 \to C^3 \to B^5$. Path nodes are grey-colored in the Fig. 1; path edges are highlighted too. The following GAs can be extracted from the path: $\{C^1, B^1\}$, $\{C^2, B^4\}$, $\{C^3, B^5\}$. Every GA corresponds to a unique value of the phase variable. The phase variable changes its value upon moving from one GA to another. On Fig. 1 related values of the phase variable are shown in brackets (the initial phase value is 0). Fig. 2 shows the example of GADD model from the previous example:

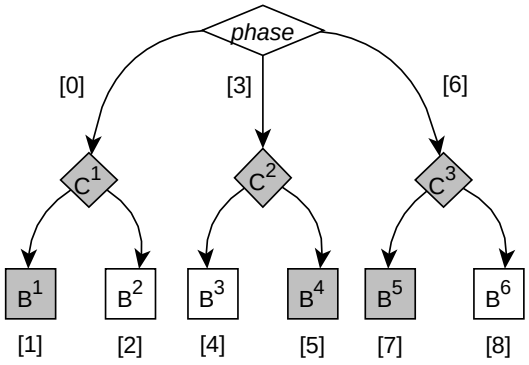

Fig. 2 GADD example

The main advantage of GADD model is path number reduction in comparison to CFG. In worst case (when CFG is a sequence of branch operators) the GADD has $O(n)$ paths, where n is the number of branches, but the CFG has $O(2^n)$.

Then the GADD is transformed into the *invariants* of the processes, which represent the cycle-accurate behavior of the processes. The invariant is a logical formula and is a kind of a SSA representation of the whole process. Every GA of the GADD contains a unique phase variable value assignment. These unique values can be used as SSA version values of the variables. The phase variable is removed from the resulting formula because it does not affect the process behavior.

Each variable that is *defined* in a GA is labeled by the corresponding phase value. Each variable that is *used* in the GA is labeled by the set of phase values of the preceding GAs. For guards intermediate variables are introduced. To determine the values of the used variables, a backward search of the GADD is used: it is obvious that the variable value was defined in one of the preceding GAs or did not change from the previous cycle. After that the process invariant formula is built as a conjunction of equality expressions representing each GA's guards and actions.

Let us see how a process invariant is built using a small example. Fig. 3 shows a part of the GADD and represents three guarded actions.

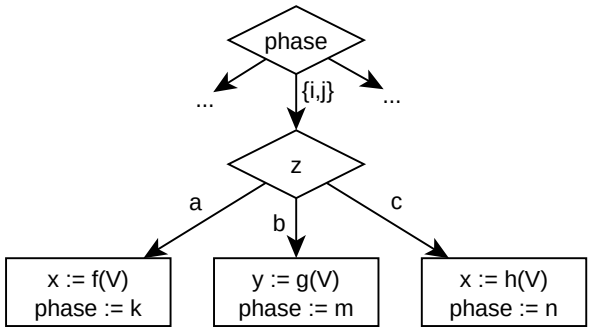

Fig. 3. Original part of the GADD

The guard conditions are: $z == a$, b and c respectively, and the actions contain definitions of variables x, y and unique definitions of $phase$. A set of the preceding phase values is $\{i, j\}$; z is a variable; a, b and c are constants; f, g and h are functions defining the values of x and y; V is a set of process variables.

On the first step we label the variables by the corresponding phase values. The result of that is shown on Fig. 4.

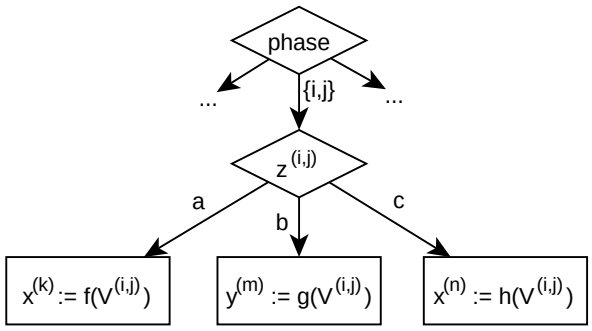

Fig. 4. GADD part with labeled variables

The used variables are now labeled by the preceding phase values $\{i, j\}$ and the defined variables are labeled by the corresponding phase values k, m, n. Phase definitions are removed.

Then we introduce and define a variable for each guard. The guard variable definition consists of a guard expression and a link to the preceding guards. This helps us restore the path from the beginning of the process to the corresponding guarded action. For example:

$$guard^{(k)} := (z^{(i,j)} == a)\ \&\ (guard^{(i)} \mid guard^{(j)})$$

When all the variables in all the GAs are labeled by phases, the remaining unknown used variables values can be determined. Let us determine the value of $z^{(i,j)}$. So we traverse the GADD backward using the preceding phase values, starting from i and j (Fig. 5). When a definition is found on some path (denoted def on Fig. 5), the traversal of this path completes and the definition value is collected. If the beginning of the process is reached, the variable preserves its value from the previous cycle.

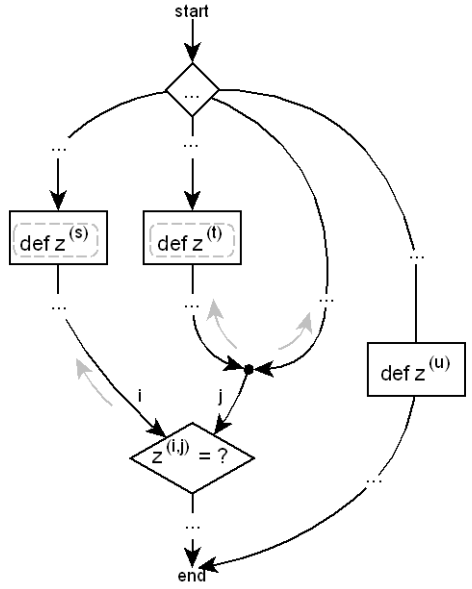

Fig. 5. Version value search (CFG view).

In the example on Fig. 5 the variable z is defined on phases s and t or may not change its value. So the value of $z^{(i,j)}$ can be determined as follows:

$$z^{(i,j)} := guard^{(s)}\ ?\ z^{(s)} : guard^{(t)}\ ?\ z^{(t)} : z$$

As the guard variables *s* and *t* are linked to their preceding phases, their corresponding conditions are incompatible and $z^{(i,j)}$ gets the proper value.

On the final step the invariant formula is built. As it was mentioned, it is a conjunction of equality expressions for every labeled variable of the process including the guard variables:

$$x^{(k)} == f(V^{(i,j)})\ \&\ y^{(m)} == g(V^{(i,j)})\ \&\ x^{(n)} == h(V^{(i,j)})$$
$$\&\ guard^{(k)} == ((z^{(i,j)} == a)\ \&\ (guard^{(i)} \mid guard^{(j)}))$$
$$\&\ guard^{(m)} == ((z^{(i,j)} == b)\ \&\ (guard^{(i)} \mid guard^{(j)}))$$
$$\&\ guard^{(n)} == ((z^{(i,j)} == c)\ \&\ (guard^{(i)} \mid guard^{(j)}))$$
$$\&\ z^{(i,j)} == (guard^{(s)}\ ?\ z^{(s)} : guard^{(t)}\ ?\ z^{(t)} : z)\ \&\ \ldots$$

After the process invariant is built, the definition and usage conditions can be collected. They are collected only for internal and output variables of the HDL model, because input variables can be only used.

If a variable is *defined* (*used*) in the action of a GA, its definition (usage) condition equals the guard variable that corresponds to this GA. If a variable is used in the guard condition of a GA, its usage condition equals the disjunction of the corresponding guard variables of the preceding GAs. The variable definition (usage) condition of the whole process is the disjunction of the variable definition (usage) conditions of the GAs.

In our example, the definition conditions for variables x and y are:

$$def(x) = guard^{(k)} \mid guard^{(n)}$$
$$def(y) = guard^{(m)}$$

The usage condition for variable *z* is:

$$use(z) = guard^{(i)} \mid guard^{(j)}$$

Then the conditions are transformed into the assertions of conflict types described above. The assertions are represented as the *Linear-time Temporal Logic* (LTL) [8] formulas and state that the abovementioned conflicts never happen.

If, for example, a variable v is defined and used both in processes $p1$ and $p2$, the corresponding RW conditions are:

$$!\ \boldsymbol{F}\ (def_{p1}(v)\ \&\ use_{p2}(v))$$
$$!\ \boldsymbol{F}\ (def_{p2}(v)\ \&\ use_{p1}(v))$$

The corresponding WW condition:

$$!\ \boldsymbol{F}\ (def_{p1}(v)\ \&\ def_{p2}(v))$$

The corresponding WRW condition:

$$\boldsymbol{F}\ ((def_{p1}(v) \mid def_{p2}(v))$$
$$\&\ (\boldsymbol{F}\ (use_{p2}(v) \mid use_{p1}(v))\ \boldsymbol{U}\ (def_{p1}(v) \mid def_{p2}(v))))$$

The corresponding UNDEF condition:

$$\boldsymbol{G}\ (!\ (use_{p2}(v) \mid use_{p1}(v))\ \boldsymbol{U}\ (def_{p1}(v) \mid def_{p2}(v)))$$

Invariants and assertions are then translated into the SMV model. Their translation is rather straightforward. It is only important to define the variable value in the next state of the model using the keyword *next*. This value equals the last version of the variable before the end of the process. For example, if the final phase values of a process are k, l, m, then the next state value of a variable *v* is defined as:

$$next(v) := v^{(k,l,m)}$$

The SMV model is checked by the nuXmv [9] tool using bounded model checking. If an assertion is violated, a counterexample is generated and a potential conflict is found. The counterexamples may be later translated into test scenarios for the original HDL description.

IV. Case Study

The method was implemented in the Retrascope [10] tool. It was applied to a range of Verilog designs from the Texas-97 [11], VCEGAR [12] and Verilog2SMV VIS [13] benchmarks and the 16-bit MIPS processor [14]. Table I contains the results of the method's application: benchmark descriptions and generated assertions amount. Here *N* means total amounts of top level modules. Most of the assertions denote only suspicious situations, so the results should be analyzed by a verification engineer to filter out the real data conflicts.

TABLE I. Benchmark descriptions and potential conflicts.

Bench	N	LOC	Assertions			
			RW	WW	WRW	UNDEF
Texas'97	17/58	69539	408	26	211	211
VCEGAR	20/34	15144	315	25	167	167
Verilog2SMV	12/20	4494	78	0	62	62
mips16	5/12	1007	10	0	9	9

Example of a RW situation, which is not a conflict (*mips16/ID_stage.v*):

```
module ID_stage
…
wire  [2:0]     ir_dest_with_bubble;
wire  [2:0]     write_back_dest;

assign ir_dest_with_bubble = ( instruction_decode_en ) ?
        ir_dest : 0;
assign write_back_dest = ir_dest_with_bubble;
```

Signal *ir_dest_with_bubble* is defined in one process and is used in the other process at the same time.

Example of a WW situation, which seems to be a real conflict (*Texas97/MPEG/prefixcode.v*):

```
module start_code_prefix(start,done…);
…
reg      monitor;
…
always @(posedge read_signal) begin
        monitor=start;
…
end
always if( start==0) begin
…
        monitor=0;
end
```

Variable *monitor* is defined simultaneously, if *read_signal* rises and at the same time *start* equals 0.

Example of an UNDEF situation, which is also not a conflict (*mips16/ID_stage.v*):

```
module ID_stage

…
reg    [15:0]    instruction_reg;
…
always @(posedge clk or posedge rst) begin
        if (rst) begin
                instruction_reg <= 0;
        end
        else begin
                if (instruction_decode_en) begin
                        instruction_reg <= instruction;
                end
        end
end
assign ir_op_code = instruction_reg[15:12];
```

Register *instruction_reg* is undefined from the start of simulation until the *clk* or *rst* rising edge.

V. Conclusion and Future Work

In this paper the approach to data access conflicts extraction from HDL descriptions has been proposed. We extract assertions from the source code and automatically translate them into the input format of the model checker. The tool generates counterexamples that are proofs of conflicts' reachability. We have implemented the approach in the Retrascope toolkit and applied it to several open source HDL benchmarks.

One direction for future research is to propagate assertions from internal variables' to interface variables. Such assertions can be used to improve protocols of unknown third-party modules or even to reconstruct protocols. Another direction is the generation of *checkers*, i.e. HDL wrappers for target modules that check their behavior through simulation.

References

[1] S. Tahar, R. Kumar. "Formal Verification of Pipeline Conflicts in RISC Processors", *Proceedings of the European Design Automation Conference (EURO-DAC)*, 1994, pp. 285-289.

[2] M. Gordon, T. Melham. "Introduction to HOL: A Theorem Proving Environment for Higher Order Logic", *Cambridge University Press*, 1993, 492 p.

[3] S. Hertz, D. Sheridan, S. Vasudevan, "Mining Hardware Assertions With Guidance From Static Analysis", *IEEE Transactions on Computer-Aided Design of Integrated Circuits and Systems*, Vol. 32, No. 6, 2013, pp. 952-965.

[4] Cadence Incisive Formal Verifier. https://community.cadence.com//CSSharedFiles/forums/storage/22/10078/IncisiveFV_ds.pdf

[5] A. V. Aho, R. Sethi, J. D. Ullman, "Compilers: principles, techniques, and tools", 1986, 796 p.

[6] J. Brandt, M. Gemunde, K. Schneider, S. Shukla, and J.-P. Talpin, "Integrating system descriptions by clocked guarded actions", *Proceedings of Forum on Design Languages (FDL)*, 2011, pp. 1-8.

[7] R. Cytron, J. Ferrante, B.K. Rosen, M.N. Wegman, F.K. Zadeck, "Efficiently computing static single assignment form and the control dependence graph", *ACM Transactions on Programming Languages and Systems*, 1991, pp. 451-490.

[8] A. Pnueli, "The temporal logic of programs", 18th Annual Symposium on Foundations of Computer Science, 1977, vol. 00, pp. 46-57.

[9] nuXmv model checker. https://nuxmv.fbk.eu

[10] Retrascope toolkit. https://forge.ispras.ru/projects/retrascope

[11] Texas-97 Verification Benchmarks. https://ptolemy.berkeley.edu/projects/embedded/research/vis/texas-97

[12] VCEGAR benchmark collection. https://www.cprover.org/hardware

[13] Verilog2SMV tool. https://es-static.fbk.eu/tools/verilog2smv

[14] Educational 16-bit MIPS Processor. https://opencores.org/projects/mips_16

Towards a Probabilistic Extension to Non-Deterministic Transitions in Model-Based Checking

Sergey Staroletov
Polzunov Altai State Technical University,
Lenin avenue 46, Barnaul, 656038, Russia
Email: serg_soft@mail.ru

***Abstract*—The more the software systems complexity increases, the harder to describe models for them; in addition, these models should be adequate. For many types of systems, we can create models by replacing complex algorithms of interaction with occurrences of certain non-deterministic events. The paper is considered a problem of modeling probabilistic transitions in Promela language (SPIN verification tool) and a technique of enhancing its grammar for the purpose of probabilistic verification. The extension is based on non-deterministic choice operator in Promela.**

***Keywords*—Model Checking, Promela, Probabilistic Model Checking**

I. Research objectives

Software engineering world has already developed a sufficient amount of testing technologies as processes of searching inconsistencies between programs and requirements for them, and they are applicable well when creating typical desktop applications or web sites with their business logic. However, for systems that need to work in the critical industries such as embedded control systems, aircraft management entities, operating system components, the testing process does not guarantee sufficient output quality of the product and the appearance of an error can lead to costly consequences. It is because the testing is not able to prove the absence of errors over all possible states and can only show their lack at a particular test.

Formal verification process (in comparison with testing) enables us to prove the infallibility of some formal model in relation to system requirements, expressed in a predicate logic, and we can talk about the correctness of the model on all data inputs and all specified methods of interaction of model entities.

This study applies formal models in Promela (*"protocol meta-language"*) for SPIN verification tool (*"simple Promela interpreter"*) [1], [2], and the system requirements are defined in terms of linear time temporal logic (LTL).

The more the software systems complexity increases, the harder to describe models for them; in addition, these models should be adequate. For many types of systems, we can create models by replacing complex algorithms of interaction with occurrences of certain non-deterministic events.

The goal of the paper is to move from the non-determinism to probabilities. The two words mean some variations of unpredicted behaviour, but when we talk about the last one, we operate with probability values as guards of program actions, and they can be either *a priori* and *a posteriori* (pre-defined before the execution and calculated after some cases of it).

Promela modeling language already includes *non-deterministic transitions in the IF clause*, but in the simulation mode the corresponding actions are selected randomly and equiprobably. It can lead to a problem of simulation of complex protocols, distributed and network software, with given initial requirements with probabilities.

In this work, an approach to extend Promela language with probability-based constructions is presented for simulating behaviours with given probabilities in the system description. To solve this problem, some SPIN verifier internals are studied and described. Moreover, a method to *probability driven programming* is shown, and some further steps to move to Probabilistic model checking are described.

II. Related work

A. Background of the proposed method

In the articles [3], [4] we considered creating a model of interoperational programs on different levels of abstraction: from the code level to the logical level as the interaction between components of a distributed system, constructed with a goal to its verification and testing. As well as we proposed methods of software development (according to the Model-driven developing approach), when the development begins with a model, then the code is generated and can be verified subsequently. For the verification, we provided methods for transforming extended automata models into Promela language. This language was chosen because the programs in it are created in accordance with the *"Actors"* approach [5] that involves the interoperation between low coupling processes that interact through messages. This approach allows modeling distributed systems, multi-threaded systems, multi-component systems that interact through API calls.

The developed model has probabilistic transitions between states of an extended finite state machine. In Promela language there are not probabilistic transitions explicitly, but there are non-deterministic conditions, which became the basis for creating the technology proposed here for transformation of the non-deterministic model into probabilistic one. In [3] it was considered a way to generate an additional duplicated code to

satisfy a given guard probability in the simulation mode, but it is a very naive approach.

B. Probabilistic model checking

According to [6], the Probabilistic model checking problem is stated as follows:
Given a property ϕ, the Problem consists of checking whether a stochastic system satisfies ϕ with a probability greater than or equal to a certain threshold θ.

Herein we consider to LTL properties ϕ. For an example to understand the problem, refer to the *Roundabout Maneuver* [7] – is a behavior of two aircraft to make *Collision Avoidance*, and it is a subject to cooperation in air traffic control. The avoidance of collision is achieved by an agreement on some common angular velocity ω_{xy} and common centre c_{xy} around which both can fly by the circle safely without coming close to each other not more than R_{safe} [7]. There is the following precondition to the entry procedure of the Maneuver and the safe property to verify:

$$isSafe ::= (x_1 - y_1)^2 + (x_2 - y_2)^2 \leqslant R_{safe}^2 \qquad (1)$$

where $x = (x_1, x_2)$ is a first planar position, $y = (y_1, y_2)$ is a second planar position.

Model checking approach can be applied to this problem by specifying an LTL property (for example, in SPIN notation):

$$[\,]\ (isSafe == 1) \qquad (2)$$

where "[]" is the "Globaly" LTL operator and 1 is an alias for true. Statement (2) in natural language means "during the execution in all the states of the program model, the rule (1) will be preserved as true".

When we move to the Probabilistic model checking, we can specify a PLTL property as

$$[\,]_{\ \theta>90\%}\ (isSafe == 1) \qquad (3)$$

and here we like to verify that the system satisfies the safe property with probability of 90% or higher (that means the system will be safe in 90% cases for some reasons when it start working from an initial state and finish in a final state; or: in 10% cases or less two aircraft can be closer than R_{safe}).

C. Probabilistic languages and models to verify

In the work [8] the Probabilistic model checking problem was faced and an approach was presented to ensure that a given labeled Markov chain satisfies a given LTL property with a given probability. In [9] the approach is extended to verify these things effectively using an LTL-BDD representation of formulas.

The authors of the publications [10], [11] state that Markovs' models cannot be useful at the system description level since they are not able to describe parallel processes. So, to evaluate aspects such as the probability of system failure they construct Discrete Time Markov Chain (DTMC) models from the composition of the Probabilistic Component Automata (PCA) representations of each component and then analyse them in tools such as PRISM [12].

In the work [13] the SMC (Statistical model checking) approach has been introduced, and the tool Uppaal [14] has been extended to check system properties using an extended automaton model. The tool offers probabilistic simulation and verification by specifying in the user interface probability distributions that drive the timed behaviors, and the engine offers computing an estimate of probabilities and comparison between estimated probabilities without actually computing them.

In the book [16] the author decided to implement classes in Scala language to allow developers to make complex probabilistic and statistical programs.

In the paper [17] the authors decided to implement from scratch a language similar to Promela with some probabilistic additions to satisfy the probabilistic model checking goals. They used SOS-rules in the Plotkin style [15] to describe the language formally. For example, this language offers to write code with PIF (probability IF clause):

$$\textbf{PIF}\ [p1] \Rightarrow P1 ... [pn] \Rightarrow Pn\ \textbf{FIP} \qquad (4)$$

That means: probabilities p1..pn lead the code P1..Pn to execute. In the current paper, we are going to follow this approach, but without creating a "yet another" language and a new tool, because now Promela language and SPIN tool are well-designed and community-approved, and new language creation instead of extension of an existing one should be well justified. Of course, it is possible to declare some inductive rules for a theorem prover for making the evidence of particular problems like it is done in [18], but extending a modeling language to some conventional structures and rules can involve additional engineers to the formal proof process of software.

D. How to create non-deterministic transitions in Promela

It is known that the programs in Promela are modeled in the form of instructions in a special language, which at the same time looks like C and also like functional languages such as Erlang (it refers to "Actors" approach). The language contains conditions in the form

```
if
  :: boolean expression1 -> actions1
  :: boolean expression2 -> actions2

  :: boolean expressionN -> actionsN
fi
```

It is considered that in order to perform a certain action, it is necessary that the corresponding logical expression was true. However, if multiple logical expressions are true in the same if construction, it is considered that the next step is one of the non-deterministic choices of them. Refer to the code snippet in Promela, modeling the *Leader Selection algorithm* (Dolev, Klawe & Rodeh [19]):

```
if      /* non-deterministic choice */
  :: Ini[0] == 0 && N >= 1 -> Ini[0] = I
  :: Ini[1] == 0 && N >= 2 -> Ini[1] = I
  :: Ini[2] == 0 && N >= 3 -> Ini[2] = I
```

```
  :: Ini[3] == 0 && N >= 4 -> Ini[3] = I
  :: Ini[4] == 0 && N >= 5 -> Ini[4] = I
  :: Ini[5] == 0 && N >= 6 -> Ini[5] = I
fi
```

with N equal to, for example, 3 and the zero value of Ini, it has four variants of non-deterministic steps in the Promela model to continue at this point. In the SPIN simulation mode, a necessary option can be selected by a user in the interactive dialog or enabled by using a random number generator with a given initial value.

If there is a software system that works in some way and we have calculated the probabilities of certain events in it, for example, transitions to different states, then to simulate such a system in Promela we can propose using a technology to increase the likelihood in the simulation mode: for events that are more likely we can proceed to simply increase the number of identical conditions and actions.

For example in this case the probabilities of both actions are identical (50 and 50 percents):

```
if
  :: boolean expression1 -> actions1
  :: boolean expression2 -> actions2
fi
```

If we want to increase the likelihood of action1, the following code

```
if
  :: boolean expression1 -> actions1
  :: boolean expression1 -> actions1
  :: boolean expression2 -> actions2
fi
```

does not change the logic of the transition, it changes the likelihood of the first step in the model. And the probabilities of selection this actions equal to 66.(6) and 33.(3) percents. To check this assumption, we can write a program in Promela, which counts the number of execution of one of the branches into p variable:

```
mtype = {s1, s2, s3};
active proctype main() {
mtype state;
int p = 0;
int count = 0;
do
::{
  state = s1;
  do :: {
    if
    :: (state == s1) -> {
      if
      :: true ->  {state = s2;  p = p + 1}
      :: true ->  {state = s2;  p = p + 1}
      :: true -> state = s3
      fi
    }
    :: (state == s2) -> state = s3;
    :: (state == s3) -> break;
    fi;}
  od
  count = count + 1;
  }
  :: (count >= 100) -> goto fin;
od
fin:
printf ("p = %d", p);
}
```

As a result, starting the model execution with different values of the random number generator, we will receive the value of p = 60 ... 70.

In the current SPIN implementation, a next running node in a non-deterministic transition is selected using seed-based random generator, see run.c:

```
/* CACM 31(10), Oct 1988 */
Seed = 16807*(Seed%127773) - 2836
*(Seed/127773);
if (Seed <= 0) Seed += 2147483647;
return Seed;
```

If we need to create some emulation of probabilistic transition with a given probability, it is possible to generate a large number of repetitive conditions [3]. However, the disadvantages of this approach are: duplicated code, generation a large number of conditions, difficulties with manual testing this code.

III. The proposed solution

We propose first to extend the Promela grammar with an annotation of probabilistic transition:

```
if
  :: [prob = value %] condition -> actions
...
fi
```

where the ”prob value” (probability value) is an integer of [0..100]. In this case, we can get rid of unwanted repetitive conditions, and perform the transition with a probability within the SPIN code of the analysis of transitions with using abstract syntax tree.

SPIN is shipped in the open source code, now available in Github repository. Promela language parser is implemented using Yacc tools. A fragment of the grammar is introducing the changes described here (modified source from spin.y):

```
options : option
| option options
;
option  : SEP
prob
sequence OS
;

prob    :/* empty */
| '[' PROB ASGN const_expr '%' ']'
;
```

where prob – is the new grammar rule for probability transition, SEP is the "::" terminal, PROB – is the new terminal symbol "prob", ASGN is the assignment ("=") and const_expr is Promela's non-terminal (grammar rule) for constant expression that is calculated at the parsing time. This grammar extension can now allow the previous code snippet as well as usual Promela constructions.

Further, we propose to extend this idea, putting the probability of not only as a constant number but the value of a variable. In this case, the probability may dynamically be recalculated during program execution on Promela. So, the following Promela grammar addition is presented:

```
prob    :/* empty */
| '[' PROB ASGN const_expr '%' ']'
| '[' PROB ASGN expr ']'
;
```

where expr – is a grammar rule for the Promela expression.

Thus we will be able, for example, simulate and verify various training and recognition algorithms. A new probability value will be received from a different process, changed in code based on a given probabilistic transition or other different cases. So, with simple grammar additions and some changing to semantic of SPIN code, we can speak of *"Probability driven programming"* in Promela.

To continue this idea, we can propose some "syntactic sugar" for probabilistic actions with Promela channels. To simulate some networking protocols it is required to specify a loss/reliability value for a channel, that means: with a given probability a channel lose/guarantee some messages and protocols should correctly handle this. Our new additions for the channels in the grammar:

```
one_decl: vis TYPE chan_loss osubt var_list
...
;
chan_loss    : /* empty */
| '[' LOSS ASGN const_expr '%' ']'
| '[' RELY ASGN const_expr '%' ']'
;
Special : varref RCV
  rargs
| varref SND msg_loss
  margs
;
msg_loss    : /* empty */
| '[' LOSS ASGN const_expr '%' ']'
| '[' RELY ASGN const_expr '%' ']'
| '[' RELY ASGN expr ']'
| '[' LOSS ASGN expr ']'
;
```

where chan_loss is the new grammar rule to define channels, msg_loss – is the new rule to annotate the message send Promela operator (SND terminal); LOSS – is our terminal symbol 'loss' (to specify channel loss values after it) and RELY – is our terminal symbol 'rely' (to specify channel reliability values after it).

So, after the modifications, the extended Promela grammar should accept the following test code with the new annotations:

```
mtype = {s1, s2, s3};
int count = 0;
/* now define a normal chan */
chan a = [1] of { short };
/* now define a chan with 30% loss value */
chan [loss = 30%] b = [1] of { short };
/* now define a chan with 70% rely
value (or 30% loss) */
chan [rely = 70%] c = [1] of { short };

int pp = 70;

active proctype main() {
  mtype state = s1;
  count = pp - 10;
  /* send to a normal chan */
  a ! 1
  /* send to a 30% loss chan */
  b ! count;
  /* send to a chan with re-defined 10%
  loss */
  c ! [loss = 10%] 3;
  /* send to a chan with 70% reliability */
  c ! 2;
  /* send to a chan with re-defined 99%
  reliability */
  c ! [rely = 99%] 4;
  /* send to a chan with re-defined loss
  with count value */
  b ! [loss = count ] 1;
  if
    :: true -> state = s2;
    /* 10% prob transition */
    :: [prob = 10%] true -> state = s3;
    /* dynamic prob transition */
    :: [prob = pp] true -> state = s3;
    /* for the others prob will be */
       calculated as 100% - all
       specified probs */
    :: true -> state = s2;
    :: true -> state = s3;
  fi
  printf ("state = %d", state);
}
```

IV. Status and perspectives of the solution

Currently, we implemented the extension to the grammar with a goal to extend the semantics and understanding of the SPIN internal logic. The advanced program simulation in Promela as well as verification code generation are in progress. Adding probabilities to the transitions and channels with losses will allow SPIN users to model some complex interactions and probabilistic algorithms. We are making some additions on internal nodes (at the parsing time), and some – on dynamic values calculation after SPIN processes are scheduled.

With regard to verification, making the addition to Promela with transitions for a given value of probability should allow us to use probabilities in the system requirements as LTL

predicates, after which it would be possible to prove the statements of the forms ”if the transition probability is given, it satisfied the requirement ...”, ”if a requirement is satisfied, then the probability is ...”; moreover, it is possible to show a counterexample as a sequence of states that can be performed too frequently or too infrequently.

Of course, it is easy to implement our approach with probabilities as given constants in the code - however, much more interesting is to represent the implementation of probability values, given by the variables in run time. We would like to experiment with it after doing some programming stuff with SPIN sources, and we are going to compare the resulting approach with existing probabilistic model checking approaches which have been mentioned in the paper.

The advantage of this approach is an attempt to solve problems of Probabilistic model checking by using such existing community-approved verification and simulation instrument with relatively little efforts of its improvements; this approach also allows verification engineers to extend the class of verifiable systems with the SPIN verifier.

REFERENCES

[1] Holzmann, Gerard J. ”The model checker SPIN.” IEEE Transactions on software engineering 23.5 (1997): 279-295.

[2] Spin - Formal Verification. http://spinroot.com

[3] S. Staroletov. Model of a program as multi-threaded stochastic automaton and its equivalent transformation to Promela model. Ershov informatics conference. PSI Series, 8th edition. International workshop on Program Understanding. Proceedings.At: Novosibirsk, Russia. 2011

[4] S. Staroletov. Model Driven Developing & Model Based Checking: Applying Together / Tools & Methods of Program Analysis TMPA-2014:Kostroma, 2014. - pp. 215-220. ISBN 975-5-8285-0719-1. Presentation: http://www.slideshare.net/IosifItkin/model-driven-developingmodelbasedchecking

[5] Hewitt, Carl, Peter Bishop, and Richard Steiger. ”Session 8 formalisms for artificial intelligence a universal modular actor formalism for artificial intelligence.” Advance Papers of the Conference. Vol. 3. Stanford Research Institute, 1973.

[6] Clarke, Edmund, Alexandre Donz, and Axel Legay. ”On simulation-based probabilistic model checking of mixed-analog circuits.” Formal Methods in System Design 36.2 (2010): 97-113.

[7] Platzer, André, ”Differential dynamic logic for hybrid systems”, Journal of Automated Reasoning, vol. 41, no. 2, pp. 143-189, 2008

[8] Courcoubetis, Costas, and Mihalis Yannakakis. ”The complexity of probabilistic verification.” Journal of the ACM (JACM) 42.4 (1995): 857-907.

[9] J. Eliosoff. Calculating the probability of an LTL formula over a labeled Markov chain. McGill University, Montreal, 2003

[10] Rodrigues, Pedro, Emil Lupu, and Jeff Kramer. ”LTSA-PCA: Tool support for compositional reliability analysis.” Companion Proceedings of the 36th International Conference on Software Engineering. ACM, 2014.

[11] Lupu, E. C., P. Rodrigues, and Jeff Kramer. ”Compositional reliability analysis for probabilistic component automata.”

[12] M. Kwiatkowska, G. Norman, and D. Parker, ”PRISM 4.0: Verification of probabilistic real-time systems,” in CAV11, ser. LNCS, G. Gopalakrishnan and S. Qadeer, Eds., vol. 6806. Springer, pp. 585591.

[13] Sen, Koushik, Mahesh Viswanathan, and Gul Agha. ”Statistical model checking of black-box probabilistic systems.” International Conference on Computer Aided Verification. Springer, Berlin, Heidelberg, 2004.

[14] David, Alexandre, et al. ”Uppaal SMC tutorial.” International Journal on Software Tools for Technology Transfer 17.4 (2015): 397-415.

[15] G. D. Plotkin. A structural approach to operational semantics. Technical Report DAIMI FN-19, Computer Science Department, Aarhus University, 1981.

[16] Pfeffer, Avi. Practical probabilistic programming. Manning Publications Co., 2016.

[17] Baier, Christel, Frank Ciesinski, and M. Grosser. ”PROBMELA: a modeling language for communicating probabilistic processes.” Proceedings. Second ACM and IEEE International Conference on Formal Methods and Models for Co-Design, 2004. MEMOCODE'04.. IEEE, 2004.

[18] Shishkin, Evgeniy. ”Construction and formal verification of a fault-tolerant distributed mutual exclusion algorithm.” Proceedings of the 16th ACM SIGPLAN International Workshop on Erlang. ACM, 2017.

[19] Dolev, Danny, Maria Klawe, and Michael Rodeh. ”An O (n log n) unidirectional distributed algorithm for extrema finding in a circle.” Journal of Algorithms 3.3 (1982): 245-260.

[20] Hahn, Ernst Moritz, et al. ”PARAM: A model checker for parametric Markov models.” International Conference on Computer Aided Verification. Springer, Berlin, Heidelberg, 2010.

The editor for teaching the proof of statements for sets

Vadim Rublev[1] and Vladislav Bondarenko[2]

[1] Department of Theoretical Computer Science, Demidov Yaroslavl State University, Yaroslavl, 150000, Russia,
roublev@mail.ru,
ORCID 0000-0002-0252- 9958
[2] Department of Theoretical Computer Science, Demidov Yaroslavl State University, Yaroslavl, 150000, Russia,
bondarencko40@gmail.com

Abstract. One of the problems of developing a computer system for teaching proof of statements for sets is the development of software that allows a student to independently conduct step-by-step proving, starting from determining initial premise and targeted statement, and which at the same time controls at each step of proof the correctness of determining the premises of elementary conclusion of step and The correctness of the text entered by the conclusion of the step. We called this software the Editor for learning to prove assertions for sets. Namely, the solution of the problems of extracting an elementary step of proof, syntactic control of the input text and logical control of the correctness of the conclusion were the main ones in the development of the Editor. It is intended to develop an automated learning system (ALS) "Elements of set theory", the purpose of which will be to teach algebra of sets and the ability to carry out evidence with the help of the Editor.

Keywords: computer training, proving statements for sets, editor for teaching the proof, step by step proof, control of step correctness

1 Introduction

At present, the problems of teaching the bulk of students in mathematical and computer Sciences are associated with underdevelopment of thinking caused by the low quality of school education. A significant mass of school graduates do not know how to read (understand what they read), do not know how to reason, because they were not taught enough. These problems can be solved only by individual training, but this approach requires a huge additional time from the teacher, exceeding several times the hours allocated by the curriculum. Therefore, it suggests a solution in the development of computer automated learning systems (ALS), with which you can not only control the knowledge, but to conduct training. Basically, many computer systems control the testing of student memory, and therefore can teach some definitions, but not their use. A similar

solution Stepik has a disadvantage in that the choice of the correct answer is always the only one (which allows you to guess, but not know), and the solution is not controlled by the system step by step, which does not give reason to consider it even testing knowledge. ALS for the exact Sciences should teach data analysis, formalization, analysis, reasoning and transformation. The use of computer algebra [1][2] underlies the construction of such systems. For example, one of the authors of this paper used this to construct ALS of computational complexity of algorithms [3].

In this paper, models of computer-based learning to prove statements for sets are considered. These models can be divided into 2 groups: proof-of-statement models for sets and training models that prepare a student for the first group models. The models of the first group are described in the proof of statements editor for sets and the study of models of the second group related to the training of using models of the first group is supposed to be.

2 The problem of constructing a proof editor of statements for sets

To solve the problem specified in the headline, select the following task sequence:

1. Limitations on the type of statements for sets for whose prove you need to build an editor.
2. Equivalent transformation of the sets included in the statement.
3. Splitting the basic statement into an equivalent set of simple statements.
4. The choice of the method of proving a simple statement and the selection of an initial set of premises in it.
5. Definition of the elementary step of the proof.
6. Control of the correctness proof by the editor.

2.1 Statement type constraints for sets

In the general case of the statement we will consider some *universal* set U and its subsets $X_1, X_2, \ldots, X_n$. The statement uses formulas for these subsets, constructed with operations *complement, intersection, union*, and brackets, changing the order of these operations, if necessary.

We restrict ourselves to statements for sets of the following form

$< \textit{Constriction of the set relation} > \{\rightarrow \mid \leftrightarrow\} < \textit{Constriction of the set relation} >$

So in example (1)

$$\overline{X_1 \cap \overline{X}_2 \cup \overline{X}_3} = (X_2 \cup X_3) \cap \overline{X}_1 \;\leftrightarrow\; X_1 \cap X_2 \cap X_3 = \emptyset \;\wedge\; X_2 \subseteq X_1 \cup X_3 \quad (1)$$

it is argued that the equality of two sets given by expressions takes place if and only if the intersection of the subsets is empty and the second subset is included in the union of the other two.

2.2 Equivalent transformation of sets included in the statement

To simplify the process of a proof conducted by a student, it is recommended to simplify the complex expressions of some sets of statements. In this case, we mean the representation of a complex expression in the form of a union of sets (or their intersections) in some cases or as the intersection of sets (and their unions) in other cases. So in example (1) transformation of the set on the left side of the set equality (it by A) denote

$$A \equiv \overline{X_1 \cap \overline{X}_2 \cup \overline{X}_3} = (\overline{X}_1 \cup X_2) \cap X_3 = \overline{X}_1 \cap X_3 \cup X_2 \cup X_3 \tag{2}$$

gives both views (2). The set of the right part of the equation (it by B) denote is already represented in (1) by an intersection, and the union is obtained by the following transformation

$$B \equiv (X_2 \cup X_3) \cap \overline{X}_1 = X_2 \cap \overline{X}_1 \cup X_3 \cap \overline{X}_1. \tag{3}$$

The reason why such representations of the set are important is the possibilities of simplifying the conduct of the proof. The representation of a set as a union of its subsets allows us to divide the further proof into separate branches, where the membership of an element to a set becomes easier by dividing it into cases of belonging to a particular subset, and the proof for each such branch is simplified and can be conducted separately. The representation in the form of an intersection simplifies the proof of the conclusion that the element does not belong to the intersection of sets, because it is sufficient to obtain a result about its non-belonging to one of the sets belonging to the intersection.

2.3 Splitting the basic statement into an equivalent set of simple statements

If there is an equivalent operation in the basic statement, the statement can be replaced by a conjunction of two statements with implications in one direction and the other. So the statement example (1) can be replaced by the conjunction of the following statements (with the replacement of the parts of the set equality by the introduced notations A and B):

$$A = B \ \rightarrow \ X_1 \cap X_2 \cap X_3 = \emptyset \ \wedge \ X_2 \subseteq X_1 \cup X_3 \tag{4}$$

$$X_1 \cap X_2 \cap X_3 = \emptyset \ \wedge \ X_2 \subseteq X_1 \cup X_3 \ \rightarrow \ A = B \tag{5}$$

Note that statement (4), having in conclusion the conjunction, can be spitted into 2 statements. In statement (5), the relation of equality of 2 sets at the end of the implication can be replaced by the conjunction of 2 inclusion, and therefore the statement (5) can also be divided into 2. As a result, we obtain the following partition of the basic statement (1):

$$A = B \ \rightarrow \ X_1 \cap X_2 \cap X_3 = \emptyset \tag{6}$$

$$A = B \ \rightarrow \ X_2 \subseteq X_1 \cup X_3 \tag{7}$$

$$X_1 \cap X_2 \cap X_3 = \emptyset \ \wedge \ X_2 \subseteq X_1 \cup X_3 \ \rightarrow \ A \ \subseteq \ B \tag{8}$$

$$X_1 \cap X_2 \cap X_3 = \emptyset \ \wedge \ X_2 \subseteq X_1 \cup X_3 \ \rightarrow \ B \ \subseteq \ A \tag{9}$$

An example of reducing the proof of the basic statement (1) to the proof of 4 simple statements (6)-(9) shows that this can be done in other cases of the basic statements.

2.4 The choice of a method of proving a simple statement and the selection of the initial set of premises in it

In a simple statement, when performing the premises of the left part of the implication, it is necessary to prove the truth of the right part of the implication(call it a *target* statement). There are 2 methods of proof when the target is the inclusion relation of sets:

- **direct** method when we prove for an *arbitrary* element of the universal set, that from the belonging of an element to the included set follows its belonging to the including set (call it a *target conclusion*), that is, the accuracy of the inclusion.
- **indirect** method, when we assume the opposite in the target statement(*exists an element of the universal set that belongs to the included set of the target relation of the inclusion of sets, but does not belong to the including set*) and by a consistent conclusion come to a contradiction with the conjunction of premises left part of the implication to this simple statement.

For example, in simple statements (7)-(9) both methods are possible. However, for statement (7) it is more rational to apply the method (perhaps indirect fewer steps of proof), and for statements (8)and (9) the direct method is more rational.

If the target statement is the equality of a set to an empty set or to a universal set, then only the indirect method is rational. In this case, the existence of its element is opposite for an empty set, and the existence of an element that does not belong to this set is opposite for the equality of a certain set to a universal set. For a simple statement (6) you need to use an indirect method and show the contradiction with the premises of the statement.

The proof of any method begins with sequential steps, each of which is based on a premise. The initial premise in the direct method of proof is that an arbitrary element of the universal set belongs to the included set of the target statement. For example, for statement (8), the initial premise
is the expression $\forall x : x \in A$.

The initial premise in the indirect method of proof is the denial of the target statement, which is expressed by the existence of an element that contradicts the target statement. For example, for (6), the initial statement premise is the expression $\exists x : x \in X_1 \cap X_2 \cap X_3$, and for (7) – statement $\exists x : x \in X_2, x \notin X_1 \cup X_3$.

In addition to the initial premise, conclusions can be based on assumptions statement related to the conditions (left side of the implication).The statement system prepares them as the initial set of premises, adding to it the initial premise. Meanwhile

1) to the equality of sets (for example, $C = D$) there correspond 4 premises (in the example, $x \in C \to x \in D$, $x \in D \to x \in C$, $x \notin C \to x \notin D$, $x \notin D \to x \notin C$);
2) to the inclusion case (for example, $X_2 \subseteq X_1 \cup X_3$) there correspond 2 premises (in the example, $x \in X_2 \to x \in X_1 \cup X_3$ and $x \notin X_1 \cup X_3 \to x \notin X_2$);
3) to the equality of a set to the empty set (for example, $X_1 \cap X_2 \cap X_3 = \emptyset$) there correspond 1 premise (in the example, $x \notin X_1 \cap X_2 \cap X_3$);
4) and the equality of a set to the universal set (for example, $X_1 \cup X_2 \cup X_3 = U$) also matches 1 premise (in the example, $x \in X_1 \cup X_2 \cup X_3$).

For each elementary conclusion of the proof, if it is true, the system adds the conclusion as a premise to the set of premises of the proof or branch of the proof (more on that in the next section).

2.5 Definition of the elementary step of the proof

The proof is conducted with the help of a sequence of steps, at each of which an elementary conclusion is drawn, based on the indicated premises for conclusion. For educational purposes, we limit ourselves to only elementary conclusions based on no more than 2 premises. For elementary conclusions, the following ideas are used:

1. If an element belongs to a certain set (for example, premises $x \in C$), the conclusion can be its belonging to any set, covering the set of the premises (in the example, the conclusion $x \in C \cup D$).
2. If an element belongs to two sets (for example, 2 premises $x \in C$ and $x \in D$), the conclusion can be an element belonging to the intersection of these sets (in the example conclusion $x \in C \cap D$).
3. If an element belongs to a set (for example, $x \in C \cap D$), it belongs to each part of it (in the example , 2 conclusions $x \in C$ and $x \in D$).
4. If an element belongs to a intersection of sets (for example, the premise $x \in C$), it does not belong to its complement (in the example the conclusion $x \notin \overline{C}$).
5. If an element does not belong to a set (for example, premise $x \notin C$), it belongs to its complement (in the example, the conclusion $x \in \overline{C}$)).
6. If an element does not belong to two sets (for example, 2 premises $x \notin C$ and $x \notin D$), it does not belong to the union of these sets (in the example the conclusion $x \notin C \cup D$).
7. If an element does not belong to a union of sets (for example, the premise $x \notin C \cup D$), it does not belong to any of these union sets (in the example, the conclusion $x \notin C$ and the conclusion $x \notin D$).

8. If an element belongs to a union of sets (for example, the premise $x \in C \cup D$), it can belong to one of these union sets (in the example, the conclusion $x \in C$ and the conclusion $x \in D$) – this conclusion is called *the splitting of the cases.*

Note that the splitting into cases can be conducted in different ways. A partition where the sets of cases do not intersect is called *alternative.* As an example of the premise $x \in C \cup D$ you can write the following division into cases: the conclusion $x \in C$ and the conclusion $x \in D \cap \overline{C}$. This is especially important when for one case, the further conclusion is easily built. Then, for the second case, additional information is obtained, which can help in the further conclusion. If the first case is also difficult, it can be divided into 3 cases: the conclusion $x \in C \cap \overline{D}$, the conclusion $x \in C \cap D$ and the conclusion $x \in D \cap \overline{C}$.

Note also that the division into alternative 2 cases of belonging to a certain or set non-belonging to this set can always be done without relying on premises (for example, the conclusion $x \in C$ and the conclusion $x \notin \overline{C}$ form 2 cases and do not require a premise).

Each conclusion, if made correctly, is added as a premise to the preceding set of premises. But when cases appear, each of them is associated with its own independent branch of proof and many premises of this branch, which is formed from the previous set of premises by adding a new premise – the case conclusion.

Each branch of the proof must end with either a white square denoting the receipt of the target conclusion, or a black square denoting the receipt of a contradiction. If all branches of the proof from the opposite ended with a contradiction, the proof of the statement was successful. If in the direct method the proof of all branches ended, but there are branches that ended in success (a white square), the proof was successful.

2.6 Editor control of the proof

The system allows the trainee to build a proof of the basic statement. But the system has to control all his or her actions, starting from splitting into simple statements, selecting the method of proof with the organization of an initial premise, performing each elementary step of the proof up to the completion of each branch of the proof.

To this purpose, the system, at the end of the above actions (by pressing a button **Verify**), builds a Boolean function corresponding to a statement for sets (simple statements into which the basic statement is splitted, or statements of the original premise, or the statement of an elementary step, as implications of conjunctions of the premises and conclusion of the elementary step or implication of the premise and disjunction of the conclusion of cases) and verifies its identity truth (truth on any argument sets). This Boolean function (let us call it *BIF* Boolean Identification Function) is constructed as follows:

1. Each set X_i is replaced by a boolean variable y_i, whose value is equal to the truth of the statement that the element x belongs to this set ($y_i \equiv (x \in X_i)$). Other are replaced in the same way. For example, the set A is replaced by

a boolean variable a, whose name is a lowercase letter, corresponding to the set name and its true value coincides with the value of the statement of the belonging of an element x to this set, i.e. $a \equiv (x \in A)$.
2. Operations on sets of complement, intersection and union are replaced accordingly by operations of negation, conjunction and disjunction for the corresponding subsets of statements.
3. The equality for sets is replaced by the equivalence operation of the corresponding statements.
4. The inclusion for sets is replaced by the operation of implication of the corresponding statements.
5. The equality of a set to the empty set is replaced by the negation of the corresponding statement for the set.
6. The equality of a set to the universal set is replaced by the corresponding statement for the set.

So in the considered example (2) of identical representations of the set A we obtain the following BIF $f_a = (\overline{y_1 \wedge \overline{y_2} \vee \overline{y_3}} \leftrightarrow (\overline{y_1} \vee y_2) \wedge y_3) \wedge (\overline{y_1 \wedge \overline{y_2} \vee \overline{y_3}} \leftrightarrow (\overline{y_1} \wedge y_3) \vee (y_2 \wedge y_3))$ and since it is identically true, then by the theorem *on the connection of expressions of the algebra of sets and the algebra of statements* and its consequences (see, for example [5]) the system confirms the correctness of transformations of the set A.

Next, for a simple statement (6), the BIF will look as follows:

$$f_6 \equiv (\overline{y_1 \wedge \overline{y_2} \vee \overline{y_3}} \leftrightarrow (y_2 \vee y_3) \wedge \overline{y_1}) \rightarrow \overline{y_1 \wedge y_2 \wedge y_3}.$$

Its identical truth also confirms the correctness of the simple statement (6).

When conducting the proof from the contrary of this statement, the student receives the initial premise. $\exists x : x \in X_1 \cap X_2 \cap X_3$ from the negation of the proved statement $\overline{X_1 \cap X_2 \cap X_3 = \emptyset}$ and BIF for verification gets the following expression: $f_{u1} \equiv y_1 \wedge y_2 \wedge y_3 \leftrightarrow \overline{\overline{y_1 \wedge y_2 \wedge y_3}}$, and since it is identically true, the initial premise is correctly built by the student.

From the received initial premise follows a conjunction of 3 elementary conclusions. $x \in X_1 \wedge x \in X_2 \wedge x \in X_5$, what is verified by the identical truth of BIF of the function of implication of the function of premise and conjunction of functions of elementary conclusions $y_1 \wedge y_2 \wedge y_3 \rightarrow y_1 \wedge y_2 \wedge y_3$.

3 Editor interface for proving assertions for sets

The editor interface is a constructor. Using a dialog with a choice of actions (Fig. 1), the trainee chooses which elements he will need for further work. Such elements will appear in the main program window (Fig. 2). Another single window is the input toolbar (Fig. 3). The proof process is divided into several stages:

1. Initially, at launch, a dialog is called up with the choice of action (Fig. 1), where learner selects one of the items he needs for the proof.
2. "Enter the basic statement" creates a field for input.

3. “Inputting identical transformations for some sets” (they are given the names A and B create two input fields with buttons for checking the transformations).

4. “Splitting the basic statement” creates a split number, an input field and a validation button.

5. “The choice of the statement to be proved” creates a dialog window in which the previously entered splits of the basic statement are displayed.

6. “Entering the initial premise and step of proving” creates verify button and input field.

After entering the text of the elementary conclusion or the initial premise into the scheme of the proof, one or several buttons are displayed in the form of a red square, pressing one of them will form a field for entering the text of the next elementary conclusion. The choice of an elementary conclusion of a white or black square, if correct, leads to the completion of the proof of the statement or its branch.

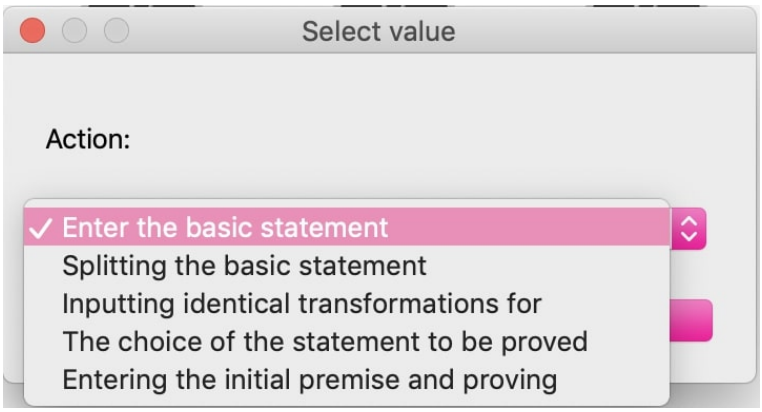

Fig. 1: Choose dialog

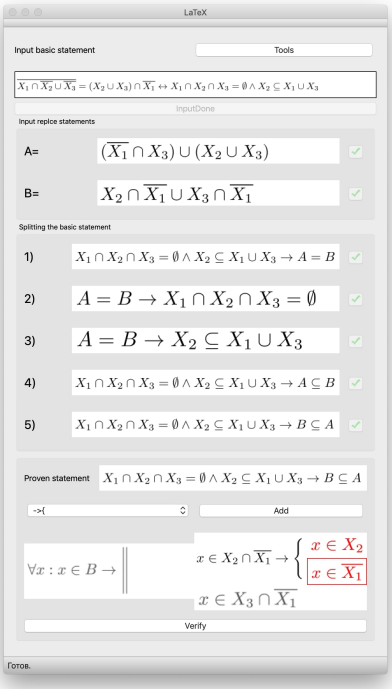

Fig. 2: A window for entering the required statements and premises of evidence

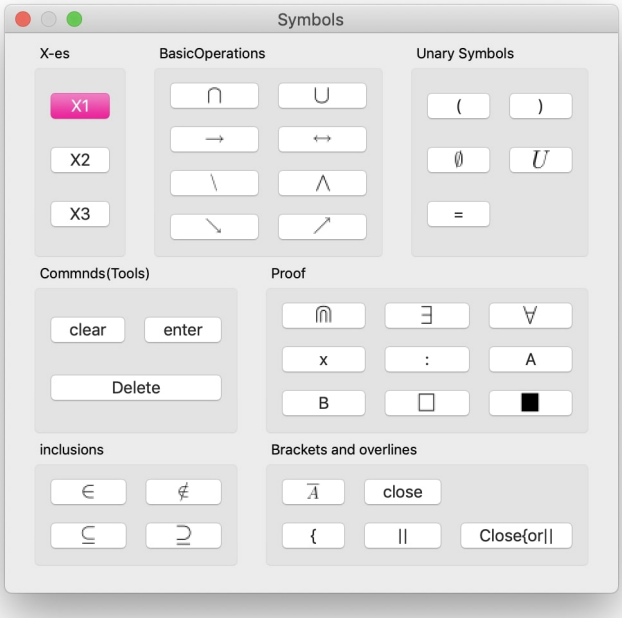

Fig. 3: Window of tools required for proof

4 Conclusion

All the tasks of developing an editor for proving statements for sets are achieved, and we hope that this will allow us to complete the development of the ALS, where this editor will be the central construction teaching this material.

References

1. Davenport J.H., Siret Y., Tournier E.: Computer algebra: systems and algorithms for algebraic computation / - Academic Press, 1988. ISBN 978-0-12-204230-0
2. Joachim von zur Gathen; Jürgen Gerhard. Modern Computer Algebra, Third Edition. — Cambridge University Press, 2013. — 808 p. — ISBN 978-1-107-03903-2.
3. Rublev V.S., Yusufov M.T.: Automated system for teaching computational complexity of algoritm cours, Convergent Cognitive Information Technologies (Selected Papers of the First International Sientific Conference Convergent Cognitive) Moscow, Russia, November 25-26, 2016 (http://ceur-ws.org/Vol-1763/). (ISSN 1613-0073 VOL-1763 urn.nbn.de: 0074-1763-4)

Local search metaheuristics for Capacitated Vehicle Routing Problem: a comparative study

Ekaterina N. Beresneva
Faculty of Computer Science
National Research University Higher School of Economics
Moscow, Russia
eberesneva@hse.ru

Scientific Advisor: Prof. Sergey Avdoshin
Software Engineering School
National Research University Higher School of Economics
Moscow, Russia
savdoshin@hse.ru

***Abstract* — This study is concerned with local search metaheuristics for solving Capacitated Vehicle Routing Problem (CVRP). In this problem the optimal design of routes for a fleet of vehicles with a limited capacity to serve a set of customers must be found. The problem is NP-hard, therefore heuristic algorithms which provide near-optimal polynomial-time solutions are still actual. This experimental analysis is a continue of previous research on construction heuristics for CVRP. It was investigated before that Clarke and Wright Savings (CWS) heuristic is the best among constructive algorithms except for a few instances with geometric type of clients' distribution where Nearest Neighbor (NN) heuristic is better. The aim of this work is to make a comparison of best-known local search metaheuristics by criteria of error rate and running time with CWS or NN as initial algorithms because there were not found any such state-of-the-art comparative study. An experimental comparison is made using 8 datasets from well-known library because it is interesting to analyze "effectiveness" of algorithms depending on type of input data. Overall, five different groups of Pareto optimal algorithms are defined and described.**

Keywords — capacitated vehicle routing problem, local search metaheuristics, LKH-3, variable record-to-record travel, simulated annealing, guided local search, tabu search.

I. Introduction

The Vehicle Routing Problem (VRP) is one of the most widely known challenges in a class of combinatorial optimization problems. VRP is directly related to Logistics transportation problem and it is meant to be a generalization of the Travelling Salesman Problem (TSP). In contrast to TSP, VRP produces solutions containing some (usually, more than one) looped cycles, which are started and finished at the same point called a "depot". As in TSP, each customer must be visited only by one vehicle. The objective is to minimize the cost (time or distance) of all tours. Despite the fact that both problems belong to the class of NP-hard tasks, VRP has higher solving complexity than TSP for the identical types of input data.

This work is aimed at analysis of VRP subcase, which is called Capacitated Vehicle Routing Problem (CVRP), where the vehicles have a limited capacity. A new constraint is that the total sum of demands in a tour for any vehicle must not exceed its capacity. In the paper we will use CVRP abbreviation having in mind the mathematical formulation that was described in our previous work [1].

There are three types of algorithms that are used to solve any subcase of CVRP: exact algorithms, constructive heuristics and metaheuristics.

• *Exact algorithms.* These algorithms find an optimal solution but take a great time for solving large instances. State-of-the-art exact methods can provide optimal solution for some SCVRP instances with up to 100 nodes, but it takes 30-40 minutes at average [2]. Due to these restrictions, researchers all over the world concentrate on heuristic methods.

• *Constructive heuristics.* They build an approximate solution iteratively, but they do not include further improvement stage. These heuristics are usually used for generation of an initial solution for improvement algorithms. A lot of experiments show that classical heuristics work much faster than to exact methods. For example, an instance of 100-150 nodes can be solved up to a few (1-2) seconds [2].

• *Metaheuristics*. These algorithms take as input some approximate initial solution and try to iteratively improve it. According to [3], metaheuristics are divided into two groups: metaheuristics based on local search and metaheuristics based on population, or natural inspired ones. The first group look for new solutions by moving at each iteration from a current state to another state in its neighborhood, while the second group works on a basis of a population of solutions which may be combined together in the hope of generating better ones, like in nature. Certain limitations are inevitable in any research, hence in this work we concentrate only on the first group of metaheuristics, because one of the most perspective algorithms for TSP – LKH-3 – belongs to this group, and it is very interesting for us to compare it with its "closest" alternatives.

Capacitated vehicle routing problems CVRP form the core of logistics planning and are hence of great practical and theoretical interest. There is no doubt that actuality of research and development of heuristics algorithms for solving CVRP is on its top, because in a real word there can be up to one thousand clients in a delivery net, that is why it is especially important to explore heuristic algorithms that allow to quickly generate near optimal solution in a polynomial time.

There are a lot of articles related to CVRP local search metaheuristics, but no works were found which compare improvement heuristics using the same input data of different types and sizes. We will compare these algorithms under criteria of quality, or error rate, and running time. Under the error rate we mean the percentage of difference in the obtained value of the solution with the optimal (or best-known) solution for the problem.

The aim of this work is to make a comparison of best-known local search metaheuristics by criteria of solution quality and running time with CWS or NN as initial algorithms as there were not found any such state-of-the-art comparative study. In addition, it is important to define sets of Pareto optimal metaheuristics for different types of input data.

The paper is structured as follows. In the second part, a general local search approach is described. After that, in the third section, some notes on a most popular local search metaheuristics are provided, including short description of chosen algorithms to be intercompared. The fourth part presents design of experiments on local search metaheuristics. of experimental results. The fifth and the sixth sections describe results of solution qualities and computing times of algorithms, respectively. The seventh part consists of definition of Pareto optimal metaheuristics and five such sets are presented. In the last part we summarize our findings and suggest areas for future work.

II. Local search approach

Local search algorithms take as input some approximate initial solution and try to iteratively upgrade it with local improvements. These changes can either improve a single route (intra-route optimization) or change more than one routes simultaneously in such a way that the overall solution is improved (inter-route optimization).

Intra-route and inter-route optimization strategies consist of different schemes, which are fully described in [5]. In this research we will use the most-known and simplest but still effective local improvement heuristics: 1-point move, 2-point move and 2-opt.

The set of all solutions that can be obtained by applying the local improvements on a solution s is called the neighborhood $N(s)$. Of course, the bigger neighborhood is, the more likely it contains a new solution that can improve current one. However, to have large neighborhoods means to have inevitably higher computational complexity since more solutions need to be generated and evaluated [6]. At the same time, local search methods must deal with the problem of being stuck in a local optimum. Thus, a lot of methods to escaping the local optimum are applied, they will be described in the next section.

So, basically, local search approach consists of the following main steps:

1. Taking as input some initial solution s.
2. Generation of a neighborhood $N(s)$.
3. Selection of the best solution s^* from $N(s)$ using some acceptance criteria.
4. Make a new s equal to s^*.
5. Checking for exceeding different limits. If stop criteria is satisfied then terminate, otherwise continue with the step 2.

III. CVRP local search metaheuristics

Local search metaheuristics are used to solve a wide range of combinatorial optimization problems. Among heuristic methods for solving TSP there is one, which is the best – it is local search metaheuristic, proposed by Lin, Kernighan and Helsgaun [7]. Also, local search algorithms are key part of most known methods for solving most subcases of VRP [3] [8] [9] [10] etc.

The most well-known schemes for solving CVRP that include local search steps are different variants of tabu search, forms of deterministic and simulated annealing, variable neighborhood search, guided local search [11]. Recently a new adoption of LKH for TSP called LKH-3 was proposed by one of the original authors, Helsgaun [12] . Also, in a recent study it was stated that improved version of record-to-record travel heuristic analyzed [13] is "… a well-performing metaheuristic", which combines strategies of deterministic annealing, tabu search, variable neighborhood search and both intra-route and inter-route optimizations described later. It was proposed by Li and others [14].

Of course, there are a lot of other metaheuristics for finding CVRP solution, however it was decided to concentrate on a set of several reputed local search algorithms that were honorably mentioned in recent studies.

As it was stated earlier, for all metaheuristics an initial solution must be obtained. For most input problems Clarke and Wright Savings (CWS) heuristic [4] is used, which is the best among construction algorithms except for a few instances with geometric type of clients' distribution. For these especial input files Nearest Neighbor (NN) heuristic is applied instead of CWS.

Thus, in this study we will intercompare following local search metaheuristics for solving classical CVRP.

A. A set of optimization operators (OPT)

As it was stated above, in this research the most-known and simplest local improvement heuristics are used. They are 1-point move, 2-point move and 2-opt.

In a tour of N vertices 1-point move operator (or relocate heuristic) moves some vertex $v_i, i \in N$ after another vertex $v_j, j \in N, i \neq j$ at the same tour. Another 2-point move operator (or exchange heuristic) swaps locations of two different vertices $v_i, i \in N$ and $v_j, j \in N, i \neq j$. And the main idea of 2-opt heuristic is to remove two edges $(v_i, v_j), i, j \in N$ and $(v_x, v_y), x, y \in N$ from the solution and replace them with two new edges (v_i, v_x) and (v_j, v_y). It is important to note that

all mentioned operators can be applied for each of intra-optimization and inter-optimization as it is shown in Fig. 1.

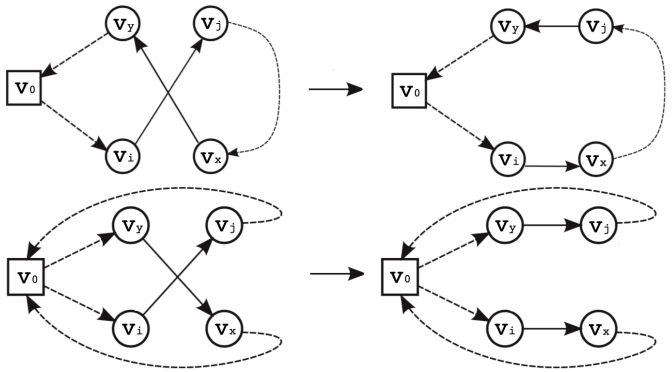

Fig. 1. Intra-route 2-opt (above) in compare to intre-route 2-opt (below).

B. Guided local search (GLS)

The guided local search metaheuristic is used to avoid local minima. It was initially proposed by [15] and later applied to CVRP by [16]. According to [17], this method is memory-based as it determines and penalizes "ineffective" edges by increasing its cost to a new $c^*(v_i, v_j) = c(v_i, v_j) + \lambda p(v_i, v_j) L$, where $p(v_i, v_j)$ counts the number of penalties of edge (v_i, v_j), L is a proxy for the average cost of an edge, computed as the costs of the starting solution divided by the number of customers, and λ controls the impact of penalties (authors suggest to always set $\lambda = 0.1$).

C. Tabu search (TS)

Tabu search originally was proposed by Glover and others [18]. The main idea of TS is as follows. If some solutions in $N(s)$ cannot be improved for several iterations or they violate the rules, they are made forbidden (or tabu) in order to prevent being in a stack of local minimum. Such forbidden solutions are put into a tabu-list, so this heuristic is also memory-based like GLS. The duration that a solution remains tabu is called its tabu-tenure and it can vary over different intervals of time.

We use recent TS algorithm that provides good results described in [19] as it was stated in [5].

D. Simulated annealing (SA)

This classical algorithm was developed in 1983 by [20]. It is based on an analogy from the annealing process of solids, where a solid is heated to a high temperature and gradually cooled in order for it to crystallize in a low energy configuration [21]. In this research we used adopted version of SA for CVRP by [22]. In SA some solution s^* from $N(s)$ at iteration i is chosen to be a new $s = \begin{cases} s^* \text{ with probability } P(s, s^*, i) \\ s \text{ with probability } 1 - P(s, s^*, i) \end{cases}$ accordingly to the probabilistic function $P(s, s^*, i) = \exp\left(-\frac{f(s) - f(s^*)}{Q_i}\right)$, where $f(s)$ is a length of solution s, Q_i is an element of an arbitrary decreasing, converging to zero, positive sequence, which specifies an analogue of the falling temperature in the crystal.

E. Lin-Kernighan-Helsgaun heuristic for CVRP (LKH-3)

LKH-3 is proposed by Helsgaun in 2017 [12]. The implementation of LKH-3 builds on the idea of transforming the problem into classical symmetric TSP. After that algorithm uses the principle of 2-opt algorithm and generalizes it. In this heuristic, the k-Opt, where $k = \overline{2..\sqrt{N}}$, is applied, so the switches of two or more edges are made in order to improve the tour. This method is adaptive, so decision about how many edges should be replaced is taken at each step [7] [23].

This algorithm was not developed by us as original source code of LKH-3 is free of charge for academic and non-commercial use and can be downloaded at [24].

F. Variable record-to-record travel heuristic (VRTR)

Li and others suggested a variable record-to-record travel heuristic, which is based on classical record-to-record travel algorithm (RTR). RTR combines approaches of deterministic annealing (which is a variant of simulated annealing heuristic) and tabu search. The main differences between VRTR and RTR are as follows. Firstly, VRTR considers 1-point, 2-point and 2-opt moves not only within individual routes as RTR does, but also between them. Secondly, "VRTR uses a variable-length neighbor list that should help focus the algorithm on promising moves and speed up the search procedure" [14].

IV. Design of experiments

All algorithms from section III were implemented as sequential algorithms in C/C++, no multi-threading was explicitly utilized. They were executed on an Intel Core i5 clocked at 1.3GHz with 4 GB RAM running the macOS 10.14.3 operating system.

The computational testing of the solution methods for CVRP has been carried out by considering eight sets of test instances from the next well-known database [25]. Total number of instances in sets A, B, E, F, G, M, P, X is 211. All instances inside one set have its own characteristics and a way of generation: cluster-based / uniform / geometric distribution of clients, real-world / imitative cases etc. The integer Euclidean metric is used for all instances. The naming scheme and data format for each instance is described here [26]. Shortly, the first letter in names shows the name of used set, the figure after letter 'n' shows the number of nodes and the figure which stands after letter 'k' presents the number of vehicles.

Experiment starts with choice of a local search metaheuristic M from set {OPT, GLS, SA, TS, LKH-3, VRTR}. After one dataset D is selected from a list of all mentioned benchmark datasets, an instance file F from chosen dataset D is taken. Next, the following steps are repeated 51 times on instance F: chosen metaheuristic M is executed on a basis of initial solution obtained by CWS or NN (as it was explained in a previous chapter). During all iterations, except the first one, solution qualities $\varepsilon_{it}(M, F)$ and computing times $t_{it}(M, F)$ (in seconds) are calculated for algorithm M on test F. The first run is not taken into account in calculations because of specifity of C++

compiler. Solution quality (or percent above best-known, or gap) is calculated using the next formula [11]:

$$\frac{F(S^0) - F_{opt}(S)}{F_{opt}(S)} \cdot 100\%,$$

where $F(S^0)$ is a length of obtained solution and $F_{opt}(S)$ is a length of optimal solution or best-known one.

Also we calculate minimal value $\varepsilon_{\min}(\mathrm{M},\mathrm{F})$ among all figures $\varepsilon_{it}(\mathrm{M},\mathrm{F})$ and sample mean $\bar{X}_t(\mathrm{M},\mathrm{F}) = \frac{1}{50}\sum_{it=1}^{50} t_{it}(\mathrm{M},\mathrm{F})$ among all figures $\mathrm{t_{it}}(\mathrm{M},\mathrm{F})$. And finally, among all $\varepsilon_{\min}(\mathrm{M},\mathrm{F})$ from one dataset average sample mean $\bar{X}_\varepsilon(\mathrm{M},\mathrm{D}) = \frac{1}{|D|}\sum \varepsilon_{\min}(\mathrm{M},\mathrm{F}), \forall \mathrm{F} \in \mathrm{D}$ is calculated, which shows average gap for algorithm M on dataset D. And among all $\bar{X}_t(\mathrm{M},\mathrm{F})$ from one dataset average sample mean $\bar{X}_t(\mathrm{M},\mathrm{D}) = \frac{1}{|\mathrm{D}|}\sum \bar{X}_t(\mathrm{M},\mathrm{F}), \forall \mathrm{F} \in \mathrm{D}$ is calculated, which shows average computing time of algorithm M on dataset D. |D| is a number of input files in dataset D.

The plan of experiment on local search metaheuristics is described in Fig. 2.

```
Input: local search metaheuristics, datasets
1:  foreach local search metaheuristic M
2:      foreach dataset D from datasets
3:          foreach instance file F from D
4:              for it ∈ {0…50} // number of runs
5:                  init_sol = run CWS or NN on F
6:                  final_sol = run M on F with init_sol
7:                  if (it != 0) // if not the first run
8:                      calculate εit(M,F), tit(M,F)
9:              calculate εmin(M,F)
10:         calculate tmin(M,F)
11:         calculate tmax(M,F)
12:         calculate X̄t(M,F)
13:         calculate st(M,F)
14:     calculate X̄ε(M,D) // average gap on dataset
15:     calculate X̄t(M,D) // average computing time
```

Fig. 2. Plan of experiment on constructive heuristics.

Each metaheuristic is subsequently launched on all instances from every mentioned dataset, so no input file is missed.

V. Computational Results on Solution Quality

Results about the best (= minimal) solution qualities $\varepsilon_{\min}(\mathrm{M},\mathrm{F})$ of metaheuristics available from experiments for set A are presented in Fig. 3. The horizontal axis represents the name of instance data. The vertical axis shows the solution quality. Results for other sets cannot be presented here as detailed as for set A, because of its size, but they are aggregated in Table 1, where average gaps $\bar{X}_\varepsilon(\mathrm{M},\mathrm{D})$ for all metaheuristics and all datasets are given. Figure 4 is a visual representation of this table. These general figures can show an approximate overall effectiveness of algorithms by criterion of solution quality. Analysis of Fig. 4 indicated a group of top-3 algorithms by criterion of solution quality: they are LKH-3, VRTR, SA. Let's take a closer look at their results.

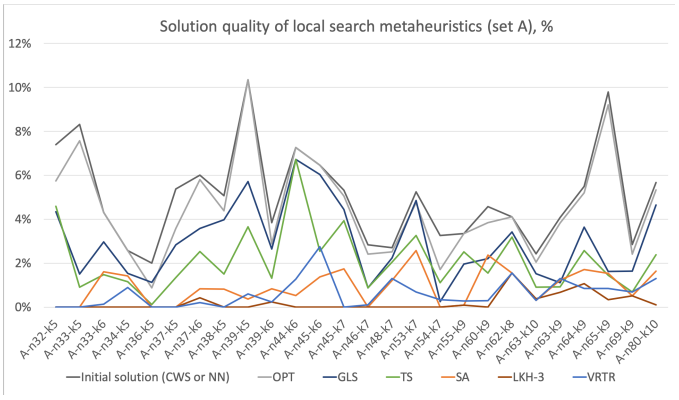

Fig. 3. Solution quality of local search metaheuristics, set A.

TABLE I. Average gap $\bar{X}_\varepsilon(M,D)$ in the dataset, %.

Average gap $\bar{X}_\varepsilon(\mathrm{M},\mathrm{D})$ in the dataset		Local search metaheuristics						
		CWS or NN	OPT	GLS	TS	SA	LKH-3	VRTR
Set (its size)	A (26)	5,0%	4,5%	3,0%	2,1%	0,9%	0,2%	0,6%
	B (23)	4,4%	3,9%	3,1%	2,5%	1,0%	0,2%	0,6%
	E (11)	7,1%	5,3%	4,1%	3,6%	0,8%	0,4%	0,8%
	F (3)	4,4%	2,7%	3,3%	3,0%	1,8%	0,1%	1,9%
	G (20)	11%	10%	8,1%	9,7%	5,2%	2,1%	2,4%
	M (4)	4,7%	2,8%	2,6%	2,1%	0,5%	0,2%	0,5%
	P (24)	8,0%	6,6%	3,5%	4,5%	0,7%	0,5%	0,9%
	X(100)	5,9%	5,4%	4,9%	4,0%	4,1%	2,0%	1,7%

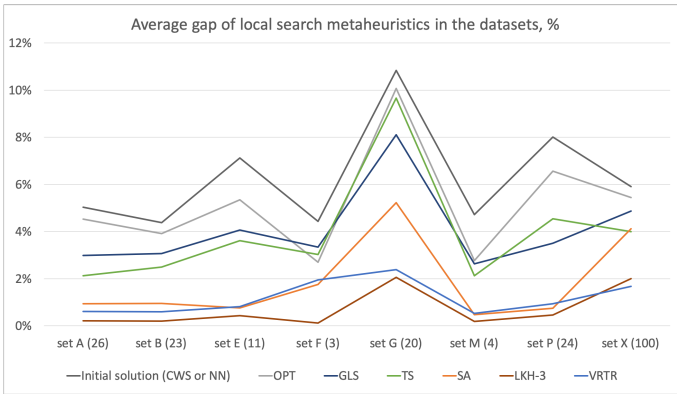

Fig. 4. Average gap of local search metaheuristics in the datasets (%).

It is clearly seen that in 7 out of 8 sets LKH-3 produces solutions with the least (= the best) solution qualities. Experiment results that are not shown here because of their large size reveal that LKH-3 produces not the best solutions in:

- 3 input files out of 26 for set A (≈12%);
- 1 input files out of 23 for set B (≈4%);
- 2 input files out of 11 for set E (≈18%);
- 1 input files out of 3 for set F (≈33%);
- 6 input files out of 20 for set G (30%);
- 0 input files out of 4 for set M (0%);
- 6 input files out of 24 for set P (≈25%);
- 61 input files out of 100 for set X (61%);

Totally, LKH-3 was not the best in quality criterion for 80 input files out of 211 (≈38%). Only 6 times SA was the best, while all other times VRTR was "the winner".

It is important to mention that LKH-3 tends to produce best solution for instances with no more than ≈100 clients in a delivery net regardless of type of distribution in the dataset. There are 86 instances with less than 102 clients, and solutions obtained using LKH-3 are the best in 86% (in 74 files).

In addition, it should be noted that LKH-3 is the best for input problems with cluster-based distribution of clients, when the number of clusters is a bit smaller than the amount of available vehicles (sets B and M). On the contrary, this algorithm is not the best for 61% of files from set X that consists of very different instances. Despite the fact that there are several files with cluster-based distribution, the amount of clusters is much less than the number of vehicles, and, as experiments showed, LKH-3 does not suits well for such cases.

VRTR nearly always takes "the second place in this race" except for set X. It can be noticed that VRTR works in a best way for instances with more than ≈320 clients in a delivery net for non-geometric distributions. There are 53 instances with more than 321 clients in set X, and solutions obtained using VRTR are the best in 89% (in 47 files). Nevertheless, if we take a range of ≈ [100; 320] clients, results show that either VRTR or LKH-3 are the best in nearly 50% of cases, so for this diapason both these algorithms can be admitted being equal.

For most of input files SA produces solutions which are nearly equal to other ones generated by VRTR. However, the situation is different for sets G and X, where SA is always worse than its closest "competitor". So, we can come to the conclusion that with SA it is better to use non-geometric input data with no more than 100 clients in a delivery net. Nevertheless, only 6 times out of 211 SA is better than LKH-3 – this fact shows superiority of LKH-3 over SA.

Other three local search metaheuristics – TS, GLS and OPT (listed in increasing size of average gaps) – were nearly always worse than top-3 group.

TS was better than LKH-3 only 3 times out of 211, better than VRTR or SA in 6 input files out of 26 from set A, in 2 input files out of 23 from set B, in 1 input file out of 24 from set P. Also, TS is slightly more effective than SA for set X, however, the difference in solution qualities between LKH-3 and TS is significant in general.

Roughly speaking, GLS is usually worse than TS, except for sets G and P. Also, GLS is better than LKH-3 only in one file, thus, it cannot compete with the algorithms from top-3 group seriously.

And the last one and the least effective by criterion of solution quality metaheuristic is OPT. It nearly always produces solutions which are better than ones obtained by simple initial algorithm but worse than other local search metaheuristics.

VI. Experimental Results on Computing Time

Results about average running times $\bar{X}_t(\mathrm{M},\mathrm{F})$ of metaheuristics available from experiments for set A are presented in Fig. 5. The horizontal axis represents the name of instance data. The vertical axis shows the running time in seconds. Results for other sets cannot be presented here as detailed as for set A, because of its size, but they are aggregated in Table 2, where average computing times $\bar{X}_t(\mathrm{M},\mathrm{D})$ for all metaheuristics and all datasets are given. Figure 6 is a visual representation of this table. These general figures can show an approximate overall effectiveness of algorithms by criterion of running time.

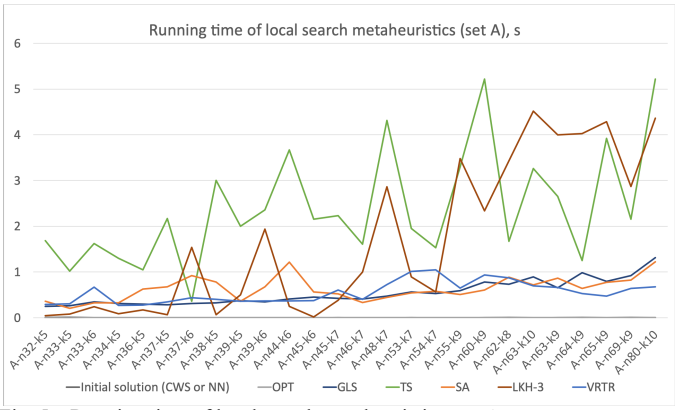

Fig. 5. Running time of local search metaheuristics, set A.

TABLE II. Average computing time $\bar{X}_t(M,D)$ in the dataset (in seconds).

Average gap $\bar{X}_\varepsilon(\mathrm{M},\mathrm{D})$ in the dataset		Local search metaheuristics						
		CWS or NN	OPT	GLS	TS	SA	LKH-3	VRTR
Set (its size)	A (26)	0,0003	0,004	0,540	2,411	0,635	1,692	0,554
	B (23)	0,0006	0,027	0,291	2,578	0,505	1,487	0,611
	E (11)	0,0008	0,016	0,311	2,172	0,857	1,930	0,851
	F (3)	0,0003	0,024	0,953	4,240	1,621	2,154	1,270
	G (20)	0,0468	0,569	7,979	16,34	15,78	8,563	9,748
	M (4)	0,0025	0,044	0,883	4,386	4,046	2,370	2,469
	P (24)	0,0008	0,023	0,367	2,216	0,566	2,166	0,554
	X (100)	0,041	0,62	7,088	65,15	56,74	37,41	9,998

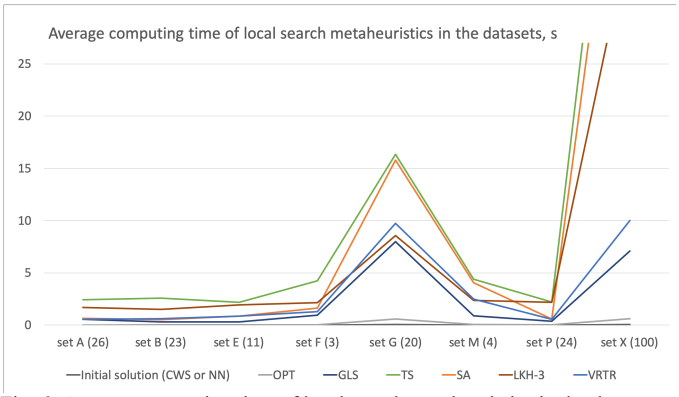

Fig. 6. Average computing time of local search metaheuristics in the datasets.

It can be seen from Table 2 and Fig. 4 that metaheuristics, which are listed in increasing size of average running times, are as follows: OPT, GLS, VRTR, SA, LKH-3, TS. Let us discuss their results in this order.

Analysis reveals that the "fastest" local search metaheuristic for all 211 instances is OPT as it was expected. Its running time is approximately 25 times bigger than computing time of initial

algorithm, however, even for 1000 clients in a delivery net the maximum running time does not exceed 3 seconds.

Next algorithm is GLS, which is approximately 300 times slower than initial one. In sets B, E, F, P, M and X it nearly always (94%) ranks #2 just after OPT. Of course, there are cases when GLS works slightly slower than others, but the number of such situations is not very significant and the difference between obtained values does not exceed 1 second. However, in sets A and G GLS works with mixed results: computing times of GLS, SA, VRTR or LKH-3 (depending on dataset) are fluctuated and too close to each other, so it is impossible to find a leader.

Average computing time of VRTR steadily goes at the third plays, except for set G with geometric instances and several rare cases from other datasets. VRTR has smooth growth of speed, and no special aspects of its work are found apart from not very stable work with geometric-inspired instances.

Next one is SA. In comparison with VRTR, SA has bigger growth of speed and the plot of its running time is more fluctuated. In sets A, B, E, F and P this algorithm executes quicker than LKH-3 but slower than VRTR. However, in sets G, M and X it shows much worse effectivity, when the number of clients in a delivery net becomes more than 100. It means that SA is better to use for instances with up to one hundred delivery points.

LKH-3 is slower than other mentioned metaheuristics (except for TS) for all datasets apart from sets G, M and those instances from set X with 322 and more delivery points. The main unique feature of LKH-3 is its variability. Linear chart of running times of LKH-3 has a lot of drastic jumps and slumps. That is why this metaheuristic has not very positive computing time rate. Nevertheless, LKH-3 can work very quickly, especially when there are no more than 50-80 clients in a net.

Last one metaheuristic to be discussed concerning its computing time is TS. As LKH-3, linear chart of running times has a lot of drastic jumps and slumps. In average, this is the slowest algorithm in this group, however, in a third of cases it can compete with LKH-3 or SA but not very significant speeding up can be noticed.

VII. Pareto Optimal Local Search Metaheuristics

The algorithm $m_0 \in \mathcal{M}$ is Pareto optimal if $(\forall m \in \mathcal{M})$ $\left((m \neq m_0) \Rightarrow \left(\bar{X}_\varepsilon(m, D) > \bar{X}_\varepsilon(m_0, D)\right) \vee \left(\bar{X}_t(m, D) > \bar{X}_t(m_0, D)\right)\right)$ Thus, our aim is to find a sets of Pareto optimal algorithms for different types of input data.

Figures from 5 to 14 are plotted using values from Table 1 and Table 2. The horizontal axis represents average computing time $\bar{X}_t(\mathrm{M}, \mathrm{D})$ in seconds. The vertical axis shows average solution quality $\bar{X}_\varepsilon(\mathrm{M}, \mathrm{D})$.

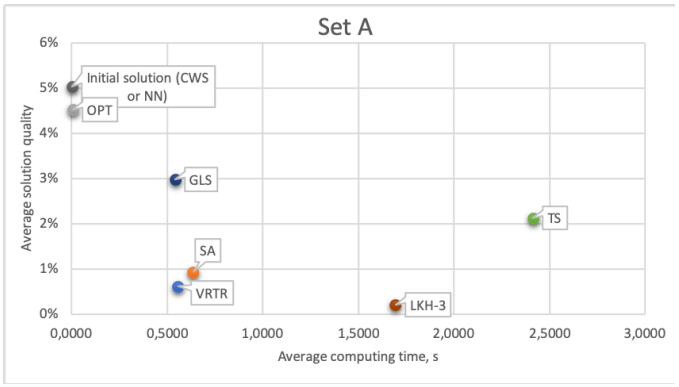

Fig. 7. Average solution quality vs. average running time, set A.

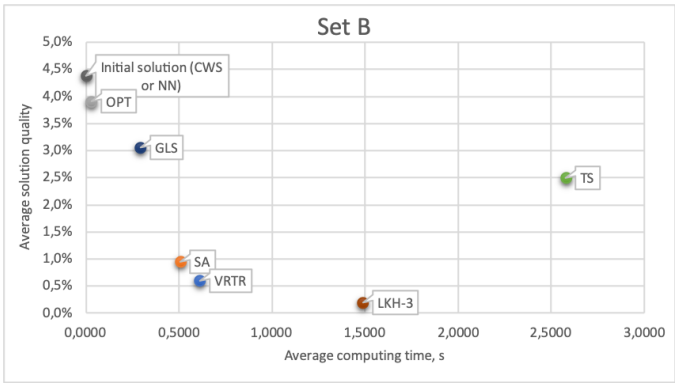

Fig. 8. Average solution quality vs. average running time, set B.

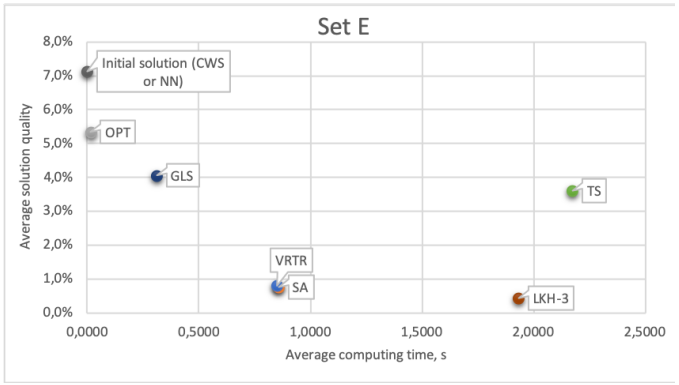

Fig. 9. Average solution quality vs. average running time, set E.

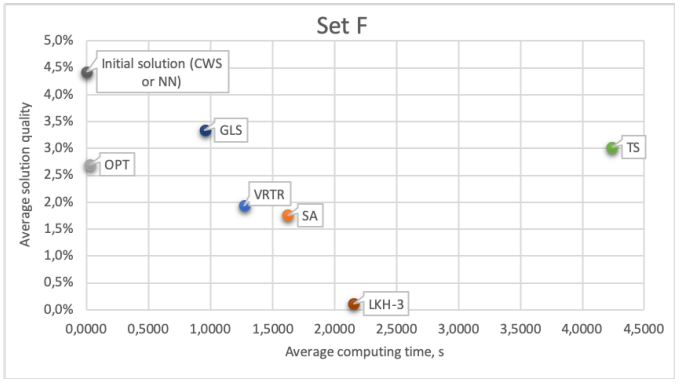

Fig. 10. Average solution quality vs. average running time, set F.

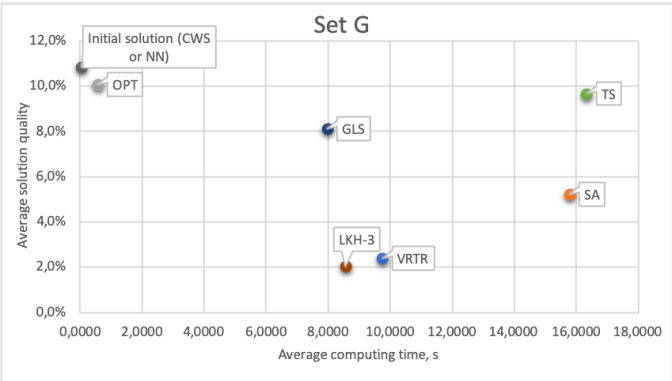

Fig. 11. Average solution quality vs. average running time, set G.

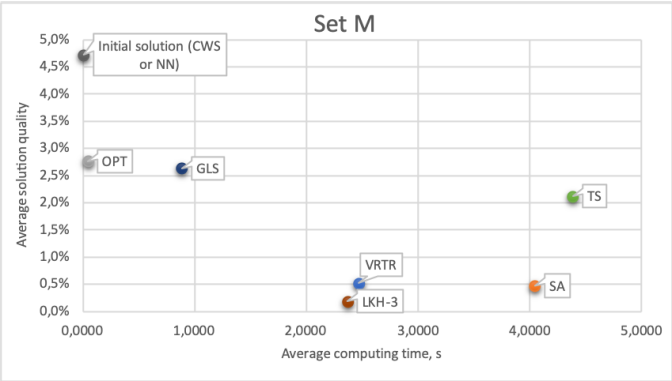

Fig. 12. Average solution quality vs. average running time, set M.

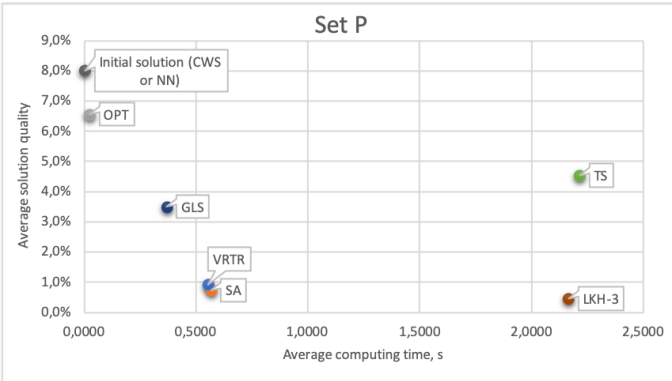

Fig. 13. Average solution quality vs. average running time, set P.

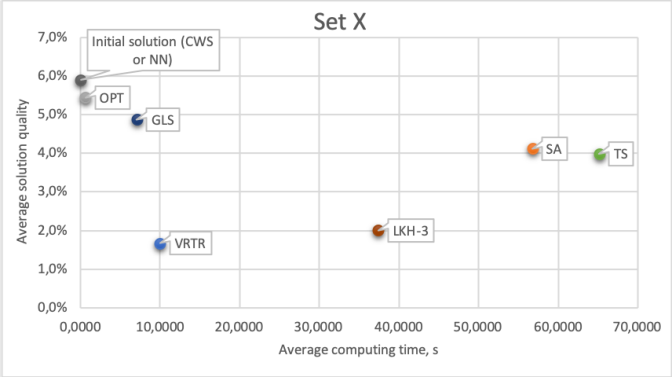

Fig. 14. Average solution quality vs. average running time, set X.

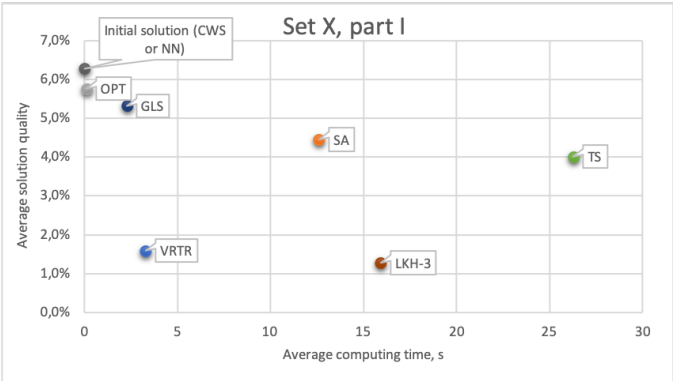

Fig. 15. Average solution quality vs. average running time, set X, part I.

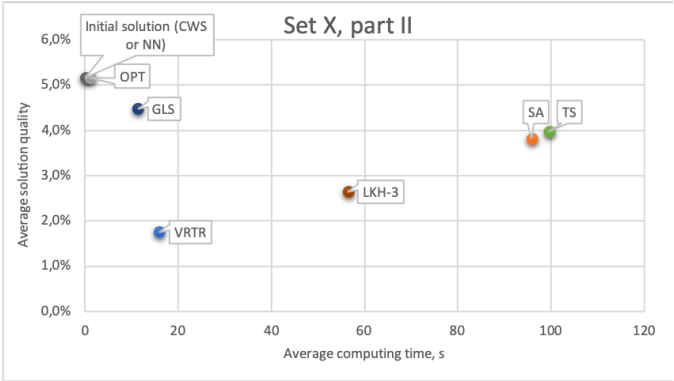

Fig. 16. Average solution quality vs. average running time, set X, part II.

To sum up information presented in Figures from 5 to 14, Table 3 is formed.

TABLE III. INVOLVEMENT OF ALGORITHMS IN PARETO OPTIMAL GROUPS FOR DIFFERENT DATASETS

Involvement of algorithms in Pareto optimal groups		Local search metaheuristics					
		OPT	GLS	TS	SA	LKH-3	VRTR
Set (its size)	A (26)	✓	✓		✓	✓	✓
	B (23)	✓	✓		✓	✓	✓
	E (11)	✓	✓		✓	✓	✓
	F (3)	✓			✓	✓	✓
	G (20)	✓	✓			✓	
	M (4)	✓	✓			✓	
	P (24)	✓	✓		✓	✓	✓
	X (100)	✓	✓				✓
	X, part I (47)	✓	✓			✓	✓
	X, part II (53)	✓	✓				✓

Table 3 shows involvement of local search metaheuristics in Pareto optimal groups for different datasets. Algorithms that belong to a group of Pareto optimal heuristics for some set are marked with a big tick. SA is marked by a small tick for set A as this metaheuristic can be in optimal by Pareto group as the difference between it and VRTR is too close, so it can be neglected. Also, it should be mentioned that two more rows are

added – they are "set X, part I" which consists of instances with up to 322 clients and "set X, part II" which is vice versa has instances with 322 and more delivery points inside input files. This division is connected with the big size of set X and with the fact that was described in section V – VRTR works in a best way for instances with more than ≈320 clients in a delivery net for non-geometric distributions but LKH-3 produces good results for instances with no more than ≈100 clients regardless of type of distribution in the dataset.

The following conclusions are made on a base of results from Table 3:

1. Sets A, B, E and P can be aggregated together because a group of Pareto optimal algorithms is the same for all these sets. We will name this aggregation as *Group_1*. It represents two different types of inputs. The first one is with clients' coordinates and demands that are formed from a uniform distribution with some outlying cases. The second one is with nodes that are formed into clusters, and the number of clusters is equal or greater than number of available vehicles. Demands are also formed from a uniform distribution with some outlying cases. All input files from *Group_1* have 101 clients in a delivery net as maximum.
2. Set F forms a second group *Group_2* with only 3 instances obtained from real goods deliveries. Number of delivery points varies from 45 to 135.
3. *Group_3* is formed of sets G and M that also have the same Pareto optimal metaheuristics. Number of delivery points varies from 100 to 483. Set G has instances with locations in a form of concentric squares, pointed stars and rays, while set M consists of only 4 input files with locations that are grouped into clusters, and the number of clusters is equal or smaller by 1 than number of available vehicles.
4. *Group_4* is formed of the first part of set X. There are 47 instances in it, and the number of instances is up to 322 clients. *Group_4* is a mix of input data types: it has different combinations of demand distribution (unitary demands, small/large values, small/large variance), depot positioning (central, eccentric, random) and customer positioning (practical cases, uniform distribution, cluster-based).
5. *Group_5* is formed of the second part of set X. There are 53 instances in it, and the number of instances is from 322 to 1001 clients. Other characteristics of this group are the same as *Group_4* has.

Above-mentioned conclusions are outlined in Table 4 with information about involvement of algorithms in Pareto optimal groups depending on types of input data. All algorithms are listed in increasing order of average computing times (from best to worst) and in decreasing order of average solution qualities (from worst to best).

TABLE IV. INVOLVEMENT OF ALGORITHMS IN PARETO OPTIMAL GROUPS DEPENDING ON TYPES OF INPUT DATA

	Number of delivery points	**Distribution of delivery points**	**Distribution of demands**	**Pareto optimal algorithms**
Group_1	Up to 101	1. Uniform (with some outlying cases). 2. Cluster-based, the number of clusters is equal or greater than number of available vehicles.	Uniform (with some outlying cases)	OPT GLS SA VRTR LKH-3
Group_2	Up to 135	Real-world	Real-world	OPT SA VRTR LKH-3
Group_3	From 100 to 483	1. Geometric (concentric squares, pointed stars and rays). 2. Cluster-based, the number of clusters is equal or smaller by 1 than number of available vehicles.	Constant or uniform	OPT GLS LKH-3
Group_4	From 100 to 322	Mixed	Mixed	OPT GLS VRTR LKH-3
Group_5	From 322 to 1001	Mixed	Mixed	OPT GLS VRTR

VIII. CONCLUSIONS

As it was expected, unfortunately, there is no one universal metaheuristic that takes the first places by both criteria of solution quality and running time. Overall, the next recommendations should be given to people who are interested in metaheuristics solving CVRP.

1. For uniform (with some outlying cases) or cluster-based distribution of clients' locations, where the number of clusters is equal or greater than number of available vehicles it is better to apply Set of optimization operators, Guided local search, Simulated annealing, Variable record-to-record travel algorithm or Lin-Kernighan-Helsgaun heuristic for CVRP depending on desired solution quality and available time for calculations. Here and elsewhere the algorithms are listed in increasing order of average computing times (from best to worst) and in decreasing order of average solution qualities (from worst to best).
2. For real-world instances it is better to use following local search metaheuristics: Set of optimization operators, Simulated annealing, Variable record-to-record travel algorithm or Lin-Kernighan-Helsgaun heuristic for CVRP.
3. For geometric (with concentric squares, pointed stars and rays) or cluster-based distribution of clients' locations, where the number of clusters is equal or smaller by 1 than number of available vehicles, it is better to apply Set of

optimization operators, Guided local search or Lin-Kernighan-Helsgaun heuristic for CVRP.

4. Finally, for mixed up combinations of demand distribution, depot positioning and customer positioning there are two recommendations. If there up to approximately 350 clients in a delivery net, it is better to use Set of optimization operators, Guided local search algorithm, Variable record-to-record travel algorithm or Lin-Kernighan-Helsgaun heuristic for CVRP. Otherwise, if there are nearly 320 delivery point and more then LKH-3 stops being so effective, so it is better to use following local search metaheuristics: Set of optimization operators, Guided local search algorithm or Variable record-to-record travelling algorithm.

Also experiments revealed absolute inefficiency of Tabu search as it is not in any of Pareto optimal groups.

In future we are planning to extend our study by conducting experiments using:

1. Population-based or nature-inspired metaheuristics as there are a lot of productive algorithms, too.
2. Other input data sets, including the most recent one with thousands of nodes in each instance. It is important to check local search metaheuristics on problems with extra-large dimensions to analyze their effectiveness.

REFERENCES

[1] E. Beresneva and S. Avdoshin, "Analysis of Mathematical Formulations of Capacitated Vehicle Routing Problem and Methods for their Solution," *Trudy ISP RAN/Proc. ISP RAS,* vol. 30, no. 3, pp. 233-250, 2018.

[2] K. Braekers, K. Ramaekers and I. Nieuwenhuyse, "The vehicle routing problem: State of the art classification and review," *Computers & Industrial Engineering,* vol. 99, pp. 300-313, 2016.

[3] B. Golden, S. Raghavan and E. Wasil, The vehicle routing problem: Latest advances and new challenges, New York: Springer, 2008.

[4] P. Toth and D. Vigo, Vehicle Routing Problems, Methods, and Applications, Philadelphia: SIAM, 2014.

[5] F. Arnold, M. Gendreau and K. Sorensen, "Efficiently solving very large-scale routing problems," *Computers and Operations Research,* vol. 107, pp. 32-42, 2019.

[6] K. Helsgaun, "An effective implementation of the Lin–Kernighan traveling salesman heuristic," *EJOR,* vol. 12, pp. 106-130, 2000.

[7] E. Zachariadis and C. Kiranoudis, "An open vehicle routing problem metaheuristic for examining wide solution neighborhoods," *Computers & Operations Research,* vol. 37, no. 4, pp. 712-723, 2010.

[8] E. Taillard, G. Laporte and M. Gendreau, "Vehicle routeing with multiple use of vehicles," *Journal of the Operational Research Society,* vol. 47, no. 8, p. 1065, 1996.

[9] S. Ropke and D. Pisinger, "An adaptive large neighborhood search heuristic for the pickup and delivery problem with time windows," *Transportation Science,* vol. 40, no. 4, p. 455–472, 2006.

[10] P. Toth and D. Vigo, "An overview of vehicle routing problems," in *The Vehicle Routing Problem*, SIAM, 2002.

[11] K. Helsgaun, "An Extension of the Lin-Kernighan-Helsgaun TSP Solver for Constrained Traveling Salesman and Vehicle Routing Problems," Roskilde University, 2017.

[12] P. Schittekat and K. Sorensen, "Deconstructing record-to-record travel for the capacitated vehicle routing problem," *Operational Research and Management Science Letters,* vol. 1, no. 1, pp. 17-27, 2018.

[13] F. Li, B. Golden and E. Wasil, "Very large-scale vehicle routing: new test problems, algorithms, and results," *Computers & Operations Research,* vol. 32, p. 1165–1179, 2005.

[14] G. Laporte and F. Demet, "Classical Heuristics for the Capacitated VRP," in *The Vehicle Routing Problem*, SIAM, 2002, pp. 109-128.

[15] C. Voudouris, E. Tsang and A. Alsheddy, "Guided local search," in *Handbook of metaheuristics*, 2010, pp. 321-361.

[16] D. Mester and O. Braysy, "Active-guided evolution strategies for large-scale capacitated vehicle routing problems," *Computers & Operations Research,* vol. 34, no. 10, p. 2964–2975, 2007.

[17] F. Arnold and K. Sorensen, "Knowledge-guided local search for the Vehicle Routing Problem," *Computers and Operations Research,* vol. 105, pp. 32-46, 2019.

[18] F. T. E. Glover, "A user's guide to tabu search," *Operations Research,* vol. 41, no. 1, pp. 1-28, 1993.

[19] E. Zachariadis and C. Kiranoudis, "A strategy for reducing the computational complexity of local search-based methods for the vehicle routing problem," *Computers & Operations Research,* vol. 37, p. 2089–2105, 2010.

[20] S. Kirkpatrick, C. Gelatt and M. Vecchi, "Optimization by simulated annealing," *Science,* vol. 220, no. 4598, p. 671– 680, 1983.

[21] NEO, "Simulated Annealing," [Online]. Available: http://neo.lcc.uma.es/vrp/solution-methods/metaheuristics/simulated-annealing/. [Accessed 27 02 2019].

[22] I. Osman, "Metastrategy simulated annealing and tabu search algorithms for the vehicle routing problem," *Annals of Operations Research,* vol. 41, pp. 421-451, 1993.

[23] S. Avdoshin and B. E.N., "The Metric Travelling Salesman Problem: The Experiment on Pareto-optimal Algorithms," *Trudy ISP RAN/Proc. ISP RAS,* vol. 29, no. 4, pp. 123-138, 2017.

[24] K. Helsgaun, "LKH-3," 2. [Online]. Available: http://akira.ruc.dk/~keld/research/LKH-3/. [Accessed 01 2019].

[25] I. Xavier, "CVRPLIB," [Online]. Available: http://vrp.atd-lab.inf.puc-rio.br/index.php/en/. [Accessed 09 05 2018].

[26] Heidelberg University, "TSPLIB," [Online]. Available: https://www.iwr.uni-heidelberg.de/groups/comopt/software/TSPLIB95/. [Accessed 09 05 2018].

The Generalized Traveling Salesman Problem: modifications and ways of solving

Mariia Gordenko
Department of Software Engineering
National Research University Higher School of Economics
Moscow, Russia
mgordenko@hse.ru

Sergey Avdoshin
Department of Software Engineering
National Research University Higher School of Economics
Moscow, Russia
savdoshin@hse.ru

***Abstract*— The Generalized Traveling Salesman problem (GTSP) is an expansion of classical Traveling Salesman problem, where vertices separated into clusters and the route should traverse each cluster once. Like TSP, GTSP has many potentially useful applications such as postal routing, material flow system design and etc. The mathematical formulation of GTSP and examples of potentially useful application are described. The GTSP has several modifications, which correspond to real tasks. In paper existing modifications are presented, also the new formulations of problem are proposed. Then the algorithms and approaches for solving GTSP are listed. There are four main approaches: exact algorithms, heuristic algorithms, reduction and transformation algorithms. In paper a focus placed on transformation and reduction algorithms. Existing algorithms for exact and non-exact transformations are described. The new modification of existing non-exact transformation based on finding center mass of graph are presented. Then the algorithm and example of reduction algorithm can be founded. The results of testing new center mass approach are also presented.**

Keywords*— *Generalized Traveling Salesman problem, Traveling Salesman problem, Routing problem

I. The Mathematical Formulations of Generalized Traveling Salesman Problem

The Generalized Traveling Salesman problem (GTSP) is a modification of classical TSP. In the given complete graph G with the set of vertices V and the set of edges E all vertices is separated into m clusters $C_1, C_2, \dots C_m$. It is needed to find the route (also called g-route) s_0 which traverse each cluster and has minimal weight. Such problem is known as NP-hard [1].

The distance (weight function) $d(v_i, v_j)$ from one vertex v_i to another vertex v_j, where $v_i, v_j \in V$ represent the edge $e_{ij} \in E$, which satisfies the triangle inequality ($v_i, v_j, v_k \in V$ and $d(v_i, v_j) \le d(v_i, v_k) + d(v_k, v_j)$).

Let $\bigcup_{i=1}^{m} C_i = V$. If some clusters C_i and C_j are intersect then $C_i \cap C_j \neq \emptyset$, otherwise, if $C_i \cap C_j = \emptyset$ then they are non-intersecting.

The path $v_{i1} \to v_{i2} \to \cdots \to v_{il} \to v_{i1}$ is a g-tour if $l = m$ and for all $h \in [1, m]$ $C_h \cap \{v_i, v_{i1}, v_{i2}, \dots, v_{il}\} \neq \emptyset$. The length of g-tour can be calculated as $s = \sum_{k=1}^{l-1} d(v_{ik}, v_{ik+1}) + d(v_{il}, v_{i1})$. It is needed to find $s_0: f(s_0) = \min_{s \in S} f(s)$ [2].

Problem defined above is a classical GTSP, where cost functions between vertices are symmetry and only one vertex from each cluster should be visited. Sometimes, such problem called E-GTSP (Equality Generalized Traveling Salesman Problem), Set-TSP or group TSP [3]. The example of classical GTSP is pictured on Fig. 1.

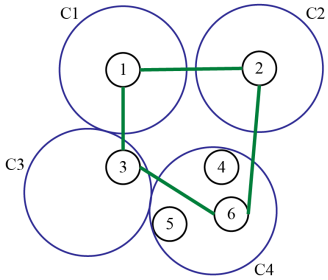

Fig. 1. The example of classical GTSP

The problem has practical useful applications, for example, airplane routing, computer file sequencing, postal delivery [4], location-based problems, urban planning, logistics problems, telecommunication problems, and railway track optimization problems.

II. Applications of the Generalized Traveling Salesman Problem

There are a wide range of applications which can be formulated mathematically as GTSP.

In article by Gilbert Laporte the five examples of applications were introduced. The problems such as location-routing, design of loop material flow systems, post-box collection or postal routing, stochastic vehicle routing and arc routing were mentioned [5].

In paper by Daniel Karapetyan such applications as "warehouse order picking with multiple stock locations, sequencing computer files, postal routing, airport selection and routing for courier planes" were listed [6]. In another article it is said that "GTSP offers a more accurate model than the TSP" [2]. This may be due to the fact that it is not necessary to visit all vertices. In some situations, it is necessary to visit only some key vertices among their small concentrations. One example is a meeting with dealers in different countries. If there are several cities in the country where dealers are present, it is not necessary to visit all of them. It is enough to visit one dealer, and he will transfer the information to the other dealers in country.

Almost the same situation occurs when somebody plans the location of the main mailboxes in the area. The main mailbox refers to the mailbox, the extraction of letters from which occurs daily. From the rest of the mailboxes, extracting letters can be done once a week. In order to understand where to place the main mailbox, the GTSP problem should be solved. Also, often there are real tasks associated with routing sites, load distribution across servers from different sites, etc. Almost all of such tasks can be solved as GTSP [2].

A wide range of situations can be modeled as a GTSP. Some situations were separates into subclasses of GTSP [5]:

- The Covering Tour Problem;
- Material Flow System Design;
- Post-box collection;
- Stochastic vehicle routing;
- Arc routing.

III. The Types of the Generalized Traveling Salesman Problem

Previously, the classical variant of GTSP was defined. However, there are real applications which require some modifications of classical GTSP. In this section all known types of GTSP are listed. The several new modifications of GTSP are proposed.

A. Generalized Traveling Salesman Problem with intersecting clusters

It is a less-known modification of GTSP, which defined in [7]. The definition of problem is similar to GTSP, but $C_1, C_2, \dots, C_m$ sets may intersect, so $C_i \cap C_j \neq \emptyset$ for some $i, j \in [1, m]$ and $i \neq j$. The example is presented on Fig. 2. The vertex v_5 lies in C_3 and C_4 cluster simultaneously.

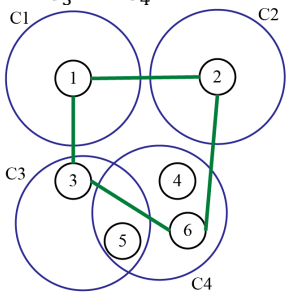

Fig. 2. The example of GTSP with intersecting clusters

B. Asymmetric Generalized Traveling Salesman Problem (A-GTSP)

If the distance function is asymmetry, so $d(v_i, v_j) \neq d(v_j, v_i)$ for some $v_i, v_j \in V$, the problem called A-GTSP (Asymmetric Generalized Traveling Salesman Problem).

C. Generalized Traveling Salesman Problem with many vertices in clusters (Many-GTSP)

In various articles, there is a mention of the problem of GTSP, where in the route $s = (v_{i_1}, v_{i_2}, \dots, v_{i_l}), l \in [m, |V|]$, where from each cluster more than one vertex can appear. However, algorithms that solve problem in this formulation were not found. There is an assumption that the problem is solved by classical methods with some modifications.

D. Dynamic Traveling Salesman (Dynamic GTSP)

The less well-known, but potentially useful problem is a Dynamic Generalized Traveling Salesman Problem (Dynamic GTSP). It is a variant of Dynamic Routing Problems and Generalized Traveling Salesman Problems at the same time. The Dynamic GTSP is a problem, where new vertices are added or deleted during the traveling. This is the main difference from the classical GTSP [8].

In the research [8] four types of Dynamic GTSP were presented. There are very few works that are devoted to this problem. In [8] the multi-agent-based approach to modeling and solving dynamic generalized traveling salesman problem is given.

E. Multi-objective Generalized Traveling Salesman Problem (MO-GTSP)

This problem is also very similar to the classical GTSP problem. However, there is some expansion. In GTSP only one characteristic is assigned to the edge, but in MO-GTSP several characteristics (for example, time, cost) are attributed to each arc, which should be minimized together [9]. The example is presented on Fig. 3.

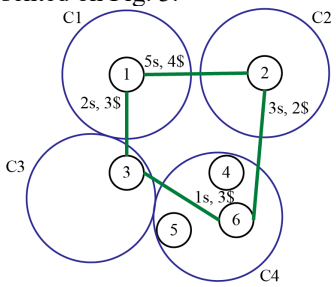

Fig. 3. The example of MO-GTSP with two functions to optimize: cost and time

F. Clustered Traveling Salesman Problem

It is an extension of TSP which has similarities with GTSP. All vertices are divided into non-intersecting clusters and solution consists of all vertices V, but vertices from one cluster should be traversed together. The example of problem and solution is presented on Fig. 4.

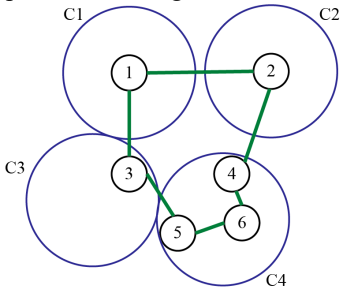

Fig. 4. The example of Clustered Traveling Salesman Problem

G. k-Generalized Traveling Salesman Problem (k-GTSP)

Previously, k-GTSP was not defined. However, other routing problem (for example, Chinese Postman problem or Traveling Salesman problem) have "-k" definition, which are very different.

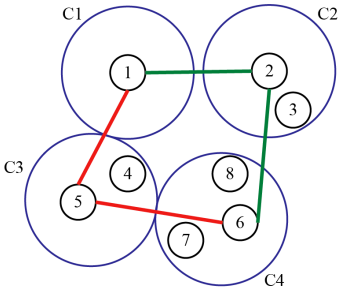

Fig. 5. The example of k-GTSP (k-GTSP with k salesmen). On figure there are 2 salesman and 2 tours (green and red)

It is possible to imagine that more than one salesman will traverse the route. Moreover, the start vertex for each salesman may be different. If the k salesman are defined, it is needed to find route with minimal weight $s = t_1 \cup \dots \cup t_k$, where t_i is route of i salesman. For all $i \in [1, m]$ $|s \cap C_i| = 1$. The example is shown on Fig. 5. In future, I will call such problem as k-GTSP with k salesmen. There is a similar

formulation for another routing problem k-CPP (k-Chinese Postman Problem) [10].

For TSP also was defined the k-TSP problem. The main idea to find the minimal weight cycle traverses exactly k vertices without repetitions [11]. Such problem can be generalized for the GTSP. In given complete graph G with the set of vertices V and the set of edges E it is needed to find minimal weight route s traverses only k clusters. The example is depicted on Fig. 6. Such problem will call k-GTSP with decreasing number of vertices.

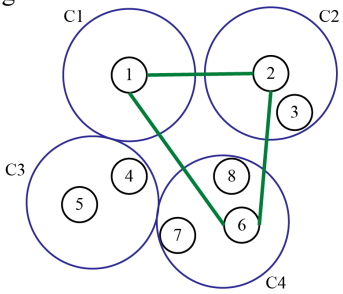

Fig. 6. The example of k-GTSP with decreasing number of vertices

It should be mentioned that problem defined above may be practically useful. For example, on the map of clusters it is necessary to choose k clusters such that the cost of traversing will be minimal. This can be useful, for example, if the supplier wants to choose the stores with minimal costs of deliver the goods.

In the literature, another formulation of the k-problem can be found. Such problems are called finding the $k-$best solutions and widely know for polynomial solvable problems. However, there is a k-TSP problem. The main idea consists of finding $k-$ best solutions. Such problem can be generalized to GTSP. It is needed to find the set of k solutions with minimal weight. The example is shown on Fig. 7. In my future work I will call such problem as k-GTSP with k best solutions.

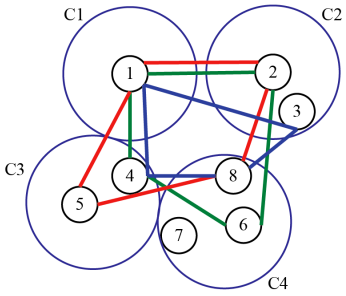

Fig. 7. The example of k-GTSP with k best solutions (3 solutions are depicted)

IV. The Ways of Solving the Generalized Traveling Salesman Problem

The GTSP is NP-hard problem and exact solution is very time expensive because requires complete search of all possible variants. Even for small tasks (for example, 20 clusters) on a personal computer, calculating the optimal route can be very time consuming.

After analyzing the sources, several groups of algorithms and approaches for solving GTSP can be distinguished:

- Exact algorithms (such as branch and bound, branch and cut algorithms, etc.);
- Heuristic algorithms (random-key genetic algorithm, mrOX genetic algorithm, BIO-inspired algorithms, generalized nearest neighbor heuristic, memetic algorithm, 2-opt local search algorithm, generalized initialization, insertion and improvement heuristic, LKH heuristic, neighborhood heuristics, etc.);
- Algorithms for transforming GTSP into related problems (exact and non-exact transformations);
- Algorithms for reduction GTSP dimension.

Below the description of transformation and reduction some algorithms are presented.

A. Transformation GTSP with intersecting clusters to GTSP with non-intersecting clusters (I-N transformation)

Suppose we are dealing with a GTSP with intersecting clusters, for some $i, j \in [1, m]$ $C_i \cap C_j \neq \emptyset$. Such type of GTSP instance G can be transformed into G' with non-intersecting clusters. The algorithm was mentioned by Y.N. Lien in [2]. The main idea of transformation is copying the vertices, which simultaneously lie in different clusters p times (p is a number of clusters, where vertex lies). Let S_v be a set of clusters in which the v vertex lies, $q_v = |S_v|$. Then it is needed to find g-tour in G'. Between copies of each vertex it is needed to construct random route. After that from g-tour in G' the g-tour in G can be obtained by deleting from g-tour copies of vertices. The correctness of algorithm was proved [2]. The cost of g-tours in G and G' are similar [2]. If some vertex should be marked as start it marked as v_0 and placed into non-intersected special cluster C_0. If there is no such restriction, then such a cluster is not allocated.

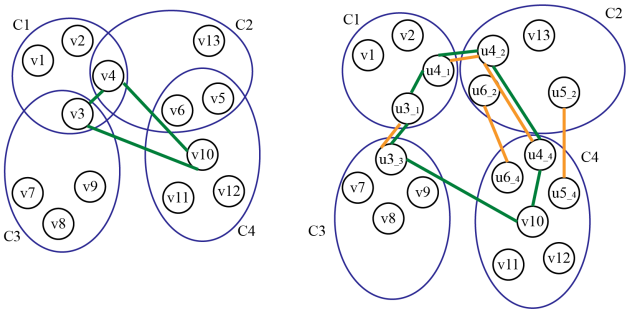

Fig. 8. The example of I-N transformation (g-tour is green, yellow route is the route between duplicated vertices)

The example of algorithm's working is presented. The Fig. 8, Table I and Table II show how the transformation is occurred.

TABLE I. *I-N Transformation. The Vertex Distribution*

	S_1	S_2	S_3	S_4	S_5	S_6	S_7	S_8	S_9	S_{10}	S_{11}	S_{12}	S_{13}
	C_1	C_1	C_1, C_3	C_1, C_2, C_4	C_2, C_4	C_2, C_4	C_3	C_3	C_3	C_4	C_4	C_4	C_2
q_v	1	1	2	3	2	2	1	1	1	1	1	1	1

TABLE II. *I-N Transformation. The Vertex Distribution into Clusters*

Cluster	Vertices
C_1	v_1, v_2, v_3, v_4
C_2	v_4, v_5, v_6, v_{13}
C_3	v_3, v_7, v_8, v_9
C_4	$v_5, v_6, v_{10}, v_{11}, v_{12}$

B. Transformation GTSP with non-intersecting clusters into standard TSP) (S-N transformation)

The GTSP with non-intersecting clusters can be transformed into standard instance of TSP [2]. Suppose we are dealing with a GTSP with non-intersecting clusters, for all $i, j \in [1, |V|]$ $C_i \cap C_j = \emptyset$.

It is needed to mark the start vertex as v_0 and put it in individual cluster C_0. In related G' problem create C' clusters, which consist of replicas of vertices:

- $v_0 \in C_0$ copies as $a_{0,0}$ and $c_{0,0}$ into $C_0{}'$ cluster.
- For all nodes from each clusters the three replicas a, b, c should be created in G' (see Fig. 9).
- For each cluster vertex e added.

After copying and doubling vertices transformation of edges are required.

The edges transform in the following ways:

- In the cluster C_0 the $c_{0,0}$ vertex connects with $a_{0,0}$ by edge with zero cost.
- All vertex in each transformed cluster $C_i{}'$ connect by edges with zero cost in the following way: $a_{i,0} \to b_{i,0} \to c_{i,0} \to a_{i,1} \to b_{i,1} \to c_{i,1} \to \cdots \to a_{i,|C_i|} \to b_{i,|C_i|} \to c_{i,|C_i|} \to a_{i,0}$. All b vertex connects with corresponding a vertex. All c vertices connect with all e vertex in each cluster and e vertex connects with all b vertices in cluster by zero cost edges.
- All intercluster edges are copies with the same cost of traverse.

The G'' problem is not presented on complete graph. After finding the solution on G'' for transforming g-tour to G' it is needed to remove incluster cycles in g-tour. The correctness of algorithm was proved [2].

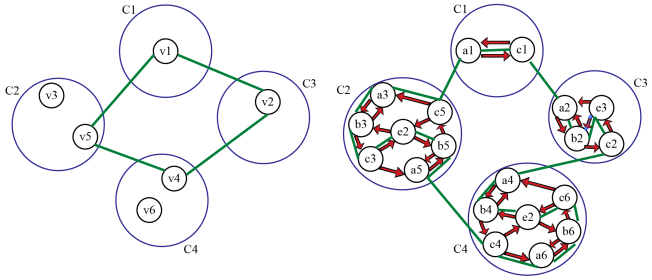

Fig. 9. The example of S-N transformation [3]

C. T-Transformation of GTSP into A-TSP

T-transformation doubles up the number of vertices [12, 13] and consists of the following steps:

- For every vertex in each cluster $v_j \in V_i, i \in [1, k]$ define two vertices v_j (entering) and v_j' (leaving). Each pair of such vertices is joined by an arc from v_j to v_j' with very high cost.
- Join all $v_j \in V_i'$ vertices in increasing order and $v_j' \in V_i'$ in decreasing order with zero cost.
- Edges between V_i copied with the same cost.

The proof of correctness such transformation is given in [12]. The example of T-transformation is shown on Fig. 10

D. Noon-Bean transformation of GTSP into ATSP

It is a way of transformation without adding any vertex. Here the cost of traversing is changed. The big constant M adds to each intercluster edges. It is guarantee that firstly the all vertices into cluster would be traversed and then the route goes to another cluster. After such solution some vertices from tour should be deleted (after the first vertex of the cluster is met, the rest should be removed). Received route is the g-tour. The correctness, proof and some computational results on GTSPlib are presented in [14] and an example of transformation is presented in my previous research [15].

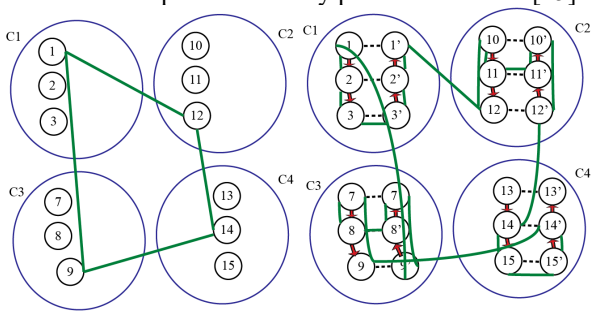

Fig. 10. The example of T-transformation

E. Spatial Transformation of GTSP to TSP

GTSP can be solved in the following way [3]:

- From each cluster V_i the vertex v_{i_j} should be selected.
- Calculate the Hamiltonian cycle in the subgraph G', constructed on the selected vertices from step 1.

Step 1 and 2 doing until all possible options for selecting vertices are completed. Then the smallest route is selected. However, such solution requires a lot of processing power and memory, especially on large-scale problems.

In article [3] the five different types of selecting vertices from clusters are shown:

1) E-Search

E-Search is known as Euclidian-Search. The main idea of this method is constructing a line connecting the first and last vertex from the original data. After that, from each cluster select only one vertex which is closest to the line. Computational time is $O(V)$ [3]. The process of E-Search is shown on Fig. 11.

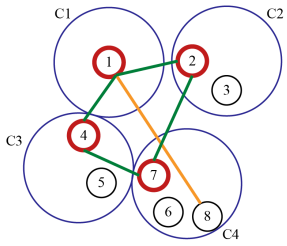

Fig. 11. The example of E-Search (yellow line - line between the first and last vertices, red vertices were selected)

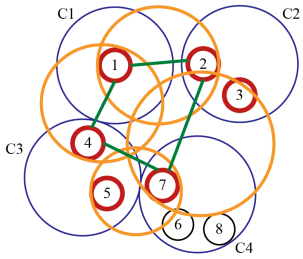

Fig. 12. R-Search example

2) R-Search

R-Search is known as Radial-Search. It is needed for the first and last vertex in the original data find from each cluster radially the nearest vertices. So, there are 2^k TSP instance, it

is needed to solve both and select the best. Computational time is $O(V)$ of selecting 2^k instances [3]. The process of R-Search is shown on Fig. 12.

3) RE-Search

It is a combination of R-Search and E-Search. Firstly, it is needed to find two vertices most radially nearest to start and end vertex in the original data. Then, for selected vertices the E-Search applied. Computational time is $O(V)$ [3].

4) D-Search

D-Search is known as Dijkstra-Search. The main idea of this method is constructing a route connecting the first and last vertex from the original data using Dijkstra algorithm. After that, from each cluster select only one vertex which is closest to the route. Computational time is $O(V^2)$ [3].

5) RD-Search

It is a combination of R-Search and D-Search. Firstly, it is needed to find two vertices most radially nearest to start and end vertex in the original data. Then, for selected vertices the D-Search applied. Computational time is $O(V^2)$ [3].

The approaches presented above have advantages and disadvantages. One of the disadvantages is the strong dependence of the minimum route weight on chosen starting and ending vertices. I propose the following search method CM-Search based on finding vertices closest to the "center of mass".

6) CM-Search

CM-Search is a Center of Mass Search. The main idea of this method is to find the center of mass of the graph G (let the mass of each vertex is equal). After that, from each cluster select only one vertex which is closest to the center mass. Computational time is $O(V)$.

However, method also has a disadvantage. The situation where all vertices are concentrated in one place, but there are several vertices that are far away from them is possible. In this case, the center of mass is shifted, and non-optimal vertices can be selected. The example of bad case shown on Fig. 13. It can be seen that the selection v_3 and v_4 instead of v_2 and v_5 is more optimal. One solution of such problem is to assign big mass to the vertices from the clusters with a larger number of vertices. This method is new and requires testing on test data.

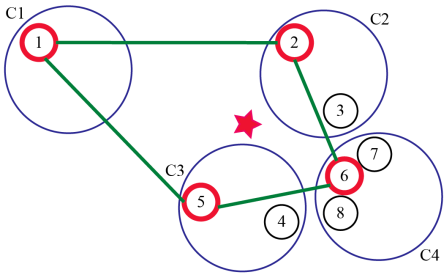

Fig. 13. CM-Search (the star is the center of mass). Bad case.

F. The Reduction Algorithm for GTSP

It is known that GTSP problems (real or, for example, from GTSPlib) have big size (several hundred of vertices). Some of vertices and edges between them are redundant. There is algorithm with running time $O(N^3)$ which can reduce size approximately to 10-15% [6].

Let $n = |V|$ the number of vertices in graph G. If graph G consists of m clusters then only m vertices should be traversed, another $n - m$ vertices are redundant. In article by Gregory Gutin the definition of redundant vertex is presented. "Let C be a cluster, $|C| > 1$. We say that a vertex $r \in C$ is redundant if for each pair x, y of vertices from distinct clusters different from C, there exists a vertex $s \in C\backslash\{r\}$ such that $d(x,s) + d(s,y) \leq d(x,r) + d(r,y)$" [6].

The example of GTSP with three clusters is defined in Table III (different colors match to different clusters). This example can be reduced.

We can define differences table as shown in original research [6]. The differences can be calculated as $dist(x,s) - dist(x.r)$. For the example from Table III the Differences table (Table IV) and Comparison distances table (Table V) can be calculated - $dist(x,r) + dist(r,y) - dist(x,s) - dist(s,y)$.

TABLE III. *THE EXAMPLE OF GTSP PROBLEM*

	v_1	v_2	v_3	v_4	v_5	v_6	v_7	v_8
v_1	-	1	2	10	7	6	7	8
v_2	1	-	3	8	8	7	10	11
v_3	2	3	-	11	10	7	6	5
v_4	10	8	11	-	1	2	1	2
v_5	7	8	10	1	-	1	3	1
v_6	6	7	7	2	1	-	2	1
v_7	7	10	6	1	3	2	-	2
v_8	6	11	5	2	1	1	2	-

TABLE IV. *THE DIFFERENCES TABLE FOR 1 CLUSTER AND* $r = v_1$

s/r	v_4	v_5	v_6	v_7	v_8
v_2	2	-1	-1	-3	-3
v_3	-1	-3	-1	1	3

TABLE V. *THE TABLE FOR COMPARISON DISTANCE THROUGH* $r = v_1$ *AND* s

	$s = v_2$	$s = v_3$
$v_4 \to v_s \to v_7$	-1	0
$v_4 \to v_s \to v_8$	-1	2
$v_5 \to v_s \to v_7$	-4	-2
$v_5 \to v_s \to v_8$	-4	0
$v_6 \to v_s \to v_7$	-4	0
$v_6 \to v_s \to v_8$	-4	2

The Comparison distances in Table V shows that vertex $r = v_1$ is not redundant.

The same calculations may be done for vertex v_2. The calculations shown in Table VI and Table VII.

TABLE VI. *THE DIFFERENCES TABLE FOR 1 CLUSTER AND* $r = v_2$

s/r	v_4	v_5	v_6	v_7	v_8
v_1	-2	1	1	3	3
v_3	-3	-2	0	4	6

TABLE VII. *THE TABLE FOR COMPARISON DISTANCE THROUGH* $r = v_2$ *AND* s

	v_1	v_3
$v_4 \to v_s \to v_7$	1	1
$v_4 \to v_s \to v_8$	1	3
$v_5 \to v_s \to v_7$	4	2
$v_5 \to v_s \to v_8$	4	4
$v_6 \to v_s \to v_7$	4	4
$v_6 \to v_s \to v_8$	4	6

The Comparison distances in Table VII shows that vertex $r = v_2$ is redundant and can be removed. The transformed GTSP is presented in Table VIII.

After removing redundant vertices from GTSP the calculations should be done again. Again, perform the calculation for the vertex $r = v_1$ (see Table IX and Table X).

TABLE VIII. *THE EXAMPLE OF GTSP PROBLEM*

	v_1	v_3	v_4	v_5	v_6	v_7	v_8
v_1	-	2	10	7	6	7	8
v_3	2	-	11	10	7	6	5
v_4	10	11	-	1	2	1	2
v_5	7	10	1	-	1	3	1
v_6	6	7	2	1	-	2	1
v_7	7	6	1	3	2	-	2
v_8	6	5	2	1	1	2	-

TABLE IX. *THE DIFFERENCES TABLE FOR 1 CLUSTER AND* $r = v_1$

	v_4	v_5	v_6	v_7	v_8
v_3	-1	-3	-1	1	3

TABLE X. *THE TABLE FOR COMPARISON DISTANCE THROUGH* $r = v_1$ *AND* s

s/r	v_3
$v_4 \to v_s \to v_7$	0
$v_4 \to v_s \to v_8$	2
$v_5 \to v_s \to v_7$	-2
$v_5 \to v_s \to v_8$	0
$v_6 \to v_s \to v_7$	0
$v_6 \to v_s \to v_8$	2

Nothing changes in Table IX and X, the vertex v_1 is not redundant. The reduction can be continued, but, further results of calculations showed that it is meaningless.

In the same way, the reduction of number of edges can be done [6].

V. THE RESULTS OF COMPUTATIONAL EXPERIMENTS

The transformation approach CM-Search E for spatial transformation of GTSP to TSP were tested on standard GTSPLib by D. Karapetyan [16]. The transformation algorithms were implemented in C++ and tested on a computer with 2,6 GHz Intel Core i5 processor. After CM-Search transformation the LKH-heuristic for finding solution were used [18]. In paper [3] was shown that the applying R-Search transformation on real-world dataset and solving transformed TSP gives the average error 8.8% (for five presented Searches it is the lowest). The main disadvantage of R-Search is computational time. The R-Search gives 2^m variants and then each variant should be solved.

The testing of CM-Search shows that the average error is 8.1%, and computational time (in average) reduced on 83% by reducing the dimension (compared to using the LKH algorithm on non-reduced problem).

VI. CONCLUSION

In paper the existing modifications of GTSP were listed and described. Three new modifications which have real applications were proposed. In next research the methods for solving k-GTSP with k salesmen, k-GTSP with k best solutions and k-GTSP with decreasing number of vertices will be proposed.

Various approaches for solving the GTSP were presented. Particular attention is paid to the algorithms for reducing the dimension and transformation algorithms. The new transformation non-exact approach CM-Search for spatial transformation of GTSP to TSP were presented and tested. Testing shown that the CM-Search significantly reduces computation time with a permissible error.

REFERENCES

[1] M. Gordenko and S. Avdoshin, "The mixed chinese postman problem," *Trudy Instituta sistemnogo programmirovaniya RAN,* vol. 29, no. 4, 2017.

[2] Y. N. Lien, E. Ma and B. W. S. Wah, "Transformation of the Generalized Traveling-Salesman Problem into the Standard Traveling-Salesman Problem," *Information Sciences,* Vols. 74 (1-2), pp. 177-189, 1993.

[3] M. Zia, Z. Cakir and D. Z. Seker, "Spatial Transformation of Equality–Generalized Travelling Salesman Problem to Travelling Salesman Problem," *ISPRS International Journal of Geo-Information,* vol. 7, no. 3, p. 115, 2018.

[4] U. Palekar and G. Laporte, "Some applications of the clustered travelling salesman problem," *Journal of the Operational Research Society,* vol. 53, no. 9, pp. 972-976, 2002.

[5] G. Laporte, A.-V. Ardavan and C. Sriskandarajah, "Some Applications of the Generalized Travelling Salesman Problem," *The Journal of the Operational Research Society,* vol. 12 (47), pp. 1461-1467, December 1996.

[6] G. Gutin and D. Karapetyan, "Generalized traveling salesman problem reduction algorithms," *arXiv preprint arXiv:0804.0735,* 2008.

[7] E. Ma, B. W. -S. Wah and Yao-Nan Lien, "Transformation of the generalized traveling-salesman problem into the standard traveling-salesman problem," *Information sciences,* vol. 74, no. 1-2, pp. 177-189.

[8] A. Baykasoğlu and Z. D. U. Durmuşoğlu, "A multi-agent based approach to modeling and solving dynamic generalized travelling salesman problem," *Journal of Intelligent & Fuzzy Systems,* vol. 31, no. 1, pp. 77-90, 2016.

[9] J. Pinxten, "Online Heuristic for the Multi-objective Generalized Traveling Salesman Problem," *Design, Automation & Test in Europe Conference & Exhibition (DATE),* pp. 822-825, 2016.

[10] A. Osterhues and F. Mariak, "On variants of the k-Chinese Postman Problem," *Operations Research and Wirtschaftsinformatik,* vol. 30, 31 August 2005.

[11] A. Horbach, "Combinatorial relaxation of the k-traveling salesman problem," *Manuskripte aus den Instituten für Betriebswirtschaftslehre der Universität Kiel,* vol. 599, 2005.

[12] V. Dimitrijević and Z. Šarić, "An efficient transformation of the generalized traveling salesman problem into the traveling salesman problem on digraphs," *Information Sciences,* vol. 102, no. 1-4, pp. 105-110, 1997.

[13] G. Laporte and F. Semet, "Computational evaluation of a transformation procedure for the symmetric generalized traveling salesman problem," *INFOR: Information Systems and Operational Research,* vol. 37, no. 2, pp. 114-120, 1999.

[14] D. Ben-Arieh, G. Gutin, M. Penn, A. Yeo and A. Zverovitch, "Transformations of Generalized ATSP into ATSP," *Operations Research Letters,* vol. 31, no. 5, pp. 357-365, 2003.

[15] M. Gordenko and S. Avdoshin, "Transformation of the Mixed Chinese Postman Problem in multigraph into the Asymmetric Travelling Salesman Problem," *International Journal of Open Information Technologies,* vol. 5, no. 6, pp. 6-11, 2017.

[16] D. Karapetyan, "GTSP Instances Library," [Online]. Available: http://www.cs.nott.ac.uk/~pszdk/gtsp.html. [Accessed 21 March 2019].

Constructive heuristics for Capacitated Vehicle Routing Problem: a comparative study

Ekaterina N. Beresneva
Faculty of Computer Science
National Research University Higher School of Economics
Moscow, Russia
eberesneva@hse.ru

Scientific Advisor: Prof. Sergey Avdoshin
Software Engineering School
National Research University Higher School of Economics
Moscow, Russia
savdoshin@hse.ru

***Abstract*— Vehicle Routing Problem (VRP) is concerned with the optimal design of routes to be used by a fleet of vehicles to serve a set of customers. In this study we analyze constructive heuristics for a subcase of VRP, where the vehicles have a limited capacity – Capacitated Vehicle Routing Problem (CVRP). The problem is NP-hard, therefore heuristic algorithms which provide near-optimal polynomial-time solutions are still actual. The aim of this work is to make a comparison of constructive heuristics as there were not found any such classification. Finally, the leader by a criterion of quality is admitted being a Clarke and Wright Savings heuristic; however, this algorithm cannot find the solution for all used instances. This fact and other ones are discussed in the paper. Our future goal is to make an experimental comparison of the most common and state-of-the-art metaheuristics using well suited constructive heuristic to build a suboptimal solution.**

Keywords*— capacitated vehicle routing problem, mathematical formulation, classical heuristics, constructive heuristics.

I. Introduction

The Vehicle Routing Problem (VRP) is one of the most widely known questions in a class of combinatorial optimization problems. VRP is directly related to Logistics transportation problem and it is meant to be a generalization of the Travelling Salesman Problem (TSP). In contrast to TSP, VRP produces solutions containing some (usually, more than one) looped cycles, which are started and finished at the same point called "depot". The objective is to minimize the cost (time or distance) for all tours. For the identical type of input data, VRP has higher solving complexity than TSP. Both problems belong to the class of NP-hard tasks.

This work is aimed at analysis of VRP subcase, which is called Capacitated Vehicle Routing Problem (Capacitated VRP, CVRP), where the vehicles have a limited capacity. It means that there is a physical restriction on transportation more than determined amount of weight for each machine. Capacitated vehicle routing problems form the core of logistics planning and are hence of great practical and theoretical interest.

There are three types of algorithms that are used to solve any subcase of CVRP:

• *Exact algorithms.* These algorithms find an optimal solution but take a great time for solving large instances. Such methods include Branch-and-Bound, Branch-and-Cut, cutting plane, column generation, cut and solve, Branch-and-Cut-and-Price, Branch-and-Price, and dynamic programming techniques. It was shown in [1] that Branch-and-Bound algorithm was able to solve random CVRP instances with up to 300 customers and four vehicles within 1000 CPU seconds in 2002. However, according to the same source some real-world CVRP instances with up to 47 vertices only were successfully solved within 1000 CPU seconds. Current situation does not differ a lot. State-of-the-art exact methods can provide optimal solution for some SCVRP instances with up to 100 nodes, but it takes 30-40 minutes at average [2]. Due to these restrictions, researchers all over the world concentrate on heuristic methods.

• *Classical heuristics.* These algorithms build an approximate solution iteratively, but they do not include further improvement stage. Different scientific works reveal that, in comparison to exact methods, classical heuristics work much faster. For example, an instance of 100-150 nodes can be solved up to a few (1-2) seconds [2]. Heuristics are divided into two groups that include constructive heuristics and improvement heuristics.

• *Metaheuristics*. Such type of algorithms is also called a framework for building heuristics. According to [3], metaheuristics either explore the solution space by moving at each iteration from a solution to another solution in its neighbourhood (metaheuristics based on local search) or evolve a population of solutions which may be combined together in the hope of generating better ones (metaheuristics based on population, natural inspired).

Actuality of research and development of heuristics algorithms for solving VRP is on its top, because such approximate algorithms can produce near-optimal solutions in a polynomial time. It is especially important in real-world tasks when there are more than one hundred clients in a delivery net. Among the best-known algorithms for CVRP there are metaheuristic proposed by Pisinger and Ropke [4], Nagata and Braysy [5], and Vidal et al [6].

There are a lot of articles related to CVRP heuristics, but no works were found which compare solution quality, or gap, of classical heuristics using the same data bases. Solution quality is calculated as the percentage of difference in the obtained

value of the solution with the optimal (or best-known) solution for the problem.

It is important to analyze classical heuristics since constructive heuristics are usually used in order to provide an initial (suboptimal) solution to improvement methods and to metaheuristics that allow to iteratively get near optimal solutions. So, we will discuss only algorithms from the first group.

The paper is structured as follows. In the second part a mathematical formulation of CVRP is given. In the third section, some notes on a classification of most popular constructive heuristics are provided, including description of chosen algorithms. The fourth part consists of design of experiments and their results. And, finally, in the fifth part conclusions and future goals are given.

II. Classical CVRP mathematical model

In the paper we will use CVRP abbreviation having in mind the mathematical formulation that was described in a previous work of authors [7].

Let a complete weighted oriented graph $G =< V, V \times V >$ is given. Let $I = \{0, 1, \dots, N\}$, where $N + 1 = |V|$. Graph vertices are indexed as $ind = V \to I, (\forall v \in V)(\forall w \in V)$ $v \neq w \Longrightarrow ind(v) \neq ind(w)$. Thus, $V = \{v_0, v_1, \dots, v_N\}$ is the set of vertices, here $i = ind(v_i), i \in I$. Let v_0 be the depot, where vehicles are located, and v_i be the destination points of a delivery, $i \neq 0$.

The distance between two vertices v_i and v_j is calculated using a distance function $c(v_i, v_j)$. Here a real-valued function $c(\cdot,\cdot)$ on $V \times V$ satisfies $\forall i, j, g \in I$ [8]:

1. $c(v_i, v_j) \geq 0$ *(non-negativity axiom).*
2. $c(v_i, v_j) = 0$ if and only if $v_i = v_j$ *(identity axiom).*
3. $c(v_i, v_j) = c(v_j, v_i)$ *(symmetry axiom).*
4. $c(v_i, v_g) \leq c(v_i, v_j) + c(v_j, v_g)$ *(triangle inequality axiom).*

Each destination point $v_i, \forall i \in I$, is associated with a known nonnegative demand, d_i, to be delivered, and the depot has a fictitious demand $d_0 = 0$. The total demand of the set $V' \subseteq V$ is calculated as $d(V') = \sum_{i'=1}^{|V'|} d_{i'}$.

Let K be a number of available vehicles at the depot v_0. Each vehicle has the same capacity – C. Let us assume that every vehicle may perform at most one route and $K \geq K_{min}$, where K_{min} is a minimal number of vehicles needed to serve all the customers due to restriction on C. Clearly, next condition must be fulfilled – $(\forall v_i \in V)\, d_i \leq C, \forall i \in I$, which prohibits goods transportation that exceed maximum vehicle capacity.

Let introduce $V^0 = \{v_0\}$, where $v_0 \in V$. Let us divide V in $K + 1$ sets: $S = \{V^0, V^1, \dots, V^K\}$, each subset, except for V^0, represent a set of customers to be served for one vehicle. $S^{all} = \{S\}$ is a set of all possible partitions of V. Let $J = \{0, 1, \dots, K\}$ be a set that keeps indexes. Then $(\forall j \in J)\, |V^j| \geq 1$. There should be no duplicates in any of subsets from S: $(\forall g \in J)(\forall j \in J)(g \neq j \Rightarrow V^g \cap V^j = \emptyset)$. Also, all subsets from S must form set V. Thus, $V = \bigcup_{j=0}^{K} V^j$. In this notation, $V^{0k} = V^0 \cup V^k, \forall k \in J\backslash\{0\}$. It is obvious that $d(V^{ok}) \leq C$.

Let introduce $M^k = \{1, N^1 \dots, N^k\}$, $N^k = |V^k|$, $\sum_{k=1}^{K} N^k = N$. Then let $M^{0k} = \{0\} \cup M^k$. Let $I^k = \bigcup_{k=1}^{K} \{i \mid i = ind(v), \forall v \in V^k\}$ be a set of vertex indices from V^k. Then $I^{0k} = \{0\} \cup I^k, \forall k \in J\backslash\{0\}$.

Let $H^k = \{p^k : M^{0k} \to I^{0k} \mid p^k(0) = 0 \;\&\; (\forall x \in M^{0k})$ $(\forall y \in M^{0k})\; x \neq y \Longrightarrow p^k(x) \neq p^k(y)\}$ be a set of codes of all possible permutations $h^k = \left(v_{p^k(0)}, v_{p^k(1)}, \dots, v_{p^k(N^k)}\right)$ of V^{0k}. These permutations represent all possible Hamiltonian cycles of graph $G^{0k} < V^{(0k)}, V^{(0k)} \times V^{(0k)} >, \forall k \in J\backslash\{0\}$.

Weight of $h^k \in H^k$ can be found according to the formula 1:

$$f(h^k) = c\left(v_{p^k(0)}, v_{p^k(N^k)}\right) + \sum_{q=0}^{N^k-1} c\left(v_{p^k(q)}, v_{p^k(q+1)}\right) \quad (1)$$

Let S' be a set of $\{V^{01}, V^{02}, \dots, V^{0K}\}$. In this notation the weight of S' is calculated as $F(S') = \sum_{k=\overline{1..K}} f(h^k),\ \forall k \in J\backslash\{0\}$.

Overall, the formulation of CVRP is to find:

$$S^0 : F(S^0) = \min_{S \in S^{all}} F(S) \quad (2)$$

III. Constructive heuristics

In this section the most popular constructive heuristics are described.

A. Sequential Insertion algorithm (SI)

Sequential Insertion algorithm [9] constructs routes subsequently, one after another.

In the first step, a new tour $tour_k, k \leq K$, is initialized with a random unrouted node $v_i, i \neq 0$, and the depot v_0. Thus, a tour (v_0, v_i, v_0) is obtained.

In the second step, another unrouted vertex $v_j, j \neq 0$, is chosen, such that its incorporation in the current tour gives the least increase in a tour length and demand of a potential node v_j does not exceed vehicle capacity. So, the next two formulae must be hold:

– $\underset{\substack{v_a \in tour_k,\\ v_{a+1} \in tour_k,\\ v_j \notin tour_k}}{\operatorname{argmin}} c(v_a, v_j) + c(v_j, v_{a+1}) - c(v_a, v_{a+1})$;

– $D_{tour_k} + d_j \leq C$, where D_{tour_k} is a total demand of current $tour_k$.

If all conditions hold then this unrouted vertex $v_j, j \neq 0$ is inserted in a tour $tour_k$ between v_a and v_{a+1}.

The second step is repeated until no more unrouted vertex $v_j, j \neq 0$, can be feasibly inserted. In this case a new tour $tour_k, k \leq K$, is initialized, and the procedure starts from the first step.

B. Improved Parallel Insertion algorithm (PI)

Parallel Insertion Improved algorithm [10] builds routes simultaneously. This method is a modification of Sequential Insertion algorithm.

In the first step, the minimum number K_{min} of feasible routes is defined as $K_{min} = \sum_{i \in |V|} d_i / C$. All these routes $tour_k \in Tours$ are initialized with K_{min} different closest to v_0 unrouted nodes $v_i, i \neq 0$. Thus, K_{min} tours (v_0, v_i, v_0) are obtained.

In the second step, a random unrouted node $v_j, j \neq 0$, is inserted in some route $tour_k$ at its best insertion position. The next two conditions must be hold – incorporation of v_j in this tour gives the least increase in a tour length among all other tours and demand of a potential node v_j does not exceed vehicle capacity. So:

- $\underset{\substack{v_a \in tour_k, \\ v_{a+1} \in tour_k, \\ v_j \notin tour_k}}{\operatorname{argmin}} c(v_a, v_j) + c(v_j, v_{a+1}) - c(v_a, v_{a+1})$;
- $D_{tour_k} + d_j \leq C$, where D_{tour_k} is a total demand of current $tour_k$.

If all conditions hold then this unrouted vertex $v_j, j \neq 0$ is inserted in a tour $tour_k$ between v_a and v_{a+1}.

The second step is repeated until no more unrouted vertex $v_j, j \neq 0$, can be feasibly inserted in some route $tour_k$. In this case a new tour $tour_k, k \leq K$, is initialized as (v_0, v_j, v_0) and adds to set of all tours $Tours$, and the procedure continues.

C. Nearest Neighbour heuristic (NN)

Nearest Neighbour heuristic constructs routes subsequently, one after another, in a greedy way.

In the first step, an unrouted node $v_i, i \neq 0$, which is closest to the depot v_0, is chosen. A new open tour $tour_k, k \leq K$, is initialized with v_i and v_0. Thus, a tour (v_0, v_i) is obtained.

In the second step, another unrouted vertex $v_j, j \neq 0$, is chosen, which is the nearest to the last added vertex and a demand of a potential node v_j does not exceed vehicle capacity. So, the next two formulae must be hold:

- $\underset{v_i \in tour_k,\ v_j \notin tour_k}{\operatorname{argmin}} c(v_i, v_j)$;
- $D_{tour_k} + d_j \leq C$, where D_{tour_k} is a total demand of current $tour_k$.

If all conditions hold then this unrouted vertex v_j is added in the end of $tour_k$ after v_i, and since that time it turns to be the last added vertex.

The second step is repeated until no more unrouted vertex $v_j, j \neq 0$, can be feasibly inserted. In this case a new tour $tour_k, k \leq K$, is initialized, and the procedure starts from the first step.

D. Clarke and Wright Savings Heuristic (CWS) [9]

In the first step, all vertices $v_i \in V, i \neq 0$, must form $|V - 1|$ routes. Thus, $|V - 1|$ tours (v_0, v_i, v_0) are obtained.

In the second step, $\forall v_i \in V, \forall v_j \in V, i \neq 0, j \neq 0, i \neq j$, saving $s(v_i, v_j)$ is calculated as $s(v_i, v_j) = c(v_i, v_0) + c(v_0, v_j) - c(v_i, v_j)$. All savings are put in a list of $\bar{S}$, $\bar{S}$ must be sorted in a non-increasing order.

In the third step, the first unused saving in a list is taken. Then, existence of two routes $tour_x$ and $tour_y$, $x \neq y$, having the next conditions, is checked:

- there is an edge (v_i, v_0) in route x and edge (v_0, v_j) in tour $tour_y$;
- $D_{tour_x} + D_{tour_y} \leq C$.

If there are such routes then $tour_x$ and $tour_y$ are combined by removing edges (v_i, v_0), (v_0, v_j) and introducing edge (v_i, v_j). After that, despite of ability or absence these routes, the current saving is skipped and the next one in the list is checked.

The last step works until K tours are left.

E. Variant of Clarke and Wright Savings Heuristic (CWS_2)

Classical variant of Clarke and Wright Savings algorithm forms good tours in the first part of its work mostly. However, it was noticed that it tends to produce less competitive tours towards the end because of periphery nodes addition. Thus, Yellow [11] and Gaskell [12] suggested improved form of savings calculation. It is $s(v_i, v_j) = c(v_i, v_0) + c(v_0, v_j) - \lambda c(v_i, v_j)$. Here λ is a parameter which responds for measuring the distance between the vertices to be joint. In one report [13] it was mentioned that the best value of λ is 0.4.

F. Two-phase methods

Two-phase methods are based on the decomposition of the CVRP solution process into two separate stages – clustering and routing. In the clustering stage, a partition of the customers into routes is made, and in the routing stage, the sequence of the customers on each subset is obtained.

1) Subgroup of Cluster-First-Route-Second heuristics

In Cluster-First-Route-Second methods, nodes are first partitioned into different subsets called clusters and then routes are determined by sequencing the customers within each subset.

a) Sweep

This Cluster-First-Route-Second method can be applied only for planar instances [9].

Clustering stage

Let us define $v_i \in V$ as $v_i = (x_i; y_i)$, where x_i and y_i are the Cartesian coordinates of point v_i.

In the first step, new normalized vertices $v_i' = (x_i'; y_i') = (x_i - x_0; y_i - y_0)$ are introduced, where the depot v_0' has new Cartesian coordinates (0; 0), $\forall i \in |V|$.

Let $\overline{v_i'} = (\theta_i, r_i)$ be a vertex with polar coordinate of v_i', where $r_i = x_i'^2 + y_i'^2$ and θ_i is calculated using formula 3:

$$\theta_i = \begin{cases} arctg\left(\frac{y_i}{x_i}\right), x_i > 0, y_i \geq 0 \\ arctg\left(\frac{y_i}{x_i}\right) + 2\pi, x_i > 0, y_i < 0 \\ arctg\left(\frac{y_i}{x_i}\right) + \pi, x_i < 0 \\ \frac{\pi}{2}, x_i = 0, y_i > 0 \\ \frac{3\pi}{2}, x_i = 0, y_i < 0 \end{cases} \quad (3)$$

In the second step, a list $\bar{V}$ of all $\overline{v_i'} = (\theta_i, r_i), \forall i \in |V|, i \neq 0$, is calculated and is sorted in increasing order by parameter θ_i.

In the next step, a new cluster is initialized with $\{v_0\}$ and maximum number of first L vertices from $\bar{V}$, such that $\sum_{i=0}^{L-1} d_i \leq C$. Parameter L is not a constant, it can be other for different clusters depending on weights of demands and total capacity. Then these used vertices are removed from $\bar{V}$, and the procedure is repeated until $\bar{V} = \emptyset$.

Routing stage

At this stage for each cluster TSP Cheapest Insertion heuristic is applied which forms a cycle.

b) Fisher and Jaikumar algorithm [14]

In contrast to Sweep algorithm, this Cluster-First-Route-Second method can be applied not only for planar instances. Instead of using a geometric method to form the clusters, it solves a Generalized Assignment Problem (GAP).

Clustering stage

In the first step $\forall k = \overline{1..K}$ a vertex $v_{seed(k)} \in V \backslash \{v_o\}$ is chosen. These K vertices form K clusters.

In the second step the cost $cost_{v_i}^k$ of allocating each node $v_i \in V, i \neq 0$, to each cluster k is calculated as $cost_{v_i}^k = c(v_o, v_i) + c\left(v_i, v_{seed(k)}\right) - c\left(v_{seed(k)}, v_0\right)$.

In the third step the algorithm solves GAP with $cost_{v_i}^k$, d_i and C, which determines a minimum cost assignment of items to a given set of bins of capacity C. The GAP can be solved using either exact or heuristic techniques.

Routing stage

The final routes are determined by solving a TSP on each defined cluster.

According to this work [15], this algorithm gives way to the algorithms described above and provides solutions with more solution quality. That is why it will not be considered in later comparison study as it was already done.

2) Subgroup of Route-First-Cluster-Second heuristics

In contrast to Cluster-First-Route-Second methods, these constructive heuristics at first solve TSP for all nodes and only then break built cycle to K routes. Unfortunately, many studies showed than these heuristics are applicable only if there is no constraint on the number of vehicles. In addition, they are not competitive with other constructive heuristics in general [9].

IV. Experiments and results

All algorithms are implemented as sequential algorithms in C++. The computational testing of the solution methods for CVRP has been carried out by considering eight sets of test instances from the next well-known database [16]. Total number of instances in sets A, B, E, F, G, M, P, X is 211. All instances inside one set have its own characteristics and a way of generation: cluster-based / uniform / geometric distribution of clients, real-world / imitative cases etc. The integer Euclidean metric is used for all instances. The naming scheme and data format for each instance is described here [17]. Shortly, the first letter in names shows the name of used set, the figure after letter 'n' shows the number of nodes and the figure which stands after letter 'k' presents the number of vehicles.

Experiment starts with the choice of a constructive heuristic H from the set {SI, FI, NN, CWS, CWS_2, Sweep}. After that one dataset D is selected from the list of all benchmark datasets. Then an instance file F from the chosen dataset D is taken as input for the algorithm H and the heuristic is executed (only 1 time because all these algorithms do not use random generations, so all obtained solutions are the same). After that we report solution quality ε(H, F) found for the algorithm H on the test F. Solution quality ε (or percent above best-known, or gap) is calculated using formula 4 [18]:

$$\frac{F(S^0) - F_{opt}(S)}{F_{opt}(S)} \cdot 100\%, \quad (4)$$

where $F(S^0)$ is a length of obtained solution and $F_{opt}(S)$ is a length of optimal solution or best-known one. And finally, among all ε(H, F) from one dataset sample mean $\bar{X}_\varepsilon(\mathrm{H}, \mathrm{D}) = \frac{1}{|D|}\sum_{F=1}^{|D|} \varepsilon(\mathrm{H}, \mathrm{F})$ is calculated which shows average gap for the algorithm H on the dataset D, where $|D|$ is a number of input files in dataset D.

The plan of experiments on constructive heuristics described in Fig. 1.

```
Input: constructive heuristics, datasets
  1: foreach constructive heuristic H
  2:     foreach dataset D from datasets
  3:         foreach instance file F from D
  4:             solution = run H on F
  5:             calculate ε(H,F)
  6:     calculate X̄ε(H,D) // average gap on
     dataset
```

Fig. 1. Plan of experiment on constructive heuristics.

It should be mentioned that each algorithm is subsequently launched on all 211 instances from 8 datasets, so no input file is missed.

A criterion of running time was not considered because all instances were solved in a time which does not exceed 1 second.

It is thought to be insignificant in comparison with time-consuming metaheuristic work.

Figures 2, 3 and 4 represent the results of experiments conducted over algorithms using sets B, P and G of widely different types. The horizontal axis represents the name of instance data. The vertical axis shows the solution quality.

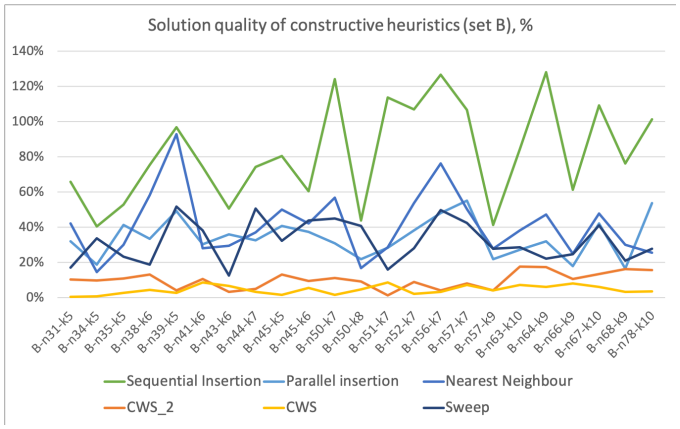

Fig. 2. Solution quality of constructive heuristics, set P.

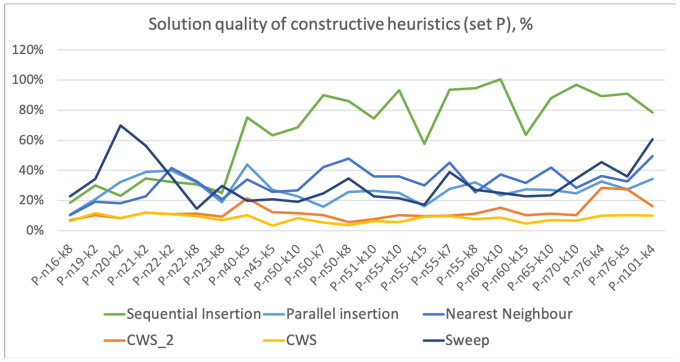

Fig. 3. Solution quality of constructive heuristics, set P.

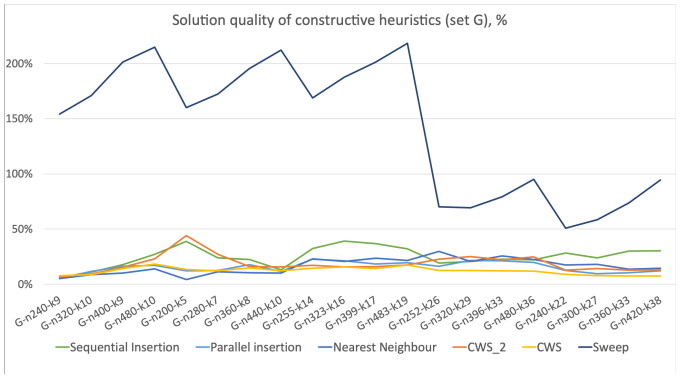

Fig. 4. Solution quality of constructive heuristics, set G.

Average gaps $\bar{X}_\varepsilon(\mathrm{H},\mathrm{D})$ of each algorithm on different data sets are presented in Table 1 and Figure 5. These general figures can show an approximate overall effectiveness of algorithms. On the basis of Table 1, all Figures 2, 3, 4, 5 and other results which cannot be shown here because of their large volume, it can be easily seen that CWS algorithm (its column is made bold in the table) is a leader for all input files, except some instances from dataset G. Its average gap varies from 3,4% till 11,0%. The closest competitor is its variant CWS_2, which has average solution quality in a range [9,8%; 20,6%]. CWS_2 algorithm is able to construct the best solutions only for some instances in set B. In all other cases this algorithm nearly always takes second place and goes behind classical CWS.

TABLE I. AVERAGE GAPS OF ALL HEURISTICS FOR EVERY SET, %.

Average gap $\bar{X}_\varepsilon(\mathrm{H},\mathrm{D})$ in the dataset		Constructive heuristic					
		SI	PI	NN	CWS	CWS_2	Sweep
Set (its size)	A (26)	68,7%	33,2%	39,7%	**5,0%**	12,7%	40,2%
	B (23)	82,3%	34,0%	41,2%	**4,3%**	9,8%	31,7%
	E (11)	70,4%	30,0%	41,5%	**6,4%**	17,5%	36,4%
	F (3)	42,5%	48,5%	74,6%	**4,4%**	20,6%	71,9%
	G (20)	24,8%	15,6%	16,3%	**11,0%**	18,4%	142,4%
	M (4)	83,0%	35,5%	44,6%	**3,4%**	12,0%	89,2%
	P (24)	66,0%	25,6%	32,2%	**6,9%**	11,3%	31,4%
	X (100)	99,7%	23,3%	27,4%	**5,9%**	11,9%	82,9%

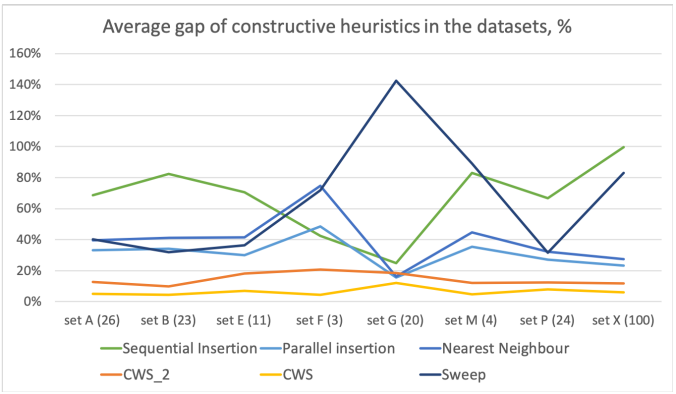

Fig. 5. Average gap of constructive heuristics in the datasets.

There is only one algorithm that have a problem with finding an answer to the given problems – it is Sweep. This heuristic is not able to construct a set of routes without exceeding the number of vehicles for some input files. All the others coped with the task – they are NN, SI, PI, CWS and CWS_2. Table 3 shows the percentage and the number of unsolved instances for all sets. In average, Sweep algorithm cannot solve the instance without over limit in more than 50% cases. It can be explained by the fact that the next vertex to be added is chosen by criteria of distance (polar angle, for real) but not the capacity.

TABLE II. PERCENTAGE OF UNSOLVED INSTANCES FOR EVERY SET, %.

Percentage of unsolved instances in the set		Constructive heuristic					
		SI	PI	NN	CWS	CWS_2	Sweep
Set (its size)	A (26)	0%	0%	0%	0%	0%	**69,0%**
	B (23)	0%	0%	0%	0%	0%	**50,0%**
	E (11)	0%	0%	0%	0%	0%	**43,5%**
	F (3)	0%	0%	0%	0%	0%	**63,6%**
	G (20)	0%	0%	0%	0%	0%	**66,7%**
	M (4)	0%	0%	0%	0%	0%	**90,0%**
	P (24)	0%	0%	0%	0%	0%	**50,0%**
	X (100)	0%	0%	0%	0%	0%	**58,3%**

It was mentioned earlier that CWS is not a leader for some instances from dataset G. There are 8 instances when NN finds the best solutions but not CWS (Fig. 4). This interesting change of the leader is connected with the type of customers' distribution – these instances have a form of rays going from the center. If we look at Fig. 6, where a solution for the instance is presented, we can see that the idea of nearest neighbor works here the best way.

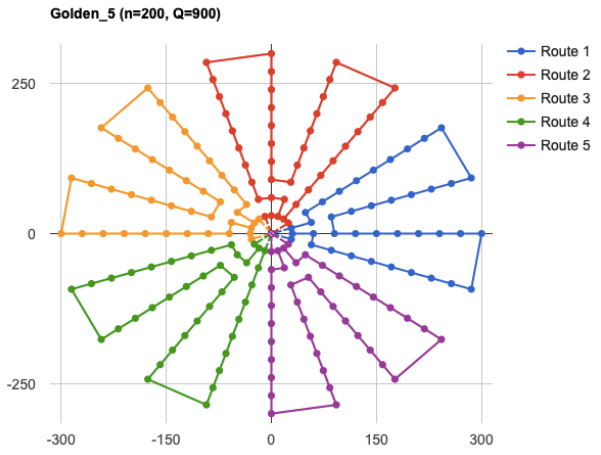

Fig. 6. Solution for instance G-n200-k5.

V. Conclusions

Overall, the next recommendation should be given to the problem which has described variant of mathematical model of CVRP. In general, for all types of clients' distribution the best algorithm to be applied is Clarke and Wright Savings, however, in case of having input data in form of concentric rays (like in Fig. 6) it is better to use Nearest Neighbor algorithm. Also, a few instances were solved best of all by Clarke and Wright Savings 2 algorithm, so it is important to have this algorithm in mind, however the difference between it and CWS is not very significant (no more than 1%).

One more conclusion is that it is unreasonable to use Sweep heuristic as it is not able to construct a set of routes without exceeding the number of vehicles for more than 50% of input files.

Finally, for our research it means that for all instances, except those 8 from set G, CWS heuristic will be used as initial algorithm for metaheuristic, otherwise – we will apply NN.

References

[1] P. Toth and D. Vigo, "Branch-and-Bound algorithms for the capacitated VRP," in *The Vehicle Routing Problem*, Philadelphia, SIAM, 2002, pp. 29-51.

[2] K. Braekers, K. Ramaekers and I. Nieuwenhuyse, "The vehicle routing problem: State of the art classification and review," *Computers & Industrial Engineering,* vol. 99, pp. 300-313, 2016.

[3] B. Golden, S. Raghavan and E. Wasil, The vehicle routing problem: latest advances and new challenges, New York: Springer, 2008.

[4] P. Pisinger and S. Ropke, "A general heuristic for vehicle routing problems," *Computers & Operations Research,* vol. 34, no. 8, pp. 2403-2435, 2007.

[5] Y. Nagata and O. Braysy, "Edge assembly-based memetic algorithm for the capacitated vehicle routing problem," *Networks,* vol. 54, no. 4, pp. 205-215, 2009.

[6] T. Vidal, T. Crainic, M. Gendreau, N. Lahrichi and W. Rei, "A hybrid genetic algorithm for multi-depot and periodic vehicle routing problems," *Operations Research,* vol. 60, no. 3, pp. 611-624, 2012.

[7] E. Beresneva and S. Avdoshin, "Analysis of mathematical formulations of Capacitated Vehicle Routing Problem and methods for their solution," *Trudy ISP RAN/Proc. ISP RAS,* vol. 30, no. 3, pp. 233-250, 2018.

[8] M. Reed and B. Simon, Methods of modern mathematical physics, London: Academic Press, 1972.

[9] G. Laporte and F. Demet, "Classical heuristics for the Capacitated VRP," in *The Vehicle Routing Problem*, SIAM, 2002, pp. 109-128.

[10] G. Laporte, Y. Nobert and M. Desrochers, "Optimal routing under capacity and distance restrictions," *Operations Research,* vol. 33, no. 5, p. 1050–1073, 1985.

[11] P. Yellow, "A computational modification to the savings method of vehicle scheduling," *Operational Research Quarterly,* no. 21, pp. 281-283, 1970.

[12] T. Gaskell, "Bases for vehicle fleet scheduling," *Operational Research Quarterly,* no. 18, pp. 281-295, 1967.

[13] B. Golden, T. Magnanti and H. Nguyen, "Implementing vehicle routing algorithms," *Networks,* no. 7, pp. 113-148, 1977.

[14] M. L. Fisher and R. Jaikumar, "A generalized assignment heuristic for vehicle routing," *Networks,* vol. 11, no. 3, pp. 109-124, 1981.

[15] T. Sultana, M. Akhand and M. Rahman, "A variant Fisher and Jaikuamr algorithm to solve capacitated vehicle routing problem," *The Proceedings of the 8th International Conference on Information Technology (ICIT),* no. 1, pp. 710-716, 2017.

[16] I. Xavier, "CVRPLIB," [Online]. Available: http://vrp.atd-lab.inf.puc-rio.br/index.php/en/. [Accessed 09 05 2019].

[17] Heidelberg University, "TSPLIB," [Online]. Available: https://www.iwr.uni-heidelberg.de/groups/comopt/software/TSPLIB95/. [Accessed 09 05 2019].

[18] P. Toth and D. Vigo, "An overview of vehicle routing problems," in *The Vehicle Routing Problem*, SIAM, 2002.

Solving the Generalized Traveling Salesman using Ant Colony algorithm with improvement local search procedures

Anastasia Inkina
School of Software Engineering
National Research University Higher School of Economics
Moscow, Russia
aninkina@edu.hse.ru

Mariia Gordenko
Department of Software Engineering
National Research University Higher School of Economics
Moscow, Russia
mgordenko@hse.ru

***Abstract*— The paper presents the research in progress in Generalized Traveling Salesman problem (GTSP) solved with ant colony algorithm. Firstly, the overview of GTSP is presented. Next, the formulation of GTSP is written. The ant colony algorithm, also, is shown. Algorithms of local search, which can improve the solution obtained by Ant Colony algorithm are identified. Test plans for algorithms and current results are provided in the next section. In conclusion, there are plans for future research.**

Keywords*— *Generalized Traveling Salesman problem, arc routing problem, local search algorithm, ant colony algorithm

I. Introduction

The Generalized Traveling Salesman problem (GTSP) is a routing problem. Most routing problem is NP-hard. In general, GTSP is NP-hard problem. The problem defined on graph and each vertex associate with cluster. It is needed to find the route with minimal weight, which traverse each cluster exactly once. It was shown, if the sequence of clusters visiting is defined that it is polynomial problem [1].

There are a lot of real-life problem, which can be solved as GTSP. For example, postal routing, airplane routing, finding optimal point for postal box and etc.

There are various algorithms for solving the GTSP. They can be divided into two big groups: exact algorithms and heuristic algorithms. Exact algorithms (such as branch-and-cut) give optimal solution, but, have exponential computational complexity, whereas, heuristic algorithms can solve GTSP in polynomial time with solution close to optimal.

In paper, the ant colony algorithm is described. The formulation on future experiments of ant colony algorithm for GTSP with using local search procedures (2-opt, 3-opt, tabu-search and etc.) are presented.

II. Defenition of Generalized Traveling Salesman Problem

The Generalized Traveling Salesman problem is defined in complete graph $G = (V, E)$.

Let V be a set of vertices, $|V| = n$; E be a set of edges between vertices from V, $|E| = m$.

Let e_{ij} be an edge between $v_i, v_j \in V$. The weight $d(v_i, v_j)$ is a cost of traversing from v_i to v_j. If $d(v_i, v_j) = d(v_j, v_i)$ for each vertex $v_i, v_j \in V$ then problem is defined as symmetric, otherwise, asymmetric. In paper, we work we symmetric GTSP.

All vertices are separated into k clusters $C_1, C_2, \dots, C_k$, $C_1 \cup C_2 \cup \dots \cup C_k = V$. If $C_i \cap C_j = \emptyset$ for all $i \neq j$, where $i, j \in [1, k]$ then problem is called as GTSP with non-intersecting clusters. The problem with intersecting clusters can be presented as GTSP with non-intersecting clusters, it was shown in research by Lien [1].

It is needed to find the route g, which traverse each cluster exactly once and has minimal possible length. Let $g = (v_{p_1}, v_{p_2}, \dots, v_{p_k}, v_{p_1})$, for each $i \in [1, k] \mid |C_i \cap \{v_{p_1}, v_{p_2}, \dots, v_{p_k}, v_{p_1}\}| = 1$. The length $L = \sum_{i=1}^{k-1} d(v_{p_i}, v_{p_{i+1}}) + d(v_{p_k}, v_{p_1})$. If $H = \{g_1, g_2, \dots\}$, it is needed to find $g_0 = \min g_i$, where $g_i \in H$.

III. Ant Colony Algorithm

There is a nature-inspired metaheuristic such as evolutionary algorithms (EA), particle swarm optimization (PSO), ant colony optimization algorithm (ACO). In research the ACO algorithm is described and tested (not all test implemented yet). It should be note, that the first mention of nature-inspired metaheuristic algorithms dates back to mid-2000.

The idea for using ACO for solving arc routing problem is not new. In previous research by Brezina Jr I. and Čičková Z. the ACO were used for solving Traveling Salesman problem [3]. In paper the impact of different parameters of algorithm on solution is shown. The computational results also were provided. The result for different amount of ant looks very interesting. If author uses 100 ants, then difference of solution from optimal is 17%. When the number of ants increases to 10000 the deference is falls to 0,83%.

In research by Camelia-M. Pintea, Petricˇa C. Pop, Camelia Chira how to apply ACO for solving GTSP were shown. However, for solving the GTSP authors choose parameters ($b = 0.5, p = 0.5, q_o = 0.5$, they will be defined) based on their experience. However, for such an algorithm, fine tuning parameters is very important and can improve the solution. This is the first task of the current research. The second task is trying to use for improving the solution various local search algorithms.

The ACO algorithm can be defined as follows (author calls it as Reinforcing Ant Colony System (RACS)) [3]:

- Let h - the number of ants. It needed randomly put h ants into vertices.
- In each iteration $(t + 1)$ every ant should be moved into another unvisited vertex and update parameters, which characterize the solution.

- Let $\tau_{ij}(t)$ is a trail intensity of e_{ij} at t time. Ant moved to the next vertex based on trail intensity and visibility of next vertex, calculates as $\eta_{ij} = \frac{1}{c_{ij}}$.
- It should be note, that trail intensity reduced each time (the process called as evaporation). It is needed for stopping unbounded increasing of trial intensity. Let $p \in [0,1]$ be an evaporation rate.
- The selection of next vertex based on probability function:

$$p_{iu}^{k}(t) = \frac{\tau_{iu}(t)(\eta_{iu}(t))^{b}}{\sum_{o \in J_i^k} \tau_{io}(t)(\eta_{io}(t))^{b}}$$

where b – importance of edge weight in ant choice,

$p_{iu}^{k}(t)$ – is a probability for choosing next vertex $u \in V_k$,

J_i^k – is unvisited vertices for v_i by ant k.

- Let q be a randomly chosen number from 0 to 1, and q_0 is the rate of acceptance (temperature level). If $q > q_0$ we choose vertex u, defined in previous stem, otherwise vertex should be chosen in following way:

$$j = argmin\left(\tau_{iu}(t)\left(\eta_{iu}(t)\right)^{b}\right), u \in J_i^k$$

TABLE I. RESULTS OF ACO TESTING

Name	Length	Optimal	Error rate	Name	Length	Optimal	Error rate	Name	Length	Optimal	Error rate
3burma14	1805	1805	0%	20rat99	587	497	18%	56a280	1395	1079	29%
4br17	31	31	0%	20rd100	4064	3650	11%	60pr299	31548	22615	40%
4gr17	1309	1309	0%	21eil101	273	249	10%	64lin318	27856	20765	34%
4ulysses16	4539	4539	0%	21lin105	8687	8213	6%	65rbg323	777	471	65%
5gr21	1765	1740	1%	22pr107	28868	27898	3%	72rbg358	985	693	42%
5gr24	353	334	6%	24gr120	3247	2769	17%	80rd400	8971	6361	41%
5ulysses22	5308	5307	0%	25pr124	41094	36605	12%	81rbg403	1460	1170	25%
6bayg29	757	707	7%	26bier127	86674	72418	20%	84fl417	12362	9651	28%
6bays29	827	822	1%	26ch130	3375	2828	19%	87gr431	133414	101946	31%
6fri26	518	481	8%	28gr137	44035	36417	21%	88pr439	75711	60099	26%
7ftv33	476	476	0%	28pr136	50651	42570	19%	89pcb442	30405	21657	40%
8ftv36	525	525	0%	29pr144	51339	45886	12%	89rbg443	1065	632	69%
8ftv38	538	511	5%	30ch150	3282	2750	19%	99d493	27488	20023	37%
9dantzig42	432	417	4%	30kroA150	13343	11018	21%	107ali535	178369	128639	39%
10att48	5645	5394	5%	30kroB150	16521	12196	35%	107att532	18612	13464	38%
10gr48	1924	1834	5%	31pr152	59826	51576	16%	107si535	18461	13502	37%
10hk48	6800	6386	6%	32u159	31938	22664	41%	113pa561	1489	1038	43%
11berlin52	4221	4040	4%	35si175	6832	5564	23%	115rat575	3287	2388	38%
11eil51	197	174	13%	39rat195	1061	854	24%	115u574	24324	16687	46%
12brazil58	16644	15332	9%	40d198	13479	10557	28%	131p654	33975	27428	24%
14st70	334	316	6%	40kroa200	18369	13406	37%	132d657	30933	22498	37%
16eil76	232	209	11%	40krob200	17391	13111	33%	134gr666	206406	163028	27%
16pr76	69540	64925	7%	41gr202	31809	23301	37%	145u724	22852	17272	32%
20gr96	33544	29440	14%	45ts225	78855	68340	15%	157rat783	4594	3262	41%
20kroA100	11238	9711	16%	45tsp225	2288	1612	42%	200dsj1000	12668019	9187884	38%
20kroB100	11529	10328	12%	46gr229	92661	71972	29%	201pr1002	162079	114311	42%
20kroC100	11283	9554	18%	46pr226	86880	64007	36%	207si1032	25100	22306	13%
20kroD100	10917	9450	16%	53gil262	1490	1013	47%	212u1060	150344	106007	42%
20kroE100	10759	9523	13%	53pr264	38080	29549	29%	217vm1084	182367	130704	40%

- After choosing the vertex the pheromone intensity trail should be updated $\tau_{ij}(t+1) = (1-p)\tau_{ij}(t) + \frac{p}{nL}$, where L – current best tour.
- After iteration the pheromone should be updated $\tau_{ij}(t+1) = (1-p)\tau_{ij}(t) + p\Delta\tau_{ij}(t)$.

After working of algorithm, we find sub-optimal solution L

Local Search Improvement Algortihms

The ants can find non-optimal solution and methods of local search can be applied for improving solution after using ACO.

The following local search procedure can be applied:

- *2-opt heuristic*. In current tour g, two edges between vertices v_i, v_j and v_k, v_l should be removed and connected in another way. If obtained tour has lowest length, then g is changed. It is repeated for all pair of vertices.
- *3-opt heuristic*. The heuristic is similar to 2-opt, but in 3-opt three edges should be removed, and vertices should be reconnected and if possible, for g tour more optimal solution should be assigned.
- *tabu-search heuristic*. It this method the neighborhood solution is used and check for optimality (if length is lower).
- *Lin-Kernighan heuristic*. It is a complex heuristic, which can be implemented by Keld Helsgaun [4].
- *In future another local search improvement heuristics can be added.*

IV. Plans for Experiments

Experiments consists of two steps:

- Testing ACO algorithms with different parameters b, p, q_0, k.
- Testing ACO with local search improvement heuristics.

The b, p, q_0, k firstly will be chosen in empirical way, after testing the results we be analyzed and method for improving and fine tune parameters will be chosen.

For testing ACO with local search improvement algorithms for each test the ACO will be applied and after that each local search algorithm will be done.

Each test should be done 10 times and we write the resulting solution and its length, considering the deviation from the optimal result:

$$e(L) = \frac{L - L_0}{L_0}$$

where L is current obtained length and L_0 is know best solution.

For testing the GTSPLib by D. Karapetyan [16] will be used.

The code of algorithms is written on C#.

V. Current Results

In Table I the results of ACO algorithm are presented. For testing the parameters $b = 1, p = 1, q_o = 1$ were used. It can be seen that the average.

The next step find the dependence between parameters and results and then find the best parameters.

VI. Conclusion

In research in progress the methods and plans for future research are presented. The methods are described, and the experiments are written.

In plan, find the optimal fine tuning of parameters for ACO and using them for testing ACO with local search heuristic.

References

[1] C. M. Pintea, P. C. Pop и C. Chira, «The generalized traveling salesman problem solved with ant algorithms» *Journal of Universal Computer Science,* #13, № 7, pp. 1065-1075, 2007.

[2] Y. N. Lien, E. Ma и B. W. S. Wah, «Transformation of the Generalized Traveling-Salesman Problem into the Standard Traveling-Salesman Problem» *Information Sciences,* T. 1/274 (1-2), pp. 177-189, 1993.

[3] J. I. Brezina и Z. Čičková, «Solving the travelling salesman problem using the ant colony optimization» *Management Information Systems,* т. 6, № 4, pp. 10-14, 2011.

[4] K. Helsgaun, «An extension of the Lin-Kernighan-Helsgaun TSP solver for constrained traveling salesman and vehicle routing problems» *Technical Report, Roskilde University,* 2017.

[5] D. Karapetyan, «GTSP Instances Library». Available: http://www.cs.nott.ac.uk/~pszdk/gtsp.html.

УДК 004.75

ADMINISTRATION OF VIRTUAL DATA PROCESSING CENTER OVER OPENFLOW

V. M. Solovyev[1], A. S. Belousov[2]

[1]Soloviev Vladimir Mikhailovich, Ph.D. in Technical Sciences, assistant professor of the department of mathematical cybernetics and computer science, head of Centre of New Information Technologies in Volga Region, Saratov State University, svm@sgu.ru.
[2]Belousov Aleksandr Aleksandrovich, Bachelor in Informatics and Computer Engineering, student of the Master's Degree in Applied Mathematics and Computer Science at the Saratov State University for the faculty of Computer Science and Information Technologi, tortyt1@gmail.com.

Abstract: This paper researches the building principles and administration of virtual data processing centers based on hyper-converged systems over OpenFlow. We provide the implementation features of these virtual centers on the basis of software-defined networking that is managed by a dedicated controller (server). We suggest the graph administration model of hyper-converged system resources compliant with required performance on one level and economic requirements on another level. Based on the proposed model, the implementation variation of greedy control algorithm of virtual data processing center over OpenFlow was examined. This algorithm assigns the requests to physical resources by using of dedicated server software. The advantages of such hyper-converged system model on performance issues were outlined, e.g., multi-threaded routing and security, elimination of the most current threats. We summarize the possibilities of transition to network infrastructure in these virtual data processing centers. Such infrastructure is focused on data and using of blockchain technology providing high reliability and content protection.

Key words: Converged Infrastructure (CI), Hyper-converged Infrastructure (HCI), Software Defined Networks (SDN), OpenFlow, Virtual Data Center (VDC), Service Level Agreement (SLA), Multi-Threaded Routing (MRT), Quality of Service (QoS), Data Oriented Network Architecture (DONA), Blockchain.

Virtual data processing center (VDPC) refers to hyper-converged infrastructure (HCI) that allows us to create virtual machines, data warehouses, switchers and routers, and communication channels. The main task of VDPC is to accept a client connection (tenant[1]) and update it with the help of virtualization technology in network topology. The basis of the mechanism of VDPC resources administration refers to a model extended for HCI tasks [1]. The network topology in this model is represented by graph $T = (C \cup M \cup K \cup L)$, C is a plurality of computing nodes, M is a plurality of data warehouses, K is a plurality of switching elements, L is a plurality of communication channels. Each of plurality has its own vectors of scalar argument defined. This argument sets up the parameters: of computing

[1]A tenant represents the requests for virtual machines, data warehouses, switchers, routers, communication channels, and all virtual communication channels.

nodes - $c \in C$, of data (memory) warehouses - $m \in M$, of crosspoints - $k \in K$ and of communication channels respectively - $l \in L$.

$$\begin{aligned} &fct(c) = (ct_1(c), ct_2(c), \ldots, ct_n(c)), \\ &fmt(m) = (mt_1(m), mt_2(m), ..., mt_n(m)), \\ &fkt(k) = (kt_1(k), kt_2(k), ..., fk_n(k)), \\ &flt(l) = (lt_1(l), lt_2(l), ..., lt_n(l)). \end{aligned} \tag{1}$$

In this model VDPC resources are specified by graph $R = (V \cup S \cup D)$,V is a plurality of applications deployed in virtual machines, S is a plurality of virtual data warehouses, D is a plurality of communication channels between virtual machines and data warehouses. Each of plurality has its own vectors of scalar argument defined. This argument sets up the parameters: of virtual machines - $v \in V$, virtual data warehouses - $s \in S$, communication channels including switching elements that provide required service level agreement (SLA[2]) - $d \in D$ respectively:

$$\begin{aligned} &fvr(v) = (vr_1(v), vr_2(v), ..., vr_n(v)), \\ &fsr(s) = (sr_1(s), sr_2(s), ..., sr_n(s)), \\ &fdr(d) = (dr_1(d), dr_2(d), ..., dr_n(d)). \end{aligned} \tag{2}$$

The parameters (2) providing SLA coincide with corresponding parameters (1) and are represented by mapping of resource requests to HCI topology:

$$O : R \to T \cup \{\oslash\} = \{V \to C \cup \{\oslash\}, S \to M \cup \{\oslash\}, D \to K \cup \{\oslash\}, L\{\oslash\}\}. \tag{3}$$

Resource requests from the expression (3) determine three relationship types between request parameters r_i and physical resources t_i, based on HCI topology:

- the requested resources correspond to resources identified by topology $r_i = t_i$,
- overload of physical resources $r_i > t_i$ that violates SLA,
- underload of physical resources $r_i < t_i$ that requires a topology reconfiguration for economic reasons.

In the last case available resources can be represented by residual graph $T_{res} = (\mathrm{C} \cup M \cup K \cup L)$ that redefines the parameters as follows:

$$\begin{aligned} &fct_{res}(c) = fct(c) - \sum_{v \in V} fvr(v), fmt_{res}(m) = fmt(m) - \sum_{s \in S} fsr(s), \\ &fkt_{res}(k) = fkt(k) - \sum_{d \in D} fdr(d), flt_{res}(l) = flt(l) - \sum_{l \in L} fdr(d). \end{aligned} \tag{4}$$

Automatic migration of HCI structures managed by controllers over OpenFlow enables us to meet both SLA and economic requirements. Migration is carried out even if it is not possible to assign the warehouse on demand, and data is added to multiple warehouses. In that case, one part of the applications can work with data warehouse, meanwhile the other part can work with data located in another physical storage. In accordance with migration plan, virtual structure relocation should comply with the following requirements:

[2]SLA (Service Level Agreement) represents a commitment about level of provided network services. This formal contract between a service provider and a client sets out agreed service quality, service description and rights of the parties. Such agreement serves as an assessment tool for quality of provided network services.

- there is no SLA violation during relocation;

- relocation is implemented at given time constraints. Automatic operation of controllers enables us to achieve it.

Input to migration is a plurality of incoming requests $Z = \{R_i\}$, a plurality of queried requests $W = \{R_i\}$, a graph of remaining resources T_{res}, and time constraint on migration τ. During migration, a new node s' and a virtual communication channel between nodes s and s' are added to graph of re quested resources R.

The administration of VDPC over OpenFlow is based on a greedy algorithm[3] of request assignment to physical resources, with the use of controller (server) software. Expression (4) describes such a greedy algorithm. As an optimization criterion, the most compact allocation of request elements (2) is applied. A similar approach is widely used in data processing centers and by cloud providers [2, 3]. The quality of VDPC administration depends on selected greedy criteria: next request - K_R, virtual node - K_V, physical node - K_C. Criteria K_V and K_C rely on cost function defined as a weighted sum of required parameters considering the resource deficit. This function represents as follows: $d(i) = (\sum_R \sum_{e \in R} r_{r,i} - \sum_{c \in C} r_{c,i}) / \sum_R \sum_{e \in R} r_{e,i}$. Then the cost function of an assignment of element e will appear as $r(e) = \sum_{i=l}^{n} d(i) r_{e,i}$. In this equation the selected element HCI is characterized by a vector of values of required resource parameters $(r_{e,1}, r_{e,2}, \ldots, r_{e,n})$. To calculate the measure of the resource deficit, firstly, it is necessary to subtract the values of available physical resources for the required resource parameter from the common value of this resource parameter in all requests. Then the measure is calculated as a quotient of this difference by total sum of required resources. We can define the cost function as weighted sum of required resource parameters considering the resource deficit. According to criterion K_V, the HCI virtual element with maximum cost function is chosen. This allows us to assign primarily the most resource-deficient elements and then assign all the other virtual elements. According to criterion K_{C}, the HCI physical element with minimum cost function is chosen. By this, we can ensure maximal utilization (loading) of computing resources. According to criterion K_{C}, the query with the maximum weighted sum of requested resources is chosen.

The general framework of administration algorithm will be as follows.

1. Scheduler[4] analyses incoming requests of resources $Z = \{R_i\}$.

2. If plurality $\{R_i\} \notin \oslash$ is not empty, the program selects another request R_i according to greedy criterion K_R. Otherwise, algorithm terminates its functioning.

3. Using the elements of request R_i, the program forms a plurality of virtual nodes $U = \{V \cup S\}$. Where it is not possible to form a plurality of virtual nodes U, it proceeds to step 14.

4. Scheduler selects another element N from formed plurality of virtual nodes U on the basis of greedy criterion K_V. Then this element is placed in queue Q which contains the elements awaiting an assignment.

[3]The greedy algorithm means optimization algorithm based on locally optimal decision that are made at each stage. Whereby, we assume that the final decision will also prove optimal.

[4]Scheduler is a program (service) driven by controller software. The principal scheduler function is to start other programs.

5. Using the elements C_i, scheduler forms a plurality of physical nodes $\{C_i\} \notin \oslash$. It is possible to assign the element N to these nodes based on correct accomplishment of mapping (3). Otherwise, if $\{C_i\} \in \oslash$, program calls the procedure of limited enumeration.

6. The program selects a physical resource from the formed plurality of physical nodes on the basis of greedy criterion K_C. It redefines the values of physical resources parameters according to functions (4).

7. Scheduler selects all virtual channels D_i that link element N to elements of request R_i to be assigned.

8. Scheduler sorts a plurality of channels $\{D_i\} \notin \oslash$ by value of the capacity in ascending order.

9. The program selects a virtual channel L_i from a plurality of channels $\{D_i\}$. It should ensure the shortest route that links element N to elements of request R_i. Where it is not possible to plot the route, it calls the procedure of virtual channel assignment on a physical resource. It redefines the values of physical resources according to functions (4).

10. Scheduler adds to queue Q the virtual nodes linked with N. By this, it follows the order of virtual channels from sorted plurality $\{D_i\}$. These channels connect the nodes.

11. Scheduler deletes N from U and Q.

12. If Q is not empty, program proceeds to step 4.

13. If U is not empty, program proceeds to step 3. Otherwise, if U is empty, program proceeds to step 1.

14. The program cancels all assignments of the elements of request R_i and removes the request from a plurality $Z = \{R_i\}$. Then it proceeds to step 2.

This algorithm contains two procedures described in [2]. The first one is a procedure of limited enumeration; the second one refers to a procedure of virtual channel assignment on a physical resource. A scheduler calls the procedure of limited enumeration if it is not possible to assign the next virtual node N from a plurality of requests to any physical resource. This procedure analyses a subset of a plurality of physical nodes $\{C_i\}$ from a graph of physical resources. Specified enumeration depth determines the subset capacity; the quantity of viewed subsets is limited. The program views only subsets whose total quantity of nodes' remaining resources allows us to assign the current element N. The procedure ensures the execution of step 5 if the program changes (selects) the enumeration depth and quantity of viewed subsets. Scheduler calls the procedure of virtual channel assignment on a physical resource when it is not possible to plot the route that links element N to element of request R_i via virtual channel. The route searching mechanism is based on modified Dijkstra's algorithm [4]. However, it can include only switching elements and communication channels of physical network to which ratios of mapping accuracy are applied (3). If it is not possible to assign a virtual

channel that connects the storage element, the storage search is accomplished. This storage should have the resources to create storage element replication. The replication requires the quantity of resources equivalent to quantity of storage element resources. All storages selected for replication creation are considered in increasing order of total route length. Furthermore, the possibility of creation of communication channel l for replication is considered. This channel provides capacity and required data-flow intensity. If the communication channel l can not provide the required parameters, program considers another variation of replication mapping. The result is the route that provides coherence between element N and replication. The parameter variations of route and communication channel provide favorable result. The same approach to virtual machines has been widely recognized and studied [5].

Analyzed HCI control algorithm over OpenFlow enables us to plan the computing resources, resources of data storage and network resources of self-organizing cloud platform (VDPC), by using of SDN technological solutions. This algorithm mechanism also complies with SLA. The algorithm allows us to use physical resources rationally by eliminating their segmentation, with the help of virtual resources migration. The algorithm enables us to administrate the hyper-converged system by specifying the data flows routing policies. Whereby, it uses the virtual network control functions of virtual and physical devices from different manufacturers. We refer to devices that support OpenFlow protocol. The proposed solution allows us to integrate different networks administrated over OpenFlow and transfer data flows between them effectively, by means of multi-threaded routing (MRT).

We can consider hyper-converged systems as applied to any computing platforms (e.g., hard, programming, cloud, neuromorphic, quantum) which provide user access to various services. These systems should be user-friendly and support multiple infrastructure layers, surely including layers of safety, reliability, communication services providing QoS for various data. Furthermore, the network behind HCI should have the opportunities to work with different types of terminals (mobile, desktop, active network, advanced UX/UI[5] etc.). This network also should have single management platform (controller, server) for the full package of services, applications, hardware, and data transfer channels. Whereby, it should select data transfer channel in real time based on QoS and applications needs for capacity and nature of traffic. Convergent technologies are not the endpoint in evolution of the next-generation computing systems. These technologies already allow us to take a content-centric approach onto prevalidated HCI infrastructure. They enable us to create computing systems that leapfrog over end-to-end paradigm toward content or data addressing paradigm (Information Centric Networking, or ICN). This paradigm implies data organization, regardless of location (server, host), through distributed network caching. Expected benefits of this approach include more efficient use of expensive network resources, scalability of computing systems and their adaptability to volatile QoS. The paradigm is based on the primitives *publish/subscribe*, that is to publish the content (make it available) and declare about it. These primitives are realized in Data Oriented Network Architecture (DONA). It works as follows: the element of such system receives a request from a similar element or host. Whereby, two scenarios are possible. If the element contains required data in cash, it will implement the request. If the DONA element does not contain the content, it will request similar elements which have data. When it gets a response, it caches the content and

[5]UX/UI (User Experience/User Interface) refers to interface design that meets current requirements

implements the request. This universal mechanism is applicable to any protocol, forming a global single mechanism of caching and content delivery. In addition, this mechanism is supported by all network nodes and aimed at all users, not just ICN users. Such a network ensures content security, not security of its delivery. It relies on a content-based model and draws on the concept of reputation, because the provider must sign the content, so users can always define it. Data Oriented Network Architecture interacts well with blockchain[6] technology that provides the high reliability of content storage and protection. Network entry is protected cryptographically. Unauthorized entry requires enormous computing resources proportional to the network size. It allows us to exclude human or machine error, missed operations, unauthorized entry etc. In future, over the course of evolution, HCI will employ other network technologies.

References

1. *By Charles Clos.* A Study of Non-Blocking Switching Networks (Manuscript received October 30, 1952). Accessed July 4, 2017, available at http://ieeexplore.ieee.org/stamp/stamp.jsp?arnumber=6770468.
2. *Zotov I. A., Kostenko V. A.* Resource Allocation Algorithm in Data Centers with a Unified Scheduler for Different Types of Resources, // Izvestiya Akademii Nauk. Teoriya i Sistemi Upravleniya, 2015, № 1, pp. 61-71.
3. *Meng Xiaoqiao, Pappas Vasileios, Zhang Li.* Improving the Scalability of Data Center Networks with Traffic-aware Virtual Machine Placement // IBM T.J. Watson Research Center 19 Skyline Drive, Hawthorne, NY 10532. Accessed July 4, 2017, available at http://ieeexplore.ieee.org/stamp/stamp.jsp?arnumber=5461930.
4. *Cormen T. H., Leiserson C. E., Rivest R. L., Stein C.* Introduction to Algorithms. Cambridge MA: MIT Press and McGrawHill, 2001. pp. 595–601.
5. *Zhao Ming, Figueiredo Renato J.* Experimental Study of Virtual Machine Migration in Support of Reservation of Cluster Resources // Advanced Computing and Information Systems Laboratory (ACIS) Electrical and Computer Engineering, University of Florida. Accessed July 4, 2017, available at http://ieeexplore.ieee.org/stamp/stamp.jsp?arnumber=5483380.

[6]The revolutionary technology of blockchain was created by Satoshi Nakamoto. This technology helps to allocate the digital content without its copying. Pertinently, it resembles a digital book whose data and their modifications are duplicated in network for several thousands of times and are regularly updated. This distributed database without central storage node is stored in network. It provides its users the hosting, such as Google Docs during collective work. Each group of blockchain transactions is a block, and miners conduct the audit of them (digital content). Therefore, this technology operates with chain of blocks created by complex cryptographic algorithms.

A Survey of Smart Contract Safety and Programming Languages

Alexey Tyurin*, Ivan Tyulyandin†, Vladimir Maltsev‡, Iakov Kirilenko¶ and Daniil Berezun‖
Mathematics and Mechanics Faculty
Saint Petersburg State University
University Embankment, 7, 199034
Saint Petersburg, Russia
*a.tyurin@2016.spbu.ru, †i.tyulyandin@2015.spbu.ru, ‡v.maltsev@2016.spbu.ru,
¶y.kirilenko@spbu.ru, ‖danya.berezun@gmail.com

***Abstract*—Blockchain technologies are gradually being found an application in many areas, especially in *FinTech*. As a result, a lot of blockchain platforms have emerged with the support of smart contracts that are intended to automate party interactions. However, it has been shown that they are prone to attacks and errors which lead to money loss. To date, there has been a wide range of approaches for making smart contracts safer that included analysis tools, reasoning models, and safer and more rigorous programming languages.**

In this paper, we provide an overview of smart contract programming languages design principles, related vulnerabilities, and future research areas. The provided overview is meant to outline the to date state of languages and to become a possible basis for future proceedings.

I. Introduction

Initially, blockchains were designed for cryptocurrency management based on transactions. Further such systems involved *smart contracts* usage to enhance transactions, making them more sophisticated. This enabled to move part of an application logic into the blockchain, thus allowing to provide customizable redeeming conditions [1], develop crowdfunding systems [2], and other applications based on blockchain technology [3]. Fundamentally smart contracts are programmable objects beyond blockchain, intended to represent *automatable*[1] and *enforceable*[2] agreements [4].

Since smart contracts are essentially programs that are executed within blockchain and written in some programming language, bugs and errors are possible. Erroneous transaction behavior can lead to a financial damage. For example, a not-reentrancy of a function has caused $40 million loss [5]. Moreover, due to the immutable nature of the blockchain, it is often impossible to fix a contract with a bad[3] behavior that is already on the chain, i.e. contracts are irrevocably committed. One possible approach to detect such unwanted behaviors and minimize the number of vulnerabilities is to provide a way to formalize smart contracts properties and vulnerabilities. It will help to specify vulnerabilities sources and facilitate reasoning about smart contracts.

In [6] provided by IOHK research[4], an ontology that provides a set of basic conceptual primitives is specified. It can be used to construct desired propositions about smart contracts. It is not intended to be the only true ontology, rather the useful one. According to the ontology, blockchain based smart contracts can be considered as computations over blockchain state, that include the changing over time state itself as well as a transition function. And we will further refer to *modality* properties as to relationships between states, possibility or necessity properties that should be maintained throughout transitions.

These concepts allow thinking about smart contract behavior abstractedly over details. For example, consider a *Deadline-dependent Transfer*, a smart contract controlling property transfer between recipients[5]. Only *Recipient 1* may transfer the *Item* during some time interval prior to the deadline, while only *Recipient 2* may transfer the *Item* once deadline has been passed. A *modality* property can be formulated in the following way. There always should be a blockchain state where at least one system participant who controls the *Item*, being transferred, exists, i.e. the absence of dead states in the blockchain.

Unfulfillment of those properties in blockchain based smart contracts may lead to money loss and malicious attacks. For example, a vulnerable sequence of smart contract library calls in Parity wallet led to $150 million freezes on wallets [7].

State inconsistency and weaknesses may be caused by a number of different reasons such as blockchain-specific behavior, execution environment bugs, a model of underlying programming language that is not amenable to proof constructions, non-intuitive representation of programs in languages with good models, unintuitive semantics of underlying programming language for people who lack programming experience etc [8]. Also, some modality properties may never be proved because of possible non-termination of a program, which basically depends on a certain programming language.

[1] "Automatable" rather than "automated" since parts of an agreement may require some human input.

[2] Enforceable either by law or by tamper-proof computer code.

[3] Here, by a "bad" contract behavior, we mean any behavior that is unexpected or undesirable by the contract owner, caused by any reason.

[4] IOHK company is one of the main customers of research in peer-to-peer networks. See https://iohk.io/about/ for details.

[5] Between users or other smart contracts

Thereby, to make smart contracts secure it is desirable to be able to specify the intended behavior and properties that they should fulfill. These properties fulfillment can be provided with machine-checkable proofs and facilitated with more intuitive programming languages accompanied by tools for static analysis and formal verification to reduce the number of errors.

To date, various approaches, languages, and tools have been proposed: extensive type systems and various programming paradigms [9], programming languages that have easily checked termination conditions [10, 11], high-level languages that encourages safer programming via abstractions [12, 13], and intermediate and low-level languages that ease formal verification and compilers development [14–16].

Smart contract programming languages design is influenced by domain ontology, encountered vulnerabilities and ease of reasoning about modality properties. So, in this paper, we concentrate on the incorporation of known approaches used in design and development of smart contracts programming languages, proceed through vulnerabilities and domain specific concepts that have been considered during design process, provide a classification of current efforts, and emphasize topics for future research.

The paper is organized as follows. Section II provides a short evaluation of similar works. Section III gives a brief summary of blockchain architecture principles relevant to languages and tools design. Section IV describes known vulnerabilities of smart contracts, classifying them for future analysis. Section V provides a survey of smart contract programming languages and their design ideas and principles, according to known vulnerabilities and blockchain architectures. In section VI we discuss possible research gaps and future work. Section VII concludes the paper.

II. Related work

Surely this paper is not the only one surveying smart contract programming languages, and we are aware of a couple of similar works.

So, [17] provides an overview of smart contracts programming languages, security properties, and verification methods along with some classification of them. However, despite a good coverage, the proposed survey is rather superficial in a sense that it describes languages through specification of their features, not going deep into design foundations that have provided the features.

Another work [18] gives an overview of some distributed ledger systems, smart contracts languages, and technologies that might facilitate safety and performance, or make new applications possible. The paper is not aimed entirely at languages, hence it leaves the description without design foundations and any classification according to whether desirable properties or design principles.

[15] also contains some overview of existing languages and their features, but the survey is performed from the perspective of comparison between them and the language proposed in the paper.

In contrast, this work is intended to enhance language coverage, provide foundations and intuition for reasoning, classification of languages, properties, and design fundamentals along with vulnerabilities that have influenced them.

III. Background

Since smart contracts are computations on a blockchain, underlying blockchain protocol basically sets the path for language and tools design. In this section, we review a few protocol details that influence further development of languages. Substantially there are two widespread blockchain architectures on top of which smart contracts are built to date — *UTxO-based* and *account-based* blockchains, that allow stateless and stateful smart contracts respectively.

A. UTxO

Unspent transaction output, UTxO, model was introduced with the emergence of Bitcoin blockchain. A typical Bitcoin transaction contains a list of inputs that specifies the funds that the transaction issuer can transfer and a list of outputs, that represent the way these funds are intended to be transferred. Each output can be used as an input for another transaction. For example, an issuer can set the amount of currency for each output or specify conditions, under which a possible receiver of funds can spend them, also they can specify themselves as the receivers to get so-called change. A set of UTxO consists of all transactions outputs that have not been yet used as inputs.

Redeeming conditions for transaction outputs in Bitcoin are defined with programs written in Bitcoin Script [10]. These programs describe properties that must be satisfied for the redeemer to be able to use these transaction outputs as their transaction inputs in order to spend the credits. The spender should provide input values to each locking script of referenced outputs of previous transaction such that all scripts evaluate to `true`, e.g. they may provide their wallet address and transaction signature to verify authority.

Such scripts are stored within transactions and are being maintained only during a transaction, thus they have no state. Further scripts have limited access to blockchain data and essentially they are pure stateless functions of transaction data, i.e. of input parameters. Despite limitations, scripts along with transaction signatures can express complex redeeming conditions such as *multi-signature* payments, deposit providing, escrow, and dispute mediation, access to external data using oracles, time-locks, payment channels, cross-chain atomic trades etc [19]. Throughout the paper, we regard these scripts as stateless smart contracts.

B. Account-based blockchains

Account-based blockchains maintain an explicit state throughout transactions. A *state* is a mapping between account addresses and balances. Within these blockchain systems, each transaction is a mapping between the states. Basically, these systems are transaction-based state machines.

ETHEREUM is an example of such a system [20]. In ETHEREUM smart contracts are similar to users' accounts in a sense that they have their own address and a balance. Smart contracts are stored inside the blockchain and essentially these contracts are lists of functions that can be invoked through users' transactions or other contracts messaging. These functions are defined with bytecode of the corresponding execution environment called *Ethereum Virtual Machine*, EVM. Since any smart contract has a balance, it is a stateful function of a data transaction (or a message) and blockchain state, in which the transaction takes place, so they can write to blockchain state or read from it. Contracts state typically involves a stored amount of currency. However, in general, it can have arbitrary persistent storage that is maintained throughout the transitions of the blockchain.

C. Preventing the Denial-of-service attacks (DOS)

Despite the underlying blockchain model, smart contracts are computations that are replicated over blockchain via consensus protocol. To prevent DOS-attacks the number of computations for every program representing a smart contract should be restricted beforehand. Restriction mechanism depends on the underlying programming languages properties. One of the main properties in the context of smart contracts is halting, i.e. whether every program that has been written in it terminates or not. BITCOIN SCRIPT program always terminates since language is not Turing-complete and it does not have loops, or recursion, or any other mechanism that provides infinite computations. However, the size of a program also affects the performance of the system behind it. Thus BITCOIN SCRIPT programs are limited by the stack size and number of computationally heavy instructions, i.e. transactions that contain a script that does not satisfy restrictions are rejected.

For programs written in languages that do not guarantee program termination, e.g. EVM bytecode, program execution is limited via a gas system. *Gas* is basically an amount of cryptocurrency specified for contract execution. Fixed units of gas are charged to a miner for every instruction being executed. If the specified amount of gas is expired, execution of the contract stops. Furthermore, EVM contracts also have a limited stack size.

IV. SMART CONTRACT WEAKNESS

In this section, programming language-level vulnerabilities that may cause unfulfillment of modality properties and possible mistakes are classified. It is worth to notice, that the most common property arising in distributed systems is that results of computations should be deterministic. While many smart contract programming languages have been designed with determinism in mind, sometimes general purpose programming languages are used for development [21]. A detailed overview of potential risks of non-determinism and causes can be found in [22].

We consider SOLIDITY language for stateful contracts, since it is the most popular smart contract programming languages and generally it was one of the first languages that revealed such weaknesses, unfortunately on its own instance. Despite originally being known as unsafe, the language is evolving and to date its compiler is able to warn about code that might misbehave. However, Solidity has provided the foundation for the design of other languages. The most famous errors that have caused contracts failure are DAO [5] and PARITY [23].

SOLIDITY vulnerabilities are classified in the following subsections based on what level they occur on and the reasons that cause them. Code examples of the weaknesses could be found in [20, 24–28]. Possible attacks are discussed in [29]. Also, it is worth to mention, that SOLIDITY is a Turing-complete language, meaning that in general fulfillment of particular modality properties can not be proved, even despite guaranteed termination due to gas limit.

A. Block content manipulation

Block of transactions in blockchains is formed by one of the participants who have the ability to influence block content. Thus, careless blocks handling may cause a number of errors.

Front-Running (Transaction-ordering dependence): It is important to be careful of transactions order. For example, Alice has deployed contract with possibility to sell a product and set a price for it. Bob wants to buy the product, and Alice wants to set a higher price. Let's assume, they want to do it at the same time. If Bob's request is the first, Alice loses money. In another case, Bob's transaction can be rejected, or Bob will spend more money than he expected.

Weak sources of randomness: Random values should be deterministic for all nodes in the network due to consensus considerations. One way to get randomness is to use pseudo-random values. Variables of contract, even the private ones, meta-variables of a block, or a hash of a previous and next block cannot be used as a source of entropy. In some blockchains (including ETHEREUM) it is possible to have influence over these variables during the validation process. A pseudo-random value in smart contract code can be predicted by a malefactor. Precalculation can be done via code analysis.

B. Contract interaction

A smart contract should be able to interact with other contracts. The following vulnerabilities appear due to the fact that smart contracts cannot rely on of each other's behavior.

Unchecked return values for low-level calls: There are three functions to send ether [30] from account to account in ETHEREUM: `send()` and `call()` that return `false` if an error occurs but the transaction execution continues, and `transfer()` that rolls back the transaction in case of error. Low-level functions `callcode()` and `delegatecall()` behave in the same way as functions `send()` and `call()`. Thus handling of `false` value of corresponding functions is needed to avoid undesirable behavior of contract. According to Luu et al. [31], 27.9% of smart contracts in ETHEREUM blockchain do not check returned values.

Reentrancy: An external contract can call back functions of a caller contract before the first invocation has finished. It can lead to undesirable recursive function interactions and allow the callee contract to take over the control flow. The example of this vulnerability is a famous DAO smart contract [5].

Callstack bound: A failure may occur when an external call is made, but the program stack has reached its limit. Stack overflow is possible in smart contract languages. In EVM call stack is limited to 1024 stack frames. If the exception is not properly handled by a contract, the malefactor can use it to attack.

C. Resource limits

If the smart contract language is Turing-complete, there is a need in metering[6] mechanism to prevent infinite execution. ETHEREUM charges a fee, named *gas*. Amount of gas is proportional to the number of executed commands by EVM. Every transaction in bounded with maximum amount of gas as well as blocks.

Infinite loops: Mistakes and misprints in operators usage may keep contracts syntactically correct but strongly affect their logic. For example, writing =+ instead of += in a loop terminating condition may lead to unexpected program behavior and even to an infinite loop. Moreover, in this case, excessive gas consumption may occur. It also includes situations when the number of memory addresses being used are significantly increase, e.g. when the number of elements in a map grows, it becomes too expensive to iterate over it.

D. Arithmetics

In SOLIDITY arithmetics is available on unsigned integers only and the language does not provide any arithmetic operations check for correctness. This class of mistakes mostly refers to common programmer errors. In the case of smart contracts, they may lead to a huge loss of assets. Thus, it is common to consider them as vulnerabilities in order to attract programmers attention.

Overflow and underflow: These vulnerabilities arise because numbers can have a fixed size. In case of ETHEREUM, maximum value for `uint(uint256)` is $2^{256} - 1$ and minimum — 0. A programmer has to manually checks overflow and underflow.

Floating points and precision: SOLIDITY does not have fixed and floating point types. Instead, a programmer has to emulate them via integers. All integer divisions are rounded down. Careless handling of such operations may cause unexpected program behavior.

E. Storage access

The following vulnerabilities are caused by negligent memory usage and access.

Uninitialized storage pointer: Local structures, arrays, and maps link to storage zero address by default. Using of these object without initialization will lead to overwriting whatever is in zero address.

[6]Metering is a way to limit and charge the execution of a smart contract.

Write to an arbitrary storage location: A smart contract can store some data and wrong variable assignment can break it. SOLIDITY has reference types. Mistake with references can lead to internal state corruption. If an array index is out of range, the exception will be thrown, and the smart contract will be reverted.

F. Internal control flow

This class of vulnerabilities is caused by a complex control flow graph structure and an ability to manipulate it.

Using of inherited functions and variables: It is possible to use inheritance in smart-contracts languages with the object-oriented paradigm. SOLIDITY allows multiple inheritance. If several super-classes have a method or variable with the same name, their behavior in sub-class depends on the inheritance order. It could shadow previously defined values or functions and lead to undesirable results.

Using of built-in functions: Programmers should be aware of using built-in functions and their behavior. E.g., someone would like to use assertions to check program invariant. SOLIDITY `assert()` function is intended for this purpose. In case of failure, this method throws an exception and does not return the remaining gas. Thus, to check for changing values, such as input data, it is recommended to use `require()` statement which in the same case does transaction rollback and returns remaining gas.

Using of deprecated functions: It is not clear what new compiler versions do with deprecated functions. Therefore, it is not recommended to use these objects.

Locked assets: Contracts should provide a way to manage assets. Suppose in the example the contract has a method to take assets but does not have code to give them back. Due to smart contract code immutability in blockchain history, it is impossible to upgrade or fix this contract. It will cause property loss.

G. Authorization

Authorization is a major part of a person identification mechanism, designed to verify the permission for actions. Incorrect or insufficient authorization can lead to the following vulnerabilities.

Incorrect initialization: When smart contract was deployed to a blockchain, it should be initialized. Often initialization contains sensitive operations such as a setting contract's owner. An error in this action may violate the logic of the smart contract. In SOLIDITY, the *constructor* is a special function, which is called once to set contract's state. In new SOLIDITY versions, constructors are denoted by a special keyword that made the definitions more obvious. But in earlier versions (less than 0.4.22) constructor is just a function with the same name as the class has. Thus, a typo in constructors' name makes it a usual function, which can be called by anybody since default modifier for function is *public*.

Function default visibility: Incorrect access modifiers usage or a lack of them can lead to undesirable behavior. For example, calling the function that changes the contract owner with public access modifier allows everyone to become its owner. Default modifier for SOLIDITY is `public`. Thus, it is strongly recommended to explicitly define visibility for all functions and variables.

V. SMART CONTRACT LANGUAGES

In this section, smart contract languages are considered with respect to their main features, paradigms, and common properties such as Turing-completeness, metering mechanism, reasoning, type system, code analyzers, etc. To reduce the number of subsections we have classified languages with respect to their level of usage.

Low-level languages: These languages are designed for direct execution by the underlying execution environment. Most concepts and principles of formal semantics, computational model, metering, logic for reasoning about programs, and typing are often introduced on that level. Furthermore, to date, smart contracts are mostly stored on the blockchain in low-level bytecode, which imposes suitability considerations. Examples of such languages are BITCOIN-SCRIPT [10], EVM [32], MICHELSON [33].

High-level: Languages with the idea of making the writing of contracts easier for developers via readability and safer high-level syntactic constructs enhanced by a type system that provides machine services abstractions. Safety aspect appears here and refers to the languages ability to guarantee the integrity of these abstractions and abstractions introduced by the programmer using definitional facilities of the language. In a safe language, such abstractions can be used abstractly while in an unsafe language they cannot: in order to completely understand how a program may (mis-) behave, it is necessary to keep in mind all sorts of low-level details such as the layout of data structures in memory and the order in which they will be allocated by the compiler. [34]. The semantics of both levels should be considered here[7] Examples of such languages are SOLIDITY [35], FLINT [12], and LIQUIDITY [36].

Intermediate-level: Languages that present a compromise between a high-level source and low-level target languages. As a general rule, they are designed in order to simplify program verification or static analysis, relying on the computation model, type system, reasoning, semantics, etc. Furthermore, they allow unification of compilation, i.e. providing a language that can be compiled for different platforms. SCILLA [15] is an example of such a language.

It is also useful to emphasize some desirable language properties that affect language design.

- *Reasoning* — language behavior model should allow to specify modality properties and facilitate proving of their (un-) fulfillment. Underlying calculus model and type system are aimed at this.
- *Safety* — language abstractions should hold integrity property. Rigorous semantics promotes this.
- *Expressivity* — basically language should be expressive to fit possible various range of use cases.
- *Readability* — language representation of a contract behavior should be intuitive, i.e. be easy to inspect and write with.

Every smart contract language has domain specific instructions or/and types, e.g. cryptographic primitives, assets types, messaging instructions. So we will not emphasize this aspect much. Notable features and models of several languages with respect to desirable properties are discussed below while a summary of a more expanded set of languages is presented in the table on the Fig. 1.

A. Low-level languages

1) BITCOIN SCRIPT*:* is an untyped[8] stack-based low-level language for stateless smart contracts development in BITCOIN and handles transaction verification process. It is intentionally non-Turing-complete with the restricted instruction set where some opcodes are removed e.g. multiplication, division, strings operations, bitwise logic, due to possible overflow vulnerabilities and implementation bugs. Everything is allocated on the stack of limited size words while a program has access to some transaction fields e.g. a hash of transaction data, time field. Thus every program is a pure function of transaction data, i.e. transactions are *self-contained*.

To our knowledge, BITCOIN SCRIPT has no formal semantics, which makes metering ad-hoc and does not enforce formal verification. Furthermore, its stack-based nature and bytecode make smart contracts less auditable since only bytecode is stored inside transactions. Metering is performed via expensive operators counting and script size evaluation. However script's input is arbitrary, hence BITCOIN SCRIPT allows specification of redemption properties like signature checking, pay-to-public-key-hash, pay-to-script-hash, multisignature checking, and arbitrary data storage inside transactions [1, 10, 48].

2) SIMPLICITY*:* is designed for extending BITCOIN SCRIPT capabilities. It is intended to enhance expressiveness, while enabling static analysis that allows to efficiently bound the number of computations, maintaining BITCOIN SCRIPT design of self-contained transactions, and providing formal semantic to facilitate reasoning about programs. It is anticipated to be used as a compilation target for high-level languages and deployed to *sidechains* [49]. SIMPLICITY is a typed non-Turing-complete combinator-based language with terms based on *Gentzen's sequent calculus*. Every SIMPLICITY type is finite: it contains finitely many values. Hence SIMPLICITY does not support recursive types and can express only finitary functions.

The core of SIMPLICITY consists of nine combinators for term construction with a corresponding denotational semantics. The language is formalized in COQ as well as a

[7] Fundamentally safeness spreads to other levels since low-level language is an abstraction of its implementation, e.g. a virtual machine.

[8] More precisely stack operates with byte vectors, which can be interpreted depending on opcode.

Language	Level	Current state	Project	Paradigm / influence	Analyzers	Metering	Turing-completeness	Main features
Bamboo	high-level	alpha (experimental)	Ethereum	functional	EVM bytecode analyzers[1]	gas system	yes	program behaves as a state automata
Bitcoin Script	low-level	under development	Bitcoin	stack-based, reverse-polish	no[2]	script size	no	Forth-like syntax, any program always terminates
Chaincode	high-level	stable	Hyperledger Fabric	general purpose languages	no[2]	timeout	yes	GO, NODE.JS and JAVA extensions for smart contracts
EOSIO	high-level	stable	EOS.IO	object-oriented, statically typed	no[2]	bound system[3]	yes	C++11 library
EVM bytecode	low-level	stable	Ethereum	stack-based	EVM bytecode analyzers[1]	gas system	yes	well researched
Flint	high-level	alpha	Ethereum	contract-oriented, type safe	EVM bytecode analyzers[1]	gas system	yes	Swift-like syntax, safety
IELE	low-level	prototype	Ethereum	register-based	tools generated by K [37]	gas system	yes	generated from formal specification, LLVM IR-like syntax, safety
Ivy	high-level	prototype (experimental)	Bitcoin	imperative	no[2]	gas system	no	can be compiled to Bitcoin Script
Liquidity	high-level	under development	Tezos	fully-typed, functional	under development	gas system	yes	OClaml-like syntax, compiled to Michelson according to formal semantics, safety
LLL	intermediate-level	under development	Ethereum	stack-based	EVM bytecode analyzers[1]	gas system	yes	Lisp-like syntax, a wrapping over EVM bytecode
Logikon	high-level	experimental	Ethereum	logical-functional	EVM bytecode analyzers[1]	gas system	yes	translated to Yul
Michelson	low-level	under development	Tezos	stack-based, strongly typed	Typecheck system	gas system	yes	programs can be verified with Coq
Plutus (PlutusCore)	high-level (low-level)	under develop	Cardano	functional	no[2]	gas system	yes	Haskell-like syntax, formal specification
Rholang	high-level	under development	RChain	functional	no[2]	rule reduction system[4]	yes	concurrent, Scala-like syntax, based on rho-calculus
Scilla	intermediate-level	under development	Zilliqa	functional	Scilla-checker	gas system	no[5]	embedded in Coq, formal specification
Simplicity	low-level	under development	Bitcoin	functional, combinator-based, typed	Bit Machine	Bit Machine cell usage	no	formal denotational and operational semantics
Solidity	high-level	stable	Ethereum	statically typed, object-oriented	EVM bytecode analyzers,[1] SmartCheck [38], ZEUS [39], Solidity* [40]	gas system	yes	JavaScript-like syntax, popularity
SolidityX	high-level	beta	Ethereum	secure-oriented	EVM bytecode analyzers[1]	gas system	yes	compiled to Solidity
Vyper	high-level	beta	Ethereum	imperative	EVM bytecode analyzers[1]	gas system	no	Python-like syntax, safety
Yul	intermediate-level	under development	Ethereum	object-oriented	EVM bytecode analyzers[1]	gas system	yes	intermediate language for future Solidity

Fig. 1. Smart contract languages

[1] Programs can be translated to EVM bytecode, and then OYENTE [31], SECURIFY [41], EVM* [40], KEVM [42], MYTHRIL [43], VANDAL [44], RATTLE [45], MANTICORE [46] can be applied.

[2] To our knowledge there is no analyzer, which works with that smart contract language.

[3] Based on the amount of EOS tokens, more tokens — more computation power.

[4] Applying one reduction rule of rho-calculus [47] costs some value, paid by user.

[5] Any in-contract computation within a transition terminates, however non well-founded recursion in SCILLA can be implemented with contracts calling themselves or via explicit continuations, i.e. blockchain level interaction. Loops constructs are planned to be implemented via well-founded recursive functions.

correctness of some functions built up from combinators, e.g. *half-adder* or *SHA-256 function*. Generally, the completeness, i.e. the notion that any function between SIMPLICITY types can be expressed with combinators, is verified in COQ.

Further, operational semantics of SIMPLICITY is defined within the abstract machine called BIT MACHINE, intended to ease bounding of the number of computations, i.e. metering. It is designed to crash at anything that resembles undefined behavior. BIT MACHINE is an abstract imperative machine which state consists of two non-empty stacks of data frames formed by an array of cells. The machine has a set of instructions that manipulate the two stacks and their data frames, and corresponding operational semantics is defined by translating a SIMPLICITY expression into a sequence of BIT MACHINE instructions. It allows computational resources measuring with respect to cells and frames, e.g. the number of executed instructions, copied cells, maximum cells in both stacks at the given point, the number of frames in both stacks. Operational semantics correctness and its correspondence to the denotational semantics are verified in COQ. Furthermore, the set of core combinators can be extended for implementing a signature checking that requires transaction data, thus SIMPLICITY programs can be built to implement the pay-to-script hash scheme [50].

Summarizing, SIMPLICITY stateless nature and rather simple functional semantics without recursion and unbounded loops facilitate equational reasoning, avoiding complex logic. It provides means for formal verification of programs as well as static analysis more capable to effectively bound the number of computational resources. To date SIMPLICITY has a HASKELL implementation under development [51].

3) EVM: is a bytecode language for *Ethereum Virtual Machine*. It is designed to support and execute arbitrary computations over ETHEREUM account-based blockchain, i.e. programs with loops and recursion.

EVM is a *stack-based*, Turing-complete machine of 256-bit words with *memory* model of word addressed byte array. The machine also has a persisted *storage* which is maintained between transactions and is a part of the blockchain state. It is a word-addressable word array. Program code is separated from data. Access to and modification of data in different types of memory is charged differently from storage — the most expensive to stack and memory being equally charged. The formal execution model and the environment is specified in ETHEREUM Yellow paper [32].

There are efforts on specifying formal semantics for EVM in OYENTE [31], F* [52], KEVM [42], and LEM [53] that focus on formal verification tools and detecting and avoiding insecure features of EVM, e.g. *delegatecall*, *overflows*, *undefined call/return*. Also, the poor human-readability of bytecode is a flaw. ETHEREUM includes many implementations of EVM, e.g. in JAVA SCRIPT, C++, PYTHON, and a promising WEBASSEMBLY implementation [54].

4) IELE*:* is a language defined within *K-framework*[9] [14]. It was designed to overcome EVM drawbacks with an idea of correctness by construction and formal verification in mind. It is intended to be secure and human-readable and to serve as a compilation target for high-level languages, thus unifying compilers construction.

IELE is a register-based untyped[10] language: instructions operate on and store their output in infinite number of virtual registers and have access to a persistent *storage* — the unbounded sparse array of arbitrary-precision signed integers. The language implementation is generated from its formal specification defined in K-framework, which provides generation of verification tools, debugger, interpreter, model checker, etc. IELE has functions and defines a call/return convention where a called function expects a specific number of parameters and returns a specific number of values or corresponding error status.[11] Furthermore, IELE avoids some insecure EVM features, e.g. by introducing *delegatecall* functionality and maintains arbitrary-precision arithmetic. Its operational semantics specifies contracts internal state, blockchain state, and transition rules, i.e. contract's code, intra-contract call stack, remaining gas, and the state of the local memory and virtual registers, storage content, balances, etc. Thus IELE makes formal verification less tedious, enhances human-readability, eliminates undefined, and implementation-defined behaviors, i.e. it is considered to be safe[12].

Gas costs for computation time are based on instructions asymptotic and the gas cost for memory is based on peak memory consumption. Gas model is designed to allow arbitrarily large valued instructions and to avoid artificial limits on the size of data or call stacks while preserving the existing goals of the EVM gas model. However, while arithmetics may cause overflows in EVM, in IELE it may cause out-of-gas exception, starting from some input size. Gas formulas are also specified in K.

5) MICHELSON *[33, 55]:* is a typed stack-based language designed to be on-chain code for stateful smart contracts in TEZOS. It is intended to be a more readable compilation target and more amenable for formal verification.

A MICHELSON program supports high-level types (e.g. *map, list, set*, etc.) and receives an input stack with parameters and storage being pushed on. It evaluates to a result stack with an output value and new storage, or can fail. The language does not support closures in a sense that every functions has empty environment. Messaging with other contracts is performed through passing a storage and not maintains the stack between calls. The types are predefined[13] and monomorphic, further

[9]Framework used to produce implementation derived from formal specifications, based on logic rules.

[10] Arbitrary-precision signed integers is the main datatype.

[11]For reference, in EVM caller sends an arbitrary byte stream containing the call arguments values since functions are represented as a set of JUMP labels.

[12] IELE is stated to be the first real-world language, that is designed and implemented using formal semantics, with a zero gap between the formal specification and the implementation.

[13] A programmer can not define their own types.

types of input, output, and storage of a contract are fixed and it is statically ensured that resulting storage type is preserved. MICHELSON has a builtin type for cryptocurrency and operations defined for this type are mandatory checked for *underflow/overflow*. Typing is done via types propagation.

Due to its computation model, MICHELSON has a straightforward semantics, based on rewriting rules defined on stack and syntax. Also, it defines what is considered as well-typed stacks and the resulting outputs. MICHELSON is currently implemented in OCAML via GADT with an interpreter defined corresponding to the semantics while leaving the type checking to OCAML. It is anticipated to replace current implementation with a one verified with either COQ or F* [56].

6) PLUTUS CORE*:* is a typed language designed for use as a transaction validation language in *UTxO*-based blockchain systems. Fundamentally it is eagerly-reduced higher-order polymorphic λ-calculus extended with iso-recursive types, higher kinds, and a library of basic types and functions, hence it has a straightforward operational semantics. The language is meant to be a compilation target, since it is difficult to write and read but it is intended to be formally verifiable in proof-assistants.

PLUTUS CORE program is a closed term, and its execution is performed by (possibly non-terminating) reduction of well-typed terms. All types can be normalized and normalization process always terminates. Further, operations on types allow to deal with sized types, i.e. sized integers or bytestrings, that allows them to be tracked in the type system to facilitate charging for the appropriate amount of gas and detecting overflows at the type level. The language has a specified abstract machine intended to be amenable for a verification reference implementation. Moreover, PLUTUS CORE has its formal specification defined in K [57, 58].

Transaction validation is performed similarly to BITCOIN SCRIPT. Validation is successful if the PLUTUS CORE program reduces to a non-error value within an allotted number of steps. But it is more extended in a sense that a program has a read-only access to world state passed through a *monad* [59, 60].

PLUTUS CORE is an on-chain language for CARDANO blockchain and is embedded into HASKELL. Furthermore the blockchain system itself is implemented in HASKELL as well as off-chain computations, e.g. wallets, it allows type checking on the level of the interaction between off-chain applications and on-chain code.

B. High-level languages

1) SOLIDITY*:* is a very rich and expressive high-level object-oriented Turing-complete language [35] for writing smart contracts for EVM with a syntax similar to JAVASCRIPT and C++. It has static types, inheritance, libraries, complex user-defined types supporting, and other features. As a consequence, that causes its prevalence as well as a large number of potential vulnerabilities (see section IV).

2) SOLIDITYX*:* is a high-level language [61] which compiles to SOLIDITY. SOLIDITYX is a *secure-oriented* language, which means that it has a defense from some vulnerabilities by default, for example, all access modifiers are *private* by default. However, SOLIDITYX is in beta development now and it is not recommended to be used in production.

3) VYPER *(aka* VIPER*):* is a high-level language for implementing smart contracts for the EVM [13]. It is PYTHON3 derived programming language. VYPER is an alternative to SOLIDITY that is aimed at code security, clarity, and unambiguity, for example, it excludes constructions that can lead to misleading code. To achieve this VYPER does not support modifiers, class inheritance, inline assembly, function overloading, operator overloading, recursive calling, infinite-length loops, binary fixed point. The language also leverages overflow checking, array bounding, and limited state modification.

4) FLINT*:* is a high-level statically-typed contract-oriented language aimed to write robust smart contracts on EVM [12]. FLINT provides a mechanism to specify actors that can interact with a contract, immutability by default, assets types, and safer semantics with overflows causing revert of a transaction and explicit states.

5) BAMBOO*:* is a high-level language compiling to the EVM [62]. Its compiler is implemented in OCAML thus BAMBOO is well amenable to formal verification. BAMBOO creates clarify state transitions and avoids reentrancy problems by default. However, it does not support loops and assignments into storage variables, except array elements, which improves the ability of contracts to be verified but complicates their development.

6) LOGIKON*:* is a high-level logical-functional language compiled to YUL [63]. LOGIKON program represents a set of logical constraints statically and formally verified.

7) IVY*:* is a language [64], designed to simplify programming of stateless smart contracts for BITCOIN. Compare to BITCOIN SCRIPT, in IVY program it is possible to use named variables, named clauses, domain-specific types, syntax sugar for function calls.

8) LIQUIDITY*:* is a functional, statically and strongly typed language, compiled down to MICHELSON. It has OCAML syntax and keeps safety guaranteed by MICHELSON, while providing high-level constraints. LIQUIDITY has a formal specification of the compilation semantics[65] and supports decompilation back from MICHELSON, based on graph produced by symbolic execution that is eventually transformed into LIQUIDITY *AST*. This feature greatly enhances readability, since stack-based MICHELSON code is rather hard to inspect manually.

9) CHAINCODE*:* is a smart contract program, written for HYPERLEDGER FABRIC [21] blockchain. CHAINCODE can be developed with GO, NODE.JS or JAVA. The code should implement a special interface to interact with the blockchain network. Unlike ETHEREUM smart contracts, CHAINCODE does not have account address or associated assets, but the smart contract can have a mapping of the real assets to the internal state. CHAINCODE has similar conception to database stored procedures. When a transaction is created, CHAINCODE is called to perform operations according to the transaction data. Possible operations are: read, update or delete data,

stored in the ledger. Also, it is possible to invoke or read the state of another CHAINCODE, if the caller has enough permissions.

C. Intermediate-level languages

1) YUL *(*JULIA *or* IULIA*):* is an intermediate language [66]. It can be compiled to a number of backends: *EVM 1.0*, *EVM 1.5* and *eWASM*. It is planning to use YUL as an intermediate language in the future versions of the SOLIDITY compiler. YUL can be used for "inline assembly" inside SOLIDITY.

2) RHOLANG*:* is a functional, concurrent, based on *rho-calculus* [47] language [67], used in project RCHAIN. A smart contract in terms of RCHAIN is a process, which has persistent state, its own code, and associated address. Execution of code is done by applying the reduction rule of rho-calculus. RHOLANG has behavioral types [68], reflection, reactive API, asynchronicity. Synchronization primitives for parallel execution of transactions are *messages* and *channels*. Messages are the way to communicate smart contracts with each other, sending values through channels. A user has to pay a cost in special tokens, named *Phlogiston*, to the node in the system for computational resources, These tokens will be used for executing smart contract's code. Rate-limiting mechanism looks like the *gas system* in ETHEREUM. Unlike EVM, where gas metering is done on the VM level, manipulations on *Phlogiston*s are injected in smart contract's source code by RHOLANG compiler.

3) SCILLA*:* is intended to be an intermediate level language as a translation target for high-level languages to facilitate program analysis and verification before compiling to executable bytecode. SCILLA is a typed language built on stateful smart contracts, i.e. contracts that have a state represented with a storage and that can communicate either with other contracts via messages or with the off-chain world by raising events or with blockchain explicitly reading blockchain data. The language design is aimed to facilitate formal reasoning providing clear and principled semantics.

Specifically, its semantics is based on communicating automata that separate contract specific computations called *transitions* and blockchain-wide interactions, i.e. messaging with other contracts, thus making transitions atomic. Atomicity is achieved through allowing only tail-calling communications which eliminate reentrancy problems. However non-tail calls are needed for some computations e.g. passing and saving some value back from the callee, it is implemented with explicit continuations mechanism. Nevertheless, possible non-terminating execution can be caused by non well-founded recursion, which is going to be handled with gas usage. Further, SCILLA specifies pure, i.e. that change the state and impure transitions and those reading blockchain data, e.g. block number with OCAML based syntax.

SCILLA has been shallow-embedded in COQ, specifying such properties as contract terminology, contract state, and transitions along with blockchain states, which allows properties verification in isolation. So its design implies leveraging of formal reasoning to prove different modality properties, e.g. safety[14], liveness[15] or termination for well-founded recursive functions. It is anticipated to enhance support for automating the proofs of safety/temporal properties.

4) LLL*:* is a Lisp-like language [69] for EVM. Main purpose of LLL is to provide a little bit higher level of abstraction upon EVM bytecode, i.e. programmer has more high-level constructions to work with stack. Also language has more functionality over the base set of EVM opcodes, such as multiary operators (they can be applied to one or more arguments, result of following code `(+ 1 2 3 4 5)` is `15`), including files, control structures, and macro definitions. LLL has an analog of variables, it makes automatic memory management for saving values.

VI. DISCUSSION

We briefly described notable approaches for specification of smart contracts intended behavior and analysis of behavioral properties. However, this survey is nevertheless incomplete. The area of blockchain and smart contracts is under active research. The community tries to apply different approaches and ways in the area of smart contract languages and their execution environments development. Some of them are Turing-completeness, paradigm (e.g. imperative, object-oriented, functional), level of abstraction, a way to limit code execution (metering systems such as ETHEREUM gas, time bounds, number of instructions) and a formal theory on which a language is based.

In the rest of the section, we discuss contributions that have not been classified in previous sections, propose aspects that may worth future researching and related work, and summarize possible pros and cons of provided aspects.

Recall that most smart contracts in blockchains are irreversible, i.e. they are hard to fix once they are deployed. One approach to mitigate this is a design pattern provided in [70, 71] that leverages using *delegatecalls*. It suggests deploying contracts with another *dispatcher* contract. The increased number of messages makes analysis and reasoning more complicated, since dispatcher contracts should be robust and safe then. Another approach is platforms that allow *upgradable* contracts [72].

Arguable concept is the representation in which contracts are deployed to a blockchain. Most of the systems included in our survey store on-chain code in a some low-level form. Such form hardens auditability, while also may serve as a uniform compilation target. That facilitates the development with different languages. There are platforms where contracts are stored as programs written in high-level safe languages [72]. Another possible approach for this is a decompilation from low-level byte code to more high level code like in MICHELSON and LIQUIDITY case. However, to our knowledge, only this couple of languages have formalized semantics of compilation, while none of the known works

[14] These are invariants that hold through the lifetime of a contract, exposing that nothing should go wrong.

[15] Basically, it states that something should eventually happen.

provides the correctness of interpretation and interpretation after compilation at all, i.e. the correctness of the compiler or the commutativity of the implied diagram.

One more problem is a metering system for smart contracts, such as ETHEREUM gas and its analogues. Gas estimation is in general undecidable. It could be useful to find mechanisms to predict gas consumption. Improper estimation may lead to vulnerabilities (e.g. DoS-attacks), or to fails during code execution (e.g. ETHEREUM out-of-gas exception). Gas consumption depends on many factors such as memory usage and blockchain state. Various adaptive methods like type system are already surveyed PLUTUS [58], rigorous semantics with asymptotic analysis as in IELE [14], or dynamic adjustment as adaptive gas cost mechanism in [73] may be promising, as well as methods based on symbolic paths exploration and resource analysis [74, 75]. For example, PLUTUS design of unbounded integers allows metering statically due to its type system, while unbounded integers in IELE allows only dynamic gas evaluation. One may apply techniques like RAML [76]. Gas reducing optimization are also worth considering. [16]

Since smart contracts use cases are yet to be researched, it is undesirable to restrict either statefulness of contracts or Turing-completeness of languages they are written in. The compromise between an ability to run arbitrary computations on the blockchain and amenability to reasoning defines future research topics. For instance, in [9] dependent types within IDRIS language are leveraged for writing provable smart contracts, that are compiled down to run on ETHEREUM. Languages based on models, which better describe interaction between contracts based on message passing may become future research objectives, e.g. languages based on process calculus [77]. Extensive type systems in such systems also worth researching, e.g. behavioral type systems or linear epistemic ones [78]. Type annotating while writing a contract with such languages is often non-trivial as well as robust and safe contracts development in general. There are researches aimed at domains formalizing, e.g. *finances* and at the design of simpler languages that are embedded in some safe language for only domain purposes [79]. Such domain specific languages tend to be visual to ease the development process for non-experts in programming. Approaches aimed at actors behavior are as well interesting. There is a DSCP contracting protocol for trading proposed in [80]. The protocol was verified using game theory and statistical models, such as Markov decision processes.

There is still another point about properties to consider. It is modality properties formulating, an i.e. specification of such a property a smart contract should satisfy. If the property unfulfillment can be proved, it would prevent some exploit, e.g. already mentioned DAO. Some such properties can be seen in [81]. It propose BITML — Bitcoin Modelling Language that leverages process calculus to describe interactions between participants and generate BITCOIN transactions according to symbolic semantics. In [82] EVM is formalized in LEM for modeling smart contracts behavior with some properties defined.

To outline the discussion, it it worth to notice that many researches avoid the infrastructure around the language, i.e. development environments, testing and deployment tools, extensive *API* libraries. However, these are essential components of successful development and a field for a plenty of practical studies, since to date only ETHEREUM has a rather complete infrastructure.

[16] Due to safety considerations, such optimization should be proven to be semantically equivalent. However we are not aware of any related results.

VII. CONCLUSION

As smart contracts platforms are intended to reasonably automate the economy, smart contracts should be safe and robust. In this paper, we have presented an overview of a to date state of smart contract programming languages. We have classified weaknesses and vulnerabilities smart contracts are prone to. Languages calculus models, semantics, and type systems have been surveyed as well as other properties according to reasoning, safety, expressiveness, and readability. At the end we have summarized related work and possible future research topics.

REFERENCES

[1] Bitcoin contract. URL: https://en.bitcoin.it/wiki/Contract (Date: 2019-01-30).

[2] Solidity-example-crowdfunding. URL: https://github.com/zupzup/solidity-example-crowdfunding (Date: 2019-01-30).

[3] D. Macrinici, C. Cartofeanu, and S. Gao, "Smart contract applications within blockchain technology: A systematic mapping study," *Telematics and Informatics*, vol. 35, no. 8, pp. 2337 – 2354, 2018.

[4] C. D. Clack, V. A. Bakshi, and L. Braine, "Smart contract templates: foundations, design landscape and research directions," *CoRR*, vol. abs/1608.00771, 2016.

[5] A 50 million hack just showed that the dao was all too human. URL: https://www.wired.com/2016/06/50-million-hack-just-showed-dao-human/ (Date: 2019-01-30).

[6] D. McAdams. An ontology for smart contracts. URL: https://cryptochainuni.com/wp-content/uploads/Darryl-McAdams-An-Ontology-for-Smart-Contracts.pdf (Date: 2019-02-07).

[7] N. Atzei, M. Bartoletti, and T. Cimoli, "A survey of attacks on ethereum smart contracts sok," in *Proceedings of the 6th International Conference on Principles of Security and Trust - Volume 10204*. New York, NY, USA: Springer-Verlag New York, Inc., 2017, pp. 164–186.

[8] G. Destefanis, A. Bracciali, R. Hierons, M. Marchesi, M. Ortu, and R. Tonelli, "Smart contracts vulnerabilities: A call for blockchain software engineering?" *ResearchGate*, 2018.

[9] Safer smart contracts through type-driven development. URL: https://publications.lib.chalmers.se/records/fulltext/234939/234939.pdf (Date: 2019-01-30).

[10] "Bitcoin script," 2019-01-30. URL: https://en.bitcoin.it/wiki/Script

[11] R. O'Connor, "Simplicity: A new language for blockchains," *CoRR*, vol. abs/1711.03028, 2017.

[12] Flint. URL: https://github.com/flintlang/flint (Date: 2019-01-30).

[13] Vyper. URL: https://github.com/ethereum/vyper (Date: 2019-01-29).

[14] T. Kasampalis, D. Guth, B. Moore, T. Serbanuta, V. Serbanuta, D. Filaretti, G. Rosu, and R. Johnson, "Iele: An

intermediate-level blockchain language designed and implemented using formal semantics," University of Illinois, Tech. Rep. http://hdl.handle.net/2142/100320, July 2018.
[15] I. Sergey, A. Kumar, and A. Hobor, "Scilla: a smart contract intermediate-level language," *CoRR*, vol. abs/1801.00687, 2018.
[16] Plutus core specification. URL: https://github.com/input-output-hk/plutus/tree/master/plutus-core-spec (Date: 2019-01-30).
[17] D. Harz and W. J. Knottenbelt, "Towards safer smart contracts: A survey of languages and verification methods," *CoRR*, vol. abs/1809.09805, 2018.
[18] P. L. Seijas, S. Thompson, and D. McAdams, "Scripting smart contracts for distributed ledger technology," Cryptology ePrint Archive, Report 2016/1156, 2016, https://eprint.iacr.org/2016/1156.
[19] Contract. URL: https://en.bitcoin.it/wiki/Contract (Date: 2019-01-30).
[20] Ethereum contract security techniques and tips. URL: https://github.com/ethereum/wiki/wiki/Safety (Date: 2019-01-29).
[21] E. Androulaki, A. Barger, V. Bortnikov, C. Cachin, K. Christidis, A. De Caro, D. Enyeart, C. Ferris, G. Laventman, Y. Manevich, S. Muralidharan, C. Murthy, B. Nguyen, M. Sethi, G. Singh, K. Smith, A. Sorniotti, C. Stathakopoulou, M. Vukolić, S. W. Cocco, and J. Yellick, "Hyperledger fabric: A distributed operating system for permissioned blockchains," in *Proceedings of the Thirteenth EuroSys Conference*, ser. EuroSys '18. New York, NY, USA: ACM, 2018, pp. 30:1–30:15.
[22] K. Yamashita, Y. Nomura, E. Zhou, B. Pi, and S. Jun, "Potential risks of hyperledger fabric smart contracts," in *2019 IEEE International Workshop on Blockchain Oriented Software Engineering (IWBOSE)*, 2019, pp. 1–10.
[23] 300m in cryptocurrency accidentally lost forever due to bug. URL: https://www.theguardian.com/technology/2017/nov/08/cryptocurrency-300m-dollars-stolen-bug-ether (Date: 2019-01-30).
[24] Smart contract weakness classification and test cases. URL: https://smartcontractsecurity.github.io/SWC-registry/ (Date: 2019-01-29).
[25] Decentralized application security project. URL: https://dasp.co (Date: 2019-01-29).
[26] Security considerations. URL: https://solidity.readthedocs.io/en/latest/security-considerations.html (Date: 2019-01-29).
[27] Vulnerabilities description. URL: https://github.com/trailofbits/slither/wiki/Vulnerabilities-Description (Date: 2019-01-30).
[28] Smart contract weakness classification and test cases. URL: https://smartcontractsecurity.github.io/SWC-registry/ (Date: 2019-01-22).
[29] N. Atzei, M. Bartoletti, and T. Cimoli, "A survey of attacks on ethereum smart contracts sok," in *Proceedings of the 6th International Conference on Principles of Security and Trust - Volume 10204*. New York, NY, USA: Springer-Verlag New York, Inc., 2017, pp. 164–186.
[30] Ether — the crypto-fuel for the ethereum network. URL: https://www.ethereum.org/ether (Date: 2019-01-30).
[31] L. Luu, D.-H. Chu, H. Olickel, P. Saxena, and A. Hobor, "Making smart contracts smarter," in *Proceedings of the 2016 ACM SIGSAC Conference on Computer and Communications Security*, ser. CCS '16. New York, NY, USA: ACM, 2016, pp. 254–269.
[32] D. G. Wood. Ethereum: A secure decentralised generalised transaction ledger. URL: https://ethereum.github.io/yellowpaper/paper.pdf (Date: 2019-01-31).
[33] Michelson language. URL: https://www.michelson-lang.com/ (Date: 2019-01-31).
[34] B. C. Pierce, *Types and Programming Languages*, 1st ed. The MIT Press, 2002.
[35] Solidity. URL: https://github.com/ethereum/solidity (Date: 2019-01-29).
[36] Liquidity. URL: https://github.com/OCamlPro/liquidity (Date: 2019-01-29).
[37] G. Rou and T. F. erbnut, "An overview of the k semantic framework," *The Journal of Logic and Algebraic Programming*, vol. 79, no. 6, pp. 397 – 434, 2010, membrane computing and programming.
[38] S. Tikhomirov, E. Voskresenskaya, I. Ivanitskiy, R. Takhaviev, E. Marchenko, and Y. Alexandrov, "Smartcheck: Static analysis of ethereum smart contracts," in *Proceedings of the 1st International Workshop on Emerging Trends in Software Engineering for Blockchain*, ser. WETSEB '18. New York, NY, USA: ACM, 2018, pp. 9–16.
[39] S. Kalra, S. Goel, M. Dhawan, and S. Sharma, "Zeus: Analyzing safety of smart contracts," 01 2018.
[40] K. Bhargavan, A. Delignat-Lavaud, C. Fournet, A. Gollamudi, G. Gonthier, N. Kobeissi, N. Kulatova, A. Rastogi, T. Sibut-Pinote, N. Swamy, and S. Zanella-Béguelin, "Formal verification of smart contracts: Short paper," in *Proceedings of the 2016 ACM Workshop on Programming Languages and Analysis for Security*, ser. PLAS '16. New York, NY, USA: ACM, 2016, pp. 91–96.
[41] P. Tsankov, A. Dan, D. Drachsler-Cohen, A. Gervais, F. Bünzli, and M. Vechev, "Securify: Practical security analysis of smart contracts," in *Proceedings of the 2018 ACM SIGSAC Conference on Computer and Communications Security*, ser. CCS '18. New York, NY, USA: ACM, 2018, pp. 67–82.
[42] E. Hildenbrandt, M. Saxena, X. Zhu, N. Rodrigues, P. Daian, D. Guth, B. Moore, Y. Zhang, D. Park, A. Stefanescu, and G. Rosu, "Kevm: A complete semantics of the ethereum virtual machine," in *2018 IEEE 31st Computer Security Foundations Symposium*. IEEE, 2018, pp. 204–217.
[43] Mythril. URL: https://github.com/ConsenSys/mythril-classic (Date: 2019-01-29).
[44] L. Brent, A. Jurisevic, M. Kong, E. Liu, F. Gauthier, V. Gramoli, R. Holz, and B. Scholz, "Vandal: A scalable security analysis framework for smart contracts," *CoRR*, vol. abs/1809.03981, 2018.
[45] Rattle. URL: https://github.com/trailofbits/rattle (Date: 2019-01-30).
[46] Manticore. URL: https://github.com/trailofbits/manticore (Date: 2019-01-30).
[47] L. G. Meredith and M. Radestock, "A reflective higher-order calculus," *Electr. Notes Theor. Comput. Sci.*, vol. 141, pp. 49–67, 2005.
[48] Bitcoin weaknesses. URL: https://en.bitcoin.it/wiki/Weaknesses (Date: 2019-01-30).
[49] A. Back, M. Corallo, L. Dashjr, M. Friedenbach, G. Maxwell, A. Miller, A. Poelstra, J. Timón, and P. Wuille, "Enabling blockchain innovations with pegged sidechains," 2014.
[50] Mediawiki. URL: https://github.com/bitcoin/bips/blob/master/bip-0016.mediawiki (Date: 2019-02-5).
[51] Simplicity. URL: https://github.com/ElementsProject/simplicity (Date: 2019-02-5).
[52] Grishchenko I., Maffei M., Schneidewind, C.: A semantic framework for the security analysis of ethereum smart contracts - technical report (2018). URL: https://secpriv.tuwien.ac.at/tools/ethsemantics. (Date: 2019-01-30).
[53] Formalization of ethereum virtual machine in lem. URL: https://github.com/pirapira/eth-isabelle (Date: 2019-01-30).
[54] Ewasm: design overview and specification. URL: https://github.com/ewasm/design (Date: 2019-01-30).
[55] Michelson: the language of smart contracts in tezos. URL: http://www.liquidity-lang.org/doc/reference/michelson.html (Date: 2019-01-30).
[56] Why michelson? URL: https://www.michelson-lang.com/

why-michelson.html (Date: 2019-02-5).
[57] Plutus core semantics. URL: https://github.com/kframework/plutus-core-semantics (Date: 2019-01-30).
[58] Plutus implementation and tools. URL: https://github.com/input-output-hk/plutus (Date: 2019-01-30).
[59] The extended utxo model. URL: https://github.com/input-output-hk/plutus/tree/master/docs/extended-utxo (Date: 2019-02-5).
[60] Is it smart to use smart contracts? URL: https://plutusfest.io/presentations/Philip-Wadler/Wadler30.pdf (Date: 2019-02-5).
[61] Solidityx. URL: https://solidityx.org/ (Date: 2019-01-30).
[62] Bamboo. URL: https://github.com/pirapira/bamboo (Date: 2019-01-30).
[63] Logikon. URL: https://github.com/logikon-lang/logikon (Date: 2019-01-31).
[64] Ivy: Bitcoin smart contracts. URL: https://github.com/ivy-lang/ivy-bitcoin (Date: 2019-01-30).
[65] Çagdas Bozman, M. Iguernlala, M. Laporte, F. L. Fessant, and A. Mebsout, "Liquidity: Ocaml pour la blockchain," *Journées Francophones des Langages Applicatifs 2018*, 2018.
[66] Yul. URL: https://solidity.readthedocs.io/en/latest/yul.html (Date: 2019-01-30).
[67] Rchain and rholang. URL: https://www.rchain.coop/platform (Date: 2019-01-30).
[68] D. Ancona, V. Bono, and M. Bravetti, *Behavioral Types in Programming Languages*. Hanover, MA, USA: Now Publishers Inc., 2016.
[69] G. Wood. LLL. URL: https://lll-docs.readthedocs.io/en/latest/index.html (Date: 2019-01-30).
[70] Upgradable contract with solidity. URL: https://gist.github.com/Arachnid/4ca9da48d51e23e5cfe0f0e14dd6318f (Date: 2019-01-30).
[71] Proxy libraries in solidity. URL: https://blog.zeppelin.solutions/proxy-libraries-in-solidity-79fbe4b970fd (Date: 2019-01-30).
[72] The pact smart-contract language. URL: http://kadena.io/docs/Kadena-PactWhitepaper.pdf (Date: 2019-01-30).
[73] T. Chen, X. Li, Y. Wang, J. Chen, Z. Li, X. Luo, M. H. Au, and X. Zhang, "An adaptive gas cost mechanism for ethereum to defend against under-priced dos attacks," *CoRR*, vol. abs/1712.06438, 2017.
[74] E. Albert, P. Gordillo, A. Rubio, and I. Sergey, "GASTAP: A gas analyzer for smart contracts," *CoRR*, vol. abs/1811.10403, 2018.
[75] M. Marescotti, M. Blicha, A. E. J. Hyvärinen, S. Asadi, and N. Sharygina, "Computing exact worst-case gas consumption for smart contracts," in *International Symposium on Leveraging Applications of Formal Methods ISoLA 2018: Leveraging Applications of Formal Methods, Verification and Validation. Industrial Practice*, Springer. Cyprus: Springer, 2018.
[76] J. Hoffmann, A. Das, and S. Weng, "Towards automatic resource bound analysis for ocaml," *CoRR*, vol. abs/1611.00692, 2016.
[77] J. Baeten, "A brief history of process algebra," *Theoretical Computer Science*, vol. 335, no. 2, pp. 131 – 146, 2005, process Algebra.
[78] H. Deyoung and F. Pfenning, "Reasoning about the consequences of authorization policies in a linear epistemic logic," 05 2012.
[79] S. Thompson and P. L. Seijas, "Marlowe: Financial contracts on blockchain," in *ISoLA 2018: Leveraging Applications of Formal Methods, Verification and Validation. Industrial Practice*, ser. Lecture Notes in Computer Science. Switzerland: Springer-Verlag Berlin, October 2018. URL: https://kar.kent.ac.uk/69846/
[80] G. Bigi, A. Bracciali, G. Meacci, and E. Tuosto, "Validation of decentralised smart contracts through game theory and formal methods," in *Essays Dedicated to Pierpaolo Degano on Programming Languages with Applications to Biology and Security - Volume 9465*. New York, NY, USA: Springer-Verlag New York, Inc., 2015, pp. 142–161.
[81] M. Bartoletti and R. Zunino, "Bitml: A calculus for bitcoin smart contracts," in *Proceedings of the 2018 ACM SIGSAC Conference on Computer and Communications Security*, ser. CCS '18. New York, NY, USA: ACM, 2018, pp. 83–100.
[82] Y. Hirai, "Defining the ethereum virtual machine for interactive theorem provers," in *Financial Cryptography and Data Security*. Cham: Springer International Publishing, 2017, pp. 520–535.

Ethereum Blockchain Analysis using Node2Vec

Aleksander Salnikov
Higher School of Economics
Moscow, Russia
salnikovsas@gmail.com

Evgenia Sivets
Higher School of Economics
Moscow, Russia
evgeniasivets@gmail.com

***Abstract*—In this work we apply Node2Vec[19] to obtain structural information from Ethereum network transaction graph[11], [12]. Given the large amount of data that is stored in the blockchain, we make use of the Google BigQuery service to extract only a small relevant subset of nodes and reconstruct transaction graph. After that the Node2Vec was used to embed this graph into a high-dimensional vector space. The space of embeddings is used to clusterize Ethereum addresses.**

The Ethereum network was chosen thanks to the property of its addresses to represent a long-term entity, in contrast to Bitcoin[1] and many other blockchains where it is not possible to establish such relationship between entities (users, etc...) and addresses[2], [3], [4], [5]. This makes us think of trying to classify Ethereum users according to their activity[6], [7], based solely on the blockchain data.

I. Introduction

A. The purposes of blockchain data analysis overview

Blockchain technology has been becoming more and more popular and complex recently. Simply speaking, blockchain can be seen as a very specific type of database — a distributed ledger. Because of blockchain being a public database that anyone can write to (following a certain set of rules) and the record will persist forever in its state, the blockchain data, as a result, implicitly contains valuable financial and social information about its users. Which ultimately draws attention of both data scientists and government regulators, giving a boost to developing blockchain analysis techniques and motivating research teams to explore the data from many different perspective.

The blockchain state has been conceptualized through graph-based data models, providing researchers with a rich toolbox of different approaches. Graph theory has been already successfully applied to solve many practical and theoretical network-related problems, which, by the way, may explain the wide adoption of network mental model towards blockchains as well. Much progress has been achieved in the field of random graph analysis, so it was just a matter of time for this ideas to make their way into blockchain state research.

The first widely adopted blockchain system was Bitcoin. Being designed to preserve privacy of its users, while preserving all information about every single transaction on the network, it expectedly became a target for researches aiming to extract users' private information from blockchain data. It has been shown that the blockchain data contains much more private information that has been previously assumed and led to deeper understanding of the privacy problem in distributed systems. Despite not being ultimately private, Bitcoin is still the first and the most popular cryptocurrency in the world.

While some subsequent developments tried to challenge the uncovered privacy-related issues in order to archive the level of privacy that Bitcoin initially expected to provide, others focused on exploring another unique properties of emerged technology. In particular, they enriched identity management functionality: making the user to be represented as an on-network entity, capable of interacting with other entities — users or special kind of programs, living in the network, named "smart-contracts". Ethereum appeared to be the first widely-adopted blockchain system that implemented these concepts, although formerly it was presented as a system for general-purpose distributed computations. Without a design decisions aiming at achieving privacy, the Ethereum data explicitly contains information about the sender and recipient for each transaction, making it more suitable for conducting research.

B. Ethereum network transaction graph model

For the purpose of our study, Ethereum network can be represented as a directed graph, where nodes represent network entities (addresses), whereas edges reflect transactions between them.

Each edge of this graph has at least the following set of attributes: transacted value and transaction time[13]. Over time new edges may be added to the graph but cannot be removed or modified[20]. Accounting for both incoming value and outgoing value that has been transacted to/from a particular node determines the node's balance at any particular moment of time.

Besides the financial transactions there are another kind of transactions related to smart-contract functionality that Ethereum provides. Smart-contract can be seen as applications that are running inside the network and may enjoy the same security guarantees that the ordinary transactions do. They facilitate the exchange of messages between network entities, with each message being a transaction carrying arbitrary app-specific data[8], [10], [11], [9]. This opens up great opportunities for a further research.

C. Obtaining Data and Data-set preparation

We used Google's BigQuery service to obtain only interesting subset of data through querying block-chain data with SQL. Google maintains the up-to-date complete Ethereum block-chain data on their servers and provides a structural

query service to allow data scientists analyze the data without the overhead of downloading gigabytes of data and keeping it up-to-date.

SQL allows to easily fetch required data. For example, to obtain every transaction that ever happened, we may write:

```
SELECT from_address, to_address, value
FROM `bigquery-public-data
 ↪ .crypto_ethereum.transactions`
```

This query will return each transaction separately.

For the sake of simplicity, we will bring individual transactions into aggregated ones based on pair of sender and receiver. The corresponding query reads:

```
SELECT from_address, to_address,
 ↪ SUM(value)
FROM `bigquery-public-data
 ↪ .crypto_ethereum.transactions`
GROUP BY from_address, to_address
```

To obtain list of every address, involved in transactions we can use the following query:

```
SELECT from_address
FROM  `bigquery-public-data.
 ↪ crypto_ethereum.transactions`
GROUP BY from_address
UNION DISTINCT
SELECT to_address
FROM `bigquery-public-data.
 ↪ crypto_ethereum.transactions`
GROUP BY to_address
```

Using full Ethereum-addresses during the calculation step would require a huge amount of memory. Since the set of network addresses is fixed and known beforehand, we may mitigate this issue by enumerating them at the pre-processing step and using integers as identifiers instead. The mapping (stored as a Python dictionary) can be easily used to resolve the network address when needed.

Also there is some interest in transaction analysis that happened over a specific period of time.

D. Nodes embedding

Let

$$G = (V, E),$$

where V — the set of all network entities, E — a set of aggregated transactions between them.

Our primary goal is to process this data using various machine learning algorithms in order to categorize them into distinct groups according to the type of their activity on the network.

Solving this problem directly on the graph model is a very hard task. Instead, one of the recent approaches – graph embedding – suggests representing network vertices into a low-dimensional vector space [16]:

$$f : V \to \mathbb{R}^d,$$

chosen so that preserving information about network topology structure[18]. Here d is the number of dimensions of our feature representation. The above requirement can be expressed in terms of maximizing the likelihood of network neighborhoods preserving:

$$\max_f \sum_{u \in V} \log P(N_S(u)|f(u)).$$

The objective can be efficiently optimized using stochastic gradient descent (SGD) [14]. The idea behind an embedding is that the neighborhood (the context) of each node to much extend determines the properties of the node itself.

Here we used the notion of node's neighborhood [17], that must be clearly specified before we may continue. More formally, we have to define a sampling strategies.

Definition 1. *For each node $u \in V$, its network neighborhood $N_S(u) \subset V$ is generated through a neighborhood sampling strategy S.*

The simplest such strategies are, for instance, Breadth-first Sampling (BFS) and Depth-first Sampling (DFS), but being deterministic they represent single node's neighborhood, failing to preserve a complex structure of a node's neighborhood. Instead, the $node2vec$ approach, that we will work with, solves this by using randomized procedure to sample many different neighborhoods for a single node.

E. Random Walks

For each node u, consider the following random walk of the fixed length ℓ with the following distribution [15]:

$$P(c_i = x | c_{i-1} = v) = \begin{cases} \pi_{vx}/Z & \text{if } (v, x) \in E \\ 0 & \text{otherwise} \end{cases}$$

Here Z is the normalizing constant, π_{vx} is transition probability between nodes v and x, defined as:

$$\alpha_{pq}(t, x) = \begin{cases} 1/p & \text{if } d_{tx} = 0 \\ 1 & \text{if } d_{tx} = 1 \\ 1/q & \text{if } d_{tx} = 2 \end{cases}$$

where d_{tx} denotes the shortest path distance between nodes t and x.

The two parameters have the following meaning:

1) return parameter p — controls the likelihood of returning to the same node
2) in-out parameter q — defines if random walk should go towards node t (when $q > 1$) or away from it ($q < 1$).

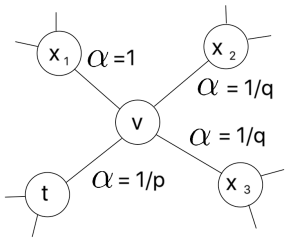

Figure 1. Illustration of the random walk procedure in node2vec. The walk from t to v is evaluating the next step.

F. Classification of addresses based on extracted features

After the feature representations has been constructed using node2vec, we can use it to estimate roles of involved entities. For the constructed features to be useful and meaningful, we need to keep the number of features as small as possible.

Using unnecessarily high number of dimensions for a feature space inherently implies ambiguities and the observed feature vectors is largely determined by random factors, making it harder or even impossible to come up with a meaningful interpretations for them.

In our case, the optimal size of feature space is appeared to be 3, leading to highly reproducible identifiable patterns in the results as shown on the scatterplot matrix below.

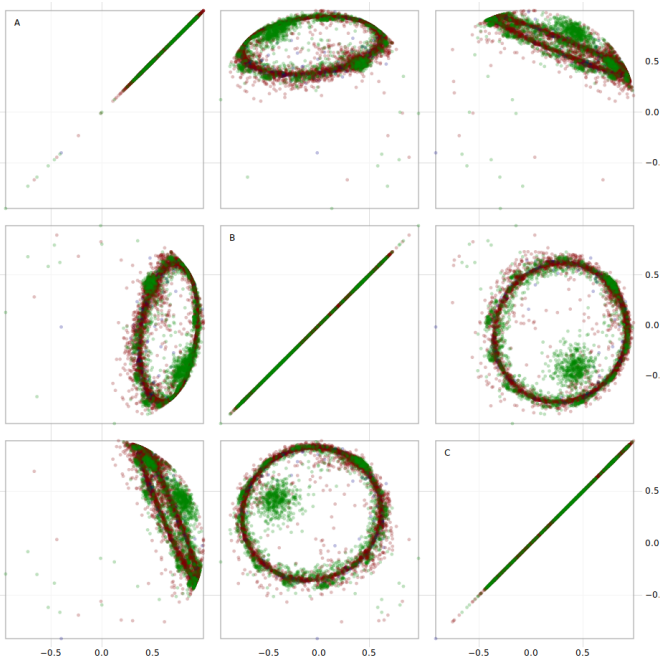

Figure 2. Scatterplot matrix for 3 dimensional embedding. The color of a node is defined by the number of other nodes it connects to: green nodes has at most 2 neighbours, red — up to 8, others are depicted blue.

The nodes on the plot are colored based on the number of connections to another nodes. An interesting pattern can be observed about how the most connected nodes are distributed over the feature space.

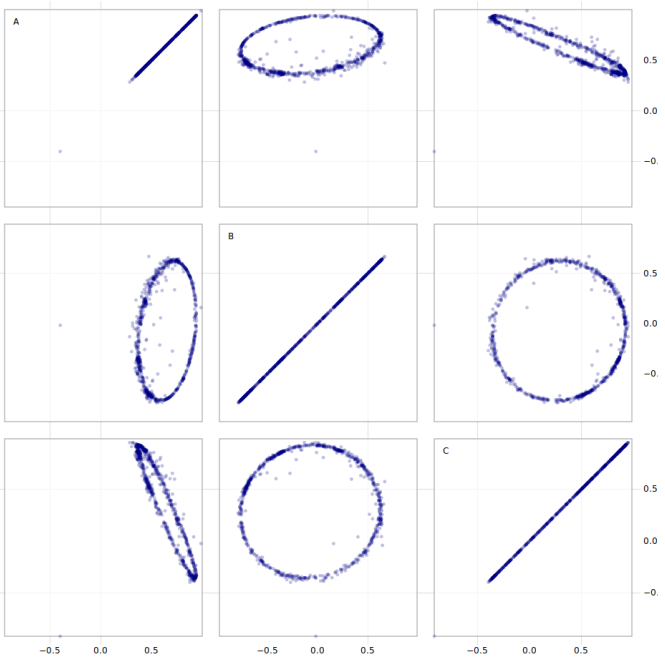

Figure 3. Scatterplot matrix for 3 dimensional embedding showing only nodes with a high number of connections

These nodes are connected to both red nodes with the latter mostly distributed around them in the feature space and green nodes cluster positioned at the center, The green nodes that connects to red ones, in contrast, distributed close to them.

That brings us the following intuition about the role of the nodes:

1. Blue nodes represents exchange hot wallets, and constantly have to interact with users. 2. Users are red nodes having moderate number of connections, mostly with an exchange, but also rarely between themselves. 3. Some of the green nodes are also users, which happen to have quite a few transactions from explored substate. 4. But the central green cluster is the internal addresses, used by blue nodes to do some financial manipulation behind the scene.

G. Clustering

On the applicability of k-means method

At first we tried to use k-means to do clustering. The results were more than questionable and highly problematic to interpret. We thoroughly investigated the structure of data to found out the underlying reason why that didn't work.

k-means method can be expressed as optimization problem:

$$\sum_{i=0}^{n} \min_{\mu_j \in C} (||x_i - \mu_j||^2),$$

where μ_j — clusters centers.

The basic idea is that at each iteration the center of mass is recalculated for each cluster obtained in the previous step, then the vectors are divided into clusters again according to which of the new centers was closer in the selected metric.

The algorithm terminates when at some iteration there is no change in the distance inside the cluster. This happens in a

finite number of iterations, since the number of possible partitions of a finite set is finite, and at each step the total square bias of V decreases, therefore looping is impossible. Using a different distance function other than (squared) Euclidean distance may stop the algorithm from converging.

But k-means clustering requires the number of clusters as a parameter. To determine an optimal number of clusters, we should use Silhouette analysis.

The silhouette of a data represent how well data is matched within its cluster but not of the neighbouring cluster. When Silhouette coefficients is near $+1$, the sample is separated from the neighboring clusters, whereas a 0 value would mean that sample is too close to the boundary and might have been assigned to the wrong cluster.

But the converging property doesn't mean the quality of clustering will be acceptable. Such proprety can be misleading, however. Another well known property of k-means is faliure to match clusters with complex geometry.

The warning sign could be too many clusters given as a result of Silhouette analysis. This step is required to determine an optimal number of clusters, since it is a parameter of k-means. The silhouette of a data represent how well data is matched within its cluster but not of the neighbouring cluster. When Silhouette coefficients is near +1, the sample is separated from the neighboring clusters, whereas a 0 value would mean that sample is too close to the boundary and might have been assigned to the wrong cluster.

Our data gives the following values of Silhouette coefficients:

Number of clusters	5	10	15	20	27
Silhouette coefficient	0.247	0.277	0.281	0.315	0.323

Table I
SILHOUETTE COEFFICIENTS

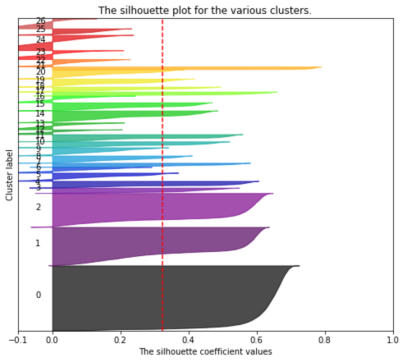

Figure 4. Silhouett analysis for K-means clustering on sample data with n clusters = 27.

And the optimal number of clusters were 27. The next warning sign was that we had to use t-SNE (t-distributed stochastic neighbor embedding) method to visualize that many clusters. It's a nonlinear dimension-reduction technique, that is designed for visualization high-dimensional data in a low-dimensional space of two dimensions. It maps each high-dimensional object to a two-dimensional point, so that similar objects get mapped to points nearby. Dissimilar objects, instead, map to distant points with high probability.

The t-SNE algorithm consists of two steps:

- Constructing a probability distribution over pairs of high-dimensional objects. For given a set of N objects $x_1, \dots, x_N$ t-SNE first computes probabilities p_{ij}, that are proportional to the similarity of objects x_i and x_j:

$$p_{i|j} = \frac{\exp(-\|x_i - x_j\|^2)/2\sigma_i^2}{\sum_{k \neq i} \exp(-\|x_i - x_k\|^2)/2\sigma_i^2},$$

$$p_{ij} = \frac{p_{j|i} + p_{i|j}}{2N}$$

- t-SNE aims to learn a d-dimensional map $y_1, y_2, \dots, y_N$ that reflects the similarities p_{ij}. It measures similarities q_{ij} between two points in the map y_i, y_j. The locations of the points y_i in the map are determined by minimizing the Kullback–Leibler divergence

$$KL = \sum_{i \neq j} p_{ij} \log \frac{p_{ij}}{q_{ij}}$$

The resulting figure is shown below.

Here we need to make some notes:

1. On the correct picture we see that there exist simple feature representation, where all addresses are located on the sphere or very close to it.

2. Addresses were distributed unevenly, mostly in a small circle area on the surface of the sphere. The central part of that area is populated with addresses having just a few transactions.

3. K-means failed to detect correctly these clusters: the circle cluster of highly active nodes has been recognized as many small clusters instead, leading to a completely incorrect result.

4. Using t-SNE can even further lead to a misperception, since it deforms cluster geometry, making the case of circle cluster broken down into many small ones harder to recognize.

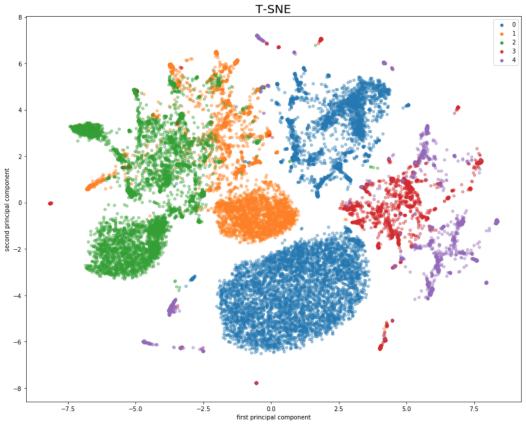

Figure 5. 16-dimensional data as returned by node2vec mapped to 2-dimensional plane.

On the figure we can see the clustered structure.

H. Technical details

We get the data about the addresses with maximum balance.

	from_address	to_address	value_eth
0	0x0a15f00eab4313f2157db0bb31b8b05ead193445	0x03098c1632399bf0ee1be9cd91ba605c6f0671d3	0.01
1	0x07283e73a2032d41fdea3886dc8c2ca27e307c25	0x08ba8a8779305da712b14d1b7121c31e9652035e	7.99
2	0x0681d8db095565fe8a346fa0277bffde9c0edbbf	0x050131ee5ecaf4174e712950ab2897991cb7115b	0.32

Figure 6. DataFrame of transactions

Using networkx we find the maximal connected component. The result was about 25000 nodes.

```
g = nx.from_pandas_edgelist(df,
  source="from_address",
  target="to_address")
Gc = max(
  nx.connected_component_subgraphs(g),
  key=len)
```

These nodes were then consecutively numbered to obtain much more concise integer ID, which will be used instead of 20-byte long addresses.

```
Gc_numbered =
nx.relabel.convert_node_labels_\
  _to_integers(
    Gc, label_attribute="address",
    ordering="decreasing degree")
df_connected_numbered =
nx.to_pandas_edgelist(Gc_numbered)
```

They were processed using node2vec to learn continuous feature representations. Running the node2vec program with training parameters dimention (d) = 16, length of walk per source (l) = 20, number of walks per source (r) = 5, context size for optimization (k) = 5:

```
../../snap/examples/node2vec/node2vec
-i:df_connected_numbered.csv
-o:node2vec_embedding.txt
-d:16 -l:20 -r:5 -k:5 -v
```

For 24936 nodes 1GB Ram is Used and real 0m31.538s Then we read embedding results into pandas DataFrame.

```
df_node2vec = pd.read_csv(
"node2vec_embedding.txt",
sep=" ", skiprows=1, header=None)
```

To analyse the results we need convert back numbered id to string type and so we change number of node into address name.

```
df_node2vec_address = df_node2vec.copy()
#create a new dataframe for renaming
#back node ids to addresses
df_node2vec_address =
df_node2vec_address.astype({0: str})
#convert id to str type and change
#node_id to address
for i, line in
  df_node2vec_address.iterrows():
    node_id = int(line[0])
    address =
    Gc_numbered.nodes[
      node_id]["address"]
    df_node2vec_address.at[i,0] =
      address
```

Then we determine how many clusters is optimal for clustering and silhouette analysis. Then we use the standard procedure for silhouette analysis and t-SNE to get graphic interpretation of clusters.

I. Results and Further research

We have studied various methods to learn feature representation. While some methods didn't appear to be acceptable for the task, the analysis of arising issues and its underlying reasons have led us to the rigid, scaling and performant approach. We are going to continue research in this direction.

References

[1] Nakamoto, Satoshi. "Bitcoin: A peer-to-peer electronic cash system." (2008).

[2] F. Reid, M. Harrigan, An analysis of anonymity in the bitcoin system, In: Proc. of IEEE Third International Conference on Privacy, Security, Risk and Trust, 2012, pp. 1318-1326.

[3] P. Koshy, D. Koshy, P. McDaniel, An analysis of anonymity in bitcoin using p2p network traffic. In Proc. of Financial Cryptography and Data Security, 2014, pp. 469-485.

[4] A. Biryukov, D. Khovratovich, I. Pustogarov, Deanonymisation of clients in bitcoin p2p network. In: Proc. of Computer and Communications Security, 2014, pp. 15-29.

[5] Monero, Monero-secure, private, untraceable, (https://getmonero.org/), accessed on Jan. 21, 2018.

[6] V. Monaco, Identifying bitcoin users by transaction behavior, In: Proc. of Biometric and Surveillance Technology for Human and Activity Identification XII, 9457(2015):945704.

[7] C. Zhao, Graph-based forensic investigation of bitcoin transactions, Master's thesis, Iowa State University, 2014, doi: https://doi.org/10.31274/etd-180810-3797.

[8] A. Kosba, A. Miller, E. Shi, Z. Wen, C. Papamanthou, Hawk: The blockchain model of cryptography and privacy-preserving smart contracts, In: Proc. of Security and Privacy (S&P), 2016, pp. 839-858.

[9] C. K. Frantz, M. Nowostawski, From institutions to code: Towards automated generation of smart contracts, In: Proc. of Foundations and Applications of Self* Systems, 2016, pp. 210-215.

[10] F. Zhang, E. Cecchetti, K. Croman, A. Juels, E. Shi, Town crier: An authenticated data feed for smart contracts, In: Proc. of the 2016 ACM SIGSAC Conference on Computer and Communications Security, 2016, pp. 270-282.

[11] Wood, Gavin. "Ethereum: A secure decentralised generalised transaction ledger." Ethereum Project Yellow Paper 151 (2014): 1-32.

[12] " The Ethereum Nodes Explorer". Accessed April 28, 2018. https://www.ethernodes.org/network/1/nodes

[13] "Etherchain - The Ethereum Blockchain Explorer". Accessed April 28, 2018. https://www.etherchain.org/charts/averageBlockUtilization

[14] B. Recht, C. Re, S. Wright, and F. Niu. Hogwild!: A lock-free approach to parallelizing stochastic gradient descent. In *NIPS*, 2011.
[15] L. Backstrom and J. Leskovec. Supervised random walks: predicting and recommending links in social networks. In *WSDM*, 2011.
[16] S. Cao, W. Lu, and Q. Xu. GraRep: Learning Graph Representations with global structural information. In *CIKM*, 2015.
[17] L. A. Adamic and E. Adar. Friends and neighbors on the web. *Social networks*, 25(3):211–230, 2003.
[18] S. Fortunato. Community detection in graphs. *Physics Reports*, 486(3-5):75 – 174, 2010.
[19] Grover, Aditya and Leskovec, Jure node2vec: Scalable feature learning for networks 2016, Proceedings of the 22nd ACM SIGKDD international conference on Knowledge discovery and data mining
[20] Buterin, Vitalik and others A next-generation smart contract and decentralized application platform

A Tool for Identification of Unusual Wallets on Ethereum Platform

Mikhail Petrov[1] Rostislav Yavorskiy[2]

National Research University Higher School of Economics
Myasnitskaya 20, Moscow, Russia
mishanayrus@gmail.com[1] ryavorsky@hse.ru[2]

Abstract. We present a tool for identifying the most suspicious Ethereum wallets by finding atypical vertices of the transactions graph. We inspect different characteristics of the wallets and the transactions they were involved in during a week. First, we identify "typical" groups of nodes. Then the nodes which are far different from all these groups are considered to be suspicious.

Keywords: Ethereum platform · cryptocurrency transactions · transactions graph.

1 Introduction

Anomaly detection is an area that has been receiving much attention in recent years. It has a wide variety of applications, including fraud detection, network intrusion detection, medical diagnosis and other fields. Usually research in this area is using attribute-value data as the medium from which anomalies are to be extracted. Some works are focused on anomaly detection in graph-based data. In our paper we are going to combine these approaches for the goal of identification of suspicios wallets in a cryptocurrency community.

1.1 Cryptocurrencies and Ether

The area of cryptocurrency is quite young. The first appearance of Ether, the transactions graph of which will be analyzed in this article, appeared in 2013. By now the analysis of the Ether community has progressed very little. One can find quite many articles on the analysis and prediction of cryptocurrencies rates, but so far few research has been focused on the analysis of exchange communities for the cryptocurrencies.

It is known that the semantics of transactions of blockchain systems can be captured by a transaction graph, see e.g. [1]. Such a graph generally consists of the states and the transactions as transitions between the states, together with conditions for the consistency and validity of transactions.

Detailed overview of cryptocurrencies could be found in [4].

1.2 Overview of anomaly detection methods

In [8] a comprehensive survey of recent anomaly detection systems and hybrid intrusion detection systems is provided, and recent technological trends in anomaly detection are also discussed. In [2] existing techniques are grouped into different categories based on the underlying approach adopted by each technique. For each category key assumptions are identified, which are used by the techniques to differentiate between normal and anomalous behavior. In [7] two techniques for graph-based anomaly detection are introduced. The authors suggest a new method for calculating the regularity of a graph, with applications to anomaly detection. Experimental results are provided which use both real-world network intrusion data and artificially-created data. In [5] several information-theoretic measures, namely, entropy, conditional entropy, relative conditional entropy, information gain, and information cost for anomaly detection are used.

1.3 Networks analysis

As it was already mentioned, see [7], some anomaly detection method use graph-based analysis. Besides standard graph analysis library networkx, we are also using statistical properties of social networks, see [3, 6].

1.4 Structure of the remaining text

The rest of the paper is organized as follows. Section 2 describes the data we worked with. Section 3 describes the methods we used to analyze transaction data. Section 4 presents a description of how the points for the strangeness rating were calculated. Section 5 shows the top 5 vertices as a result of calculating the suspiciousness rating with the rating values.

2 The data analyzed

In this paper data on all transactions for a week was downloaded using the open etherium API. Significant characteristics for the community analysis were chosen, and an ether exchange graph was constructed based on them. The vertices of this graph are the participants in the platform and also the edges are the transactions between these participants. Further in the received graph, the characteristics of the vertices were calculated, clusters were found, and associative rules based on them were constructed. As a result, taking into account the data on graph vertices, clustering, and associative rules, the suspiciousness rating of vertices was constructed.

Since in this paper we were focused on identifying suspicious and untypical members in the ether exchange community, only those characteristics that were useful for analyzing and constructing the graph were extracted from the set of parameters.

2.1 Ethereum API

Ethereum API provides information about each block, all transactions and every members of the network. JSON RPC API of the Ethereum platform currently supports four programming languages: C++, Go, Python, and Parity. Also there is an option to access the data via web interface at *https://etherscan.io*, which we used.

For our study all transactions executed during a particular week have been downloaded. That was done using the timestamp field of the blocks and the method eth_getBlockByNumber().

Totally information about 3,382,252 transactions were collected.

2.2 Format of Ethereum transaction data

All transactions were selected from each block and then the following four parameters were saved for each transaction:

- address of the sender;
- address of the receiver;
- date and time of the transaction;
- the amount of the internal currency (wei) that is transferred.

These characteristics of transactions allow us to construct the graph of an ether exchange. The vertices in this graph are the addresses of wallets which are either senders or receivers of these transactions, the edges correspond to the transactions themselves.

In this paper we analyze only total amount sent from node A to node B and ignore details about the number of transactions and distribution of the amount between them.

In addition to the total volume transmitted between a pair of wallets, the frequency of interactions between participants (the number of transactions sent) could be considered too.

2.3 Transactions graph

The resulting set of transaction on ether exchange was processed and presented as a graph. The first step to getting the graph was renaming vertices, since addresses do not make any sense. In order to save memory and more clarity, they were numbered with the help of natural numbers, and the dictionary with addresses mapping in the vertex numbers was saved in the file.

Next, we summed the weights of the edges between identical pairs of sender and receiver, recorded the graph as an adjacency list with edge weights and the total number of transactions between vertices. As a result, we obtained an undirected graph with positive and negative edge weights. The graph has 1,577,010 vertices and 4,963,980 edges. To analyze this graph we used networkx, a common library of the Python language. All further operations for calculating the various characteristics of the graph have been done with the help of this library.

3 Analysis

Our anomaly detection analysis consists of the following four parts:

1. **Graph connectivity analysis.** During this step we put off wallets for which too few information is available, so no meaningful analysis could be conducted for them.
2. **Analysis of the vertex characteristics.** Here we compute degree, centrality and containing k-core for each vertex of the transaction graph.
3. **Cluster analysis.** The clustering is performed based on the vectors obtained in the previous section.
4. **Association rules** are used to find patterns that can be traced in this graph.

After each part all the vertices are ranged according to their suspiciousness, and then these ratings are merged into one.

3.1 Connectivity analysis

The next step was to analyze the connectivity components of the obtained graph. The graph has 35,628 connectivity components. These components can be divided into three groups:

- The main component of a large community. In this component there are 1,474,024 vertices. Most likely, it is a graph of the interaction of people of some large service or exchange, but the exact meaning is not yet clear. This component has the biggest interest for analysis and will continue to be the first in priority.
- The second type is a small groups of ten to a thousand people. Most likely, these groups are small companies in which payment occurs in the cryptocurrency, or small communities that pay cryptocurrency for some services. This group also deserves attention for analysis, but to a lesser extent.
- The third class includes groups of up to ten people. These are some local exchanges of money, betting between people. This group has no interest for analysis, since it does not contain any meaningful information.

As was mentioned above, the first group has the greatest interest for analyzing, therefore it will be analyzed in the future. The remaining connectivity components are stored in separate files and their analysis is possible in future work.

3.2 Vertex Characteristics

Since the main purpose of the work is to distinguish atypical and suspicious vertices, then we must determine the typical aspects of the obtained community. Taking into account that the received connectivity component can have multiple chains of elements with a degree equal to two, therefore the graph has many

vertices that are just a link in the chain of transmission of the cryptocurrency, it was decided to allocate the k-cores of the graph of this component. A k-core of a graph G is a maximal subgraph of G in which all vertices have degree at least k. To do this, we run a search of the value of k-cores from 1 to 50 and used the method *k_core* for each value. If the k-core was not found for the value of n, then it will not be found for n + 1, since any k+1-core is also a k-core. Therefore, if such a situation arises in searching the k-cores, then the search can be stopped.

The algorithm stopped at k equal to 15, which means that the k-kernels from 1 to 14 were found. Since the sizes of k-cores beginning with k equal to 8 are already sufficiently small and the 3-core is quite large, 4, 5, 6, and 7 core were chosen as an optimal from the point of view of time for analyzing the graph. Based on the selected k-cores we can calculate new characteristics of the vertices. Three kinds of centrality were calculated for each vertex in the core: betweenness centrality, closeness centrality and degree centrality. Also we add vertex degree as a characteristic. On the basis of the obtained data, we can form a vector that will describe the vertices of the graph (participants of the cryptocurrency community), split each characteristic into groups of segments and create binary vectors for deriving associative rules.

As a result, we obtained a 5-dimensional vector characterizing the vertices of the graph: 3 kinds of centralities; number of the k-core, which vertex belongs; degree of a vertex. Also, the dimensionality of these vectors could be increased by adding distance to the hubs for each of the characteristics, but this operation is planned for the next stages of the work. The resulting vectors can be clustered now.

3.3 Clustering

Based on the vectors obtained in the previous section, clustering is performed using the standard k-means method. Since for this method it is necessary to initially know the number of clusters we must first determine this number. To determine the optimal number of clusters all numbers from 0 to 200 in steps of 10 were chosen, clustering was performed and the result were checked with Silhouette and the shoulder methods.

Table 1. The Silhouette Coefficients

Number of clusters			
Coefficient value			
10	20	30	40
0.6768368853142156	0.7095846965311733	0.8111177029982155	0.8702494303581093
50	60	70	80
0.9146516160235698	0.9293358278581296	0.9387072507702181	0.9478746102234425
90	100	110	120
0.9505421030096185	0.950768946865395	0.7874773068611389	0.7884553347797727
130	140	150	160
0.7698049042610146	0.7467290976039868	0.7992449839069017	0.7467532658132512
170	180	190	
0.7044007926707637	0.6867901637311503	0.665831212711668	

As you can see, this method shows that the most optimal number of clusters is $n = 100$, but not too far from 50 to 100. The result of the shoulder method is shown below:

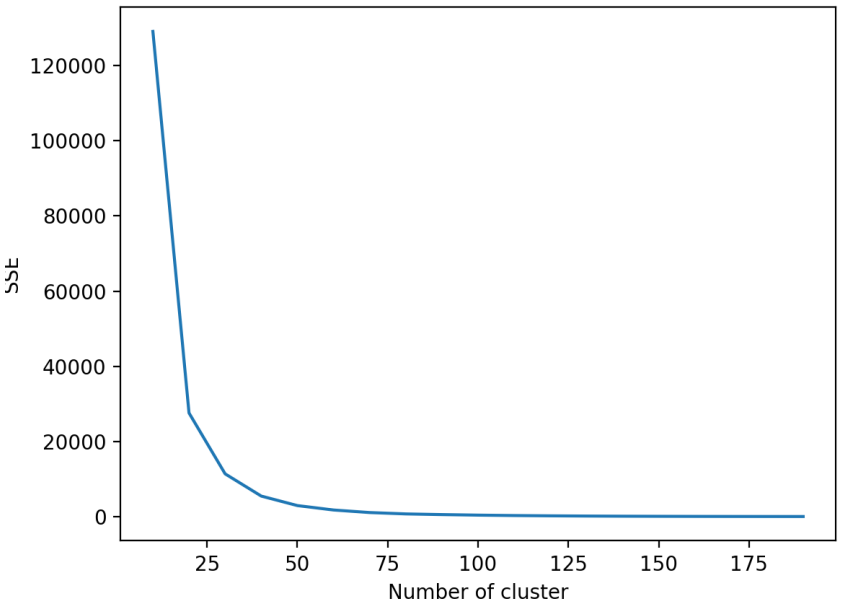

This chart shows that the optimal amount is $n = 30$. Since the optimal number of clusters depends very much on the type of data, both methods do not always correctly indicate the right result, so the combined solution of the two methods was chosen as the right answer. As a result, the optimal number of clusters was chosen to be 50 and clustering was performed for it using the k-

means method. Distribution of the cluster size can be seen in the figure number 3:

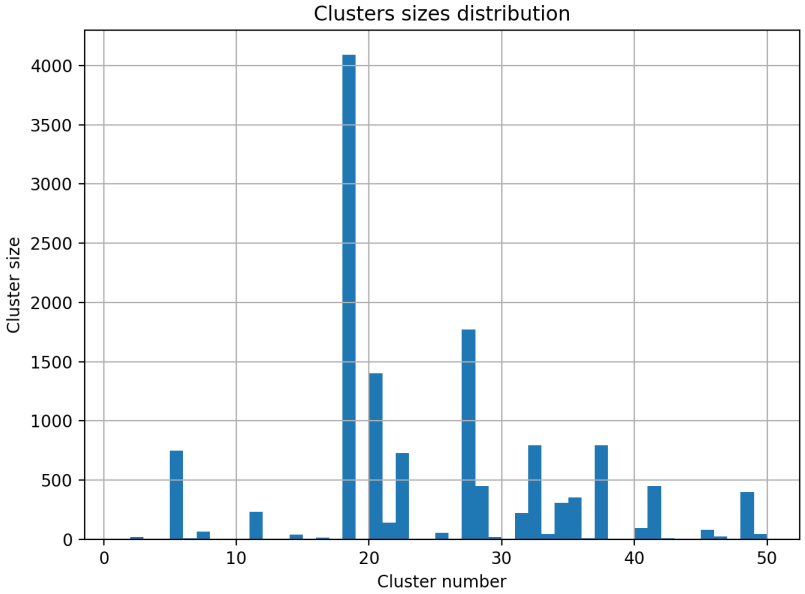

It can be seen from the distribution diagram that one strongly dominant in terms of the size of the elements cluster, two clusters slightly above the average level, about 15 clusters of medium size and the other clusters of a very small size were obtained. These results will be used in the next chapter to build associative rules.

3.4 Association Rules

Now based on all of the characteristics of the community we can try to find patterns that can be traced in this graph. For example, it may happen that if the vertex belongs to the 4-core, then its degree must necessarily be higher than 7. To do this, it is necessary to generate binary vectors in which the element at the i-th position will report whether this element belongs to a certain group or not. Having formed such vectors, we can find patterns, but on first step we need to form the groups themselves. For this, it is necessary to analyze the distribution of the characteristics of the vectors. To achieve this, we should construction distribution histograms for each of the characteristics. The first and third graphs of distributions are strongly shifted to the left, and the thresholds

between the groups are not visible, so we need to look at the left parts closer:

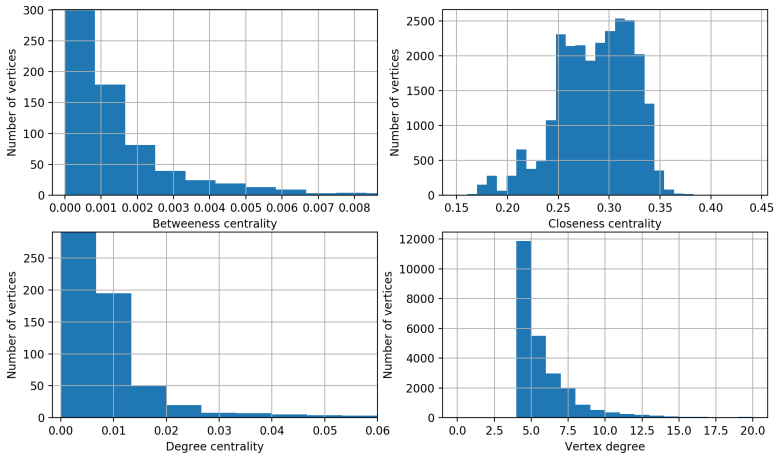

From the received observations it is possible to break each of the characteristics into ranges of values into which approximately equal number of elements will fall. These ranges will also form groups for finding associative rules. The result is the following groups:

Table 2. Groups

Degree centrality	Betweenness centrality	Closenness centrality
$0 < x \leq 0.005$	$0 < x \leq 0.0005$	$0 < x \leq 0.2$
$0.005 < x \leq 0.015$	$0.0005 < x \leq 0.001$	$0.2 < x \leq 0.3$
$0.015 < x$	$0.001 < x$	$0.3 < x \leq 0.4$
		$0.4 < x$

Generation of binary vectors is now carried out. To search for associative rules we used the mlxtend library, which is the apriori method to search for frequent sets of attributes, and then search for associative rules. In our script the rules with a minimum support = 0.8 are taken so that the existing patterns are highly probable. As a result of the launch, two associative rules were found:

Table 3. New rules table

Number	Antecedants	Consequents	Antecedent support	Consequent support
0	1 deg. cen. group	1 bet. cen. group	0.997946	0.994034
1	1 bet. cen. group	1 deg. cen. group	0.994034	0.997946
Support	Confidence	Lift	Leverage	Conviction
0.993876	0.995922	1.001899	0.001884	1.463008
0.993876	0.999841	1.001899	0.001884	12.922448

To get more associative rules, we need to decrease the support threshold, but then there will be less probabilistic associative rules, which will contradict the goal of finding typical signs of this community.

4 Top strangeness rating

Now, when there is a whole set of characteristics of the vertices (clustering results, clustered vectors, associative rules), we can start isolating their typical values and finding all the values that will go beyond this framework. For each overshoot of these boundaries points are entered, which will award the vertices with these atypical characteristics. For each "suspicious" characterization points from 1 to 100 will be given depending on the criticality. At the end, the promised rating of the suspicious vertices of the community graph will be obtained.

Let's start with the simplest - associative rules. Here everything is simple, because if a vector does not obey this rule, then it is atypical for this community. Here, the scores in the scores will be determined by the value of the support of the associative rule multiplied by one hundred.

The next will be the scoring of vertices whose vectors are too far from the center of their clusters. We can calculate the average distance to the center of each cluster and the variance. Accordingly, if the distance of the vector does not fall within the range of the mean ± variance, then this vector is atypical. Points will be calculated according to the following formula:

$$\frac{|mean - distance|}{difference_{max}},$$

$mean$ is the average distance to the center in the cluster
$distance$ - the point to the center of a particular windbreaker
$difference_{max}$ is the maximum difference between the average and the distance from the vector to the center inside the cluster

Next will be scoring the vertices, whose characteristics of the vectors also go beyond the limits of the mean ± variance. Here the same normalized formula will be used, as well as with distances.

The last will be awarded for belonging to atypical small clusters. Since the sizes of some clusters reach even one, this clearly indicates the atypicality of

the vertices in such clusters. Here we can not use the metric, as in the previous two cases, because the dimensions are too scattered, the average is quite heavily shifted to the left and the variance is several times larger than the average, which moves the left border to the minus. With a normal distribution, the segment of the mean ± variance covers approximately 68 percent of the values and for a given number of clusters equal to 50 these 68 percent are 34. Therefore, it was decided to score points to the vertices contained in the 16 smallest clusters. Since the number is 16 the vertice that hit the latest one will get 6.25 points; which falls in the second from the end - 12.5 and so on up to 100. As a result of summation of the values on the vertices we get the rating of the suspicious vertices of the community graph for the exchange of ether.

5 Conclusion

5.1 Result

As a result of this work the open API Ethereum platform was used to download data on all transactions for the week. A community graph on ether exchange was built for the week. Further, the analysis of the obtained graph, the separation of the characteristics of vertices, clustering of vertices according to the selected characteristics and the derivation of associative rules were carried out. The result of the work is the algorithm for constructing the rating of the suspicious vertices of the community graph. Since the algorithm generates a rating based on deviations from the standard values inside the similar wallets groups, the algorithm finally reveals the most suspicious wallets that differ from the general background. These wallets most likely have large transaction volumes on the balances or passing through them.

After summing up all the points by the nodes the rating of the suspicious vertices for the exchange of the Ether was obtained. Below are the top of 5 values of this rating:

Table 4. Top 5 suspicious vertices

Value	Node number
499.66345040230755	311861
488.3862740302283	633953
481.4078191332377	16010
457.7035133901014	314045
437.19194102533953	1627

As you can see, there are vertices with a fairly large number of points at the top of the rating, given that the maximum is 700 points. This indicates that the same vertices received points of 4 or more rules. Hence, it is stands out of

the general background immediately by several characteristics, which proves its strangeness.

References

1. Christian Cachin, AD Caro, Pedro Moreno-Sanchez, Björn Tackmann, and Marko Vukolic. The transaction graph for modeling blockchain semantics. Technical report, Cryptology ePrint Archive, Report 2017/1070, 2017.
2. Varun Chandola, Arindam Banerjee, and Vipin Kumar. Anomaly detection: A survey. *ACM computing surveys (CSUR)*, 41(3):15, 2009.
3. Aric Hagberg, Pieter Swart, and Daniel S Chult. Exploring network structure, dynamics, and function using networkx. Technical report, Los Alamos National Lab.(LANL), Los Alamos, NM (United States), 2008.
4. Jan Lansky. Possible state approaches to cryptocurrencies. *Journal of Systems Integration*, 9(1):19–31, 2018.
5. Wenke Lee and Dong Xiang. Information-theoretic measures for anomaly detection. In *Security and Privacy, 2001. S&P 2001. Proceedings. 2001 IEEE Symposium on*, pages 130–143. IEEE, 2001.
6. Mary McGlohon, Leman Akoglu, and Christos Faloutsos. Statistical properties of social networks. In *Social network data analytics*, pages 17–42. Springer, 2011.
7. Caleb C Noble and Diane J Cook. Graph-based anomaly detection. In *Proceedings of the ninth ACM SIGKDD international conference on Knowledge discovery and data mining*, pages 631–636. ACM, 2003.
8. Animesh Patcha and Jung-Min Park. An overview of anomaly detection techniques: Existing solutions and latest technological trends. *Computer networks*, 51(12):3448–3470, 2007.

Vulnerabilities Detection via Static Taint Analysis

Nikita Shimchik
Ivannikov Institute for System Programming of the Russian Academy of Sciences (ISP RAS)
Moscow, Russian Federation
shimnik@ispras.ru

Valery Ignatyev
Ivannikov Institute for System Programming of the Russian Academy of Sciences (ISP RAS), CMC MSU
Moscow, Russian Federation
valery.ignatyev@ispras.ru

***Abstract*—Due to huge amounts of code in modern software products, there is always a variety of subtle errors or flaws in programs, which are hard to discover during everyday use or through conventional testing. A lot of such errors could be used as a potential attack vector if they could be exploited by a remote user via manipulation of program input. This paper presents the approach for automatic detection of security vulnerabilities using interprocedural static taint analysis. The goal of this study is to develop the infrastructure for taint analysis applicable for detection of vulnerabilities in C and C++ programs and extensible with separate detectors. This tool is based on the Interprocedural Finite Distributive Subset (IFDS) algorithm and is able to perform interprocedural, context-sensitive, path-insensitive analysis of programs represented in LLVM form.**

According to our research it is not possible to achieve good results using pure taint analysis, so together with several enhancements of existing techniques we propose to supplement it with additional static symbolic execution based analysis stage, which has path-sensitivity and considers memory region sizes for filtering results found by the first stage. The evaluation of results was made on Juliet Test Suite and open-source projects with publicly known CVE.

***Index Terms*—static code analysis, taint analysis, vulnerabilities**

I. Introduction

In the paper we consider a specific subset of all possible software vulnerabilities – ones which are caused by utilizing unchecked user-provided data in critical functions or code instructions. This class includes, but is not limited to vulnerabilities allowing such important attacks as SQL Injection, Buffer Overflow and XSS attacks.

One group of methods used to represent and discover such vulnerabilities is called taint analysis. In general, taint analysis starts from so-called taint sources – pre-defined functions, which provide special "tainted" data. For example, we may say that the result of a *read()* call will contain untrusted data and thus call it a taint source. Besides that, any value dependent on tainted data is declared to be tainted itself.

There are also so-called taint sinks – special functions or instructions which should never accept tainted data as arguments. Continuing our example, it is not safe to use values, obtained from *read()* call, as a buffer index, since this may lead to a memory corruption and a variety of other problems, thus we may call any pointer dereference instruction a taint sink.

Taint analysis is expected to report such potentially dangerous data flows for a manual or automated verification.

Taint analysis may be performed both as a part of dynamic and static analysis and each approach has its own advantages and drawbacks.

Dynamic analysis is performed during program execution and thus has low false positive rate, but it requires a lot of test runs and it could be close to impossible to explore all possible execution paths in a non-trivial program due to path explosion problem – this is important since some vulnerabilities could actually be hidden on complex execution paths, which are hard to discover using dynamic analysis or testing.

Static analysis on the contrary doesn't execute the analysed program, but processes some kind of model instead. Depending on a specific algorithm, this could enable an analyzer to explore almost all possible execution paths, which is a significant advantage in terms of security, but is also likely to increase amount of false positives due to inconsistencies between program and its model.

In this work the term "taint analysis" will be used to refer to "static taint analysis" and we define taint sources as all functions providing untrusted data and taint sinks as all instruction parameters or function call arguments which may cause undesired program behavior if one allow an attacker to pick an arbitrary value for it.

We propose some extensions to the interprocedural context-sensitive taint analysis algorithm originally defined in [1]. Implementation of the algorithm is based on the LLVM compiler infrastructure and uses LLVM bitcode as an intermediate representation.

The paper is organized as follows. In Section II we briefly discuss the general idea of IFDS algorithm and its application to the taint analysis problem. Section III describes several approaches developed to make memory model used by taint analysis more precise and our improvements of indirect calls resolution. Section IV summarizes our attempts to decrease false positive ratio by performing additional verification step for all reported vulnerabilities. Section V reports experimental results. In the last section, we summarize the results of the work and present directions of future research.

II. Related Work

A. IFDS Framework

Reps et al. [2] introduced an efficient, context-sensitive and flow-sensitive dataflow analysis framework which is able to solve a large class of interprocedural dataflow problems.

This class of problems is called IFDS (Interprocedural, Finite, Distributive, Subset) problems and consists of all dataflow problems in which the set of dataflow facts is a finite set and dataflow functions distribute over the meet operator (either $\cup$ or $\cap$). The algorithm solves an IFDS problem in a polynomial time by transforming it into a problem of reachability along interprocedurally realizable paths. The complexity of the algorithm is shown to be $O(ED^3)$ in general case and $O(ED)$ for locally separable problems, where E is the number of edges in the interprocedural control flow graph and D is the number of dataflow facts.

According to the algorithm, the program should be represented as a directed super graph $G = (N, E)$, which contains a union of all functions' control flow graphs (CFG) with some special nodes and edges described below.

- There is a single entry and exit node for every function in a program.
- Every call statement is represented with two adjacent nodes: a call-site node and a return-site node. For every such statement there is an intraprocedural edge from call-site to the corresponding return-site node, an interprocedural edge from the call-site to the corresponding called function's entry node and an interprocedural edge to the return-site coming from the corresponding called function's exit node.

The general idea of the algorithm is to construct a directed exploded super graph $G_e = (N_e, E_e)$ with $N_e = N \times D$ set as nodes (where N is the set of super graph nodes and D is the set of dataflow facts) in which any node (s, d) is reachable from a special start node iff the dataflow fact d holds at node s.

Later several extensions to the IFDS algorithm were proposed by Naeem et al. [3], such as constructing nodes of a super graph on demand (which is important when dealing with large D sets) and exploiting existing subsumption relationships between elements of D set to perform more efficient analysis. It has been reported that these extensions are often necessary when applying the IFDS algorithm to non-separable problems, such as alias set analysis.

B. IFDS based taint analysis

Flowdroid [4] is one of the most well-known implementations of the IFDS framework for data leaks detection in Android applications. It demonstrates a possibility to perform taint analysis in terms of IFDS framework and also explains how to combine on-demand backward alias analysis with a regular forward taint analysis. In Flowdroid, dataflow set D is defined as the set of access paths, plus a special "true" fact $[\emptyset]$. An access path consists of a base value (such as a local variable or parameter) with potentially empty ordered list of fields and could be written e.g. like $\langle x; f, g\rangle$ which corresponds to `x.f.g` Java expression, where x is the name of the base object, f is the name of the dereferenced field of x object and g is one of the fields of $x.f$ object.

Dataflow fact $x.f$ holds at node s iff an object, which is accessible through this access path at s, may contain tainted data here. $x.f$ being tainted implies the fact that all object, accessible through this object (such as already mentioned $x.f.g$), are also considered tainted.

III. Taint analysis stage

Our experience with the development of vulnerabilities detection tool based on taint analysis shows that resulting warnings contain a lot of false positives. Particular results evaluation makes it possible to discover 2 main roots of the problem: path-insensitivity and inaccurate sizes of tainted objects. It's unclear how to resolve both issues without complex memory model, which would allow to build path and object size conditions. We deal with it by using external symbolic execution engine, forcing it to execute the exploded graph subset corresponding to any specific warning.

Initial warning set is generated by the tool based on [1] and is greatly inspired by Flowdroid design. It uses LLVM as intermediate representation. Due to a low-level nature of LLVM bitcode, we use another definition of access path: an access path consists of a base value (which is an actual LLVM value) and an ordered list of dereference offsets. This definition is suitable for referencing both structure fields (since in LLVM bitcode it is possible to calculate a fixed offset for any structure field) and memory locations, accessible with a help of simple pointer arithmetics. In this paper we will use $[\textit{pointer}, \textit{offset}]$ to denote value, accessible through dereference of *pointer* value plus *offset* bytes, $[\textit{integer}]$ to denote value of the *integer*, and $[\emptyset]$ to denote a special "true" fact. It is possible to specify a list of offsets to define a sequence of consecutive dereferences.

Let's consider an example on Fig.1, written in C language.

```
extern void *a;
extern void *b;

void source(int *pointer) {
  scanf("%d", pointer);
}

void sink(int size) {
  memcpy(a, b, size);
}

void foo(int *t) {
  source(t);
  sink(*t);
}
```

Fig. 1. Example of program with interprocedural taint flow

Omitting insignificant details, it is possible to say that

- *scanf* function call is a taint source, since it changes the value pointed to by the *pointer* parameter to an arbitrary value chosen by the user.

- *memcpy* function call copies *size* bytes from the object pointed to by *b* variable to the object pointed to by *a* variable. We may call it a taint sink, since it is dangerous to specify *size* values greater than actual size of objects pointed to by *a* or *b*.
- *source* function's entry-to-exit subgraph can be summarized with the path edge $(\textit{source-Entry}, [\emptyset]) \rightarrow (\textit{source-Exit}, [\textit{pointer}, 0])$, i.e. value of $[\textit{pointer}, 0]$ becomes unconditionally tainted.
- *sink* function's subgraph can be summarized with the path edge $(\textit{sink-Entry}, [\textit{size}]) \rightarrow (\textit{Sink}, [\textit{size}])$, i.e. tainted data would reach a taint sink if the value of $[\textit{size}]$ is known to be tainted at the entry of the *sink* function.
- *foo* function's subgraph can be summarized as $(\textit{foo-Entry}, [\emptyset]) \rightarrow (\textit{source-callsite}, [\emptyset])$
  $\rightarrow (\textit{source-retsite}, [t, 0])$
  $\rightarrow (\textit{sink-callsite}, [t, 0])$
  $\rightarrow (\textit{Sink}, [\textit{size}])$, i.e. tainted data unconditionally reaches a taint sink.

Unlike in known implementations and Flowdroid we don't store the whole exploded super graph, because it requires too much memory for regular industrial project with millions lines of code even if this graph is constructed on-demand. To solve this issue another analysis mode was developed, which doesn't require exploded super graph edges to be constructed. The existing IFDS analysis engine was supplemented with function summaries (similar to [3]) and explicit taint traces, which makes it possible to show user where the tainted data originate from and how did it get to the taint sink without the need to store the graph itself.

As we've noticed during analysis of selected open source projects, the majority of taint sources is usually located "far" from each other in a program and thus their taint flow subgraphs are rarely intersecting. To decrease memory consumption, we have added an ability to run a separate analysis for every taint source. Therefore, exploded graph nodes and summaries can be cleared, but the total analysis time could increase since parts of the program graph can be potentially analyzed more than once.

The second significant difference with other implementations is that each request for a set of aliases for any specific tainted value is handled in a separate local environment with its own IFDS solver and exploded super graph. The graph is cleared after the call and only the resulting aliases set is preserved so that it could be reused both in main taint analysis and when calculating other aliases sets.

Remaining improvements are discussed in following subsections III-A and III-B with more details.

A. Unresolved function calls

When examining a call site we assume that it is trivially easy to determine the called function by the generated bitcode. Unfortunately, C and C++ programs contain calls, whose targets couldn't be determined until runtime. There are three main sources of such unresolved calls, described below:

1) virtual functions;
2) external functions;
3) indirect calls.

C++ virtual function is a member function declared within a base class and overridden by the method in the derived class. When performing a virtual call, the called function is determined by the actual type of the object and may vary in runtime. Such calls were already handled in the previous implementation of the algorithm [1] by adding interprocedural edges to all possible overrides.

Another case of a call with unknown called function is an external call. There are two main kinds of external calls: library functions and system calls. In both cases the analyzed program doesn't contain called functions' definitions and thus we cannot add any "call-site to entry" and "exit to return-site" edges to the call and has to rely on "call-site to return-site" intraprocedural edge only.

By default we assume that an external function can change values of all its arguments, unless it contradicts with language semantics, so the corresponding facts are not propagated further. We also assume that external function doesn't change value of any global variable and leave it tainted. Usually such assumptions lead to an undertainting and thus we've developed several ways to deal with this issue:

1) Since there is a limited number of system functions and most of them are well-documented, it is possible to create summaries (models) for most frequently used ones manually. Our tool also provides the list of external functions encountered during analysis, which makes it possible for user to prepare summaries for them. It's also possible to specify custom sources, sinks and propagators using similar files in JSON format – those summaries are applied at "call-site to return-site" edges.
2) For an open-source library it is possible to compile it into LLVM bitcode and then link it together with the analyzed program's representation using *llvm-link* program, which is a part of LLVM infrastructure.
3) If some specific parameter of an external function has type with *const* qualifier, which specifies that its value should remain unchanged after invocation, we derive a rule for propagating taint through the corresponding argument in every call of this function. Unfortunately, a lot of type-related information, including constancy, is lost during compilation, so we had to add several modifications to the Clang compiler in order to store this information in the LLVM metadata.

Lastly, there is another type of calls where the memory address of the called function is calculated at runtime – such calls are named indirect calls. It is possible to say that a virtual call is just a special case of such indirect call. C developers sometimes use indirect calls to simulate virtual calls functionality available in C++ and thus it could be important to support such calls. For example, such technique is used in security-critical OpenSSL library.

We've evaluated several ways to handle indirect calls, described below. Firstly, we make the following assumptions

for an indirect call:

(A) the indirect call is never used for invocation of any external function, thus the analyzed program contains definitions for all possible candidate functions;
(B) the set of all possible candidates is completely determined by the program itself, which means that for all possible target function there is a path in the program where the address of the given target is taken and transferred to the indirect call instruction.

If (A) is considered to be false, such indirect call is actually an external call and should be handled as appropriate, otherwise we can examine following approaches:

1) The naive approach is to take every function definition with compatible parameter types and consider as a candidate. The problem of this approach is that all functions with 0 parameters are indistinguishable and most functions with 1-2 parameters are divided into large clusters. If we also assume (B) to be true, this approach could be slightly improved by excluding functions, whose address was never explicitly taken in the program.
2) Another approach relies on the assumption that both functions and variables in a program are usually named according to their semantics. In this case it should be possible to compare similarity between call instruction and different call candidates to choose the most likely called function. Unfortunately, the function and variable names are virtually never plain equal and while it should be possible to write an automated heuristic, its results would be unreliable due to lack of formal specifications regarding naming. Such a heuristic would need to put "encrypt_string", "EncryptString", "EncryptUTF", "encstr" names into the same similarity cluster, but differentiate between "encrypt" and "decrypt" function names. Common abbreviations, such as "Context – ctx" and "Source – src" may also pose a problem.
   Right now we use a semi-automated solution, where the naive approach is used to generate a *.txt* file with "expression name" $\rightarrow$ "{called function names}" mapping, which can be filtered by a user for further analysis runs.
3) Assuming both (A) and (B) are true, it should be possible to implement an interprocedural backward-dataflow analysis to find possible candidates for an arbitrary indirect call. We suppose that one of the problems of such analysis is that its results are used to add missing interprocedural edges to the super graph, but at the same time they are dependent on the super graph structure, thus it should be performed as an iterative process. We don't have a working implementation of this approach by now.

B. Memory model

As it was already mentioned in Section III, we use an access path based memory model with an access path defined as a combination of base value and an ordered list of dereference offsets.

In the current implementation, offsets are represented with either constant integers or a special λ-offset, which is used to denote an unknown offset. This λ-offset has a special behavior: given any pointer *ptr* and a constant offset a, access path $[ptr, \lambda]$ is considered to be subsuming $[ptr, a]$, i.e. the statement `b = ptr[a]` would propagate taint from either one of these access paths to $[b]$, but the statement `ptr[a] = 0` would remove taint from the second one only.

Usage of arbitrary integer offsets instead of object fields in access paths, what is required to achieve complete support of all C++ features, leads to an extremely large D set, which has a great impact on worst-case complexity of the algorithm. Thus it is necessary either to make sure that transfer functions would work with a limited subset of D for any given program, or to limit path length in the exploded super graph.

While this special offset enables us to give a simple and efficient representation for complex expressions like `s->packet+len+left`, where `s->packet` is a pointer and `len` and `left` are non-constant offsets, it inevitably leads to an overtaint problem, because λ-offset doesn't restrict the set of possible values and any two λ-offsets are considered to be equal.

While it is possible to extend this model to achieve more precise analysis, it's required to keep reasonable size of the D set. We've evaluated following approaches:

1) A relatively simple extension of the model is to introduce "unknown non-negative" offset λ_+, which is included into "unknown" λ-offset. Let us assume that an instruction writes tainted data into a single element with unknown index of an array field of an object. As a result the whole object becomes tainted, because resulting access path will be equal to $[this, offsetof(field) + \lambda] = [this, \lambda]$. If the used index is nonnegative, because it corresponds to an unsigned variable, it's possible to achieve better precision, tainting only consequent part of the object with the help of λ_+.
   This approach has allowed us to slightly decrease amount of false positives on LibTIFF library, but it hasn't proved to make any difference in other cases, since buffers are usually accessed via pointers and this situation seems to be rather an exception.
2) The access path is the core of used memory model. It's possible to use interval domain to get better granularity and precision. The model requires to define a number of predicates, such as that one access path corresponds to the memory region included into region of another access path. Since AP construction and predicate calculation for interval domain is significantly slower and the total number of created access paths (the size of the D set) grows significantly too, the total analysis time becomes unacceptable.
3) We also tried to implement another extension of memory model which uses symbolic expressions instead of integer offsets in access path. But this approach requires to gather constraints for these offsets using LLVM-instructions which are usually ignored by the

IFDS engine, because values of these variables are not tainted. Therefore it's better to build a dedicated symbolic execution engine and integrate it with existing IFDS engine or to build taint analysis immediately on symbolic execution [5]. Because of this we decided to use an existing symbolic execution tool as a second analysis stage.

4) We also considered using a region based memory model, similar to the one proposed in [6], since that would allow us to merge all aliases in a single data fact, instead of propagating them independently. We don't have a working implementation of this approach.

IV. Analysis results refinement stage

One of the likely reasons of false positives is the lack of path-sensitivity in the IFDS algorithm. Let's consider a modified example based on a typical buffer overflow test from the Juliet Test Suite for C/C++ on Fig.2.

```
extern int globalFive;
int data = -1;

if(globalFive == 5)
{
  fscanf(stdin, "%d", &data);
}

if(globalFive != 5)
{
  int buffer[10] = { 0 };
  if (data >= 0)
  {
    buffer[data] = 1;
  }
}
```

Fig. 2. Example for path insensitivity problem

There is a single taint source *fscanf(data)* and a single taint sink *buffer[data]*. Due to path-insensitivity of the algorithm, it reports a dangerous data flow between those instructions, but in reality there is no realizable path from source to sink, because that would require variable *globalFive* to be equal to 5 and not to be equal to 5 at the same time.

There are different ways to solve this issue. We propose performing a two-stage analysis: the first step is done by a relatively fast and simple analyzer, which is able to detect most errors in the program but also produces a high amount of false positives and a second one is performed by a slower but more precise path-sensitive analyzer, whose task is to confirm or reject reports from the first stage.

Similar two-staged approach, consisting of static and guided dynamic analysis was proposed for example in [7] [8]. Preliminary static analysis helps to avoid path explosion problem in dynamic analysis, since it is necessary to check only those execution paths, which were already discovered by the first stage.

We propose an analogical combination of two static analyses: IFDS-based analysis and symbolic execution. Unlike building taint analysis using static symbolic execution without IFDS framework, as we have already done for C# in [5], or as it is done for C and C++ in Svace [9], two-staged approach allows to deal with following issues. Every general purpose static analyzer is required to balance between analysis precision and performance. We can enable very detailed and precise analysis because it's necessary to handle only minimal amount of possible dangerous paths, found by the previous stage. Hence states explosion problem together with conditions simplification for analyzer with states merging are solved.

We decided to use an existing symbolic execution engine for a second stage and the main requirement was that it should work with program representation in LLVM bitcode format to ease exchanging data between stages.

As an experiment, we consider a simpler form of report confirmation – a path confirmation. In this case the only task of the second analyzer is to confirm that the source-sink path is realizable and it doesn't need to know anything about the vulnerability itself. Hereafter we plan to built more precise condition for each type of detected error. For example, considering usage of tainted data as an array index, we can ensure proper sanitizing by building condition to check if the index is out of bounds.

A. KLEE

KLEE [10] is a well-known open-source symbolic execution engine which is actively developed since 2008 and has more than one hundred related publications [11].

It analyses programs in LLVM format and is able to mix both concrete and symbolic execution. To enable symbolic execution, the program should be explicitly annotated with special functions, which are used to mark symbolic values to be created, conditions to be checked etc. This should be done either manually, or by linking the program with a special implementation of system libraries, such as *uClibc* [12].

We have tested a simple way to transfer information about taint sources and sinks in program to KLEE by instrumenting bitcode file with necessary special functions calls.

The path confirmation problem was modeled as follows:

Every warning trace contains an ordered list of instructions (tracepoints) in a program along the path from source to sink, which are important to demonstrate to user the taint flow. For every tracepoint except the last one corresponding to the sink, a special global variable *tracepoint_i_j* is created, where *i* is the index number of the current report trace and *j* is an index number of the tracepoint.

At the first tracepoint of every trace *i* we insert an LLVM instruction, corresponding to the assignment

```
tracepoint_i_1 = 1;
```

At every other tracepoint *j* of the trace *i* we insert LLVM instructions, corresponding to the code

```
if (tracepoint_i_(j-1))
```

```
    tracepoint_i_j = 1;
```

At the sink we insert an equivalent of the code

```
if (tracepoint_i_(j-1))
    klee_report_error(...);
```

In this terms, the error would be reported iff KLEE has found a realizable path which visits all tracepoints of the trace in a proper order.

Unfortunately, while the concept seemed to be working for simple test cases (and even there were some difficulties with external functions), the general idea has proved to be not so easy to properly implement.

In particular, we encountered following issues:

- KLEE doesn't support memory regions with symbolic size. It means that it's necessary to explicitly specify size for every input string and memory buffer, which is inappropriate for us. This problem is addressed in [13]
- KLEE as is can't start analysis from an arbitrary point of the program. It is acceptable for tests generation, but it is not very suitable for our purpose, since we are interested in simulating of a relatively small subpath from source to sink. In addition many libraries don't have any entry point at all. The problem is addressed in [14]
- By design KLEE uses program traversing strategy which is aimed to increase code coverage. However, we were not satisfied with the existing "covering-new" heuristic and would need to implement another one for directed symbolic execution similar to [15].
- By default, KLEE works on self-contained isolated programs that don't use any external code (e.g. C library functions), but in practice most programs use external functions calls. To solve this issue, it is possible to link the program with the library or model representation or to automatically generate stub definitions for unknown functions.

After successful experiments on artificial tests, we've tried KLEE to automatically confirm our reports on the relatively small library LibTIFF, but we haven't managed to find a way to reach even the taint source.

As a conclusion, we've decided that it would be too hard to adapt this tool to our problem and it is better to use a pure static analysis approach.

B. Svace

Svace [16] is a static analysis tool for bug detection developed at the Institute for Systems Programming, Russian Academy of Sciences. It supports analyzing program written in various programming languages, including C, C++, C# and Java.

Unlike the previous tool, it performs purely static analysis, which means that it doesn't necessarily require a full model of the analyzed program and is suitable to analyze libraries without executable files.

We started with creating a symbolic execution based checker for Svace, which analyses the modified LLVM bitcode file to confirm the existence of a realizable source-sink path for traces of warnings reported by the first stage.

For the proof of concept, report traces are represented in a following manner:

1) Temporarily we don't use any tracepoints, other than the first corresponding to the source and the last one corresponding to the sink.
2) All unique sources appearing in any reported source-sink pair are sorted and enumerated. If tainted data from the source haven't reached any sink, such source is ignored.
3) For every source, a global variable *source_i_tainted* is created, where *i* is the source's index number.
4) A special function call `taint_variable(source_i_tainted)` is inserted after every source statement in the program to tell the analyzer that the variable is tainted.
5) A special function call `check_tainted(source_i_tainted)` is inserted before every sink statement appearing in a source-sink pair, where *i* is the corresponding source's index number.

For every function containing either *taint_variable* or *check_tainted* call, a summary is created. Summary contains intraprocedural reachability condition of the corresponding source or sink. Similar summaries are created for every caller function and contain conjunction of call reachability condition and condition from the callee translated into the caller context. Error condition is equal to the conjunction of the current path condition, the source reachability condition and the sink reachability condition. The resulting condition is passed to a solver for every function call, containing sink. If the resulting condition is UNSAT checker classifies corresponding report as false positive.

Hereafter we plan to check the reachability condition of the whole path or set of paths, instead of source to sink subpath. For example the entry point can be considered as the entry of nearest function containing source to sink path. We also want to filter out sanitized taints by checking corresponding security conditions.

V. Testing results

First of all, we performed empirical evaluation of some of the memory usage enhancements mentioned in Section III. We have launched analysis 4 times on *libssl* library from OpenSSL version 1.0.1f with following configurations:

1) Baseline configuration, with most enhancements disabled
2) Default configuration
3) Default configuration without separate sources analysis
4) Default configuration with full exploded graph instead of currently used taint traces

This library contains 3 taint sources and was chosen for the demonstration because it contains a well-known "Heartbleed" (CVE-2014-0160) vulnerability, which was successfully found by the analyzer. Also we have to mention the fact that baseline

TABLE I
EVALUATION OF MEMORY CONSUMPTION

Configuration	# Reports	Time	Memory
(1)	75	45 s	938 Mb
(2)	75	55 s	318 Mb
(3)	75	53 s	467 Mb
(4)	75	45 s	580 Mb

configuration exceeds 20 Gb RAM usage limit on a full *openssl* executable – it contains 162 taint sources and has a huge taint flow graph mostly because of extensive use of cryptographic library *libcrypto*. Thus mentioned enhancements seem to be necessary for the analysis of programs with vast taint flow graphs.

Another launch without "const" qualifier handling in external function calls mentioned in Subsection III-A shows decreased amount of reported warnings from 75 to 67, amount of covered functions from 141 to 136 and the decrease of the number of performed algorithm iterations from 3.61 millions to 3.02 millions.

Regarding two-stage analysis concept, we've performed an evaluation on the set of artificial tests, which was created during development of the first stage analyzer. While these tests were not designed to test path confirmation, that allowed us to find some obvious implementation flaws and compare analysis time of both stages.

TABLE II
EVALUATION OF ANALYSIS TIME ON ARTIFICIAL TESTS

Stage	# Tests	# Passed	Time
First	266	263	1m 16s
Both	175	167	15m 38s

Second stage analyzer has been launched for 175 tests in which first stage analyzer produced at least a single report to be confirmed.

Out of 8 tests, incorrectly filtered out by the second stage analysis:

- 3 were caused by the lack of indirect and virtual calls support in the second stage analyzer
- 3 were caused by incorrect interpretation of traces produced by a backward analysis checker
- 2 has failed because of merged or duplicated reports, which seems to be an implementation issue

The substantial slowdown of the second stage analyzer is most likely caused by the fact that Svace is a general-purpose tool and performs a lot of actions which are not necessary for the path confirmation checker. Also, it requires more time to bootstrap and initialize analysis, which makes difference because every test file was analyzed in a separate instance.

We've also checked two-stage approach on Juliet 1.3 test suite for C/C++ [17] with and without work-in-progress Svace checker. The first stage was launched on a program which consists of all unix tests from CWE121_Stack_Based_Buffer_Overflow, CWE122_Heap_Based_Buffer_Overflow, CWE126_Buffer_Overread and CWE127_Buffer_Underread directories. There were 2240 taint sources in the analyzed program. Some tests use a hardcoded index instead of user-provided data for buffer overflow – such overflows cannot be discovered by the analyzer since there are no taint sources.

TABLE III
EVALUATION OF TWO-STAGE ANALYSIS ON JULIET TEST SUITE

Stage	# Reports	True positive rate	Time	Memory
First	1982	43%	8m 58s	1.7 Gb
Second	1404	43%	9m 37s	7.5 Gb
Second*	804	72%	9m 52s	7.7 Gb

*We don't have a working solution for security conditions checking right now. For the purpose of proof of concept, we've implemented a simple addition to the current path confirmation checker, which should check that all LLVM values corresponding to the access paths from the reported trace are able to have arbitrary high values. This is not a proper implementation of security conditions checking, but is enough to demonstrate filtering out most false positives on this particular test suite.

As it can be seen from the evaluation data, path confirmation checker alone is not enough to improve analysis results on the selected test suite, because it doesn't contain tests with unrealizable paths between source and sink. Also, the current version of the checker was able to confirm path only for 1404 warnings from the first stage analyzer results, which has to be investigated.

However, if supported with a security conditions checker, this approach seems to be able to significantly decrease amount of false positives among reported warnings without affecting performance of the analysis.

Unfortunately, current implementation of the path confirmation checker is not yet able to confirm real vulnerabilities, which are known to be detectable by the first stage analyzer.

In case of OpenSSL library and CVE-2014-0160 vulnerability, the second stage analysis appears to lose information about taint sinks in several functions. This is most likely caused by imperfection of the checker and will try to fix it in the nearest future.

In case of LibTIFF library and CVE-2018-15209 vulnerability, the taint path could not be confirmed because it requires handling of indirect calls which is not yet supported by the checker.

Therefore our testing shows that the concept seems to be promising, but still requires further refinement.

VI. CONCLUSION

Performing taint analysis for vulnerability detection via pure IFDS approach has several limitations in comparison to existing buffer overflow checkers, such as [9]: it doesn't make any assumptions about buffer size and is unable to detect several cases even from Juliet Test Suite, because there are

no taint sources. For example, if a constant array index is used to access memory outside of array bounds. Moreover, considering error detection problem, pure static taint analysis generate too many alarms to be able to find few vulnerabilities uncaught in an industrial project. The majority of false alarms are introduced by path-insensitivity and overtainting due to inconsistencies between a program and its memory model. Our experience shows that addons to simple and efficient memory model used by IFDS lead to unreasonable analysis slowdown and offer just a minimal results improvement. Therefore a postprocessing of results is required.

Proposed approach with two-staged analysis looks promising, but requires a lot of enhancements to achieve industrial-level quality and there are no guaranties that it is even possible.

We are going to continue our research by developing other types of report confirmation in Svace infrastructure, since despite all listed limitations, the tool has a potential to discover serious vulnerabilities, such as "Heartbleed" in OpenSSL and CVE-2018-15209 in LibTIFF.

References

[1] V. Koshelev, A. Izbyshev, and I. Dudina., "Interprocedural taint analysis for LLVM-bitcode," *Trudy ISP RAN / Proc. ISP RAS*, vol. 26, pp. 97–118, 2014, (in Russian).

[2] T. Reps, S. Horwitz, and M. Sagiv, "Precise interprocedural dataflow analysis via graph reachability," *POPL '95*, pp. 49–61, 1995.

[3] N. A. Naeem, O. Lhoták, and J. Rodriguez, "Practical extensions to the IFDS algorithm," *Compiler Construction 2010*, pp. 124–144, 2010.

[4] S. Arzt, S. Rasthofer, C. Fritz, A. Bartel, J. Klein, Y. L. Traon, D. Octeau, and P. McDaniel, "FlowDroid: precise context, flow, field, object-sensitive and lifecycle-aware taint analysis for android apps," *PLDI '14*, pp. 259–269, 2014.

[5] M. V. Belyaev, N. V. Shimchik, V. N. Ignatyev, and A. A. Belevantsev, "Comparative analysis of two approaches to static taint analysis," *Programming and Computer Software*, vol. 44, no. 6, pp. 459–466, 2018.

[6] Z. Xu, T. Kremenek, and J. Zhang, "A memory model for static analysis of C programs," *Leveraging Applications of Formal Methods, Verification, and Validation*, pp. 535–548, 2010.

[7] A. Y. Gerasimov, L. V. Kruglov, M. K. Ermakov, and S. P. Vartanov, "An approach of reachability determination for static analysis defects with help of dynamic symbolic execution," *Trudy ISP RAN / Proc. ISP RAS*, vol. 29, pp. 111–134, 2017, (in Russian).

[8] A. Y. Gerasimov, "Directed dynamic symbolic execution for static analysis warnings confirmation," *Programming and Computer Software*, vol. 44, no. 5, pp. 316–323, 2018.

[9] I. A. Dudina and A. A. Belevantsev, "Using static symbolic execution to detect buffer overflows," *Programming and Computer Software*, vol. 43, no. 5, pp. 277–288, 2017.

[10] C. Cadar, D. Dunbar, , and D. Engler, "KLEE: Unassisted and automatic generation of high-coverage tests for complex systems programs," *OSDI '08*, pp. 209–224, 2008.

[11] Publications • KLEE. [Online]. Available: http://klee.github.io/publications/ [Accessed: 20-Mar-2019]

[12] klee/uclibc: KLEE's version of uClibc. [Online]. Available: https://github.com/klee/klee-uclibc [Accessed: 2-Apr-2019]

[13] M. Šimáček, "Symbolic-size memory allocation support for Klee," Master's thesis, Masaryk University, Faculty of Informatics, Brno, 2018. [Online]. Available: https://is.muni.cz/th/mdedh/ [Accessed: 21-Mar-2019]

[14] D. A. Ramos and D. Engler, "Under-constrained symbolic execution: Correctness checking for real code," *Proceedings of USENIX Security Symposium '15*, pp. 49–64, 2015.

[15] P. D. Marinescu and C. Cadar, "KATCH: High-coverage testing of software patches," *Proc. of 9th Joint Mtg. on Foundations of Software Engineering (FSE) '13*, pp. 235–245, 2013.

[16] V. P. Ivannikov, A. A. Belevantsev, A. E. Borodin, V. N. Ignatiev, D. M. Zhurikhin, and A. I. Avetisyan, "Static analyzer Svace for finding defects in a source program code," *Programming and Computer Software*, vol. 40, no. 5, pp. 265–275, 2014.

[17] Software assurance reference dataset. [Online]. Available: https://samate.nist.gov/SARD/testsuite.php [Accessed: 20-Mar-2019]

C# parser for extracting cryptographic protocols structure from source code

1st Ilya Pisarev
Information security departmen
Southern Federal University
Taganrog, Russian Federation
ilua.pisar@gmail.com

2nd Liudmila Babenko
Information security departmen
Southern Federal University
Taganrog, Russian Federation
lkbabenko@sfedu.ru

***Abstract*—Cryptographic protocols are the core of any secure system. With the help of them, data is transmitted securely and protected from third parties' negative impact. As a rule, a cryptographic protocol is developed, analyzed using the means of formal verification and, if it is safe, gets its implementation in the programming language on which the system is developed. However, in the practical implementation of a cryptographic protocol, errors may occur due to the human factor, the assumptions that are necessary for the possibility of implementing the protocol, which entail undermining its security. Thus, it turns out that the protocol itself was initially considered to be safe, but its implementation is in fact not safe. In addition, formal verification uses rather abstract concepts and does not allow to fully analyze the protocol. This paper presents an algorithm for analyzing the source code of the C# programming language to extract the structure of cryptographic protocols. The features of the implementation of protocols in practice are described. The algorithm is based on the searching of important code sections that contain cryptographic protocol-specific constructions and finding of a variable chain transformations from the state of sending or receiving messages to their initial initialization, taking into account possible cryptographic transformations, to compose a tree, from which a simplified structure of a cryptographic protocol will be extracted. The algorithm is implemented in the C# programming language using the Roslyn parser. As an example, a cryptographic protocol is presented that contains the basic operations and functions, namely, asymmetric and symmetric encryption, hashing, signature, random number generation, data concatenation. The analyzer work is shown using this protocol as an example. The future work is described.**

Keywords—cryptographic protocols, C#, parser, verification, tree, analysis, source code.

I. INTRODUCTION

The problem of verifying the security of cryptographic protocols is relevant nowadays despite the existence of a large number of already verified protocols. The need to use self-written protocols that use lightweight cryptography for IoT, mobile robots, as well as the imperfection of formal verification of protocols is a new challenge for verification methods, in particular, the possibility of verifying the security of cryptographic protocols implementation. The primary task in this matter is to extract the structure of the protocol from the source code. At the moment there are works in which the problem of extracting an abstract model from the source code of programming languages C [1-3], Java [4-6], F# [7-12] is being considered. Most of them require a special programming style for the possibility of use these algorithms or the use of additional annotations in the source code. The paper proposes to analyze the source code of the C # programming language. There are no other works in which code analysis would be carried out, not involving the use of annotations or a special programming style.

II. CRYPTOGRAPHIC PROTOCOLS

Cryptographic protocols are a set of cryptographic algorithms and functions, with a correct combination of which is obtained a secure process of transferring messages between the parties. Protocol security is defined as complying with security requirements, the main of which are mutual authentication of the parties, protection against time attacks such as replay attacks, privacy and integrity of the transmitted data. Below is an example of a test protocol that does not have a special meaning, but contains all the basic cryptographic algorithms and functions: asymmetric and symmetric encryption, hashing, signature, random number generation.

1. *A->B:* $E_{pkB}(A, Na)$
2. *B->A:* $E_{pkA}(Na, Nb, B)$
3. *A->B:* $E_{pkB}(Nb, k)$
4. *B->A:* $E_k(M1, E_{pkA}(M2)), Hash(M1)$
5. *A->B:* $E_k(M1, M2, M3), Sign_{skA}(M1, M2, M3)$
6. *B->A:* $E_k(M3)$

At the beginning of this protocol, messages 1-3 use the Needham–Schroeder public key protocol (NSPK) [13] for mutual authentication of the parties. In message 3, in addition to the random number Nb, the key k is also transmitted for further communication between the parties using a symmetric cipher. In message 4, M2 data is transmitted, asymmetrically encrypted on partys' A public key, and some M1 data. All this is encrypted symmetrically using the key k, after which the data hash M1 is applied. In message 5, side A applies its M3 data to the previously sent data M1 and M2, encrypts all this symmetrically on key k, applies a signature and sends this

message to side B. In message 6, B sends A M3 data encrypted symmetrically on key k.

III. Features Of The Cryptographic Protocols Implementation

There are a number of problems with the implementation of cryptographic protocols. One of the problems is the dynamic size of messages. In the programming language, the transfer of messages between the parties is implemented using sockets. In this case, the party that receives the message must know in advance the size of the buffer to receive. For example, in the protocol described in the previous paragraph, in the first three messages random numbers and identifiers of the parties with a fixed length are used. In this case, everything is simple and at the reception of the message by the party, it will expect a previously calculated static message length. However, messages 4-6 use data M1, M2, M3, which may have different lengths. For example, in message 4, M1 data can be a video file, the length of which can vary from 1 MB to several GB. And the question is how to tell the receiving party the size of the receiving buffer. There are various options for how this can be done, for example, to add information about its length to the beginning of a message, to put a mark at the end of the message. Let us consider in more detail the option with the addition of information about the length of the message. This option involves the use of additional data before the main message, which will contain the size of the future message. An example of a message with additional size information is shown in Figure 1.

Figure 1 – Additional information about the size of the message

The receiving party in this case receives a fixed array of bytes, which contains the size of the message, after which the second portion takes the rest of the message knowing in advance its length.

```
A send: Buffer size, Message
B receive(4 bytes): Buffer size
B receive(Buffer size): Message
```

Since *Message* is usually encrypted and, in the context of a protocol, its transmission is protected, the question arises of how to protect information in *Buffer size*. All security requirements are important for us, except secrecy. To ensure them, you can, for example, use the signature of this area with timestamps. Thus, the transmission, for example, message 4, will have the following form when implementing the protocol:

$$\texttt{B->A:}\ \ Buffer\ size, T, Sign_{skB}(Buffer\ size, T),$$
$$E_k(M1, E_{pkA}(M2)), Hash(M1)$$

Another way is to get data into a fixed-length buffer until the buffer becomes empty. In this case, problems can also arise as shown in Figure 2.

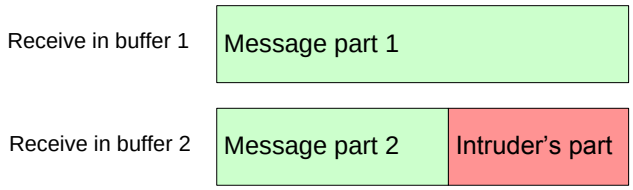

Figure 2 – Intruders' attack on the addition of real data

The result is that the message will be received longer than necessary and in some implementations, in which further processing of the message by the receiving party is tied to the use of the message length, some data may be imperceptibly corrupted when decrypting and dividing the data into the message elements (random numbers, keys, etc.). In order to avoid this, various methods of controlling the length of a message are also used. Thus, some protocols are changed and supplemented during implementation, and for their initial analysis, for example, by means of formal verification this is not taken into account.

IV. Source Code Analysis Algorithm

As an example for describing the operation of the algorithm, the previously considered protocol was taken and implemented in the C # programming language in the form of a client server application.

1. *A->B:* $E_{pkB}(A, Na)$
2. *B->A:* $E_{pkA}(Na, Nb, B)$
3. *A->B:* $E_{pkB}(Nb, k)$
4. *B->A:* $E_k(M1, E_{pkA}(M2)), Hash(M1)$
5. *A->B:* $E_k(M1, M2, M3), Sign_{skA}(M1, M2, M3)$
6. *B->A:* $E_k(M3)$

The analysis algorithm uses the C # Roslyn source code parser [14]. With it you can get the tree structure of the source code, and you can use filters. We need these filters:

1. *InvocationExpressionSyntax* - call expressions.
2. *VariableDeclarationSyntax* - declaration of variables.
3. *AssignmentExpressionSyntax* - an assignment expression.
4. *IfStatementSyntax* - statement with a condition statement.

Using filters, you can get the desired expression, after which you can view the tree structure of this expression. For example, using "*AssignmentExpressionSyntax*" we can find the expression "*M1enc1 = RSA.Encrypt (M1, true)*". The derived linear tree structure of the expression is shown in Figure 3.

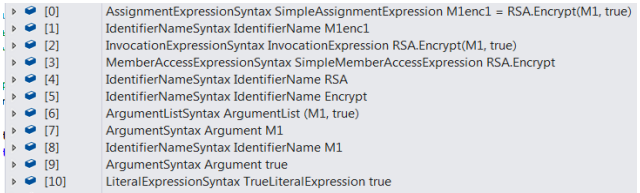

Figure 3 – Tree structure of expression in a linear form.

The main purpose of using this parser is to find the transition from one variable to another. In this case, we are interested in the transition *M1enc1 -> M1*. This is achieved by searching for data such as "*IdentifierName*" together with the use of a black list of expressions. For example, it uses the call of the "*Encrypt*" method, as well as the previously declared object of the asymmetric encryption class "*RSA*", which are present in the black list, and *M1enc1* and *M1* that we need can be obtained from here, where the first element will be the variable to which the value will be assigned, and the rest of those that are lower and not included in the black list will be the new value assigned.

The algorithm is based on the definition of important code sections containing constructs specific to cryptographic protocols. Ultimately, the task is to find a chains of variables transformation from the state of sending or receiving messages (socket send/receive) to their initial initialization (static initialization, load from file, etc.), while taking into account possible cryptographic transformations (hash, encryption, etc.). In the course of building a chain, a tree is constructed, the nodes of which are variables with additional information about them, including data type definitions for the final leaves of the tree and cryptographic algorithms in the tree nodes. The tree structure allows you to describe all the chains of data transformations, since the data in the message is combined in various ways, the chains can be strongly branched and joined. Below is a fragment of the source code for the implementation of a part of the cryptographic protocol (messages 1-3) from participant A.

```
...
Socket socA =
new Socket(ipAddress.AddressFamily,
SocketType.Stream, ProtocolType.Tcp);

socA.Connect(remoteEP);

RNGCryptoServiceProvider rng = new
RNGCryptoServiceProvider();

byte[] A = new byte[] { 132, 114 };
byte[] B = new byte[] { 15, 245 };

byte[] Na = new byte[64];
rng.GetBytes(Na);

byte[] M1 = new byte[2 + 64];

Array.Copy(A, 0, M1, 0, A.Length);
Array.Copy(Na, 0, M1, 2, Na.Length);

//1
byte[] M1enc;
using (RSACryptoServiceProvider RSA =
new RSACryptoServiceProvider())
{
      RSA.ImportParameters(
rsaPB.ExportParameters(false));
      M1enc = RSA.Encrypt(M1, true);
}

socA.Send(M1enc);

//2
byte[] MGet2Encr = new byte[256];
socA.Receive(MGet2Encr);

byte[] MGet2;
using (RSACryptoServiceProvider RSA = new
RSACryptoServiceProvider())
{
      RSA.ImportParameters(
rsaSA.ExportParameters(true));
      MGet2 = RSA.Decrypt(MGet2Encr, true);
}

byte[] BFromServer = new byte[2];
byte[] NaGet = new byte[64];
Array.Copy(MGet2, 0, BFromServer, 0, 2);
Array.Copy(MGet2, 0, NaGet, 0, 64);

if (!NaGet.SequenceEqual(Na) &&
!B.SequenceEqual(BFromServer))
{
      socA.Shutdown(SocketShutdown.Both);
      socA.Close();
      return;
}

byte[] Nb = new byte[64];
Array.Copy(MGet2, 64, Nb, 0, 64);

byte[] k = new byte[32 + 16];
rng.GetBytes(k);

byte[] M3 = new byte[0];
M3 = Nb.Concat(k).ToArray();

//3
byte[] M3enc;
using (RSACryptoServiceProvider RSA = new
RSACryptoServiceProvider())
{
      RSA.ImportParameters(rsaPB.ExportParame
      M3enc = RSA.Encrypt(M3, true);
}
socA.Send(M3enc);
...
```

First you need to define the declaration and initialization:

1. Objects of class Socket.
2. Class objects of the standard library cryptographic algorithms, such as the *RSACryptoServiceProvider* asymmetric encryption algorithm, the *RNGCryptoServiceProvider* random number generator, etc.

The variables of the class object *Socket: [socA]*, classes of cryptographic algorithms are defined: *[rng, RSA]*.

To find variable of the *Socket* class object, the sending and receiving messages is searched. In this case, there are 3 such constructions. At this stage, you can construct an interaction scheme of the following form:

1. *A-> B: M1*
2. *B-> A: M2*
3. *A-> B: M3*

To determine the structure of the message, it is necessary to build a tree, the nodes of which contain variables with additional information. Consider an example for determining the content of the first message. The order of the algorithm is as follows:

1. The expression of the first message *socA.Send (M1enc)* is taken as the root of the tree. It is necessary to understand the contents of the variable *M1enc*.
2. First you need to find the declaration of the variable *M1enc* using the filter *VariableDeclarationSyntax*. However, in our case, the variable is declared, but not initialized (line 23). In this case, the filter *AssignmentExpressionSyntax* is used and you can find in line 29 the assignment of the value to our variable. *M1enc* is added as a child node with the "*var*" tag, which means it is just a variable.
3. The simplest case of assignment is when the value of one variable is assigned to another. In this case, the situation is more difficult. The variable *M1enc* is assigned the value of the result of the work of the *Encrypt* method for an object of the asymmetric encryption class *RSACryptoServiceProvider*, which takes two parameters as input: what to encrypt and flag whether to use optimal asymmetric encryption with addition (OAEP padding). At the current stage, we remember that the content of the variable *M1* was asymmetrically encrypted and assigned to the variable for sending message 1. In the tree structure, this is displayed as adding a child node *M1* with the note "*AsymENC*", which means that the value of the variable *M1* is encrypted using an asymmetric cipher.
4. Similar to paragraph 2, we are looking for the initialization of the variable *M1*. Using the first filter, you can find out that the variable is a one-dimensional array (line 17). Using the second filter, you must find the assignment of values to our array. These are lines 19 and 20. Two children *Na* and *A* with the mark "*var*" are added to node *M1*.
5. For variable *A*, the final value can be found using the first *VariableDeclarationSyntax* filter (line 11). This is where static initialization occurs in the source code. It is enough for a person to simply understand that this is the initial value, but for the automated determination of this fact it is necessary to understand that this is not a variable. One way to solve this problem is to re-search the right side of the expression, and since more in the design code of the assignment is not detected, this value is final. In the tree structure for node A, the initialization leaf is added "*new byte [] {132, 114};*" marked "*DATA*", which means the presence of some semantic data in the variable *A*.
6. For the *Na* variable, the search is carried out further. Using filters, we look for the declaration of the array and its initialization. The declaration occurs in line 14, and initialization occurs in line 15 by calling some method of the *rng* variable, which in turn is an object of the *RNGCryptoServiceProvider* class of random numbers, thus, the value of this variable is defined as a random number. The last leaf "*rng.GetBytes (NaPrev);*" is added to the tree structure marked "*RANDOM*", which means generating a random number.
7. Further search initialization for current leaves gives nothing, therefore the structure of the tree is considered final. The output tree view is shown in Figure 4 in the "*Full tree*" area and it corresponds to the following chain: *Send (M1enc) -> M1enc = E (M1) -> M1 = {A, Na} -> A = new byte [] {132, 114}, Na = rand ()*. You can also see short tree structure and result message from it.

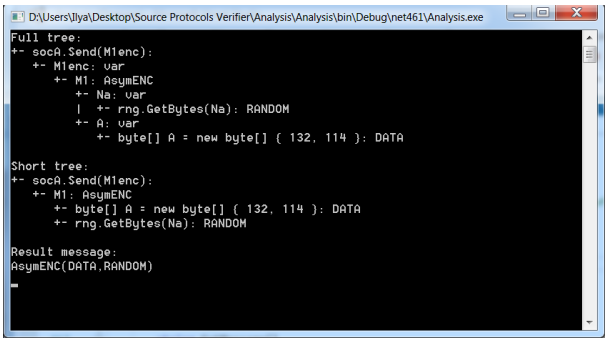

Figure 4 –Output for composing the structure of a single message

V. Return Data Problem

At the moment there is a problem in determining the returned data. For example, in message 1, a random number *Na* is sent, and then in the second message it is sent back. By default, there are currently two data concepts: *DATA* and *RANDOM*. All that is not a random number - is considered semantic data, for example: keys, identifiers, transferred files, etc. And at this stage, all values are considered different. For example, for the following protocol:

1. *A->B: Ek(Na,A)*
2. *B->A: Ek(Nb,B)*

The result of the work will be as follows:

1. *A->B: SymENC(RANDOM, DATA)*
2. *B->A: SymENC(RANDOM, DATA)*

And in our context, the default *DATA* in the first message is different from the one in the second message. If the protocol takes the following form:

1. A->B: Ek(Na,A)
2. B->A: Ek(Nb,Na)

There is a problem. *Na* just comes back, and on the receiving side we need to understand that this is the same data. For example, when processing message 2 (lines 34-58), we can trace the separated parts. In line 50, the value of the random number *Na* is obtained, after which it is checked for coincidence with what was sent in line 52. Most often in the context of cryptographic protocols, returned values are used for mutual authentication. There can be 2 types: the return of the same number or the return of a function from this number. In both cases, the return value is checked for a match with the one sent earlier. In our case, this is line 53. However, another value is checked here — identifier *B*. In this case, one of the solutions to this problem would be to find the situation when the variable was sent, and then a value is checked for a match with this variable. In this case, you can assume that this is the case of the return value. However, there may be a number of problems, in particular, just the occurrence of an error in writing code, or simply the absence of such a check of the return value. At the moment, the abstract notion of the type of the *RETURN* variable is used. This means that a variable of this type was returned in the current message.

VI. Protocol Output Structure

Using the algorithm presented in the preceding paragraphs, the complete output structure of the protocol is constructed according to the messages. It is obtained both in short form for formal verification, and in full form for dynamic verification. The full view contains the last variable, before serving in the cryptographic function, the names of the last variables and their initial initialization, for example, static in the code or loading data from a file. Dynamic analysis will be considered in further work and therefore the contents of the full protocol can be changed.

Short view:

```
1) A->B: AsymENC(DATA,RANDOM)
2) B->A: AsymENC(RETURN,RANDOM,DATA)
3) A->B: AsymENC(RETURN,RANDOM)
4) B->A: SymENC(DATA,AsymENC(DATA)),
    HASH(DATA)
5) A->B: SymENC(RETURN,RETURN,DATA),
    Sign(RETURN,RETURN,DATA)
6) B->A: SymENC(RETURN)
```

Full view:

```
1) A->B: AsymENC(DATA,RANDOM)
M1 | byte[] A = new byte[] { 132, 114 }
| rng.GetBytes(Na)

2) A->B: AsymENC(RETURN,RANDOM,DATA)
M2 | socB.Receive(MGet1) |
rng.GetBytes(Nb) | byte[] B = new
byte[] { 15, 245 }

3) A->B: AsymENC(RETURN,RANDOM)
M3 | socA.Receive(MGet2Encr) |
rng.GetBytes(k)

4) A->B: SymENC(DATA,AsymENC(DATA)),
HASH(DATA)
ForEncM4 | byte[] M1forSend =
File.ReadAllBytes("Mess1.txt") |
M2forSend | byte[] M2forSend =
File.ReadAllBytes("Mess2.txt") |
M1forSend | byte[] M1forSend =
File.ReadAllBytes("Mess1.txt")

5) A->B: SymENC(RETURN,RETURN,DATA),
Sign(RETURN,RETURN,DATA)
ConcatMess5 | socA.Receive(MGet4) |
socA.Receive(MGet4) | byte[] M3forSend
= File.ReadAllBytes("Mess3.txt") |
ConcatMess5 | socA.Receive(MGet4) |
socA.Receive(MGet4) | byte[] M3forSend
= File.ReadAllBytes("Mess3.txt")

6) A->B: SymENC(RETURN)
M3From5 | socB.Receive(MGet5)
```

VII. Future Work

Future work primarily includes a segmentation of DATA semantic data into classes:

1. Party identifiers
2. Keys
3. Timestamps
4. Authentication Codes
5. Data received from the user

It is also an important point to determine the ownership of a key by any of the parties in the case of asymmetric encryption, and to the list of parties in the case of symmetric encryption. Support for protocols involving more than two parties will also be needed. In addition, a complete solution to the problem of accurately determining the returned data is necessary to make it possible to build a complete structure of a cryptographic protocol and its further analysis using formal verification tools. After obtaining the structure of the cryptographic protocol, it is necessary to develop an algorithm for automated translation into the specification language of the most well-known protocol verification tools, such as Avispa [15], Scyther [16], ProVerif [17], and others. It is also necessary to improve the parser. At the moment, the structure can only be retrieved from areas of code where all functions for sending and receiving messages are combined into one block, for example, into the body of a function or class method. In the future, it is planned to improve the parser to work with complex code structures.

VIII. Conclusion

An algorithm was presented for analyzing the source code of the C # programming language for extracting the structure of cryptographic protocols, based on identifying important code sections that contain cryptographic protocol-specific constructions and determining the chain of variable

transformations from the sending or receiving status to their initial initialization, taking into account possible cryptographic transformations to compose a tree, from which it is possible to get simplified structure of a cryptographic protocol. An example of a protocol containing all cryptographic functions is given. The output structure of the cryptographic protocol is shown. For the further possibility of the application of formal verification of protocols and dynamic analysis, it is necessary to make an additional classification of semantic data, determine whether the keys belong to any party or parties, and also solve the problem with the returned values.

ACKNOWLEDGMENT

The work was supported by the Ministry of Education and Science of the Russian Federation grant № 2.6264.2017/8.9.

REFERENCES

[1] Chaki S., Datta A. ASPIER: An automated framework for verifying security protocol implementations //Computer Security Foundations Symposium, 2009. CSF'09. 22nd IEEE. – IEEE, 2009. – С. 172-185.

[2] Goubault-Larrecq J., Parrennes F. Cryptographic protocol analysis on real C code //International Workshop on Verification, Model Checking, and Abstract Interpretation. – Springer, Berlin, Heidelberg, 2005. – С. 363-379.

[3] Goubault-Larrecq J., Parrennes F. Cryptographic protocol analysis on real C code. – Technical report, Laboratoire Spécification et Vérification, Report LSV-09-18, 2009.

[4] Jürjens J. Using interface specifications for verifying crypto-protocol implementations //Workshop on foundations of interface technologies (FIT). – 2008.

[5] Jürjens J. Automated security verification for crypto protocol implementations: Verifying the jessie project //Electronic Notes in Theoretical Computer Science. – 2009. – Т. 250. – №. 1. – С. 123-136.

[6] O'Shea N. Using Elyjah to analyse Java implementations of cryptographic protocols //Joint Workshop on Foundations of Computer Security, Automated Reasoning for Security Protocol Analysis and Issues in the Theory of Security (FCS-ARSPA-WITS-2008). – 2008.

[7] Backes M., Maffei M., Unruh D. Computationally sound verification of source code //Proceedings of the 17th ACM conference on Computer and communications security. – ACM, 2010. – С. 387-398.

[8] Bhargavan K. et al. Cryptographically verified implementations for TLS //Proceedings of the 15th ACM conference on Computer and communications security. – ACM, 2008. – С. 459-468.

[9] Bhargavan K., Fournet C., Gordon A. D. Verified reference implementations of WS-Security protocols //International Workshop on Web Services and Formal Methods. – Springer, Berlin, Heidelberg, 2006. – С. 88-106.

[10] Bhargavan K. et al. Verified interoperable implementations of security protocols //ACM Transactions on Programming Languages and Systems (TOPLAS). – 2008. – Т. 31. – №. 1. – С. 5.

[11] Bhargavan K. et al. Verified implementations of the information card federated identity-management protocol //Proceedings of the 2008 ACM symposium on Information, computer and communications security. – ACM, 2008. – С. 123-135.

[12] Bhargavan K. et al. Cryptographically verified implementations for TLS //Proceedings of the 15th ACM conference on Computer and communications security. – ACM, 2008. – С. 459-468.

[13] Needham R. M., Schroeder M. D. Using encryption for authentication in large networks of computers //Communications of the ACM. – 1978. – Т. 21. – №. 12. – С. 993-999.

[14] Capek P., Kral E., Senkerik R. Towards an empirical analysis of. NET framework and C# language features' adoption //Computational Science and Computational Intelligence (CSCI), 2015 International Conference on. – IEEE, 2015. – С. 865-866.

[15] Viganò L. Automated security protocol analysis with the AVISPA tool //Electronic Notes in Theoretical Computer Science. – 2006. – Т. 155. – С. 61-86.

[16] Cremers C. J. F. The scyther tool: Verification, falsification, and analysis of security protocols //International Conference on Computer Aided Verification. – Springer, Berlin, Heidelberg, 2008. – С. 414-418.

[17] Küsters R., Truderung T. Using ProVerif to analyze protocols with Diffie-Hellman exponentiation //Computer Security Foundations Symposium, 2009. CSF'09. 22nd IEEE. – IEEE, 2009. – С. 157-171.

Fabless-companies data security while using cloud services

Adelina Akhmedzianova
Kazan Federal University
Kazan,Russia
iadelina.ah@gmail.com

Alexey Budyakov
Bauman Moscow State Technical University
Moscow, Russia
alexbb@mail.ru

Sergey Svinarev
Rostov Law Institute of the Ministry of Internal Affairs of the Russian Federation
Rostov-on-Don, Russia
squire@inbox.ru

***Abstract*—Cloud storage services like Google Drive and Yandex.Disk are increasingly popular to store and transmitting service information in corporate purposes, especially in fabless companies, which do not have hardware and other resources for sensitive data storage and exchange. These services allow synchronizing and accessing data from multiple devices. However, privacy of data stored in a cloud is a concern. To allow data access from multiple devices, current solutions derive the encryption keys solely from user-chosen passwords, which result in low entropy keys. Moreover existing solutions do not provide verification of the relevance of the data contained in the cloud. In these terms, fabless companies need a more appropriate solution. Method being developed has integration with the Yandex.Disk cloud and intended to improve the confidentiality of information stored in a cloud and consists of user-side encryption, two-factor authentication scheme using single-time passwords. Provision is made to ensure the confidentiality of information during transmission to users not having installed software. The resulting solution also can be further used to create cross-platform software. Limitations of considered scheme and further research are presented.**

Keywords—cloud services, data security, encryption

I. INTRODUCTION

The high demand for using cloud storage services can be demonstrated by the example of fabless-companies. These companies are engaged in the development of semiconductor chips and other high-tech devices, so employees during their work process develop intellectual property objects – information in the limited-access category that have high economic value [1]. Many fabless-companies are small and it is widespread practice that engineers of the companies work remotely in collaboration, so there is the reason cloud storage services are preferable.

At present, cloud storage solutions like Google.Drive and Yandex.Disk are becoming more and more popular, bringing innovation not only in terms of minimizing the cost of resources but also in terms of optimization of company processes. These solutions are widely used for both personal purposes and corporate purposes for storage and transmission different types of data, including proprietary information.

Cloud services have a number of advantages like absence of need physical storages and opportunity to provide multiple access to files. However, security policy of cloud storages do not provide an appropriate level of data protection, including protection from cloud service providers themselves [2].

Currently some solutions partially solve the problem of providing security data storage in cloud services: Boxcyptor [3], CarotDAV [4], Mega [5]. These software applications are powerful tools for ensuring the confidentiality of data storage in the clouds, but most of them do not meet the requirements in terms of easy access to the system, providing high level of data availability to multiple users, adaptability to the needs of the particular organization.

For example, the service [3] does not provide the relevance of files in the presence of multiple user access. Additionally, the encryption keys are generated only once when the user registers. The service [5] uses its own cloud storage and does not interact with other cloud storages.

The common disadvantages of existing solutions include the fact that they do not provide secure transmission of keys between users and the absence of version control – these tasks are completely left on the shoulders of users. Thus, the existing solutions in the field of data security in cloud services have a number of drawbacks, so they can not be used in organizations interested in providing the secure storage of processed data in cloud services – in particular, in fabless-companies.

This paper presents the approach to develop the software solution providing the security of data storage in the Yandex.Disk cloud storage service. The main part of paper divided into three sections. The first section presents the main requirements for the system. The second section describes the main functionalities of the system: two-factor authentication scheme, client-side encryption and directly interaction with cloud storage service directly by using API interface. In the third section is proposed the technique of generation and safe distribution of the encryption keys that takes into account the features of the scope of the system. In the last section, the limitations of the approach are described and options for the future work directions are proposed.

II. MATERIALS AND METHODS

A. Requirements

The main task of our system is to ensure the security of data stored in the cloud services. The most effective way to achieve this task is client-side encryption. However, client-side encryption additionally leads to the task of secure encryption key exchange between multiple users and task of secure transfer data to users who have no access to the system.

In order to design the solution it is necessary to define the main requirements that it must meet in order to be successful. An effective solution should meet the following requirements:

- providing convenient and effective tools to quickly upload files from computer to cloud storage and download files from cloud storage to a computer in safe mode;
- integration with cloud storage service using API interface;

• ensuring the confidentiality of data (data encryption, key generation and exchange) taking into account the features of the scope of the system;

• ensuring the availability of data (including in relation to people who have no access to the system);

• ensuring the relevance of data (confirmation of the relevance of the file when it is loaded);

• providing an intuitive user interface;

• reducing the number of required actions from the user.

B. The basic functionality

Requirements from Section A allow to describe basic functionality of solution. In general, the solution can be used to perform the following scenarios:

1. Uploading a file to the cloud storage service;

2. Downloading a file from the cloud storage service;

3. Transfer a file to a person who has no access to the solution (but has the right to access the file).

Let's describe each scenario more detailed.

Scenario 1. Uploading a file to the cloud storage service. In order to upload a new file to the cloud storage, firstly user has to be verified by entering a one-time password from his own token. After successful verification user should select the document needs to be uploaded. Then the solution generates an encryption key, encrypts the selected file and upload it directly to user's folder in the cloud storage. If the user wants to update an existing file, in the solution will be additionally performed a comparison of the keys of both versions of file (normally they must be equal). After successful uploading the file to the file's parameters will be added meta information about the last uploading. Fig.1 shows the conceptual scheme of the Scenario 1.

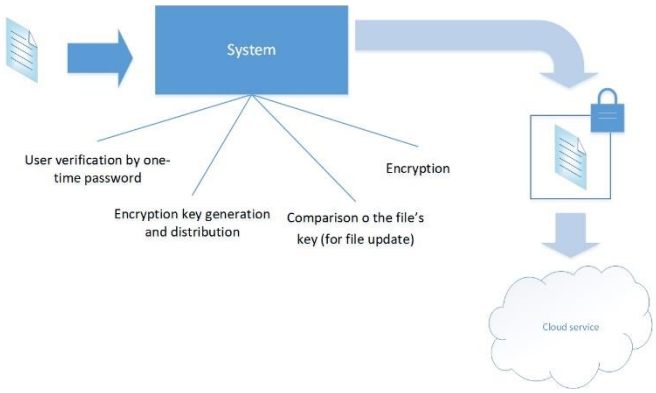

Fig.1. Conceptual scheme of Scenario 1 "Uploading a file to the cloud storage service"

Scenario 2. Downloading a file from the cloud storage service. In order to download file from the cloud storage, user must select the file has to be downloaded from the list of available files, provided by the solution. Then user has to be verified by entering a one-time password from his own token. Then in the solution is performing checking of the relevance of the file and, if it necessary, requests to get the latest version of this file are sent to users who have access to this file. Then user has to enter the encryption key, after which the document is decrypted. After successful downloading the file to the file's parameters will be added meta information about the last downloading. Fig.2 shows the conceptual scheme of the Scenario 2.

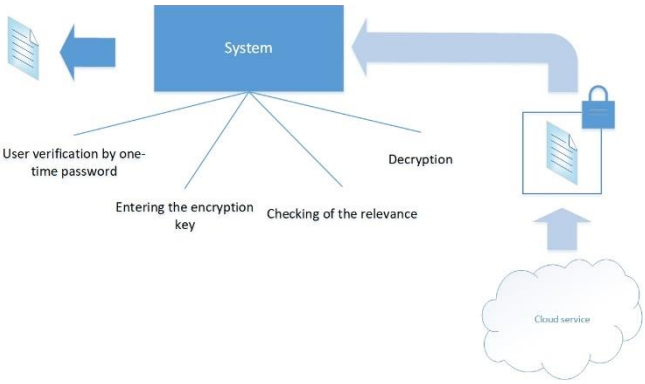

Fig.2. Conceptual scheme of Scenario 2 "Downloading a file from the cloud storage service"

Scenario 3. Transfer a file to a person who has no access to the system. In order to transfer a file to a legitimate person without an installed application, other user with access to the solution has to download the file according to Scenario 2 and sent this file via secure messenger.

The advantage of the solution is the fact that users do not interact with cloud storage service, but only with one solution. Interaction with cloud service is provided through Rest API interface, where the following methods are possible:

- view a list of files in a user's folders;
- view and add meta information parameters of the file;
- upload and download files.

Therefore, data processing takes place on the side of our solution, data storage – on the side of cloud service. The fragment of system sequence diagram, which shows the interaction between our solution and cloud storage service according to Scenario 1 "Uploading a file to the cloud storage service" is provided on Fig.3.

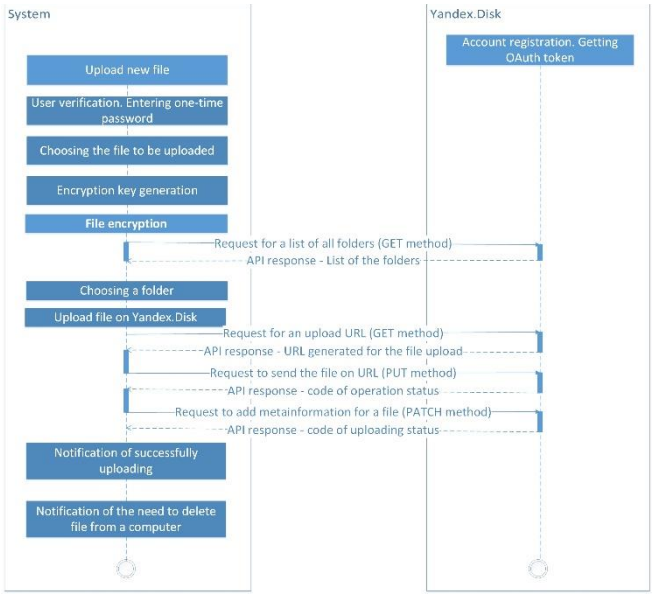

Fig.3. Sequence diagram for Scenario 2"Uploading the file to a cloud service"

C. Approach for data encryption

The task of providing the confidentiality of data is traditionally solved by the implementation of cryptographic algorithms. There is no need to separate the sender, who

applies encryption, and the receiver, who applies decryption of files, so it is advisable to use symmetric cryptographic algorithms in this case. DES is one such algorithm. DES is a block cipher operating on 64-bit blocks of plaintext using a 64-bit key [6].

In addition, to the implementation of the encryption, the solution according to the requirements should provide the secure transfer of encryption keys. Transferring method must be appropriate to the specifics of the scope of the solution: in the cloud data storage users should be able to instantly access all the files available in their cloud folders.

At the time, we consider two approaches to generate encryption keys: by hardware random number generator (Fig. 4) and by extracting bits from the image data (Fig. 5).

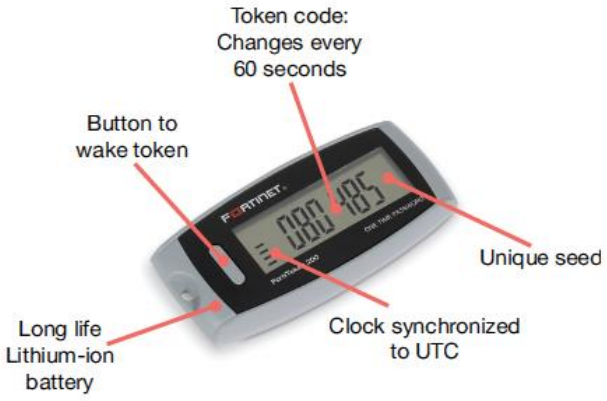

Fig.4. Example of one-time random number generator

Using image files as source files for a key generation has the advantage of improving the convenience in transferring encryption keys between users and implemented in different ways: generating encryption keys directly from the image or getting a key as result of converting the bits of the source file.

Method of generating encryption keys directly from the image, provided by the user, do not ensure a high degree of data confidentiality [7]. Image-keys distribute to users by uploading them into a cloud storage. Storing image-keys in a cloud service raises the probability of a brute-force attack.

More appropriate way to generate encryption key from the image as a result of some transformations. Currently the most popular method of hiding information in the media files is a steganography, the essence of which is to use files as a digital containers to hide data [8]. But using stenography methods in our solution leads to the complexity of the user interface and to the need for additional training in the rules of storage result images.

A modification of method of stenography is the reverse approach, when the encryption key is extracted from the source image by transformations without pre-treatment of this image. In order to generate the key from the source image we must set the sequence of positions. The encryption key consists of the bits standing in positions from a given sequence. In order to increase the resistance to attacks of this sequence should be non-trivial: for example, a sequence of positions of a fractal curve can be used (Fig.5).

If we define a set of positions in fractal curve, the bits from the original image located at these positions will make up the resulting encryption key. The most important limitation of the proposed approach is the need to ensure the confidentiality of the solution source code.

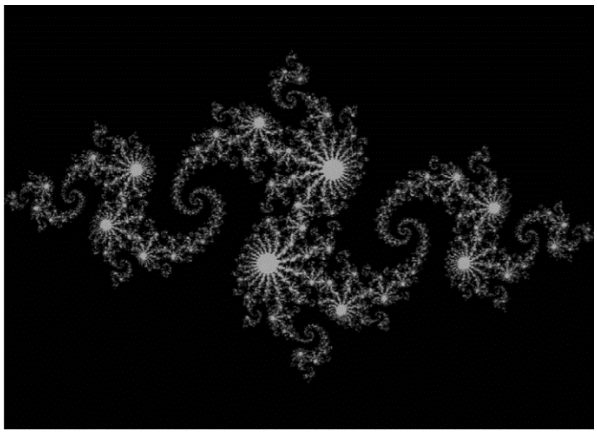

Fig.5. Julia Set visualization

Advantages and disadvantages of considered two-factor authentication schemes will be investigated and compared to choose one for realization.

III. Conclusion

Nowadays privacy of data stored in a cloud services is a concern. The organizations interested in data security while using cloud storages (including fabless-companies) need such solution. This paper purposes an approach to the development of a solution providing security of data stored in the cloud services. The proposed approach has advantages over existing solutions. The approach ensures not only the implementation of the encryption functions but also the method of secure and convenient key generation and distribution. A system developed according to the described method will have an intuitive user interface. The number of actions required from the user is reduced because of direct interaction with cloud service by API interface. The main limitation of the approach is the need to protect program source code from unauthorized access and modification. The method proposed in this paper can be used as a basis for the development of a cross-platform application.

References

[1] Jeorge S.Hurtarte, Evert A.Wolsheimer, Lisa M.Tafoya, “Understanding Fabless IC Technology”. Newnes, 2007, pp.25-32

[2] ‘Terms of Use of Yandex.Disk Service’, 2018. [Online]. Available: https://yandex.com/legal/disk_termsofuse/.

[3] ‘Boxcryptor. Encryption software to secure cloud files’, 2018. [Online]. Available: https://www.boxcryptor.com

[4] ‘WebDAV Client CarotDAV’, 2018. [Online]. Available: http://rei.to/carotdav_en.html.

[5] ‘MEGA’,2019. [Online]. Available: https://mega.nz.

[6] W.Stallings, “Cryptography and Network Security: Principles and Practice”, 6th ed. Prentice Hall Press Upper Saddle River, New Jersey: 2013, pp. 68-89.

[7] Omer A.Shqeer, “Judgment of Extracting Encryption Keys From Image Data”, IJCSNS vol.14, no.2, pp.116-119.

[8] S.Katzenbeisser, Fabien A.P.Petitcolas, “Information Hiding Techniques for Steganography and Digital Watermarking”. Boston: Artech House, 2000, pp.43-71.

[9] J.Sanders, E.Kandrot “CUDA by Example: an introduction to general-purpose GPU programming”. Addison-Wesley Professional,2010, pp.46-57.

Artificial Intelligence in Web Attacks Detecting

Maxim Gromov
Tomsk State University,
36, Lenin ave., Tomsk, 634050, Russia
maxim.leo.gromov@gmail.com

Svetlana Prokopenko
Tomsk State University,
36, Lenin ave., Tomsk, 634050, Russia
s.prokopenko@sibmail.com

Natalia Shabaldina
Tomsk State University,
36, Lenin ave., Tomsk, 634050, Russia
nataliamailbox@mail.ru

Alexander Sotnikov
Tomsk State University,
36, Lenin ave., Tomsk, 634050, Russia
sotnikhtc@gmail.com

***Annotation* – In this paper, the problem of web attacks detecting is considered. We propose to use neural networks to solve the problem. Such approach allows to pre-process user data only once. Experimental results confirm the feasibility of the application of artificial intelligence in web attacks detection.**

***Index Terms* – Web application, attack, neural network.**

I. INTRODUCTION

WEB APPLICATIONS are widely used. Users trust web applications transfer, processing and storage of personal and commercial data. Therefore security of web applications is a hot topic.

As a rule, web applications are verified and tested, in particular, the security of applications is checked. But even in this case, a valid user (who in fact has no malicious intents) may accidentally enter data that actually is an attack on the application. It happens due to the fact that the variety of possible attacks is very large. And at the moment of application development not all attacks are known for developers.

Usually known types of attacks are considered for testing of safety/security. But during exploitation, new types of attacks dangerous for the application may appear. In this case, it becomes necessary to eliminate this vulnerability of the application. It can be done, for example, by adding of a new filter to the application which detects such attacks.

The detection of web application vulnerabilities can be done in different ways. There are mathematical approaches based on automata equations and inequalities solutions [1-5]. These approaches require the description of a part of the program and all kinds of user data by automata. Then the solutions of corresponding automata equation or inequality describe possible attacks on this web application. But these mathematical approaches are not general, because in some cases they can lead to attacks' skipping. In other cases the solutions include not only attacks but also safe data [2].

Furthermore, there is a tool called Stranger [6, 7]. This tool uses an attack pattern and a source code of a web application and draws a conclusion whether the application is vulnerable to the given attack. Unfortunately, Stranger is applicable to programs written in PHP ver. 3 or lower versions.

If new type of attacks appear and the application is vulnerable to these attacks, new filters should be added to the source code of the web application. These filters may be implemented based on the PHP function `preg_replace`. Filters indicate attacks and stop the execution of the application, or modify user data. Such user data modification should not lead to the loss of data meaning but should remove the threat. During exploitation, the web application is regularly upgraded with new filters. So the web application source code is regularly changed. To the best of our knowledge, there are no other ways to protect web applications from new vulnerabilities.

Our paper is devoted to web attacks detection. For this purpose we propose to exploit neural networks. Attack detection is considered as a text classification process. This approach requires only attack patterns and there is no necessity in the source code of the application. Thus this approach can be applied for web attacks detection on applications that are developed in any programming language. When new types of attacks appear, one only needs to retrain the neural network.

II. PROBLEM STATEMENT

All modern web applications are interactive. Usually it is assumed that users interact with the applications. The user enters arbitrary data in specific fields. Since entered data is processed by the application, it may be unsafe for the application. User data can lead to database structure or contents disruption, unauthorized access to data, etc.

To avoid situations described above, it is possible to act in two ways. The first way is to analyze the source code of a web application in order to detect and fix vulnerabilities in the application. The second way is to pre-process user data in order to detect and prevent possible attacks on the web application. Both cases require the knowledge of the type of attacks.

Feasibility of neural networks to pre-process user data is experimentally investigated in this paper.

III. THEORY

In this research, we consider a web application to be vulnerable if it admits unauthorized access to data, their modification, etc. Users interact with the web application by issuing requests to the web server (via form fields or

URL requests). These requests contain transmitted users' data. In this case, an attack is user data that is generated in a special way.

The attack can be detected and neutralized using built-in filters, for example, using the PHP `preg_replace` function. Each type of attack should be described by a regular expression, and the filter function should be called for this expression (Fig. 1a).

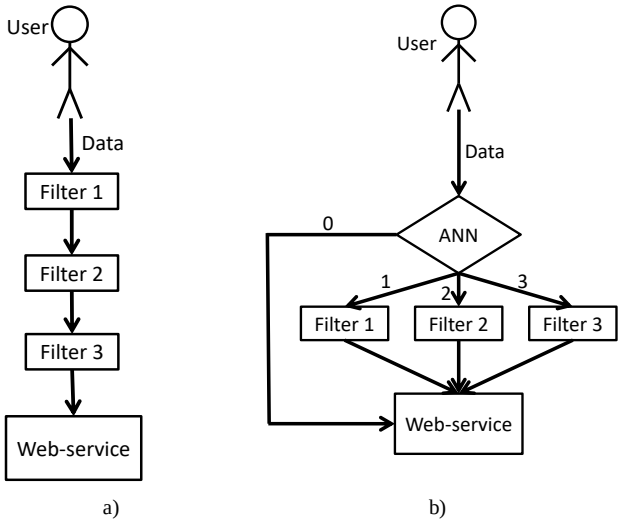

Fig. 1. Attacks' filtering workflow. Classical approach (a), proposed approach (b)

We propose another approach. The idea is to create a function that detects an attack and determines attack's type. Neural network will be used for this purpose [8]. This approach allows to avoid multiple calls of the filtering function and call it with the desired regular expression only once (Fig. 1b).

Since the considered problem is similar to the problem of text messages classification, an appropriate neural network structure is chosen (Fig. 2). The network includes the following layers. The first one is embedding layer, which is designed to map text strings to dense vectors. Next layers are two recurrent layers LSTM (1) and LSTM (2) for analyzing sequences and extracting key features from dense vectors. The activation functions of the recurrent layers are linear. Then dropout layer comes that controls overfitting followed by dense layer. Dense layer is a classical features' classification layer. An activation function of the dense layer is sigmoid. Since this network is used for classification problem, the function categorical cross-entropy is used as a cost function during network training.

The variety of possible attacks is large. Therefore we consider only three types of classical attacks for experiments: two types of SQL injections and one type of XSS attacks.

An SQL injection is an injection of a malicious code into an SQL request in order to gain unauthorized access to a database [9]. An XSS attack (cross-site scripting) is an insertion of malicious code into the page being formed [10]. For example, the malicious code can be written in JavaScript.

The neural network needs to be trained before using. The training set is formed as follows.

Three types of text strings were generated. The first type of strings contains strings with SQL injections of the kind `OR 1=1`. The second one contains strings of common SQL injections. And the third type of strings contains XSS attacks. In each case, the attacks were masked by randomly generated text. We also generated strings without attacks and strings that are similar to attacks but are not attacks in fact.

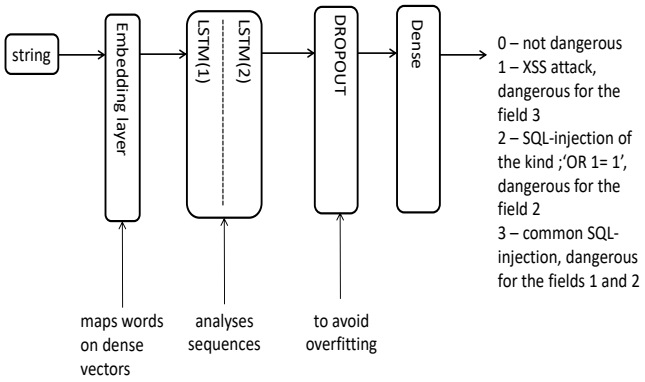

Fig. 2. Neural network structure

IV. EXPERIMENTAL RESULTS

A. An Example of a Web Application and Attacks

In order to develop attack patterns and to train the neural network, we implemented user password change web application. Moreover, we may not experiment with real web applications since these experiments can lead to data corruption stored and processed by the application. The created web application is implemented using the web server solution stack XAMPP [11]. The graphical user interface of this application has a web form with three fields, in which the user enters a login, an old-password and a new-password.

The following two database queries are made in the PHP part of the web application when transferring data from the form to the web server:

```
SELECT pswrd FROM users WHERE login = '".$login."';
UPDATE users SET pswrd = '".$newpass."' WHERE login = '".$login."';
```

For this web application, we consider various SQL injections. An example of one of them is as follows.

Suppose that a user does not know the structure of database queries, but knows names of tables. The user wants to drop the table containing information about logins and passwords. In order to drop the table, the user types the following text in the new-password field:

```
'; drop table users; --
```

It implies the following database query:

```
UPDATE users SET pswrd = ''; drop table users; -- ' WHERE login = '".$login."';
```

As a result of the malicious query, the table `users` is dropped.

B. Experiments to Detect Web Attacks Using a Neural Network

To experiment on web attacks detecting using neural network, the source code of the web application is not required and the purpose of the application is not essential. Therefore, similar to the experiments described in the previous subsection, we consider a web application with graphical user interface form containing three fields (1, 2 and 3). Users type data to these fields. The web application processes data from the specified fields in different ways. The method of data processing is essential for the experiment. These fields are sensitive to the attacks of different types.

The data from the first field is substituted as values of variables in the logical expression for the **WHERE** directive of the SQL query, for example,

```
SELECT * FROM users WHERE login = '".$login."'
```

In the example above, the data from field 1 is substituted for the `$login` variable.

Data from the second field is inserted into SQL query of the general form.

Data from the third field is displayed unchanged in the browser.

To detect and classify attacks, the neural network takes user data string as an input, and returns a class number of the string (Fig. 2):

0 denotes that the user data string does not contain an attack;

1 denotes that the user data string contains an XSS attack. The string is dangerous for the field 3;

2 denotes that the user data string contains an SQL injection of the form `";' OR 1 = 1 '"`. The string is dangerous for the field 2;

3 denotes that the user data string contains an SQL injection of the general form. The string is dangerous for fields 1 and 2.

To train the neural network, the following training set was generated:

– one million different strings with XSS attacks,

– one million different strings with the SQL injection of the form `";' OR 1 = 1 '"`;

– one million different strings with common SQL injection.

Each attack was masked by random text data.

Moreover, strings that resemble attacks but are not attacks were generated. For example, instead of the tag `<SCRIPT>` a non-existent tag `<ASCRIPT>` was used, etc. One million strings of pseudo-attacks for each type of attacks were generated. Therefore, three millions of such pseudo-attacks were generated.

Additionally, one million text strings with no attacks and pseudo-attacks were generated.

Totally seven million text strings (data that user could type in the fields of the web application form) were generated. Each generated string was of the length 100 characters.

To train the neural network all string were shuffled. The type of the string (SQL injections of the kind `OR 1=1`, common SQL injection, XSS attack, and the string without any attack) was kept with the corresponding string. This information was used to train the network and to assess the accuracy of recognition of the attack type.

The Keras over TensorFlow framework was used to implement the neural network. For the experiments we used the computer with the following parameters: processor Intel Core i5-3470 3.2 GHz, 8 GB of RAM, 1 TB hard drive, video card GeForce GTX 650 Ti with CUDA support, operating system Windows 7.

After training the network by 10% of an artificially generated sample of seven million strings, the neural network could classify the attacks with the accuracy of 99.97%.

V. CONCLUSION

In this paper, we considered the problem of web application security. To the best of our knowledge the only approach to solve the problem is to add new filters to the source code of the application. Each filter should detect specific attack and/or modify user data. In contrast to this approach in the paper we suggested to perform two-step pre-processing of user data to detect and filter an attack on the web application.

At the first step an attack is detected and classified. At the second step the user data is filtered by the appropriate filter. Note that in the classical approach user data passes through several filters (Fig. 1a). It happens because it is not known a priori whether the data contain an attack. The type of the attack also is not known. In our approach, user data passes through one filter (Fig. 1b), since the type of attack was recognized at the first step.

As a future work, one could consider the problem of embedding of a trained neural network into a web application. In addition, it is interesting to investigate the problem of neural network training on the fly.

ACKNOWLEDGMENT

This work was carried out with the financial support of grant RNF No. 16-49-03012 "Reliability, security and trust in systems used as services: scalable solutions for effective analysis and management."

REFERENCES

[1] Anton V. Kolomeets, Natalia V. Shabaldina, Ekaterina V. Darusenkova, Nina V. Yevtushenko. Using Models of Finite Transition Systems for Checking Web-Service Security //18th International Conference of Young Specialists on Micro/Nanotechnologies and Electron Devices EDM 2017 : proceedings Erlagol, 29 june - 3 july 2017. Novosibirsk: NSTU publisher, 2017. P. 151-154.

[2] Shabaldina N., Yevtushenko N., Yu F. Towards checking WEB-services security: using automata equations and inequalities // Proceedings of the XII Conference Computer-aided technologies in applied mathematics (ICAM 2018), June 4-8, 2018. P. 90

[3] P. Linz. An Introduction to Formal Languages and Automata, Johnes & Barlett Learning, 2012

[4] L. Kari, “On language equations with invertible operations,” Theoret. Comput. Sci. 132 (1994), L. Kari and G. Thierrin, “Maximal and Minimal Solutions to Language Equations,” Journal of computer and system sciences 53, (1996)

[5] B. A. Trahtenbrot, Ya. M.Barzdin: Finite automata (Behavior and synthesis). Nauka, Moscow 1970 (in Russian).

[6] An Automata-based PHP String Analysis Tool. https://vlab.cs.ucsb.edu/stranger/
[7] F. Yu, M. Alkhalaf, and T. Bultan. Stranger: An automata-based string analysis tool for php. In TACAS, pages 154-157, 2010.
[8] Artificial neural network. https://en.wikipedia.org/wiki/Artificial_neural_network
[9] SQL Injection Cheat Sheet. https://www.netsparker.com/blog/web-security/sql-injection-cheat-sheet/
[10] XSS Filter Evasion Cheat Sheet. https://www.owasp.org/index.php/XSS_Filter_Evasion_Cheat_Sheet
[11] XAMPP. https://www.apachefriends.org

SQLite RDBMS Extension for Data Indexing Using B-tree Modifications

Anton Rigin[1], Sergey Shershakov[2]
Faculty of Computer Science
National Research University – Higher School of Economics
Moscow, Russia
[1]amrigin@edu.hse.ru, [2]sshershakov@hse.ru

The B-tree structure has several modifications which are, by default, not supported in the popular open-source RDBMS SQLite. In the scope of this work an extension for SQLite is developed, based on some modifications of the B-tree structure. The modifications of the base structure were developed as a C++ library. The library is connected to the SQLite using the C-C++ cross-language API. The SQLite extension also implements the novel algorithm for selecting the best possible index structure (B-tree or one of its modifications) for some table of a database.

Keywords—B-tree; data indexing; SQLite; DBMS; RDBMS; multiway tree

I. INTRODUCTION

Last decades, the amount of data volume is growing substantially which exposes the well-known problem of big data [1].

Many companies and laboratories need to collect, store and process big data. There exist many algorithmic and software solutions to cope with these problems. One of these solutions is using indices which are usually represented by data structures such as hash tables and trees.

Using indices creates a new problem – when data are stored on slow carriers, it is more efficient to load data batches from a storage instead of splitting to individual elements. Multiway trees solve this problem. One type of them is a B-tree which was initially described by Bayer and McCreight in 1972 [2]. The B-tree also has several modifications. In this paper, the following B-tree modifications are considered: B^+-tree [3], B^*-tree [4] and B^{*+}-tree (the latter is developed by the author of this paper data structure, which combines the main B^+-tree and B^*-tree features) [5].

This paper extends the research made in the framework of the term project [5].

One of the popular open-source relational database management systems (RDBMS) is SQLite [6]. It is used in mobile phones, computers and many other devices. However, this RDBMS does not support using B^+-tree or B^*-tree as data index structures by default.

The main goals of the work are the following:

- to add B-tree modifications such as B^+-tree, B^*-tree and B^{*+}-tree to SQLite;
- to develop and implement an algorithm that would allow selecting the most appropriate indexing data structure (B-tree, B^+-tree, B^*-tree or B^{*+}-tree) when a user manipulates a table.

The work includes linking of B-tree modifications from a C++ library (developed by the author of this work previously) to SQLite using a C-C++ cross-language API and developing an algorithm for selecting an indexing data structure.

The rest of the paper is organized as follows. Firstly, B-tree, B^+-tree, B^*-tree and B^{*+}-tree are shortly described. After this, the SQLite, its indexing algorithms and extensions are presented. Then, the B-tree modifications C++ library and connecting it to the SQLite RDBMS is described. After this, our previous researches conducted using this library are presented. These researches have proved the main theoretical B-tree modifications complexity hypotheses and they show the abilities of this library. Then, the indexing approach, the methods for outputting the index representation and information and the development of algorithm of selecting the best index structure for table are discussed, after which the experiment conducted using the developed in this work SQLite extension is described. After this, the main points of the paper are summarized in conclusion and used references are presented.

II. B-TREE AND ITS MODIFICATIONS

A. B-tree

The B-tree is a multiway tree. It means that each node may contain more than one data key. Furthermore, each node except of the leaf nodes contains more than one pointer to the children nodes. If some node contains k keys than it contains exactly $k + 1$ pointers to the children nodes [2].

The B-tree depends on its important parameter which is called B-tree order. The B-tree order is such a number t that:

- for each non-root node, the following is true: $t - 1 \leq k \leq 2t - 1$, where k is the number of keys in the node [2];
- for root node in the non-empty tree the following is true: $1 \leq k \leq 2t - 1$, where k is the number of keys in the node [2];
- for root node in the empty tree the following is true: $k = 0$, where k is the number of keys in the node [2].

B-tree operations complexities are the following (t is the tree order, n is the tree total keys count):

- for the searching operation: time complexity is $O(t\log_t n)$, memory usage is $O(t)$ and disk operations count is $O(\log_t n)$ [2];
- for the nodes split operation (the part of the insertion operation): time complexity is $O(t)$, memory usage is $O(t)$ and disk operations count is $O(1)$ [2];
- for the insertion operation (includes the nodes split operation): time complexity is $O(t\log_t n)$, memory usage is $O(t\log_t n)$ for simple recursion and $O(t)$ for tail recursion and disk operations count is $O(\log_t n)$ [2];
- for the deletion operation: time complexity is $O(t\log_t n)$, memory usage is $O(t\log_t n)$ for simple recursion and $O(t)$ for tail recursion and disk operations count is $O(\log_t n)$ [2].

B-tree is usually used as the data index [2].

The example of B-tree is shown on the Fig. 1.

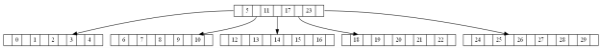

Fig. 1. The B-tree example, tree order $t = 6$.

B. B-tree Modifications

B^+-tree is the B-tree modification in which only leaf nodes contain real keys (real data), other nodes contain router keys for searching real keys. Leaf nodes in B^+-tree contain $t \leq k \leq 2t$ keys, where t is the tree order, the rules for other nodes are the same as in B-tree [3]. Keys deletion in B^+-tree is expected to be faster than in B-tree since it is always performed on the leaf nodes.

B^*-tree is the B-tree modification in which each node (except of the root node) is filled at least by 2/3 not 1/2 [4]. Keys insertion in B^*-tree is expected to be faster than in B-tree.

B^{*+}-tree is the B-tree modification developed by the author of this paper which combines the main B^+-tree and B^*-tree features together. In this data structure only leaf nodes contain real keys (real data) as in B^+-tree and each node (except of the root node) is filled at least by 2/3 as in B^*-tree.

III. Implementation and Tools

A. SQLite and Its Extensions

The SQLite is the popular open-source C-language library which implements the SQLite relational database management system (RDBMS) [6]. The SQLite default index algorithms are hash-table and B-tree. The SQLite does not implement B^+-tree and B^*-tree based indices.

Nevertheless, SQLite supports loading its extensions at run-time, which can add new functionality to the SQLite. For example, it can be a new index structure implementation. One of such extensions is the R-tree. The R-tree is a B-tree modification which allows to index geodata. It is loaded by the SQLite as the extension and delivered together with the SQLite RDBMS default build.

B. B-tree Modifications C++ Library

The B-tree modifications C++ library was developed by the author of this paper previously. It contains B-tree, B^+-tree, B^*-tree and B^{*+}-tree implementations written in C++ [5].

In the current work this library is connected to the SQLite as the run-time loadable extension. For this goal the C-C++ cross-language API is implemented. It is possible to do using the *extern "C" { ... }* C++ statement. The other tasks are to implement base SQLite extension's methods and to use Makefiles to make this extension run-time loadable correctly. The extension provides module for creating virtual tables (tables which encapsulate callbacks instead of simple reading from database and writing to database) based on this module.

C. Research Conducted Using the Library

The B-tree modifications C++ library was previously used for conducting a research on the performance of multiway trees in the problem of structured data indexing by the author of this paper [5].

The CSV files with random content were generated for the indexing, with sizes of 25000, 50000, 75000, 100000 rows. The value of the first cell of each row was considered as a key ("name") of the row and was saved in the tree together with the bytes offset of the row in the indexed CSV file. The charts of different dependencies were built using the Python 2.

The chart with the indexing time dependence on the tree order for a file where the "names" (keys) of the rows are uniformly distributed, with the size of 25000 rows is shown on the Fig. 2.

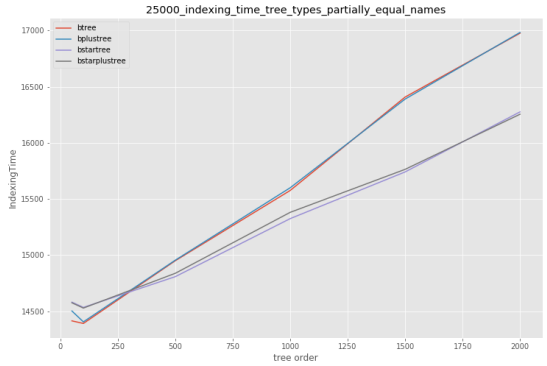

Fig. 2. The chart with the indexing time dependence on the tree order for a file where the "names" (keys) of the rows are uniformly distributed, with the size of 25000 rows.

According to this chart, B*-tree and B*+-tree have a better time performance on the keys insertion than B-tree and B+-tree, as expected. These results are confirmed by the experiments with other parameters (for example, on the larger files with different keys).

However, the better time performance of B*-tree and B*+-tree on the keys insertion has a cost of a larger memory usage as shown on the Fig. 3.

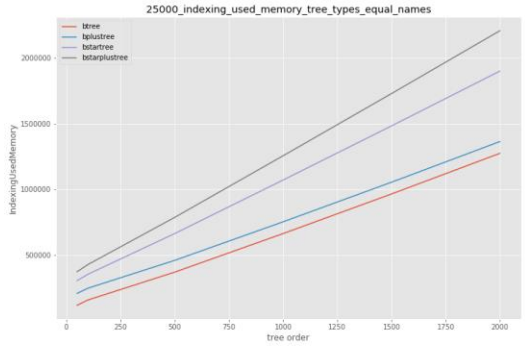

Fig. 3. The chart with the indexing memory usage dependence on the tree order for a file where all the "names" (keys) of the rows are equal, with the size of 25000 rows.

Also, indexing using B*-tree or B*+-tree requires more disk operations than indexing using B-tree or B+-tree as shown on the Fig. 4.

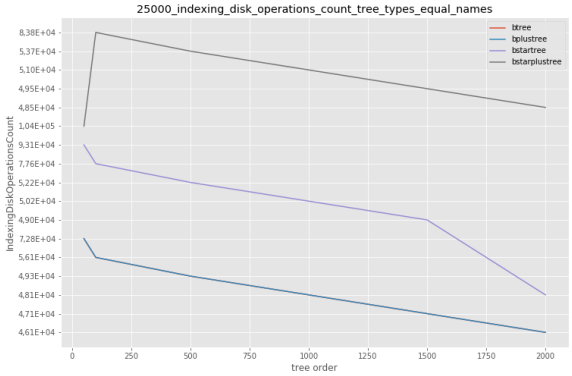

Fig. 4. The chart with the indexing disk operations count dependence on the tree order for a file where all the "names" (keys) of the rows are equal, with the size of 25000 rows.

The monotonous dependence of the keys searching on the tree order is not detected as shown on the Fig. 5.

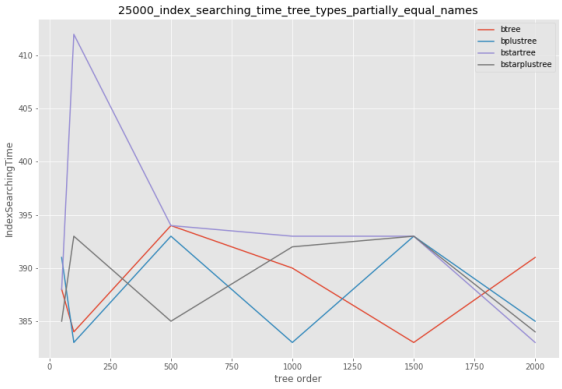

Fig. 5. The chart with the index searching time dependence on the tree order for a file where the "names" (keys) of the rows are uniformly distributed, with the size of 25000 rows.

The B*-tree and B*+-tree require more memory during the keys searching than the B-tree and B+-tree as shown on the Fig. 6.

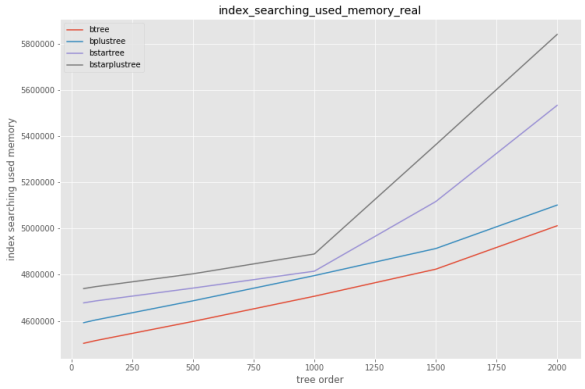

Fig. 6. The chart with the index searching memory usage dependence on the tree order for a file with real (not randomly generated) data.

In addition, the B^{+}-tree and B^{*+}-tree have a better time performance on the keys removing than B-tree and B^{*}-tree as expected and shown on the Fig. 7. This chart also proves that the B^{*+}-tree has the best time performance on the keys removing among all the considered in this paper multiway trees and that the dependence of keys removing time on the tree size is logarithmic.

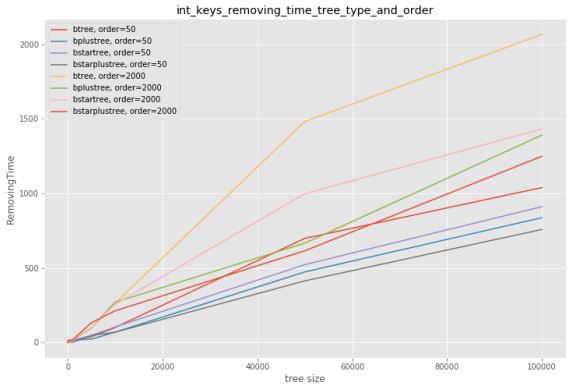

Fig. 7. The chart with the keys removing time dependence on the tree size.

Therefore, the main theoretical hypotheses were confirmed [5].

IV. Working with Indices While Manipulating DB Data

A. Table Creation, Data Search and Updating

In the current work B-tree modifications based indices are built over the existing SQLite table implementation which is represented in the storage as pages of a B-tree by default.

The table creation and main data operations (inserting, searching, deleting and updating) use the methods presented in the Table I.

TABLE I. Main Extension Methods

Method	Purpose
btreesModsCreate(sqlite3*, void*, int, const char* const*, sqlite3_vtab**, char**)	Creates a new table.
btreesModsUpdate(sqlite3_vtab*, int, sqlite3_value**, sqlite_int64*)	Inserts, deletes or updates a value of a row in the table.
btreesModsFilter(sqlite3_vtab_cursor*, int, const char*, int, sqlite3_value**)	Searches for a row in the table.

The extension with the B-tree modifications based indices provides module for creating virtual tables. User should create a virtual table using the module called *btrees_mods* in order to use one of the B-tree modifications as index for the table. When a user creates such virtual table, the *btreesModsCreate()* method of the extension is called and the matching real table is created in the database. Also, a B-tree or one of its modifications is created using the algorithm of selecting the best index's structure (see the section V) and the information about the created table and index's structure (including the name of the file with the B-tree or its modification and the attributes of the primary key of the table) is stored in a special table.

When a user inserts a row into a table, the *btreesModsUpdate()* method of the extension is called and a corresponding record for the index structure is created. The record consists of the primary key value of this row and the row id. This record is saved as a data key into the index structure (B-tree or one of its modifications).

When a user searches for a row in a table, the *btreesModsFilter()* method of the extension is called and the value of the primary key of the row being searched is compared with the keys of the index structure. During the key searching only the primary key value part of the tree's keys is compared with the value of the primary key of the row being searched. If the necessary tree's key is found, the row id is extracted from the key and a row found in the table by the row id is considered as a result of the searching.

When a user deletes a row from a table, the *btreesModsUpdate()* method of the extension is called, the primary key of the deleted row is found in the index structure using the same approach as in the search case. The found key is deleted from the index structure.

When a user updates the value of the primary key of a row in a table, the *btreesModsUpdate()* method of the extension is called. The old value of the primary key is deleted from the index structure and the new value is inserted to the index structure.

B. Index Structure's Graphical Representation and Main Information Outputting

Also, the several methods are available to output the index structure's graphical representation and main information. They are presented in the Table II.

TABLE II. INDEX STRUCTURE'S INFORMATION AND GRAPHICAL REPRESENTATION OUTPUTTING EXTENSION METHODS

Method	Purpose
btreesModsVisualize(sqlite3_context*, int, sqlite3_value**)	Outputs the graphical representation of the table's index structure (tree) into the GraphViz DOT file. It is called after the SQL query such as *SELECT btreesModsVisualize("btt", "btt.dot");*, where *btt* is the table name, *btt.dot* is the outputting GraphViz DOT file name.
btreesModsGetTreeOrder(sqlite3_context*, int, sqlite3_value**)	Outputs the order of the tree used as the table's index structure. It is called after the SQL query such as *SELECT btreesModsGetTreeOrder("btt");*, where *btt* is the table name.
btreesModsGetTreeType(sqlite3_context*, int, sqlite3_value**)	Outputs the type of the tree (1 – B-tree, 2 – B^+-tree, 3 – B^*-tree, 4 – B^{*+}-tree) used as the table's index structure. It is called after the SQL query such as *SELECT btreesModsGetTreeType("btt");*, where *btt* is the table name.

C. SQLite Extension's Usage Example

The developed in this work SQLite extension's usage example is presented on the screenshot (Fig. 8).

```
SQLite version 3.26.0 2018-12-01 12:34:55
Enter ".help" for usage hints.
Connected to a transient in-memory database.
Use ".open FILENAME" to reopen on a persistent database.
sqlite> .load ./btrees_mods
sqlite> CREATE VIRTUAL TABLE btt USING btrees_mods(id INTEGER PRIMARY KEY, a INTEGER, b TEXT);
sqlite> INSERT INTO btt VALUES (4, 2, "ABC123");
sqlite> INSERT INTO btt VALUES (7, 3, "def");
sqlite> SELECT * FROM btt WHERE id = 4;
4|2|ABC123
sqlite> SELECT * FROM btt WHERE id = 7;
7|3|def
sqlite> SELECT * FROM btt WHERE id = 4 OR id = 7;
4|2|ABC123
7|3|def
sqlite> .tables
btrees_mods_idxinfo  btt                  btt_real
sqlite> SELECT * FROM btt_real;
4|2|ABC123
7|3|def
sqlite> SELECT * FROM btrees_mods_idxinfo;
btt|1|0|id|INTEGER|4|tree_18291557263097.btree
sqlite> DROP TABLE btt;
sqlite> .tables
btrees_mods_idxinfo
sqlite> SELECT * FROM btrees_mods_idxinfo;
sqlite> .exit
```

Fig. 8. SQLite extension's usage example.

V. ALGORITHM OF SELECTING THE BEST INDEX STRUCTURE

In this work an algorithm for selecting the best index structure for a table is developed and implemented in the following way.

The algorithm considers B-tree and its modifications (B^+-tree, B^*-tree and B^{*+}-tree) for using as an index structure. The best index structure is defined by the step 6 of the algorithm.

The algorithm is executed at the start of each operation on the table (search, insertion, deletion or update of the table's row) which uses the *btrees_mods* module. The algorithm consists of the following steps.

1. If the current total count of the operations on the tree is equal to 0 or more than 10000 or not a multiple of 1000, then exit the algorithm, otherwise go to step 2.
2. If the current count of the modifying operations on the tree (key insertions, key deletions) is less than 10 % of the current total count of the operations on the tree, then exit the algorithm, otherwise go to step 3.
3. If the current count of the key insertion operations is more than 90 % of the current count of the modifying operations on the tree, then select the B^*-tree as the index structure and go to step 6, otherwise go to step 4.
4. If the current count of the key insertion operations is not less than 60 % of the current count of the modifying operations on the tree, then select the B^{*+}-tree as the index structure and go to step 6, otherwise go to step 5.
5. Select the B^+-tree as the index structure and go to step 6.
6. If the new index structure was selected in the steps 3 – 5, then rebuild the existing index structure into the new selected index structure (which is considered as the best index structure) saving all the data stored in the existing index structure.

The tree order of the B-trees and their modifications used in the SQLite extension developed in this work equals 100.

VI. EXPERIMENT CONDUCTED USING THE DEVELOPED SQLITE EXTENSION

The experiment on the counting the empirical computational complexity is conducted using the developed in this work SQLite extension. The operations' times were counted using the SQLiteStudio GUI manager [7]. The results are presented in the Table III.

TABLE III. EXPERIMENT RESULTS

Operation on the table	Total execution time (ms)	Mean execution time per row (ms)
Table creation	21	-
First 500 rows insertion	9128	18.3
Next 500 rows insertion	9802	19.6
1001st row insertion (including the B-tree into the B^*-tree rebuilding)	50	50
Next 499 rows insertion	9168	18.4
Last 500 rows insertion	8933	17.9

Operation on the table	Total execution time (ms)	Mean execution time per row (ms)
First 500 rows deletion	9888	19.8
Next 500 rows deletion (including the B^*-tree into the B^{*+}-tree rebuilding)	9974	19.9
Next 500 rows deletion	9784	19.6
Last 500 rows deletion (including the B^{*+}-tree into the B^+-tree rebuilding)	9201	18.4
1000 rows insertion	18113	18.1
Next 4800 rows insertion (including the B^+-tree into the B^{*+}-tree rebuilding)	86465	18

According to the data in the Table III, the key insertion on the B^*-tree is faster than on the B-tree as expected. The key deletion on the B^+-tree and B^{*+}-tree is faster than on the B-tree and B^*-tree respectively. Also, the key insertion on the B^{*+}-tree is slightly faster than on the B^+-tree.

VII. Conclusion

The big data problem currently affects the world. There are many mathematical and software solutions for collecting, storing and processing big data including the data indexing. Many of the index data structures are tree-based ones such as B-tree and its modifications. B-tree is used as an index structure in many DBMSs including the popular open-source RDBMS SQLite. However, the SQLite does not support its modifications which may be more appropriate for some tasks than the original B-tree. In the current work this problem is elaborated.

Firstly, the B-tree modifications C++ library is connected to the SQLite as the extension using C-C++ cross-language API. After this, the algorithm of the best index selecting is developed and implemented and the experiment is conducted using the developed in this work SQLite extension.

This work tests new data indexing approaches using the SQLite as an example. The results of the work can be used by researchers and professors in this field and their students. The SQLite B-tree modifications extension can be used by all the developers who use this DBMS.

Acknowledgment

This work is supported by RFBR according to the Research project No. 18-37-00438 “mol_a”.

References

[1] J. Manyika *et al.*, “Big data: The next frontier for innovation, competition, and productivity,” McKinsey Global Institute, May 2011. Accessed: Jan. 20, 2019. [Online]. Available: https://www.mckinsey.com/~/media/McKinsey/Business%20Functions/McKinsey%20Digital/Our%20Insights/Big%20data%20The%20next%20frontier%20for%20innovation/MGI_big_data_exec_summary.ashx

[2] R. Bayer and E. McCreight, “Organization and maintenance of large ordered indexes,” *Acta Informatica*, vol. 1, no. 3, pp. 173 – 189, 1972.

[3] K. Pollari-Malmi. (2010). B^+-trees [PDF paper]. Available: https://www.cs.helsinki.fi/u/mluukkai/tirak2010/B-tree.pdf

[4] “B^*-tree.” NIST Dictionary of Algorithms and Data Structures. Available: https://xlinux.nist.gov/dads/HTML/bstartree.html (accessed Dec. 24, 2018).

[5] A. Rigin, “On the Performance of Multiway Trees in the Problem of Structured Data Indexing,” (in Russian), coursework, Dept. Soft. Eng., HSE, Moscow, Russia, 2018.

[6] “SQLite Home Page.” SQLite.org. Available: https://www.sqlite.org/ (accessed Jan. 20, 2019).

[7] “SQLiteStudio”. SQLiteStudio. Available: https://sqlitestudio.pl/ (accessed: Jan. 26, 2019).

Supporting evolutionary concepts to organize information search in the Internet

1st Alexander Marenkov
I nstitute YurInfor-MSU Moscow
Malaya Pirogovskaya 5, Moscow,
119435, Russian Federation
qwex-x@rambler.ru

2nd Senior Researcher Sergey Kosikov
I nstitute YurInfor-MSU Moscow
Malaya Pirogovskaya 5, Moscow,
119435, Russian Federation
kosikov.v@gmail.com

3rd Candidate of Technical Sciences Larisa Ismailova
I nstitute YurInfor-MSU Moscow
Malaya Pirogovskaya 5, Moscow,
119435, Russian Federation
lyu.ismailova@gmail.com

***Abstract*—Problem domain (PD), which are modeled in information systems, are subject to changes; they have the dynamics that must be taken into account when designing and further using an information system. In this case, the arising changes in the problem domain may not only affect the specific data but change the content of the meta descriptions of the problem domain. This instability is especially characteristic of the information from the Internet. This requires additional domain modeling tools and information system support for saving the actual connection between the information system and the problem domain.**

The paper proposes an approach to modeling dynamic PD based on the support of evolutionary concepts. It also considers the possibility of using the approach to develop a prototype of a system for supporting information search in the Internet and processing the data found.

Keywords—concept, extension, intensional, problem domain, domain dynamics

I. INTRODUCTION

When researching the PD one should adhere to the hypothesis, which forms the possibility of allocating indivisible atomic objects, on the one hand, in this problem domain, and the connections between these objects, on the other hand. In its turn, the connected objects can form new objects in the PD, and it is possible to include the connections between objects themselves into the number of objects [4]. The dynamic nature of the PD requires a formalized description of changes as a basis for developing tools. The changes may be extensional (changing the scope of concepts in the description of the problem domain) and intensional (changing the content of the concepts, i.e., the researcher's understanding of the problem domain).

The indicated above is characteristic of such an information resource as the Internet, as well. Numerous changes of concepts are seen in the Internet environment, which today penetrate many spheres of human activity, be it information gathering, training, communication, job, leisure, etc. Constantly new information appears, the existing information is deleted or is affected by modifications. Network pages are identified by a URL, which can be considered as an individual identifier of the information page. The change in the content of a page can both keep the classification attributes of a page (extensional changes) and lead to their change (intensional changes).

The changes may also be related to a modification of the PD. This happens when the Internet user formulates information queries. When the query is performed, a dynamic web page is created in accordance with its own classification of resources. Different queries may classify the same Internet resources into different classes according to the setting the classifying characteristics.

The paper proposes an approach to the formalization of variable classifications of objects based on the evolutionary concept technique. An evolutionary concept is understood as a concept supplied with a spectrum of its potential transformations, keeping a given set of semantic characteristics of the concept. The paper discusses ways to specify the general definition of the evolutionary concept regarding the Internet.

II. THE TASK OF SUPPORTING EVOLUTIONARY CONCEPTS

Ensuring the work with evolutionary concepts is a critical opportunity when developing information systems in dynamic problem domains. For this reason, the task of supporting evolutionary concepts for describing dynamic objects is given a priority and is considered as the task to form a set of tools that provide for the following:

- representation of objects, allowing to account the dynamics of both extensions and intensions of the introduced concepts;
- ability to compute the assigning of objects bound to the point of correlation;
- ability to store descriptions of objects with the support to linking with the object data about the nature of its dynamics and extracting objects according to such data.
- The need to support the work in the Internet environment makes additional requirements to the developed tools. These requirements are as follows:
- dynamic invocation to the address of the resource in the Internet to check the validity of the link;
- dynamic information retrieval by link and comparison with a set of stored samples to determine the presence of changes and define their nature;

- construction and re-construction of the classification of dynamic objects, including the case when modifying the intentions of concepts in the problem domain.

It is feasible to solve the problem by combining the expressive capabilities of semantic networks and applicative computing systems. In this case, it seems possible to provide a combination of the representation flexibility and the power of computational tools enough to support evolutionary concepts.

The possibility of using the approach to develop a prototype of a system for supporting information search in the Internet and processing the data found is under consideration.

III. References

[1] Storing RDF at relational database. URL: http://infolab.stanford.edu/~melnik/rdf/db.html

[2] Current status of RDF, URL: http://www.w3.org/standarts/techs/rdf#w3c_all

[3] Quillan M. R. Semantic memory // BOLT BERANEK AND NEWMAN INC CAMBRIDGE MA. 1966. №. SCIENTIFIC-2.

[4] Wolfenhagen V. E. Logic. Lecture notes: the technique of reasoning. Moscow. JurInfoR Center JSC, 2002.

[5] Wolfengagen V. E., Ismailova L. Y., Kosikov S. V. The Presentation of Evolutionary Concepts // First International Early Research Career Enhancement School on Biologically Inspired Cognitive Architectures. Springer, Cham, 2017. C. 113-125.

[6] Wolfengagen, V. 2010. Semantic Modeling: Computational Models of the Concepts // In Proceedings of the 2010 International Conference on Computational Intelligence and Security (CIS '10). IEEE Computer Society, Washington, DC, USA, 42-46. DOI=10.1109/CIS.2010.16. URL:http://dx.doi.org/10.1109/CIS.2010.16

Deriving test suites with guaranteed fault coverage against nondeterministic Finite State Machines with timed guards and timeouts

Aleksandr Tvardovskii
National Research Tomsk State University
Tomsk, Russia
tvardal@mail.ru

Nina Yevtushenko
Ivannikov Institute for System Programming RAS
Moscow, Russia
evtushenko@ispras.ru

***Abstract*—The behavior of many information and control systems nowadays is nondeterministic and depends on time aspects. In this paper, we adapt classical FSM based test derivation methods for initialized nondeterministic FSMs with timed guards and timeouts (TFSMs). A proposed approach and appropriate fault model are based on the FSM abstraction of the given TFSM specification that can be used to describe the behavior of a TFSM and allows to adapt classical FSM based test derivation methods when deriving tests for TFSMs. We study properties of such an abstraction for a nondeterministic TFSM and justify that our method allows to derive test suites with guaranteed fault coverage with respect to the defined fault model.**

Keywords—Finite State Machine, timeout, timed guard, nondeterministic Timed Finite State Machine, test derivation

I. INTRODUCTION

Finite State Machines (FSMs) are widely used for analysis and synthesis of discrete event systems [1]. In particular, FSM based approaches can be effectively used when deriving test sequences for determining whether a given implementation considered as a "black box" conforms to its specification and a number of methods exist for deriving complete test suites with respect to various fault models [see, for example, 2-5] without the explicit enumeration of possible FSMs under test. Well-known W-method [2] and many its derivatives have been developed including those for FSMs with the nondeterministic behavior (see, for example, [4, 6]). Researchers often consider the case when the specification is a nondeterministic FSM, while an implementation FSM is deterministic and conforms to the specification if the implementation behavior is contained in that of the specification. In other words, the specification nondeterminism occurs according to the optionality of the informal requirements' description and the behavior of a conforming implementation must not violate the specification.

Nowadays time aspects become very important when describing the behavior of digital and hybrid control systems, and, respectively, similar to automata [7] classical FSMs were extended with time variables [see, for example, 5, 8-12]. When the behavior of a system under test is described by a Timed Finite State Machine (TFSM), classical FSM-based methods have to be modified and extensions to the W-based methods are considered in the context of systems with timed constraints [8], [13]. In [10], Merayo et al. consider timed possibly nondeterministic FSMs where time elapsed when an output has to be produced after an input has been applied to the FSM under test is limited. The model also takes into account input timeouts at states. However, the authors do not consider test derivation; yet establish a number of conformance relations. El-Fakih et al. [9] consider test derivation and assessment for FSMs with timed guards; such an FSM has a single clock that is reset at every transition. In the thesis by Zhigulin [12], a method is proposed for deriving complete test suites for FSMs with timeouts. The author considers a traditional fault domain assuming that the number of states of an implementation TFSM (Implementation Under Test, IUT) does not exceed that of the state reduced specification TFSM as well as the maximal finite timeout of the IUT does not exceed that of the specification. However, as we further show, two reduced TFSMs with timeouts can be equivalent but not isomorphic and this fact violates the main idea of W-based methods of checking the isomorphism or homomorphism between transitions of the specification and implementation under test. In [11], the authors show that the behavior of a deterministic TFSM can be adequately described by its FSM abstraction and this is a hint that a fault model can be derived based on such abstraction for which well elaborated FSM based methods with guaranteed fault coverage can be applied. Such a fault model is considered in [14] for deriving a complete test suite against deterministic TFSMs.

In this paper, we consider FSMs with timed guards, timeouts and output delays (TFSM) which generalize the TFSM model that has only timed guards or only input timeouts [10]. Moreover, in our case, a TFSM can be nondeterministic. Timed guards describe the system behavior depending on a time instance when an input is applied. If no input is applied until an (input) timeout expires then the system can spontaneously move to another state. An output delay describes a time for processing a given transition.

We propose a method for deriving a test suite with guaranteed fault coverage against a complete possibly nondeterministic specification FSM with timed guards, input timeouts and output delays with respect to the reduction relation assuming that an implementation TFSM under test is deterministic. The fault model and a procedure for deriving a complete test suite are based on the FSM abstraction of a given TFSM specification since according to [11], the behavior of a TFSM can be completely described by its corresponding (untimed) FSM abstraction.

The structure of the paper is as follows. Section 2 contains the preliminaries for classical and timed FSMs. It also contains the explanation how the behavior of a TFSM can be described using an appropriate FSM abstraction. In Section 3, existing test derivation methods for nondeterministic FSMs with respect to the reduction relation are considered. Section 4 contains the review of related works on test derivation against Timed FSM models. In Section 5, a method is proposed for deriving a complete test suite against a

nondeterministic FSM with timed guards and timeouts by determining an appropriate fault model based on the FSM abstraction of the given TFSM specification; the section also contains an example of a test derivation procedure. Section 6 concludes the paper.

II. Preliminaries

This section contains basic definitions of classical Finite State Machines and Timed Finite State Machines as their extension. We also show how the behavior of a TFSM can be adequately described by the corresponding FSM abstraction and establish some useful properties of such FSM abstractions.

A. Finite State Machines

The model of a Finite State Machine (FSM) [1] is used for describing the behavior of a system that moves from state to state under input stimuli and produces a predefined output response. Formally, an initialized FSM is a 5-tuple $\mathsf{S} = (S, I, O, h_\mathsf{S}, s_0)$ where S is a finite non-empty set of states with the designated initial state s_0, I and O are input and output alphabets, and $h_\mathsf{S} \subseteq (S \times I \times O \times S)$ is the transition (behavior) relation. A transition (s, i, o, s') describes the situation when an input i is applied to S at the current state s. In this case, the FSM moves to state s' and produces the output (response) o. FSM S is *nondeterministic* [15] if for some pair $(s, i) \in S \times I$, there can exist several pairs $(o, s') \in O \times S$ such that $(s, i, o, s') \in h_\mathsf{S}$; otherwise, the FSM is *deterministic*. FSM S is *complete* if for each pair $(s, i) \in S \times I$ there exists $(o, s') \in O \times S$ such that $(s, i, o, s') \in h_\mathsf{S}$; otherwise, the FSM is *partial*. FSM S is *observable* if for every two transitions $(s, i, o, s_1), (s, i, o, s_2) \in h_\mathsf{S}$ it holds that $s_1 = s_2$. In the following, we consider complete observable possibly nondeterministic FSM specifications, while an implementation is a complete deterministic FSM. A complete nondeterministic FSM is reduced if for every two different states, the sets of traces do not coincide. The unique reduced form exists for any complete nondeterministic FSM and can be derived similar to that for complete deterministic FSMs [15].

A trace or an *Input/Output sequence* α/γ, written often as an I/O sequence, of the FSM S at state s is a sequence of consecutive input/output pairs starting at the state s. Given a trace α/γ, α is the *input projection* of the trace (input sequence) while γ is the corresponding *output projection* (output sequence), i.e., a possible output response of the FSM when the sequence α is applied at state s. Given a complete nondeterministic FSM, there can exist several output responses for an input sequence at a given state.

Given states s and p of complete FSMs S and P, state p is a *reduction* of s (written, $p \leq s$) if the set of I/O sequences of FSM P at state p is contained in the set of I/O sequences of FSM S at state s. FSM P is a *reduction* of FSM S if the reduction relation holds between the initial states of the machines.

B. Timed Finite State Machines

A timed FSM (TFSM) is enriched with timed guards and timeouts [11]. The timed guards at a state have less time upper bounds than the timeout at the state (if any) and describe the behavior at a given state for inputs which arrive at different time instances. Correspondingly, an initialized TFSM is a 6-tuple $\mathsf{S} = (I, S, O, h_\mathsf{S}, \Delta_\mathsf{S}, s_0)$ where S is a finite non-empty set of states with the designated initial state s_0, I and O are input and output alphabets, $h_\mathsf{S} \subseteq S \times I \times O \times S \times \Pi \times Z$ is the *transition relation* and Δ_S is the timeout function. The set Π is a set of *input timed guards* and Z is the set of output delays which are non-negative integers. The *timeout function* is the function $\Delta_\mathsf{S}: S \to S \times (N \cup \{\infty\})$ where N is the set of positive integers: for each state this function specifies the maximum time for waiting for an input. If no input is applied until an (input) timeout expires then the system can spontaneously move to another state. By definition, for each state of TFSM exactly one timeout is specified. An input timed guard $g \in \Pi$ describes the time domain when a transition can be executed and is given in the form of interval $<min, max>$ from $[0; T)$, where $< \in \{(, [\}, > \in \{),]\}$ and T is the input timeout at the current state. We also denote the largest finite boundary of timed guards and timeouts as B_S. The transition $(s, i, o, s', g, d) \in S \times I \times O \times S \times \Pi \times Z$ means that TFSM S being at state s accepts an input i applied at time $t \in g$ measured from the initial moment or from the moment when TFSM S has produced the last output; the clock then is set to zero and S produces output o exactly after d time units. Given state s of TFSM S such that $\Delta_\mathsf{S}(s) = (s', T)$, if no input is applied before the timeout T expires, the TFSM S moves to state s'. If $\Delta_\mathsf{S}(s) = (s', \infty)$ then $s' = s$, and this means that the TFSM can stay at state s indefinitely long waiting for an input.

Given TFSM S, S is a *complete* TFSM if the union of all input timed guards at any state s under every input i equals $[0; T)$ when $\Delta_\mathsf{S}(s) = (s', T)$. In this paper, we consider only complete TFSMs and the question about the interpretation of undefined transitions in partial machines and their augmentation is out of the scope of this paper [16].

TFSM S is a *deterministic* TFSM if for each two transitions $(s, i, o_1, s_1, g_1, d_1), (s, i, o_2, s_2, g_2, d_2) \in h_\mathsf{S}$, $s_1 \neq s_2$, $d_1 \neq d_2$ or $o_1 \neq o_2$, it holds that $g_1 \cap g_2 = \varnothing$, otherwise, TFSM S is *nondeterministic*. In this paper, we consider the system specification as a complete observable possibly nondeterministic TFSM while the behavior of an implementation under test (IUT) is described by a complete deterministic TFSM. In other words, the specification describes a set of permissible possible behaviors and a conforming implementation must be one of them.

Example. Consider a TFSM S in Figure 1 with two states, one input and three outputs, where $\Delta_\mathsf{S}(a) = (b, 2)$, i.e., the timeout at state a is 2. For state b, $\Delta_\mathsf{S}(b) = (b, \infty)$, and this loop is not shown in the figure. If input i is applied to the TFSM at state a at time instance 1 measured from the initial moment then S moves to state b producing output o_2 after one time unit. However, if any input is not applied to TFSM until time value reaches 2 then S moves to state b using a timeout transition. At state b, TFSM S can wait for an input indefinitely long.

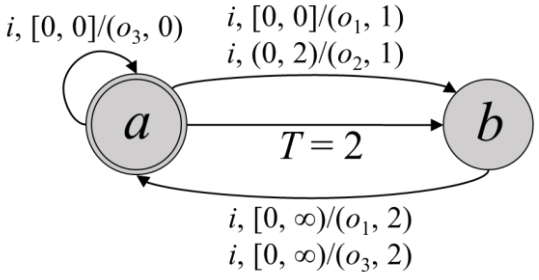

Fig. 1. Timed Finite State Machine S

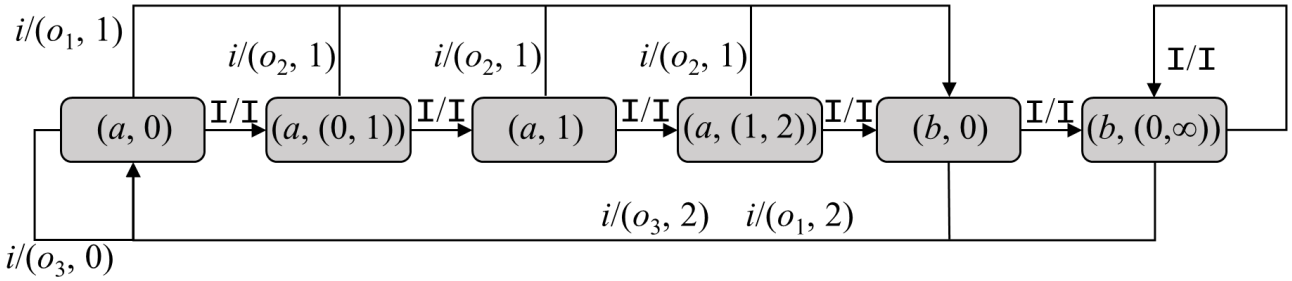

Fig. 2. FSM abstraction $\mathsf{A_S}$ of TFSM S (Figure 1)

A *timed input* is a pair (i, t) where $i \in I$ and t is a real; a timed input (i, t) means that input i is applied to the TFSM at time instance t measured from the initial moment or from the moment when TFSM S has produced the last output. A timed output is a pair (o, d) where $o \in O$ and d is the output delay measured from the moment when an input has been applied. In order to determine the output response of the TFSM at state s to a timed input (i, t), state s', which is reached by the TFSM by timeout transitions at time instance t, is calculated first [12]. State s' is a state where TFSM moves from state s via timeout transitions such that the maximum sum Σ of all timeouts starting from state s is less than t. At the second step, a transition (or several transitions for nondeterministic TFSM) (s', i, o, s'', g, d) such that $t - \Sigma \in g$ is considered. According to this transition, the machine produces the output (o, d) to a timed input (i, t) applied at state s and moves to the next state s''.

A sequence of timed inputs $\alpha = (i_1, t_1) \dots (i_n, t_n)$ is a *timed input sequence*, a sequence of timed outputs $\gamma = (o_1, d_1) \dots (o_n, d_n)$ is a *timed output sequence*. The TFSM is initialized and the clock is equal to 0 at the initial moment. Given a timed input sequence $(i_1, t_1) \dots (i_n, t_n)$, an input i_1 is applied when clock value is equal to t_1; after applying the input the clock is set to 0 and the machine produces an output o_1 when clock value is equal to d_1. After producing the output o_1 the clock is reset and the machine is waiting for another input i_2 that is applied when clock value equals t_2. After applying the input i_2 the clock is set to 0 and the machine produces an output o_2 when clock value is equal to d_2. After producing the output o_2 the clock is reset and the machine is waiting for another input i_3, etc. A sequence $\alpha/\gamma = (i_1, t_1)/(o_1, d_1) \dots (i_n, t_n)/(o_n, d_n)$ of consecutive pairs of timed inputs and timed outputs starting at the state s is a *timed I/O sequence* or a *timed trace* of TFSM S at state s. Note that time of the first timed input in the sequence is counted from startup of the system at state s while time of all next inputs is counted from the time instance when a previous output was produced. Similar to FSMs, α is an applied timed input sequence while γ is the corresponding output response of the TFSM to sequence α of applied inputs. Given a state of a complete nondeterministic TFSM, there can exist several output responses to a timed input sequence.

Similar to FSMs, the set of all timed traces at the initial state determines the behavior of an initialized TFSM.

Example. Consider TFSM S in Figure 1 again. If a timed input sequence $(i. 2.5).(i, 0)$ is applied to S at state a then TFSM first moves to state b by timeout when clock value reaches 2. The clock is reset and output $(o_1, 2)$ or $(o_3, 2)$ is produced, the system moves back to state a and the clock is reset When the next input $(i, 0)$ is immediately applied, the TFSM moves either to state a with timed output $(o_3, 0)$ or to state b with timed output $(o_1, 1)$.

Given states s and p of complete TFSMs S and P, state p is a *reduction* of s (written, $p \leq s$) if the set of timed I/O sequences of TFSM P at state p is contained in the set of timed I/O sequences of TFSM S at state s. TFSM P is a *reduction* of TFSM S if the reduction relation holds between the initial states of the machines.

C. FSM abstraction

The behavior of a TFSM can be adequately described using a classical FSM that is called the *FSM abstraction* of the TFSM and is derived similar to [11]; however, in [11], output delays are not considered.

Given a complete observable possibly nondeterministic TFSM $\mathsf{S} = (S, I, O, \lambda_\mathsf{S}, \Delta_\mathsf{S}, s_0)$, the largest finite boundary of timed guards and timeouts B_S and maximum output delay D, we derive the FSM abstraction of TFSM S as the FSM $\mathsf{A_S} = (S_A, I \cup \{\mathtt{I}\}, O_A, \lambda_{A\mathsf{S}}, s_0)$ where $S_A = \{(s, 0), (s, (0, 1)), \dots, (s, (B_\mathsf{S} - 1, B_\mathsf{S})), (s, B_\mathsf{S}), (s, (B_\mathsf{S}, \infty)): s \in S\}$, $O_A = \{(o, 0), (o, 1), \dots, (o, D): o \in O\} \cup \{\mathtt{I}\}$. The input $\mathtt{I}$ is a special input of the FSM abstraction. Given state (s, t_j), $t_j = 0, \dots, B_\mathsf{S}$, of FSM $\mathsf{A_S}$ and input i, a transition $((s, t_j), i, (o, d), (s', 0))$ is a transition of the FSM abstraction $\mathsf{A_S}$ if and only if there exists a transition $(s, i, o, s', g_i, d) \in \lambda_\mathsf{S}$ such that $t_j \in g_i$. Given state (s, g_j), $g_j = (0, 1), \dots, (B_\mathsf{S} - 1, B_\mathsf{S}), (B_\mathsf{S}, \infty)$, of FSM $\mathsf{A_S}$ and input i, a transition $((s, g_i), i, (o, d), (s', 0))$ is a transition of $\mathsf{A_S}$ if and only if there exists a transition $(s, i, o, s', g, d) \in \lambda_\mathsf{S}$ such that $g_i \subseteq g$. In other words, transitions under input $i \in I$ correspond to timed inputs (i, t) where t is 'hidden' as the second item of states of the FSM abstraction $\mathsf{A_S}$. Transitions under the special input $\mathtt{I}$ correspond to the clock change between non-integer and integer values, or to a timeout transition between states. Given state s such that $\Delta_\mathsf{S}(s) = (s', T)$, transitions $((s, n), \mathtt{I}, \mathtt{I}, (s, (n, n + 1)))$ and $((s, (n - 1, n)), \mathtt{I}, \mathtt{I}, (s, n))$ are in the transition relation $\lambda_{A\mathsf{S}}$ if and only if $n < T$. Transition $((s, (n - 1, n)), \mathtt{I}, \mathtt{I}, (s', 0)) \in \lambda_{A\mathsf{S}}$ if and only if $n = T < \infty$. In [11], it is shown that the FSM abstraction of complete and deterministic TFSM S is also complete and deterministic. In the same way, it can be shown that the FSM abstraction of a complete observable nondeterministic TFSM S is complete observable and nondeterministic.

Example. For a deterministic TFSM S in Figure 1 the corresponding FSM abstraction is shown in Figure 2. FSM abstraction $\mathsf{A_S}$ has states $(a, 0)$, $(a, (0, 1))$, $(a, 1)$, $(a, (1, 2))$, $(b, 0)$, $(b, (0, \infty))$. Transitions $((a, 0), i, (o_1, 1), (b, 0))$ and $((a, 0), i, (o_3, 0), (a, 0))$ exist in FSM abstraction $\mathsf{A_S}$ since TFSM S has transitions $(a, i, o_1, b, [0, 0], 1)$ and $(a, i, o_3, a, [0, 0], 0)$. FSM abstraction $\mathsf{A_S}$ has transition $((a, (0, 1)), i, (o_2, 1), (b, 0))$ since TFSM S has transition $(a, i, o_2, b, (0, 2), 1)$. Transition $((a, 0),$

I, I, (*a*, (0, 1))) of A_S corresponds to clock change at state *a* from time instance 0 to the interval (0, 1).

A timed input sequence α of TFSM S can be transformed into a corresponding input sequence α_{FSM} of the FSM abstraction A_S. In this case, each timed input (*i*, *t*) is replaced by sequence I.I … I.*i* of inputs of the FSM abstraction where the number of inputs I equals the number of clock transitions between a non-integer and integer values for the time duration *t*. At the same time the response of the FSM abstraction to sequence I.I…..I.*i* equals I.I…..I.(*o*, *d*), where the number of inputs I is the same as for the timed input (*i*, *t*) and (*o*, *d*) is the response of the TFSM to timed input (*i*, *t*). Thus, the output sequence of the FSM abstraction γ_{FSM} can be transformed into corresponding timed output sequence γ by removing all outputs I. The following statement can be established.

Proposition 1. A timed trace α/γ exists for TFSM S if and only if there exists a trace $\alpha_{FSM}/\gamma_{FSM}$ for the FSM abstraction A_S.

Proposition 2. There exists a timed trace α/γ at state *s* of a possibly nondeterministic TFSM S if and only if the FSM abstraction A_S has a trace $\alpha_{FSM}/\gamma_{FSM}$ at state (*s*, 0).

Indeed, all the transitions under input I are deterministic and correspond to the clock change between integer and non-integer value and equal to increasing of timed variable while transitions at state (*a*, *g*) of abstraction under another input *i* corresponds to transitions of TFSM at state *a* at time (or timed interval) *g*.

Example. Consider TFSM S in Figure 1 and its FSM abstraction in Figure 2. Timed trace (*i*, 2.5)/(o_1, 2).(*i*, 0)/(o_3, 0) of TFSM S corresponds to trace I/I.I/I.I/I.I/I.I/I.*i*/(o_1, 2).*i*/(o_3, 0) of FSM abstraction A_S, and vice versa.

According to Proposition 2, all the trace features of a TFSM are preserved for its FSM abstraction and thus, the set of reductions of a TFSM can be analyzed based on a set of reductions of a classical FSM. The following statement establishes necessary and sufficient conditions for two TFSM states to be in the reduction relation.

Proposition 3. State *s* of TFSM S is a reduction of state *p* of TFSM P if and only if state (*s*, 0) of the FSM abstraction A_S is a reduction of state (*p*, 0) of FSM A_P.

Thus, the conclusion about the reduction relation between two TFSMs can be drawn based on their FSM abstractions and there exist methods for checking the reduction relation between two FSM states or between two FSMs.

III. Fault Models and Test Suites

FSM based testing can be preset and adaptive. We first consider the preset testing where *test cases* are (timed) input sequences derived from the given TFSM specification to determine whether a given IUT, which is assumed to have the FSM behavior, conforms to the given specification. In this section, classical FSM based test derivation methods are adapted for test derivation against Timed FSMs.

In this paper, an implementation FSM P conforms to the specification if FSM P is a reduction of the specification FSM. In other words, an implementation FSM P conforms to the specification FSM if for each input sequence the output response of the FSM P is contained in the set of output responses of the specification FSM to this input sequence. In this case, the *fault model* $FM_m^{FSM} = <S, \leq, \Im_m>$ is considered where S is the specification that is a complete observable, possibly nondeterministic FSM, ≤ is the reduction relation, $\Im_m$ is the fault domain which contains each deterministic complete FSM with at most *m* states over the same input alphabet as the specification. Here we notice that differently from the paper [17] where only deterministic FSMs are considered, the specification can be nondeterministic and the conformance relation is not the equivalence but the reduction relation. Correspondingly, different transfer and separating sequences have to be used when deriving a test suite with guaranteed fault coverage.

A test suite is *complete* with respect to the $FM_m^{FSM} = <S, \leq, \Im_m>$ if for each FSM $P \in \Im_m$ such that P is not a reduction of S, the test suite has a sequence for which an output response of P is not in the set of output responses of S to this sequence.

A complete test suite with respect to FM_m^{FSM} can be derived using an appropriate modification of the so-called state counting reduction (SCR) method for nondeterministic FSMs which was proposed in [6]; the proposed method is based on *deterministically-transfer* (*d-transfer*) and separating sequences. A state *s* is *deterministically reachable* (*d-reachable*) from the initial state of the FSM S if there exists an input sequence α such that for any output response β to α, the machine S moves from the initial state to state *s* when α is applied. In this case, α is a *d-transfer* sequence for state *s*. States s_1 and s_2 of an FSM S are *separable* if there exists an input sequence α such that the sets of output responses of the FSM at states s_1 and s_2 to α do not intersect; in this case, sequence α is called a *separating* sequence for states s_1 and s_2. If a sequence separates each pair of different states of the FSM S then this sequence is a separating sequence for FSM S. Again, differently from [17], not each input sequence is a *d*-transfer of the nondeterministic specification and separable states and separating sequences for the nondeterministic specification are defined in a different way according to [15].

If FSM S has a separating sequence γ and each state is *d*-reachable from the initial state, the procedure for deriving a complete test suite w.r.t. the fault model $FM_n^{FSM} = <S, \leq, \Im_n>$ where *n* is the number of states of S, has the following steps:

1. A *d-cover* set of the FSM S is derived. This set contains a *d*-transfer sequence for each state of the FSM S.
2. Each sequence of the *d*-cover set is appended with the separating sequence γ of the FSM S and every input that also is appended with the separating sequence γ.

If an adaptive test suite is derived, an adaptive distinguishing sequence can be used instead of a separating sequence while *d*-transfer sequences can be replaced by adaptive transfer sequences (if they exist). Adaptive distinguishing (separating) and *d*-transfer sequences can be shorter then preset, moreover, they exist more often.

An input sequence α is *adaptive* if the next input depends on the outputs of the FSM. Such an input sequence can be represented by an FSM called a *test case* [18]. At each state of a test case, either there are transitions for one input with all outputs or there are no transitions and in the latter case, a state is called *terminal*. Given a test case (TC) D for FSM S, an adaptive distinguishing sequence defined by DTC D is applied in the following way. If input i_1 is defined at the initial state d_0

of D then the first input i_1 is applied to FSM S and DTC D moves to the i_1o-successor d_1 of state d_0 if the output o is the response of S to the input i_1. The next input to apply is the input defined at state d_1, etc. The procedure terminates when a terminal state is reached.

A test case represents an *adaptive separating* sequence for states s_1 and s_2 of the FSM S if each input-output sequence from the initial to the terminal state of the test case is possible at most at one of states s_1 or s_2. In the former case, the state s_1 is identified, while in the latter case it will be state s_2. States s_1 and s_2 of the FSM S are *adaptively separable* if there is a test case that represents an adaptive separating sequence for states s_1 and s_2. In this case, the corresponding trace from the initial state to a terminal state of an adaptive separating test case allows to determine what was a state of the FSM S before the experiment.

If an adaptive sequence separates each pair of states of the FSM S, then such a sequence is an *adaptive separating sequence* for the FSM S.

A test case can also represent an adaptive sequence from the initial state of the FSM S to the state s if each input-output sequence of the test case from the initial to a terminal state is ended at state labeled by s [18, 19]. In this case, the state s is *adaptively reachable* from the initial state. The above steps for deriving a complete adaptive test suite are almost the same as for preset testing listed above; the only difference is that adaptive distinguishing sequences are used instead of separating sequences while using adaptive transfer sequences instead of d-transfer sequences.

If FSM S has no (adaptive) separating sequence or S has states which are not d-reachable from the initial state then a complete test suite cannot be derived using the above procedure. In this case, the so-called state counting (SCR) method should be applied [6].

Below, we describe the main steps of the general SCR-method with respect to fault model $FM_m^{FSM} = <\mathsf{S}, \leq, \Im_m>$.

1. Determine subset S_d of all d-reachable states and derive *d-cover* of the FSM S which contains a d-transfer sequence for each state of S_d.
2. Determine the set $R = \{R_1, R_2, \ldots, R_p\}$ of maximal subsets of pairwise separable states; for each subset $R_j \in R$, denote R_{jd} a subset of all d-reachable states of R_j. For each subset $R_j \in R$, derive a distinguishing set W_j that contains a separating sequence for each pair of different states of R_j.
3. For each state s_k of S_d, derive a set of input sequences N_k: an input sequence $\alpha \in N_k$ if for each *I/O* sequence α/β at state s_k, it holds that α/β traverses states of some $R_j \in R$ at least $m - |R_{jd}| + 1$ times and this does not hold for any proper prefix of α. Concatenate each prefix of sequence α with each sequence of the set W_j.
4. Concatenate each d-transfer sequence with each sequence of each set W_j that was used at Step 3 when terminating an input sequence of the set N_k, $k = 1, \ldots, p$.

Here we notice that in general case, complete test suites derived by SCR method are much longer than for the case when the specification FSM has a separating sequence and the derivation method is much more complex. To minimize our efforts for deriving a complete test suite w.r.t. the fault model $FM_m^{FSM} = <\mathsf{S}, \leq, \Im_m>$, the adaptive testing can be used instead of the preset [18].

It is known that a test suite can be usually shorter if the specification FSM has a sequence, which separates every two states [6]. In this case set W_j contains only one separating sequences α and $R = \{S\}$. However, such a separating sequence does not always exist and thus, we are obliged to use a set of separating sequences for test derivation. Adaptive distinguishing (separating) sequences exist more often than the preset and are usually shorter, thus, adaptive distinguishing sequences can be preferable for test derivation. Anyway, using adaptive distinguishing sequences can increase the size of subsets of pairwise distinguishable states, and thus, sets W_j and the sets N_k of transfer input sequences, and correspondingly, minimize a complete test suite.

In the next section, we consider an existing approach for adaptation classical FSM based test derivation methods for Timed FSM.

IV. Related work on TFSM based tesing

The problem of deriving a complete test suite against a nondeterministic FSM with timed guards with respect to reduction relation has been considered in [19]. The proposed approach is based on the FSM abstraction of TFSM but that abstraction is a bit different from that considered in the 'Preliminaries' section. In that case, one-to-one mapping between sets of states of TFSM and corresponding FSM abstraction has been established. The latter allows to inherit the above described steps for deriving a complete test with respect to the fault domain which contains each deterministic complete TFSMs with timed guards with at most m states over the same input alphabet as the specification TFSM S and the largest boundary B_S for input timed guards. However, in general case, this approach cannot be applied for FSMs with time guards and timeouts since the one-to-one mapping between transitions of two state reduced equivalent TFSMs with timeouts not always can be established.

In [14], it is shown that initialized reduced deterministic TFSM specification and TFSM implementation with timeouts can be equivalent yet not isomorphic; moreover, they can have different number of states. The latter violates the main assumption of W-based methods about checking the correspondence between FSM transitions. As an example, consider TFSMs in Figure 3.

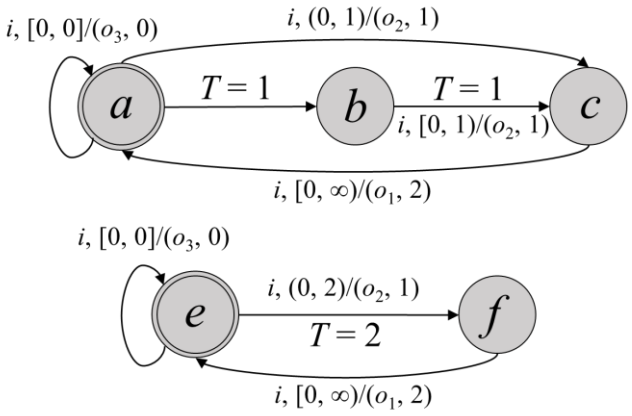

Fig. 3. Two reduced deterministic complete TFSMs R and Q

Each state in R and Q is reachable from the initial state and each two different states of each machine are not equivalent, i.e., both TFSMs are connected and state reduced. By direct inspection, one can assure that equivalent machines in Figure 3 have different number of states and thus, are not isomorphic.

On the other hand, according to Proposition 1, the necessary relationship holds between transitions of their FSM abstractions. For example, reduced forms of FSM abstractions of TFSMs R and Q (Figure 3) are isomorphic. FSM abstraction A_R and its reduced form is shown in Figure 4. Thus, in order to derive a complete test suite for deterministic TFSMs, corresponding fault domain contains every TFSM P over the same input alphabet as S such that the reduced form of the FSM abstraction of P has at most $m > 1$ states. A similar approach can be applied for the test derivation against nondeterministic FSMs with timeouts and timed guards; in the next section, corresponding fault model and test derivation method are proposed.

domain and vice versa a number of timed FSMs which have more states than the specification TFSM, are included into the fault domain.

Example. Consider TFSM specification S (Figure 1) with two states. Fault domain $\aleph_m$ from fault model $FM_m^{TFSM} = <S, \leq, \aleph_m>$ contains TFSM R (Figure 3) with 3 states since the FSM abstraction A_R has not more states than the FSM abstraction A_S. At the same time, in Figure 5 the TFSM specification Y and its non-conforming implementation Y′ are shown such that both TFSMs have three states and the finite timed guards' boundary two. However, the fault domain $\aleph_m$ does not contain Y′ since the reduced form of its FSM abstraction has more states than A_Y. Thus, it can happen that nonconforming implementations with the same number of states as the specification TFSM can pass a complete test suite with respect to $<S, \leq, \aleph_m>$.

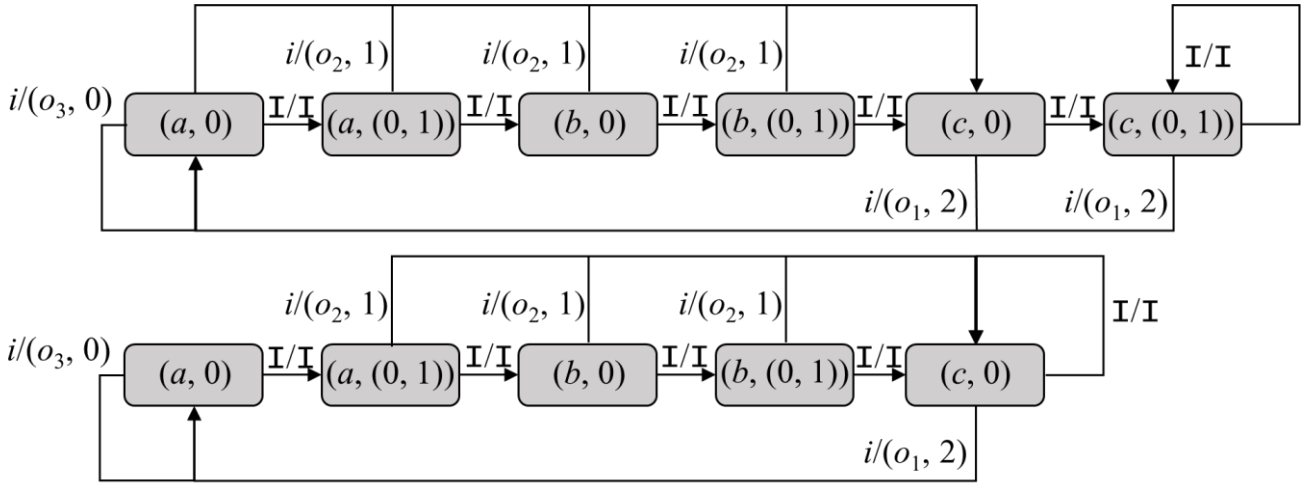

Fig. 4. The FSM abstraction A_R of TFSMs R (Figure 3) and its reduced forms

V. Test Derivation Method for Nondeterministic FSM with Timed Guards and Timeouts

In order to derive a test suite with guaranteed fault coverage for a nondeterministic TFSM we propose a fault model based on the FSM abstraction of the TFSM and apply the SCR-method.

Given a nondeterministic TFSM S with n states (Figure 1), two deterministic equivalent TFSM implementations R and Q (Figure 3) which are reductions of S can have different number of states. However, the reduced forms of their abstractions are isomorphic and are reductions of FSM abstraction A_S. Another example in Figure 5 demonstrates that for nondeterministic TFSM Y there can exist a deterministic TFSM Y′ with the same number of states and the boundary B_S, such that FSM abstraction $A_{Y'}$ has more states than A_Y.

Given a TFSM specification S, we consider the fault model $FM_m^{TFSM} = <S, \leq, \aleph_m>$, where S is the complete nondeterministic observable TFSM specification, $\leq$ is the reduction relation, $\aleph_m$ is the fault domain that contains each deterministic complete TFSM P over the same input alphabet as the specification such that the reduced form of its FSM abstraction A_P has at most $m > 1$ states.

It can well happen that some timed FSMs with less states than the specification TFSM are not included into the fault

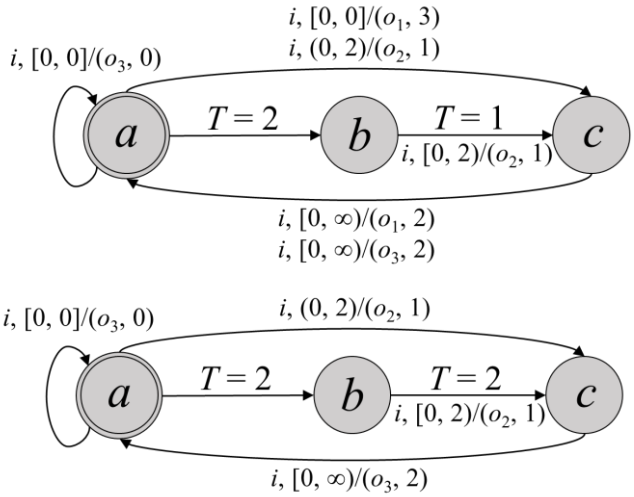

Fig. 5. TFSM Y and its non-conforming implementation Y′

Note that the FSM abstraction of TFSM S can have non-separable states, i.e. the FSM abstraction can have a pair of states for which a separating sequence does not exist while the specification TFSM S has a separating sequence, i.e., all states of the TFSM S are pairwise separable. For example, TFSM S in Figure 1 has a separating sequence (i, 1) while the corresponding FSM abstraction A_S has a pair of non-separable

states (b, 0) and (b, (0, ∞)), for which the sets of input/output sequences coincide. In order to derive a complete test suite for such FSM, the SCR method can be used.

As mentioned above, similar to a deterministic FSM abstraction [14], a nondeterministic FSM abstraction can be minimized using the method from [15]. As an example, for FSM abstraction $\mathsf{A_S}$ (Figure 2) of TFSM S (Figure 1), equivalent states (b, 0) and (b, (0, ∞)) can be merged into one state. However, unlike deterministic machines, such optimization does not always allow to merge pairs of non-separable states of the FSM abstraction of the specification and thus, the SCR method is still used for test derivation.

Algorithm for deriving a complete test suite w.r.t $FM_m^{TFSM} = <\mathsf{S}, \leq, \aleph_m>$ where m is the number of states of the reduced form of the FSM abstraction of S

Input: The complete observable possibly nondeterministic specification TFSM S

Output: A complete test suite TS with respect to the fault model $FM_m^{TFSM} = <\mathsf{S}, \leq, \aleph_m>$, where $\aleph_m$ contains every TFSM P over the same input alphabet as S such that FSM abstraction of P has at most $m > 1$ states

Step 1. Derive the reduced form of the FSM abstraction $\mathsf{A_S}$ of TFSM S.

Step 2. Derive a test suite TS_A with respect to the fault model $FM_m^{FSM} = <\mathsf{A_S}, \leq, \Im_m>$ using the SCR-method described above, where m is number of states of the FSM abstraction $\mathsf{A_S}$.

Step 3. According to Proposition 1, transform test cases of the test suite TS_A into corresponding timed sequences over the TFSM S and obtain the test suite TS.

Proposition 4. The test suite TS returned by Algorithm 1 is complete with respect to the fault model $FM_m^{TFSM} = <\mathsf{S}, \leq, \aleph_m>$.

Proof. Let TFSM P which is not a reduction of specification TFSM S be in the set $\aleph_m$, and a test suite TS is returned by the above algorithm. By definition of the fault domain $\aleph_m$, the reduced form of the FSM abstraction $\mathsf{A_P}$ has at most m states. Since P is not a reduction of S, the FSM $\mathsf{A_P}$ is not a reduction of $\mathsf{A_S}$ (Proposition 3). Thus, a test suite TS_A derived at Step 2 contains an input sequence α_{FSM}, which separates FSMs $\mathsf{A_P}$ and $\mathsf{A_S}$. By Proposition 2, for each response of the FSM $\mathsf{A_P}$ to sequence α_{FSM} there exists the corresponding timed input sequence α of the TFSM P that will demonstrate that P is not a reduction of the TFSM S. The latter guarantees that each non-conforming implementation P of the set $\aleph_m$ is detected by the test suite TS.

The fault domain in the above algorithm can be extended and for TFSM S and the reduced form of its FSM abstraction $\mathsf{A_S}$ with n states, a complete test suite can be derived by SCR-method with respect to $\aleph_m$ when $m > n$. However, in this case length of a complete test suite significantly increases.

In the worst case, the length of derived by SCR-method test suite exponentially depends on number of states of FSM and can be more complex for FSM with timed aspects. In practice length of adaptive d-transfer sequences does not exceed number of states FSM while length of an adaptive distinguishing sequence usually polynomial depends on the number of states of FSM [19]. Respectively, similar results can be derived for a TFSM when proposed algorithm is used and the boundary on timed guards is not too big. Note that length of the test suite significantly depends on timed aspects of TFSM such as boundary of timed guards and value of timeouts [19].

We note again that the FSM abstraction of TFSM S can have non-separable states while all states of the TFSM are pairwise separable. However, we underline that the FSM abstraction inherits d-reachability of states from the specification TFSM and the following proposition holds.

Proposition 5. States (s, 0), (s, (0, 1)), (s, 1), (s, (1, 2)) … of FSM abstraction $\mathsf{A_S}$ are d-reachable if and only if state s is d-reachable in TFSM S.

The statement is implied by Proposition 1 and Proposition 2 due to a deterministic transition under the special input $\mathtt{I}$. Respectively, all states of FSM abstraction $\mathsf{A_S}$ are d-reachable if and only if all states of TFSM S is d-reachable.

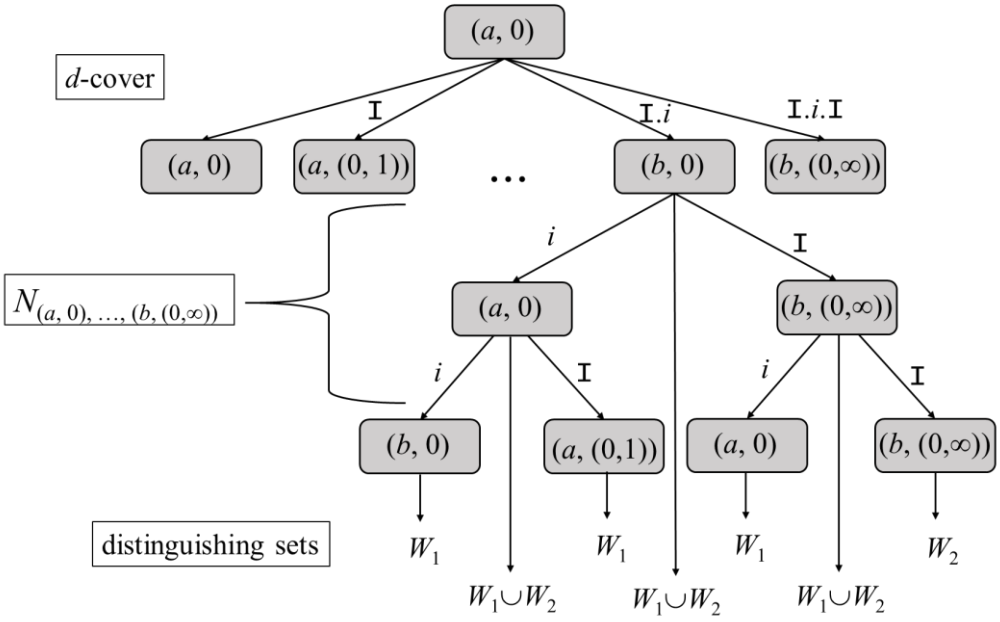

Fig. 6. A fragment of test suite TS_A for the FSM abstraction

Example. Consider TFSM S in Figure 1 and its FSM abstraction A_S in Figure 2. We derive a complete test suite w.r.t. the fault model $FM_6^{TFSM} = <S, \leqslant, \aleph_6>$. For state ($b$, 0) of A_S there exists a d-transfer sequence I.i and respectively, state b of TFSM S has a timed d-transfer sequence (i, 0,5). Other states of FSM abstraction are d-reachable from states (a, 0) and (b, 0) by a sequence of I inputs. Thus, all states of A_S are d-reachable from the initial state and for the FSM abstraction A_S, S_d = {(a, 0), (a, (0, 1)), (a, 1), (a, (1, 2)), (b, 0), (b, (0, ∞))}.

Given FSM A_S, we can also determine two maximal subsets of pairwise separable states R_1 = {(a, 0), (a, (0, 1)), (a, 1), (a, (1, 2)), (b, 0)}, R_2 = {(a, 0), (a, (0, 1)), (a, 1), (a, (1, 2)), (b, (0, ∞))} and corresponding distinguishing sets $W_1 = W_2$ = { i, I.i, I.I.i}. Note that $R_1 = R_{1d}$ and $R_2 = R_{2d}$ since all states of A_S are d-reachable.

Consider state (b, 0) and the set $N_{(b, 0)}$ of input sequences derived at Step 3 of the SCR-method when a test suite is derived with respect to the fault model <S, ≤, $\Im_6$>. Input/Output sequences with the input projection of the set $N_{(b, 0)}$ should traverse states of some R_j at least 2 = 6 - 5 + 1 times while this does not hold for any proper prefix of the input sequence, and respectively, $i.i$ is in the set $N_{(b, 0)}$ which traverses states (a, 0) and (b, 0) of R_1. Other sequences at state (b, 0) are i.I (traverses (a, 0), (a, (0, 1))), I.i (traverses (b, (0, ∞)), (a, 0)), I.I (traverses (b, (0, ∞)), (b, (0, ∞))) and thus, $N_{(b, 0)}$ = {$i.i$, i.I, I.i, I.I, i, I}.

A fragment of the tree that is obtained when deriving a test suite, is shown in Figure 6. One of test sequences of TS_A is I.$i.i.i$.I.I.i and a corresponding timed input sequence of test TS is (i, 0,5).(i, 0).(i, 0).(i, 1) where (i, 0,5) is a d-transfer sequence and (i, 1) is a separating sequence from W_1. Each sequence of the test suite is applied to TFSM implementation at the initial state. First input i is applied when clock is equal to 0,5; after applying the input the clock is set to 0 and the machine produces corresponding output when clock value is equal to 1 when an implementation is conforming. After producing the output o_2 the clock is reset and the machine is waiting for the next input i that is immediately applied after resetting the clock. After applying this input the clock is reset again and the machine produces an output o_1 or o_3 when clock value is equal to 2. After producing any of outputs the clock is reset and the machine is waiting for a next input, etc.

VI. Conclusions

In this paper, we have proposed an approach for deriving complete test suites with respect to the reduction relation against nondeterministic Finite State Machines with timed guards and timeouts. Both, a proposed approach and a corresponding fault model are based on the FSM abstraction of machines with timed guards and timeouts and this allows inheriting the known FSM based SCR-method when deriving test suites with guaranteed fault coverage for nondeterministic TFSMs.

Acknowledgment

This work is partly supported by RFBR project N 19-07-00327/19.

References

[1] Gill A. Introduction to the Theory of Finite-State Machines, 272 p. 1964.

[2] Chow T.S. Test design modeled by finite-state machines. IEEE Trans. Software Eng., 1978, vol. 4, no. 3, pp. 178–187.

[3] Dorofeeva R., El-Fakih K., Maag S., Cavalli A., Yevtushenko N. FSM-based conformance testing methods: A survey annotated with experimental evaluation. Inf. Software Technol., 2010, vol. 52, pp. 1286–1297.

[4] Hierons R.M., Merayo M.G., Nunez M. Testing from a Stochastic Timed System with a Fault Model. Journal of Logic and Algebraic Programming, 2009, Vol. 72(8), pp. 98-115.

[5] Krichen M. and Tripakis S. Conformance testing for real-time systems. Formal Methods Syst. Des., 2009, vol. 34, no. 3, pp. 238–304.

[6] Petrenko A., Yevtushenko N. Conformance tests as checking experiments for partial nondeterministic FSM. In: Grieskamp, W., Weise, C. (eds.) FATES 2005, Springer, Heidelberg, 2006, LNCS, vol. 3997, pp. 118–133. doi:10.1007/11759744_9

[7] Alur R. and Dill D.L. A theory of timed automata. Theoretical Computer Science 126, 1994, pp. 183–235.

[8] Springintveld J., Vaandrager F., and D'Argenio P. Testing timed automata. Theor. Comput. Sci., 2001, vol. 254, nos. 1–2, pp. 225–257.

[9] El-Fakih K., Yevtushenko N., and Fouchal H., Testing timed finite state machines with guaranteed fault coverage. Proceedings of the 21st IFIP WG 6.1 International Conference on Testing of Software and Communication Systems and 9th International FATES Workshop, 2009, pp. 66–80.

[10] Merayo M.G., Nunez M., and Rodriguez I. Formal testing from timed finite state machines. Comput. Networks: Int. J. Comput. Telecommun. Networking, 2008, vol. 52, no. 2, p. 432–460.

[11] Bresolin D., El-Fakih K., Villa T., and Yevtushenko N. Deterministic timed finite state machines: Equivalence checking and expressive power, Int. Conf. GANDALF, 2014, pp. 203–216.

[12] Zhigulin M., Yevtushenko N., Maag S., Cavalli A. FSM-Based Test Derivation Strategies for Systems with Time-Outs. 11th International Conference On Quality Software, Madrid, 2011, pp. 141–150.

[13] En-Nouaary A., Dssouli R., Khendek F. Timed Wp-Method: Testing Real-Time Systems. IEEE TSE 28(11), 2002, 1023–1038.

[14] Tvardovskii A., El-Fakih K, Yevtushenko N. Deriving Tests with Guaranteed Fault Coverage for Finite State Machines with Timeouts. LNCS, 2018, Vol. 11146, pp. 149–154.

[15] Starke P. Abstract Automata / P. Starke // American Elsevier, 1972, 419 p.

[16] Villa T., Kam T., Brayton R.K., Sandgiovanni-Vincentelli A. Synthesis of Finite State machines: Logic Optimization, Springer, 1997, 520 p.

[17] Lee D., Yannakakis M. Principles and methods of testing finite state machines - a survey. Proceedings of the IEEE, 1996, Vol. 84(8), pp. 1090–1123.

[18] Yevtushenko N., El-Fakih K., and Ermakov A., On-the-fly construction of adaptive checking sequences for testing deterministic implementations of nondeterministic specifications. Lect. Notes Comput. Sci., 2016, vol. 9976, pp. 139–152.

[19] Tvardovskii A.S., Gromov M.L., El-Fakih Khaled, Evtushenko N.V. Testing Timed Nondeterministic Finite State Machines with the Guaranteed Fault Coverage. Automatic Control and Computer Sciences, 2017, Vol. 51, № 7, pp. 724–730.

Simulating Petri Nets with Inhibitor and Reset Arcs*

Pavel Pertsukhov
PAIS Lab, Faculty of Computer Science
National Research University Higher School of Economics
Moscow, Russia
papertsukhov@edu.hse.ru

Alexey Mitsyuk
PAIS Lab, Faculty of Computer Science
National Research University Higher School of Economics
Moscow, Russia
amitsyuk@hse.ru

***Abstract*—Event logs of software systems are used to analyse their behaviour and inter-component interaction. Artificial event logs with desirable specifics are needed to test algorithms supporting this type of analysis. Recent methods allow to generate artificial event logs by simulating ordinary Petri nets. In this paper we present the algorithm generating event logs for Petri nets with inhibitor and reset arcs. Nets with inhibitor arcs are more expressive than ordinary Petri nets, and allow to conveniently model conditions in real-life software. Resets are common in real-life systems as well. This paper describes the net simulation algorithm, and shows how it can be applied for event log generation.**

***Index Terms*—Petri nets, inhibitor arcs, reset arcs, simulation, event logs**

I. Introduction

Recently, process analytics evolved into an advanced field of computer-based technology. Automated methods have been created to find bottlenecks and inefficiencies in process models of information systems.

One particular technology that helps to automate process analysis is process mining [1]. Experts in this technology employ algorithms and methods which use the records of a system behaviour, which are called "event logs" or "system logs". This information can be explored to discover a model of how the real process behaves [1]. An existing process model runs can be aligned to the records of an event log to check if the model conforms to the real system behaviour [2]. The field also provides an expert with method to improve/repair processes and process models.

The process simulation methods are also applied in the field of process analytics [3].

Recently, it has been stated that process mining and simulation form "a match made in heaven" [4]. In particular, process model simulation can be applied to look in the future of a process, and to test *what-if* alternative scenarios possible because of process change. Moreover, the development of process mining algorithms is impossible without sample models and event logs with a suitable characteristics [1]. Sample event logs can be generated using the process model simulation methods [5]–[8]. Process mining and simulation can also be matched in other way. The results of process discovery and conformance checking can be applied to improve simulation models.

Various modelling formalisms are employed in the field of process analytics [1], [3]. Among them, the language of Petri nets is one of the most well-established, well-researched, simple, and commonly-used modelling languages [9]. Lots of process discovery and analysis techniques are based on this language [1].

A strength of the Petri net language is that on top of simply defined P/T-nets many extensions have been built. These are high-level Petri nets: Coloured Petri nets [10], Nested Petri nets [11], Object nets [12] etc. Method to simulate Petri nets of various types have been proposed in literature. However, for many types of Petri nets still there are no simulation techniques/tools.

This paper presents an approach and a tool to simulate Petri nets with reset and inhibitor arcs. The addition of these arc types improves the net expressiveness significantly. Thus, these nets are used when the process can not be (conveniently) modelled by P/T-nets.

This paper is organized as follows. Section II defines models and event logs. In Section III the main contribution is presented: algorithms to simulate Petri nets with inhibitor and reset arcs. These algorithms are implemented in the tool which is described in Section IV. Finally, Section V concludes the paper.

II. Petri Nets and Event Logs

In this section, we define process models and event logs. Let $\mathbb{N}$ denote the set of all non-negative integers, and $\mathbb{N}_+ = \mathbb{N} \setminus \{0\}$.

A. Ordinary Petri nets

Petri nets are directed bipartite graphs which allows for modelling and representation of processes in information systems [13]. More formally, an *ordinary Petri net* is a triple $N = (P, T, F)$, where P and T are two disjoint sets of places and transitions, and $F \subseteq (P \times T) \cup (T \times P)$ is a flow relation.

As graphs, Petri nets have convenient visual representation. Fig. 1 shows an example model. Places are shown by circles, transitions are shown by boxes, the flow relation is depicted

*This work is supported by the Basic Research Program at the National Research University Higher School of Economics.

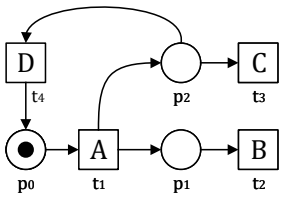

Fig. 1. An ordinary labelled Petri net

using ordinary directed arcs. In Fig. 1, there are three places (p_0, p_1, p_3) and four transitions (t_1, t_2, t_3, t_4).

Transitions are labelled with activity names from the set $\mathcal{A} \cup \{\tau\}$. In the example, $\mathcal{A} = \{A, B, C, D\}$. Labels are placed inside the transition boxes. An Petri net can contain invisible (*silent*) process actions which are labelled with τ. Labels are assigned to transitions via a *labelling function* $\lambda \colon T \to \mathcal{A} \cup \{\tau\}$.

A state of an ordinary Petri net is called its *marking*. It is a function $M \colon P \to \mathbb{N}$ assigning natural numbers to places. In figures, a marking M can be designated by putting $M(p)$ black tokens into a place p of the net. By M_0 we denote the initial marking. For example, the initial marking of the net from Fig. 1 consists of a single token in the place p_0.

A transition represents an activity of a process. It is enabled in a current marking if in each of its input places (for $t \in T$ input places are $\bullet t = \{p \mid (p,t) \in F\}$) there enough tokens, that is $\forall p \in \bullet t \colon M(p) \geq 1$. An enable transition may fire that changes a marking of the net. It consumes tokens from the input places, and produces tokens to output places (for $t \in T$ input places are $t\bullet = \{p \mid (t,p) \in F\}$).

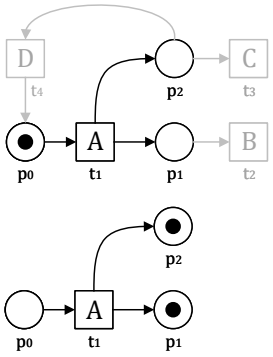

Fig. 2. An ordinary labelled Petri net

Consider a model from Fig. 1. t_1 is the only one transitions is enabled in the initial marking. It may fire, that corresponds to an occurrence of activity "A". Then, the transition consumes a single token from p_0 and produces tokens to p_1 and p_2. Fig. 2 illustrates this firing. The firing is local, each transition fires independently from other transitions.

B. Petri nets with Inhibitor and Reset Arcs

In this paper, we consider Petri nets with arcs of two additional types: reset and inhibitor arcs. These nets also contain places, transitions, and ordinary control flow arcs.

A *labelled Petri net with weights, inhibitor and reset arcs* (WIR Petri net) is a tuple $N_{WIR} = (P, T, F, W, R, I, \lambda)$, where

- (P, T, F) is an ordinary Petri net,
- $W \in F \to \mathbb{N}_+$ is an arc weight function,
- $R \subseteq P \times T$ is a function defining reset arcs,
- $I \subseteq P \times T$ is an inhibiting relation,
- and $\lambda \colon T \to \mathcal{A} \cup \{\tau\}$ is a labelling function.

Fig. 3 shows an example WIR Petri net.

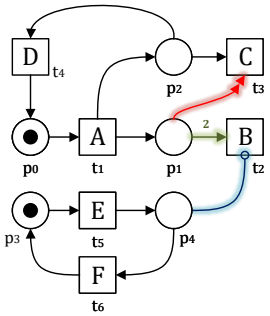

Fig. 3. A WIR Petri net

A *reset arc* removes all tokens from the place no matter of their number. These arcs also called *clear* arcs [14].

In Fig. 3, there is a reset arc from the place p_1 to the transition t_3 labelled with "C". Reset arcs are denoted with double arrows at the end. Note that the net contains a loop of two actions "A" (t_1) and "D" (t_4). The possible sequence of firings is $< t_1,\ t_4,\ t_1,\ t_4,\ t_1,\ t_4,\ t_3 >$. Before the last step, p_1 will contain 3 tokens all of which will be removed by the firing of t_3.

An *inhibitor arc* [15], [16] can be from a place to a transition. This transition can not fire if there is a token in place connected with the transition using an inhibitor arc. $\circ t = \{p \mid (p,t) \in I\}$ denotes the set of inhibiting places for t. That is, an inhibiting place allows to prevent the transition firing. Transitions consume no tokens through inhibitor arcs.

Inhibitor arcs are shown with small circles instead of arrows at the end. In Fig. 3, there is a reset arc from the place p_4 to the transition t_2 labelled with "B". Thus, t_2 can not fire if there is a token in p_4 no matter how many tokens are in p_1. The whole part of the model that consists of places p_3 and p_4, transitions t_5 and t_6 is a switch with two possible states: open (there is a token in p_3) / closed (there is a token in p_4).

The firing of t_5 closes the switch and deprecates the firing of t_2. Thus, only t_3 is able to clear tokens from the place p_1

if there is a token in p_2. The firing of t_3 will end the process, because it will consume and remove all tokens from the upper part of the net.

The firing of t_6 opens the switch. Then, t_2 may consume tokens from p_1 independently of tokens in other places. Note that the arc from p_1 to t_2 has a weight of 2. Thus, each firing of t_2 consume exactly 2 tokens, and t_2 can not fire if there is only one token in p_1.

Note that a particular WIR Petri net can contain zero number of reset and inhibitor arcs.

Marking of a WIR Petri net is defined in the same way as for an ordinary Petri net. But the firing rule is slightly different for WIR Petri nets. Each marking change is called *step*. In this paper, we assume that each step consists of a single transition firing. The step from Fig. 2 is denoted by $M_0[t_1\rangle M'$, where $M'(p_1) = M'(p_2) = M'(p_3) = 1$ and $M'(p_0) = M'(p_4) = 0$.

C. Event Logs

In this paper, we apply process model simulation to generate event logs with records of the behaviour.

We define an *event log* as a finite multiset of traces $L \in \mathcal{B}(\mathcal{A}^*)$ [1]. A trace $\sigma \in \mathcal{A}^*$ is a finite sequence of events from the set $\mathcal{A}$. Note that transitions of a WIR Petri net are labelled with elements of $\mathcal{A}$. The only transitions which firing leaves no events are silent τ-transitions.

Technically, we record the event logs in XES (Extensible Event Stream) format[2] that will be considered in more detail in Section IV.

III. Petri net Simulation Algorithm

This section describes the algorithm to simulate labelled WIR Petri nets.

The main idea is to iterate over all transitions and fire one of them at each iteration, recording corresponding events to the log. This procedure is performed in the main generating function called $generateTrace$ (see Algorithm 1).

This algorithm works as follows. We have $maxIterations$ attempts to reach the final marking of the net. By default this number is 10. The function $moveToInitialState$ initiates the trace generation by setting a marking of the to M_0. Then, we create an empty trace by calling $createTrace$.

At each step of the main loop, the algorithm chooses an enabled transition in the $chooseNextTransition$, and fire it (function $fire$). The function $fire$ changes a marking of the net and writes an event to trace. Then we call the function $isCompleted$ to check if we reached the final marking and update $replayCompleted$. This loop iterates until we reach the final marking ($replayCompleted = true$) or exceed the specified limit of steps for one trace $maxNumberOfSteps$.

When we can not find an enabled transition which is ready to fire, we clear the unfinished trace and begin a new attempt. If no one of ten attempts succeeded, we return NULL which will be recorded as an empty trace to the event log. Note that there is a setting of the prototype tool that removes all empty and unfinished traces.

[1]Here $\mathcal{B}(\mathcal{A}^*)$ denotes all multisets over $\mathcal{A}^*$, where $\mathcal{A}^*$ — all finite sequences with elements from $\mathcal{A}$.

[2]http://www.xes-standard.org/

Algorithm 1 One trace generation

Input: transitions, initialMarking, finalMarking, settings as $\{maxNumberOfSteps, maxIterations, isRemovingUnfinishedTraces\}$
Output: generated trace or NULL

```
1: function GENERATETRACE
2:     trace ← NULL;
3:     replayCompleted ← false;
4:     addTraceToLog ← false;
5:     iteration ← 0;
6:     repeat
7:         MOVETOINITIALSTATE();
8:         trace ← CREATETRACE();
9:         stepNumber ← 0;
10:
11:        while stepNumber < maxNumberOfSteps
12:                and not replayCompleted do
13:
14:            transition ← CHOOSENEXTTRANSITION();
15:            if transition = NULL then
16:                trace ← NULL;
17:                break;
18:            end if
19:
20:            FIRE(transition, trace);
21:            replayCompleted ← ISCOMPLETED(finalMarking);
22:            stepNumber ← stepNumber + 1;
23:        end while
24:
25:        iteration ← iteration + 1;
26:    until (iteration >= maxIterations or
27:        not isRemovingUnfinishedTraces or replayCompleted)
28:
29:    if not replayCompleted
30:            and isRemovingUnfinishedTraces then
31:        trace ← NULL;
32:    end if
33:    return trace;
34: end function
```

The *chooseNextTransition* function selects an enabled transition using a specified rule. The most basic implementation of this function is shown in Algorithm 2. Here, the random transition among all enabled and noise transitions is selected. This algorithm is based on the algorithm for ordinary Petri nets [17], and thus, is able to add noise to the event log. More complex rules to select the enabled transition can be applied. For example, priorities of preferences can be assigned to the transitions which affect the order of their firing. If there is no enabled transition, then NULL is returned.

Algorithm 2 Looking for the next transition

Input: allTransitions, noiseTransitions
Output: selected transition or NULL

```
1: function CHOOSENEXTTRANSITION(allTransitions, noiseTransitions)
2:     enabledTransitions ← FINDENABLEDTRANSITIONS();
3:
4:     return random transition among enabledTransitions
5:     and noiseTransitions or NULL;
6: end function
```

To check if a transition t is enabled, we ensure that all input places connected with t with the help of ordinary arcs have enough tokens. Besides that, we check that places connected with t with the help of inhibitor arcs don't contain any tokens. Reset arcs don't affect if a transition is enabled or not. Algorithm 3 shows how this is done.

Algorithm 3 Finding enabled transitions

Input: allTransitions
Output: list of enabled transitions

```
1: function FINDENABLEDTRANSITIONS(allTransitions)
2:     enabledTransitions ← ∅;
3:
4:     for transition in allTransitions do
5:         enabled ← true;
6:         for arc in transition.inputArcs do
7:             if arc.place.numberOfTokens < arc.weight then
8:                 enabled ← false;
9:                 break;
10:            end if
11:        end for
12:        if not enabled then
13:            continue;
14:        end if
15:        for arc in transition.inhibitorArcs do
16:            if arc.place.numberOfTokens > 0 then
17:                enabled ← false;
18:                break;
19:            end if
20:        end for
21:        if enabled then
22:            enabledTransitions.add(transition)
23:        end if
24:    end for
25:    return enabledTransitions;
26: end function
```

Algorithm 4 shows the transition firing function. This function produces and consumes tokens, and then adds an event corresponding to this transition to the trace. The basic implementation is shown which considers only transition names. There are much more complicated implementations of this function for time-driven, resources, and priorities generation modes.

Algorithm 4 Firing function

```
1: function FIRE(transition, trace)
2:     for arc in transition.inputArcs do
3:         arc.place.consumeToken(arc.weight)
4:     end for
5:
6:     for arc in transition.inputResetArcs do
7:         arc.place.consumeAllTokens()
8:     end for
9:
10:    log transition to trace or perform some noise event
11:
12:    for arc in transition.outputArcs do
13:        arc.place.produceTokens(arc.weight)
14:    end for
15: end function
```

IV. Prototype Tool

The presented event log generation algorithm has been implemented as a prototype tool. It is written in Java and in Kotlin programming languages. In this section, we consider the tool.

The tool consists of two parts: *Generation Setup* unit and *Generation* unit.

A. Preparing for Generation

In preparation part we receive settings from the GUI (see Fig. 4) or read a JSON (see Fig. 5) file. Settings from JSON are validated. Then we load the model from a PNML[3] file and prepare this model for generation. Inhibitor and reset arcs could be either specified in settings file, or loaded from the PNML file. The initial and final markings are loaded in the same manner.

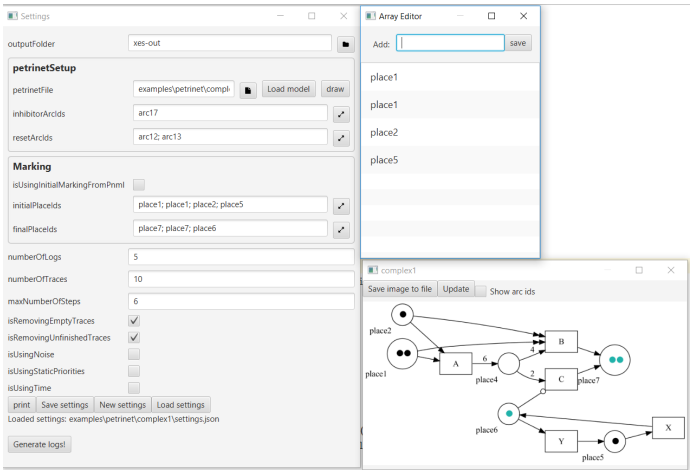

Fig. 4. Tool GUI

After that we create an instance of special class $GenerationHelper$, which encapsulates the main code for choosing transitions, looking for enabled transitions, handling noise and artificial log events if it is needed. There are different helpers for simple generation, generation with priorities, and generation with time.

Also we convert each transition to a special loggable transition-related class which is used during generation. They contain methods of event recording to a trace. Such a class also consumes tokens from input places and produces tokens to output places. Methods to check if a transition is enabled are also here.

B. Generation

A singleton class is used to record the event log. We set-up this logging class. It uses the OpenXES[4] library with the help of which we can write XES log files. The XES format is common for the field of process mining [1]. OpenXES library creates a separate file for each log.

A fragment of the example output in XES file is shown in Fig. 6. This example contains two traces with names "$Trace\ 4$" and "$Trace\ 5$". These names should be unique.

[3]www.pnml.org/
[4]http://www.xes-standard.org/openxes/start

```
{
  "petrinetSetup" : {
    "petrinetFile" : "examples\\petrinet\\complex1\\complex1.pnml",
    "marking" : {"isUsingInitialMarkingFromPnml": false...},
    "inhibitorArcIds" : [ "arc17" ],
    "resetArcIds" : [ "arc12", "arc13" ]
  },
  "outputFolder" : "xes-out",
  "isRemovingEmptyTraces" : true,
  "isRemovingUnfinishedTraces" : true,
  "numberOfLogs" : 5,
  "numberOfTraces" : 10,
  "maxNumberOfSteps" : 6,
  "isUsingNoise" : false,
  "noiseDescription" : {
    "noiseLevel" : 5,
    "isSkippingTransitions" : true,
    "isUsingExternalTransitions" : true,
    "isUsingInternalTransitions" : true,
    "internalTransitionIds" : [ ],
    "existingNoiseEvents" : [ {
      "activity" : "NoiseEvent",
      "executionTimeSeconds" : 600,
      "maxTimeDeviationSeconds" : 120
    } ]
  },
  "isUsingStaticPriorities" : false,
  "staticPriorities" : {"maxPriority": 1...},
  "isUsingTime" : false,
  "timeDescription" : {"generationStart": "2019-04-07T22:27:06.991Z"...}
}
```


Fig. 5. Generation settings in JSON


```
<trace>
    <string key="concept:name" value="Trace 4"/>
    <event>
        <string key="concept:name" value="B"/>
    </event>
    <event>
        <string key="concept:name" value="D"/>
    </event>
    <event>
        <string key="concept:name" value="D"/>
    </event>
</trace>
<trace>
    <string key="concept:name" value="Trace 5"/>
    <event>
        <string key="concept:name" value="D"/>
    </event>
    <event>
        <string key="concept:name" value="B"/>
    </event>
    <event>
        <string key="concept:name" value="D"/>
    </event>
</trace>
```


Fig. 6. Fragment of XES file

The first trace is of the three events: “B”, “D”, and “D”. Note that XES is XML-based, and is easy-to-read for a machine or a human.

Then we use a $Generator$ class to launch the main generation method (see Algorithm 1), passing a $generationHelper$ to this class.

C. Tool Usage

Let us test our tool on the model from Fig. 7.

The initial marking consists of the four tokens (shown as black dots): one token lies in $place2$, one is in $place5$, and two tokens are in $place1$. Our goal is to reach the final marking (shown as green dots): two tokens in $place7$, and one token in $place6$.

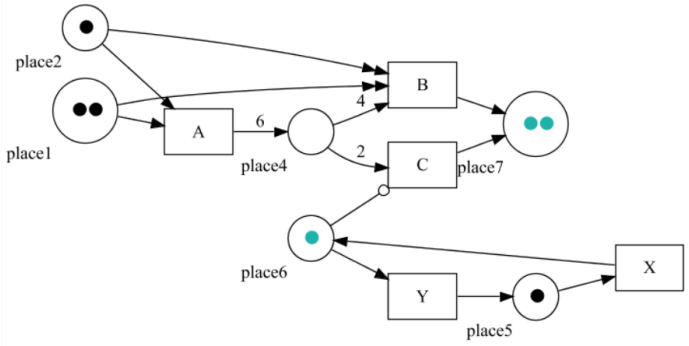

Fig. 7. Petri net used for log generation

Transition C is enabled only when place $place6$ is empty. C consumes 2 tokens from $place4$ and produces a token to $place7$.

Transition B removes all tokens in places $place1$ and $place2$. When fire this transition consumes 4 tokens from $place4$ and produces a token to $place7$. Thus, B can not fire before A.

At each step either X or Y is enabled, so these transitions may produce a trace of any length.

We set-up our tool to remove unfinished traces and limited max number of steps to 10.

The result of the generation is shown in Fig. 8.

Let us look at some trace, for example: $\langle A, X, B, Y, C, X \rangle$. First fired transition was A, and it produced 6 tokens to $place4$. Then X fired. It consumed a token from $place5$ and produced one to $place6$. C can not fire in this marking. Thus, B fires. 4 of 6 tokens was consumed from $place4$, and one token

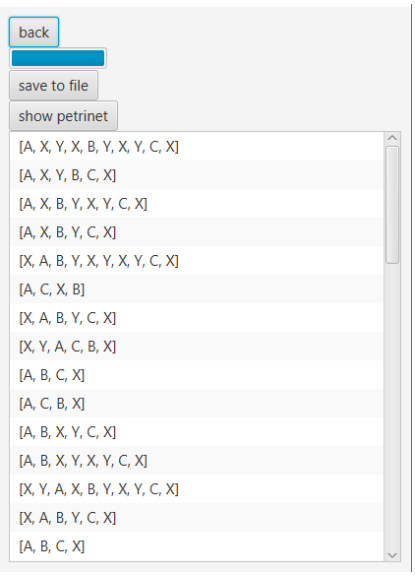

Fig. 8. Resulting traces

produced to $place7$. Then Y fired and "opened" C. C has been fired just after Y was fired, when a token has been removed from $place6$. B and C were fired once each, and produced 2 tokens in total to $place7$. $place1$ and $place2$ were cleared by B. The last event was X, which placed a token to $place6$. At the end of this run all tokens lie in the final marking.

V. Conclusions

In this paper, we have presented the algorithm to simulate a process model in the form of weighted labelled Petri net with inhibitor and reset arcs. This algorithm can be applied to generate event logs from the event log. Proposed algorithm continues the previous works on Petri net simulation with the purpose of generating artificial event logs. The prototype implementation is based on Gena tool[5].

We have plans for future work. Firstly, we plan to comprehensively evaluate the proposed algorithm on artificial and real-life process models. For now, we just tested it on sample models to check algorithm validity. Secondly, we also plan to improve the prototype implementation and make it stable and usable. Thirdly, Gena is able to simulate timed process models, models with resources, data, add noise to an event log [8], [17]. Recently, an extension for Gena to simulate the multi-agent system has been proposed [18]. We plan to merge these extensions and the algorithm presented in this paper. Then, it will be possible to simulate WIR Petri nets with time/resources, and data.

References

[1] Wil M. P. van der Aalst, *Process mining: Discovery, Conformance and Enhancement of Business Processes*. Springer, 2011.

[2] J. Carmona, B. F. van Dongen, A. Solti, and M. Weidlich, *Conformance Checking - Relating Processes and Models*. Springer, 2018.

[3] M. Weske, *Business Process Management: Concepts, Languages, Architectures*. Springer, 2007.

[4] W. M. P. van der Aalst, "Process mining and simulation: a match made in heaven!," in *SummerSim*, pp. 4:1–4:12, ACM, 2018.

[5] A. Burattin and A. Sperduti, "PLG: A framework for the generation of business process models and their execution logs," in *Business Process Management Workshops*, vol. 66 of *Lecture Notes in Business Information Processing*, pp. 214–219, Springer, 2010.

[6] A. Burattin, "PLG2: multiperspective process randomization with online and offline simulations," in *BPM (Demos)*, vol. 1789 of *CEUR Workshop Proceedings*, pp. 1–6, CEUR-WS.org, 2016.

[7] T. Jouck and B. Depaire, "Ptandloggenerator: A generator for artificial event data," in *BPM (Demos)*, vol. 1789 of *CEUR Workshop Proceedings*, pp. 23–27, CEUR-WS.org, 2016.

[8] A. A. Mitsyuk, I. S. Shugurov, A. A. Kalenkova, and W. M. P. van der Aalst, "Generating event logs for high-level process models," *Simulation Modelling Practice and Theory*, vol. 74, pp. 1–16, 2017.

[9] W. Reisig, *Understanding Petri Nets - Modeling Techniques, Analysis Methods, Case Studies*. Springer, 2013.

[10] K. Jensen and L. M. Kristensen, *Coloured Petri Nets - Modelling and Validation of Concurrent Systems*. Springer, 2009.

[11] I. A. Lomazova, "Nested petri nets: Multi-level and recursive systems," *Fundam. Inform.*, vol. 47, no. 3-4, pp. 283–293, 2001.

[12] R. Valk, "Object petri nets: Using the nets-within-nets paradigm," in *Lectures on Concurrency and Petri Nets*, vol. 3098 of *Lecture Notes in Computer Science*, pp. 819–848, Springer, 2003.

[13] W. M. P. van der Aalst and K. M. van Hee, *Workflow Management: Models, Methods, and Systems*. MIT Press, 2002.

[14] C. Lakos and S. Christensen, "A general systematic approach to arc extensions for coloured petri nets," in *Application and Theory of Petri Nets*, vol. 815 of *Lecture Notes in Computer Science*, pp. 338–357, Springer, 1994.

[15] R. Janicki and M. Koutny, "Semantics of inhibitor nets," *Inf. Comput.*, vol. 123, no. 1, pp. 1–16, 1995.

[16] H. C. M. Kleijn and M. Koutny, "Process semantics of p/t-nets with inhibitor arcs," in *ICATPN*, pp. 261–281, 2000.

[17] I. S. Shugurov and A. A. Mitsyuk, "Generation of a Set of Event Logs with Noise," in *Proceedings of the 8th Spring/Summer Young Researchers Colloquium on Software Engineering (SYRCoSE 2014)*, pp. 88–95, 2014.

[18] R. A. Nesterov, A. A. Mitsyuk, and I. A. Lomazova, "Simulating behavior of multi-agent systems with acyclic interactions of agents," *Proceedings of the Institute for System Programming*, vol. 30, pp. 285–302, 2018.

[5]https://pais.hse.ru/research/projects/gena

Computing Transition Priorities for Live Petri Nets

Kirill Serebrennikov
Faculty of Computer Science
National Research University Higher School of Economics
Moscow, Russia
cyrilsilver94@gmail.com

***Abstract*—In this paper we propose an approach to implementation of the algorithm for computing transition priorities for live Petri nets. Priorities are a form of constraints which can be imposed to ensure liveness and boundedness of a Petri net model. These properties are highly desirable in analysis of different types of systems, ranging from business processes systems to embedded systems. The paper covers the design considerations of the implementation, including an approach to handling the high time complexity of the algorithm and optimizations introduced in the original algorithm. Analysis of design decisions is provided. On the basis of the actual implementation an application for computing priorities was developed. It can be used for further analysis of the algorithm applicability for real life cases.**

Keywords—formal methods, Petri nets, coverability graph, priority relation, cyclic behavior

I. Introduction

Petri nets are widely applicable for modeling and analysis of various distributed systems ranging from business processes systems to biological systems. Regardless the nature of such systems their models always have some properties of liveness and boundedness. Properties of liveness include reiteration of all subprocesses and return to some initial state of the system. Properties of boundedness are those related to finiteness of the set of possible states.

In most of the cases it is highly desirable for the system to have finite set of states, i.e. its model should be bounded. Let us take, for example a Petri net shown in Fig. 1. This Petri net is a model of a simple producer/consumer system, where the left cycle represents a producer, the right cycle – a consumer, and the place p_3 between them is a buffer. This net is live, i.e. in every reachable marking each transition can eventually fire. The net is unbounded, since the number of tokens in p_3 can be arbitrary large. It means that the buffer overflow will eventually occur. Thus, it is desirable to transform the model into live and bounded preserving the original structure of the net.

The problem of transformation of a given live and unbounded Petri net into live and bounded one without modification of its structure was considered in [1] and [2]. The authors focused on two approaches to control of Petri net behavior: through priority-based and through time-based constraints on transition firings. Algorithms for computation of priorities and time intervals were proposed by them. This paper continues their study.

The proposed algorithms are based on construction of the spine tree which is a subgraph of the reachability tree, containing exactly all feasible cyclic runs in a net. It represents the behavior that should be saved in a transformed Petri net to preserve the liveness property of the original net. The procedure of obtaining those cyclic runs each of which contains all transitions and is reachable from the initial marking was introduced in [3]. It is based on the construction of the coverability graph that is finite by definition but can be extremely large. This fact affects negatively the overall time complexity of the algorithms.

Nevertheless, the performance of these algorithms may be optimal for the majority of real life cases. In this paper we target implementation considerations of the above mentioned algorithms. The study is focused on computation of transition priorities leaving apart computation of time intervals since these two procedures have common foundation. The main contributions of this paper are:

1. An approach to implementation design of the transition priority computation algorithm based on construction steps optimization and adoption of parallelization;
2. A brief analysis of the actual implementation coded in Java programming language;
3. A Java application with command line interface built upon the algorithm implementation that can be used for running experiments and researching the applicability of the algorithm in practical cases.

The source code of the application along with usage instructions can be found in the repository[1].

The structure of the paper is as follows. In Section II the main theoretical preliminaries are provided. Section III contains a brief description of the algorithm under consideration. In section IV the approach to implementation design is described and results of implementation analysis are presented. Section V concludes the paper.

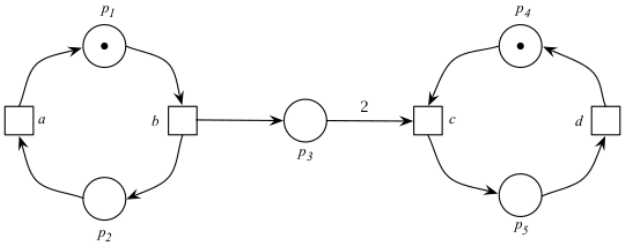

Fig. 1. Example of a marked Petri net

II. Preliminaries

For a more detailed introduction to the concepts presented in this section see e.g. [4].

Let $\mathbb{N}$ denote the set of natural numbers (including 0). We define a marked Petri net as a tuple

$$(P, T, pre: T \times P \longrightarrow \mathbb{N}, post: T \times P \longrightarrow \mathbb{N}, m_0: P \longrightarrow \mathbb{N})$$

where P and T are finite disjoint sets of places and transitions, respectively. $pre(t,p)$ is a number of tokens required to present on place p to enable transition t. The firing of t adds $post(t,p) - pre(t,p)$ tokens to p. Graphically,

[1] https://github.com/molassar/PN-transition-priority-computer

places are denoted by circles and transitions by squares. There is a directed arc from p to t if $pre(t,p) > 0$. The arc is annotated with $pre(t,p)$ if $pre(t,p) > 1$. Similarly, there is a directed arc from t to p if $post(t,p) > 0$. It is annotated with $post(t,p)$ if $post(t,p) > 1$. The pre-set of a transition t is the set of places p satisfying $pre(t,p) > 0$. The post-set of t is a set of places p satisfying $post(t,p) > 0$. A marking of a net is a mapping $m: P \longrightarrow \mathbb{N}$. The initial marking m_0 is represented by $m_0(p)$ tokens on place p.

An initial run is a sequence of transition firings, starting with the initial marking. Reachable markings are all those markings which can be reached by the initial run. A cyclic run is a finite run starting and ending at the same marking.

A reachability graph of a Petri net is a labeled directed graph in which vertices correspond to reachable markings of the net. A directed edge from vertex v to vertex v' is labeled with transition t which is enabled by marking m represented by v and leads to marking m' represented by v'.

A Petri net is bounded if, for each place p, the number of tokens on p does not exceed some fixed bound $k \in \mathbb{N}$, i.e. for each reachable marking m the following is true: $m(p) \leq k$. Thus, a Petri net is bounded if and only if its reachability graph is finite.

A marking m' strictly covers a marking m if and only if for each place $p \in P$, $m'(p) \geq m(p)$ and $m' \neq m$.

In case of unbounded nets coverability graphs provide finite information about behavior. The construction of coverability graph is based on the notion of the generalized marking which is formally a mapping: $P \longrightarrow \mathbb{N} \cup \{\omega\}$, where ω denotes an arbitrary number of tokens on a place. A coverability graph is defined constructively: it is constructed successively like the reachability graph starting from the initial marking. However, in case of the coverability graph when a marking m' represented by a current leave v' in the reachability graph strictly covers a marking m represented by a vertex v, lying on the path from the root to v', then in coverability graph the vertex v' gets a marking m_w, where $m_w(p) = \omega$, if $m'(p) > m(p)$, and $m_w(p) = m'(p)$, if $m'(p) = m(p)$. Fig. 2 shows a coverability graph of the example shown in Fig. 1.

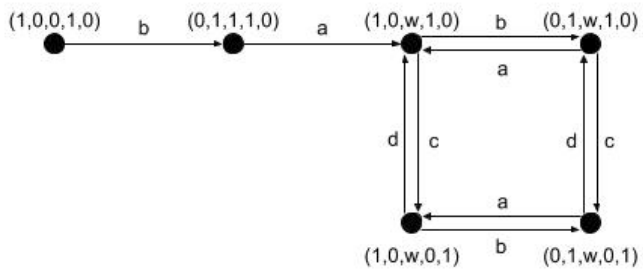

Fig. 2. A coverability graph of the Petri net of Fig. 1

The coverability net of a Petri net $N = (P, T, pre, post, m_0)$ is a new Petri net $N' = (P', T', pre', post', m_0')$ which is constructed on the basis of a coverability graph (V, E, v_0) of the original net. The transitions of N' are mapped to the transitions of N by a labeling function λ': $T' \longrightarrow T$. The coverability net is formally defined as:

- $P' = V$,
- $T' = E$,
- $pre'((v', t, v''), v) = 1$ if $v = v'$,
- $pre'((v', t, v''), v) = 0$ if $v \neq v'$,
- $post'((v', t, v''), v) = 1$ if $v = v''$,
- $post'((v', t, v''), v) = 0$ if $v \neq v''$,
- $m_0'(v) = 1$ if $v = v_0$,
- $m_0'(v) = 0$ if $v \neq v_0$,
- $\lambda'(v, t, v') = t$.

The extended coverability net is the coverability net that contains additional places to capture the token count change for ω-marked places of the original net. For each unbounded place p in the original net a place p is added to the extended coverability net. If transition t is in the pre-set of p in the original net N, then all transitions $t' \in T'$ with $\lambda'(t') = t$ are in the pre-set of the added place p. Arc weights are taken into account. The same holds for the post-sets of added places. The initial marking of added places coincides with the initial marking of these places in the original net. Fig. 3 demonstrates the extended coverability net constructed upon the coverability graph shown in Fig. 2.

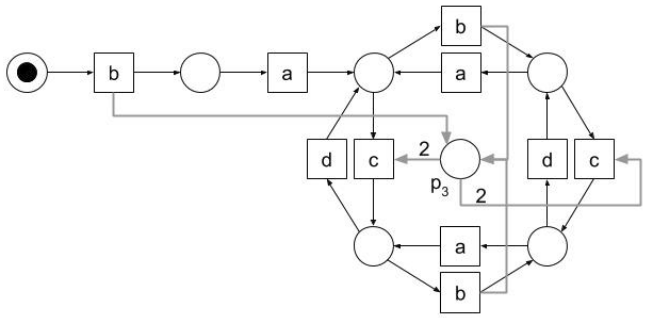

Fig. 3. The extended coverability net of the Petri net of Fig. 1

We define the set of all minimal feasible cyclic runs together with prefixes leading to the cycles in a Petri net N as

$$C(N) = \{\tau\sigma \mid \tau\sigma^* \text{ is an initial run in } N,$$
$$\tau \text{ does not include } \sigma \text{ and}$$
$$\sigma \text{ includes all transitions in } N\}$$

where σ is a minimal feasible cyclic run in N and τ is a finite initial run leading to σ. A spine tree is a subgraph of a reachability tree that contains exactly all runs from $C(N)$. The spine tree contains the behavior that should be saved in course of transformation in order to keep a Petri net live. For the Petri net in Fig. 1 $C(N)$ = {*babacd*, *babcad*, *babcda*, *babacbd*, *babcabd*, *babacbad*}. Thus, the spine tree of the net has the construction as shown in Fig. 4.

A priority relation for a Petri net N is a partial order $(T, \ll)$, i.e., the relation is reflexive, antisymmetric and transitive. A priority relation $\ll$ can be specified by assigning a priority label $\pi(t) \in \mathbb{N}$ to each transition t. Thus, $t \ll t'$ if and only if $\pi(t) < \pi(t')$. A Petri net with priorities is a Petri net together with a priority relation. In a Petri net with priorities if Q is a set of all transitions enabled in a marking m then only transitions with the highest priority may fire.

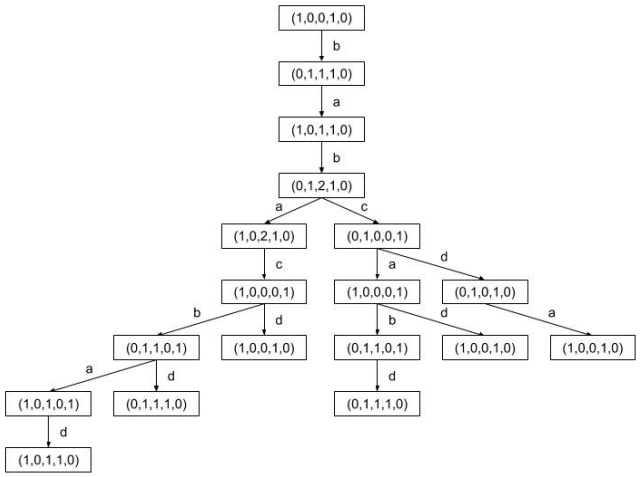

Fig. 4. The spine tree of the Petri net of Fig. 1

III. Algorithm overview

Let *N* be a live and unbounded Petri net. The task is to check, if it is possible to transform this net into live and bounded by adding priorities to its transitions. To accomplish the task we should find those transition priorities, which exclude runs leading to unboundedness.

It is possible to distinguish two major stages in the algorithm. The first is the search for cyclic runs in a Petri net. The presence of cyclic runs is a necessary condition for existence of transition priorities for a given Petri net. On the second stage the spine tree is built with the cyclic runs found on the previous stage forming its skeleton. The whole algorithm has the following sequence of actions:

1. Given a Petri net build its coverability graph;
2. Given the coverability graph constructed on the previous step build a coverability net;
3. Transform the coverability net into an extended coverability net;
4. Find behavioral cycles of the extended coverability net;
5. If the set of cyclic runs computed on the previous step is not empty build a spine tree in which the cyclic runs form the skeleton;
6. Given the spine tree build a spine-based coverability tree in which all leaves are colored in either red or green[2];
7. Traverse the spine-based coverability tree. For each non-red node *a* with its incoming edge labeled after transition t_1 if there exists a red sibling *b* with its incoming edge labeled after transition t_2 add (t_1, t_2) to the priority relation;
8. Assign priority labels to the transitions on the basis of the priority relation computed on the previous step.

The steps 1-4 form the first stage of the algorithm – search for cyclic runs. The procedure was introduced in [3]. The second stage – computation of a priority relation through spine tree construction – is represented by the steps 5-7. It was described in [1].

[2] For the complete algorithm see [1]

IV. Implementation approach

A. Cyclic Runs Search

The problem of the search for cyclic runs in a Petri net can be reduced to the search for cyclic runs in its extended coverability net. The original algorithm for the cyclic runs search is comprised of four steps. We have reduced the number of steps to two by optimizing the construction phases of coverability and extended coverability nets.

The first step is the construction of a coverability graph. This step can not be avoided since the coverability graph is the foundation for the rest of the algorithm. Since the coverability graph can grow exponentially the overall time complexity of the algorithm is also exponential. We have chosen parallelization to target the problem. The implementation of coverability graph construction and traversal steps was designed to be easily parallelized.

```
1  procedure buildCG(m0,T)
2
3  Input:  Initial marking m0 ∈ M,
4              M - set of generalized markings;
5          set of transitions T
6  Output: Directed graph G = (V,E), |V| = |M|
7
8  G = initGraph()
9  root = Node(marking: m0, parentNode: null)
10 Q = makequeue(root)
11 while Q is not empty:
12     node = dequeue(Q)
13     m = marking(node)
14     v = Vertex(label: label(m))
15     incidentFrom = listIncidentFrom(G,v)
16     if incidentFrom is empty:
17         fireableT = filter(T, predicate: isFireableFrom(m))
18         for each t ∈ fireableT:
19             mn = fire(m,t)
20             parentNode = node
21             while parentNode is not null:
22                 mp = marking(parentNode)
23                 if isStrictlyCoveredBy(mn,mp):
24                     mn = generalize(mn,mp)
25                     break
26                 parentNode = parentNode(parentNode)
27             u = Vertex(label: label(mn))
28             e = Edge(label: label(t))
29             addIncidentFrom(G,v,e,u)
30             newNode = Node(marking: mn, parentNode: node)
31             enqueue(Q,newNode)
```

Listing 1. Pseudocode of the algorithm for building the coverability graph

Listing 1 demonstrates the pseudocode of the algorithm for building the coverability graph. Each node is processed in the following way: the set of transitions is filtered to find the transitions enabled by the marking corresponding to a node, then all the filtered transitions are fired to produce new generalized markings. Directed arcs are added from the vertex labeled by the marking of the node to the vertices labeled by the produced generalized markings. New nodes are generated from the obtained markings for further processing. Processing of a node does not depend on processing of other nodes so this task can be scheduled in parallel. The actual implementation of the pseudocode has the time complexity

$$O(|V| * |T| * d(CG) * |P|)$$

where $|V|$ is the number of vertices in a coverability graph, $|T|$ - the cardinality of the transition set of a Petri net, $d(CG)$ – depth of the coverability graph, i.e. the distance from the root to the most distant vertex, and $|P|$ - the cardinality of the set of places.

We have made two implementations of the algorithm: single-threaded and parallel. For the parallel implementation the fork/join Java framework was used. It is based on the

divide and conquer approach and uses a pool of threads. We have also conducted a benchmarking of the two implementations with the use of JMH open source tool. Coverability graph construction for the Petri net in Fig. 1 was benchmarked. The single shot time mode was selected for the test. In this mode the time for a single operation is measured. Thus the "cold" performance of an algorithm is estimated, since no preliminary warm-up is conducted. This mode is most similar to the real-life usage scenario of the algorithm The results are presented in Table 1.

The results in Table 1 demonstrates that the single-threaded implementation performs slightly better for the Petri net of Fig. 1. The probable reason is the low complexity of the net. The time complexity of processing a single node is

$$O(|T| * d(CG) * |P|)$$

and, hence, there are strong reasons to believe that with increase in concurrency of the model and in number of transitions and places the parallel implementation will outperform the single-threaded one. Further experiments should be conducted.

TABLE I. BENCHMARK RESULTS FOR IMPLEMENTATIONS OF THE COVERABILITY GRAPH CONSTRUCTION ALGORITHM

Benchmark Mode	Single-Threaded Score	Parallel Score
Single shot time	5080.768 us/op	7632.496 us/op

The construction of the coverability net and the extended coverability net was optimized: we used coverability graph built on the previous stage and a separate data structure for capturing the number of tokens on unbounded places to find all feasible cyclic runs. The pseudocode of the cyclic runs search procedure is presented in Listing 2.

Again, the algorithm was designed to be easily parallelized. Processing of each node in the actual implementation has the time complexity

$$O(|E|)$$

where $|E|$ is the number of edges in the coverability graph. Table 2 demonstrates benchmark results of parallel and single-threaded implementations of the cyclic runs search algorithm. For the purposes of benchmarking the Petri net of Fig. 1 was searched for cyclic runs. Again, the single-threaded solution has higher performance and this time the gap is larger. However, as it was mentioned earlier further experiments should be conducted since the model is very simple.

TABLE II. BENCHMARK RESULTS FOR IMPLEMENTATIONS OF THE CYCLIC RUNS SEARCH ALGORITHM

Benchmark Mode	Single-Threaded Score	Parallel Score
Single shot time	11366.737 us/op	19647.215 us/op

B. Priorities computation

The rest of the algorithm is based on the construction of the spine tree of a Petri net and its traversal. The procedure of constructing the spine tree from the list of cyclic runs is quite straightforward and we omit its description here. Similarly, the algorithm for the construction of the spine-based coverability tree was described in details in [1] and we have mostly followed this description in the process of implementation design. In the spine-based coverability tree the red leaves (ω-leaves) are those nodes which strictly cover some markings preceding them in their branches. To guarantee boundedness they should be cut off. This is achieved with priorities. Listing 3 demonstrates the pseudocode for computing priority relation on the basis of the spine-based coverability tree.

```
procedure cyclicRunsSearch(G,m0,upm0,T)

Input:  Coverability graph G;
        initial marking m0 ∈ M,
            M - set of generalized markings;
        initial marking of unbounded places upm0;
        set of transitions T
Output: List of all cyclic runs L

L = initEmptyList()
root = Node(marking: m0, unboundedPlaces: upm0,
            transition: null, parentNode: null)
Q = makequeue(root)
while Q is not empty:
    node = dequeue(Q)
    m = marking(node)
    upm = unboundedPlaces(node)
    t = transition(node)
    // check for cyclic run
    prefix = initEmptyPrefix()
    cycle = initEmptyCycle()
    hasCycleOccurred = false
    addTransition(cycle,t)
    curNode = parentNode(node)
    while curNode is not null:
        mCur = marking(curNode)
        upmCur = unboundedPlaces(curNode)
        tCur = transition(curNode)
        if markingsAreEqual((m,upm),(mCur,upmCur)):
            hasCycleOccurred = true
        if tCur is not null:
            if hasCycleOccurred:
                addTransition(prefix,tCur)
            else:
                addTransition(cycle,tCur)
        curNode = parentNode(curNode)
    if hasCycleOccurred:
        run = Run(prefix: prefix, cycle: cycle)
        if containsAllTransitions(T,run):
            addRun(L,run)
            continue
    // no cyclic run was detected
    v = Vertex(label: label(m))
    incidentFrom = listIncidentFrom(G,v)
    for each (e,u) in incidentFrom:
        tForE = transitionForEdge(e)
        mForU = markingForVertex(u)
        // check if transition tForE from
        //  marking m to marking mForU is not
        //  in the sequence represented by node
        if isNotInSequence(node,tForE,mForU):
            // calculate marking of unbounded places
            upmn = fireForUnbounded(upm,tForE)
            if for every marking in upmn marking >= 0:
                newNode = Node(marking: mForU,
                               unboundedPlaces: upmn,
                               transition: tForE,
                               parentNode: node)
                enqueue(Q,newNode)
```

Listing 2. Pseudocode of the algorithm for cyclic runs search

It was proved in [1] that if the relation $\ll$ constructed for the live and unbounded Petri net (N, m_0) is a partial order (i.e. antisymmetric), then $\ll$ is a priority relation for N, and the Petri net $(N, \ll, m_0)$ is live and bounded. However, it is possible for the algorithm in Listing 3 to produce relations with contradictory pairs, thus violating the antisymmetric property. In [2] it is suggested to remove such contradictory pairs from the relation. In this case the Petri net with the resulting priority relation should be checked for boundedness and liveness.

The concluding step of the algorithm implementation is computation of priority labels of transitions. For transitions

which are not included in the priority relation the highest priority is assigned since this means that the order of their occurrence is not important. For the rest of transitions a topological sorting is used to order the transitions in the ascending priority and assign a label to each of them with respect to their position. This is possible because the priority relation can be represented as a directed acyclic graph. It should be noted that the obtained priorities can be stronger than it is required since topological sorting does not take into account relative independence of transitions in the priority relation.

```
procedure computePR(treeRoot)

Input:  Root of spine-based coverability tree treeRoot
Output: Priority relation PR = {(t1,t2) : t1 ∈ T, t2 ∈ T},
            T - set of transitions

PR = initEmptyRelation()
Q = makequeue(treeRoot)
while Q is not empty:
    node = dequeue(Q)
    childNodes = children(node)
    redNodes = filter(childNodes, predicate: isRed())
    greenNodes = filter(childNodes, predicate: isGreen())
    yellowNodes = filter(childNodes, predicate: isYellow())
    enqueueAll(Q,yellowNodes)
    for each rn in redNodes:
        // get transition represented by incoming arc of node
        tr = transitionOfIncArc(rn)
        for each yn in yellowNodes:
            ty = transitionOfIncArc(yn)
            addToRelation(PR,(ty,tr))
        for each gn in greenNodes:
            tg = transitionOfIncArc(gn)
            addToRelation(PR,(tg,tr))
```

Listing 3. Pseudocode of the algorithm for priority relation computation

V. Conclusion

In this paper we have proposed an approach to implementation design of the algorithm for computing transition priorities for live Petri nets. In the worst case the performance of the algorithm may be not optimal for the task since it is based on construction and traversal of the coverability graph which can grow exponentially. However, it may prove optimal for the majority of real-life system models. The presented approach targets the drawbacks of the algorithm. The main proposed methods are the use of parallel computing and the optimization of construction steps.

Priority constraints can be helpful in analysis of technical systems, since they ensure liveness and boundedness of such systems. For the purposes of computing priorities an application was developed. This application is based on the algorithm implementation presented in the paper and can be used for further studies on the problem.

However, it should be noted that the application inherits the weak points of the algorithm it is based on, i.e. the high time complexity. Hence, further experiments should be conducted to determine the limits of applicability of the application and the algorithm in particular.

VI. Acknowledgments

This work is supported by the Basic Research Program at the National Research University Higher School of Economics.

References

[1] I. Lomazova, L. Popova-Zeugmann Controlling Petri Net Behavior using Priorities for Transitions. *Fundamenta Informaticae*, Vol. 143, No 1-2, pp. 101–112, 2016.

[2] I. Lomazova, L. Popova-Zeugmann, A. Bartels Controlling Boundedness for Live Petri Nets. *Proceedings of the 4th International Conference on Control, Decision and Information Technologies*, pp. 236-241, 2017.

[3] J. Desel, On Cyclic Behaviour of Unbounded Petri Nets. In: Application of Concurrency to System Design (ACSD). *13th International Conference on Application of Concurrency to System Design*, pp. 110–119. IEEE, 2013.

[4] W. Reisig, Understanding Petri Nets. Springer-Verlag Berlin Heidelberg, 2013.

[5] T. Cormen, C. Leiserson, R. Rivest, C. Stein, Introduction to Algorithms. The MIT Press, 2009.

[6] B. Goetz, T. Peierls, J. Bloch, J. Bowbeer, D. Holmes, D. Lea, Java Concurrency in Practice. Addison-Wesley Professional, 2006.

Method for Building UML Activity Diagrams from Event Logs

Natalia Zubkova* and Sergey Shershakov†
Laboratory of Process-Aware Information Systems (PAIS Lab)
National Research University Higher School of Economics
Moscow 101000, Russia
Email: *nszubkova@edu.hse.ru, †sshershakov@hse.ru

***Abstract*—UML Activity Diagrams are widely used models for representing software processes. Models built from event logs can provide valuable insights into real flows in systems and suggest ways of improving those systems. This paper proposes a novel method for mining UML Activity Diagrams (AD) from event logs. The method is based on a framework that consists of three nested stages involving a set of model transformations. The initial model is inferred from an event log using one of the existing mining algorithms. Then the model, if necessary, is transformed into an intermediate form and, finally, converted into the target UML AD by the newly propsed algorithm. The transforming algorithms, except one used at the last stage, are parameters of the framework.**

***Index Terms*—Process mining, Petri Nets, UML Activity Diagrams, Process Discovery**

I. Introduction

Process mining techniques [1] aim at analyzing and improving real-life processes by taking information from event logs. Event logs are generally produced by process-aware information systems (PAIS) that support these processes. One particular problem of process mining is *process discovery*; its goal is to build a model of a process, based on the data in an event log. Such models can be expressed in different notations. For example, transition systems (TS) naturally represent sequences of events (*traces*) as they are recorded in event logs. However, if a process contains concurrent behavior, transition systems tend to be very complex and as large as the event log itself. This occurs due to the fact that similar patterns are not joined together and concurrency is expressed in the form of interleaving.

There are other types of models that allow to represent concurrency patterns, namely choice and parallelism, and that are widely used in the field of process mining. *Petri nets (PN), BPMN, Fuzzy maps* and *UML Activity Diagrams (AD)* are examples of such models. Unified Modeling Language (UML) [2] is a standart for defining, documenting and visualizing artifacts, especially in the software engineering domain. Particularly, UML Actitity Diagrams are used, among other, to represent and analyse actual or expected behavior of software systems. AD is not the only UML class that allows to represent concurrency [3]. For instance, *UML State Machine Diagrams* have their own semantics to illustrate concurrency. However, they reflect different *states* of a system which are not explicitly represented in event logs. These states, therefore, have to be mined using different techniques, i.e. encoding states with trace prefixes. Given that event logs contain information representing *activities* performed by process participants and supporting systems, we regard Activity Diagrams as the desired class of target models in this paper.

In our work, we propose a framework for building UML Activity Diagrams from event logs, consisting of a number of steps. The frameworks *essential* part is the algorithm for converting Petri nets into UML ADs. Other intermediate models (namely, TS and PN) can be synthesised using different algorithms which are parameters of the framework. Here we consider the algorithm of regions [4] as a means to generate Petri nets which are consequently converted into target UML ADs. ADs are usually more compact than Petri nets and are more easily interpretable. Moreover, generated diagrams can be imported and used in different visual modeling and design tools used in the software engineering domain, i. e. Sparx Enterprise Architect, and be later included as part of bigger software models.

The contributions of this paper are as follows: (1) a framework for generating UML AD from event logs, (2) a novel method for UML AD sythesis from a Petri nets as intermediate models, (3) implementation of the proposed framework specified by a particular set of sythesis algorithms.

The rest of the paper is organized as follows. Section II gives a brief overview of related work. Section III defines necessary concepts needed for the explanation of the proposed approach. The framework is described in Section IV and the PN-to-UML AD conversion algorithm is presented in Section V. Section VI contains models derived from real-life event logs. Finally, Section VII concludes the paper and outlines possible directions for future work.

II. Related work

There exist many approaches to construct Petri nets from event logs [1], [5], [6]. The algorithm of regions and its extensions are described, particularly, in [4], [7], [8]. The algorithm produces a Petri net from a given TS that serves as an input of the algorithm. The behavior of the derived PN is guaranteed to be equivalent to the TS. Previously, Petri nets have also been used as intermediate models for constructing other types of target models, such as BPMN in [9].

The similarity between UML Activity Diagrams and Petri nets are studied in numerous works. Arlow et al. present UML specification in application to Unified Process including UML AD structural elements, and also mention that UML AD are based on the Peti Net techniques [10]. In [11] authors formalize AD semantics and compare them to semantics of Petri Nets. There are many works dedicated to the transformation of UML Activity Diagrams into Petri nets; the reverse transformation is studied scantily. In [12] the author describes an approach to translate UML AD into Petri nets. Agarwal [13] developed a method for transforming AD into Petri nets for verification purposes. The author considers a set of UML patterns and indicates corresponding Petri net instances.

III. Preliminaries

$\mathcal{B}(X)$ is the set of all multisets over some set X. For a given set X, X^+ is the set of all non-empty finite sequences over X.

A. Trace, Event Log

Let Z be a set of activities. A *trace* is a finite sequence $\sigma = \langle a_1, a_2, ..., a_i, ..., a_n \rangle \in Z^+$.By $\sigma(i) = a_i$ we denote i-th element. $L \in \mathcal{B}(Z^+)$, such that $|L| > 0$, is an *event log*. Here, $|L|$ is the number of all traces.

B. Labeled Petri Net, Well-structured Labeled Petri Net

A *labeled Petri net (PN)* is a tuple $PN = \{P,\ T,\ F,\ l\}$, where P is a set of places, T is a set of transitions, $P \cap T = \emptyset$, $F \subseteq (P \times T) \cup (T \times P)$ is the flow relation, l is the labeling function $l : T \to \Lambda$, and Λ is a set of labels. In process mining, labels of transition represent events.

Given $p \in P$, the set $p^\bullet = \{y | (p, y) \in F\}$ is the *postset* of p.

In this paper by Petri net we denote a *well-structured* Petri net, i.e. a hierarcical Petri net that can be recursively divided into parts having single entry and exit points [14].

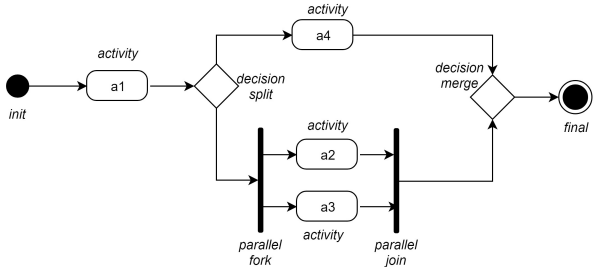

Fig. 1: An Activity Diagram example

C. UML Activity Diagram

A UML Activity Diagram is a tuple $AD = \{N, E, NT\}$, where

- NT is a set of node types $NT = \{control, object, executable\}$
- N is a set of nodes. $n \in N : n = (\lambda, type), \lambda \in \Lambda, type \in NT$
- E is a set of edges. $e \in E : e = (n_1, n_2), n_1, n_2 \in N$

Similar definition was used in [15]. In this paper we mainly focus on the following elements of the UML AD (see Fig. 1):

1) A is a set of *activity* nodes, $a \in A : a = (\lambda, executable)$
2) F is a set of *parallel* nodes, $f \in F : f = (control)$
3) D is a set of *decision* nodes, $d \in D : d = (control)$
4) $init$ and $final$ are initial and final nodes, both of type $control$.

UML decision nodes should be equipped with guards that indicate the conditions under which the decision is made. In this paper, we regard non-deterministic Petri nets as intermediate models[1]. The proposed conversion algorithm does not assume the presence of guard information in the event log and uses only the input Petri net. Thus, the produced Activity Diagram is non-deterministic as well.

IV. Framework

The proposed framework is illustrated in Fig. 2. The framework consists of a number of nested stages related to individual steps of the proposed method. At every step a transformation from one entity, event log or process model, into another is made. There exist numerous approaches to construct both Petri nets and transition systems. Models obtained from the same event log, but using different algorithms, represent the same process. However, they vary in details that are usually represented by *quality metrics* [16]. Depending on the task, specific combinations of quality metrics can be considered.

The long path of the framework (I) includes first building a TS needed for the algorithm of regions. Here, various techniques for *TS construction* can be used, for instance, *prefix tree sythesis* [17], *frequency based reduction* [18], neural approach [19] etc. However, the TS synthesis can be bypassed and a Petri net can be generated directly from the event log (II). There are many algorithms for that, i. e. *Inductive miner* [14], $\alpha-$*algorithm* [5], *ILP-miner* [20] and other. Finally, in III the generated Petri net is converted into a UML Activity Diagram.

A. Proposed implementation

In this paper we consider the full version of the framework with the following parameters.

1) Prefix tree builder, unlimited window, for TS construction.
2) The algorithm of regions for converting the TS into a PN.
3) The PN-to-UML AD converter described in the following section.

This following paragraph gives a brief overview of the algorithms used in steps 1 and 2.

Prefix tree builder [17] is an algorithm for TS synthesis. Event logs usually do not explicitly contain states that are needed for the construction of a transition system. A *state function* is introduced in order to infer such states. This

[1]There exists an extension to Petri nets that adds guards to its semantics. However, most of the process mining algorithms consider Petri nets without guards. Here we follow the same approach.

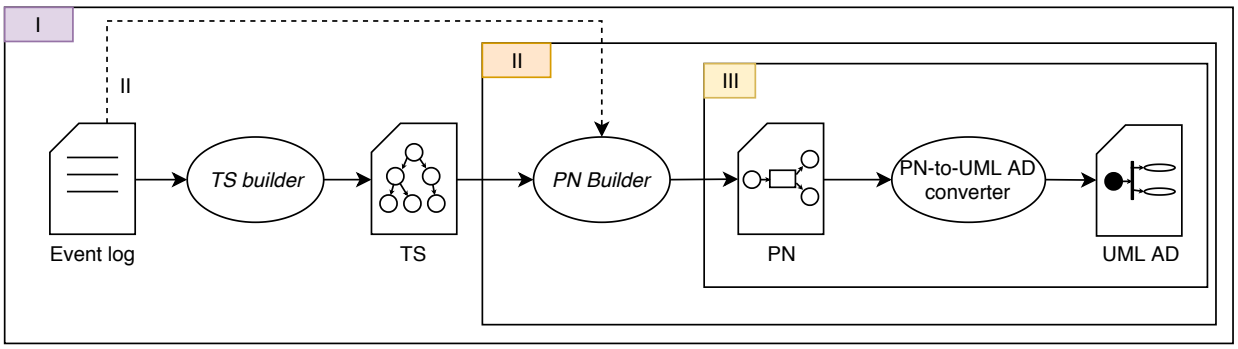

Fig. 2: Proposed framework. I-III are nested staged of the framework.

- I – II + TS construction from event log.
- II – III + PN synthesis from event log.
- III – AD synthesis for a given PN.

function maps events in an event log onto states of a TS. Let E be a set of events in an event log, and S be a set of states in a transition system. For each event $e \in E$ the state function produces a state $s \in S$ regarding either pre- or posthistory of the state s. A prefix tree is a special type of transition systems, for which the state function consideres prehistory (prefix) of the state s. Informally, a transition (s, e, s') appears if $prehistory_{s'} = prehistory_s + e$. If the prefix size is unlimited, the size of the generated TS can be equivalent to the size of the event log.

The algorithm of regions [8] used in 2 is based on finding equivalent behaviors in a given transition system. These behavioral fragments are grouped into so-called *regions*. Intuitively a region is equivalent to a place in a Petri net. Placing a token in such a place means allowing such a behavior to appear – via activating a post-transition. In UML Acitivity Diagrams transitions are translated into *activities*. Thus, considering a transitive dependence between an initial TS and an AD, one can ascertain a link between equivalent behavioral fragments in TS (regions) and corresponding nodes in AD.

V. PN to UML AD conversion algorithm

The PN-to-UML AD conversion algorithm is based on the idea of converting places and transitions of a given Petri net into corresponding elements of the target UML Activity Diagram. UML AD specification notes that an activity diagram can only have a single entry point, whereas the inception of a process modeled by a Petri net can be determined by placing tokens in multiple places (an initial marking). Here, we consider all places without incoming edges as a potential starting place. Then a single starting point (*init* node) in an Activity Diagram is constructed and connected to the following activities. Final places are also not explicitly indicated in Petri nets, however it is sensible to regard those without outgoing edges as such, corresponding *final* nodes are inserted in the AD.

While translating a Petri net into a UML activity diagram the algorithm considers special patterns, namely parallelisms and decisions. Such patterns can be translated into equivalent patterns in an Activity Diagram. A similar approach was used in [12], [13] for the reverse transformation.

In order to describe the proposed transformation we illustrate it on a running example (Fig. 3). We consider different types of AD nodes and describe the according transformations as follows.

A. Transformation functions

- Let $\alpha : (T, l) \to (A, l)$ be a function transforming transitions of the Petri net into *activities* of the constructed UML AD, tagged by the same labels;
- Let $\phi : P \to D$ be a function transforming appropriate positions of the PN into *decision* nodes of the UML AD;
- Let $\xi : T \to F$ and $\psi : P \to F$ be functions transforming PN transitions and sets of PN places into UML *parallel* nodes accordingly.

B. Building a UML Activity Diagram

UML Activity Diagram construction includes the following procedures.

1) *Constructing activity nodes*
   The semantics of Petri nets suggests that transitions, which model events in Petri nets, correspond to *activities* in Activity Diagrams. So the first transformation step of the algorithm is turning transitions of a given Petri net into UML AD *activities*, i.e. for each transition $t \in T$ we create an activity $a = \alpha(t)$ in the AD.
2) *Detecting parallel forks*
   We now need to connect nodes and identify more complex behaviors. In a Petri net a concurrent pattern occurs if a transition has multiple outgoing edges, allowing tokens to appear in *all* of the following places when the transition is fired (see Fig. 4). Considering a transition $t \in T$ of a Petri net, let T^* be a set of transitions reachable from t in one step. For each transition $t \in T$, if t has
   a) 0 outgoing edges, then activity $\alpha(t)$ is connected to a final node;

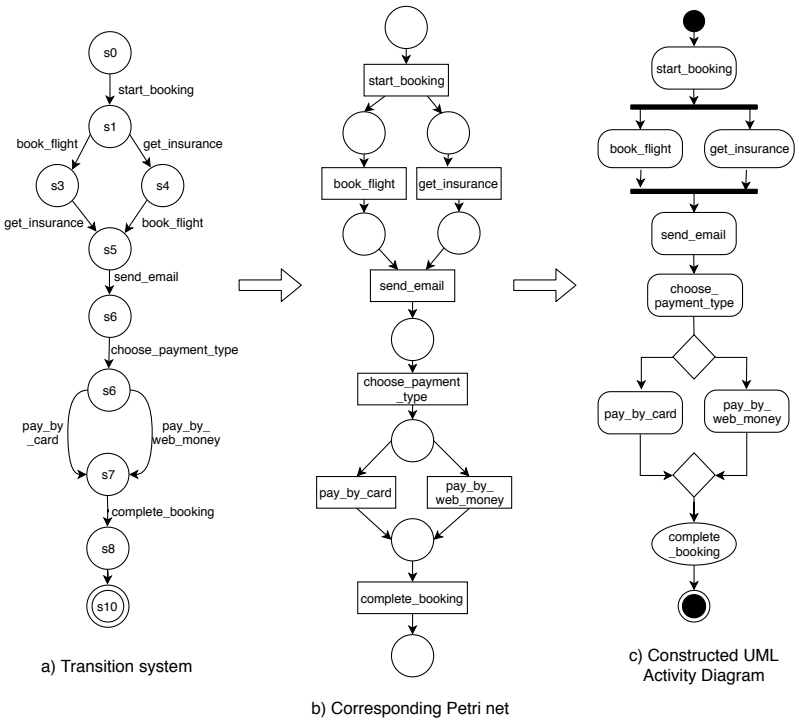

Fig. 3: Example models.

b) 1 outgoing edge, then activity $\alpha(t)$ is connected to $\alpha(t^*$, for each $t^* \in T^*$;
c) > 1 outgoing edge, activity $\alpha(t)$ is connected to a fork node $\xi(t)$, and $\xi(t)$ is then connected to $\alpha(t^*$, for each $t^* \in T^*$.

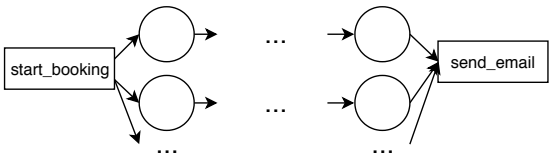

(a) In Petri net.

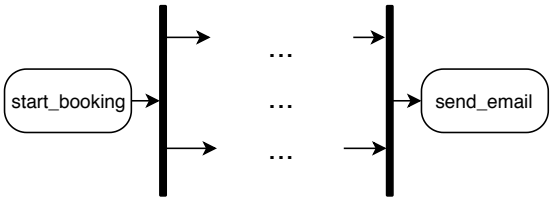

(b) In corresponding UML Activity Diagram.

Fig. 4: Concurrency pattern.

3) *Detecting parallel join*
In order for the model to be more interpretable, for each parallel fork there should be a reciprocal parallel join. So for each fork, described in 2 we need to find the corresponding join. This is done according to the following steps.

a) For each maximum set of places $\{p_1, ..., p_n\} \subseteq P$ that have coinciding postsets ($p_1^\bullet = ... = p_n^\bullet$) and $n > 1$, a $\psi(P)$ join node is inserted in the AD.
b) For each transition t immediately preceding each place from S, the activity $\alpha(t)$ is connected to $\psi(P)$.
c) Join node $\psi(P)$ is then connected to $\alpha(t')$, $\forall t' \in T'$, where T' is a set of transitions immediately following places $\{p_1, ..., p_n\}$.

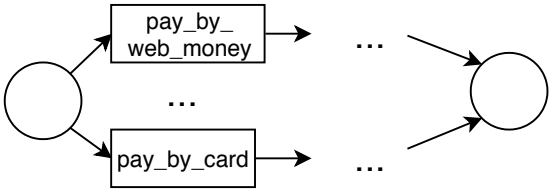

(a) In Petri net.

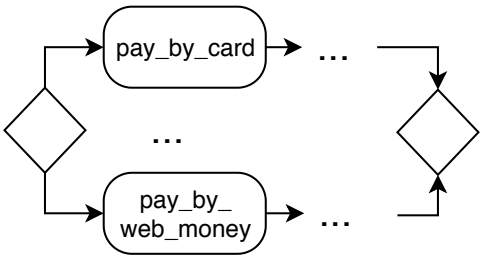

(b) In corresponding UML Activity Diagram.

Fig. 5: Choice pattern.

4) *Detecting decision splits and merges*
A decision pattern in a Petri net occurs if a place has multiple outgoing edges allowing *only one* consecutive transition to fire (see fig. 5). So for each place $p \in P$, that has more than one outgoing edge a *decision* node $\phi(p)$ is inserted into the AD and is connected to $\alpha(\tilde{t})$, $\forall \tilde{t} \in \tilde{T}$, where $\tilde{T}$ are transitions connected to p (both before and after). Likewise, if the place p has multiple *incoming* edges, a reciprocal *merge node* $\phi(p)$ is inserted into the AD.

Applying the steps 1–4 to an input Petri net, the target UML Activity Diagram is constructed.

VI. Application

In this section we provide example of models obtained from real logs. *Log1* and *Log2* consist of 243 and 1132 traces respectively. For observability purposes intermediate transition systems were reduced using a frequency reduction algorithm described in [18].

In 6 models were generated with window size 1 and frequency reduction parameter 0.04. *Log1* contains information about bank operations.

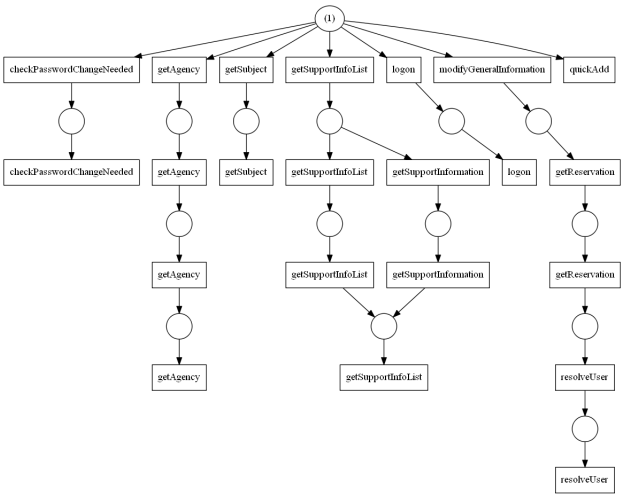

(a) Petri net

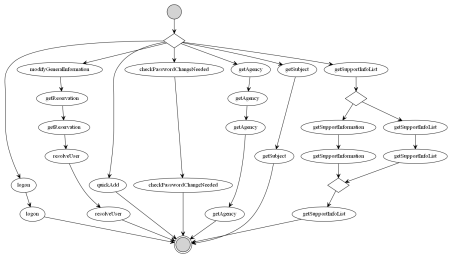

(b) UML AD

Fig. 6: *Log1*.

In 7 models were generated on a log containing information about building permit applications from five Dutch municipalities. Transistion system was built with unlimited window parameter and reduced with frequency reduction parameter of 0.15.

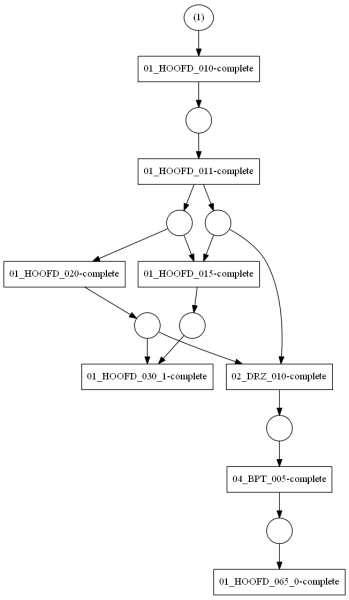

(a) Petri net

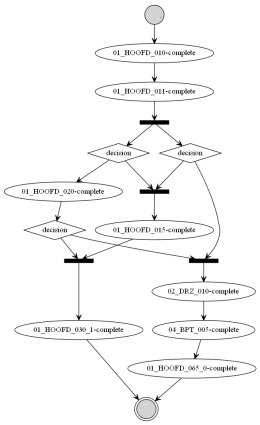

(b) UML AD

Fig. 7: *Log2*.

VII. Conclusion

In this paper we proposed a method based on a framework to build UML Activity Diagrams from event logs and introduced a novel algorithm for converting a well-structured Petri net into a UML Activity Diagram. The method is implemented as a part of the `LDOPA`[2] library. Future work includes studying the executuion semantics of Petri nets and UML activity diagrams with guards. Moreover, the framework can be further investigated by implementing different TS and PN synthesis algorithms.

Acknowledgment

This work is supported by the Basic Research Program of the National Research University Higher School of Economics.

[2]Available at https://prj.xiart.ru/projects/ldopa

REFERENCES

[1] Wil Van der Aalst. Data Science in Action. In *Process Mining*, pages 3–23. Springer, 2016.

[2] UML specification. https://www.omg.org/spec/UML/About-UML/. Accessed: 2019-03-01.

[3] Concurrecy in UML. https://www.omg.org/ocup-2/documents/concurrency_in_uml_version_2.6.pdf. Accessed: 2019-03-05.

[4] Josep Carmona, Jordi Cortadella, and Michael Kishinevsky. A Region-Based Algorithm for Discovering Petri Nets from Event Logs. volume 5240, pages 358–373, 09 2008.

[5] Wil MP Van Der Aalst and Boudewijn F Van Dongen. Discovering Petri Nets from Event Logs. In *Transactions on Petri Nets and Other Models of Concurrency VII*, pages 372–422. Springer, 2013.

[6] A Weijters, Wil M. P. Aalst, and Alves A K Medeiros. *Process Mining with the Heuristics Miner-algorithm*, volume 166. 01 2006.

[7] Eric Badouel, Luca Bernardinello, and Philippe Darondeau. Polynomial algorithms for the synthesis of bounded nets. In *Colloquium on Trees in Algebra and Programming*, pages 364–378. Springer, 1995.

[8] Jordi Cortadella, Michael Kishinevsky, Luciano Lavagno, and Alexandre Yakovlev. Deriving Petri nets from finite transition systems. *IEEE transactions on computers*, 47(8):859–882, 1998.

[9] Anna A. Kalenkova, Wil M. P. van der Aalst, Irina A. Lomazova, and Vladimir A. Rubin. Process mining using bpmn: relating event logs and process models. *Software & Systems Modeling*, 16(4):1019–1048, Oct 2017.

[10] Jim Arlow and Ila Neustadt. *UML2 and the Unified Process: practical object-oriented analysis and design*. Pearson Education, 2005.

[11] Rik Eshuis and Roel Wieringa. A comparison of Petri net and Activity diagram variants. In *Proc. of 2nd Int. Coll. on Petri Net Technologies for Modelling Communication Based Systems*, volume 93, 2001.

[12] Dirk Fahland. Translating UML2 Activity diagrams to Petri nets. *Berlin, Germany: Humboldt-Universitat zu Berlin*, 2008.

[13] Bhawana Agarwal. Transformation of UML Activity diagrams into Petri nets for verification purposes. *International Journal Of Engineering And Computer Science*, 2(3):798–805, 2013.

[14] Sander JJ Leemans, Dirk Fahland, and Wil MP van der Aalst. Discovering block-structured process models from event logs-a constructive approach. In *International conference on applications and theory of Petri nets and concurrency*, pages 311–329. Springer, 2013.

[15] Kseniya Davydova and Sergei Shershakov. Mining hybrid uml models from event logs of soa systems. 29(4), 2017.

[16] Joos CAM Buijs, Boudewijn F Van Dongen, and Wil MP van Der Aalst. On the role of fitness, precision, generalization and simplicity in process discovery. In *OTM Confederated International Conferences" On the Move to Meaningful Internet Systems"*, pages 305–322. Springer, 2012.

[17] Wil MP Van der Aalst, Vladimir Rubin, HMW Verbeek, Boudewijn F van Dongen, Ekkart Kindler, and Christian W Günther. Process mining: a two-step approach to balance between underfitting and overfitting. *Software & Systems Modeling*, 9(1):87, 2010.

[18] Sergey A Shershakov, Anna A Kalenkova, and Irina A Lomazova. Transition systems reduction: balancing between precision and simplicity. In *Transactions on Petri Nets and Other Models of Concurrency XII*, pages 119–139. Springer, 2017.

[19] Timofey Shunin, Natalia Zubkova, and Sergey Shershakov. Neural approach to the discovery problem in process mining. In *Analysis of Images, Social Networks and Texts*, pages 261–273. Springer International Publishing, 2018.

[20] Jan Martijn EM Van der Werf, Boudewijn F van Dongen, Cor AJ Hurkens, and Alexander Serebrenik. Process discovery using integer linear programming. In *International conference on applications and theory of petri nets*, pages 368–387. Springer, 2008.

“Life” in Tensors: Implementing Cellular Automata on Graphics Adapters

Shalyapina Natalia
National Research Tomsk State University
Tomsk, Russia
nat.shalyapina@gmail.com

Gromov Maxim
National Research Tomsk State University
Tomsk, Russia
maxim.leo.gromov@gmail.com

***Abstract*— This paper presents an approach to the description of cellular automata using tensors on the example of the cellular automata of Conway's Game of Life. This approach allows to attract various frameworks for organizing scientific calculations on high-performance graphics adapter processors, that is, to automatically build parallel software implementations of cellular automata. In our work, we use the Keras and TensorFlow frameworks to organize computations on NVIDIA graphics adapters. Since these frameworks were created to build neural networks, the functioning of the cellular automata of Conway's Game of Life is described by a specially constructed neural network. The resulting acceleration from such a parallel implementation of the cellular automata is estimated experimentally.**

Keywords*— *Cellular automata, Conway's Game of Life, tensor

I. Introduction

The use of automata in description of a dynamic systems’ behavior has been known for a long time. The key point of this approach to the description of systems is a representation of the object under study in the form of a discrete automatic device – automaton (State Machine or Transition System). Under the influence of input sequences (or external factors) an automaton changes its state and produces reactions. There are many types of such automata: the Moore and Mealy machines [1], the cellular automaton [2], and others. The knowledge of the features of the object under study can provide enough information to select the appropriate type of automaton for the object’s behavior description. In some cases, it is convenient to use an infinite model. But finite models are mostly common. In the latter case, the sets of states, input actions (or states of the environment), and output reactions are finite.

Our work deals with *cellular automata* (CA). The theory of cellular automata began to take shape quite a long time ago. The work of John von Neumann [3] might be considered as the first work of the cellular automata theory. Today, a large number of studies devoted to cellular automata are known [4, 5]. Note that a major part of these works is devoted to the simulating of spatially distributed systems in physics, chemistry, biology, etc. [6]. The goal of the simulation is to find the states of the cells of a CA after a predetermined number of CA cycles. The resulting set of states in some way characterizes the state of the process or object under study (fluid flow rate at individual points, concentration of substances, etc.). Thus, the task of simulating a certain process or object by a cellular automaton can be divided into two subtasks. First, the researcher must select the parameters of the automaton (the dimension of the grid of cells, the shape of the cells, the type of neighborhood, etc.). And secondly, programmatically implement the behavior of the selected cellular automaton. Our work is focused on the second task – the software implementation of the cellular automaton.

In itself, the concept of a cellular automaton is quite simple and the idea of software implementation is obvious. However, the number of required calculations and the structure of these calculations suggest the use of modern supercomputers with a large number of cores and supporting large-block parallelism. In this case, the cell field of the automaton is divided into separate blocks. Processing of blocks is done in parallel and independently from each other. At the end of each processing cycle, the task of combining the processing results of each block arises. This problem was solved in [7] in the original way. The experimental study in [7] of the efficiency of parallelization was carried out on clusters with 32 and 768 processors. Despite the high effectiveness of this approach, it has some issues. First, this approach assumes that a researcher has an access to a cluster. Supercomputers are quite expensive and usually are the property of some collective access center [8]. Of course, after waiting a certain time in the queue, access to the cluster is possible. But another difficulty arises: a special skill is needed to write parallel programs in order to organize parallel sections of the program correctly. And this leads to the fact that it takes a certain number of experiments with the program to debug it before use. The latter means multiple times of waiting in a queue for a cluster, which, of course, delays the moment of launching true (not debugging) experiments with cellular automata.

We offer an alternative approach for software implementation of cellular automata, which is based on the use of modern graphics adapters. Modern graphics adapters are also well-organized supercomputers, consisting of several specialized computational cores and allowing execution of operations in parallel. Compared to clusters, graphics adapters are available for a wide range of users and we believe that their capabilities are enough to simulate cellular automata. The fact is that if we exclude extravagant and exotic examples of cellular automata, the process of modeling their behavior does not imply branching or return to the previous state. Exactly these restrictions are imposed on programs for graphics adapters. In addition, there are

special source development kits (frameworks) that can exploit multi-core graphics adapters and help a researcher quickly and efficiently create a software product, without being distracted by thinking about parallelizing data flows and control flows. In particular, such frameworks include Keras [9] and ThensorFlow [10].

In this paper, we demonstrate an approach for software implementation of cellular automata on graphics adapters. To do this, we use the well-known frameworks' combination Keras-over-TensorFlow.

In order to use these tools, we propose to describe the set of states of an automaton cells' by the main data structure used in these frameworks, namely, the *tensor*. Then we describe the process of evolution of the automaton in terms of tensor operations. Since Keras was developed as a tool for building (and learning) neural networks, a special neural network is built to implement the operations on tensors. The network takes as an input the tensor of the current set of states of the CA cells and builds the tensor of the subsequent set of states. A well-known cellular automaton, the Conway's Game of Life, is used as a demonstration.

The work is structured as follows. Section II presents the basic concepts and definitions concerning the theory of cellular automata. Section III provides a description of the game Conway's Game of Life, its features and rules of operation. Section IV is devoted to a detailed presentation of the proposed approach for software implementation of cellular automata on graphics adapters. The results of computer experiments with the implementation of the Conway's Game of Life and comparison with the results of a classical sequential implementation are presented in Section V.

II. Preliminaries

The Moore machine (finite, deterministic, fully defined) is a 6-tuple $A = \langle S, \hat{s}, I, O, \varphi, \psi \rangle$, where S is the finite nonempty set of states of the machine with a distinguished initial state $\hat{s} \in S$, I is the finite set of input stimuli (input signals), O is a finite set of output reactions (output signals), $\varphi: S \times I \to S$ is a fully defined transition function, $\psi: S \to O$ is a fully defined function of output reactions. If at some moment of time the Moore machine $\langle S, \hat{s}, I, O, \varphi, \psi \rangle$ is at the certain state $s \in S$ and the input signal $i \in I$ arrives, then the machine changes its state to the state $s' = \varphi(s, i)$, and the signal $o = \psi(s')$ appears at its output. The machine starts its operation from the initial state $\hat{s}$ with the output signal $\psi(\hat{s})$. It is important to note that originally Moore defined the machine so that the output signal of the machine is determined not by the final state of the transition, but by the initial one (i.e. in the definition above instead of $o = \psi(s')$ should be $o = \psi(s)$). However, for our purposes it is more convenient to use the definition we have specified.

Let $\mathbb{Z}$ be the set of integers. Consider the set of all possible integers pairs $(i, j) \in \mathbb{Z} \times \mathbb{Z}$. With each pair (i, j) we associate some finite set of pairs of integers $N_{i,j} \subseteq \mathbb{Z} \times \mathbb{Z}$, called *the neighborhood of the pair* (i, j). Pairs of $N_{i,j}$ will be called *neighbors* of the pair (i, j). The sets $N_{i,j}$ must be such that the following rule holds: if the pair (p, q) is the neighbor of the pair (i, j), then the pair $(p + k, q + l)$ is the neighbor of the pair $(i + k, j + l)$, where k and l are some integers. Note that the cardinalities of all neighborhoods coincide and the sets will have the same structure. For convenience, we assume that all neighbors from $N_{i,j}$ are enumerated with integers from 1 to $|N_{i,j}|$, where $|N_{i,j}|$ is the cardinality of the set $N_{i,j}$. Then we can talk about the *first*, *second*, etc. *neighbor* of some pair (i, j). If the pair (p, q) is the n-th neighbor of the pair (i, j), then the pair $(p + k, q + l)$ is the n-th neighbor of the pair $(i + k, j + l)$.

Consider the set of Moore machines of the form $A_{i,j} = \langle S, \hat{s}_{i,j}, S^{|N_{i,j}|}, S, \varphi, \psi \rangle$ such that $\psi(s) = s$. Here i and j are some integers, B^n is the n-th Cartesian power of B. The machines corresponding to the neighbors of the pair (i, j) are called *neighbors* of the machine $A_{i,j}$. Neighboring machines will be numbered as well as the corresponding neighboring pairs (that is, the first neighbor, the second, etc.). We specifically note that (i) for each machine $A_{i,j}$ the set of states is the same, i.e. S; (ii) for each machine $A_{i,j}$, the set of output signals coincides with the set of states, that is, also S; (iii) as an output signal, the machine gives its current state; (iv) all machines have the same transition function and the same function of output reaction; (v) as an input signal, machines take tuples of states (of their neighbors), the number of elements in the tuple coincides with the number of neighbors, that is, equals $|N_{i,j}|$; (vi) machines differ only in their initial states. Let at a given time moment the current state of the first neighbor of the machine $A_{i,j}$ is equal to s_1, the state of the second neighbor is s_2, ..., the state of the n-th neighbor is s_n, where $n = |N_{i,j}|$. Then the tuple $(s_1, s_2, ..., s_n)$ is the input signal of the machine $A_{i,j}$ at this very moment. All machines accept input signals, change their states and provide output signals simultaneously and synchronously. That is, some global clock signal is assumed.

The resulting set $\{A_{i,j} | (i, j) \in \mathbb{Z} \times \mathbb{Z}\}$ of the Moore machines is called a *two-dimensional synchronous cellular automaton* (or simply *cellular automaton* – CA). Each individual Moore machine of this set will be called a *cell*. The set of states of all cells the CA at a given time moment will be called *the global state of the cellular automaton at this time moment*.

The transition rules of cells from one state to another (the function φ), the type of neighborhood of the cells (the sets $N_{i,j}$), the number of different possible cell states (the set S) define the whole variety of synchronous two-dimensional cellular automata.

For clarity, one can draw cellular automata on the plane. For this, the plane is covered with figures. Coverage can be arbitrary, but of course, it is more convenient to do it in a regular way. Classic covers are equal squares, equal triangles and equal hexagons. The choice of one or another method of covering the plane is dictated by the original problem a CA is used for and the selected set of neighbors. Next, the cover figures are assigned to the cells of the cellular automaton in a regular manner. For example, let the

plane be covered with equal squares, so that each vertex of each square is also the vertex of the other three squares of the coverage (Fig. 1a). Choose the square of this coverage randomly and associate it with the cell $A_{0,0}$. Let the cell $A_{i,j}$ be associated with a certain square. Then we associate the cell $A_{i+1,j}$ with the square on the right, the cell $A_{i-1,j}$ with the square on the left, the cell $A_{i,j+1}$ with the square above, and the cell $A_{i,j-1}$ with the square below (Fig. 1b). Cell states will be represented by the color of the corresponding square (Fig. 1c)

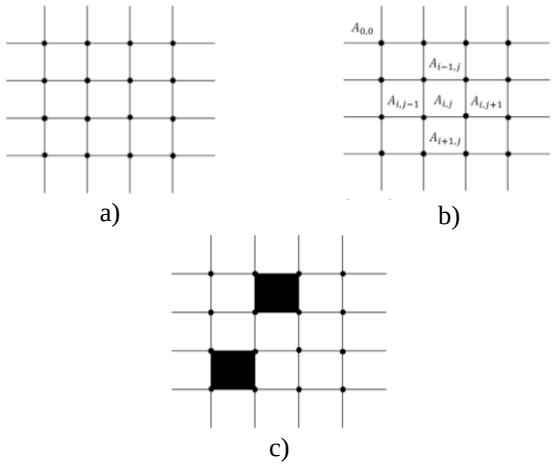

Fig. 1. A CA represented on a plane covered by equal squares: a) the coverage of the plane; b) association of the cells with the squares; c) colour representation of cells' states (for the case $|S| = 2$, «white» – state 0, «black» – state 1)

The resulting square based representation of a CA on a plane is classical one. In our work we consider only this representation.

For the square based representation of a CA, the neighborhoods shown in Fig. 2 are the most common.

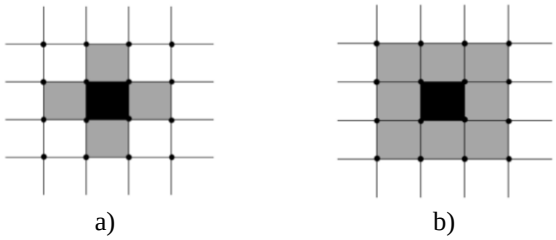

Fig. 2. The neighborhood (grey cells) of a cell (the black one) by a) von Neumann, b) Moore

If a given cellular automaton models a process (for example, heat transfer), then the various global initial states $\{\hat{s}_{i,j} | (i,j) \in \mathbb{Z} \times \mathbb{Z}\}$ of the cellular automaton correspond to different initial conditions of the process. According to the definition of cellular automata introduced by us, the set of cells in it is infinite. However, from the point of view of practice, especially in the case of an implementation of a cellular automaton, a set of cells have to be made finite. In this case, some of the cells lack some neighbors. Therefore, for them the set of neighbors and the transition function are modified. Such modifications determine the boundary conditions of the process being modeled.

III. CONWAY'S GAME OF LIFE

In the 70s of the 20th century, the English mathematician John Conway proposed a cellular automaton called the Conway's Game of Life [l3].

The cells of this automaton are interpreted as biological cells. The state "0" corresponds to the "dead" cell, and the state "1" – "alive". The game uses the Moore's neighborhood (Fig. 2b), i.e. each cell has 8 neighbors. The rules for the transition of cells from one state to another are as follows:

- if a cell is "dead" and has three "alive" neighbors, then it becomes "alive";
- if a cell is "alive" and has two or three "alive" neighbors, then it remains "alive";
- if a cell is "alive" and has less than two or more than three neighbors, then it becomes "dead".

For the convenience of perception, the behavior of each cell of the cellular automaton Conway's Game of Life can be illustrated using the transition graph (Fig. 3).

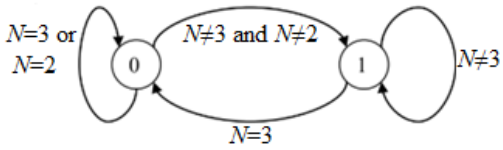

Fig. 3. Cell Transition Graph of the Conway's Game of Life, where N is the number of "alive" neighbors

Despite the simplicity of the functioning of the automaton, it is an object for numerous studies, since the variation of the initial configuration leads to the appearance of various images of its dynamics with interesting properties. One of the most interesting among them are moving groups of cells – gliders. Gliders not only oscillate with a certain periodicity, but also move the space (plane). Thus, as a result of experiments, it was established that on the basis of gliders logical elements AND, OR, NOT can be built. Therefore any other Boolean function can be implemented. It was also proved that using the cellular automata Conway's Game of Life it is possible to emulate the operation of a Turing machine [l3].

IV. FEATURES OF CONWAY'S GAME OF LIFE PARALLEL IMPLEMENTATION

According to our definition, a set of states of a cell is finite. It is obvious that, in this case, without loss of generality, we can assume that the set of states is the set of integers from 0 to $|S|$ - 1, where $|S|$ – is the cardinality of the set of states. Therefore, the global state of the cellular automaton can be represented as a matrix $\boldsymbol{A}$. The element $\boldsymbol{A}_{i,j}$ of this matrix is equal to the current state of the cell $\boldsymbol{A}_{i,j}$. We call the matrix $\boldsymbol{A}$ *the matrix of the global state* of the cellular automaton. If there are no restrictions on the number

of cells, then matrix $\boldsymbol{A}$ will be infinite. As have already been mentioned, the number of cells has to be limited from a practical point of view, that is, it is necessary to somehow choose the finite subset of cells. After that, only selected cells are considered. In this case, the ability to describe the global state of the cellular automaton by the matrix is determined by which cells are selected. We assume that the following set of cells is selected: $\{A_{i,j} | (1 \le i \le m) \wedge (1 \le j \le n)\}$, where m and n – two fixed natural numbers. In this case, the global state matrix is obtained naturally.

Since we use the Keras and TensorFlow frameworks for implementation of a CA, we should work with concepts defined in them. The main data structure in TensorFlow is a multidimensional matrix which in terms of this framework is called a tensor. However, in many cases, such a matrix may not correspond to any tensor. The tensor in the n-dimensional space must have n^{p+q} components and is represented as $(p + q)$-dimensional matrix, where (p, q) is the rank of the tensor. And, for example, a 2 by 3 matrix does not follow these restricions. But the convenience of data manipulation provided by the framework justifies some deviations from strictly defining the tensor. Therefore, in the case when we are talking about the software implementation of a cellular automaton using TensorFlow, we will consider the the notion of the global state matrix of a CA and the notion of *the global state tensor of a CA* as equivalent.

Thus, the evolution of the global state of a cellular automaton can be represented (within TensorFlow) as a transformation of the components of the global state tensor. Such a transformation will be called *the evolution of the tensor*.

Thus, the logic of the transition of the cellular automaton from a given global state to the next global state will be described using operations on tensors. In particular, for the software implementation of Conway's Game of Life in our work such operations are the convolution of tensors and the "restriction" of the components value. Let us consider a small example.

Let some initial global state of the cellular automaton (Fig. 4) be given.

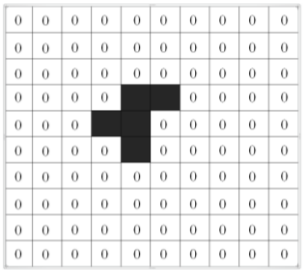

Fig. 4. Some initial global state of the finite state machine for the Conway's Game of Life

Black cells are a "alive" cell (state 1), zero means that the cell is "dead" (state 0). The corresponding tensor of the global state has the form (1):

$$\boldsymbol{T} = \begin{bmatrix} 0 & 0 & 0 & 0 & 0 & 0 & 0 & 0 & 0 & 0 \\ 0 & 0 & 0 & 0 & 0 & 0 & 0 & 0 & 0 & 0 \\ 0 & 0 & 0 & 0 & 0 & 0 & 0 & 0 & 0 & 0 \\ 0 & 0 & 0 & 0 & 1 & 1 & 0 & 0 & 0 & 0 \\ 0 & 0 & 0 & 1 & 1 & 0 & 0 & 0 & 0 & 0 \\ 0 & 0 & 0 & 0 & 1 & 0 & 0 & 0 & 0 & 0 \\ 0 & 0 & 0 & 0 & 0 & 0 & 0 & 0 & 0 & 0 \\ 0 & 0 & 0 & 0 & 0 & 0 & 0 & 0 & 0 & 0 \\ 0 & 0 & 0 & 0 & 0 & 0 & 0 & 0 & 0 & 0 \\ 0 & 0 & 0 & 0 & 0 & 0 & 0 & 0 & 0 & 0 \end{bmatrix} \quad (1)$$

The next state of a cell of the cellular automaton of the Conway's Game of Life depends on the number of living neighbors of this cell. We suggest using convolution to count the number of living neighbors of a cell. Since set of neighbors in the Conway's Game of Life are specified by the Moore neighborhood, the convolution kernel will have the form (2):

$$\boldsymbol{S} = \begin{bmatrix} 1 & 1 & 1 \\ 1 & 0{,}5 & 1 \\ 1 & 1 & 1 \end{bmatrix} \quad (2)$$

Note the special role of the element $\boldsymbol{S}_{22} = 0{,}5$. This element corresponds to the cell for which the number of living neighbors is calculated. Let the number of living neighbors of a certain dead cell be calculated. Then it will turn out to be integer because component $\boldsymbol{S}_{22}$ will be multiplied by the state of the dead cell (and it is equal to 0), and in the sum the number $\boldsymbol{S}_{22}$ will not participate. It will turn out to be half-integer in the case when the number of living neighbors of a living cell is calculated. This is important when the cell has two living neighbors. Then the dead cell must remain dead, and the living cell must live. That is, if after the convolution the counted number of living neighbors turns out to be 2 (the cell is dead, it has 2 living neighbors), then in its place should be 0 in the tensor of the global state of the cellular automaton in the next cycle. If, after convolution, the counted number of living neighbors is 2.5 (the cell is alive, and it has 2 neighbors), then in its place should be 1 in the tensor of the global state of the cellular automaton in the next cycle.

Constructing a convolution with the kernel $\boldsymbol{S}$ of the tensor $\boldsymbol{T}$, we obtain the new tensor $\boldsymbol{C}$, where at the intersection of the i-th row and j-th column there is an element corresponding to the number of living neighbors for the cell $\boldsymbol{A}_{i,j}$. Note that we obtain a tensor $(m-2) \times (n-2)$ when constructing a convolution with a kernel of size 3×3 of an arbitrary tensor of the size $m \times n$. In order to save the initial dimensions of the global state tensor of a cellular automaton, we will set the elements in the first and last row and in the first and last column of the global automaton tensor to 0. We will append these zero rows and columns to the result after the convolution is completed. Appended elements in the formula (3) are highlighted in gray. The mentioned fact suggests that some of the subsequent computations are superfluous (namely computations on the appended elements). The amount of extra computations for

the global state tensor with dimensions $m \times n$ will be $(2m - 2) + (2n - 2)$. Then, the part of extra computations in the amount of useful computations is $\frac{(2m-2)+(2n-2)}{(m-1)(n-1)} = O(\frac{1}{m} + \frac{1}{n})$.

$$C = \begin{bmatrix} 0 & 0 & 0 & 0 & 0 & 0 & 0 & 0 & 0 & 0 \\ 0 & 0 & 0 & 0 & 0 & 0 & 0 & 0 & 0 & 0 \\ 0 & 0 & 0 & 1 & 2 & 2 & 1 & 0 & 0 & 0 \\ 0 & 0 & 1 & 3 & 3,5 & 2,5 & 1 & 0 & 0 & 0 \\ 0 & 0 & 1 & 3,5 & 4,5 & 4 & 1 & 0 & 0 & 0 \\ 0 & 0 & 1 & 3 & 2,5 & 2 & 0 & 0 & 0 & 0 \\ 0 & 0 & 0 & 1 & 1 & 1 & 0 & 0 & 0 & 0 \\ 0 & 0 & 0 & 0 & 0 & 0 & 0 & 0 & 0 & 0 \\ 0 & 0 & 0 & 0 & 0 & 0 & 0 & 0 & 0 & 0 \\ 0 & 0 & 0 & 0 & 0 & 0 & 0 & 0 & 0 & 0 \end{bmatrix} \quad (3)$$

Taking into account the agreement on the half-integer value of the number of living neighbors, the integer part of the value of the tensor component ***C*** determines the number of living neighbors of the cell, and the presence of the fractional part means that the cell was alive in the previous step.

According to the rules of the Conway's Game of Life it is necessary to transform the tensor ***C*** in order to determine the global state of the cellular automaton in the next step. Components with values in the range [2.5, 3.5] should take the value 1 (cells are alive). The remaining components should become 0 (cells are dead). Among the classical operations on tensors there is no operation that would allow to express the required transformation. However, the frameworks used in our work (Keras and TensorFlow) were created primarily for the problems of the theory of artificial intelligence, namely, for implementing of neural networks. The data flow in them is the flow of tensors (a tensor as an input, a tensor as an output). Computational elements, that change data, are layers of the neural network.

So, for example, in our case for the convolution we use a two-dimensional convolution layer with the kernel ***S*** (formula (2)). Any tool for neural network implementation ought to have the special type of layers – activation layers (layer of non-linear transformations). These layers calculate activation functions (some non-linear functions) of each element of the input tensor and put the result into the output tensor. Keras and TensorFlow offer a standard set of non-linear activation functions. In addition, it is possible to create custom activation functions. We built our own activation function based on a function from a standard set of functions, called a *Rectified Linear Unit (ReLU)*. The function *ReLU* is defined as follows (formula (4)). Its graph is shown in Figure 5:

$$ReLU = max(0, x) \quad (4)$$

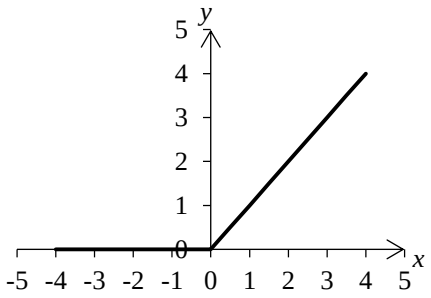

Fig. 5. Diagram of *ReLU* function

Taking into account the required transformation of the components of the tensor ***C*** described above, we suggested the function presented in (5):

$$\delta = ReLU\big(4(x - 2{,}125)\big) - ReLU\big(4(x - 2{,}125)\big) - ReLU\big(4(x - 2{,}125)\big) + ReLU\big(4(x - 2{,}125)\big) \quad (5)$$

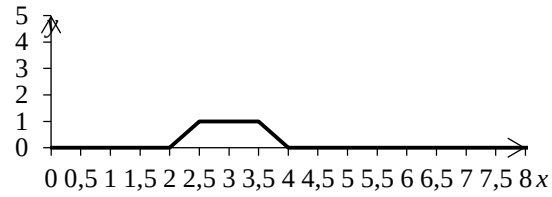

Fig. 6. Diagram of the transition function of the Conway's Game of Life

As a result of applying the function δ to each component of the tensor ***C***, the tensor of the global state of the cellular automaton will take the following form (formula (6)).

$$\boldsymbol{T}' = \begin{bmatrix} 0 & 0 & 0 & 0 & 0 & 0 & 0 & 0 & 0 & 0 \\ 0 & 0 & 0 & 0 & 0 & 0 & 0 & 0 & 0 & 0 \\ 0 & 0 & 0 & 0 & 0 & 0 & 0 & 0 & 0 & 0 \\ 0 & 0 & 0 & 1 & 1 & 1 & 0 & 0 & 0 & 0 \\ 0 & 0 & 0 & 1 & 0 & 0 & 0 & 0 & 0 & 0 \\ 0 & 0 & 0 & 1 & 1 & 0 & 0 & 0 & 0 & 0 \\ 0 & 0 & 0 & 0 & 0 & 0 & 0 & 0 & 0 & 0 \\ 0 & 0 & 0 & 0 & 0 & 0 & 0 & 0 & 0 & 0 \\ 0 & 0 & 0 & 0 & 0 & 0 & 0 & 0 & 0 & 0 \\ 0 & 0 & 0 & 0 & 0 & 0 & 0 & 0 & 0 & 0 \end{bmatrix} \quad (6)$$

Thus, the software implementation of the Conway's Game of Life using the frameworks Keras and TensorFlow is a two-layer neural network. The first layer is convolutional, with the kernel from formula (2). The second layer is the activation layer with the activation function from formula (5).

V. EXPERIMENTAL RESULTS

We have implemented the described approach for the cellular automaton of the Conway's Game of Life in the Python.

Based on the frameworks Keras and TensorFlow, a two-layer neural network was created. The first layer is

convolutional with the kernel of the form (2), the second layer is the activation layer with the activation function of the form (5). Naturally, network training is not required. We set all parameters in advance. In this case, the neural network is a way of presenting the necessary transformations of the global state tensor of the cellular automaton, which is provided by Keras + TensorFlow. The resulting program was launched on a graphics adapter with CUDA support. For comparison with the classical implementation of the cellular automaton of the Conway's Game of Life on a uniprocessor system, we used the implementation of [11].

R-pentamino [12] located in the middle of the field (Fig. 4) was used as the initial global state of the cellular automaton of the Conway's Game of Life in the experiments.

We took a square game field (the matrix of the global state of the cellular automaton) with dimensions $m \times m$, where m varied from 10 to 350 with the step 10. For each m, we calculated 1000 subsequent global states of the cellular automaton. The execution time was measured. The calculations were repeated 10 times. Time was averaged. All experiments were conducted on a computer with the following characteristics: Intel Core i5-3470@3.2 GHz processor, 8 GB RAM, Windows 7-x64 OS, GeForce GTX 650 Ti graphics adapter (1024 MB RAM, 928 MHz base frequency, 768 CUDA cores).

Dependence diagrams of the program execution time on the "length" of the square field side m of the game are shown in Figures 7 and 8. We also built regressions. The regression curves are shown in Figures 7 and 8 as well. A second-degree polynomial was chosen as the regression hypothesis.

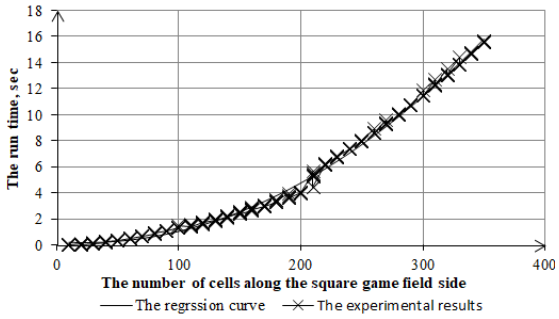

Fig. 7. Results of experiments with a single-threaded implementation

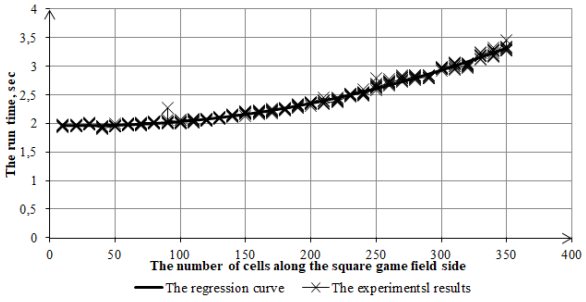

Fig. 8. Results of experiments with CUDA (Keras+TensorFlow) implementation

It can be noted that for small values of m, the execution time of a single-threaded program is smaller than the execution time of the multiprocessor (on the graphics adapter) implementation proposed by us. However, as m grows, the situation changes and the proposed multiprocessor implementation begins to outperform the classical single-threaded implementation. We associate this with the overhead of transferring data from the computer's general RAM to the graphics adapter's RAM and returning the result from the graphics adapter's memory to the computer's memory. When the dimensions of the game field of the Conway's Game of Life are small, the time of actual calculations of the global states of the cellular automaton is much less than the time of transmission of information. As the field size grows, the computation time of the cellular automaton state becomes significant, the data transfer time is leveled, and the multiprocessor implementation on the graphics adapter begins to significantly outrun the single-threaded speed.

Obviously, the dependence of the execution time of programs on the "length" m of the square field side of the Conway's Game of Life must be parabolic. With the growth of m, the number of cells grows as m^2, each cell needs to be processed once per cycle. Therefore, operations of fixed duration must be of the m^2 order. According to the obtained results we constructed regression polynomials of the second degree. Regression curves are in good agreement with experimental data (Fig. 7, 8). It may seem that for a multithreaded implementation the dependency should be different. However, we note that when the number of cells becomes much more than the number of cores in a multi-core system (in our case, the graphics adapter had 768 cores), then processing will be performed block by block: first comes one block of 768 cells, then another, etc. Thus, m^2/K operations will be done, where K is the number of cores, that is, also of the order of m^2.

VI. CONCLUTIONS

In this paper, a tensor approach to the software implementation of cellular automata is described and programmatically implemented. The approach is focused on launching programs on multi-core graphics adapters. Programs are implemented in Python using the frameworks Keras and TensorFlow. These frameworks allow automatically generate and run multi-threaded programs on multi-core graphics adapters. These frameworks were created for the problems of the artificial neural networks theory. The data flow is the flow of tensors, and the converting nodes are the layers of the neural network. Therefore, the proposed approach should be implemented within these frameworks as some kind of neural network. For the Conway's Game of Life we proposed a two-layer neural network with certain parameters.

The effectiveness of using the developed approach was shown during a series of computer experiments. If the number of cells in the automaton is equal to the number of cores, then the maximum acceleration can be observed. If

the number of cells exceeds the number of cores, then the parallel sections of the program are executed sequentially. This means that with a very large size of the playing field the type of dependence will be parabolic when using a graphics adapter. The latter is confirmed by regression analysis.

REFERENCES

[1] D. Harris and S. Harris. *Digital Design and Computer Architecture*. Morgan Kaufmann, 2012. 721 p.

[2] T. Toffolli, N. Margolus. *Cellular Automata Machines*. MIT Press, 1987. 279 p.

[3] J. von Neumann *Theory of Self-Reproducing Automata*. University of Illinois Press, 1966. 403 p.

[4] O. Bandman. *Simulation Spatial Dynamics by Probabilistic Cellular Automata*. Lecture Notes in Computer Science, 2002, vol. 2493, 10–19 pp.

[5] G.G. Malinetski, M.E. Stepantsov Modelirovanie diffusionnykh protsessov s pomoshchyu kletochnykh avtomatov s okrestnostyu Margolusa (*Modeling of Diffusion Processes by Cellular Automata with Margolus Neighborhood*), Zhurnal vychislitelnoy matematiki i matematicheskoy phiziki (Comput. Math. Math. Phys.), 1998, vol. 38, No. 6, 1017–1021 pp. (in Russian).

[6] J.R. Weimar. *Cellular Automata for Reaction-Diffusion Systems*. Parallel Computing, 1999, vol. 23, No. 11, 1699–1715 pp.

[7] Y.G. Medvedev. *Razrabotka i issledovanie trehmernoj kletochno-avtomatnoj modeli potoka vyazkoj zhidkosti* (*Development and Research of a Three-Dimensional Cellular Automaton Model of a Viscous Fluid Flow*). PhD thesis, Novosibirsk, 2005, 108 p (in Russian).

[8] *Vychislitelnyj klaster* «*SKIF Cyberia*» (*Computing Cluster* «*SKIF Cyberia*»). URL: https://cyberia.tsu.ru (12.05.2019).

[9] *Keras: the Python Deep Learning Library*. URL: https://keras.io (12.05.2019).

[10] *TensorFlow*. URL: https://www.tensorflow.org (12.05.2019).

[11] *Sozdanie igry «Zhizn'» na C++* (*Implementation of the Game "Life" using C++*) URL: https://code-live.ru/post/cpp-life-game (12.05.2019).

[12] M. Gardner *The Fantastic Combinations of John Conway's New Solitaire Game "Life"*. Scientific American, 1970, vol. 223, no 4, 120–123 pp.

Modeling of angular stabilization system on processors with scalable architecture

Dmitry Melnichuk
Department of Mathematical Support of Computer and Information Systems
Saratov State University
Saratov, Russia
melnichukdv@sgu.ru

***Abstract*—A numerical simulation of the effect of typical nonlinearities on the output vector functions of a nonlinear stabilization system of a moving control object is performed. The efficiency of parallelization of computations in the implementation of similar tasks is investigated on the example of cluster systems with Intel Xeon Phi coprocessors.**

***Index Terms*—hybrid dynamical systems, processors with scalable architectures**

I. Introduction

Currently, cluster systems are widely used, in the nodes of which one or several processors with a large number of cores are used. Examples include computing systems with new Intel Xeon processors with scalable architecture or computing systems with Intel Xeon Phi coprocessors that are used as virtual cluster nodes. Parallel computational architectures of this class are effective only when solving problems with a significant parallelism resource. In this case, classes of mathematical models that are effectively implemented on Intel Xeon Phi, will be effectively implemented on modern scalable Intel Xeon architectures. For the problems of modeling of hybrid dynamical systems (HDS) [1, 2] a significant resource of parallelism is typical, since in this class of mathematical models the (theoretically infinite-dimensional) phase space of control objects with space-distributed parameters is isolated. For dynamic balancing of computational load on cluster systems, the MPI-MAP parallelization pattern was previously implemented [3]. The purpose of this work is to study the effectiveness of the software implementation on parallel computing systems of the class of modeling problems of the influence of typical nonlinearities and nonstationarity on the output vector function of the HDS. As an example, we consider a similar [4] system of angular stabilization of the movable control object (the rocket taking into account the deformations of its body), but providing stabilization both with respect to the vertical direction and with respect to the longitudinal axis.

II. Parallel algorithms for modeling of hybrid dynamical systems

HDS are systems of ordinary differential equations and partial differential equations connected by means of boundary conditions and constraint's conditions under appropriate initial conditions [1, 2]. HDS with piecewise continuous input vector function $\mathbf{x}(t)$, $\mathbf{x} : \mathbb{R} \to \mathbb{R}^{N_x}$ and continuous output vector function $\mathbf{y}(t)$, $\mathbf{y} : \mathbb{R} \to \mathbb{R}^{N_y}$ correspond to equations similar to [2, 4]

$$\begin{gathered}\dot{\mathbf{y}} = \mathbf{f}(\mathbf{x}, \mathbf{y}, \mathbf{h}, \mathbf{p}, \boldsymbol{\mu}, \boldsymbol{\mu}_t t) \\ \dot{\mathbf{u}} = \mathbb{F}(\mathbf{u}, \mathbf{x}, \mathbf{y}, \dot{\mathbf{y}}, \boldsymbol{\mu}, \boldsymbol{\mu}_t t), \mathbf{r} \in \Omega \\ \mathbb{G}(\mathbf{u}, \mathbf{y}, \boldsymbol{\mu})|_S = 0, S = \partial\Omega;\ \mathbf{h} = \int_S \mathbb{H}(\mathbf{u}, \boldsymbol{\mu}) dS \\ \mathbf{y}(0) = \mathbf{y}_0,\ \mathbf{u}(\mathbf{r}, 0) = \mathbf{u}_0(\mathbf{r})\end{gathered} \tag{1}$$

Here $\mathbf{r} \in \mathbb{R}^{N_r}$ are independent spatial coordinates of individual points of the object with space-distributed parameters, $\Omega \subset \mathbb{R}^{N_r}$ is an area occupied by an object with space-distributed parameters, $\mathbf{h} : \mathbb{R} \to \mathbb{R}^{N_h}$, $\mathbf{f} : \mathbb{R}^{N_x} \times \mathbb{R}^{N_y} \times \mathbb{R}^{N_h} \times \mathbb{R}^{N_p} \times \mathbb{R}^{N_\mu} \times \mathbb{R}^{N_t} \to \mathbb{R}^{N_y}$, $\mathbf{u}(\mathbf{r}, t)$, $\mathbf{u} : \mathbb{R}^{N_r} \times \mathbb{R} \to \mathbb{R}^{N_u}$ are distributed output vector function, operators $\mathbb{F} : (\mathbb{R}^{N_r} \times \mathbb{R} \to \mathbb{R}^{N_u}) \times (\mathbb{R} \to \mathbb{R}^{N_x}) \times (\mathbb{R} \to \mathbb{R}^{N_y}) \times (\mathbb{R} \to \mathbb{R}^{N_y}) \times \mathbb{R}^{N_\mu} \times \mathbb{R}^{N_t} \to (\mathbb{R}^{N_r} \times \mathbb{R} \to \mathbb{R}^{N_u})$, $\mathbb{G} : (\mathbb{R}^{N_r} \times \mathbb{R} \to \mathbb{R}^{N_u}) \times (\mathbb{R} \to \mathbb{R}^{N_y}) \times \mathbb{R}^{N_\mu} \to (\mathbb{R}^{N_r} \times \mathbb{R} \to \mathbb{R}^{N_g})$, $\mathbb{H} : (\mathbb{R}^{N_r} \times \mathbb{R} \to \mathbb{R}^{N_u}) \times \mathbb{R}^{N_\mu} \to (\mathbb{R} \to \mathbb{R}^{N_h})$ correspond to partial differential equations, boundary conditions, and coupling conditions; $\mathbf{p} \in \mathbb{R}^{N_p}$ are feedback parameters; $\boldsymbol{\mu} \in \mathbb{R}^{N_\mu}$ are parameters of model nonlinearities; $\boldsymbol{\mu}_t \in \mathbb{R}^{N_t}$ are parameters characterizing the unsteadiness of the system from the point of view of the automatic control theory; the point at the top indicates the time t differentiation. When $\boldsymbol{\mu} = \boldsymbol{\mu}_t = 0$ HDS (1) becomes linear stationary. The main theorems on the stability of linearized HDS are formulated and proved in [1, 2]. In work [4] on the basis of an asymptotic method of many scales the fact of stabilization of nonlinear HDS on the basis of parametric synthesis on the linearized model is proved, and adaptive algorithms of parametric synthesis are offered. After parametric synthesis, numerical simulation of the effect of typical nonlinearities and unsteadiness on the output vector function of a nonlinear HDS is performed (1). In this case, the input vector function $\mathbf{x}(t)$ and the initial conditions $\mathbf{y}_0$, $\mathbf{u}_0(\mathbf{r})$ are fixed, and the components of the vectors $\boldsymbol{\mu}$ and $\boldsymbol{\mu}_t$ change with a fixed step within a parallelepiped. The element-by-element transformation of sequence $(\boldsymbol{\mu}_j, \boldsymbol{\mu}_{t_j})$, $j = 1, 2, 3, ...$ into a sequence of values characterizing the maximum and standard deviations of function $\mathbf{y}(t; \boldsymbol{\mu}_j, \boldsymbol{\mu}_{t_j})$ from $\mathbf{y}(t; 0, 0)$ is parallelized

$$
\begin{aligned}
&(\boldsymbol{\mu}_j, \boldsymbol{\mu}_{t_j}) \to (v_{1_j}, v_{2_j})^T,\ j = 1, 2, 3, ... \\
&v_1 = \max_{0 \le t \le t_{\max}} |\mathbf{y}(t; \boldsymbol{\mu}, \boldsymbol{\mu}_t) - \mathbf{y}(t; 0, 0)|,\ t_{\max} \gg 1 \\
&v_2 = \left[t_{\max}^{-1} \int_0^{t_{\max}} |\mathbf{y}(t; \boldsymbol{\mu}, \boldsymbol{\mu}_t) - \mathbf{y}(t; 0, 0)|^2 dt \right]^{1/2}
\end{aligned} \tag{2}
$$

The transformation (2) can be adapted to the "two-layer" MPI-OpenMP scheme, where a separate MPI-MAP executing process performs the transformation of

$$
\{(\boldsymbol{\mu}_j, \boldsymbol{\mu}_{t_j}),\ j = \overline{1, m}\} \to \{(v_{1_j}, v_{2_j})^T,\ j = \overline{1, m}\} \tag{3}
$$

by parallelizing calculation of the values on the right side (3) based on OpenMP.

Numerical integration of the initial boundary value problem (1) is realized on the basis of the Galerkins projection method [4] with the subsequent application of the BDF method to the resulting Cauchy problem for the system of ordinary differential equations.

III. Model of stabilization system

The equations of the angular stabilization system are similar [4], but take into account the stabilization of the object (see Fig. 1) both in the vertical direction and relative to the

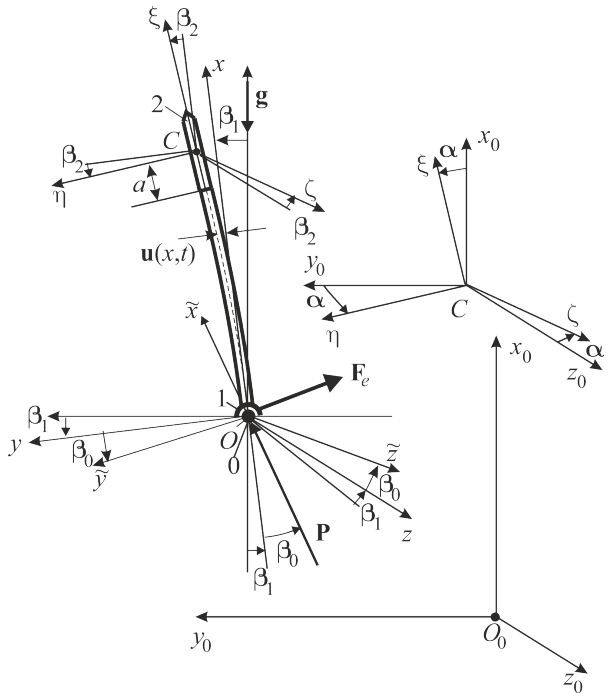

Fig. 1. Structural scheme.

longitudinal axis, as well as a smooth change in the time of the thrust force of the rocket engine. The rotation of the coordinate system is characterized by angles $\boldsymbol{\alpha} = (\alpha_1, \alpha_2, \alpha_3)^T$ (in order $\alpha_3, \alpha_2, \alpha_1$), and

$$
A(\alpha) = \begin{bmatrix} \cos\alpha_3 & -\sin\alpha_3 & 0 \\ \sin\alpha_3 & \cos\alpha_3 & 0 \\ 0 & 0 & 1 \end{bmatrix} \cdot
$$

$$
\cdot \begin{bmatrix} \cos\alpha_2 & 0 & \sin\alpha_2 \\ 0 & 1 & 0 \\ -\sin\alpha_2 & 0 & \cos\alpha_2 \end{bmatrix} \begin{bmatrix} 1 & 0 & 0 \\ 0 & \cos\alpha_1 & -\sin\alpha_1 \\ 0 & \sin\alpha_1 & \cos\alpha_1 \end{bmatrix}
$$

$$
B(\alpha) = \begin{bmatrix} 1 & 0 & -\sin\alpha_2 \\ 0 & \cos\alpha_1 & \cos\alpha_2 \sin\alpha_1 \\ 0 & -\sin\alpha_1 & \cos\alpha_2 \cos\alpha_1 \end{bmatrix}
$$

The object moves with respect to a fixed coordinate system $O_0 x_0 y_0 z_0$ under the action of force $\mathbf{P}$, attraction to the Earth and external disturbing horizontal force $\mathbf{F}_e = (0, F_{e_{y0}}, F_{e_{z0}})^T$. The coordinate system $Oxyz$ is connected to the body 1 (see Fig. 1), and $\mathbf{r}_1 = (x_1, y_1, z_1)^T$ and $\boldsymbol{\beta}_1 = (\beta_{1,1}, \beta_{1,2}, \beta_{1,3})^T$ characterize its linear and angular displacements relative to $O_0 x_0 y_0 z_0$. Linear $\mathbf{r}_2 = (x_2, y_2, z_2)^T$ and angular $\boldsymbol{\beta}_2 = (\beta_{2,1}, \beta_{2,2}, \beta_{2,3})^T$ displacement of body 2 with respect to $Oxyz$ is caused by the elastic displacement $\mathbf{u} = (u_x, u_y, u_z)^T = \mathbf{u}(x, t)$ of the centerline of the hull. The rotation angle $\boldsymbol{\alpha} = (\alpha_1, \alpha_2, \alpha_3)^T$ of the body 2 relative to $O_0 x_0 y_0 z_0$ measures the gyrostabilizer, and the control moments of the forces $M_j^{(c)}$, $j = 1, 2, 3$ are formed. Under the action of $M_2^{(c)}$ and $M_3^{(c)}$ body 0 rotates at angles $\boldsymbol{\beta}_0 = (0, \beta_{0,2}, \beta_{0,3})^T$ relative to $Oxyz$. The moment $M_1^{(c)}$ acts on the body 1 and compensates for the rotation of the movable object relative to the x axis. Let $\omega_0 = (\omega_{0_x}, \omega_{0_y}, \omega_{0_z})^T$, $\Omega_1 = (\Omega_{1_x}, \Omega_{1_y}, \Omega_{1_z})^T$, $\Omega_2 = (\Omega_{2_\xi}, \Omega_{2_\eta}, \Omega_{2_\zeta})^T$ be the relative and absolute angular velocities of bodies 0, 1, 2; $\mathbf{Q} = (Q_1, Q_2, Q_3)^T$, $\mathbf{M}$=$(M_1, M_2, M_3)^T$ be the internal forces and moments acting in the cross sections of the body. In dimensionless variables and parameters the equations of motion of the HDS have the form

$$
\begin{aligned}
&\boldsymbol{\Omega}_1 = B(\mu_1 \boldsymbol{\beta}_1) \dot{\boldsymbol{\beta}}_1 \\
&\boldsymbol{\Omega}_2 = A^T(\mu_1 \boldsymbol{\beta}_2) \boldsymbol{\Omega}_1 + B(\mu_1 \boldsymbol{\beta}_2) \dot{\boldsymbol{\beta}}_2 \\
&\omega_{0_x} = -\dot{\beta}_{0,2} \sin(\mu_1 \beta_{0,3}),\ \omega_{0_y} = \dot{\beta}_{0,2} \cos(\mu_1 \beta_{0,3}) \\
&\omega_{0_z} = \dot{\beta}_{0,3},\ m_1 \ddot{\mathbf{r}}_1 = A(\mu_1 \boldsymbol{\beta}_1) \mathbf{Q}(0, t) - \mathbf{F}_e + \\
&+ a_x [(1 + m_2) A(\mu_1 \boldsymbol{\beta}_1) \boldsymbol{\Phi}(0, \boldsymbol{\beta}_0) + m_1 \boldsymbol{\Phi}(\boldsymbol{\beta}_1, \boldsymbol{\beta}_0)] \\
&J_0(\dot{\boldsymbol{\Omega}}_1 + \dot{\boldsymbol{\omega}}_0) + J^{(1)} \dot{\boldsymbol{\Omega}}_1 + \\
&+ \mu_1 \boldsymbol{\Omega}_1 \times (J_0 \boldsymbol{\omega}_0 + J^{(1)} \boldsymbol{\Omega}_1) = \\
&= \mathbf{M}(0, t) - (M_c^{(1)}, 0, 0)^T,\ J^{(1)} = \mathrm{diag}\{J_{1k}, J_1, J_1\} \\
&J_0[\dot{\Omega}_{1_y} + \dot{\omega}_{0_y} + \mu_1(\Omega_{1_z} \omega_{0_x} - \Omega_{1_x} \omega_{0_z})] = \\
&= M_2^{(c)} \cos(\mu_1 \beta_{0,3}) + M_3^{(c)} \sin(\mu_1 \beta_{0,3}) \sin(\mu_1 \beta_{0,2}) \\
&J_0[\dot{\Omega}_{1_z} + \dot{\omega}_{0_z} + \mu_1(\Omega_{1_x} \omega_{0_y} - \Omega_{1_y} \omega_{0_x})] = \\
&= M_3^{(c)} \cos(\mu_1 \beta_{0,2}) \\
&\mathbf{w}_2 = A^T(\mu_1 \boldsymbol{\beta}_1) \ddot{\mathbf{r}}_1 + \dot{\boldsymbol{\Omega}}_1 \times \mathbf{R}_2 + \mu_1 (\boldsymbol{\Omega}_1 \cdot \mathbf{R}_2) \boldsymbol{\Omega}_1 - \\
&- \mu_1 \boldsymbol{\Omega}_1^2 \mathbf{R}_2 - 2\mu_1 \boldsymbol{\Omega}_1 \times \dot{\mathbf{r}}_2 + \ddot{\mathbf{r}}_2 \\
&J^{(2)} \dot{\boldsymbol{\Omega}}_2 + \mu_1 \boldsymbol{\Omega}_2 \times J^{(2)} \boldsymbol{\Omega}_2 = \\
&= -A^T((\mu_1 \beta_{2,1}, 0, 0)^T) \mathbf{M}(1, t) + \\
&+ (a, 0, 0)^T \times A^T((\mu_1 \beta_{2,1}, 0, 0)^T) \mathbf{Q}(1, t) \\
&m_2 \mathbf{w}_2 = a_x m_2 [\boldsymbol{\Phi}(0, \mu_1 (0, \beta_{2,2}, \beta_{2,3})^T) - \\
&- \boldsymbol{\Phi}^*(0, \mu_1 \boldsymbol{\beta}_1)] - A(\mu_1 (0, \beta_{2,2}, \beta_{2,3})^T) \mathbf{Q}(1, t) \\
&\boldsymbol{\Phi}(\boldsymbol{\alpha}, \boldsymbol{\beta}) = \mu_1^{-1} (A(\mu_1 \boldsymbol{\alpha}) A(\mu_1 \boldsymbol{\beta}) - E)(1, 0, 0)^T = \\
&= (\Phi_1(\boldsymbol{\alpha}, \boldsymbol{\beta}), \Phi_2(\boldsymbol{\alpha}, \boldsymbol{\beta}), \Phi_3(\boldsymbol{\alpha}, \boldsymbol{\beta}))^T \\
&E = \mathrm{diag}\{1, 1, 1\},\ J^{(2)} = \mathrm{diag}\{J_{2k}, J_2, J_2\}
\end{aligned} \tag{4}
$$

$$
\begin{aligned}
&\mathbf{R}_2 = (1+a,0,0)^T + \mu_1 \mathbf{r}_2,\ \boldsymbol{\Phi}^*(\boldsymbol{\alpha},\boldsymbol{\beta}) = \\
&= \mu_1^{-1}(A^T(\mu_1\boldsymbol{\alpha})A^T(\mu_1\boldsymbol{\beta}) - E)(1,0,0)^T = \\
&= (\Phi_1^*(\boldsymbol{\alpha},\boldsymbol{\beta}), \Phi_2^*(\boldsymbol{\alpha},\boldsymbol{\beta}), \Phi_3^*(\boldsymbol{\alpha},\boldsymbol{\beta}))^T \\
&\boldsymbol{\Phi}^{**}(\boldsymbol{\alpha},\boldsymbol{\beta}) = \mu_1^{-1}(A(\mu_1\boldsymbol{\alpha})A(\mu_1\boldsymbol{\beta}) - E)(0,1,0)^T = \\
&= (\Phi_1^{**}(\boldsymbol{\alpha},\boldsymbol{\beta}), \Phi_2^{**}(\boldsymbol{\alpha},\boldsymbol{\beta}), \Phi_3^{**}(\boldsymbol{\alpha},\boldsymbol{\beta}))^T \\
&\alpha_2 = -\mu_1^{-1}\arcsin(\mu_1\Phi_3(\boldsymbol{\beta}_2,\boldsymbol{\beta}_1)) \\
&\alpha_3 = \tfrac{1}{\mu_1}\arcsin\tfrac{\mu_1\Phi_2(\boldsymbol{\beta}_2,\boldsymbol{\beta}_1)}{\cos(\mu_1\alpha_2)} \\
&\alpha_1 = -\tfrac{1}{\mu_1}\arcsin\tfrac{\mu_1\Phi_3^{**}(\boldsymbol{\beta}_2,\boldsymbol{\beta}_1)}{\cos(\mu_1\alpha_2)} \\
&M_1^{(c)} = \mathbb{S}_1[\alpha_1],\ f_1(z) = \operatorname{tg} z \\
&M_3^{(c)} = \mathbb{S}_3[\alpha_3] - p_1\dot{\beta}_{0,3} - p_2\mu_2^{-1}f_1(\mu_2\beta_{0,3}) \\
&M_2^{(c)} = \mathbb{S}_2[\alpha_2] - p_6\dot{\beta}_{0,2} - p_7\mu_2^{-1}f_1(\mu_2\beta_{0,2}) \\
&\mathbb{S}_1[\alpha] = \mu_3^{-1}f_2(\mu_3\mathbb{S}_1^{(L)}[\alpha]) \\
&\mathbb{S}_1^{(L)}[\alpha] = p_{11}d\alpha/dt + p_{12}\alpha,\ f_2(z) = \operatorname{th} z \\
&\mathbb{S}_3[\alpha] = \mu_3^{-1}f_2(\mu_3\mathbb{S}_3^{(L)}[\alpha]) \\
&\mathbb{S}_3^{(L)}[\alpha] = p_3 d\alpha/dt + p_4\alpha + p_5\textstyle\int_0^t \alpha(\xi)d\xi \\
&\mathbb{S}_2[\alpha] = \mu_3^{-1}f_2(\mu_3\mathbb{S}_2^{(L)}[\alpha]) \\
&\mathbb{S}_2^{(L)}[\alpha] = p_8 d\alpha/dt + p_9\alpha + p_{10}\textstyle\int_0^t \alpha(\xi)d\xi
\end{aligned}
$$

$$
\begin{aligned}
&u'_x = [(1-\mu_1^2({u'_y}^2 + {u'_z}^2))^{1/2} - 1]/\mu_1 \\
&L_{21} = \mu_1 u'_y, L_{31} = \mu_1 u'_z \\
&L_{11} = (1 - L_{21}^2 - L_{31}^2)^{1/2} \\
&L_{33} = (1 - L_{31}^2)^{1/2}, L_{12} = -L_{21}/L_{33} \\
&L_{22} = L_{11}/L_{33} \\
&L_{32} = 0, L_{13} = -L_{31}L_{22}, L_{23} = L_{31}L_{12} \\
&\kappa_1 = u'_z(L_{12}L'_{22} - L_{22}L'_{12}) \\
&\kappa_2 = u'_z L_{22}L'_{11} - u''_y L_{23} - u''_z L_{33} \\
&\kappa_3 = -u'_y L'_{11}/L_{33} + u''_y L_{22} \\
&\ddot{u}_y + (A^T(\mu_1\boldsymbol{\beta}_1)\ddot{\mathbf{r}}_1)\cdot(0,1,0)^T - (\mu_1\dot{\Omega}_{1_x}u_z - \\
&-\dot{\Omega}_{1_z}(x+\mu_1 u_x)) + \mu_1[(x+\mu_1 u_x)\Omega_{1_x} + \\
&+\mu_1 u_z\Omega_{1_z}]\Omega_{1_y} - \mu_1^2(\Omega_{1_x}^2 + \Omega_{1_z}^2)u_y + \\
&+2\mu_1(\Omega_{1_x}\dot{u}_z - \Omega_{1_z}\dot{u}_x) = \\
&= L_{21}(Q'_1 + \mu_1(\kappa_2 Q_3 - \kappa_3 Q_2)) + \\
&+L_{22}(Q'_2 - \mu_1(\kappa_1 Q_3 - \kappa_3 Q_1)) + \\
&+L_{23}(Q'_3 + \mu_1(\kappa_1 Q_2 - \kappa_2 Q_1)) - \\
&-a_x[\Phi_2^*(0,\boldsymbol{\beta}_1) + ((m_2+1-x)u'_y)'] \\
&\ddot{u}_z + (A^T(\mu_1\boldsymbol{\beta}_1)\ddot{\mathbf{r}}_1)\cdot(0,0,1)^T + \mu_1\dot{\Omega}_{1_x}u_y - \\
&-\dot{\Omega}_{1_y}(x+\mu_1 u_x) + \mu_1[(x+\mu_1 u_x)\Omega_{1_x} + \\
&+\mu_1 u_y\Omega_{1_y}]\Omega_{1_z} - \mu_1^2(\Omega_{1_x}^2 + \Omega_{1_z}^2)u_z - \\
&-2\mu_1(\Omega_{1_x}\dot{u}_y - \Omega_{1_y}\dot{u}_x) = \\
&= L_{31}(Q'_1 + \mu_1(\kappa_2 Q_3 - \kappa_3 Q_2)) + \\
&+L_{33}(Q'_3 + \mu_1(\kappa_1 Q_2 - \kappa_2 Q_1)) - \\
&-a_x[\Phi_3^*(0,\boldsymbol{\beta}_1) + ((m_2+1-x)u'_z)'] \\
&Q''_1 - \mu_1^2(\kappa_2^2 + \kappa_3^2)Q_1 = \\
&= \mu_1\{-a_x(m_2+1-x)(\kappa_2^2+\kappa_3^2) + \\
&+\kappa'_3 Q_2 - \kappa'_2 Q_3 + 2\kappa_3 Q'_2 - 2\kappa_2 Q'_3 - \\
&-\mu_1\kappa_1(\kappa_2 Q_2 + \kappa_3 Q_3) - ((\dot{u}'_x)^2 + (\dot{u}'_y)^2 + (\dot{u}'_z)^2) + \\
&+(\Omega_{1_x}L_{11} + \Omega_{1_y}L_{21} + \Omega_{1_z}L_{31})^2 - \\
&-(\Omega_{1_x}^2 + \Omega_{1_y}^2 + \Omega_{1_z}^2) + \\
&+2[L_{11}(\Omega_{1_y}\dot{u}'_z - \Omega_{1_z}\dot{u}'_y) - L_{21}(\Omega_{1_x}\dot{u}'_z - \Omega_{1_z}\dot{u}'_x) + \\
&+L_{31}(\Omega_{1_x}\dot{u}'_y - \Omega_{1_y}\dot{u}'_x)]\}
\end{aligned}
\tag{5}
$$

$$
\begin{aligned}
&u_y(0,t) = 0,\ u'_y(0,t) = 0 \\
&u_y(1,t) = y_2 - a\Phi_2(0,\boldsymbol{\beta}_2) \\
&u'_y(1,t) = \cos(\mu_1\beta_{2,2})\mu_1^{-1}\sin(\mu_1\beta_{2,3}) \\
&u_z(0,t) = 0,\ u'_z(0,t) = 0 \\
&u_z(1,t) = z_2 - a\Phi_3(0,\boldsymbol{\beta}_2) \\
&u'_z(1,t) = -\mu_1^{-1}\sin(\mu_1\beta_{2,2}) \\
&x_2 = u_x(1,t) + a\Phi_1(0,\boldsymbol{\beta}_2) \\
&Q'_1(0,t) + \mu_1(\kappa_2(0,t)Q_3(0,t) - \kappa_3(0,t)Q_2(0,t)) = \\
&= \ddot{\mathbf{r}}_1 \cdot A(\mu_1\boldsymbol{\beta}_1)(1,0,0)^T + a_x\Phi_1^*(0,\boldsymbol{\beta}_1) \\
&Q'_1(1,t) + \mu_1(\kappa_2(1,t)Q_3(1,t) - \kappa_3(1,t)Q_2(1,t)) = \\
&= a_x\Phi_1^*(\boldsymbol{\beta}_2,\boldsymbol{\beta}_1) + \mu_1 a(\Omega_{2_\eta}^2 + \Omega_{2_\varsigma}^2) + \\
&+(1,0,0)^T \cdot A^T(\mu_1\boldsymbol{\beta}_2)\mathbf{w}_2
\end{aligned}
\tag{6}
$$

$$
\begin{aligned}
&M_1 = I_k\left(\beta_{2,1} + \gamma\dot{\beta}_{2,1} - \textstyle\int_0^1 \kappa_1 dx\right) \\
&M_2 = \kappa_2 - \gamma\dot{u}''_z,\ M_3 = \kappa_3 + \gamma\dot{u}''_y \\
&Q_2 = -M'_3 + \mu_1(\kappa_2 M_1 - \kappa_1 M_2) \\
&Q_3 = M'_2 + \mu_1(\kappa_3 M_1 - \kappa_1 M_3)
\end{aligned}
\tag{7}
$$

$$
\begin{aligned}
&\boldsymbol{\beta}_1(0) = \dot{\boldsymbol{\beta}}_1(0) = \boldsymbol{\beta}_2(0) = \dot{\boldsymbol{\beta}}_2(0) = \beta_{0,2}(0) = \\
&= \dot{\beta}_{0,2}(0) = \beta_{0,3}(0) = \dot{\beta}_{0,3}(0) = \mathbf{r}_1(0) = \\
&= \dot{\mathbf{r}}_1(0) = y_2(0) = \dot{y}_2(0) = z_2(0) = \dot{z}_2(0) = \\
&= u_y(x,0) = \dot{u}_y(x,0) = u_z(x,0) = \dot{u}_z(x,0) = 0
\end{aligned}
\tag{8}
$$

Here $\mathbf{x}(t) = (F_{e_{y0}}(t), F_{e_{z0}}(t))^T$ and $\mathbf{y}(t) = (\beta_{1,3}(t), \beta_{2,3}(t), \beta_{1,2}(t), \beta_{2,2}(t), \beta_{1,1}(t), \beta_{2,1}(t))^T$ are input and output vector functions, $\mathbf{p} = (p_1, p_2, ..., p_{12})^T$ are feedback parameters, (4) are ordinary differential equations, (5) are partial differential equations, (6) are boundary conditions, (7) are constraints conditions, (8) are initial conditions. The set of parameters $\boldsymbol{\mu} = (\mu_1, \mu_2, \mu_3)^T$ characterizes typical nonlinearities, and the parameter $\boldsymbol{\mu}_t = \{\mu_4\}$, $\mu_4 \geq 0$ characterizes a smooth change in the characteristic overload according to the law

$$
\begin{aligned}
&a_x(t) = a_x^{(\min)} + (a_x^{(\max)} - a_x^{(\min)})e^{-\mu_4 t}, \\
&t \geq 0, a_x^{(\min)} < a_x \leq a_x^{(\max)}
\end{aligned}
\tag{9}
$$

At $\boldsymbol{\mu} = 0$, the model equations are linearized and decomposed into three independent subsets corresponding to the motion in the $O_0x_0y_0$ and $O_0x_0z_0$ planes (by virtue of symmetry, they pass into each other), as well as to the rotation relative to the longitudinal axis. In this case, $p_{5+j} = p_j$, $j = \overline{1,5}$, correspond to the stabilization system in the vertical direction, and p_{11}, p_{12} correspond to the stabilization system with respect to the longitudinal axis.

IV. Numerical simulation results

In the numerical simulation of the output vector functions of the nonlinear angular stabilization system, the components of the input vector function were given as $F_{e_{y0}}(t) = 1(t)$, $F_{e_{z0}}(t) = 1(t) - 1(t-1)$, where $1(t)$ is the unit jump function of Heaviside. For stabilization system with a set of parameters

$$
\begin{aligned}
&J_0 = 0.02, m_1 = 0.3, J_1 = 0.07, m_2 = 0.2, J_2 = 0.05,\\
&a = 0.166667, a_x^{(\min)} = 0.2, a_x^{(\max)} = 2, \gamma = 0.01,\\
&J_{1k} = 0.1, J_{2k} = 0.05, J_k = 2, \mu_1 = 0.08, \mu_2 = 0.15,\\
&\mu_3 = 0.055, \mu_4 = 0.05
\end{aligned} \tag{10}
$$

the feedback parameters of the stabilization system in the direction of vertical $p_1 = p_6 = 6.347$, $p_2 = p_7 = 13.12$, $p_3 = p_8 = 17.59$, $p_4 = p_9 = 14.03$, $p_5 = p_{10} = 5.951$ were chosen on the basis of an adaptive algorithm of parametric synthesis of the family of linearized models of HDS [4]. Since the stabilization of the object with respect to the longitudinal axis is intended to compensate for the slow accumulation of errors due to nonlinear effects, the feedback parameters $p_{11} = 0.04$, $p_{12} = 1$ are selected in the central part of the stability region.

Figure 2 presents the results of numerical simulation of the components $\beta_{1,2}$ and $\beta_{1,3}$ of the output vector functions of the original nonlinear unsteady HDS (shown as a solid line) and its linear stationary analog at $\mu_1 = \mu_2 = \mu_3 = \mu_4 = 0$ (shown as a dashed line). The significant difference of the results is explained by the fact that the dimensionless overload a_x decreases smoothly, with the decrease of a_x in the considered range of overload changes in the linear stationary system, the attenuation of transients decreases, and the characteristic value of the output vector function increases. Nevertheless, parametric synthesis based on the linearized model allows to stabilize the original nonlinear system in the vertical direction in the entire range of overloads. As follows from the results presented in Fig. 3, the selected values of the feedback parameters p_{11} and p_{12} allow to stabilize the movable control object with respect to the longitudinal axis, i.e. to allow compensate for the slow accumulation of errors due to nonlinear effects. Fig. 4 shows the dependences of the parameters $\mu_3 \in [0, 0.055]$ and $\mu_4 \in [0, 0.05]$ at fixed μ_1 and μ_2 maximum v_1 and standard v_2 deviations (see (2)) of the output vector function of the nonlinear HDS on the output vector function of the linearized HDS for $t_{\max} = 250$. As follows from the data presented in Fig. 4, when changing the overload according to (9) the greatest influence on the output vector function of the nonlinear HDS has parameter μ_4, characterizing the unsteadiness of the system.

Similar data characterizing the efficiency of stabilization with respect to the vertical, longitudinal axis, as well as the influence of the parameters of nonlinearity and unsteadiness on the output functions of the stabilization system with parameters

$$
\begin{aligned}
&J_0 = 0.00003, m_1 = 0.0667, J_1 = 0.00009728, m_2 = 0.333,\\
&J_2 = 0.00345, a = 0.166667, a_x = 1, \gamma = 0.01,\\
&p_1 = p_6 = 4.098, p_2 = p_7 = 9.553, p_3 = p_8 = 7.687,\\
&p_4 = p_9 = 7.714, p_5 = p_{10} = 3.269, J_{1k} = 0.002,\\
&J_{2k} = 0.005, J_2 = 2, \mu_1 = 0.08, \mu_2 = 0.2,\\
&\mu_3 = 0.04, \mu_4 = 0.05, p_{11} = 0.05, p_{12} = 1
\end{aligned} \tag{11}
$$

are shown in Fig. 5-7.

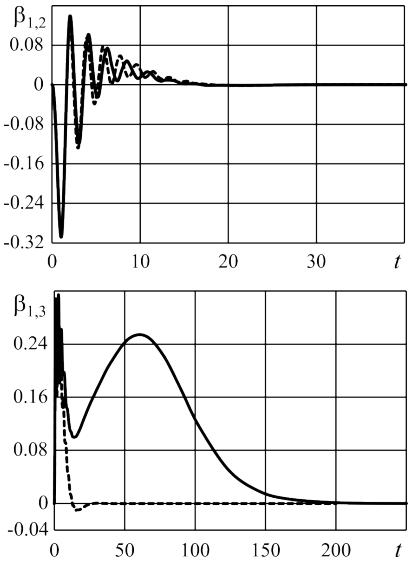

Fig. 2. Stabilization in the vertical direction.

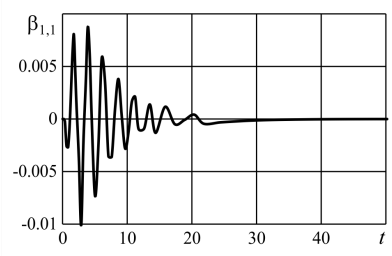

Fig. 3. Stabilization with respect to the longitudinal axis.

Similarly to the previously discussed non-linear stabilization system allows to compensate for errors in the entire range of overload (Fig. 5, 6). The greatest influence on the output vector function of the nonlinear HDS has the parameter μ_4, which characterizes the unsteadiness of the system.

V. Efficiency analysis of parallel algorithms

Consider the effectiveness of the implementation on computer systems with coprocessors Intel Xeon Phi parallel algorithm (2), (3) modeling the effect of typical nonlinearities and unsteadiness on the output functions of the HDS. The data corresponding to the modeling of a nonlinear stabilization system with parameters (10) are presented in Table I. The calculations were performed on a cluster of faculty of Computer Science and Informational Technologies and Volga Region Center of New Information Technologies of SSU. The four-dimensional grid of change of parameters $\mu_1, \mu_2, \mu_3, \mu_4$ dimension $6 \times 9 \times 9 \times 9$ was used. As follows from the results shownin the Table I , in this case the use of a single Intel Xeon Phi coprocessor is more efficient than the use of two quad-core CPUs. The most profitable strategy of using coprocessors is parallelization based on OpenMP inside the coprocessor and parallelization based on MPI-MAP between coprocessors.

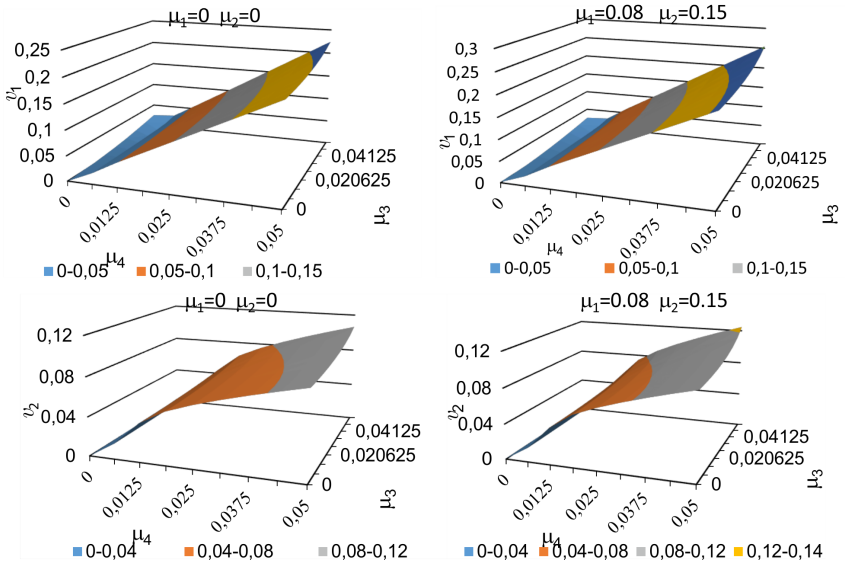

Fig. 4. Maximum and standard deviations.

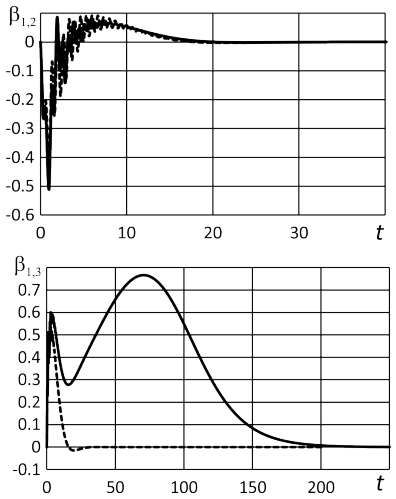

Fig. 5. Stabilization in the vertical direction.

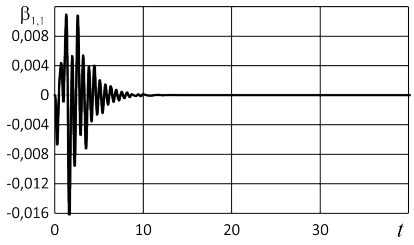

Fig. 6. Stabilization with respect to the longitudinal axis.

Similar data for the stabilization system with parameters for the stabilization system with a set of parameters (11) are presented in Table II. And in this case, using one Intel Xeon Phi processor is more efficient than using two quad-core CPUs. The most profitable strategy for the use of coprocessors is the parallelization based on OpenMP within the coprocessor and parallelization based on MPI-MAP between the coprocessors.

TABLE I
TIME OF MODELING THE IMPACT OF NONLINEARITIES, SEC.

Grid $6 \times 9 \times 9 \times 9$					
Processor, serial/parallel	Test 1	Test 2	Test 3	Test 4	Test 5
Intel Xeon E5-2603 v2, serial	16411	16325	16470	16531	16314
2 processors Intel Xeon E5-2603 v2, OpenMP	2480	2471	2501	2492	2485
Coprocessor Intel Xeon Phi 5110P, OpenMP	1667	1635	1673	1649	1655
2 coprocessors Intel Xeon Phi 5110P, MPI-MAP/OpenMP	1023	1015	1032	1008	1040

TABLE II
TIME OF MODELING THE IMPACT OF NONLINEARITIES, SEC.

Grid $6 \times 9 \times 9 \times 9$					
Processor, serial/parallel	Test 1	Test 2	Test 3	Test 4	Test 5
Intel Xeon E5-2603 v2, serial	9637	9597	9645	9657	9675
2 processors Intel Xeon E5-2603 v2, OpenMP	1443	1470	1430	1412	1467
Coprocessor Intel Xeon Phi 5110P, OpenMP	1052	1042	1063	1037	1055
2 coprocessors Intel Xeon Phi 5110P, MPI-MAP/OpenMP	703	699	710	707	705

Analogique evidence of the effectiveness of the implementation of the parallel algorithm (2), (3) using a single Intel Xeon Phi coprocessor (OpenMP) and two Intel Xeon Phi coprocessors (MPI-MAP OpenMP) for a more detailed

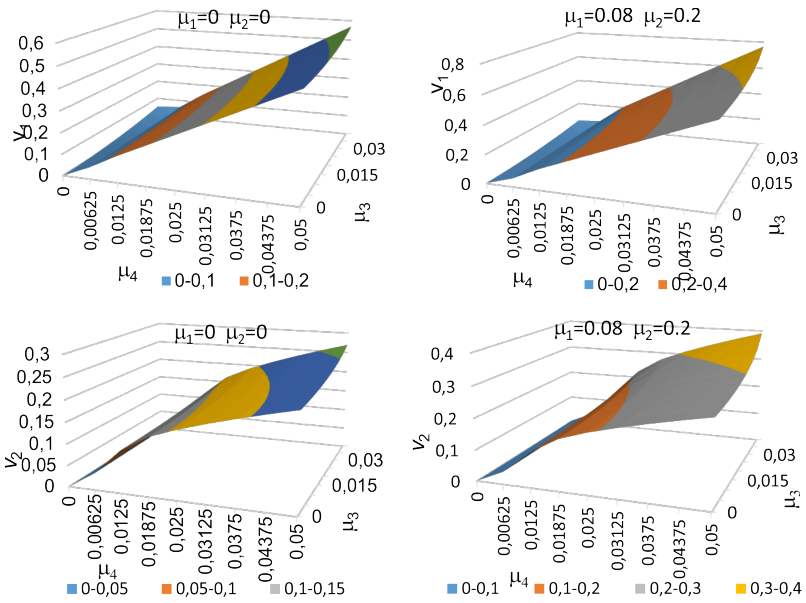

Fig. 7. Maximum and standard deviations.

meshes, changing parameters $\mu_1, \mu_2, \mu_3, \mu_4$ are given in Table III for stabilization system with parameters (10) and in Table IV for the stabilization system with parameters (11).

TABLE III
TIME OF MODELING THE IMPACT OF NONLINEARITIES, SEC.

Processor, serial/parallel	Test 1	Test 2	Test 3	Test 4	Test 5
Grid $6 \times 16 \times 16 \times 16$					
Coprocessor Intel Xeon Phi 5110P, OpenMP	8953	9005	8934	8902	8985
2 coprocessors Intel Xeon Phi 5110P, MPI-MAP/OpenMP	4726	4753	4715	4703	4744
Grid $12 \times 16 \times 16 \times 16$					
Coprocessor Intel Xeon Phi 5110P, OpenMP	18132	18243	18025	18187	18053
2 coprocessors Intel Xeon Phi 5110P, MPI-MAP/OpenMP	9478	9529	9435	9501	9439

TABLE IV
TIME OF MODELING THE IMPACT OF NONLINEARITIES, SEC.

Processor, serial/parallel	Test 1	Test 2	Test 3	Test 4	Test 5
Grid $6 \times 16 \times 16 \times 16$					
Coprocessor Intel Xeon Phi 5110P, OpenMP	5671	5634	5654	5754	5698
2 coprocessors Intel Xeon Phi 5110P, MPI-MAP/OpenMP	2988	2969	2967	3031	3002
Grid $12 \times 16 \times 16 \times 16$					
Coprocessor Intel Xeon Phi 5110P, OpenMP	11205	11278	11154	11174	11237
2 coprocessors Intel Xeon Phi 5110P, MPI-MAP/OpenMP	5777	5809	5735	5741	5798

As follows from the Table III and IV results, with an increase in the average number of nodes on the grid measurement, the multiplicative contribution to the acceleration of the MPI-MAP pattern quickly tends to the number of coprocessors used.

VI. CONCLUSIONS

The proposed parallel algorithm is effective on cluster systems with nodes using processors with a large number of cores. In particular, it is effective on cluster systems with Intel Xeon Phi coprocessors.

REFERENCES

[1] Andreichenko D. K., Andreichenko K. P. On the theory of hybrid dynamical systems. Jour-nal of Computer and Systems Sciences International, 2000, vol. 39, no. 3, pp. 383-398.

[2] Andreichenko D. K., Andreichenko K. P. *Modelirovanie, analiz i sintez kombinirovannykh dinamicheskikh sistem. Uchebnoe posobie* [Modeling, analysis and synthesis of combined dynamical systems. Tutorial]. Saratov, Rait-Ekspo Publ., 2013. 144 p. ISBN 978-5-4426-0018-6 (in Russian).

[3] Andreichenko D. K., Andreichenko K. P., Melnichuk D. V. *Pattern MPI-MAP i modeliro-vanie nelinejnyh kombinirovannyh dinamicheskih sistem* [Pattern MPI-MAP and modeling of nonlinear hybrid dynamical systems] *Problemy upravleniya, obrabotki i peredachi in-formacii* [Problems of control, information processing and transmission]. Saratov, Rait-Ekspo Publ., 2015, vol.2, pp. 19-26. ISBN 978-5-4426-0049-0 (in Russian).

[4] Andreichenko D. K., Andreichenko K. P., Melnichuk D. V., Portenko M. S. Adaptive Algorithm of Parametric Synthesis of Hybrid Dynamical Systems. *Izv. Saratov Univ. (N. S.), Ser. Math. Mech. Inform.*, 2016, vol. 16, iss. 4, pp. 465475 (in Russian). DOI: 10.18500/1816-9791-2016-16-4-465-475.